General Disclaimer

One or more of the Following Statements may affect this Document

- This document has been reproduced from the best copy furnished by the organizational source. It is being released in the interest of making available as much information as possible.

- This document may contain data, which exceeds the sheet parameters. It was furnished in this condition by the organizational source and is the best copy available.

- This document may contain tone-on-tone or color graphs, charts and/or pictures, which have been reproduced in black and white.

- This document is paginated as submitted by the original source.

- Portions of this document are not fully legible due to the historical nature of some of the material. However, it is the best reproduction available from the original submission.

Produced by the NASA Center for Aerospace Information (CASI)

VOLUME I

AN ANALYTICAL STUDY

OF

MEASURED RADIOMETRIC DATA

by

Ronald A. Porter

12 December 1969

Prepared Under Contract No. 952397 by

RADIOMETRIC TECHNOLOGY, INC.
179 - Fifth Street
Cambridge, Massachusetts 02141

for

JET PROPULSION LABORATORY
California Institute of Technology
Pasadena, California



N70-20193
(ACCESSION NUMBER)
363
(PAGES)
CR-108769
(NASA CR OR TMX OR AD NUMBER)
(THRU)
1
(CODE)
13
(CATEGORY)
FACILITY FORM 602

VOLUME I

AN ANALYTICAL STUDY OF MEASURED RADIOMETRIC DATA

by

Ronald A. Porter

12 December 1969

Prepared Under Contract No. 952397 by

RADIOMETRIC TECHNOLOGY, INC.
179 - Fifth Street
Cambridge, Massachusetts 02141

for

JET PROPULSION LABORATORY
California Institute of Technology
Pasadena, California

PRECEDING PAGE BLANK NOT FILMED.

ACKNOWLEDGEMENTS

The author wishes to acknowledge the cooperation and assistance of the following individuals who made valuable contributions to this study in the indicated areas:

Mr. D. K. Agrawal	- analysis of portions of reduced data.
Dr. N. E. Gaut (Environmental Research & Technology, Inc.)	- generation of calculated sky brightness temperatures.
Mr. P. Morgenstern (Walden Research Corp.)	- derivation of diffuse emissivities of Salines.
Mrs. N. C. Spencer	- computer programming for data reduction and plotting.

Mrs. Spencer's contributions are particularly appreciated due to the complex requirements imposed by the programming aspects of the study.

TABLE OF CONTENTS

Section	Title	Page
I	INTRODUCTION	1
II	CRITIQUE AND ERROR ANALYSIS OF MEASURED DATA	4
	A. Calculation of Sky Brightness Temperatures	5
	1. Theory	6
	2. Atmospheric Models	8
	3. Computer Output	11
	4. Plotted Data	12
	B. Review of Radiometer Calibration Methods	22
	1. Two-Load Calibration Method	22
	2. Attenuator Calibration Method	27
	C. Segregation of Valid Data	30
	D. Radiometer Errors	32
III	DATA REDUCTION METHODS	37
	A. Conversion of Output Voltages to Apparent Temperatures	37
	B. Conversion of Apparent Temperatures to Brightness Temperatures	39
	C. Conversion of Brightness Temperatures to Emissivities	41
	1. Specular Emissivities	41
	2. Determination of Emissivities of Rough Surfaces	42
	D. Computer Programs Employed in Data Reduction	46
	1. RADIOP Modifications	47
	2. Antenna Pattern Correction	48
	3. EMISS Program	49
	4. Program for Plotting Apparent and Brightness Temperatures versus Nadir Angle (PLOTER)	50

TABLE OF CONTENTS (Continued)

Section	Title	Page
	5. Program for Calculating Emissivities for a Lambert Surface	50
IV	STUDY RESULTS AND ANALYSIS	53
	A. Sea Water - Data Results and Analysis	53
	1. 9.5 GHz Data	54
	2. 16.5 GHz Data	60
	3. 94 GHz Data	74
	B. Analysis of Theoretical Sea Water Data	85
	1. Dielectric Permittivities of Sea Water	85
	2. Theoretical Emissivities of Sea Water	93
	C. Additional Analysis of Sea Water Data	93
	1. Analysis to Show The Utility of Converting Apparent Temperatures to Brightness Temperatures	93
	2. Frequency, Polarization and Angular Dependence of Sea Water Brightness Temperatures	108
	3. Influence of Sea Surface Temperatures on Brightness Temperatures	110
	4. Effects of Sea Surface Roughness on Brightness Temperatures	110
	D. Salines - Data Results and Analysis	119
	1. 9.5 GHz Data	119
	2. 16.5 GHz Data	133
	3. 94 GHz Data	149
	4. Comparison of Derived and Calculated Brightness Temperatures - Salines	162
	5. Comparison of Specular and Diffuse Emissivities - Salines	162
	E. Quartz Sand - Data Results and Analysis	168

TABLE OF CONTENTS (continued)

Section	Title	Page
	1. 9.5 GHz Data - Quartz Sand	168
	2. 16.5 GHz Data - Quartz Sand	183
	3. 94 GHz Data - Quartz Sand	196
	4. Comparison of Derived and Calculated Brightness Temperatures - Quartz Sand	208
	F. Limestone - Data Results and Analysis	208
	1. 9.5 GHz Data - Powdered Limestone	215
	2. 9.5 GHz Data - Pebbled Limestone	215
	3. 16.5 GHz Data - Pebbled Limestone	229
	4. Comparison of Derived and Calculated Brightness Temperatures - Pebbled Limestone	239
	5. 94 GHz Data - Pebbled Limestone	248
	6. Polarization and Frequency Dependence of Brightness Temperatures and Emissivities - Limestone	258
	G. Influence of Surface Roughness on Brightness Temperatures of Solid Materials	259
	H. Effects of Surface and Subsurface Temperatures on Brightness Temperatures and Emissivities	261
	1. Limestone	262
	2. Salines	262
	3. Quartz Sand	263
V	DETERMINATION OF DIELECTRIC CONSTANTS OF SPECULAR MATERIALS	264
	A. Theoretical Considerations	264
	B. Method for Calculation of e' and T	268
	C. Analysis of Limestone Calculations	275
VI	CONCLUSIONS	283

TABLE OF CONTENTS (continued)

Section	Title	Page
	A. Correction of Calibration Errors	283
	B. Sea Water Data	283
	C. Salines Data	284
	D. Quartz Sand Data	285
	E. Limestone Data	285
	F. Other Conclusions	286
VII	RECOMMENDATIONS	288
	REFERENCES	290
A	APPENDIX A - ANTENNA PATTERN CORRECTION	A-1
B	APPENDIX B - COMPUTER PROGRAMS FOR ANTENNA PATTERN CORRECTION	B-1
C	APPENDIX C - CALCULATION OF EMISSIVITY FOR SPECULARLY REFLECTING MATERIALS	C-1
D	APPENDIX D - COMPUTER PROGRAM FOR CALCULATION OF e' AND T	D-1

I. INTRODUCTION

The objective of this study was to perform an analysis of microwave radiometric data, obtained during a field measurement program, conducted at several locations in California in 1966. Measurements were performed with three radiometers, operating at 9.5, 16.5 and 94 GHz, mounted in a mobile van. This program was conducted by the Raytheon Company, under contract to the Jet Propulsion Laboratory. Supporting investigations were performed at the time by the following organizations:

Marine Advisers, Inc. La Jolla, California.	- Correlative measurements during sea water observations.
Mackay School of Mines, University of Nevada, Reno, Nevada.	- Geological measurements on solid materials.
Laboratory for Insulation Research, Massachusetts Inst. of Technology Cambridge, Massachusetts.	- Laboratory measurements of dielectric permittivities on all materials observed in the program.

The radiometers employed in the measurements were conventional Dicke-type, double-sideband units with internal calibration circuitry furnishing two absolute references, at ambient temperature and at approximately 400 degrees Kelvin. The minimum detectable temperature sensitivities and antenna characteristics are listed below for purposes of reference.

Operating Frequency	Temperature Sensitivity	Integration Time	Antenna* Diameter	3-db Beamwidth
9.5 GHz	0.4°K rms	1 sec.	19 in.	5.5°
16.5 "	0.5 " "	1 "	16 "	3.7°
94 "	1.2 " "	3 "	6 "	1.6°

*Prime-focus paraboloidal antennas.

Materials observed in the field program were as follows:

Ocean Water	- at Tidewater Oil Co., drilling pier, Ventura, Calif.
Salines	- at Devil's Golf Course, Death Valley, California.
Quartz Sand	- at Osborne Lookout, Brawley, California.
Limestone (Powdered and Pebbled)	- Phizer Co., quarry, Lucerne Valley, California.

Preliminary data reductions and analyses were performed in 1966 at Raytheon Co.; the results of this work were presented in References (1) and (2) reports. These documents, together with associated computer cards and other data, formed the basis for the current study. The detailed objectives of this study were as follows:

1) Perform a critique and error analysis of measured radiometric data.

2) Convert apparent temperatures to brightness temperatures, by correcting for radiations received via antenna sidelobes and backlobes.

3) Convert brightness temperatures to emissivities, for both specular and diffuse surfaces.

4) Analyze measured data by correlation with data obtained by Marine Advisers, Inc., University of Nevada and the Massachusetts Institute of Technology.

5) Analyze the contributions of subsurface temperatures to brightness temperatures.

6) Investigate the development of techniques for determining the dielectric constants of specular and diffusely reflecting surfaces, and apply these to the measured radiometric data.

Most of the above objectives have been realized; however, due to excessive efforts required in the computer programming and data reduction areas, it was necessary to limit the amount of work devoted to Items (5) and (6). Nonetheless, a comprehensive study was performed in the critical areas represented by the preceding four Items.

Early in the study it was realized that a new reduction of the raw data was necessary, due to the unstable character of certain data. The cause of this instability lay in the radiometer calibration scheme, which utilized two calibration temperatures above the dynamic range of the input signal. A third calibration point was introduced, at the low end of the dynamic range, in the form of a calculated value of zenith sky brightness temperature. A different value was used for each data "Run", based on prevailing atmospheric conditions. The new output voltage-apparent temperature conversion curve was represented by a best-fit-straight-line drawn between the three calibration points. In this manner all negative and excessively positive apparent sky temperatures were eliminated. Stabilization of the apparent sky temperatures automatically improved the prime(surface) data.

The new apparent temperatures were converted to brightness temperatures with the aid of a special computer program which permitted separation of radiations received via the antenna sidelobes and backlobes. Following this operation, specular emissivities were derived from the brightness temperatures. In the case of the Saline material, diffuse emissivities were derived using appropriate scattering coefficients. Both brightness temperatures and emissivities were subsequently analyzed in terms of angular, polarization, temperature and frequency dependence. Correlations were performed to determine the effects of influencing factors, such as surface roughness, surface temperature and certain environmental conditions. In addition, comparisons were made in many cases with theoretical data. A set of conclusions and recommendations for further studies are also presented in the report.

This report consists of three volumes. All written material is contained in this Volume, together with typical brightness temperature and emissivity data. Volume II contains the remaining sea water information and Volume III includes the balance of the solid material data. Although approximately 15 percent of the measured radiometric data was discarded, in the course of segregation of valid data, a considerable mass of quantitative information is represented by the remaining data.

Based on the results obtained in the study, it is felt that information presented in this report will be of considerable value in the application of microwave radiometry to remote sensing of earth resources.

II. CRITIQUE AND ERROR ANALYSIS OF MEASURED DATA

An analysis was performed to determine possible errors in radiometer calibrations, involved in the original data reduction work at Raytheon Co., and to furnish a means of correcting such errors. A variety of errors were discovered with the result that a third calibration point, consisting of a calculated value of zenith sky brightness temperature, was considered necessary. This additional calibration point was obtained individually for each data "Run" (a "Run" being defined as a single pass with the radiometer from zenith to nadir, or vice-versa).

In addition to the above, the calibration method employed in each radiometer was reviewed and calibration circuit losses corrected where necessary. Two different calibration methods were employed, each providing a 2-point calibration. The 9.5 and 16.5 GHz radiometers both utilized a method involving a series combination of a "Hot Load" and a precision variable attenuator. Two separate waveguide "loads", at different temperatures, were employed in the 94 GHz radiometer for most of the field measurements.

Following data reduction and conversion of apparent temperatures to brightness temperatures, valid data was segregated from data containing gross errors on the basis of a tolerance assigned to calculated values of zenith sky brightness temperatures. Data runs with zenith sky brightness temperature values falling outside the assigned tolerance were excluded from further analysis.

An error analysis was performed on each radiometer to establish over-all errors inherent in the equipment and in the data reduction technique. This work included a review of Reference (3) report and a comparison of apparent temperatures obtained in the current data reduction with those obtained during the original data reduction, performed in 1966. The latter analysis provided a useful set of information concerning the improvements achieved in the current data reduction.

A. CALCULATION OF SKY BRIGHTNESS TEMPERATURES

Calculated sky brightness temperatures were employed as a basis for a third calibration point, for conversion of radiometer output voltages to apparent temperatures. Only the zenith values of sky brightness temperatures were used in this manner; calculations for the zenith-pointing condition are considered to be more accurate than at any other zenith angle. A computer program was utilized to calculate a set of sky brightness temperatures, from zenith to 80 degrees off the zenith, for each set of recorded environmental data.

The approach used in the sky brightness temperature calculations is described in the paragraphs below.

Using measured values of air temperature, pressure, and humidity as inputs, obtained during the Field Measurement Program, reasonable atmospheric temperature, pressure, and humidity profiles were established to altitudes beyond which the effective sky brightness temperatures were expected to be less than one (1) degree Kelvin, at 9.5, 16.5 and 94 GHz. A sufficient number of profiles were generated to represent the range of conditions covered by the sets of input atmospheric data. Approximately 140 sets of measured values were furnished for this purpose.

With the above profiles as inputs, sky brightness temperatures were calculated for clear sky, fog and cloud conditions as applicable, at 9.5, 16.5 and 94 GHz, for each set (or group of sets) of input data, for zenith angles in the range 0 to 80 degrees. To conserve effort, an attempt was made to group sets of data that were reasonably similar so that a given group was represented by an appropriate atmospheric model.

The resultant data was tabulated by Run No., Date and Time, in terms of sky brightness temperature as a function of zenith angle, for each frequency. The input data, together with the atmospheric profile information, was also tabulated and arranged for easy cross-referencing with the sky brightness temperatures. In addition, computer cards containing the above information, were prepared.

Information contained in References (5) thru' (12) was used in this work.

1. Theory

The atmospheric constituents of consequence are oxygen, water vapor and small water droplets (small with respect to λ, where λ is the wavelength of the radiation being monitored). The attenuation coefficients for each of the constituents are given below.

a. Oxygen

$$\gamma_{O_2} = C_1 \, P \, T^{-3} \, \nu^2 \sum_N S_N \exp\,(-E_N/kT) \qquad (1)$$

where,

γ_{O_2} = absorption coefficient for oxygen

ν = frequency in gigacycles

P = atmospheric pressure in millibars

T = atmospheric temperature in degrees Kelvin

N = rotational quantum number

C_1 = 2.0058 for γ_{O_2} in decibels/km.

E_N = energy of rotational state N

k = Boltzmann's constant

$\sum_N$ = summation taken over all rotational levels with significant populations

$$S_N = F_N + \mu_{N+}^2 + E_{N-}\mu_{N-}^2 + F_o \mu_{N_o}^2$$

in which N+ and N- refer to the transitions $N \rightarrow N+1$ and $N \rightarrow N-1$ respectively and the F's and μ's have the meanings

$$F_{N\pm} = \frac{\Delta\nu}{(\nu_{N\pm} - \nu)^2 + \Delta\nu^2} + \frac{\Delta\nu}{(\nu_{N\pm} + \nu)^2 + \Delta\nu^2}$$

$$F_o = \frac{\Delta\nu}{\nu^2 + \Delta\nu^2}$$

$$\mu_{N+}^2 = \frac{N(2N+3)}{N+1}$$

$$\mu^2_{N-} = \frac{(N + 1)\ (2N + 1)}{N}$$

$$\mu^2_{N_o} = \frac{2(N^2 + N + 1)\ (2N + 1)}{N(N + 1)}$$

$\Delta\nu$ = α P[0.21 + 0.78β] $\left[\frac{300}{T}\right]^{0.85}$

$\nu_{N\pm}$ = resonance frequency for given transition

α = 1.44 MHz/mb

β = 0.25 for z H_1 (P 356 mb)

β = 0.25 + 0.50 $(h-H_2)/(H_2-H_1)$ for H_1 z H_2

β = 0.75 for z H_2 (P 25.3 mb)

where z, H_1 and H_2 are similar units and represent distance above the earth's surface.

b. Water Vapor

$$\gamma_{H_2O} = 1.570 \times 10^3 \frac{\rho_{H_2O}\ \nu^2\ e^{-642/T}}{T^{5/2}} \left[\frac{\Delta\nu}{(\nu_{1.35} - \nu)^2 + \Delta\nu^2} + \right.$$

$$\left. + \frac{\Delta\nu}{(\nu_{1.35} + \nu)^2 + \Delta\nu^2} \right] + 1.11 \times 10^{-2} \frac{\rho_{H_2O}\ \nu^2\ \Delta\nu}{T^{3/2}} \qquad (2)$$

where,

γ_{H_2O} = absorption coefficient for water vapor in db/km.

ρ_{H_2O} = water vapor density in g/m^3

ν = frequency in gigahertz

T = atmospheric temperature in degrees Kelvin

$\nu_{1.35}$ = resonance frequency of lowest water vapor line

$$\Delta\nu = 2.62 \left(\frac{P}{1013.25} \right) \left(\frac{T}{300} \right)^{-0.626} \left(1. + 0.015 \frac{\rho_{H_2O}\, T}{P} \right) \text{ GHz}$$

c. Cloud, Fog and Haze

For conditions where "a" the drop diameter is considerably smaller than λ the wavelength,

$$\gamma_{CLOUD} = \frac{M\left\{10^{(0.0122(291 - T)-6}\right\}}{\lambda^2} \qquad (3)$$

where,

M = liquid water concentration in g/m^3

T(z) = atmospheric temperature at level z in degrees Kelvin.

λ = wavelength of the radiation in cm.

2. Atmospheric Models

In order to calculate a brightness temperature, it was necessary to know or assume the vertical distribution of temperature, pressure, water vapor density, and liquid water concentration. For the first three quantities, two methods were used.

Method (1) involved the use of radiosonde data taken over the time periods of the measurements for those weather stations closest to the radiometer measurement sites. The stations available were the following:

03131 San Diego, Calif.	elevation	124	meters
23114 Edwards AFB, Calif.	"	724	"
23169 Las Vegas, Nev.	"	660	"
93104 China Lake, Calif.	"	660	"
93116 San Nicolas Is.	"	174	"
93214 Vandenburg AFB Calif.	"	100	"

The above stations represented the closest active radiosonde stations for the four radiometer sites:

1.	Ventura, Calif.	elevation	0	meters
2.	Brawley, Calif.	"	-33	"
3.	Death Valley, Calif.	"	-250	"
4.	Lucerne Valley, Calif.	"	967	"

The second method for determining the vertical distribution of pressure, temperature and humidity was based solely upon the reported surface conditions. The surface temperature was lapsed at $6.5^{\circ}K$ per kilometer up to the assumed tropopause near 10 km, then allowed to remain steady up to 19 km, and finally was elevated at the rate of $1.8^{\circ}K$ per km up to 30 km. The surface moisture was allowed to decrease with a scale height of 2.2 km up to 18 km and assumed zero above. (This scale height now appears to be too large, based upon the evidence of many radiosondes around the Southern California region).

In both modeling methods, the reported surface conditions and heights were incorporated into the modeled atmospheres.

For each of the radiometer sites, there was a preferred radiosonde station or perhaps as many as three which were searched for on a given observation day. The preferences in order are listed below:

Ventura	- 03214, 93116, 93131
Brawley	- 03131
Death Valley	- 23169
Lucerne Valley	- 23114, 93104

On days where no radiosonde data could be found, the surface-based model only was used.

For clouds, fog, and haze, relatively poor observations were taken at the radiometer. Therefore, models were constructed based upon what the subjective notes on hydrometeors really meant. Nine categories of haze, fog, and clouds were finally constructed. They are listed below in terms of the liquid water concentration M at height H:

1) Light haze

$M(1) = 10^{-5}$ g/m^3	H (1) = 0 meters
$M(2) = 10^{-5}$	H (2) = 100
M (3) = 0	H (3) = 200

2) Medium haze

M (1) = 10^{-4} g/m^3	H (1) = 0
M (2) = 10^{-4}	H (2) = 100
M (3) = 0	H (3) = 200.

3) Heavy haze

M (1) = 10^{-3} g/m^3	H (1) = 0. meters
M (2) = 10^{-3}	H (2) = 100
M (3) = 0	H (3) = 200

4) Light fog (visibility approx. 2000 ft.)

M (1) = 0.032 g/m^3	H (1) = 0
M (2) = 0.032	H (2) = 25
M (3) = 0	H (3) = 100

5) Medium fog (visibility approx. 400 ft.)

M (1) = 0.32 g/m^3	H (1) = 0 meters
M (2) = 0.32	H (2) = 37.5
M (3) = 0	H (3) = 10

6) Heavy fog (visibility approx. 100 ft.)

M (1) = 3.2 g/m^3	H (1) = 0 meters
M (2) = 3.2	H (2) = 50
M (3) = 0	H (3) = 100

7) Light overcast (sun image visible)

M (1) = 0 g/m^3	H (1) = 300 meters
M (2) = 0.33	H (2) = 400
M (3) = 0.33	H (3) = 600
M (4) = 0	H (4) = 650

8) Medium overcast (no sun, light sky)

M (1) = 0 g/m^3	H (1) = 400 meters
M (2) = 0.67	H (2) = 550
M (3) = 0.67	H (3) = 850
M (4) = 0	H (4) = 900

9) Heavy overcast

M (1) = 0 g/m^3	H (1) = 500 meters
M (2) = 1	H (2) = 1000
M (3) = 1	H (3) = 3000
M (4) = 0	H (4) = 3200

Judgments were made as to which condition above was closest to the recorded conditions for any given radiometer site observation. These conditions were then inserted into the clear sky models previously mentioned and the opacities and brightness temperatures computed.

3. Computer Output

Results are both printed and punched. Printed output is self-explanatory. Punched output is in the following format:

Card 1 : Radiosonde station number, month, day, year, time of radiometer observation, run number, model atmosphere number, radiometer site by assigned numbers, number of levels in atmosphere model, card sequencing number.
Format: (9I5, 33X, 2A1)

Cards 2 thru' 4 : Pressure in millibars at each level in model atmosphere sequentially, card sequencing number.
Format: (13F6.1, 2A1)

Cards 5 thru' 7 : Height of each level in model atmosphere in meters, card sequencing number.
Format: (13F6.0, 2A1)

Cards 8 thru' 10 : Temperature in degrees Kelvin at each level in model atmosphere, card sequencing number.
Format: (13F6.1, 2A1)

Cards 11 and 12 : Water vapor density in g/m^3 at each level in model atmosphere, card sequencing number.
Format: (13F6.2, 2A1)

Card 13 : Number of levels with non-zero condensed water values, level with condensed water information, liquid water concentration g/m^3, card sequencing number.

Format: (I2, 9(Z1, 1PE7.1), 4X, 2A1)

Cards 14 thru' 22 : Zenith angle, T_{H_2O} for 9.5 GHz, T_{O_2} for 9.5 GHz, T_{Cloud} for 9.5 GHz, T_{Total} for 9.5 GHz, T_{H_2O} for 16.5 GHz, T_{O_2} for 16.5 GHz, T_{Cloud} for 16.5 GHz, T_{Total} for 16.5 GHz, T_{H_2O} for 94 GHz, T_{O_2} for 94 GHz, T_{Cloud} for 94 GHz, T_{Total} for 94 GHz, card sequencing number.

Format: (13F6.2, 2A1)

When the results from the atmosphere derived from a radiosonde are punched, the radiosonde station number will appear and the model atmosphere number will be 1. When the model derived from only surface data is punched these two numbers will appear as 0 and 2, respectively.

The card sequencing numbers are to the base 36 using the 10 arabic numerals plus 26 alphabetic characters. They run sequentially from 0 to ZZ and then start over again.

4. Plotted Data

Figures 1 thru' 9 show plots of calculated sky brightness temperatures for each measurement site and radiometer frequency. Curves representing extreme values of sky brightness temperatures, for each site, are shown in each plot. In most cases, clear sky conditions are implied by the curves, although some cloudy conditions are represented in Figures 2 and 3 (Ventura site).

It will be observed that, for clear sky conditions, the zenith brightness temperatures lie in the range 3 - 3.5°K at 9.5 GHz; 6 - 8.5°K at 16.5 GHz; and 62 - 85°K at 94 GHz. Considerably higher zenith brightness temperatures

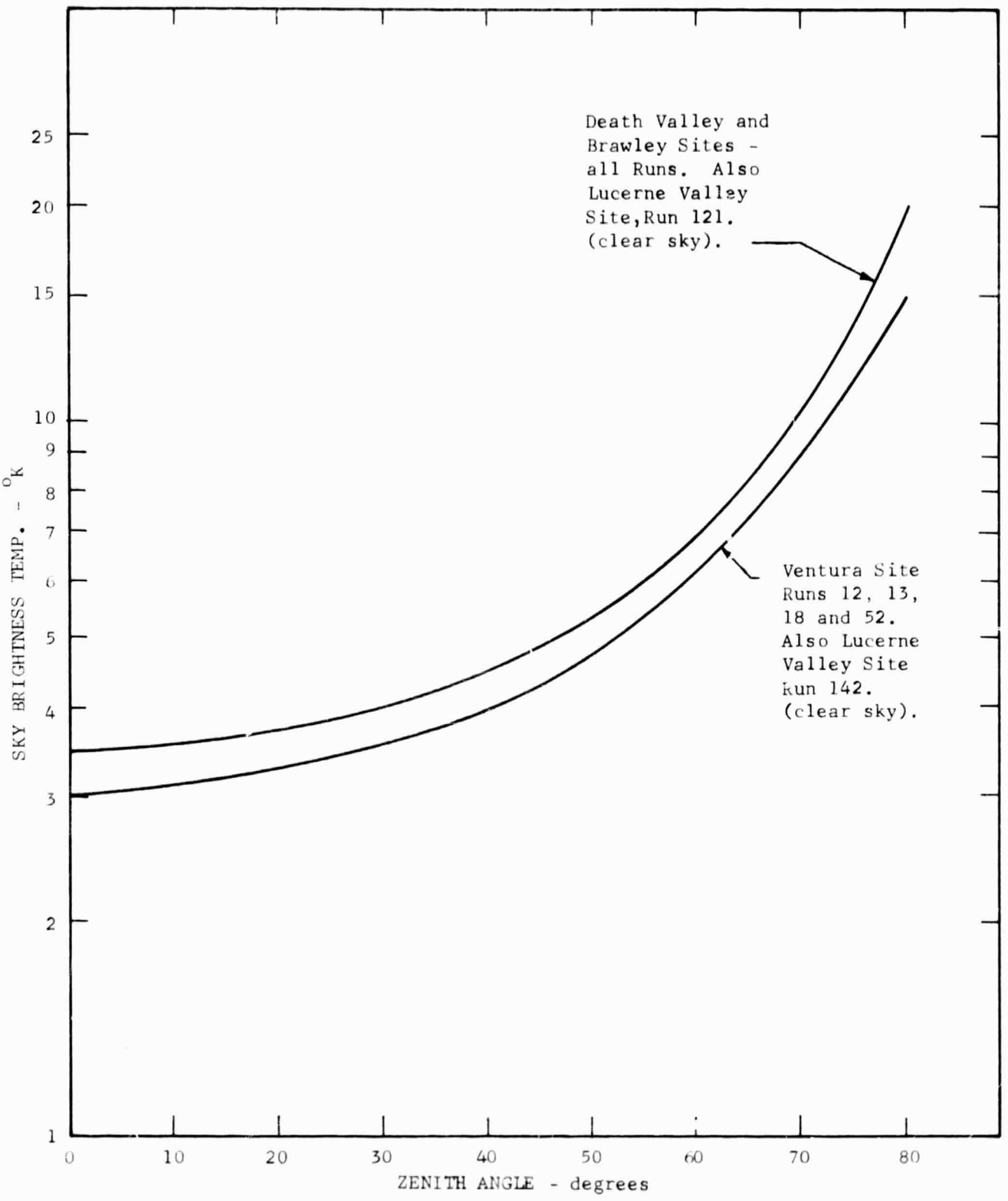


Figure 1 - Calculated Sky Brightness Temperatures, from Recorded Environmental Conditions - 9.5 GHz

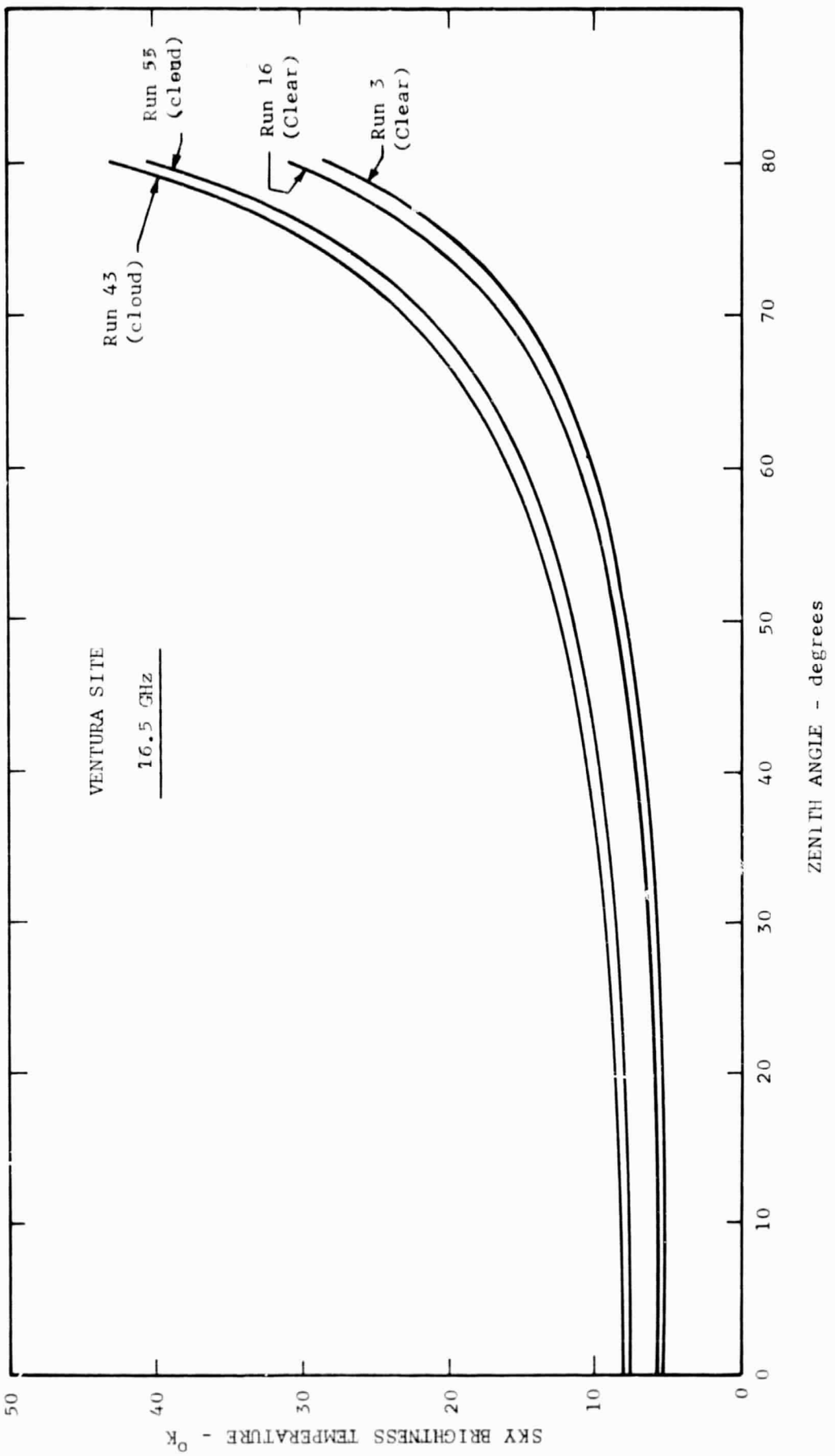


Figure 2 - Calculated Sky Brightness Temperatures, from Recorded Environmental Conditions - 16.5 GHz

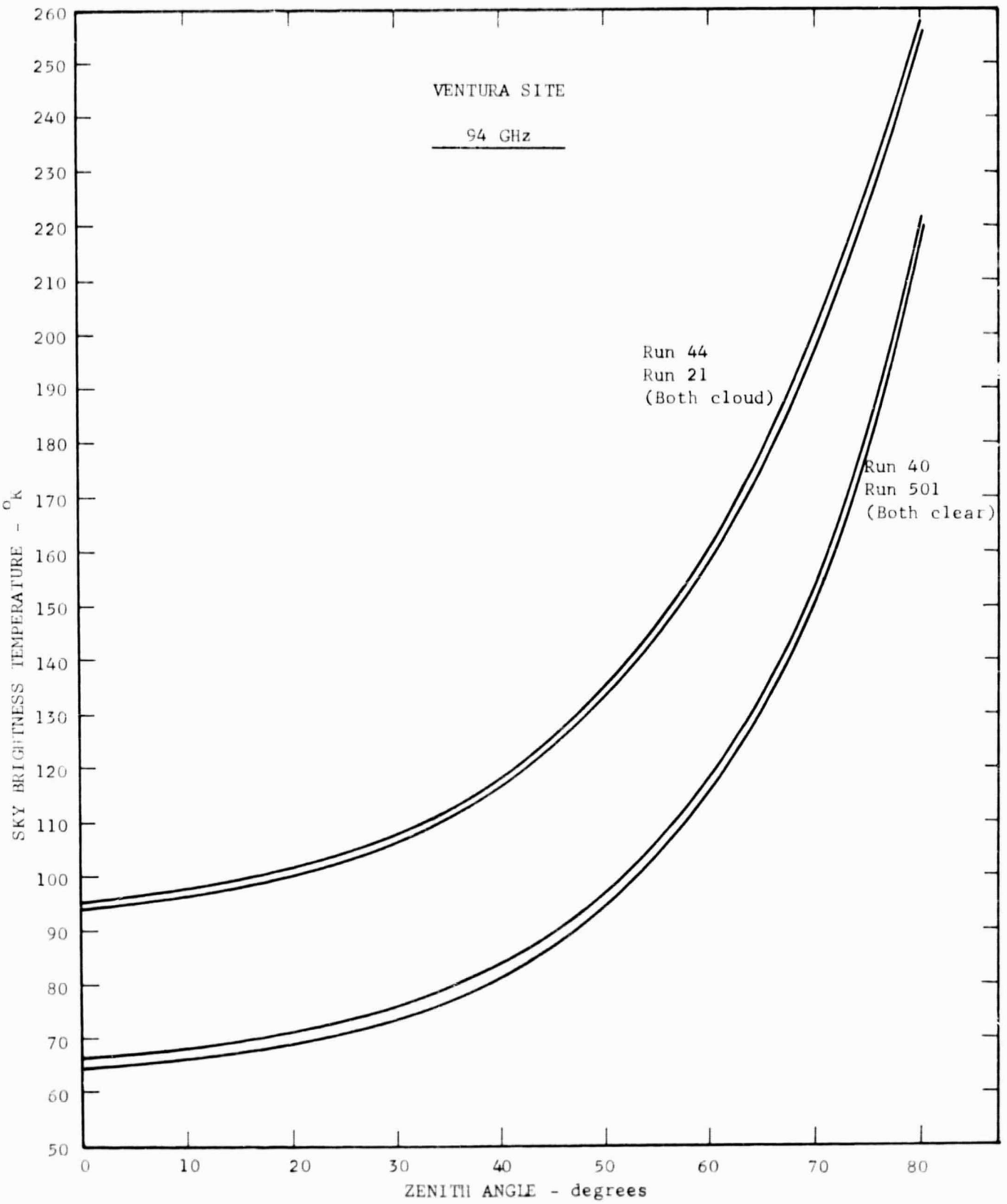


Figure 3 - Calculated Sky Brightness Temperatures, from Recorded Environmental Conditions - 94 GHz

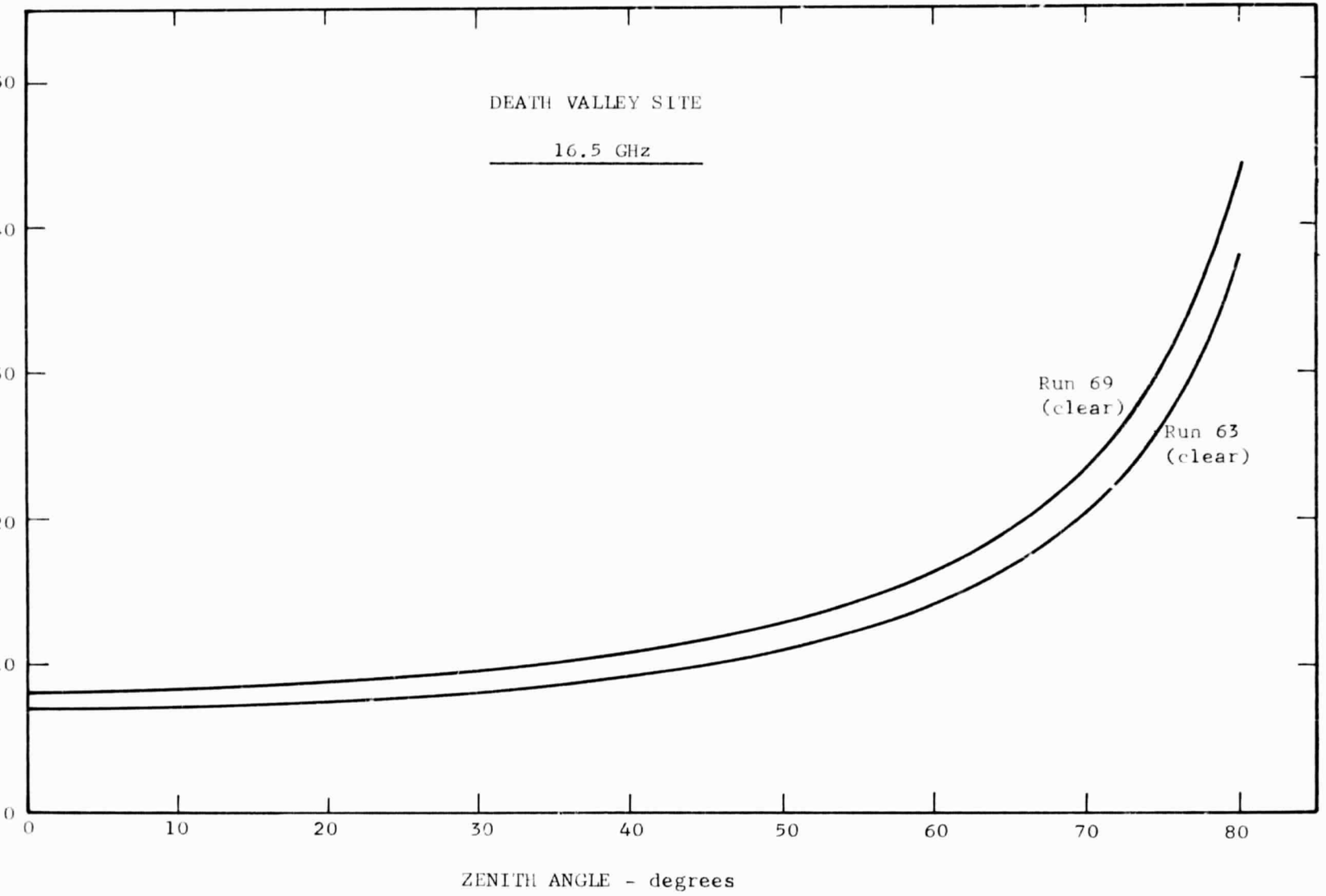


Figure 4 - Calculated Sky Brightness Temperatures, from Recorded Environmental Conditions - 16.5 GHz

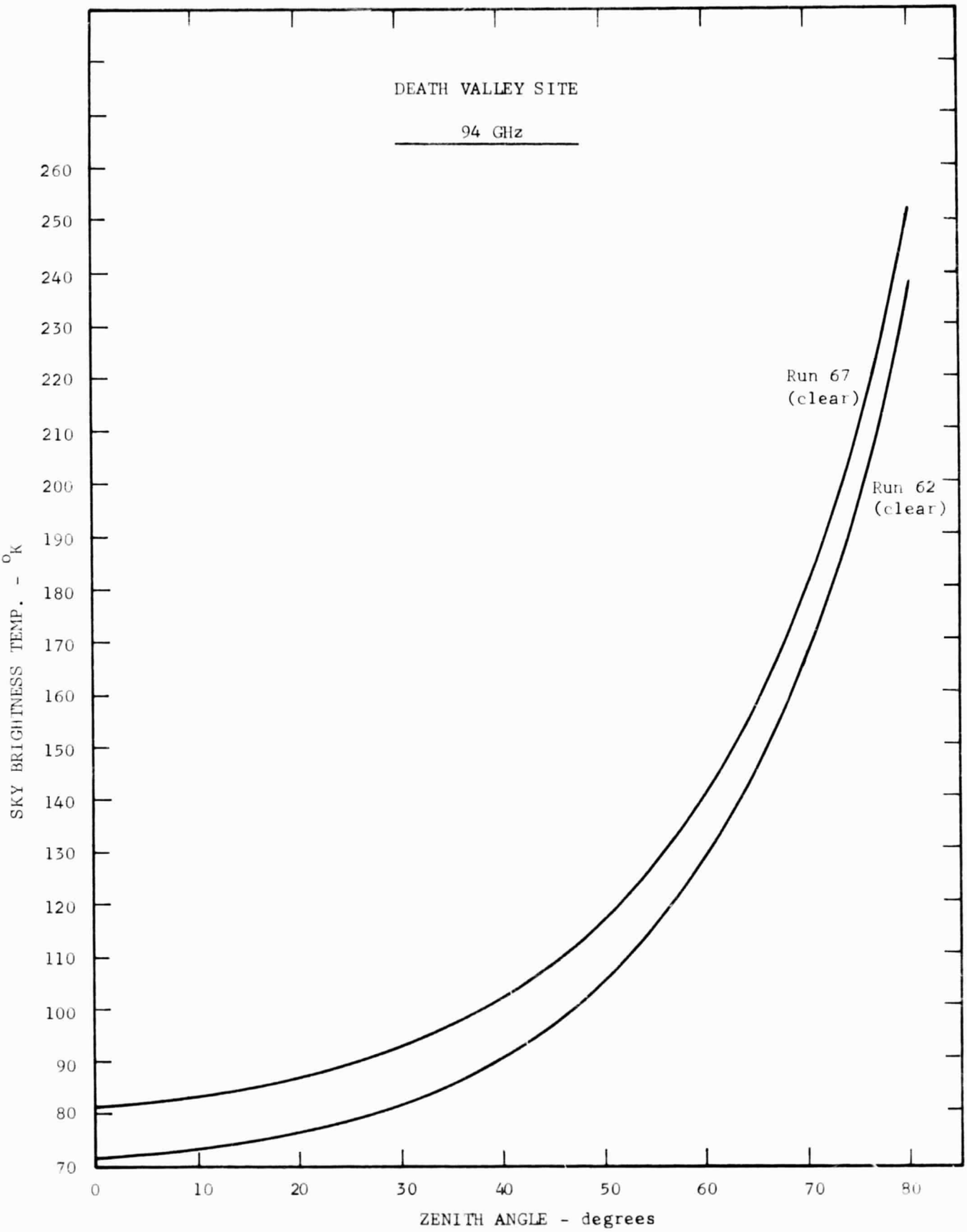


Figure 5 - Calculated Sky Brightness Temperatures, for Recorded Environmental Conditions - 94 GHz

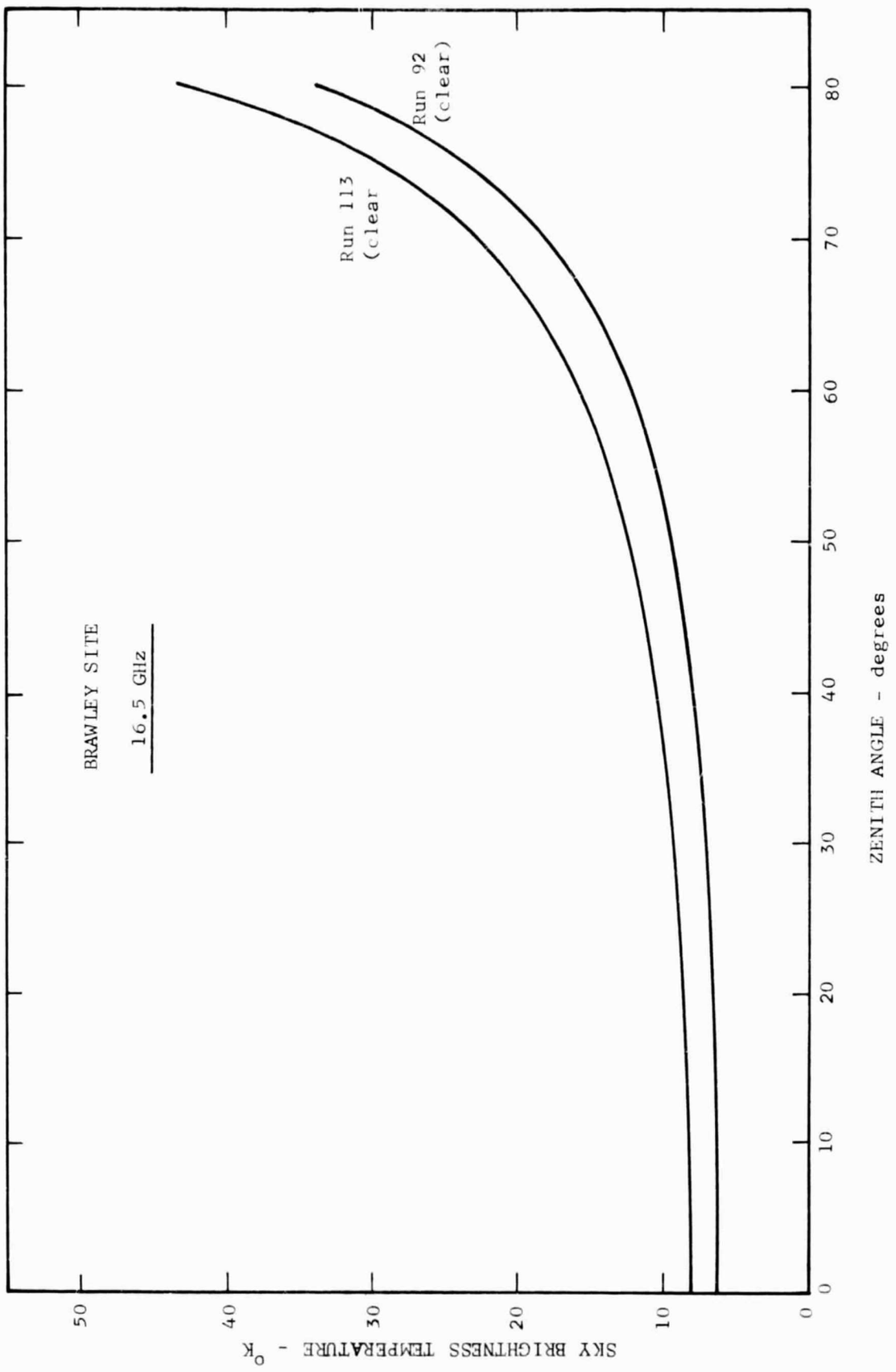


Figure 6 - Calculated Sky Brightness Temperatures, from Recorded Environmental Conditions - 16.5 GHz.

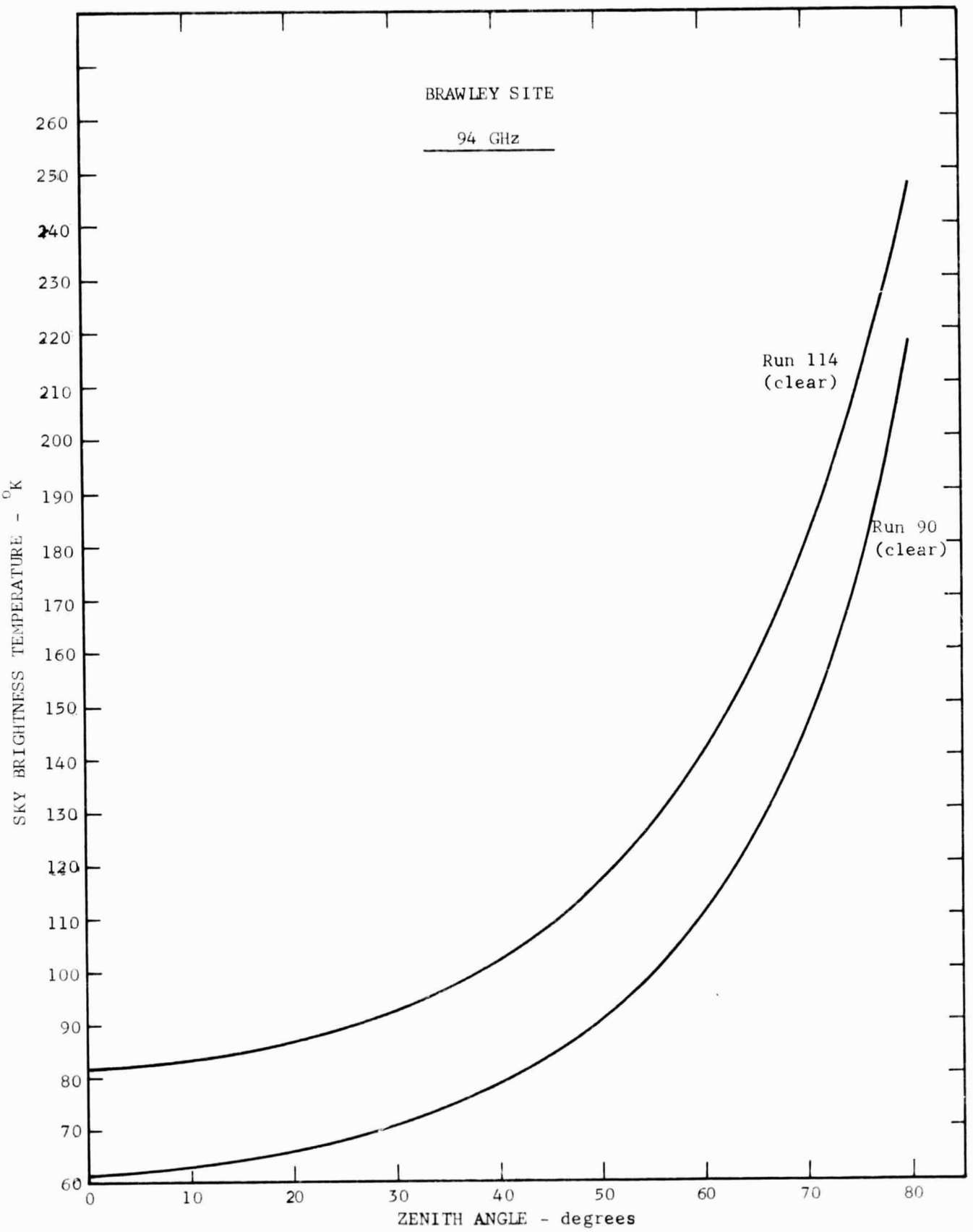


Figure 7 - Calculated Sky Brightness Temperatures, from Recorded Environmental Conditions - 94 GHz

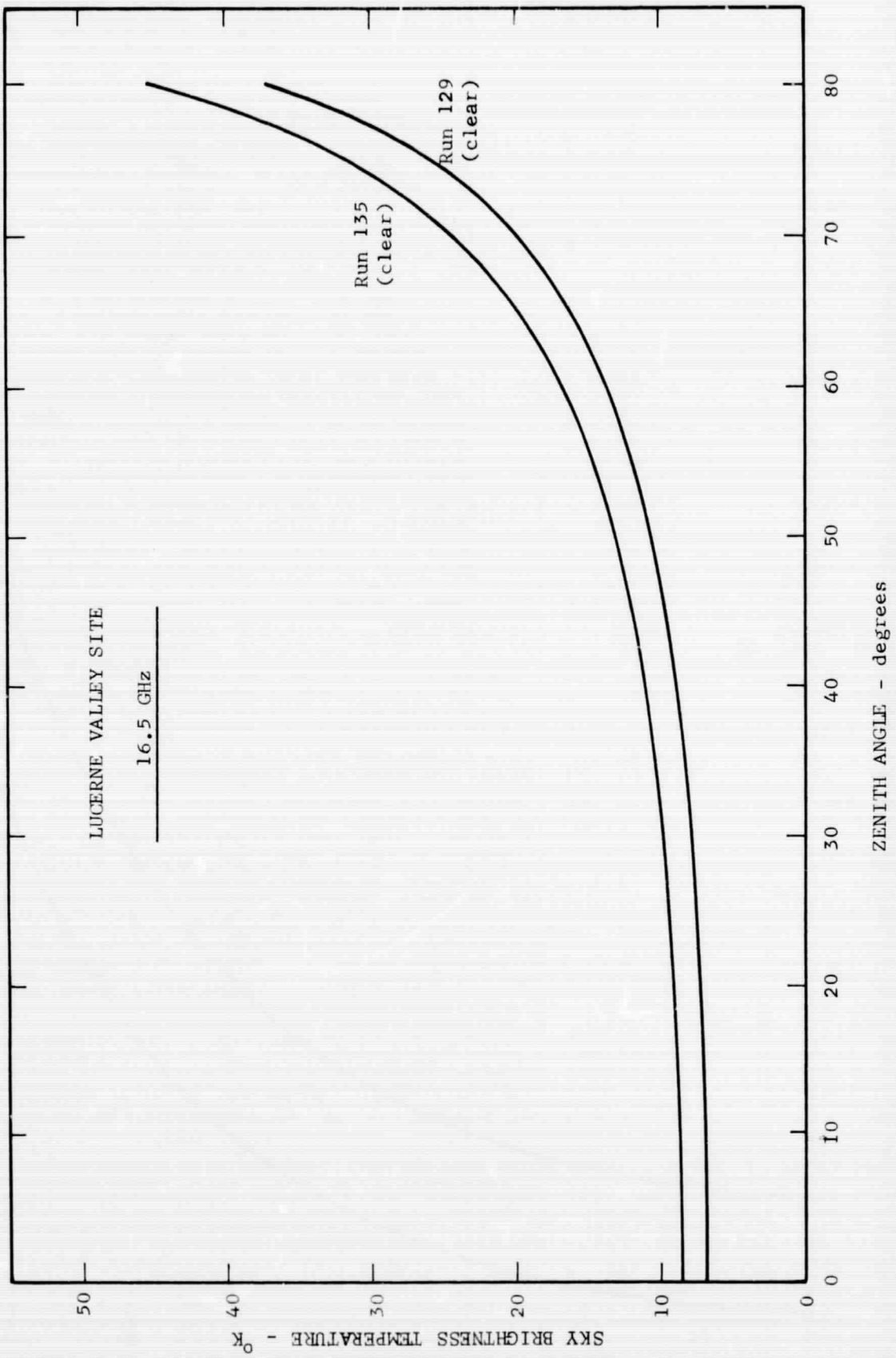


Figure 8 - Calculated Sky Brightness Temperatures, from Recorded Environmental Conditions - 16.5 GHz

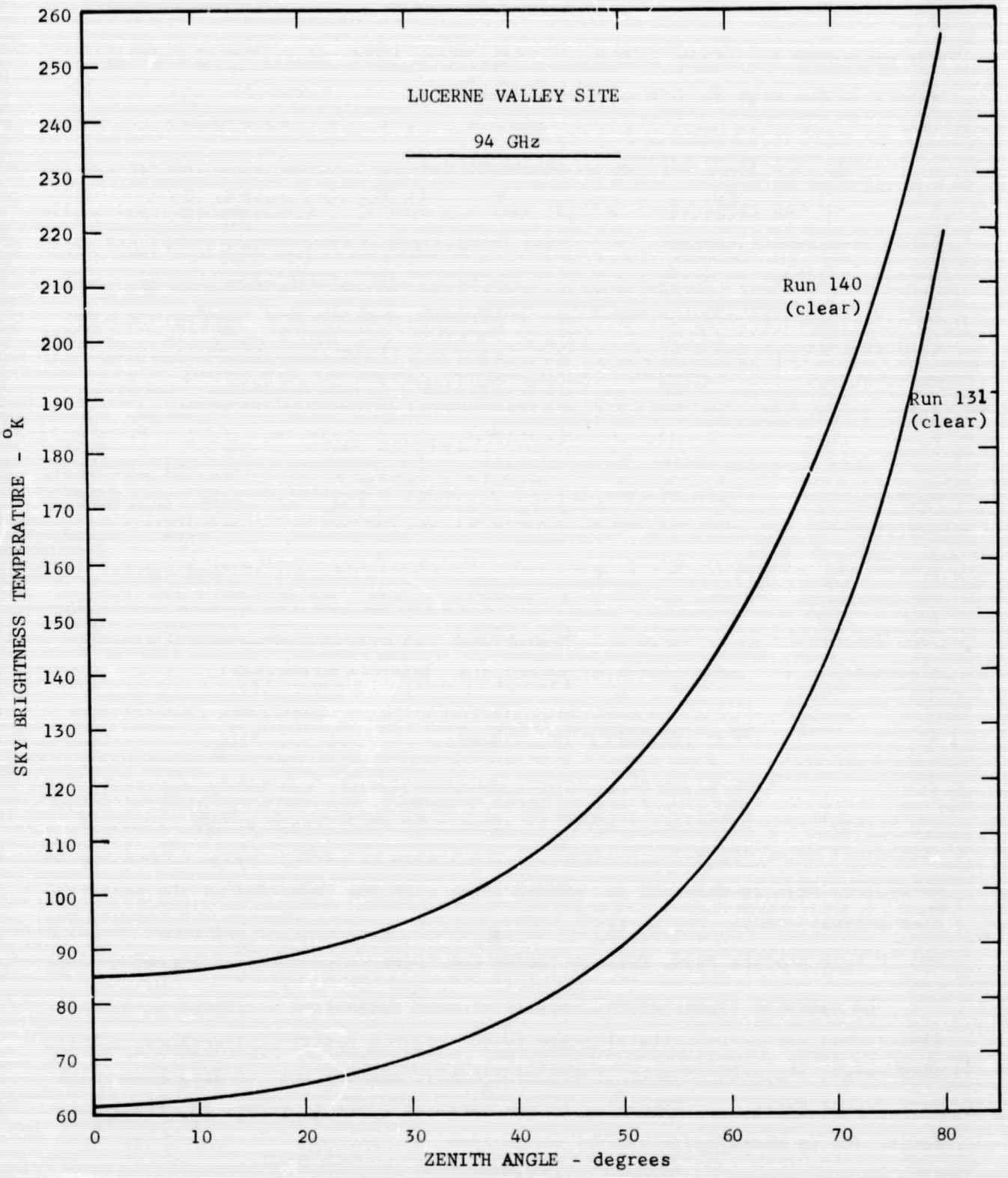


Figure 9 - Calculated Sky Brightness Temperatures, from Recorded Environmental Conditions - 94 GHz

are evidenced for cloudy conditions, especially at 94 GHz. Figure 3 shows values in the rage 93 - 96°K at this frequency.

B. REVIEW OF RADIOMETER CALIBRATION METHODS

Two calibration methods were employed in the radiometers used in the field measurement program. All three radiometers were originally designed for 2-point calibration utilizing a variable attenuator in series with a Hot Load; the latter consisted of a waveguide termination mounted in a temperature-controlled oven operating at a nominal temperature of 400°K. The calibration temperatures were obtained by setting the attenuator at minimum and maximum attenuations, in turn.

Since the above method was cumbersome, due to the need for frequent manual adjustment of a component situated approximately twenty feet above the ground, a modification procedure was instituted early in the measurement program to convert the 94 GHz radiometer to a 2-load, remotely selectable, calibration scheme. This was accomplished early in the sea water measurements, at the Ventura site. In the case of the 9.5 and 16.5 GHz radiometers, it was necessary to utilize the attenuator - Hot Load method throughout the field measurements.

1. Two-Load Calibration Method

Figure 10 shows a 2-point input calibration scheme consisting of two waveguide terminations (loads) at accurately known temperatures, and a mechanical waveguide selector switch. The losses of all microwave components and waveguides were re-measured in January 1967, with the exception of the antenna feed losses. These were estimated on the basis of equivalent waveguide length present in each antenna feed. The new losses for these components are listed in Table I.

The measured input-output response of each radiometer was found to be very linear over the dynamic signal range (0-400 degrees Kelvin). Therefore, within this range, the scale factor used in radiometer calibration and data conversion is a linear function. Referring to the response curve in Figure 10, the scale factor (K) is given by,

$$K = \frac{T_{C1} - T_{C2}}{E_{C1} - E_{C2}} \text{ degrees Kelvin per volt} \qquad (4)$$

Figure 10 - Two-Load Calibration Scheme Used in 94 GHz Radiometer

TABLE I

RADIOMETER INPUT COMPONENT LOSSES

Item	9.5 GHz		16.5 GHz		94 GHz	
	Loss (db)	Factor	Loss (db)	Factor	Loss (db)	Factor
1. Antenna feed* (L_a in Figure	0.250	1.059	0.350	1.084	1.000	1.259
2. Antenna flange to input of ferrite chopper (L_{S1} in Figure	0.087	1.020	0.280	1.066	0.460	1.112
3. Cold Load to input of ferrite chopper ($L_{S1,2a}$ in Figure	0.287	1.068	0.300	1.071	2.920	1.959
4. Hot Load to input of ferrite chopper ($L_{S1,2b}$ in Figure	0.316	1.075	0.330	1.079	2.220	1.667

*These values have been estimated from losses in equivalent lengths of waveguide.

Similarly, for an output voltage E_A,

$$K = \frac{T_{C2} - T_A}{E_{C2} - E_A}, \text{ degrees Kelvin per volt} \qquad (5)$$

where,

T_{C1} is the apparent temperature of the maximum (Hot Load) calibration signal, referred to the antenna feed input, degrees K.

T_{C2} is the apparent temperature of the minimum (Cold Load) calibration signal, referred to the antenna feed input, degrees K.

T_A is the apparent temperature of the material under observation, at the antenna feed, degrees K.

E_{C1} is the radiometer output when the input signal is T_{C1}, volts.

E_{C2} is the radiometer output when the input signal is T_{C2}, volts.

E_A is the radiometer output when the input signal is T_A, volts.

The radiometer temperature sensitivity can be readily calculated from knowledge of T_{C1} and T_{C2}, as well as the mean values of E_{C1} and E_{C2}. The minimum detectable temperature sensitivity, ΔT, of a radiometer is defined as the root-mean-square output signal fluctuation in the absence of an input signal. This definition implies that the radiometer input is terminated in its characteristic impedance for the requisite output reading. This results in an effective null input signal condition, which represents maximum sensitivity in a Dicke-type radiometer.

Based on the above definition, the rms temperature sensitivity of a given radiometer is expressed by,

$$\Delta T = \frac{E_{out\ p/p}}{6} \times K, \text{ degrees Kelvin rms} \qquad (6)$$

The factor "6" is used to convert peak-to-peak noise voltages to rms voltages, in accordance with common practice. Equation (6) may be expressed in terms of known quantities. Thus,

$$\Delta T = \left(\frac{E_{C2\ p/p}}{6} \right) \frac{\left(T_{C1} - T_{C2} \right)}{\left(E_{C1} - E_{C2} \right)_{mean}}, \text{ degrees K rms} \qquad (7)$$

In practice, approximately ten (10) printouts are taken for E_{C1} and E_{C2} during the sensitivity check. The peak-to-peak fluctuation of E_{C2} is then noted for use in the first term of the above Equation. Following this, the mean values of E_{C1} and E_{C2} are determined. With values of T_{C1} and T_{C2} established, from equations presented elsewhere in this Section, the rms temperature sensitivity can be calculated.

As is well known, a microwave signal with an apparent temperature T_A, is affected by transmission through a lossy medium, such as a waveguide component, in accordance with Equation (8).

$$T_{out} = T_A \left(\frac{1}{L} \right) + T_o \left(1 - \frac{1}{L} \right), \text{ degrees K} \qquad (8)$$

or

$$T_{out} = T_o + (T_A - T_o)\frac{1}{L}, \text{ degrees K} \qquad (9)$$

As indicated in Table I, the losses of WGS2 and WGS1, from the Cold Load and Hot Load to the input of the ferrite switch, were measured in combination. This combined loss is indicated in the equations to follow by the symbols $L_{S1,2a}$ for the Cold Load path and $L_{S1,2b}$ for the Hot Load path, respectively. Since the loss in WGS2 is considerably higher than in WGS1, in the X-band and W-band channels, the temperature of WGS2 is associated with $L_{S1,2a}$ and $L_{S1,2b}$.

An inversion of Equation (9) provides an expression for apparent temperature T_A. Thus,

$$T_A = L(T_{out} - T_o) + T_o, \text{ degrees K} \qquad (10)$$

Using the above basic expressions, a set of equations can be established successively at Points (1), (2) and (3) in Figure 10. The Hot Load calibration temperature, referred to Point (3), is given by

$$T_{C1} = L_a \left[L_{S1} (T_{S2} - T_{S1}) + \frac{L_{S1}}{L_{S1,2b}} (T_{HL} - T_{S2}) + T_{S1} - T_a \right] + T_a, {}^oK \qquad (11)$$

The Cold Load calibration temperature, referred to Point (3), is given by

$$T_{C2} = L_a \left[L_{S1}(T_{S2} - T_{S1}) + \frac{L_{S1}}{L_{S1,2a}} (T_{CL} - T_{S2}) + T_{S1} - T_a \right] + T_a, {}^oK \qquad (12)$$

The conversion of radiometer output voltages, E_A, to apparent temperatures, T_A, at the antenna feed horn is accomplished by means of an inverted form of Equation (5). Thus,

$$T_A = T_{C2} - K(E_{C2} - E_A), \text{ degrees K} \tag{13}$$

Note that E_{C2} rather than E_{C1} is used in this expression. The reason is that the value of E_{C2}, representing the Cold Load, is closer to the value of E_A. This optimizes the accuracy of the conversion. The value of K is determined by means of Equation (4). Finally, as in the case of the radiometer sensitivity calculation, approximately ten (10) printouts are taken for E_{C1}, E_{C2} and E_A. The mean values of these quantities are then determined prior to insertion in Equation (13) for calculation of the apparent temperature, T_A.

2. Attenuator Calibration Method

This was the original method used in radiometer calibration and is shown diagrammatically in Figure 11. The 2-point calibration was achieved by adjusting the variable attenuator to minimum and maximum settings, in turn, to obtain the high temperature calibration value, T_{C1}, and low temperature value, T_{C2}, respectively. The calibration expressions involved in this scheme are as follows:

$$T_{C1} = L_a \left[L_{S1}(T_{att.} - T_{S1}) + \frac{L_{S1}}{L_{S1b}} (T_{HL} - T_{att.}) + T_{S1} - T_a \right] + T_a, \ ^oK \tag{14}$$

$$T_{C2} = L_a \left[L_{S1}(T_{att.} - T_{S1}) + \frac{L_{S1}}{L_{S1a}} (T_{HL} - T_{att.}) + T_{S1} - T_a \right] + T_a, \ ^oK \tag{15}$$

The terms appearing in the above equations are shown in Figure 11. The conversion of radiometer output voltages to apparent temperatures at the antenna feed horn is accomplished by means of Equations (13) and (4).

Figure 11 - Variable Attenuator Calibration Method Used in 9.5 and 16.5 GHz Radiometers.

When losses were re-measured in early 1967, the losses of WGS1 and WGS2, shown in Figure 11 were lumped together. These are listed in Table I. For the attenuator method, it is necessary to have a separate value for the loss of S_1 between the attenuator and ferrite switch. Since this was not measured directly, it will be assumed that this loss is equal to that in the straight-through path in S_1 (between the antenna and ferrite chopper). The circuit losses involved in the attenuator method are shown in Table II.

Table II

CIRCUIT LOSSES FOR ATTENUATOR CALIBRATION

METHOD

Freq. ⟶ / Loss Component	9.5 GHz Loss(db)	9.5 GHz Factor	16.5 GHz Loss(db)	16.5 GHz Factor	94 GHz Loss(db)	94 GHz Factor
L_a	0.250	1.059	0.350	1.084	1.000	1.259
L_{S1}	0.087	1.020	0.280	1.066	0.460	1.112
$L_{att.(max.)}$	30	1000	30	1000	30	1000
L_{S1a}	30	1000	30	1000	30	1000
$L_{att.(min.)}$	0.300	1.071	0.500	1.121	0.500	1.121
L_{S1b}	0.387	1.093	0.780	1.197	0.960	1.247

Using the losses given in the above Table, in Equations (14) and (15), the actual expressions used in calibrating the three radiometers are given below, for the attenuator method.

9.5 GHz Radiometer

$$T_{C1} = 1.059 \left[1.020(T_{att.} - T_{S1}) + 0.933(T_{HL} - T_{att.}) + T_{S1} - T_a \right] + T_a, \ ^oK \quad (16)$$

$$T_{C2} = 1.059 \left[1.020(T_{att.} - T_{S1}) + 0.001(T_{HL} - T_{att.}) + T_{S1} - T_a \right] + T_a, \ ^oK \quad (17)$$

16.5 GHz Radiometer

$$T_{C1} = 1.084 \left[1.066(T_{att.} - T_{S1}) + 0.890(T_{HL} - T_{att.}) + T_{S1} - T_a \right] + T_a, \ ^oK \quad (18)$$

$$T_{C2} = 1.084 \left[1.066(T_{att.} - T_{S1}) + 0.001(T_{HL} - T_{att.}) + T_{S1} - T_a \right] + T_a, \ ^oK \quad (19)$$

94 GHz Radiometer

$$T_{C1} = 1.259 \left[1.112(T_{att.} - T_{S1}) + 0.892(T_{HL} - T_{att.}) + T_{S1} - T_a \right] + T_a, \ ^oK \quad (20)$$

$$T_{C2} = 1.259 \left[1.112(T_{att.} - T_{S1}) + 0.001(T_{HL} - T_{att.}) + T_{S1} - T_a \right] + T_a, \ ^oK \quad (21)$$

C. SEGREGATION OF VALID DATA

At the outset of the study it was intended to accept or reject measured data for further analysis solely on the basis of a comparison of measured sky brightness temperatures with calculated values, after assigning suitable tolerance limits to the calculated data. Unfortunately, the assignment of such tolerances proved to be a very difficult matter due to insufficient information on the variability of sky brightness temperatures with atmospheric conditions. Thus, to avoid the use of arbitrary tolerance limits, an alternate approach was devised. This approach is empirical in nature since it is based on an examination of the distributions of measured zenith sky brightness temperatures and comparisons of average values with calculated values. It is felt that reasonable tolerances have been obtained in this manner.

Table III lists the tolerances assigned to calculated zenith sky brightness temperatures, together with measured data discarded as a result of a review of same. Some of the measured data was discarded for other reasons i.e., Runs 112, 505, 113, 506, 114 and 507 were rejected due to the lack of sufficient information. These Runs included only two zenith angles - 0 and 140 degrees. The purpose of these measurements was to observe diurnal effects on brightness temperatures. Unfortunately, most of the data was lost in the mail (in 1966) between the field site and Raytheon Co. Thus, a complete analysis of diurnal effects is not possible.

Apart from the above six Runs, fifteen Runs have been discarded due to unsatisfactory sky brightness temperatures. These two groups of Runs constitute approximately 15% of the total complement of data.

Table III

TOLERANCES ASSIGNED TO CALCULATED ZENITH

SKY BRIGHTNESS TEMPERATURES

Site	Radiometer Freq.(GHz)	Sky Condition	Mean Calc. T_{so} (°K)*	Assigned Tolerance(°K)	Discarded Measured Data
Ventura	9.5	Clear	3.0	±2	18
(Sea Water)	16.5	Clear	5.7	±3	16,33
	16.5	Cloud	7.8	±3	None
	94	Clear	60	±20	None
	94	Cloud	95	±25	53
Death Valley	9.5	Clear	3.5	±2	None
(Salines)	16.5	Clear	7.4	±3	None
	94	Clear	75	±10	None
Brawley	9.5	Clear	3.5	±3	98,99,106,111
(Quartz Sand)	9.5	Cloud	3.5	±3	112,505
	16.5	Clear	7.1	±3	110
	16.5	Cloud	7.8	±3	113,506
	94	Clear	72	±20	None
	94	Cloud	95	±25	114,507
Lucerne Valley	9.5	Clear	3.3	±3	126,127
(Limestone)	9.5	Cloud	3.5	±3	120
	16.5	Clear	7.7	±3	None
	94	Clear	74	±20	None
	94	Cloud	80	±20	115,118,119

* T_{so} = zenith sky brightness temperature.

D. RADIOMETER ERRORS

The results of the radiometer accuracy analysis, presented in Reference (3) report, were reviewed and found to be somewhat inapplicable to this study. The reason for this conclusion is that the radiometer input and calibration losses, listed in Table I of the report, have been replaced by more up-to-date values, given in Tables I and II of Section II - B. Most of the new loss values were obtained by careful, repetitive measurements; very few estimated values are involved in the new losses.

An exception to the above comment, concerning the results given in the referenced report, is the variable error established for each radiometer. Since the variable error, or relative accuracy, is independent of the calibration circuitry the voltage errors given on page 13 of that report are considered to be valid. The averaged relative rms voltage errors, and corresponding apparent temperature errors obtained with appropriate conversion factors, are listed in Table IV.

Table IV

RADIOMETER RELATIVE ERRORS[3]

Frequency (GHz)	Run No.	Average RMS Voltage Error (mv)	Conversion Factor (^{o}K/mv)	Average RMS App. Temp. Error (^{o}K)
9.5	18	0.97	0.600	0.58
16.5	3	0.40	1.046	0.42
94	29	0.77	0.494	0.38

The above errors are considered to be fairly small and indicate that, if it is possible to achieve reasonable absolute accuracy, a typical data run obtained with these radiometers should follow a fairly smooth curve. Unfortunately, it is difficult, if not impossible, to obtain a reasonable estimate of the absolute accuracy of a radiometer, unless an external calibration source of known accuracy is employed. Such a calibration was not performed on these radiometers. In the absence of measured absolute calibration

data, it is felt that close agreement between measured and theoretical zenith sky brightness temperatures, together with good data consistency from Run to Run, are more significant than calculated estimates of absolute accuracy. Information relative to this item has been presented in the preceding Section.

It is interesting to note the effects of the updated losses on the two calibration points in each radiometer. Table V shows a comparison of the original and current calibration data. Both minimum and maximum calibration temperatures are listed; these were selected, wherever possible, from records taken on different days during sea water measurements. In the case of the 9.5 GHz radiometer, the average change is relatively small; however, both the 16.5 and 94 GHz radiometers show negative-going shifts of several degrees for the maximum calibration temperature. Thus, the value of the K-Factor has been reduced slightly in the latter radiometers i.e., the slope of the conversion curve has been reduced to a small extent at these frequencies. The net effect tends to raise the values of the apparent temperatures for given output voltages; this is due to the "lever" effect when the calibration curve is pivoted about the minimum calibration temperature.

Somewhat more significant results have been obtained in a comparison of apparent temperatures, obtained in the original data reduction (in 1966) and those obtained currently. These are listed in Tables VI and VII for the sea water measurements. Referring to the 16.5 GHz data in Table VI, the average shift from the original to the current data is $-6.2^{\circ}K$ and $-2.5^{\circ}K$ for zenith angles of 0° and 130°, respectively. At 94 GHz the shift is positive at the same angles i.e., $+ 8.6^{\circ}K$ and $+12.1^{\circ}K$, respectively. It is inappropriate to comment on the 9.5 GHz radiometer, due to the sparseness of sea water data at this frequency. Similarly, referring to the 16.5 GHz data in Table VII, the average shift is again negative i.e., $-15.4^{\circ}K$ and $-8.6^{\circ}K$ at 0° and 130°, respectively. At 94 GHz, a positive shift is shown again i.e., $+28.3^{\circ}K$ and $+18.7^{\circ}K$, at the same angles. Thus, it appears that the net effect of the change in radiometer calibration and input losses is to depress the apparent temperature readings at 16.5 GHz and raise them at 94 GHz.

TABLE V

COMPARISON OF ORIGINAL AND CURRENT
CALIBRATION DATA (SEA WATER MEASUREMENTS)

Radiometer Freq.(GHz)	Run No.	Min. Cal. Temp.(^{o}K)		Max. Cal. Temp.(^{o}K)	
		Original	Current	Original	Current
9.5	12	318.66	318.51	404.92	405.66
	13	318.99	318.75	404.09	404.72
	18	309.09	309.00	407.17	408.08
	52	320.75	320.51	405.71	406.34
	Average	change:	- 0.18^{o}K		+0.73^{o}K
16.5	3	311.63	311.04	397.62	391.91
	6	298.98	298.27	401.31	394.50
	14	299.85	299.96	394.04	388.54
	27	324.24	323.55	402.29	396.95
	30	320.40	320.44	399.96	395.26
	Average	change:	- 0.37^{o}K		-5.61^{o}K
94	502	296.56	297.58	395.62	386.26
	53	298.08	299.00	395.56	386.32
	58	294.96	296.66	396.82	387.48
	41	295.02	295.21	394.48	384.73
	38	292.18	293.93	389.72	380.82
	Average	change:	+ 1.11^{o}K		-9.32^{o}K

Table VI

COMPARISON OF ORIGINAL AND CURRENT

APPARENT TEMPERATURES - SEA WATER MEASUREMENTS

(HORIZONTAL POLARIZATION)

Radiometer Freq.(GHz)	Run No.	Zenith Angle = 0° Apparent Temp.(°K)			Zenith Angle = 130° Apparent Temp.(°K)		
		Orig.	Current	Diff.	Orig.	Current	Diff.
9.5	13	7.0	5.2	-1.8	97.3	106.1	+8.8
	Average shift:			-1.8°K			+8.8°K
16.5	3	2.0	8.3	+6.3	99.7	101.9	+2.2
	7	2.8	9.6	+6.8	108.5	113.5	+5.0
	9	-9.2	8.8	+18.0	107.6	114.7	+7.1
	11	-15.4	9.0	+24.4	84.0	105.6	+21.6
	17	3.7	8.8	+5.1	72.5	91.7	+19.2
	55	45.3	12.3	-33.0	122.7	109.3	-13.4
	59	15.1	11.9	-3.2	85.9	96.1	+10.2
	43	62.0	13.2	-48.8	135.7	106.0	-29.7
	26	41.3	11.0	-30.3	126.9	109.0	-17.9
	28	3.0	10.8	+7.8	117.0	101.6	-15.4
	37	30.8	9.8	-21.0	119.2	102.8	-16.4
	Average shift:			-6.2°K			-2.5°K
94	502	67.1	68.6	+1.5	221.4	218.4	-3.0
	61	69.5	83.3	+13.8	250.6	254.1	+3.5
	41	60.8	82.1	+21.3	207.4	234.3	+26.9
	40	147.6	80.0	-67.6	233.7	259.2	+25.5
	29	44.9	70.7	+25.8	275.9	263.5	-13.4
	31	38.7	70.2	+31.5	223.4	235.7	+12.3
	21	71.2	105.4	+34.2	256.0	288.7	+32.7
	Average shift:			+8.6°K			+12.1°K

Table VII

COMPARISON OF ORIGINAL AND CURRENT

APPARENT TEMPERATURES - SEA WATER MEASUREMENTS

(VERTICAL POLARIZATION)

Radiometer Freq.(GHz)	Run No.	Zenith Angle = 0° Apparent Temp.(°K)			Zenith Angle = 130° Apparent Temp.(°K)		
		Orig.	Current	Diff.	Orig.	Current	Diff.
9.5	12	7.1	5.0	-2.1	206.4	191.6	-15.8
	52	4.3	5.1	+0.8	146.7	104.3	-42.4
	Average shift:			-0.6			-29.1
16.5	4	1.4	8.5	+6.1	149.7	157.2	+7.5
	8	-1.1	9.9	+11.0	156.6	156.4	-0.2
	14	14.6	9.3	-5.3	142.5	155.2	+12.7
	27	23.1	10.6	-12.5	163.0	144.4	-19.6
	30	27.0	9.8	-17.2	183.3	171.5	-12.8
	32	25.9	9.4	-16.5	170.3	162.1	-8.2
	511	-2.6	9.3	+11.9	184.3	175.3	-9.0
	49	24.4	10.4	-14.0	191.0	189.4	-1.6
	45	56.7	11.1	-45.6	193.0	166.9	-26.1
	25	57.3	12.1	-45.2	181.4	161.8	-19.6
	36	49.1	10.2	-38.9	178.8	162.4	-16.4
	39	28.9	9.9	-19.0	174.6	164.6	-10.0
	Average shift:			-15.4			-8.6
94	58	95.7	102.8	+7.1	148.2	196.1	+47.9
	38	85.0	75.5	-9.5	212.9	180.4	-32.5
	501	18.1	72.4	+54.3	149.4	170.9	+21.5
	34	74.1	72.3	-1.8	147.9	155.5	+7.6
	22	0.4	103.5	+103.1	173.9	207.8	+33.9
	24	68.3	84.8	+16.5	173.5	207.8	+34.3
	Average shift:			+28.3			+18.7

III. DATA REDUCTION METHODS

The purpose of this Section is to describe the data reduction techniques used in the study. Since the radiometer calibration and input loss values were updated as a result of a re-measurement of losses and since it was decided to employ a third calibration point, consisting of calculated values of zenith apparent sky temperatures, it was necessary to re-reduce all raw data. The various stages involved in this process are described in the sections to follow.

A. CONVERSION OF OUTPUT VOLTAGES TO APPARENT TEMPERATURES

As stated in the preceding Section, the conversion of radiometer output voltages, E_A, to apparent temperatures, T_A, at the antenna feed horn is accomplished by means of Equation (13). This expression is based on the assumption of a linear input-output response curve in the radiometer in question. Since the radiometers used in the field measurements exhibited a very linear response, over the dynamic signal range (0 - 400°K), the application of Equation (13) is valid.

The straight-line characteristic, used in converting output voltages to apparent temperatures, was obtained by passing a best fit straight line through three (3) calibration points, consisting of a maximum point at approximately 400°K, an intermediate point at approximately 300°K and a low value somewhere in the range 3 - 96°K, depending on operating frequency. The third point was calculated for each Run in the manner described in Section II-A. The exact value used for the third point was equated with the original voltage reading obtained for the zenith-pointing condition.

Using the above three calibration temperatures and their corresponding voltages, the constants $\underline{a}$ and $\underline{b}$, of the straight line $y = a + bx$ which fits these three points "best" in a least squares sense, were then established. For a description of the method of least squares see Reference (13) p. 466. Briefly, in a function of the form $y = a + bx$ the principle of least squares states that the best values of the unknowns $\underline{a}$ and $\underline{b}$ are those which make the following expression a minimum:

$$f(a,b) = \sum (a + bx - y)^2 \qquad (22)$$

In this application, for three points,

$$f(a,b) = (a + bx_1 - y_1)^2 + (a + bx_2 - y_2)^2 + (a + bx_3 - y_3)^2. \qquad (23)$$

For f(a,b) to be a minimum its partial derivatives with respect to a and b must each be zero:

$$\frac{\partial f}{\partial a} = 2(a + bx_1 - y_1) + 2(a + bx_2 - y_2) + 2(a + bx_3 - y_3) = 0 \qquad (24)$$

$$\frac{\partial f}{\partial b} = 2(a + bx_1 - y_1)x_1 + 2(a + bx_2 - y_2)x_2 + 2(a + bx_3 - y_3)x_3 = 0 \qquad (25)$$

dividing through by 2 and summing,

$$3a + (x_1 + x_2 + x_3)b - (y_1 + y_2 + y_3) = 0 \qquad (26)$$

$$(x_1 + x_2 + x_3)a + (x_1^2 + x_2^2 + x_3^2)b - (x_1y_1 + x_2y_2 + x_3y_3) = 0 \qquad (27)$$

The unknowns, a and b, can be solved from these two equations. The x_1 terms correspond to the voltages and y_1 terms to the temperatures of the three points. Since initial and final calibration measurements were taken, this process is repeated and two values of a and b are calculated. An interpolated value of a and b between these two values is used to find the apparent temperature T_A at each angle from the expression

$$T_A = aE + b \qquad (28)$$

where, E is the recorded voltage.

In the computer data printouts, the value of a is printed out with the comment K - FACTOR and b is printed out with the comment Y INTERCEPT.

Since the first step in the data reduction process involved the derivation of apparent temperatures, the calculated zenith sky brightness temperatures had to be converted to apparent temperatures prior to their use as third calibration points. Thus, it was necessary to add an increment to the zenith brightness temperatures for each Run. The increments were obtained by performing all conversions to apparent temperatures and corrections for antenna pattern effects on a preliminary basis. The difference between zenith apparent and brightness temperatures was noted for each Run and averaged for each frequency and measurement site. This average increment was then added to the calculated zenith brightness temperatures to obtain "calculated values" of zenith apparent temperatures. These values were then used as third calibration points for final conversion of radiometer output voltages to apparent temperatures. Table VIII lists the incremental values used in the above procedure.

B. CONVERSION OF APPARENT TEMPERATURES TO BRIGHTNESS TEMPERATURES.

This conversion, in effect, separates radiations received by the radiometer from its environment, via the antenna sidelobes and backlobes, from the total radiation received by the antenna main lobe and the lesser lobes. The radiometer measures the weighted average of the brightness temperatures incident on the antenna, the weighting function being the antenna power pattern. Thus, to obtain brightness temperatures from apparent temperatures, an inversion of Equation (29) is necessary:

$$T_A = \frac{\int T_B(\theta)F(\theta)d\Omega}{\int F(\theta)d\Omega} \qquad (29)$$

in which,

T_A is the apparent temperature, ^oK

T_B is the brightness temperature, ^oK

$F(\theta)$ is the antenna power pattern, over angle θ

and $d\Omega$ is an elemental cone from within which energy is incident on the antenna.

Table VIII

INCREMENTAL VALUES ADDED TO CALCULATED

ZENITH SKY BRIGHTNESS TEMPERATURES FOR

THIRD CALIBRATION POINT

Observed Material and Location	Radiometer Freq. (GHz)	Average Incremental Value (^{o}K)
Sea Water (Ventura)	9.5	2.3
	16.5	2.8
	94	11.8
Salines (Death Valley)	9.5	3.6
	16.5	4.5
	94	14.9
Quartz Sand (Brawley)	9.5	0.3
	16.5	3.6
	94	14.4
Limestone (Lucerne Valley)	9.5	2.8
	16.5	3.1
	94	13.1

The procedure for the above is described in Appendix A - Antenna Pattern Correction. The radiometer antenna patterns are also included in this Appendix. A description of the program used for the conversions is given in Appendix B - Computer Programs For Antenna Pattern Correction. All apparent temperatures were converted to brightness temperatures with the aid of the programs described in this Appendix.

C. CONVERSION OF BRIGHTNESS TEMPERATURES TO EMISSIVITIES.

The emissivities of surface materials were derived from brightness temperatures on the basis of two separate procedures. The first, and most commonly used, procedure involved inversion of the basic expression for specular brightness temperatures, given in Equation (30). The second procedure involved a somewhat more complex method, based on consideration of differential scattering coefficients from rough surfaces, as indicated in Equation (32).

1. Specular Emissivities

The brightness temperature of a material, observed by a radiometer, can be related to its microwave radiative properties and its environment by the relation,

$$T_B = \epsilon_\varphi T + (1 - \epsilon_\varphi) T_{S\varphi}, \ ^oK \qquad (30)$$

in which,

ϵ_φ = emissivity at incidence angle φ

T = thermodynamic temperature of the material, ^oK

and $T_{S\varphi}$ = sky brightness temperature at zenith angle φ, ^oK.

The term $(1 - \epsilon_\varphi)$ is a substitution for reflectivity, ρ_φ. This substitution is permissible when thermal equilibrium conditions prevail at the surface and the material is homogeneous.

If the material temperature, T, and sky brightness temperature, $T_{S\varphi}$, are measured, the specular emissivity may be derived from an inversion of Equation (30). Thus,

$$\epsilon_{\varphi} = \frac{T_B - T_{S\varphi}}{T - T_{S\varphi}} \tag{31}$$

The specular emissivities of all materials were derived routinely by means of this expression.

2. Determination of Emissivities of Rough Surfaces

The primary contributions to the brightness temperatures of natural rough terrain surfaces are:

1) Radiation from the surface governed by its temperature, T, and emissivity ϵ,

and 2) Reflection of radiation emitted by the terrestrial atmosphere.

The contributions of the sun to the brightness temperature of rough surfaces has not been included since it is usually less than $0.1^{\circ}K$ at microwave frequencies[14]. Hence, the total brightness temperature (corrected for antenna pattern) sensed by a radiometer looking at nadir angle, φ, may be expressed as:

$$T_B(\varphi) = \epsilon(\varphi)T + \frac{\pi}{4}\int \gamma(\varphi,\varphi',\psi)\ T_S(\varphi')\ d\Omega' \tag{32}$$

where,

$T_B(\varphi)$ = the brightness temperature at nadir angle φ, $^{\circ}K$

$T_S(\varphi')$ = the sky brightness temperature at zenith angle φ', $^{\circ}K$

T = the thermometric ground temperature, $^{\circ}K$

$\epsilon(\varphi)$ = the surface emissivity at incidence angle φ

$\gamma(\varphi,\varphi',\psi)$ = the differential scattering coefficient[15] of the surface for radiation incident at angle φ', to emerge in direction φ with respect to the normal, and ψ with respect to the plane of incidence

$d\Omega'$ = $\sin\varphi'\ d\varphi'\ d\psi$.

Equation (32) permits the calculation of surface emissivities from observed brightness temperature and material temperature data, provided the bistatic scattering can be specified. Because the calculation of the scattering coefficient, γ, is extremely difficult for natural surfaces, it is more convenient to use simple empirical laws. Peake[16] has recently catalogued various empirical models for diffuse scattering and notes that a number of different types of diffuse surfaces can be accommodated quite well by these models. The approach followed in the current study was to select the most appropriate of these for inferring the emissities of the Saline materials. In the most general case, horizontal and vertical polarizations must be treated separately, by relations of the type given in Equation (32), since the emissivity and reflectivity of the surface are polarization dependent.

a. Method of Analysis

The data collected during May 1966 on the Saline material were reviewed to determine an appropriate bistatic scattering model. Two features of these data strongly suggested the selection of a scattering model based on the assumption of a Lambert surface. The first of these was the observation that the measured surface brightness temperatures were nearly independent of incidence angle. Secondly, the measured brightness temperatures did not differ appreciably between horizontal and vertical polarizations. Both of these factors, when combined with the inherent uncertainties of the measurement, led to the selection of the Lambert surface approximation.

The emissivity for such a surface, obeying Kirchhoff's law, is given by

$$\epsilon(\varphi) = 1 - \gamma_o/4 \tag{33}$$

Furthermore, in circumstances involving clear air, or uniform moderate cloud cover, the sky brightness temperature can be written as

$$T_S(\varphi') = T_{air}(1 - e^{-\alpha \sec \varphi'}), {}^oK \tag{34}$$

where,

T_{air} = is an "effective" air temperature, ^{o}K

$e^{-\alpha}$ = transmission through the atmosphere at zenith (i.e., α = optical depth of the atmosphere at zenith).

Since nearly all of the measurement Runs satisfied this condition, the total brightness temperature can be expressed as[14],

$$T_B(\varphi) = (1 - \gamma_o/4)T + (\gamma_o/4)\, T_{air} F_2(e^{-\alpha}) \tag{35}$$

where,

$$F_2(e^{-\alpha}) = 1 - e^{-\alpha} + \alpha e^{-\alpha} - \alpha^2 \int_{\alpha}^{\infty} e^{-t} \frac{dt}{t} \tag{36}$$

Wulfsberg[17] has reported an approximation to the "effective" air temperature used in Equations (34) and (35), namely,

$$T_{air} = (1.12\, T_{surf} - 50),\ ^{o}K \tag{37}$$

where,

T_{surf} = is the ground level thermometer temperature of the air, ^{o}K.

Hence, Equation (35) can be used to solve for γ_o, from which the emissivities may be derived by means of Equation (33).

Calculations of the optical depth of the atmosphere necessitate a knowledge of the upper atmosphere thermodynamic structure during the measurement Runs. Because these conditions were generally not known for this study, the following approximate methods were used. The one-way attenuation at zenith or optical depth, α, of the atmosphere may be estimated roughly from

$$T_{ant} = T_{air}(1 - e^{-\alpha}),\ ^{o}K \tag{38}$$

where, T_{ant} is the antenna (or apparent) temperature. For frequencies up to 40 GHz, Hogg and Semplak[18] have calculated sky noise temperatures (T_{ant}) using typical models for dry, average, and humid atmospheres. Estimates of T_{ant} for the current analysis were obtained by interpolation from these models using the surface humidities observed during the field measurements. Table IX presents the values of optical depth derived by this procedure for 9.5 and

TABLE IX

ENVIRONMENTAL CONDITIONS AND OPTICAL DEPTH ESTIMATES

Run No.	Frequency (GHz)	Surface Temp. (^{o}F)	Humidity (gm/m^{3})	Optical Depth (nepers)
83	9.5	104	2.6	0.009
81	9.5	104	1.5	0.009
79	9.5	108	1.7	0.009
78	9.5	108	2.3	0.009
80	9.5	108	1.7	0.009
82	9.5	105	2.1	0.009
71	16.5	112	5.1	0.024
69	16.5	110	6.1	0.026
65	16.5	110	1.8	0.015
73	16.5	114	4.0	0.021
63	16.5	114	2.7	0.021
66	16.5	113	2.6	0.021
70	16.5	112	5.1	0.024
72	16.5	112	4.5	0.022
75	94.0	112	2.6	0.288
76	94.0	112	2.6	0.285
77	94.0	112	2.6	0.264
74	94.0	114	3.4	0.280
68	94.0	106	6.4	0.286
67	94.0	104	6.6	0.304
64	94.0	110	1.8	0.277
62	94.0	107	5.6	0.261

16.5 GHz.

Because the Hogg and Semplak model calculations did not extend beyond 40 GHz, a different procedure was used for estimating optical depth for the 94 GHz data. This method consisted of substituting the calculated zenith brightness temperature for T_{ant} in Equation (38) and solving for α. The optical depth values derived by this technique are also given in Table IX.

D. COMPUTER PROGRAMS EMPLOYED IN DATA REDUCTION

Five separate computer codes, all written in FORTRAN IV for use on an IBM 360/75 computer, were used to analyze the radiometric data. The original data was first processed by a modified version of RADIOP, as described in Reference (4), to find the apparent temperatures. Calculated sky brightness temperatures were added to this program, to be used as third calibration points for conversion of data into apparent temperatures. The apparent temperatures which were calculated in this way were input to an existing program (APTEMP & APCOR4) for conversion to brightness temperatures. Since the third calibration point had to be an apparent temperature and not a brightness temperature, it was necessary to find the incremental correction to convert calculated zenith sky brightness temperatures to apparent temperatures. By taking the correction which the brightness temperature program gave for a zenith angle of 0^{o} and adding this number to the original sky brightness temperature, a calculated value of apparent sky temperature was established for each Run.

The RADIOP program was then run again with this corrected third calibration point, and the apparent temperatures which were produced were put through the program for conversion to brightness temperatures. This second set of brightness and apparent temperatures were used for all future processing. Next, a program entitled EMISS was used to calculate specular emissivities from brightness temperatures. The apparent temperatures and brightness temperatures were input to a plotting routine (PLOTER) which produced plots of the apparent and brightness temperatures versus nadir angle on an SC-4020 (Stromberg Carlson high-speed microfilm recorder). The final program to be run (EMIS2) processed only the Saline data. A Lambert surface was assumed

and emissivities were calculated from this model. It was not possible to generate plotting programs for either the specular or diffuse emissivities - these were plotted by hand.

1. RADIOP Modifications

All plotting instructions contained in the original program were discarded since they referred to a Calcomp plotter which was not available. In addition, it was not desired to plot the data until brightness temperatures had been calculated.

The program signal KELOPT which appears in column 74 of card #1 was allowed to be 2, to handle some cases where the original data was punched in a different format from normal.

The print-out was changed so that one could tell which method of calibration had been used - a Cold Load and a Hot Load, or a Hot Load and an attenuator.

The antenna, attenuator and switch losses were changed to agree with more recent calculations of their values.

The above changes were all relatively minor, the main change consisted of adding a third calibration point and finding the best fit straight line which passes through the three points. Two extra cards were added to the input cards. These cards were numbers 5 and 6 - therefore all cards after number 4 in the original write-up must have 2 added to them to correspond with the new data decks e.g. card #7 rather than card #5 contains the comment information.

The first additional card, card #5, contains the voltage and the corresponding sky brightness temperature. The format of this card is (2F9.2). The sky brightness temperatures were obtained from a separate set of calculations; the corresponding voltage was the recorded voltage for a zenith angle of 0^{o}. Card #6, in the same format as above, contains the correction to be added to the temperature on card #5 to convert it from a brightness temperature to an apparent temperature. The first time the program is run, this number is zero. After the program has been run to convert the apparent

temperatures, calculated in this manner to brightness temperatures, this value is found. Using this temperature, together with the other two calibration temperatures, the constants a and b of the straight line $y = a + bx$, which fits these three points best in a least squares sense, are then calculated. The value of a is printed out with the comment K - FACTOR, DEG. K/MV and b is printed out with the comment Y INTERCEPT.

Punched output is produced which serves as input to the program for computing brightness temperatures. The first card punched contains the following information and identifies the run and material TARG, DATE, IFREQ, POL, M, FDATA(M,3), NO in format (2A5,3A2,I2,I1,A3,13x,I5,F10.5, 20x,I10) (see original RADIOP write-up for a description of these parameters). The following cards contain the zenith angles (TZEN) and apparent temperatures (TAA). The format of these cards is (11F7.2). The printed output is essentially that of RADIOP. Two pages are printed, one with calibration information, the other with apparent temperature information and emissivities. In the case of the Quartz Sand data, a third page is provided to present specular emissivities as a function of antenna beam incidence angle which is, in turn, derived from nadir angle and sand dune slope angle.

2. Antenna Pattern Correction

APTEMP and APCOR4 are programs used for antenna pattern correction and conversion to brightness temperature. Those programs were generated under a separate study. The APTEMP program, which calculates the correction matrix, was not altered in any manner. The APCOR4 program was modified to accept the punched data from RADIOP. This program uses zenith angles evenly spaced in the cosine of the angle so that an interpolation is necessary to go from the original input apparent temperatures to those listed at these points. The original program had been designed to use a third order interpolation; however, this order of interpolation tended to overemphasize the lack of smoothness in the apparent temperatures; the brightness temperature conversion program requires relatively smooth data to provide meaningful results. Therefore, the interpolation was changed to first order. The punched output from this program consisted of a first card bearing title information in format (62A1), the second card contained the number of iterations IT, the number of angles M, and the frequency FREQ in

format (I3,I5,F7.1). The next card, and as many following cards as necessary, contains the zenith angles, (ZANT(I), I=1,M) in format (10F8.3). The following set of cards contains apparent temperatures (TA(I),I=1,M) in format (10F8.3) and the last set consists of brightness temperatures (TB(I), I=1,M) in format (10F8.3). The printed output is the same as that furnished in the previous study.

3. EMISS Program

EMISS is a program which calculates specular emissivities from the brightness temperatures calculated by APCOR4. It is also a modified version of RADIOP. All of the calibration calculations and the calculation of apparent temperatures have been deleted from RADIOP. The output from APCOR4 (described in the preceding section) is appended to the end of each original data deck and all of the original data (including calibration information) is used as input. This procedure was used since there were many boxes of data cards which would have had to be reproduced if it had been desired to use only some of the information contained in each deck. Some of the information was clearly needed since the emissivities depend on the surface temperature and slope angle of the surface, for each zenith angle. In this way the original data decks could be used in RADIOP and also after appending the data from APCOR4 (these cards appear after a #7 card which contains NOSEC=9 and before the eights control card) to the end of each separate data deck. The calculated brightness temperatures are not at the original zenith angles. Therefore, it is necessary to interpolate to find the values at the original angles. A first order interpolation is used.

The output for this program is similar to that for RADIOP. The first page contains run identification information. The calibration information printed out by RADIOP does not appear on page 1 in this case.

The second page contains a list of the zenith angles, brightness temperatures and specular emissivities at these angles and some additional input data.

In the case of sloped surfaces, such as the Quartz Sand dunes, there is a third page of information which contains the emissivity data. The second page contains the zenith angle, brightness temperature, and additional input data; the third page contains the zenith angle, nadir angle, slope angle, incidence angle and emissivity. There is no punched output from this program.

4. Program for Plotting Apparent and Brightness Temperatures versus Nadir Angle (PLOTER)

This program uses the punched output from APCOR4 to produce a plot of apparent and brightness temperatures versus nadir angle. The routine was designed to work with an SC-4020 (Stromberg Carlson High-Speed Microfilm Recorder) and will not work with any other plotting systems such as Calcomp. A number of subroutines are called which are described in the "Programmer's Reference Manual S-C 4020", Document #9500056, October 1964. The only subroutine which does not appear in this manual is IDFRMV which was designed by the particular computer installation for separation and identification of frames of output. The input to this program consists of a title card which identifies the run and contains the surface temperature of the material. The format of this card is (15A4,A2,F10.5). The next card contains the iteration number, the number of angles M, and the radiometer frequency. The format of this card is (I3,I5,F7.1). The next set of cards contains the zenith angles (ZANT(I), I=1,M) in format (10F8.3). The following set of cards contains the apparent temperatures (TA(I), I=1,M) in format (10F8.3). Any number of input decks can be run one after another. Nadir angles (TNAD(I),I=1,M) are computed for the zenith angles. The nadir angles appear on the abscissa of the graph and the brightness and apparent temperatures are the ordinates. The temperature of the surface appears as a dotted line in the graph.

The output from the program consists of a number of plots, and printed output which contains the title information, iteration number, number of angles and frequency, zenith angles, apparent temperatures, brightness temperatures and temperature of the surface. This printout can normally be ignored and is printed as a check to be certain cards have not gotten out of order. A number of integers, representing the number of characters plotted, are also printed out to serve as further checks. As a rule one can simply look at the plotted output and ignore all printed output.

5. Program for Calculating Emissivities for a Lambert Surface

The equations used in this work are as follows:

$$\frac{\gamma_o}{4} = \frac{T_b(\theta) - T_{surf}}{T_{air}F_2 - T_{surf}} \qquad (39)$$

where,

$$F_2 = 1 - e^{-\alpha} + \alpha e^{-\alpha} - \alpha^2 \int_{\alpha}^{\infty} \frac{e^{-t}}{t}\, dt$$

α is the optical depth of the atmosphere in nepers

$T_b(\theta)$ is the brightness temperature

T_{surf} is the temperature of the surface

$T_{air} = 1.12T - 50.$

and T is the air temperature at the surface.

The emissivity ϵ is equal to $1 - \gamma_o/4$.

The program input consists of:

Card # 1 Format (F10.3) TF - the value of t which is to be used for infinity in the evaluation of the numerical integral for $\frac{e^{-t}}{t}\, dt$. (A value of t = 20 was found to be more than adequate such that the contribution to the integral from 20 to infinity was negligible.)

Card # 2 Format (I5) KASES is the number of cases to be run.

The following cards are repeated for each case to be run:

Card # 3 Format (62A1,F10.4) TITLE(I), I=1,62,TS

This card is output from APCOR4 and contains title information and the temperature of the surface T_{surf}.

Card # 4 Format(I3,I5,F7.1) IT, MM, FREQ

This card is output from APCOR4, IT is the iteration number, MM is the number of angles, FREQ is the frequency.

Card # 5 Format (10F8.3) (Zant(I), I=1,MM)

This card is output from APCOR4 and contains the values of the zenith angles.

Card # 6 Format (10F8.3) (TA(I), I=1,MM)

This card is output from APCOR4 and contains the values of the apparent temperatures.

Card # 7 Format (10F8.3) (TB(I), I= 1,MM)

This card is output from APCOR4 and contains the brightness temperatures.

Card # 8 Format (2F10.3) ALPHA, TSA
ALPHA is the optical depth of the atmosphere, TSA is the air temperature of the surface.

The integral involved in F2 is performed using Gauss's quadrature formula with 32 points. For a description of the method see, for example, Reference (13) p. 145. This formula gives an exact result if e^{-t}/t is a polynomial of the 63rd degree or lower.

The output consists of a heading containing the number of the run, its polarization and frequency, and the target material. A line containing the value of the optical depth of the atmosphere is printed out, the next line contains the air temperature of the surface, and the next line contains the temperature of the surface. Next, at each zenith angle greater than or equal to 90^{o} the angle, the brightness temperature, the emissivity and γ_o are printed out.

IV. STUDY RESULTS AND ANALYSIS

Since a considerable volume of data was generated in the study it was necessary to arrange it in a systematic manner for ease of examination, correlation and detailed analysis. Thus, all measured data is arranged in four groups in this Volume, by observed material, in chronological order - Sea Water, Salines, Quartz Sand, Limestone. Within each group the data is arranged by radiometer frequency - 9.5, 16.5 and 94 GHz, in that order. Within each frequency data is grouped by antenna polarization - horizontal and vertical, in that order. A typical set of data, for a particular material, consists of two (2) data Runs arranged as follows:

1) A plot of brightness, apparent and surface temperatures versus antenna beam nadir angle, for horizontal polarization.

2) A computer tabulation of environmental and calibration data for the above Run, labelled "Page 1".

3) Computer tabulation of brightness and surface temperatures, with certain correlative information, labelled "Page 2".

4) In the case of Quartz Sand, derived emissivities are tabulated on "Page 3".

5) Computer tabulation of brightness and apparent temperatures, together with the correction involved in converting apparent temperatures to brightness temperatures, for the above Run.

6) A set of the above Items for vertically polarized data.

7) A plot of derived specular emissivities versus incidence angle for both Runs, together with calculated emissivities for comparison purposes. In the case of the Saline material, diffuse emissivities are furnished in a separate plot.

The above sets of data are supplemented with a variety of tables and plots generated during the course of correlation and analysis. Due to the large amount of reduced data, it has been necessary to restrict presentation of plots and tabulations in this Volume to typical Runs - the remaining information is contained in Volumes II and III.

The computer outputs require explanations as to symbols and headings; these are presented below:

1) All Machine Plots

T_B - brightness temperature, indicated by symbol X.

T_A - apparent temperature, indicated by rounded square.

T - surface temperature, indicated by dashed line.

Note: All data plotted at a nadir angle of 0^o represents extrapolated information and should be ignored.

2) Sea Water Printouts

Page 1 - Self explanatory

Page 2 - Wave direction units should be "degrees", not "seconds".

3) Solid Material Printouts

These comments include Salines, Quartz Sand and Limestone, except as noted:

Page 1 - Self explanatory.

Page 2 - Columns headed "1/2 IN TEMP", "3 IN TEMP", "6 IN TEMP" and "12 IN TEMP" refer to subsurface temperatures. Columns headed "1 FT TEMP", "2 FT TEMP" and "3 FT TEMP" refer to air temperatures above the surface.

Page 3 - Applies to Quartz Sand Only and is self-explanatory.

A. SEA WATER - DATA RESULTS AND ANALYSIS

Figures 12 and 13 show views of the ocean surface at the Ventura oil drilling pier under calm and rough seas, respectively.

1. 9.5 GHz Data

The sea water data, obtained at this frequency, is very limited due to radar interference experienced during observations. Figure 14, together with Tables X thru' XII, presents measured data for horizontal polarization. Relatively low brightness temperatures are represented by

The computer outputs require explanations as to symbols and headings; these are presented below:

1) All Machine Plots

T_B - brightness temperature, indicated by symbol X.
T_A - apparent temperature, indicated by rounded square.
T - surface temperature, indicated by dashed line.

Note: All data plotted at a nadir angle of 0^o represents extrapolated information and should be ignored.

2) Sea Water Printouts

Page 1 - Self explanatory
Page 2 - Wave direction units should be "degrees", not "seconds".

3) Solid Material Printouts

These comments include Salines, Quartz Sand and Limestone, except as noted:

Page 1 - Self explanatory.

Page 2 - Columns headed "1/2 IN TEMP", "3 IN TEMP", "6 IN TEMP" and "12 IN TEMP" refer to subsurface temperatures. Columns headed "1 FT TEMP", "2 FT TEMP" and "3 FT TEMP" refer to air temperatures above the surface.

Page 3 - Applies to Quartz Sand Only and is self-explanatory.

A. SEA WATER - DATA RESULTS AND ANALYSIS

Figures 12 and 13 show views of the ocean surface at the Ventura oil drilling pier under calm and rough seas, respectively.

1. 9.5 GHz Data

The sea water data, obtained at this frequency, is very limited due to radar interference experienced during observations. Figure 14, together with Tables X thru' XII, presents measured data for horizontal polarization. Relatively low brightness temperatures are represented by

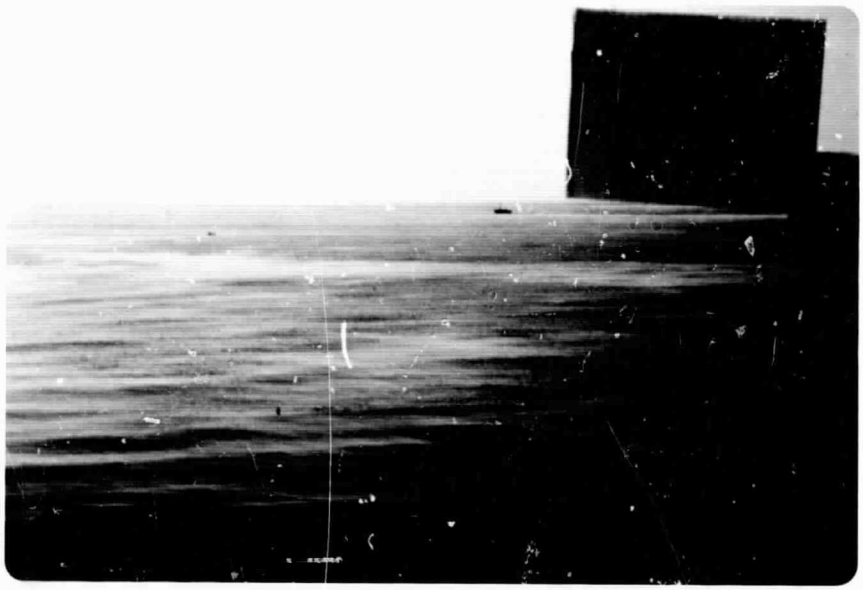


Figure 12 - Sea Water, Ventura, California (Calm Sea, Wave Height 1-3 ft.)



Figure 13 - Sea Water, Ventura, California (Rough Sea, Wave Height 1-5 ft.)

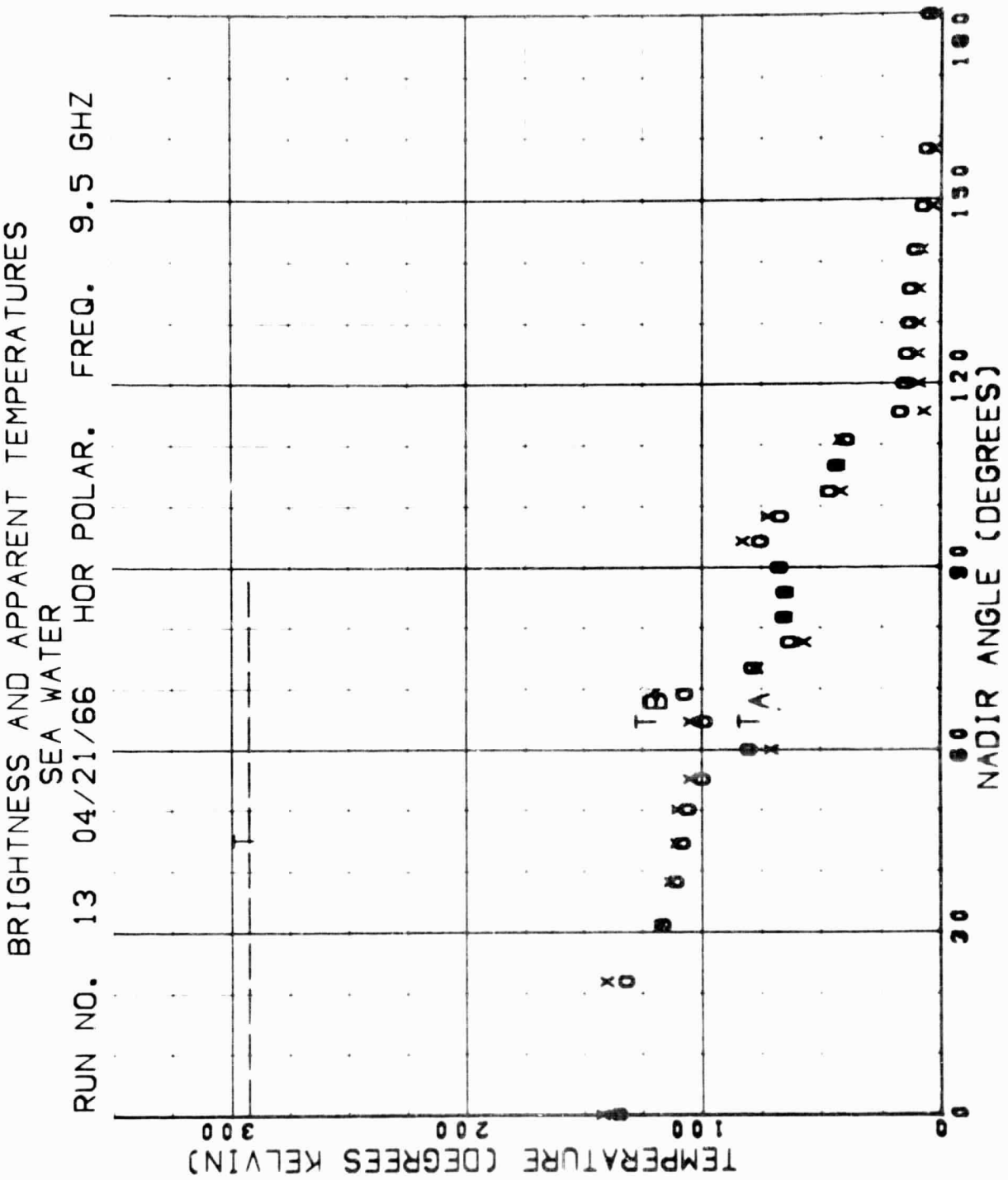


Figure 14 - Measured Sea Water Brightness Temperatures, 9.5 GHz, Hor. Pol.

PAGE 1 RUN 13

TARGET MATERIAL	SEA WATER
DATA DATE	04/21/66
START TIME	1155
FREQUENCY,GHZ	9.5
POLARIZATION	HOR
ANTENNA AZIMUTH,DEG	010
BAROMETRIC PRESSURE,IN.HG.	30.02
RELATIVE HUMIDITY,0/0	66
AIR TEMPERATURE,DEG F	58
WIND DIRECTION	
WIND SPEED,MPH	
INTEGRATION TIME,SEC	0001

THIRD CALIBRATION POINT 5.40DEG.K 6653.00MV.

INITIAL CALIBRATION DATA		
MINIMUM CAL.TEMP,DEG.K	31[illegible].75	
MAXIMUM CAL.TEMP.DEG.K	404.72	
K-FACTOR,DEG.K/MV.	0.90354	
Y INTERCEPT	-6006.04	
FINAL CALIBRATION DATA		
MINIMUM CAL.TEMP,DEG.K	317.03	
MAXIMUM CAL.TEMP.DEG.K	405.28	
K-FACTOR,DEG.K/MV.	0.89216	
Y INTERCEPT	-5930.96	

CALIBRATION CONSTANTS	INITIAL	FINAL	UNITS
REF VOLTAGE	6278.0	6278.0	MV.
HOT LOAD	404.12	404.78	DEG.K
ATTENUATOR	317.01	315.37	DEG.K
WAVE GUIDE SWITCH	313.33	310.47	DEG.K
ANTENNA	290.55	290.63	DEG.K
AVERAGE CAL.DATA-MIN.	7000.20	7007.00	MV.
-MAX.	7095.13	7099.27	MV.

COMMENTS
SUNNY SLIGHT HAZE SEA CALM LIGHT SWELL

Table X - Environmental and Calibration Data, Sea Water, 9.5 GHz, Hor. Pol.

TARGET MATERIAL SEA WATER
DATA DATE 04/21/66
START TIME 1155
FREQUENCY,GHZ 9.5
POLARIZATION HOR

ZENITH ANGLE DEG	BRIGHTNESS TEMP DEG K	EMISSIVITY HORIZONTAL	TIME	READINGS MV	WATER TEMP DEG K	WAVE PERIOD SEC	WAVE DIR SEC	WAVE HEIGHT IN
0.0	2.7			6653.				
10.0	3.0			6653.				
20.0	3.3			6685.				
30.0	3.9			6655.				
40.0	8.6		1201	6660.				
50.0	9.5			6662.				
55.0	9.5							
60.0	9.5			6664.				
65.0	10.2			6666.				
70.0	42.0			6697.				
75.0	42.5			6695.				
80.0	59.1			6702.				
82.0	72.6			6724.				
84.0	77.9			6724.				
86.0	82.6			6732.				
88.0	75.0			6733.				
89.0	71.2							
90.0	67.4			6722.				
91.0	66.7	-0.021		6705.	288.0	235		10
92.0	66.0	-0.042		6713.	288.0	225		30
94.0	64.6	-0.088		6720.	288.0	225		24
96.0	64.9	-0.062		6723.	288.2	215		18
98.0	65.2	-0.034		6721.	288.1	235		24
100.0	61.3	0.012		6717.	288.1	235		12
105.0	69.6	0.110	1215	6720.	288.1	230		12
110.0	111.3	0.284		6769.	288.2	230		12
115.0	106.4	0.346		6760.	287.8	225		12
120.0	70.3	0.220		6737.	288.2	230		12
125.0	105.1	0.343		6760.	288.1	225		12
130.0	109.2	0.361	1220	6767.	287.9	200		24
140.0	112.6	0.372		6771.	288.0	225		12
150.0	120.2	0.409		6779.	287.9	215		12
160.0	140.6	0.482		6800.	288.3	235		12

Table XI - Brightness Temperatures, Sea Water, 9.5 GHz, Hor. Pol.

RUN NO. 13 04/21/66 HOR POLAR. 9.5 GHZ SEA WATER

ITERATION NUMBER 0

ZENITH ANGLE (DEG)	BRIGHTNESS TEMP. (DEG K)	APPARENT TEMP. (DEG K)	CORRECTION TEMP. (DEG K)
0.0	2.70	5.22	-2.5227
21.79	3.39	6.29	-2.8942
31.00	3.95	7.62	-3.6694
38.21	8.30	10.99	-2.6850
44.42	9.27	12.48	-3.2164
49.99	9.47	13.32	-3.8503
55.15	9.58	14.20	-4.5133
60.00	9.47	15.02	-5.5510
64.62	7.26	16.91	-9.6440
69.08	41.74	39.35	2.3890
73.40	42.91	43.66	-0.7457
77.63	41.86	46.54	-4.6787
81.79	72.00	66.87	5.1271
85.90	82.96	75.51	7.4513
90.00	67.37	67.32	0.0509
94.10	64.53	65.25	-0.7176
98.21	65.24	65.75	-0.5050
102.37	57.22	63.28	-6.0602
106.60	77.08	78.85	-1.7703
110.92	121.26	107.22	14.0360
115.38	104.98	98.98	5.9991
120.00	70.81	80.00	-9.1933
124.85	104.99	99.97	5.0168
130.01	109.93	106.07	3.8560
135.58	110.59	108.18	2.4173
141.79	113.21	111.17	2.0406
149.00	117.69	116.53	1.1592
158.21	140.45	132.17	8.2778
180.00	142.26	135.41	6.8467

Table XII - Brightness and Apparent Temperatures, Sea Water, 9.5 GHz, Hor. Pol.

ABS. CORRECTION = 4.33E 00 DEG. K

this data - the sea surface values range from 67 to 141°K while the sky temperatures fall in the range 2.7 to 67°K. The data is generally bumpy due to radar interference.

Figure 15 and Tables XIII thru' XV, show vertically polarized data at 9.5 GHz. Here the surface brightness temperatures are, in general, higher than those mentioned above, falling in the range 131 to 298°K. The latter value is shown as being above the surface temperature (288°K); this is due to an exaggeration caused by the antenna pattern correction program and should be ignored. Such exaggerations at the Brewster Angle are not considered to be serious since data at this angle is of limited practical value.

Figure 16 presents plots of derived sea water emissivities for the above data Runs. The vertical component reaches unity emissivity and, since the horizontal component displays relatively low values, a very strong polarization effect is evident at incidence angles of 45° to 85°. The agreement between derived and calculated emissivities is better for vertical than for horizontal polarization. This is fairly typical for emissivities in this frequency region.

2. 16.5 GHz Data

Data obtained at this frequency is considered to be the most consistent of the three frequencies used in the observations; it is also free of radar interference, which affected the 9.5 GHz data. Figure 17 and Tables XVI thru' XVIII present measured data for horizontal polarization. The surface brightness temperatures range from 77 to 139°K, being fairly close to the 9.5 GHz values. The sky brightness temperatures lie in the range 9 to 132°K, being somewhat higher than at 9.5 GHz, for similar atmospheric conditions. This is to be expected since atmospheric absorption generally increases with frequency.

Figure 18, together with Tables XIX thru' XXI, furnish data for vertical polarization. It will be noted that the plot follows a fairly smooth curve and the surface brightness temperatures range from 129 to 228°K; the sky brightness temperatures lie between 6 and 160°K, covering a somewhat broader range of values than for the above-mentioned Run.

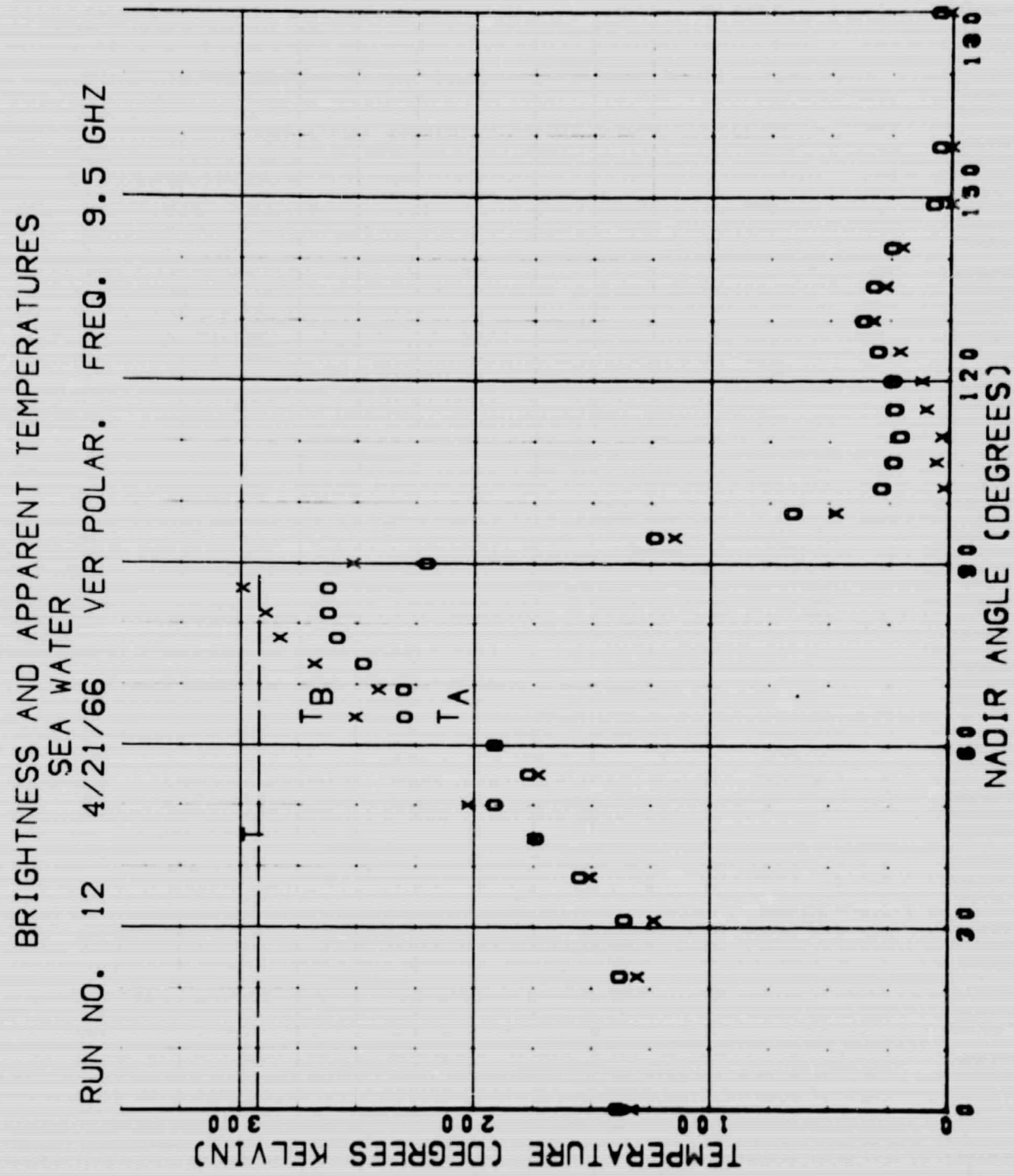


Figure 15 - Measured Sea Water Brightness Temperatures, 9.5 GHz, Vert. Pol.

REPRODUCIBILITY OF THE ORIGINAL PAGE IS POOR.

PAGE	1	RUN 12
TARGET MATERIAL		SEA WATER
DATA DATE		4/21/66
START TIME		1[illegible]
FREQUENCY,GHZ		9.5
POLARIZATION		VER
ANTENNA AZIMUTH,DEG		1[illegible]
BAROMETRIC PRESSURE,IN.HG.		30.[illegible]3
RELATIVE HUMIDITY,%		66
AIR TEMPERATURE,DEG F		58
WIND DIRECTION		SE
WIND SPEED,MPH		1
INTEGRATION TIME,SEC		1

THIRD CALIBRATION POINT 5.4[illegible]DEG.K 6642.[illegible]MV.

INITIAL CALIBRATION DATA		
MINIMUM CAL.TEMP.,DEG.K	318.51	
MAXIMUM CAL.TEMP.,DEG.K	415.66	
K-FACTOR,DEG.K/MV.	.[illegible]96 83	
Y INTERCEPT	-6333.25	
FINAL CALIBRATION DATA		
MINIMUM CAL.TEMP.,DEG.K	317.22	
MAXIMUM CAL.TEMP.,DEG.K	415.79	
K-FACTOR,DEG.K/MV.	.[illegible]90719	
Y INTERCEPT	-[illegible]26.62	

CALIBRATION CONSTANTS	INITIAL	FINAL	UNITS
REF.VOLTAGE	6275.[illegible]	6277.[illegible]	MV.
HOT LOAD	415.39	415.14	DEG.K
ATTENUATOR	317.[illegible]9	315.57	DEG.K
WAVE GUIDE SWITCH	312.19	309.92	DEG.K
ANTENNA	296.33	289.05	DEG.K
AVERAGE CAL. DATA--MIN.	6275.2[illegible]	6893.4[illegible]	MV.
-MAX.	7165.6[illegible]	7[illegible]98.[illegible]	MV.

COMMENTS

Table XIII - Environmental and Calibration Data, Sea Water 9.5 GHz, Vert. Pol.

Table XIV - Brightness Temperatures, Sea Water, 9.5 GHz, Vert. Pol.

TARGET MATERIAL	SEA WATER
DATA DATE	4/21/66
START TIME	1030
FREQUENCY, GHZ	9.5
POLARIZATION	VER

ZENITH ANGLE DEG	BRIGHTNESS TEMP DEG K	EMISSIVITY VERTICAL	TIME	READINGS MV	WATER TEMP DEG K	WAVE PERIOD SEC	WAVE DIR SEC	WAVE HEIGHT IN
0.0	1.0			6649.				
10.0	-0.3			6648.				
20.0	-1.6			6647.				
30.0	-3.3			6647.				
40.0	22.4			6673.				
50.0	32.3			6681.				
55.0	21.9							
60.0	11.5			6660.				
65.0	0.1			6668.				
70.0	3.9			6664.				
75.0	4.5			6662.				
80.0	28.1		1120	6676.				
82.0	50.8			6717.				
84.0	83.8			6734.				
86.0	118.4			6777.				
88.0	135.3			6835.				
89.0	218.8							
90.0	252.2			6880.				
91.0	263.7	0.650	1120	6898.	288.0	4	230	12
92.0	275.3	0.876		6941.	288.0	4	230	12
94.0	298.4	1.061		6925.	288.0	3	225	24
96.0	295.0	1.034		6945.	288.1	3	230	12
98.0	290.3	1.010		6928.	287.8	10	220	24
100.0	287.1	0.997		6926.	287.8	3	230	12
105.0	274.0	0.952		6921.	287.5	5	220	30
110.0	247.2	0.857		6893.	287.8	5	215	30
115.0	250.3	0.865		6897.	287.9	2	230	18
120.0	191.5	0.651		6852.	287.9	4	215	24
125.0	173.7	0.571		6836.	287.8	5	220	12
130.0	202.7	0.667		6853.	288.0	2	220	12
140.0	157.8	0.510		6818.	287.9	2	240	8
150.0	124.3	0.438		6790.	287.8	2	215	12
160.0	130.9	0.458	1140	6796.	287.8	3	215	24

RUN NO. 12 4/21/66 VER POLAR. 9.5 GHZ SEA WATER

ITERATION NUMBER 0

ZENITH ANGLE (DEG)	BRIGHTNESS TEMP. (DEG K)	APPARENT TEMP. (DEG K)	CORRECTION TEMP. (DEG K)
0.0	1.02	4.96	-3.9372
21.79	-1.78	4.50	-6.2844
31.00	-3.45	6.91	-10.3651
38.21	20.46	24.27	-3.8084
44.42	27.03	31.91	-4.8868
49.99	32.28	36.14	-3.8566
55.15	21.18	29.89	-8.7085
60.00	11.50	24.00	-12.5032
64.62	9.64	22.94	-13.2934
69.08	3.39	20.51	-17.1202
73.40	5.67	23.65	-17.9762
77.63	2.55	28.22	-25.6656
81.79	47.31	65.04	-17.7329
85.90	115.19	123.83	-8.6474
90.00	252.20	220.90	31.3040
94.10	299.49	262.69	36.7957
98.21	289.75	262.80	26.9488
102.37	283.52	258.94	24.5761
106.60	268.27	247.81	20.4569
110.92	241.46	230.31	11.1518
115.38	251.13	230.00	21.1325
120.00	191.49	191.70	-0.2069
124.85	172.86	177.25	-4.3849
130.01	202.74	191.60	11.1412
135.58	174.70	173.82	0.8850
141.79	150.91	155.06	-4.1443
149.00	123.57	136.17	-12.5994
158.21	130.66	138.10	-7.4345
180.00	133.23	139.09	-5.8591

Table XV - Brightness and Apparent Temperatures, Sea Water, 9.5 GHz, Vert. Pol.

ABS. CORRECTION = 1.29E 01 DEG. K

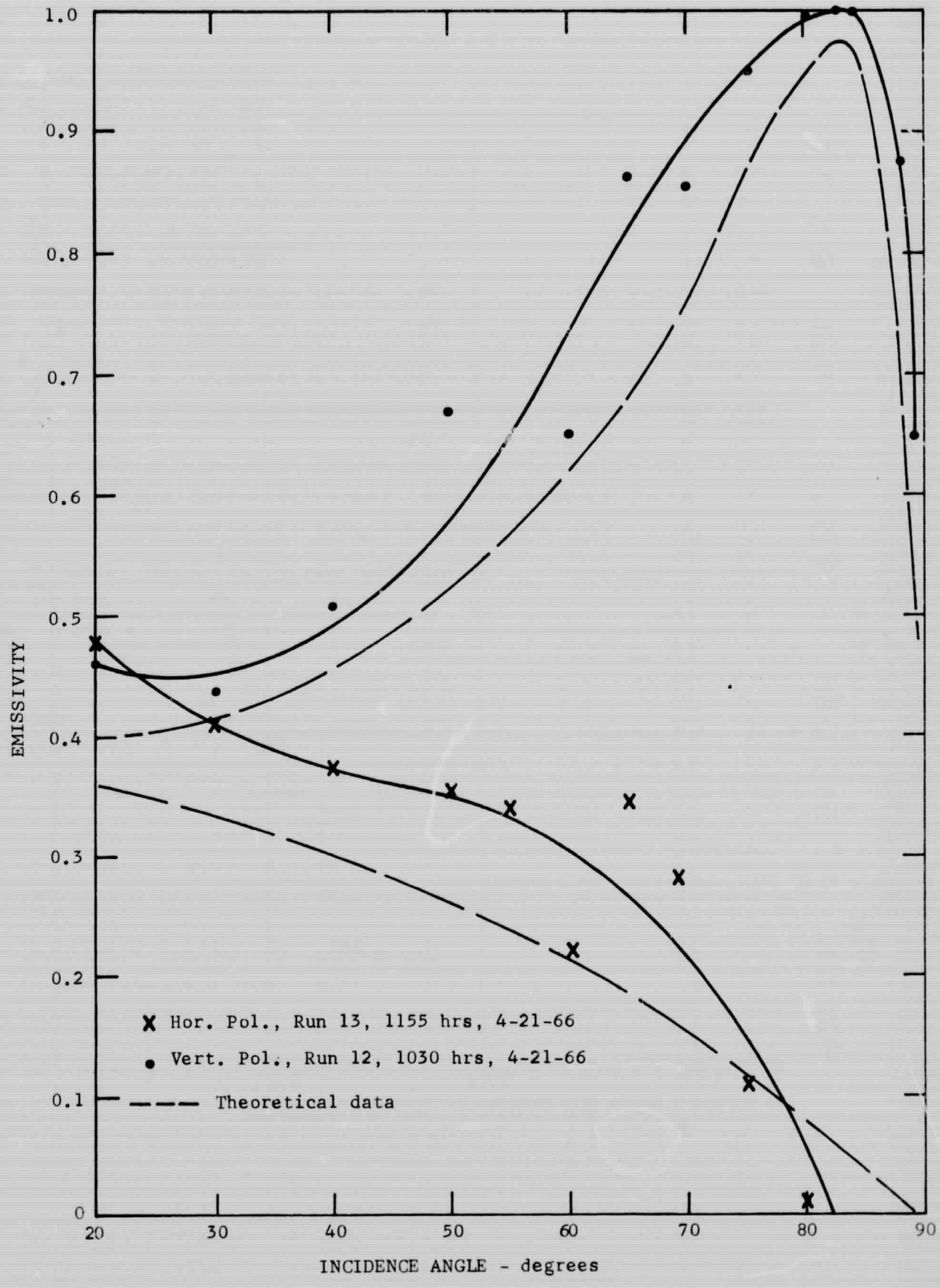


Figure 16 - Derived and Theoretical Specular Emissivities, Sea Water - 9.5 GHz

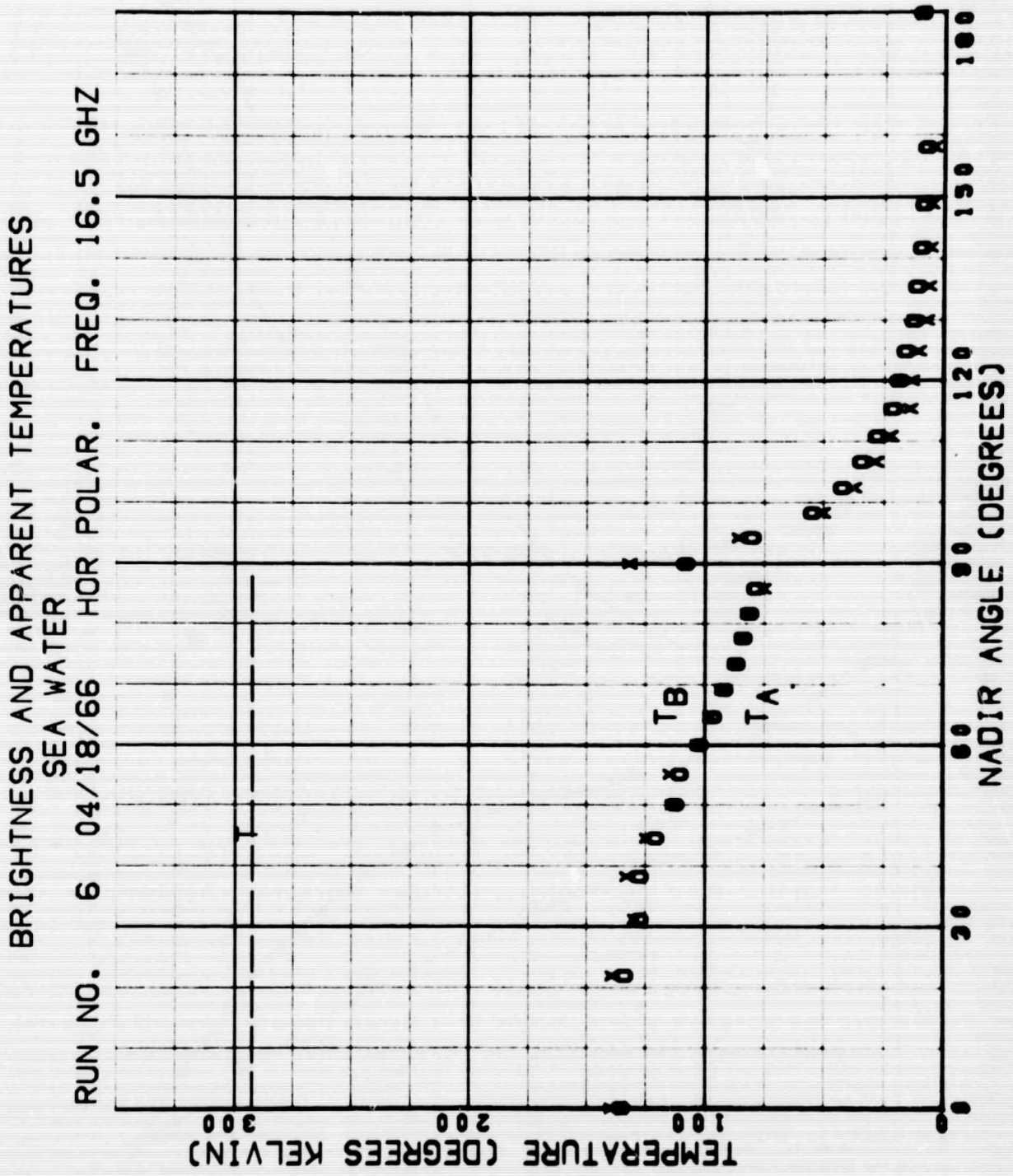


Figure 17 - Measured Sea Water Brightness Temperatures, 16.5 GHz, Hor. Pol.

PAGE 1 RUN 4

TARGET MATERIAL	SEA WATER
DATA DATE	04/18/66
START TIME	1510
FREQUENCY,GHZ	16.5
POLARIZATION	HOR
ANTENNA AZIMUTH,DEG	310
BAROMETRIC PRESSURE,IN.HG.	29.77
RELATIVE HUMIDITY,%	65
AIR TEMPERATURE,DEG F	57
WIND DIRECTION	SOUTH
WIND SPEED,MPH	3
INTEGRATION TIME,SEC	0003

THIRD CALIBRATION POINT 9.30DEG.K 6727.00MV.

INITIAL CALIBRATION DATA	
MINIMUM CAL.TEMP,DEG.K	298.27
MAXIMUM CAL.TEMP.DEG.K	394.50
K-FACTOR,DEG.K/MV.	1.22472
Y INTERCEPT	-8229.11
FINAL CALIBRATION DATA	
MINIMUM CAL.TEMP,DEG.K	298.27
MAXIMUM CAL.TEMP.DEG.K	394.50
K-FACTOR,DEG.K/MV.	1.22234
Y INTERCEPT	-8214.48

CALIBRATION CONSTANTS	INITIAL	FINAL	UNITS
REF.VOLTAGE	6313.0	6313.1	MV.
HOT LOAD	397.30	397.30	DEG.K
ATTENUATOR	297.44	297.44	DEG.K
WAVE GUIDE SWITCH	298.62	298.62	DEG.K
ANTENNA	287.93	287.93	DEG.K
AVERAGE CAL.DATA-MIN.	6961.27	6967.13	MV.
-MAX.	7342.33	7341.13	MV.

COMMENTS
SUNNY SLIGHT HAZE VIS TO HOR WAVE PER 12 DIR 30 DEG RIGHT OF LOS AT 4-5 FT

Table XVI - Environmental and Calibration Data, Sea Water, 16.5 GHz, Hor. Pol.

TARGET MATERIAL SEA WATER
DATA DATE 04/18/66
START TIME 1510
FREQUENCY, GHZ 16.5
POLARIZATION HOR

Table XVII - Brightness Temperatures, Sea Water, 16.5 GHz, Hor. Pol.

ZENITH ANGLE DEG	BRIGHTNESS TEMP DEG K	EMISSIVITY HORIZONTAL	TIME	READINGS MV	WATER TEMP DEG K	WAVE PERIOD SEC	WAVE DIR SEC	WAVE HEIGHT IN
0.0	9.4		1515	6727.				
10.0	7.2			6727.				
20.0	5.1			6725.				
30.0	5.7			6729.				
40.0	6.1			6727.				
50.0	7.6			6730.				
55.0	10.5							
60.0	13.6			6735.				
65.0	15.0			6737.				
70.0	23.8			6743.				
75.0	32.0			6749.				
80.0	44.9		1520	6758.				
82.0	52.3			6765.				
84.0	59.5			6773.				
86.0	86.9			6796.				
88.0	109.6			6803.				
90.0	132.3			6808.				
92.0	104.5	-0.029		6794.	288.2			
94.0	76.6	-0.051		6784.	288.2			
96.0	78.3	0.040		6786.	288.2			
98.0	81.5	0.123		6786.	288.2			
100.0	82.9	0.156		6788.	288.2			
105.0	86.0	0.211		6789.	288.2			
110.0	91.7	0.257		6794.	288.2			
115.0	97.3	0.301		6799.	288.2			
120.0	102.9	0.325		6803.	288.2			
125.0	114.6	0.375		6811.	288.2			
130.0	113.7	0.378		6812.	288.2			
140.0	130.6	0.441		6824.	288.2			
150.0	131.0	0.443		6824.	288.2			
160.0	139.3	0.474	1530	6831.	288.2			

RUN NO. 6 04/18/66 HOR POLAR. 16.5 GHZ SEA WATER

ITERATION NUMBER 0

ZENITH ANGLE (DEG)	BRIGHTNESS TEMP. (DEG K)	APPARENT TEMP. (DEG K)	CORRECTION TEMP. (DEG K)
0.0	9.41	9.41	0.0009
21.79	4.68	7.34	-2.6620
31.00	5.85	8.53	-2.6782
38.21	5.87	9.48	-3.6050
44.42	6.72	11.09	-4.3721
49.99	7.61	12.84	-5.2285
55.15	10.90	15.97	-5.0695
60.00	13.56	18.91	-5.3527
64.62	14.26	21.13	-6.8667
69.08	22.48	27.76	-5.2799
73.40	28.75	34.01	-5.2603
77.63	37.36	42.29	-4.9324
81.79	50.53	54.68	-4.1551
85.90	85.78	80.25	5.5238
90.00	132.32	108.40	23.9248
94.10	75.24	78.78	-3.5366
98.21	81.80	81.10	0.6994
102.37	84.36	83.65	0.7044
106.60	86.99	86.70	0.2902
110.92	92.97	91.89	1.0835
115.38	97.74	96.66	1.0781
120.00	102.89	101.92	0.9718
124.85	114.63	110.52	4.1038
130.01	113.68	112.58	1.1039
135.58	124.69	120.73	3.9594
141.79	133.05	127.25	5.8032
149.00	129.93	127.47	2.4641
158.21	139.32	133.98	5.3383
180.00	139.47	135.39	4.0796

ABS. CORRECTION = 4.14E 00 DEG. K

Table XVIII - Brightness and Apparent Temperatures, Sea Water, 16.5 GHz, Hor. Pol.

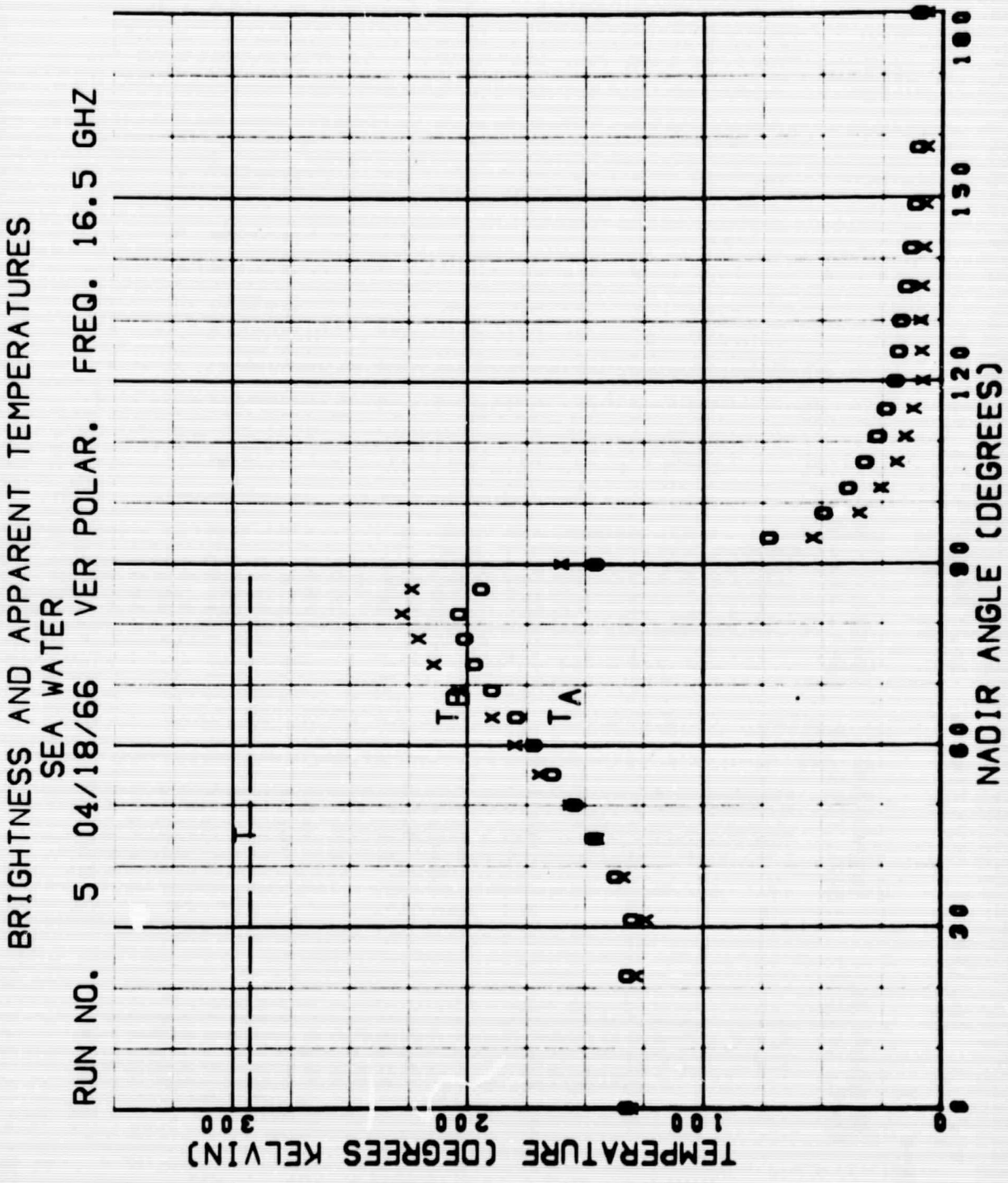


Figure 18 - Measured Sea Water Brightness Temperatures, 16.5 GHz, Vert. Pol.

Table XIX - Environmental and Calibration Data, Sea Water, 9.5 GHz, Vert. Pol.

PAGE 1 RUN 5

TARGET MATERIAL	SEA WATER
DATA DATE	04/10/66
START TIME	1535
FREQUENCY,GHZ	16.5
POLARIZATION	VER
ANTENNA AZIMUTH,DEG	016
BAROMETRIC PRESSURE,IN.HG.	29.77
RELATIVE HUMIDITY,%	65
AIR TEMPERATURE,DEG F	57
WIND DIRECTION	SOUTH
WIND SPEED,MPH	3
INTEGRATION TIME,SEC	0003

THIRD CALIBRATION POINT 9.330DEG.K 6737.03MV.

INITIAL CALIBRATION DATA

MINIMUM CAL.TEMP,DEG.K	297.85
MAXIMUM CAL.TEMP.DEG.K	393.97
K-FACTOR,DEG.K/MV.	1.25111
Y INTERCEPT	-8412.97

FINAL CALIBRATION DATA

MINIMUM CAL.TEMP,DEG.K	297.85
MAXIMUM CAL.TEMP.DEG.K	393.97
K-FACTOR,DEG.K/MV.	1.22125
Y INTERCEPT	-8218.31

CALIBRATION CONSTANTS	INITIAL	FINAL	UNITS
REF.VOLTAGE	6311.[illegible]	6311.[illegible]	MV.
HOT LOAD	396.88	396.88	DEG.K
ATTENUATOR	297.13	297.13	DEG.K
WAVE GUIDE SWITCH	299.61	299.61	DEG.K
ANTENNA	287.71	287.71	DEG.K
AVERAGE CAL.DATA-MIN.	6968.73	6973.[illegible]	MV.
-MAX.	7044.46	7152.27	MV.

COMMENTS

SUNNY SLIGHT HAZE WAVE DIR [illegible] DEG RIGHT OF LOS

Table XX - Brightness Temperatures, Sea Water, 16.5 GHz, Vert. Pol.

TARGET MATERIAL	SEA WATER
DATA DATE	04/18/56
START TIME	1535
FREQUENCY, GHZ	16.5
POLARIZATION	VER

ZENITH ANGLE DEG	BRIGHTNESS TEMP DEG K	EMISSIVITY VERTICAL	TIME	READINGS MV	WATER TEMP DEG K	WAVE PERIOD SEC	WAVE DIR SEC	WAVE HEIGHT IN
0.0	6.3		1535	6737.				
10.0	6.3			6736.				
20.0	6.3			6737.				
30.0	6.9			6738.				
40.0	7.7			6740.				
50.0	9.0			6743.				
55.0	8.5							
60.0	8.1			6745.				
65.0	12.1			6748.				
70.0	15.8			6752.				
75.0	21.3			6757.				
80.0	30.4			6765.				
82.0	35.2			6770.				
84.0	44.9			6778.				
86.0	56.5		1545	6788.				
88.0	109.4			6809.				
90.0	160.2			6848.				
92.0	191.2	0.461		6875.	289.2			
94.0	222.3	0.715		6887.	288.2			
96.0	225.8	0.744		6892.	288.2			
98.0	227.9	0.762		6895.	288.2			
100.0	225.2	0.756		6895.	288.2			
105.0	217.1	0.734		6892.	288.2			
110.0	206.2	0.699		6886.	288.2			
115.0	190.3	0.647		6876.	288.2			
120.0	180.0	0.614		6870.	288.2			
125.0	169.0	0.574	1550	6863.	288.2			
130.0	156.5	0.528		6856.	288.2			
140.0	137.3	0.462		6843.	288.2			
150.0	124.2	0.419		6835.	288.2			
160.0	120.0	0.435	1555	6838.	288.2			

RUN NO. 5 04/18/66 VER POLAR. 16.5 GHZ SEA WATER

ITERATION NUMBER 0

ZENITH ANGLE (DEG)	BRIGHTNESS TEMP. (DEG K)	APPARENT TEMP. (DEG K)	CORRECTION TEMP. (DEG K)
0.0	6.33	9.27	-2.9383
21.79	6.33	9.76	-3.4324
31.00	6.93	11.00	-4.0722
38.21	7.49	12.53	-5.0403
44.42	8.31	14.56	-6.2505
49.99	9.01	16.65	-7.6367
55.15	8.66	17.93	-9.2756
60.00	8.09	19.14	-11.0526
64.62	11.82	22.94	-11.1242
69.08	15.01	26.89	-11.8770
73.40	18.89	31.67	-12.7802
77.63	25.26	38.68	-13.4167
81.79	34.22	49.17	-14.9561
85.90	54.06	72.08	-18.0212
90.00	160.18	145.62	14.5595
94.10	223.76	194.55	29.2063
98.21	228.17	203.84	24.3299
102.37	221.23	201.46	19.7739
106.60	214.57	197.18	17.3919
110.92	203.91	189.68	14.2264
115.38	189.54	179.64	9.8996
120.00	179.96	172.04	7.9250
124.85	169.39	163.95	5.4438
130.01	156.48	154.52	1.9549
135.58	145.19	146.00	-0.8020
141.79	134.08	137.51	-3.4284
149.00	124.39	130.47	-6.0777
158.21	128.86	131.93	-3.0719
180.00	130.55	132.46	-1.9091

ABS. CORRECTION = 1.01E 01 DEG. K

Table XXI - Brightness and Apparent Temperatures, Sea Water, 16.5 GHz, Vert. Pol.

Plots of derived and theoretical emissivities are shown in Figure 19. Rather close agreement is shown for vertical polarization, except at the Brewster Angle. The disparity here is probably due to ocean surface roughness effects. Although the separation between the vertical and horizontally polarized curves is not as great as at 9.5 GHz, there is a rather strong polarization effect at this frequency, indicating a high degree of specularity to the ocean surface.

3. 94 GHz Data

Data obtained at 94 GHz is rather interesting since this frequency is removed from 16.5 GHz by almost an order of magnitude. Thus, an assessment of the frequency dependence of the observations is facilitated. Figure 20 and Tables XXII thru' XXIV present horizontally polarized data. The brightness temperatures are rather high, ranging from 147 to 234^{o}K for the surface and from 67 to 256^{o}K for the atmosphere. The high surface brightness temperatures are partly due to relatively high emissivities for sea water at 94 GHz and partly to the high sky brightness temperatures at this frequency. It will be recalled, from Equation (30), that atmospheric radiation, reflected from the surface, contributes to the total observed brightness temperature.

Figure 21 and Tables XXV thru' XXVII show the vertically polarized data. It will be noted that the surface brightness temperatures approach the thermodynamic temperature at the Brewster Angle and range from 208 to 282^{o}K. The Brewster Angle itself is quite broad; this is probably due to the relatively high values of sky brightness temperature at nadir angles of 90^{o} to 130^{o}. This characteristic is not evident at the two lower frequencies.

Figure 22 shows derived and theoretical sea water emissivities at 94 GHz. In contrast with emissivities at the lower frequencies, there is better agreement, between the derived and theoretical emissivities, for horizontal polarization than for vertical polarization. This may be due to a more pronounced surface roughness effect on the vertically polarized observations at this frequency.

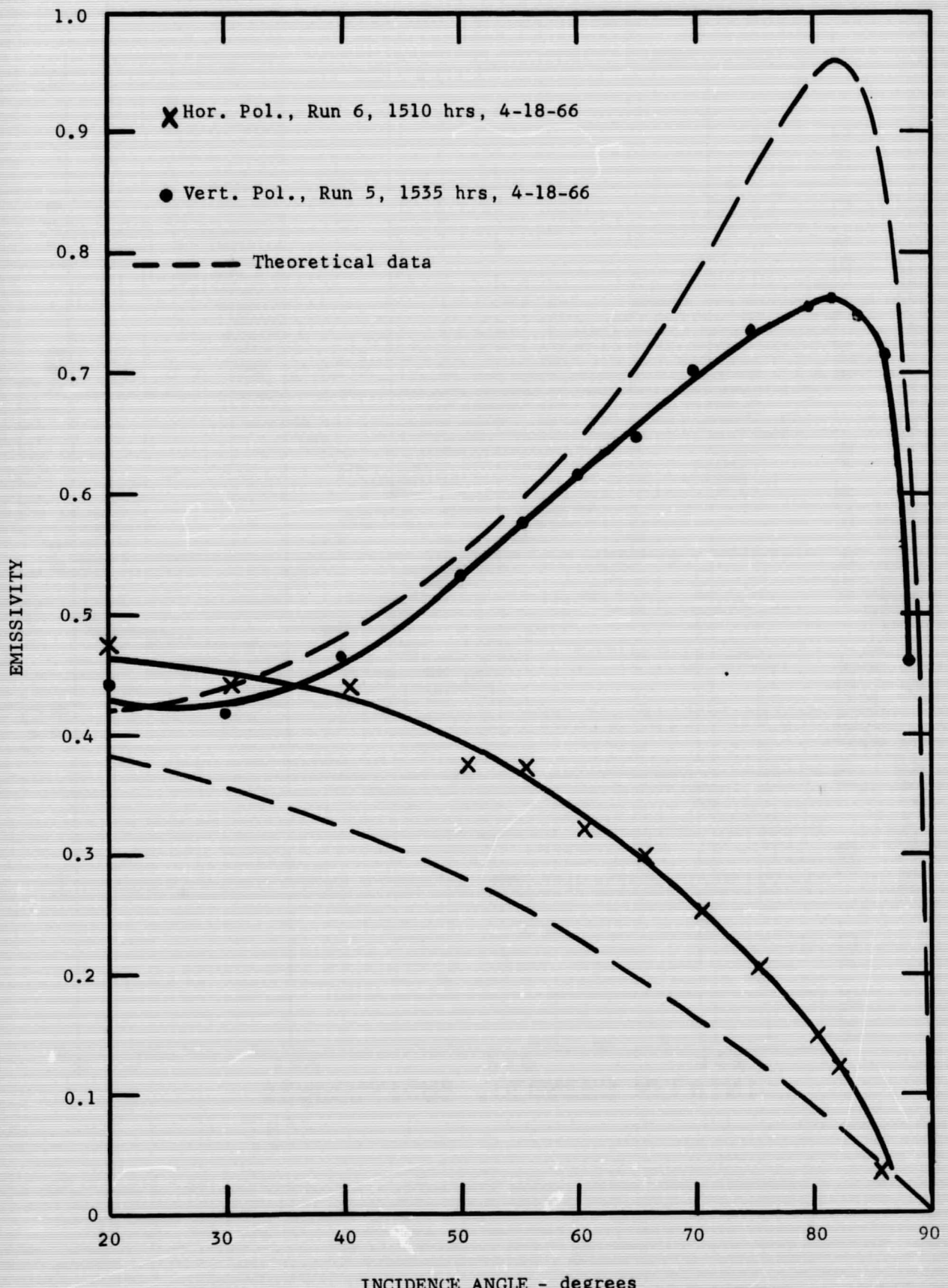


Figure 19 - Derived and Theoretical Specular Emissivities, Sea Water - 16.5 GHz

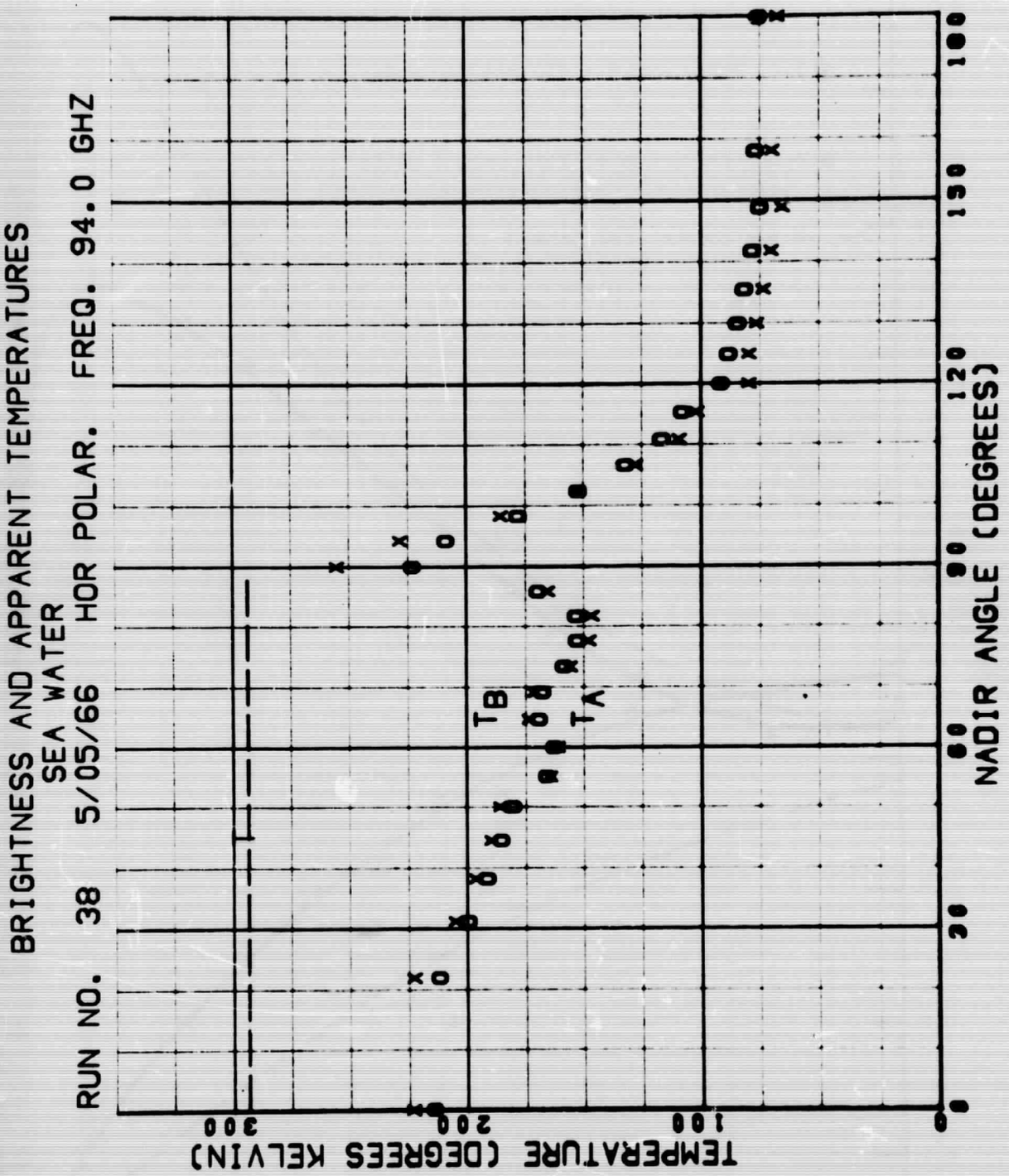


Figure 20 - Measured Sea Water Brightness Temperature, 94 GHz, Hor. Pol.

PAGE 1 RUN 38

TARGET MATERIAL	SEA WATER
DATA DATE	5/05/66
START TIME	1345
FREQUENCY,GHZ	94.0
POLARIZATION	HOR
ANTENNA AZIMUTH,DEG	20
BAROMETRIC PRESSURE,IN.HG.	30.15
RELATIVE HUMIDITY,0/0	63
AIR TEMPERATURE,DEG F	61.0
WIND DIRECTION	WEST
WIND SPEED,MPH	12
INTEGRATION TIME,SEC	3

THIRD CALIBRATION POINT 73.40DEG.K 6616.00MV.

INITIAL CALIBRATION DATA	
MINIMUM CAL.TEMP,DEG.K	293.93
MAXIMUM CAL.TEMP.DEG.K	380.82
K-FACTOR,DEG.K/MV.	0.67041
Y INTERCEPT	-4359.71

FINAL CALIBRATION DATA	
MINIMUM CAL.TEMP,DEG.K	299.65
MAXIMUM CAL.TEMP.DEG.K	387.72
K-FACTOR,DEG.K/MV.	0.58191
Y INTERCEPT	-3776.01

CALIBRATION CONSTANTS	INITIAL	FINAL	UNITS
REF.VOLTAGE	6245.0	6245.0	MV.
HOT LOAD	394.47	401.06	DEG.K
WAVE GUIDE SWITCH	297.85	301.09	DEG.K
ANTENNA	290.75	290.75	DEG.K
COLD LOAD	289.79	295.33	DEG.K
AVERAGE CAL.DATA-MIN.	6930.40	7000.60	MV.
-MAX.	7078.60	7157.80	MV.

COMMENTS
CLOUD COVER.HEAVY SWELL

Table XXII - Environmental and Calibration Data, Sea Water, 94 GHz, Hor. Pol.

Table XXIII - Brightness Temperatures, Sea Water, 94 GHz, Hor. Pol.

TARGET MATERIAL: SEA WATER
DATA DATE: 5/05/66
START TIME: 1345
FREQUENCY, GHZ: 94.0
POLARIZATION: HOR

ZENITH ANGLE DEG	BRIGHTNESS TEMP DEG K	EMISSIVITY HORIZONTAL	TIME	READINGS MV	WATER TEMP DEG K	WAVE PERIOD SEC	WAVE DIR SEC	WAVE HEIGHT IN
0.0	67.3		1347	6616.				
10.0	68.4		1350	6601.				
20.0	69.6			6618.				
30.0	66.0			6614.				
40.0	71.3			6622.				
50.0	76.3			6630.				
55.0	78.0							
60.0	79.7			6641.				
65.0	102.4			6668.				
70.0	113.2			6683.				
75.0	137.1			6715.				
80.0	171.2		1355	6756.				
82.0	187.7			6781.				
84.0	208.8			6812.				
85.0	219.1							
86.0	229.5			6830.				
88.0	242.6			6845.				
89.0	249.1							
90.0	255.7		1358	6854.				
91.0	233.7	-0.391		6855.	288.8	4	235	48
92.0	211.6	-0.670		6822.	288.8			
95.0	161.3	-0.829		6748.	288.9	4	240	48
100.0	147.3	-0.202		6742.	289.1	4	230	54
105.0	153.0	0.105		6747.	289.2	4	240	54
110.0	167.8	0.310	1405	6770.	289.4	4	235	36
115.0	173.2	0.379		6775.	289.4	4	240	48
120.0	161.1	0.388		6764.	289.4	3	230	24
125.0	165.0	0.412		6770.	289.2	4	240	36
130.0	186.1	0.516		6796.	289.3	3	240	48
140.0	194.5	0.565		6812.	289.4	4	245	60
150.0	207.1	0.632		6832.	289.4	3	240	36
160.0	223.0	0.698	1410	6858.	289.2	3	245	30

RUN NO. 38 5/05/66 HOR POLAR. 94.0 GHZ SEA WATER

ITERATION NUMBER 0

ZENITH ANGLE (DEG)	BRIGHTNESS TEMP. (DEG K)	APPARENT TEMP. (DEG K)	CORRECTION TEMP. (DEG K)
0.0	67.31	75.48	-8.1729
21.79	69.79	76.77	-6.9780
31.00	65.49	74.91	-9.4107
38.21	70.37	78.32	-7.9482
44.42	73.75	81.53	-7.7870
49.99	76.34	84.52	-8.1758
55.15	79.54	88.12	-8.5781
60.00	79.69	91.51	-11.8166
64.62	101.75	107.56	-5.8140
69.08	109.25	116.78	-7.5312
73.40	127.81	132.26	-4.4507
77.63	152.27	152.30	-0.0353
81.79	185.41	178.21	7.1956
85.90	228.84	208.94	19.9034
90.00	255.70	223.29	32.4102
94.10	165.38	169.50	-4.1133
98.21	146.74	153.11	-6.3690
102.37	148.12	152.72	-4.5998
106.60	156.02	158.17	-2.1460
110.92	171.06	167.70	3.3633
115.38	173.38	169.30	4.0872
120.00	161.08	162.64	-1.5581
124.85	164.38	165.87	-1.4907
130.01	186.15	180.38	5.7630
135.58	189.97	185.45	4.5235
141.79	196.39	191.45	4.9373
149.00	205.17	199.52	5.6495
158.21	222.90	212.25	10.6442
180.00	223.64	214.78	8.8585

ABS. CORRECTION = 7.39E 00 DEG. K

Table XXIV - Brightness and Apparent Temperatures, Sea Water, 94 GHz, Hor. Pol.

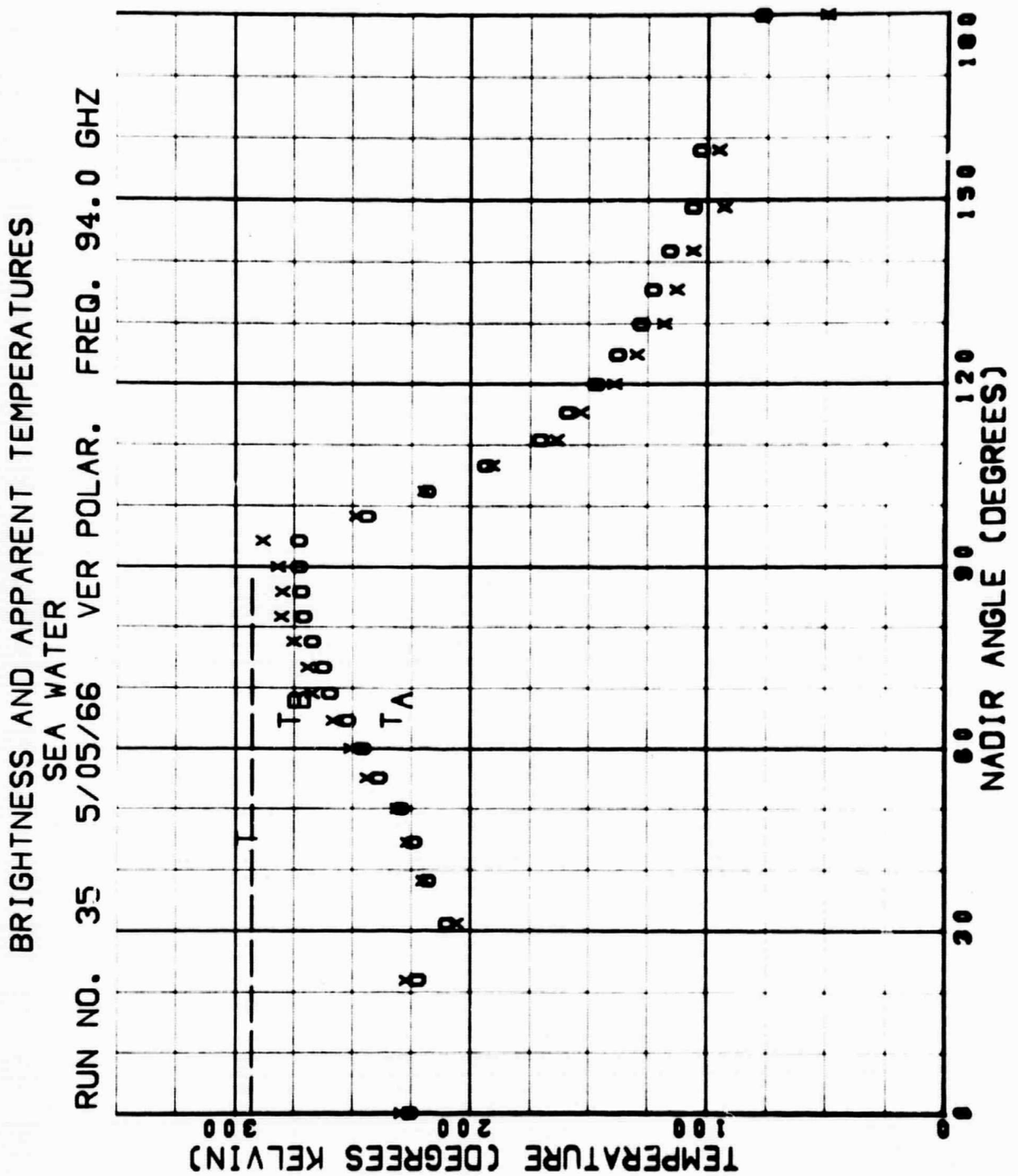


Figure 21 - Measured Sea Water Brightness Temperatures, 94 GHz, Vert. Pol.

Table XXV - Environmental and Calibration Data, Sea Water, 94 GHz, Vert. Pol.

TARGET MATERIAL	SEA WATER
DATA CATE	5/05/66
START TIME	1050
FREQUENCY,GHZ	94.0
POLARIZATION	VER
ANTENNA AZIMUTH,DEG	200
BAROMETRIC PRESSURE,IN.HG.	
RELATIVE HUMIDITY,0/0	
AIR TEMPERATURE,DEG F	
WIND DIRECTION	
WIND SPEED,MPH	
INTEGRATION TIME,SEC	3

THIRD CALIBRATION POINT 73.40DEG.K 6657.00MV.

INITIAL CALIBRATION DATA

MINIMUM CAL.TEMP,DEG.K	301.25
MAXIMUM CAL.TEMP.DEG.K	386.83
K-FACTOR,DEG.K/MV.	0.82734
Y INTERCEPT	-5430.55

FINAL CALIBRATION DATA

MINIMUM CAL.TEMP,DEG.K	301.08
MAXIMUM CAL.TEMP.DEG.K	387.70
K-FACTOR,DEG.K/MV.	0.67285
Y INTERCEPT	-4405.74

CALIBRATION CONSTANTS	INITIAL	FINAL	UNITS
REF,VOLTAGE	6239.0	6240.5	MV.
HOT LOAD	401.12	400.71	DEG.K
WAVE GUIDE SWITCH	301.71	302.70	DEG.K
ANTENNA	295.35	292.30	DEG.K
COLD LOAD	298.76	296.67	DEG.K
AVERAGE CAL.DATA-MIN.	6914.40	6994.80	MV.
-MAX.	7040.53	7124.53	MV.

COMMENTS
CLEAR,SUNNY,LIGHT HAZE.SCATTERED CLOUDS TOWARD HORIZON.HEAVY SWELLS NO WHITECAPS. WATER SAMPLE 5 TAKEN AT 120 DEGREES

Table XXVI Brightness Temperatures, Sea Water, 94 GHz, Vert. Pol.

TARGET MATERIAL	SEA WATER
DATA DATE	5/05/66
START TIME	1050
FREQUENCY, GHZ	94.0
POLARIZATION	VER

ZENITH ANGLE DEG	BRIGHTNESS TEMP DEG K	EMISSIVITY VERTICAL	TIME	READINGS MV	WATER TEMP DEG K	WAVE PERIOD SEC	WAVE DIR SEC	WAVE HEIGHT IN
0.0	50.3		1050	6657.				
10.0	71.0			6671.				
20.0	91.6			6688.				
30.0	93.0			6692.				
40.0	108.0			6709.				
50.0	117.9			6722.				
55.0	128.4							
60.0	139.0			6746.				
65.0	154.3							
70.0	169.5			6780.				
75.0	202.0			6819.				
80.0	236.3		1055	6859.				
82.0	250.8			6878.				
84.0	270.1			6908.				
85.0	279.3							
86.0	288.4			6918.				
88.0	285.2			6926.				
89.0	283.6							
90.0	282.0		1100	6922.				
91.0	281.6	-0.381		6922.	288.8	4	230	24
92.0	281.2	-1.098		6925.	288.8			
95.0	280.4	0.123		6927.	288.8	3	225	18
100.0	278.3	0.797	1105	6928.	289.0	2	230	12
105.0	271.9	0.802		6920.	289.0	4	230	30
110.0	268.1	0.825		6919.	289.1	3	220	12
115.0	259.2	0.779		6910.	289.0	2	220	10
120.0	251.3	0.749		6902.	288.9	3	230	12
125.0	243.9	0.719	1110	6894.	289.0	3	225	12
130.0	231.3	0.663		6882.	289.0	3	220	18
140.0	222.2	0.631		6871.	289.1	2	225	12
150.0	209.4	0.589		6856.	289.0	3	230	18
160.0	227.4	0.698	1115	6883.	288.9	3	225	24

RUN NO. 35 5/05/66 VER POLAR. 94.0 GHZ SEA WATER

ITERATION NUMBER 0

ZENITH ANGLE (DEG)	BRIGHTNESS TEMP. (DEG K)	APPARENT TEMP. (DEG K)	CORRECTION TEMP. (DEG K)
0.0	50.34	76.99	-26.6499
21.79	95.34	102.76	-7.4154
31.00	92.68	106.04	-13.3601
38.21	105.90	115.92	-10.0173
44.42	113.04	122.66	-9.6142
49.99	117.85	128.07	-10.2207
55.15	129.64	137.71	-8.0680
60.00	138.99	146.77	-7.7766
64.62	153.22	158.88	-5.6656
69.08	163.64	170.55	-6.9076
73.40	191.12	193.28	-2.1619
77.63	219.74	218.31	1.4331
81.79	248.74	244.20	4.5397
85.90	288.53	273.12	15.4130
90.00	282.00	272.99	9.0122
94.10	280.41	272.08	8.3263
98.21	280.49	271.52	8.9714
102.37	275.38	267.55	7.8352
106.60	269.61	262.89	6.7130
110.92	267.75	260.01	7.7398
115.38	258.42	252.72	5.6974
120.00	251.32	246.20	5.1177
124.85	244.20	239.37	4.8336
130.01	231.33	229.46	1.8723
135.58	226.93	224.38	2.5447
141.79	220.35	218.33	2.0217
149.00	206.12	210.11	-3.9968
158.21	227.21	222.78	4.4212
180.00	229.70	225.79	3.9087

ABS. CORRECTION = 7.32E 00 DEG. K

Table XXVII - Brightness and Apparent Temperatures, Sea Water, 94 GHz, Vert. Pol.

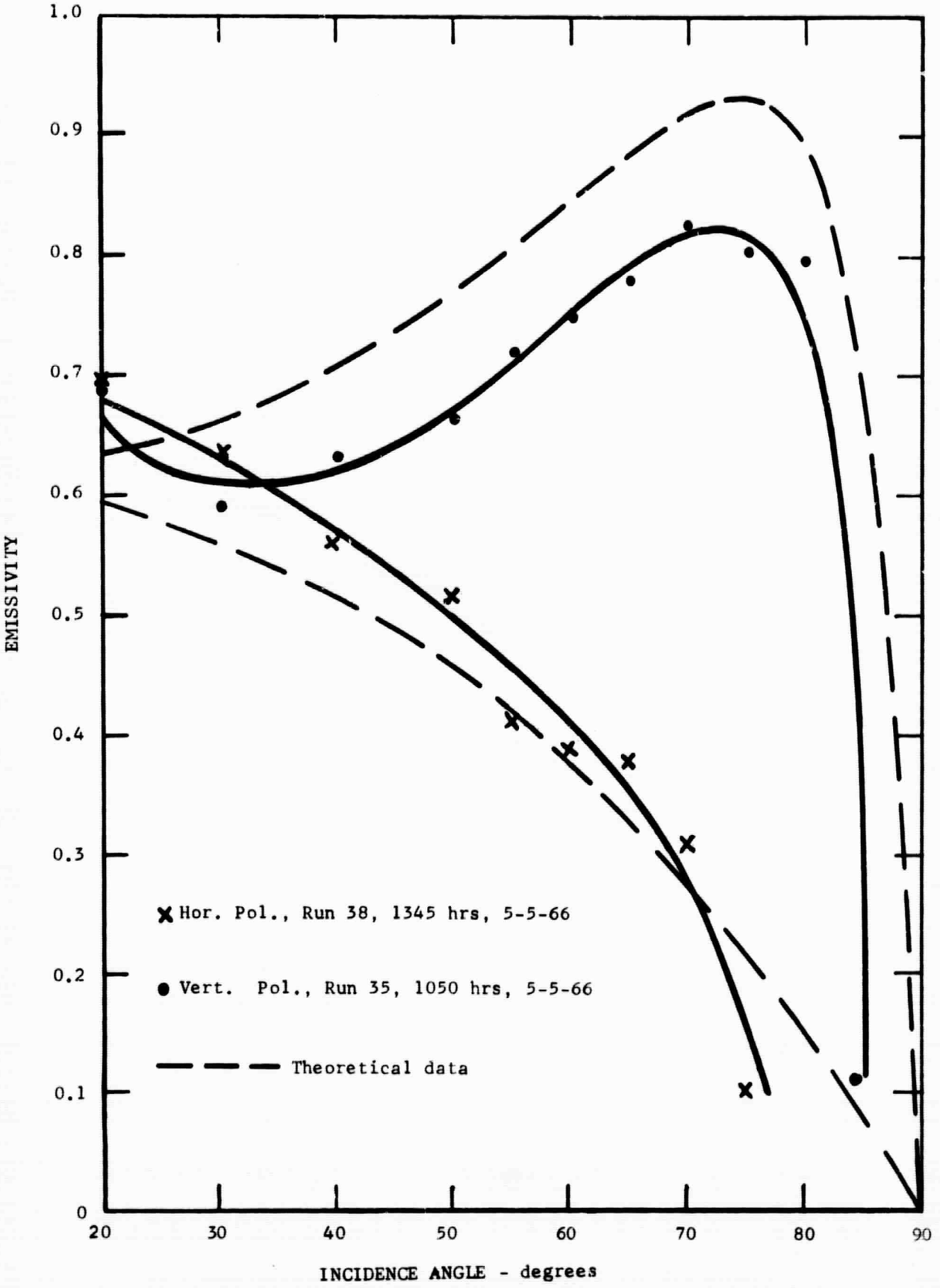


Figure 22 - Derived and Theoretical Specular Emissivities, Sea Water - 94 GHz.

B. ANALYSIS OF THEORETICAL SEA WATER DATA

A comprehensive analysis of any measured data is often facilitated by comparison with theoretical information. In the case of sea water, a considerable amount of theoretical data was generated in the study. This information has been utilized in the interpretation of measured brightness temperatures and derived emissivities.

1. Dielectric Permittivities of Sea Water

The real and imaginary parts of the dielectric permittivity are given by [19,20]:

$$e' = e_\infty + \frac{e_s - e_\infty}{1 + \left(\frac{\lambda_s}{\lambda}\right)^2} \tag{40}$$

$$e'' = \frac{(e_s - e_\infty)(\lambda_s/\lambda)}{1 + \left(\frac{\lambda_s}{\lambda}\right)^2} + \frac{1.8\sigma}{f} \tag{41}$$

where,

e_s = static permittivity

λ_s = relaxation wave length

e_∞ = high frequency limit of the permittivity

λ = wavelength, which at 14 GHz is 2.14 cm.

e_o = permittivity of free space

i.e, $e_o = 8.85 \times 10^{-12}$ farad/meter

σ = static conductivity in units of 10^3 mho/cm

and, f = frequency, GHz.

The conductivity varies with temperature according to,

$$\sigma(T) = .59\,[80.625714 + 1.702\Delta t + 0.0075714286\Delta t^2] \tag{42}$$

where, $\Delta t = T - 293$

in which, T is in degrees Kelvin.

Reference (1) report furnished a variety of information on the characteristics of the sea water at the Ventura measurement site. This data was prepared by Marine Advisers, Inc., and included, among other items, salinities and conductivities measured during the radiometric observations, together with a plot of the static dielectric constant versus temperature for sodium chloride solutions of four (4) different normalities. A portion of the accompanying discussion is reproduced here for purposes of convenience:

> "Sea water salinities display relatively small fluctuations, e.g., of the samples taken, the salinities ranged from 33.643 parts per thousand to 33.722 parts per thousand. A Sodium Chloride solution can often-times be substituted for sea water when studying the properties of sea water. Such a solution exhibits, in many ways, characteristics closely approximating those of natural sea water. In discussion of dielectric constants, experiments suggest that one may expediently make such a substitution. The mean salinity observed on the survey was 33.664 parts per thousand. If one were to regard all dissolved compounds (excluding dissolved gases) in sea water to be Sodium Chloride, the normality of the NaCl sea water would be 0.578 N.
>
> Hasted, Ritson, and Collie[19] have made measurements to determine the dielectric constants of various water-salt solutions for several normalities and temperatures at wave lengths of 10 cm, 3 cm and 1.25 cm. Figure 23 shows a graph prepared from applicable sections of their data. It is notable that the small variations of salinities encountered during the field measurements produce only negligible changes in the dielectric constant, K. Temperature is the dominant controlling variable for sea water, as far as dielectric constant is concerned.
>
> The .66N NaCl solution plot in Figure 23 is linear. Only two points each were available for plotting the 0.5N and 1N figures. However, the underlying theory and the linear trend of the 0.66N plot suggest that these other curves are straight lines. With this in mind, a straight line curve corresponding to a 0.578N NaCl solution was interpolated linearly between the 0.5N and 0.66N plots. Temperatures of

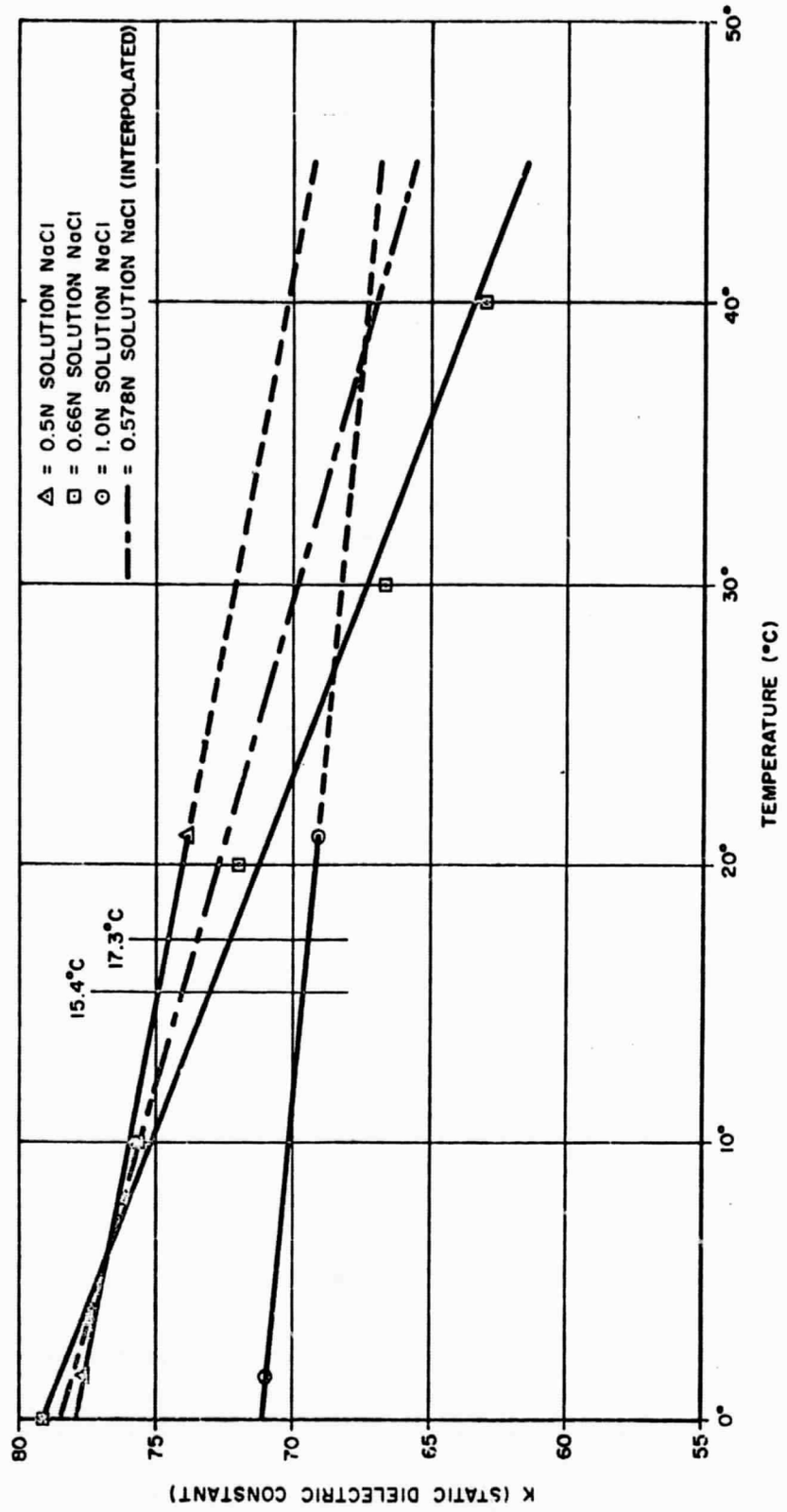


Figure 23 - Static Dielectric Constant Vs. Temperature for NaCl Water Solutions of Selected Normalities

water samples taken in the field ranged between 15.4°C and 17.3°C; these temperatures are indicated on Figure 23. At 15.4°C, the dielectric constant, K = 74.2; at 17.3°C, K = 73.5. Hence, the dielectric constant changes by only 0.7 over the temperature range experienced.

L. N. Liebermann[21] gives a value of K equal to 78 for sea water but does not state at what temperature. It is customary in oceanographic measurements, however, to give values of parameters measured at 0°C. Hence, if Liebermann's value of K is for 0°C sea water, his value differs from the value predicted by Figure 23 by only 0.5, thus lending support to the accuracy of Figure 23. The mean value of K obtained during the field program (measured from Figure 23) is 73.9."

From the interpolated straight-line plot by Marine Adivsers, Inc., the following values of e_s are obtained:

$$e_s = 70.86 \text{ at } 26.2^\circ C$$

and

$$e_s = 73.76 \text{ at } 16^\circ C$$

Marine Advisers did not furnish the correct values of λ_s at either these temperatures or for the average salinity of the sea water. The following procedure was adopted to assign correct values to λ_s. Using data in Reference (19) at 21°C, λ_s is plotted as a function of normality (N) in Figure 24. A straight line characteristic was obtained; the slope of the line gives the change in λ_s for a unit change in normality.

Thus,

$$\frac{\Delta\lambda_s}{\Delta N} = - .16 \text{ cm/N}$$

Reference (19) has also given the variation of λ_s with temperature at 0.66N. A correction has been applied to these values to correspond to 0.578N. This plot is given in Figure 25. From this λ_s is obtained as follows:

$$\lambda_s = 1.95 \text{ at } 26.2^\circ C$$

and

$$\lambda_s = 1.48 \text{ at } 16^\circ C$$

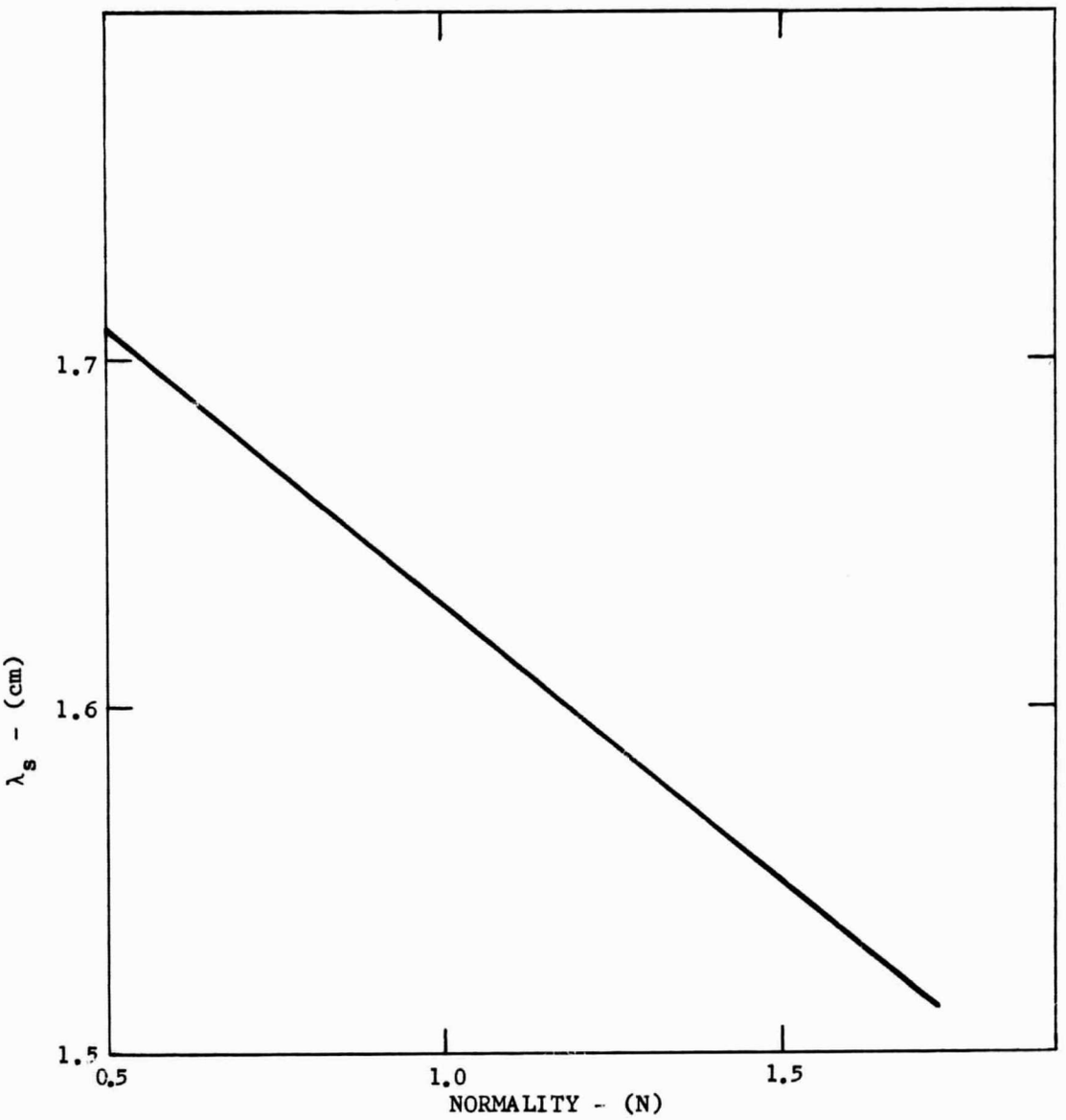


Figure 24 - Variation of λ_s with Normality for NaCl Solution at 21°C.

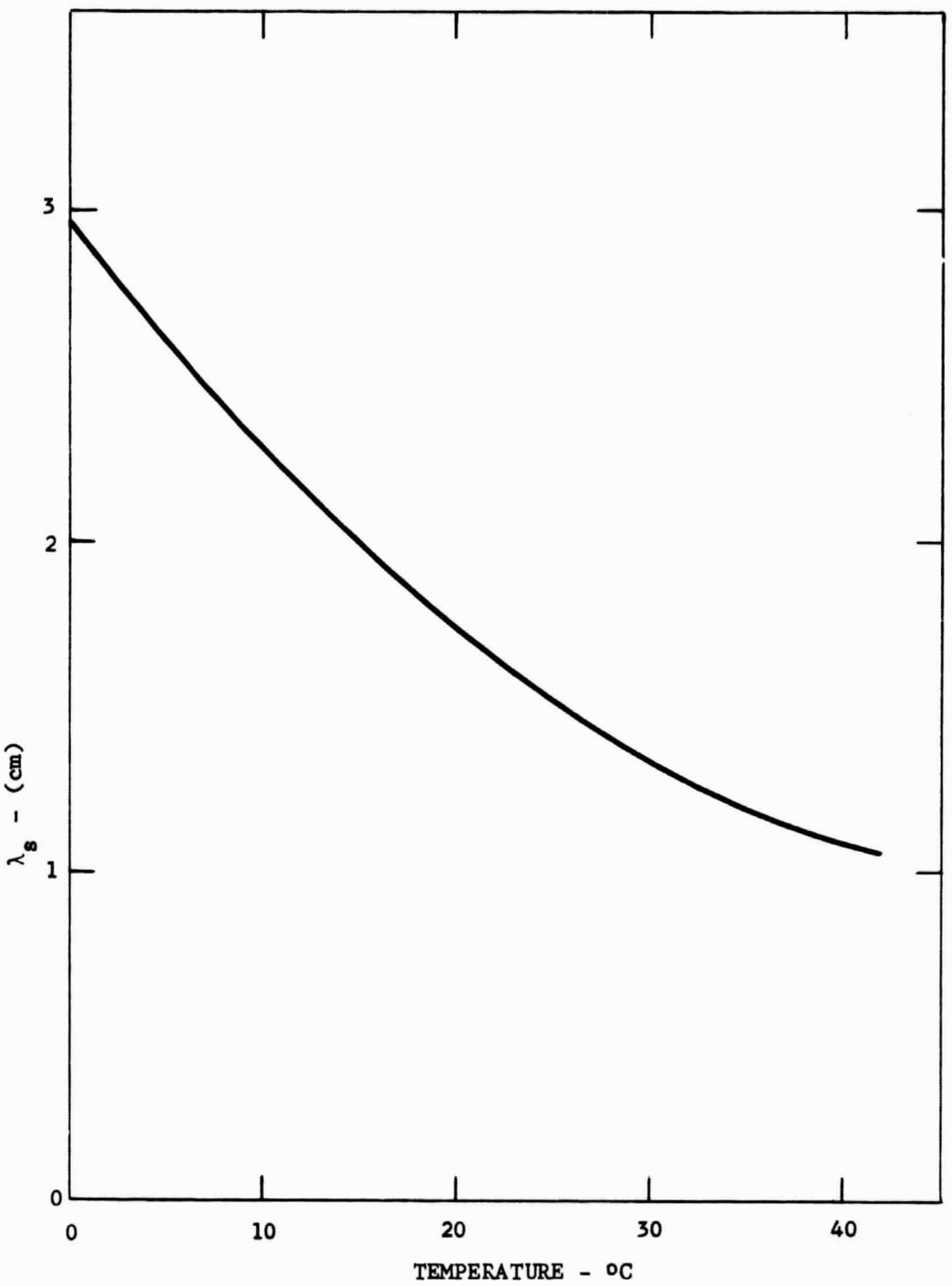


Figure 25 - Variation of λ_s with Temperature at 0.578N NaCl Solution.

The real and imaginary parts of dielectric permittivity have been calculated using Equations (40) and (41); the values are given in Table XXVIII.

TABLE XXVIII

CALCULATED DIELECTRIC PERMITTIVITIES OF SEA WATER

Frequency (GHz)	Temperature (^{o}K)	e'	e"
9.5	288.4	52.634	38.100
16.5	287.7	34.987	37.820
16.5	290.0	36.943	37.878
16.5	292.7	39.039	37.754
94	288.2	6.606	11.340
94	292.4	7.025	12.490

The above data shows that, within a given frequency, the dielectric permittivity of sea water increases with temperature; this is evident at both 16.5 and 94 GHz. In addition, the permittivity is inversely proportional to frequency, the variation in e' being greater than in e".

It is worth mentioning that the correction for conductivity, appearing in Equation (41), has a relatively small effect at the frequencies involved in this study; the magnitude of the correction is inversely proportional to frequency. According to the data obtained by Marine Advisers, Inc., the conductivity of sea water varies from 0.0004363 mho/meter to 0.0004122 mho/meter, with a mean value of 0.0004243 mho/meter. The correction to e", for conductivity at 14 GHz,* is as follows for the indicated temperatures:

Temp. (^{o}C)	Correction
26.2	6.88
16.0	5.62

The above correction is slightly larger at 9.5 GHz and smaller at 16.5 and 94 GHz, in proportion to frequency.

*This frequency was used for measurements of dielectric permittivities at Massachusetts Institute of Technology.

Reference (1) report also presented measured values of dielectric permittivities, obtained at the Massachusetts Institute of Technology. These measurements were made at 14 GHz. Table XXIX furnishes a comparison of dielectric permittivities calculated from the Marine Advisers data and measured by MIT. Since the MIT measurements were made at a temperature of 26.2°C, it is appropriate to refer to the tabulated data at this temperature. There is excellent agreement between the calculated and measured values of e', the deviation of the calculated value being only 4%. The e" values do not agree as well, the calculated value being 25% higher than the measured value. This deviation considered to be partly due to the basis used by Marine Advisers for deriving e". Calculations performed with the aid of References (19) and (20), show a value of 36.6 for e" (see Table C-I in Appendix C). This is only +16.5% higher than the measured value and is comparable to the measurement error of approximately ±15%.

TABLE XXIX

COMPARISON OF CALCULATED AND MEASURED

VALUES OF SEA WATER DIELECTRIC PERMITTIVITIES

Frequency: 14 GHz

Temperature (°C)	Calculated From Static Diel. Permittivity*		Measured Values**	
	e'	e"	e'	e"
16.0	51.7	37.5	42.9 (Calculated in Ref.(1) report)	34.2
26.2	41.2	39.4	43.0	31.4

*Derived by Marine Advisers, Inc.

**Measured by Massachusetts Institute of Technology.

2. Theoretical Emissivities of Sea Water

The dielectric permittivities listed in Table XXVIII have been used in calculations of specular emissivities of sea water at the indicated temperatures. The expressions employed for this purpose are given in Appendix C. Figures 26 thru' 32 show plots of theoretical emissivities, for both polarizations, at 9.5, 16.5, 94 and 14 GHz. Tabulations of the emissivities, shown in these plots, are given in Appendix C.

The plotted emissivities exhibit relatively low values for both polarization at incidence angles of 0 to 50 degrees, at both 9.5 and 16.5 GHz. The corresponding values are approximately 0.2 higher at 94 GHz. Thus, at a temperature of 290°K, sea water brightness temperatures should be approximately 60°K higher, in this region, due to direct emission.

Table XXX summarizes the calculated emissivities at incidence angles of 20° and 60°. The frequency dependence of the emissivities is quite clear, with approximately the same degree of upward shift at each incidence angle, for both polarizations. Within each frequency, however, it is evident that emissivities are inversely proportional to temperature. This is the obverse to the temperature dependence of permittivity. Finally, comparing the permittivity data given in Table XXVIII with the above information, it is clear that emissivity is inversely proportional to permittivity.

C. ADDITIONAL ANALYSIS OF SEA WATER DATA

A considerable amount of additional analysis was performed on the sea water data; the results of this work are presented in the following subsections.

1. Analysis to Show The Utility of Converting Apparent Temperatures to Brightness Temperatures.

This analysis indicates the improvement obtained by performing antenna pattern corrections and converting apparent temperatures, T_A, to brightness temperatures, T_B. The improvement is assessed by a comparison of derived T_B's with calculated values. The latter were obtained with the aid of Equation (30), for which the emissivities were calculated by means of infor-

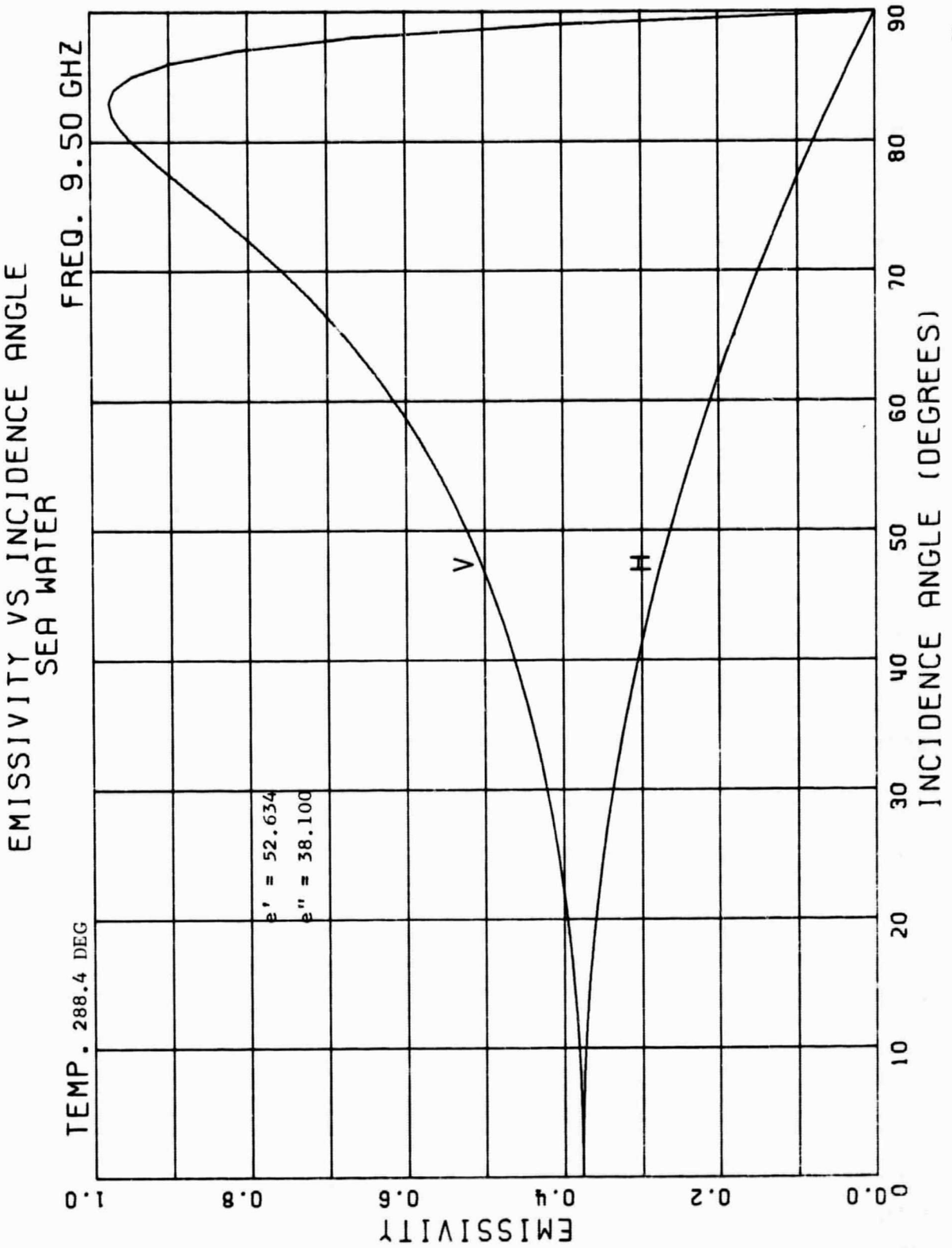


Figure 26 - Theoretical Emissivity of Sea Water - 9.5 GHz

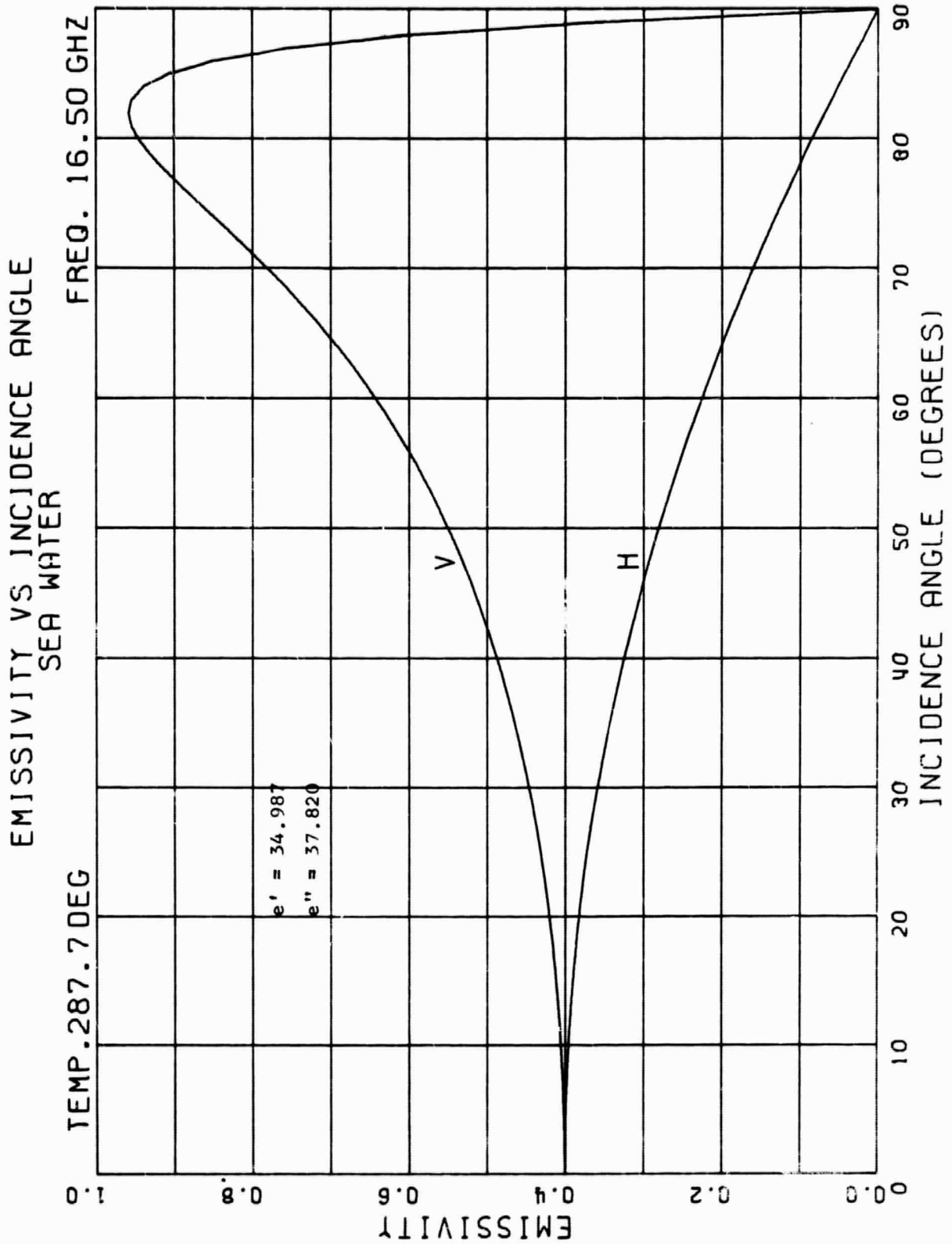


Figure 27 - Theoretical Emissivity of Sea Water - 16.5 GHz.

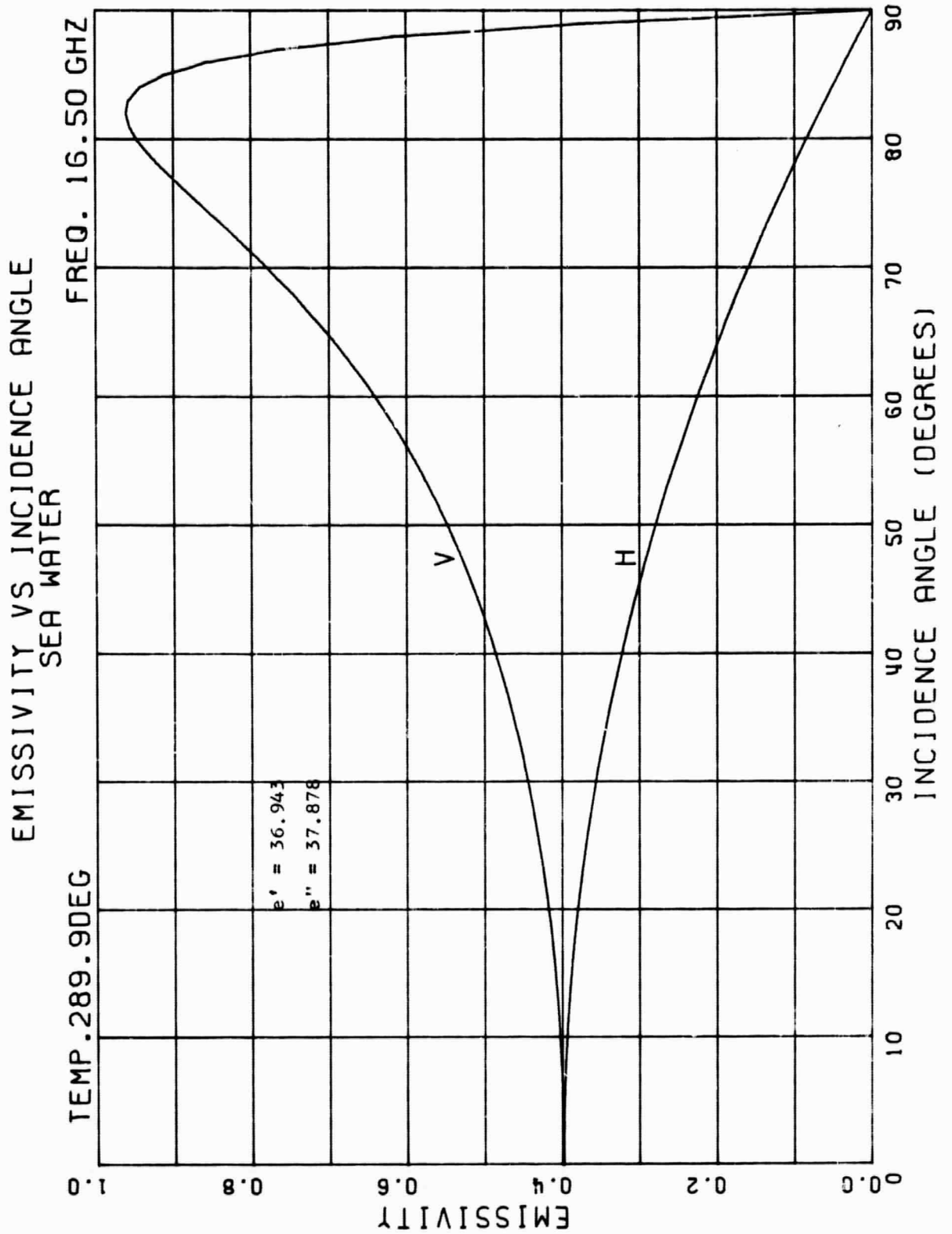


Figure 28 - Theoretical Emissivity of Sea Water - 16.5 GHz

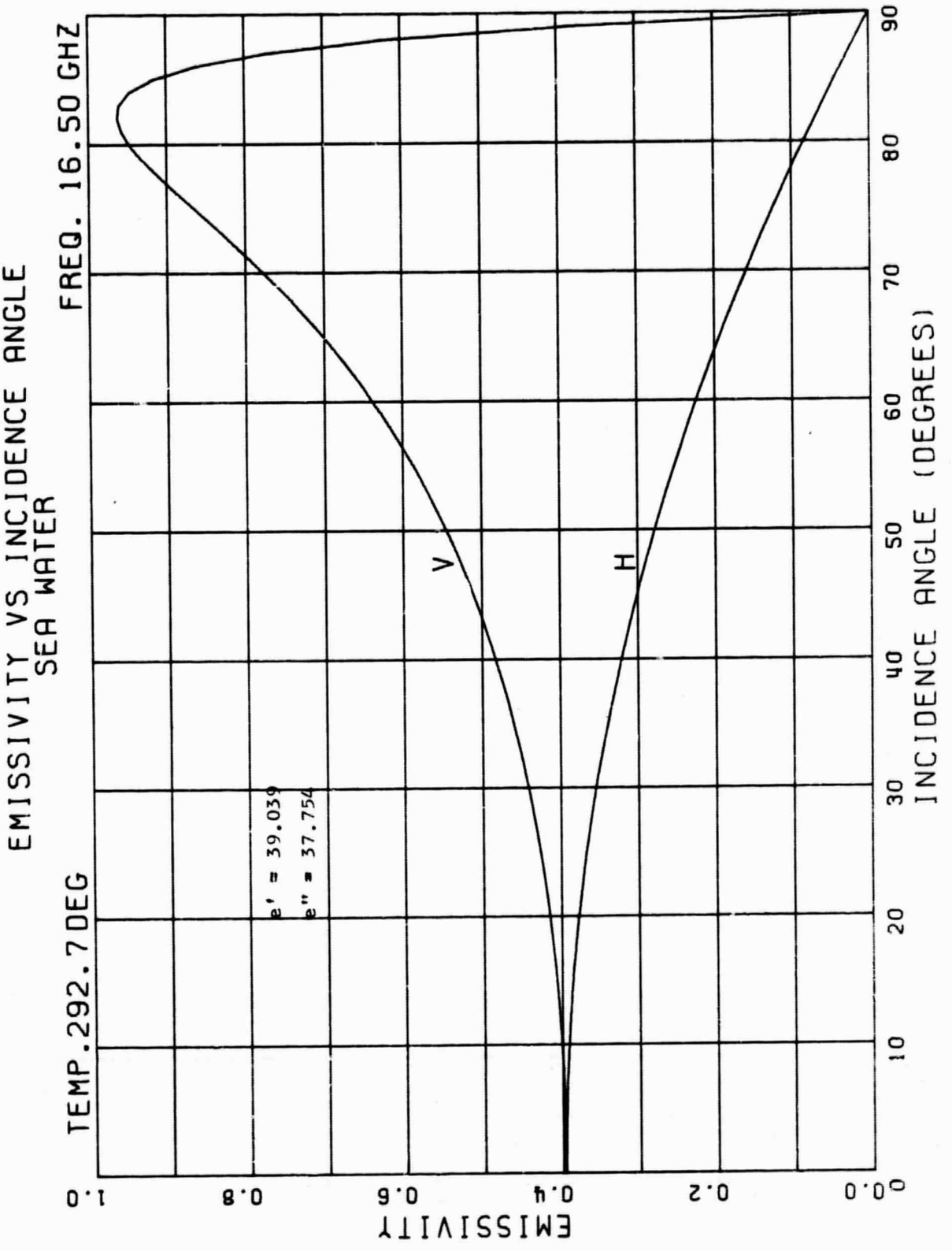


Figure 29 - Theoretical Emissivity of Sea Water - 16.5 GHz

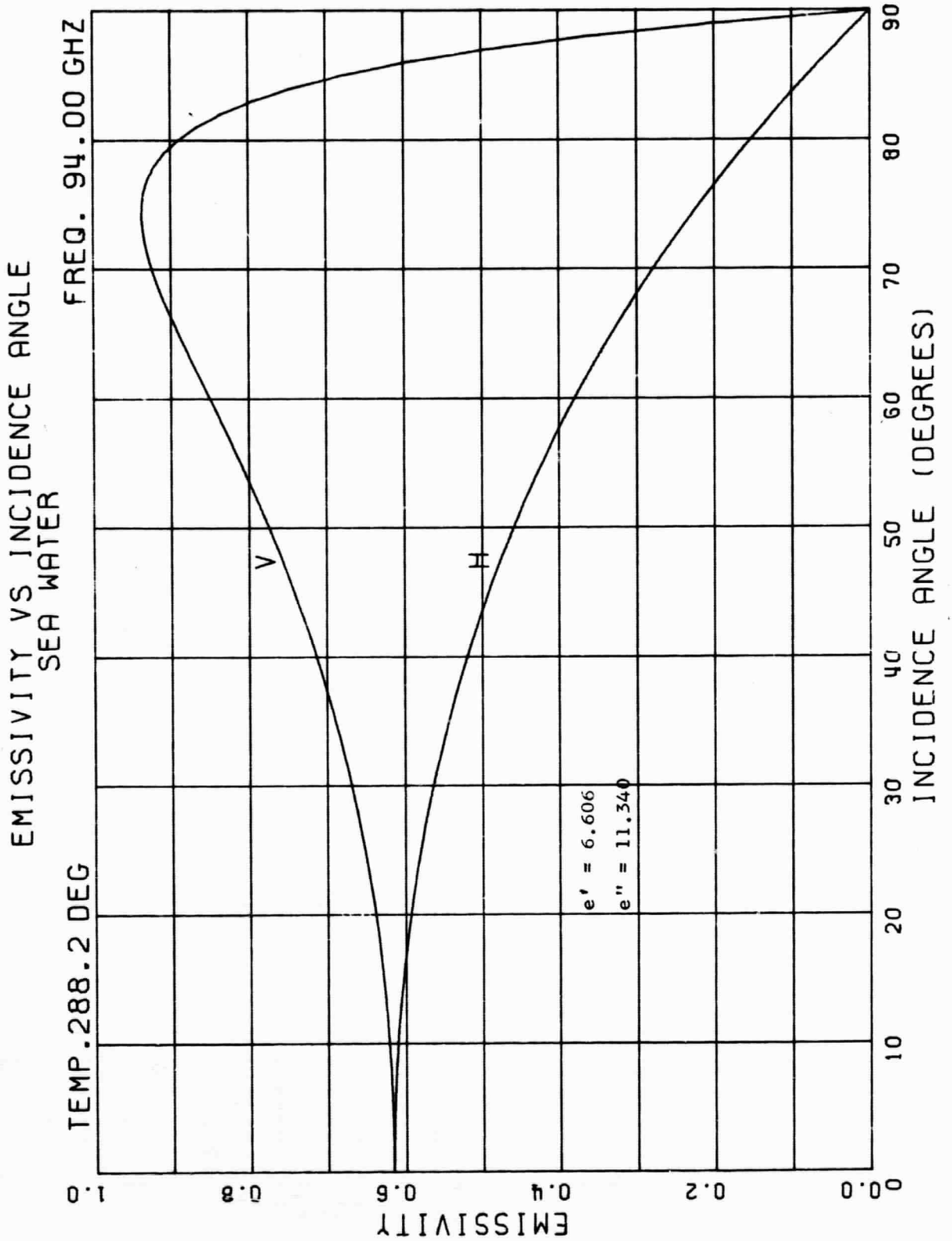


Figure 30 - Theoretical Emissivity of Sea Water - 94 GHz

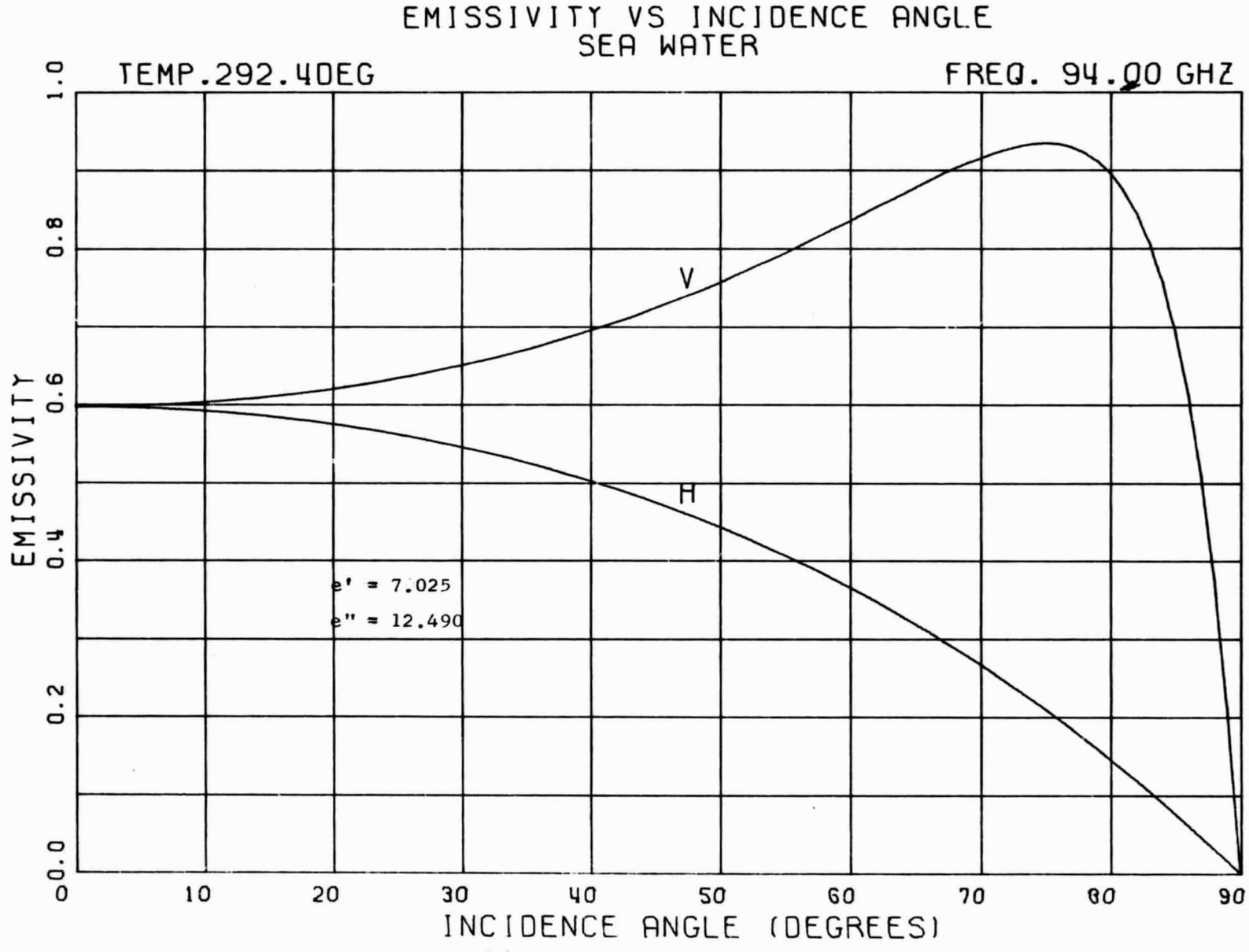


Figure 31 - Theoretical Emissivity of Sea Water - 94 GHz

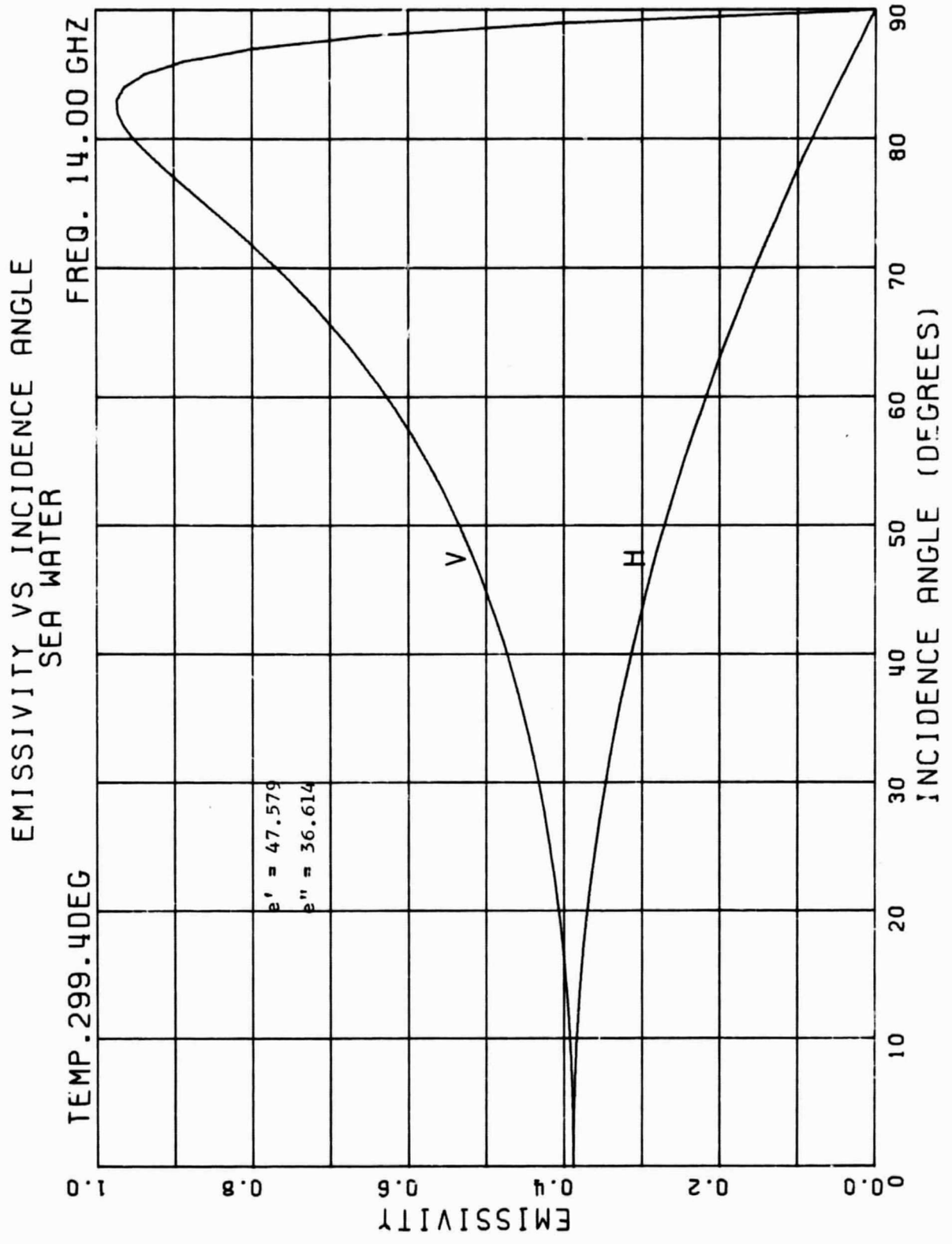


Figure 32 - Theoretical Emissivity of Sea Water - 14.0 GHz

TABLE XXX

FREQUENCY DEPENDENCE OF CALCULATED EMISSIVITIES

Incidence Angle = 20°

Frequency (GHz)	Temperature (°K)	Emissivity	
		Vert. Pol.	Hor. Pol.
9.5	288.4	0.396	0.359
16.5	287.7	0.420	0.382
16.5	289.9	0.418	0.380
16.5	292.7	0.415	0.378
94	288.2	0.639	0.593
94	292.4	0.621	0.575
Incidence Angle = 60°			
9.5	288.4	0.614	0.211
16.5	287.7	0.642	0.226
16.5	289.9	0.640	0.224
16.5	292.7	0.637	0.223
94	288.2	0.850	0.380
94	292.4	0.836	0.366

mation given in Subsection B. The emissivities were obtained for surface temperatures at, or near, those measured and for a conductivity corresponding to the mean salinity recorded during the ocean measurements. In addition, to provide a valid basis for comparison of derived and calculated T_B's, experimental surface temperatures and sky brightness temperatures were used in the calculated quantities.

a. Comparisons at 9.5 GHz

Figure 33 shows a comparison of derived and calculated T_B's at 9.5 GHz. On the average, the derived values are approximately 10^oK higher than the calculated values. This is not unexpected since the calculated T_B's do not take surface roughness into account and, hence, tend to be lower.

b. Comparison at 16.5 GHz

Figures 34 and 35 show horizontal and vertically polarized comparisons, respectively. For horizontal polarization, there is fair agreement between derived and calculated T_B's; the former being about 10^oK higher than the latter. For vertical polarization, the agreement is excellent between nadir angles of 35^o and 55^o.

c. Comparison at 94 GHz

Figure 36 and 37 show comparisons for horizontal and vertically polarized T_B's. The differences between derived and calculated values are similar to those at 16.5 GHz, with good agreement for vertical polarization.

d. Summary - 9.5, 16.5 and 94 GHz

Based on comparisons at 16.5 and 94 GHz, it appears that conversion of T_A's to T_B's is worthwhile since reasonably good agreement exists between derived and calculated T_B's at these frequencies, especially for vertical polarization. An equally positive comment cannot be made with

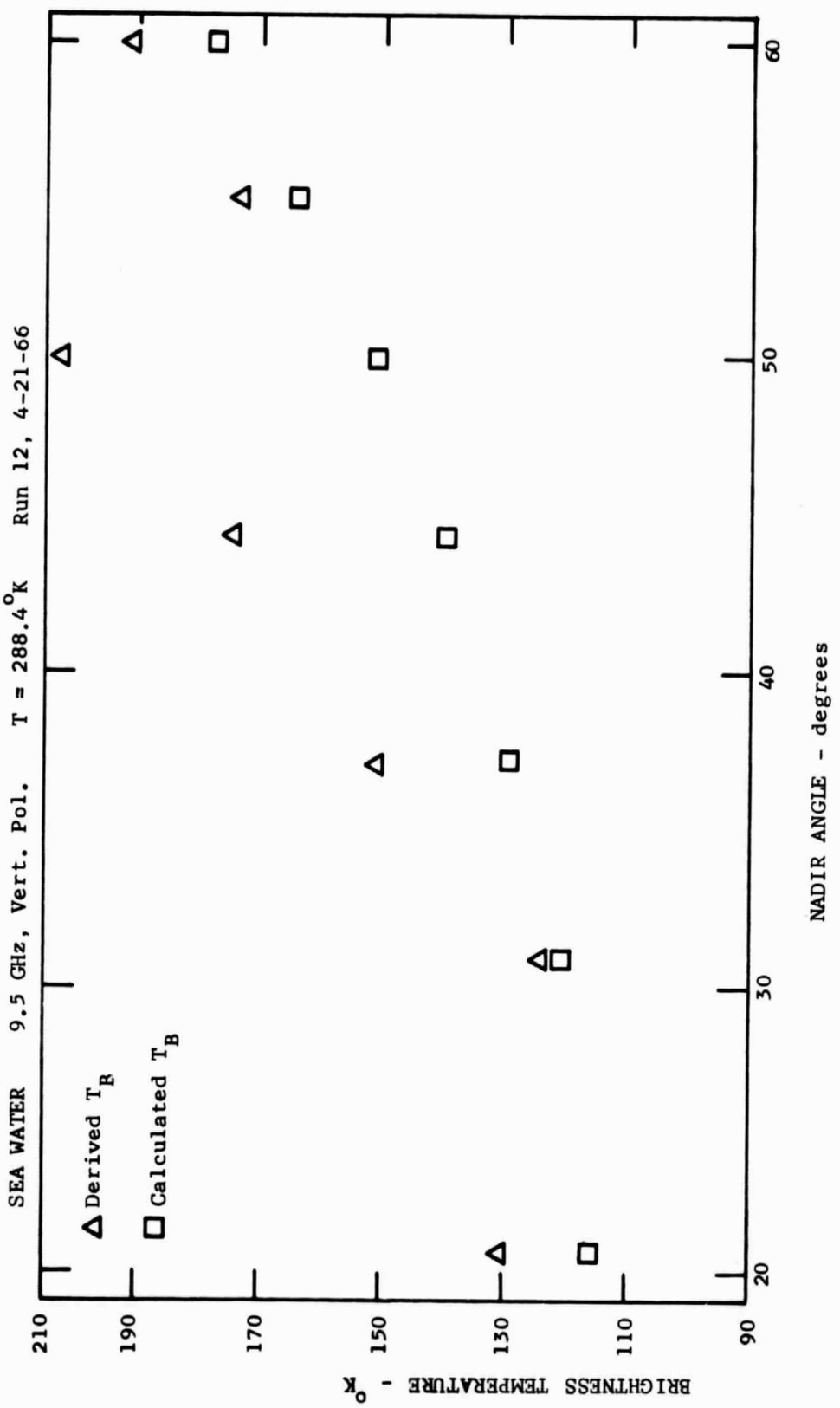


Figure 33 -Comparison of Derived and Calculated Brightness Temperatures at 9.5 GHz (Sea Water)

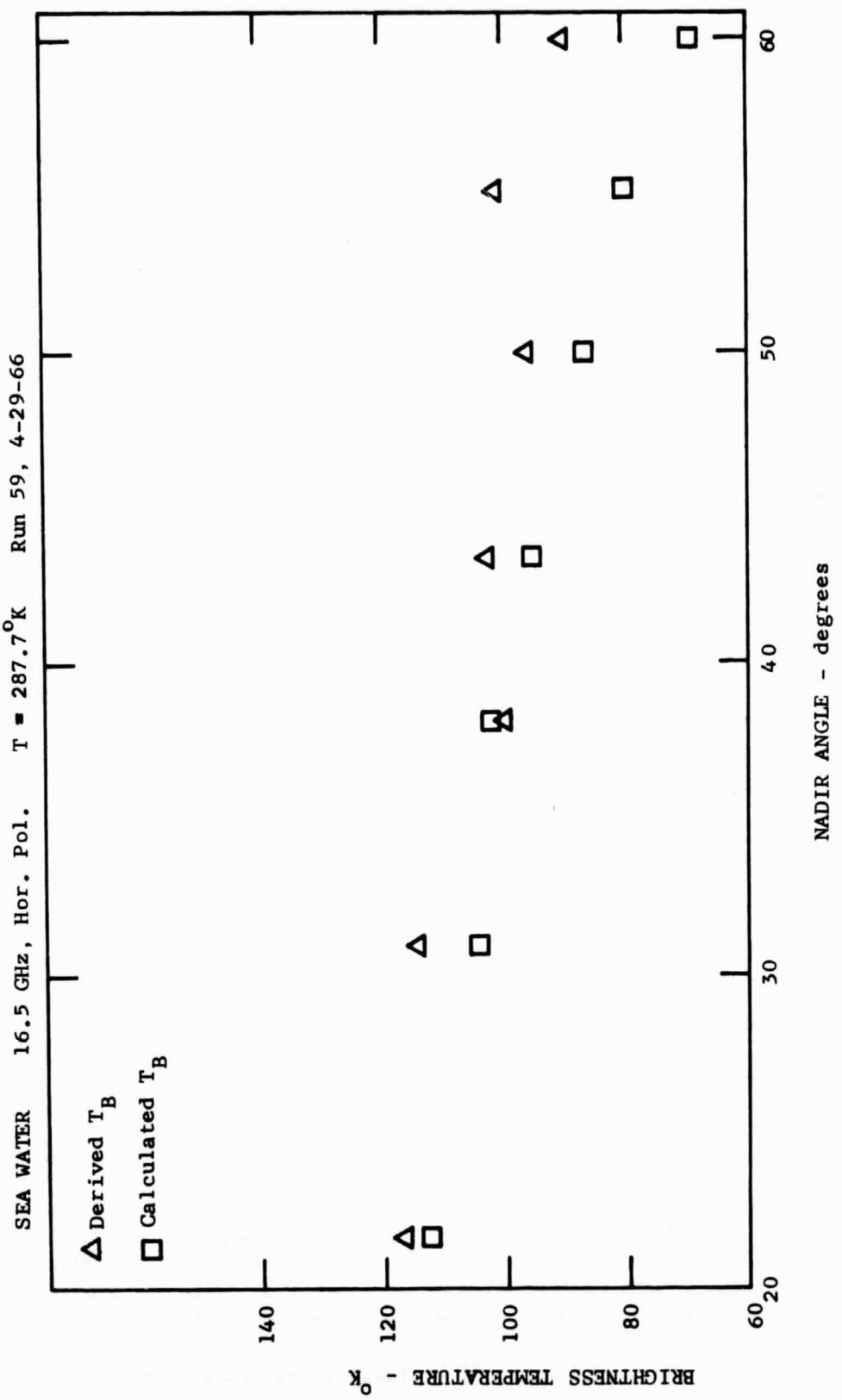


Figure 34 -Comparison of Derived and Calculated Brightness Temperatures at 16.5 GHz (Sea Water)

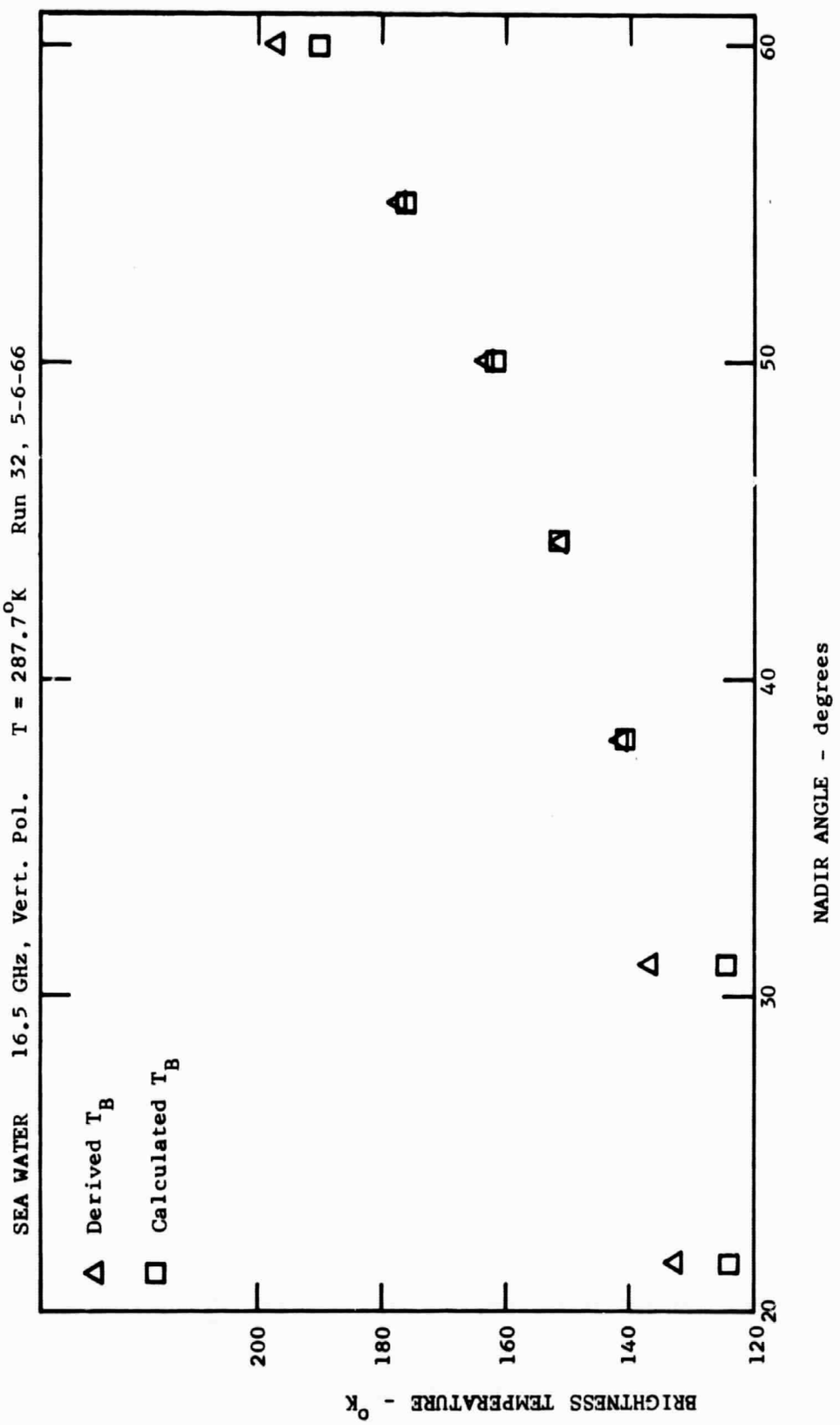


Figure 35 - Comparison of Derived and Calculated Brightness Temperatures at 16.5 GHz (Sea Water)

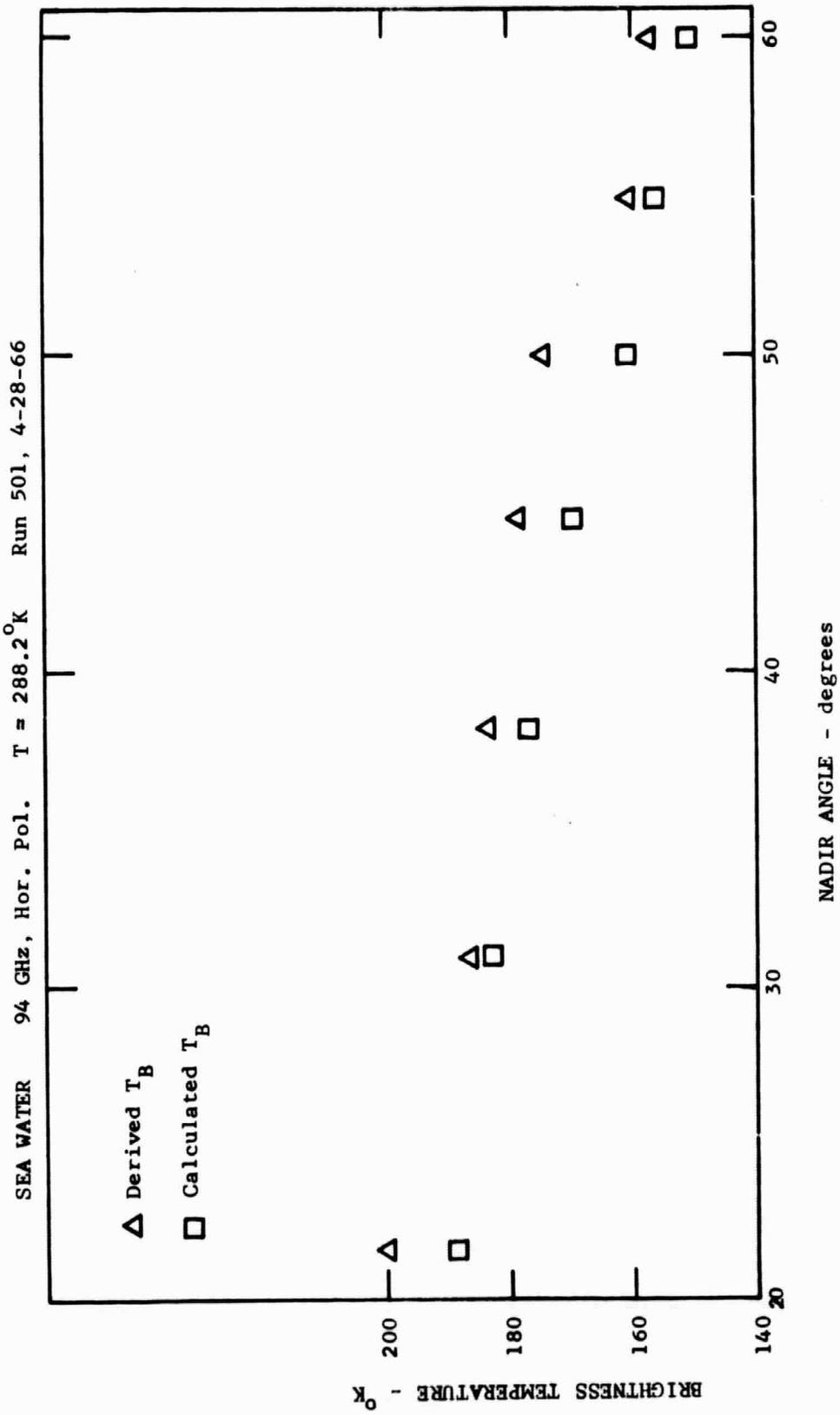


Figure 36 - Comparison of Derived and Calculated Brightness Temperatures at 94 GHz (Sea Water)

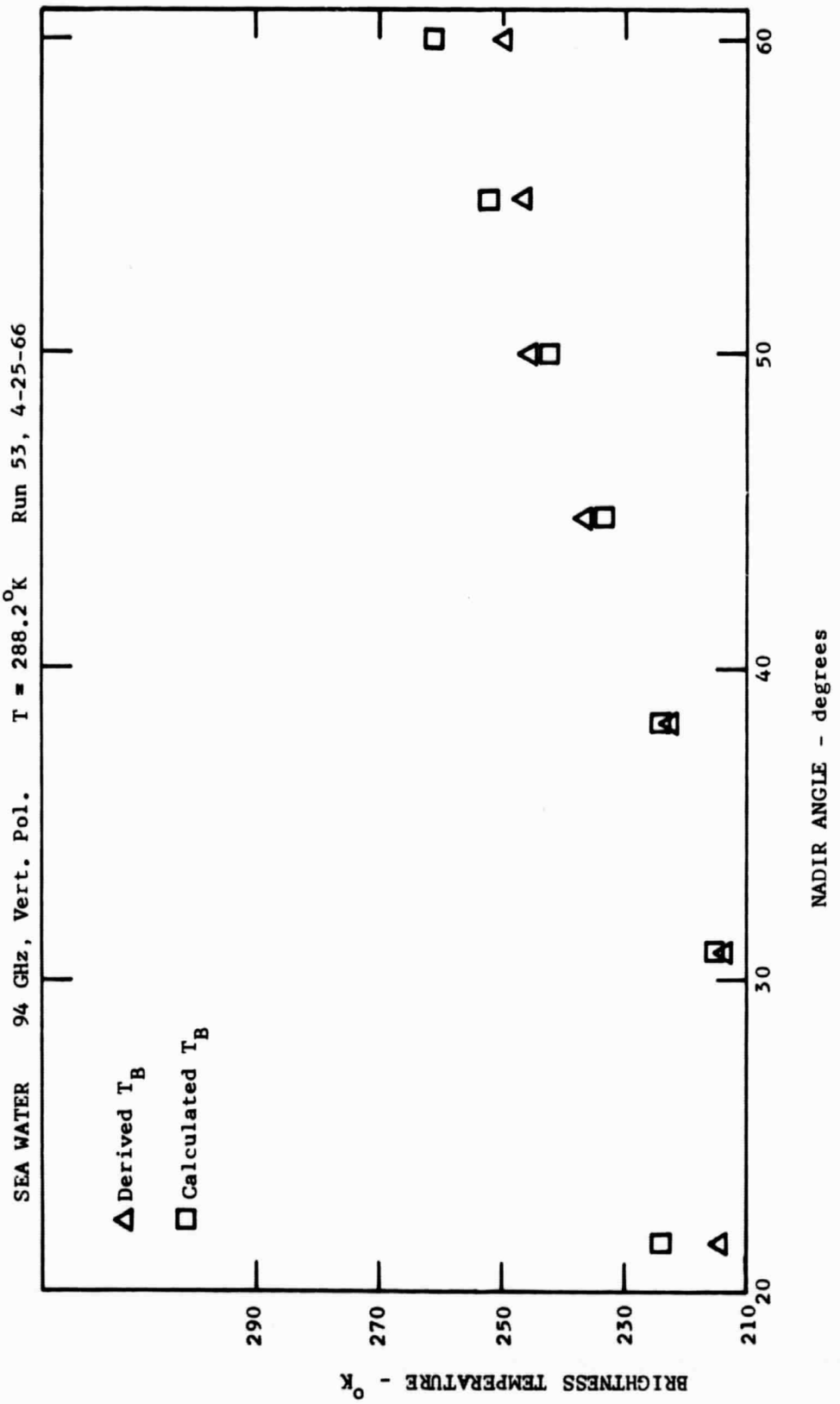


Figure 37 - Comparison of Derived and Calculated Brightness Temperatures at 94 GHz (Sea Water)

regard to 9.5 GHz T_B's due to the lack of sufficient data.

2. Frequency, Polarization and Angular Dependence of Sea Water Brightness Temperatures

An examination of measured and calculated data reveals the following results for the position of the Brewster Angle, taken at peak value:

Frequency (GHz)	Brewster Angle (deg.)	
	Measured*	Theoretical
9.5	86.0	83.2
16.5	81.5	83.0
94	79.0	75.5
* Averaged over several Runs.		

The above Table shows good agreement between measured and theoretical data with the same trend versus frequency for each category i.e., the Brewster Angle position is inversely proportional to frequency. This is because the dielectric permittivity of sea water varies in a similar manner with frequency.

A summary of sea water T_B's is given in Table XXXI, to show the frequency, polarization and angular dependence of measured data.

It will be noted that, at a given frequency the horizontally polarized T_B's decrease with increasing nadir angle; the opposite is true for vertically polarized data. These trends are in agreement with theory.

At a given nadir angle and polarization, the brightness temperatures increase with frequency. The one exception to this is the horizontally polarized data at 9.5 GHz and nadir angle of 20°; however, this value can safely be ignored since it is based on very limited data. The increase in T_B's with frequency is consistent with the fact that sea water emissivities and sky radiation both increase with frequency.

TABLE XXXI

FREQUENCY, POLARIZATION AND ANGULAR DEPENDENCE OF

SEA WATER BRIGHTNESS TEMPERATURES

Frequency (GHz)	Nadir Angle (deg.)	Brightness Temperature (^{o}K)*		% Polarization**
		Hor. Pol.	Vert. Pol.	
9.5	20	140.6	82.8	--
	60	70.8	131.9	30
16.5	20	133.3	129.5	--
	60	97.8	186.3	31
94	20	221.3	230.6	2
	60	187.8	253.0	15

* Averaged over several Runs.

** Defined as, % Pol. = $\left(\frac{V - H}{V + H}\right)$ x 100.

The percentage polarization is practically impossible to assess at a nadir angle of 20^{o}, at all frequencies. This may be explained by the inherently small separation between vertical and horizontally polarized emissivities at this angle and finite errors in the measured data. The latter have clearly caused a cross-over of polarizations at the lower frequencies. At a nadir angle of 60^{o}, the percentage polarization is similar at 9.5 and 16.5 GHz and is at a fairly high value. However, at 94 GHz, the percentage polarization is only one-half that shown at the lower frequencies. Thus, the generally higher T_B values at 94 GHz are accompanied by a convergence of the horizontal and vertical polarization components. This is due to a combination of several effects relating, basically, to sea water emissivities, surface roughness and sky radiation, each of which tends to increase T_B's at this frequency.

3. Influence of Sea Surface Temperatures on Brightness Temperatures

An attempt has been made to correlate brightness temperatures with sea surface temperatures. Due to the lack of sufficient data no correlation was possible at 9.5 GHz. At 94 GHz, the surface roughness effects masked the surface temperature effects. At 16.5 GHz, some correlation was possible; the results in Table XXXII show that, for both polarizations, there is an inverse relationship between brightness temperature and surface temperature. This is, very likely, due to the inverse relationship between emissivity and temperature.

4. Effects of Sea Surface Roughness on Brightness Temperatures

This analysis utilizes data at two frequencies - 16.5 and 94 GHz, under calm and rough sea conditions. Calm seas are defined as having wave heights varying from 1 to 3 ft., and wind velocities from 2 to 15 mph; rough sea surface conditions are defined by wave heights of 1 to 5 ft., and wind velocities of 8 to 30 mph. Figure 38 and 39 show plots of brightness

TABLE XXXII

INFLUENCE OF OCEAN SURFACE TEMPERATURES

ON BRIGHTNESS TEMPERATURES

Frequency: 16.5 GHz

Surface* Temperature (^{o}K)	Nadir Angle(deg.)	Brightness Temperature (^{o}K)*	
		Hor. Pol.	Ver. Pol.
288.2	20	137.3	133.9
289.1	"	128.5	125.1
292.7	"	134.2	129.2
288.2	60	99.4	187.0
289.1	"	97.6	186.9
292.7	"	96.4	185.1

* Average over several runs

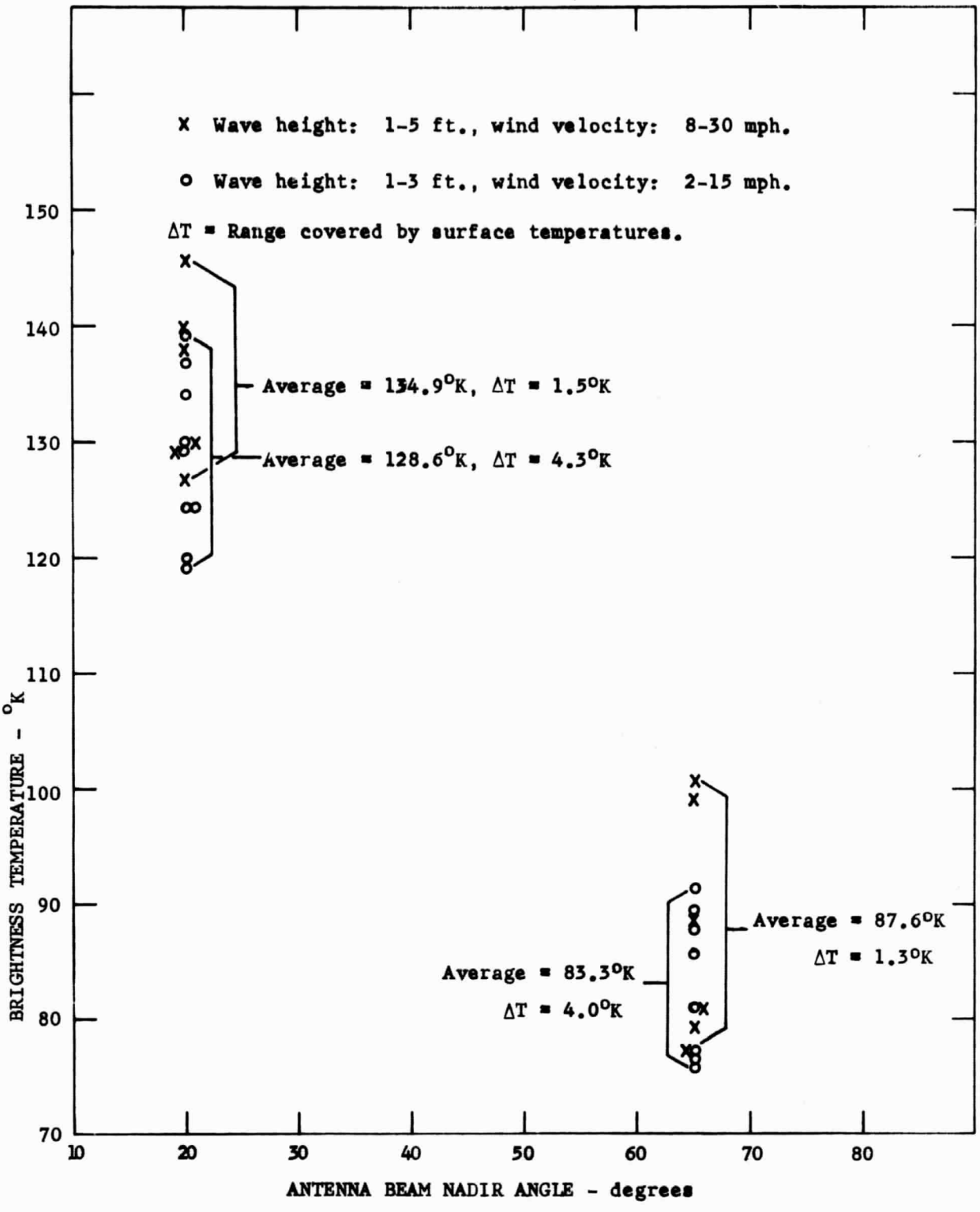


Figure 38 - Effects of Wave Height on Brightness Temperatures (16.5 GHz, Hor. Pol.).

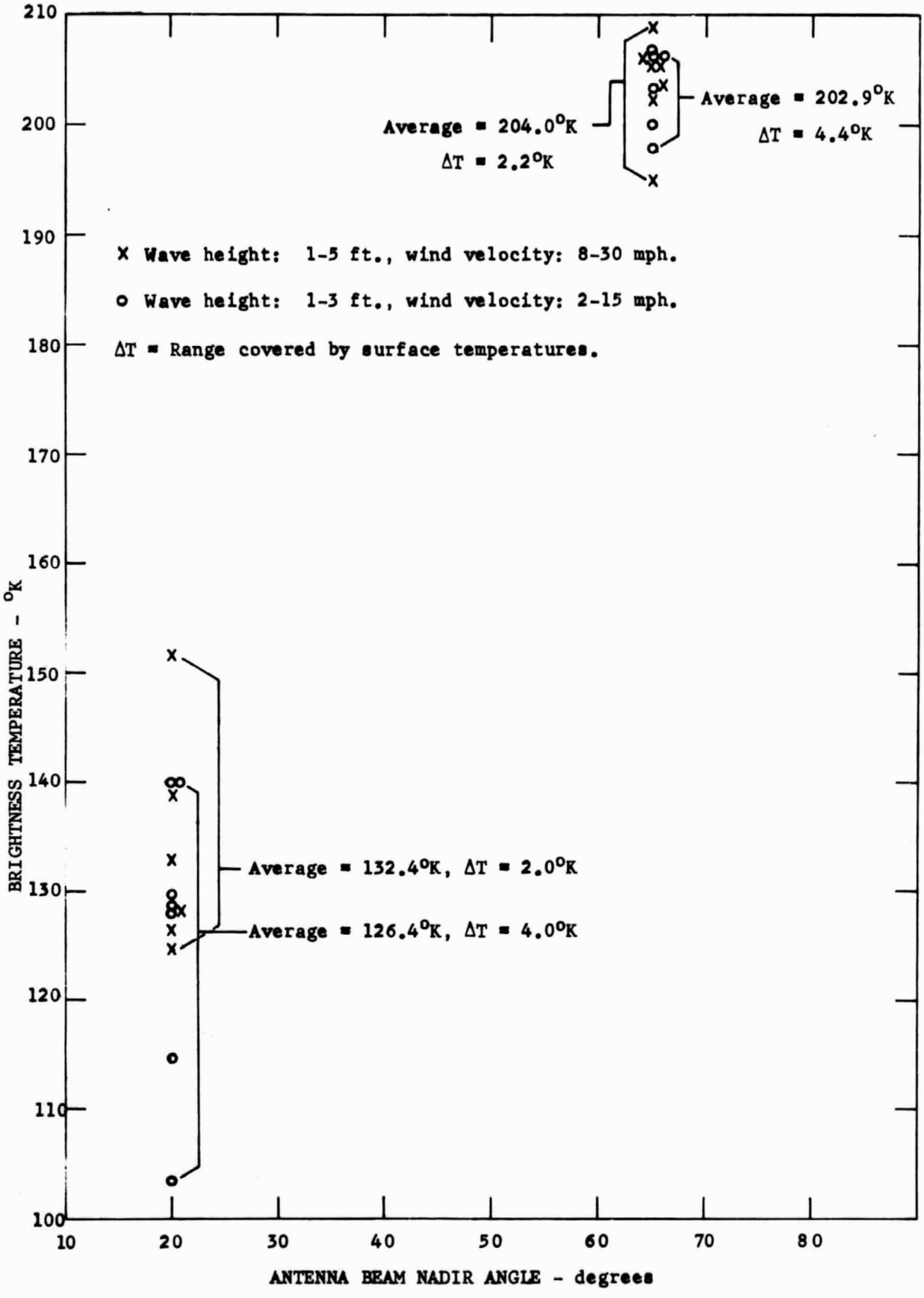


Figure 39 - Effects of Wave Height on Brightness Temperatures (16.5 GHz, Vert. Pol.).

temperatures, T_B, at horizontal and vertical polarizations, respectively, at 16.5 GHz. Figures 40 and 41 show similarly plotted data, at nadir angles of 20^o and 65^o, at 94 GHz. The following comments can be made concerning these results:

1) At 16.5 GHz and a nadir angle of 20^o the average increase in T_B, from calm to rough seas, is 6^oK for both polarizations. At a nadir angle of 65^o, the increase is only approximately 4^oK for horizontal polarization and 1^oK for vertical polarization. The last-mentioned item agrees with information given in Reference (22).

2) Since the recorded surface temperatures cover a smaller range in each of the above cases, except at a nadir angle of 65^o, vertical polarization, it appears that the above effects are due to surface roughness rather than surface temperature variations.

3) Although there are fewer data points at 94 GHz, the increase in T_B, from calm to rough seas, is considerably greater than at 16.5 GHz, for both polarizations. However, since the values at a nadir angle of 65^o, horizontal polarization, overlap very little weight should be attached to this portion of the data. The important feature, nonetheless, is the clear separation of calm and rough T_B's at a nadir angle of 20^o, for both polarizations.

4) At both frequencies, the horizontally polarized data is affected to a greater extent by sea surface roughness.

The emissivities of calm and rough seas have been derived with the aid of an inverted form of Equation (30). The results are listed in Tables XXXIII and XXXIV for horizontal and vertical polarizations, respectively. The following observations are worthy of note with regard to this information:

1) At 94GHz, the emissivities show small increases in most cases from calm to rough seas, at a given polarization and angle. Relatively inconsistent results are evident for emissivities at 16.5 GHz, with a trend toward an inverse relationship between emissivity and degree of roughness. However, no positive conclusions are possible, pro or con this observation, due to the closeness of most of the values.

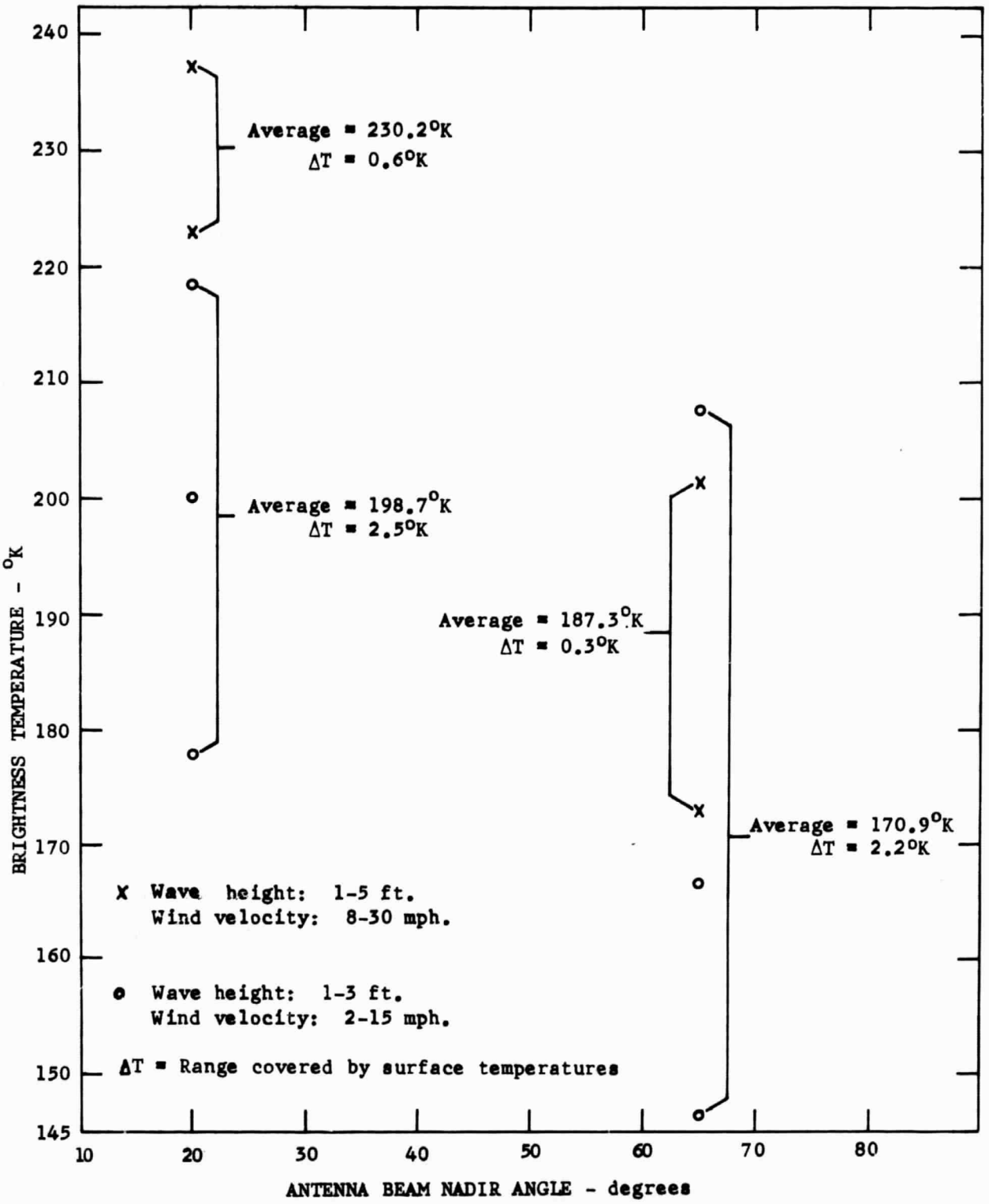


Figure 40 - Effects of Wave Height on Brightness Temperatures (94 GHz, Hor. Pol.).

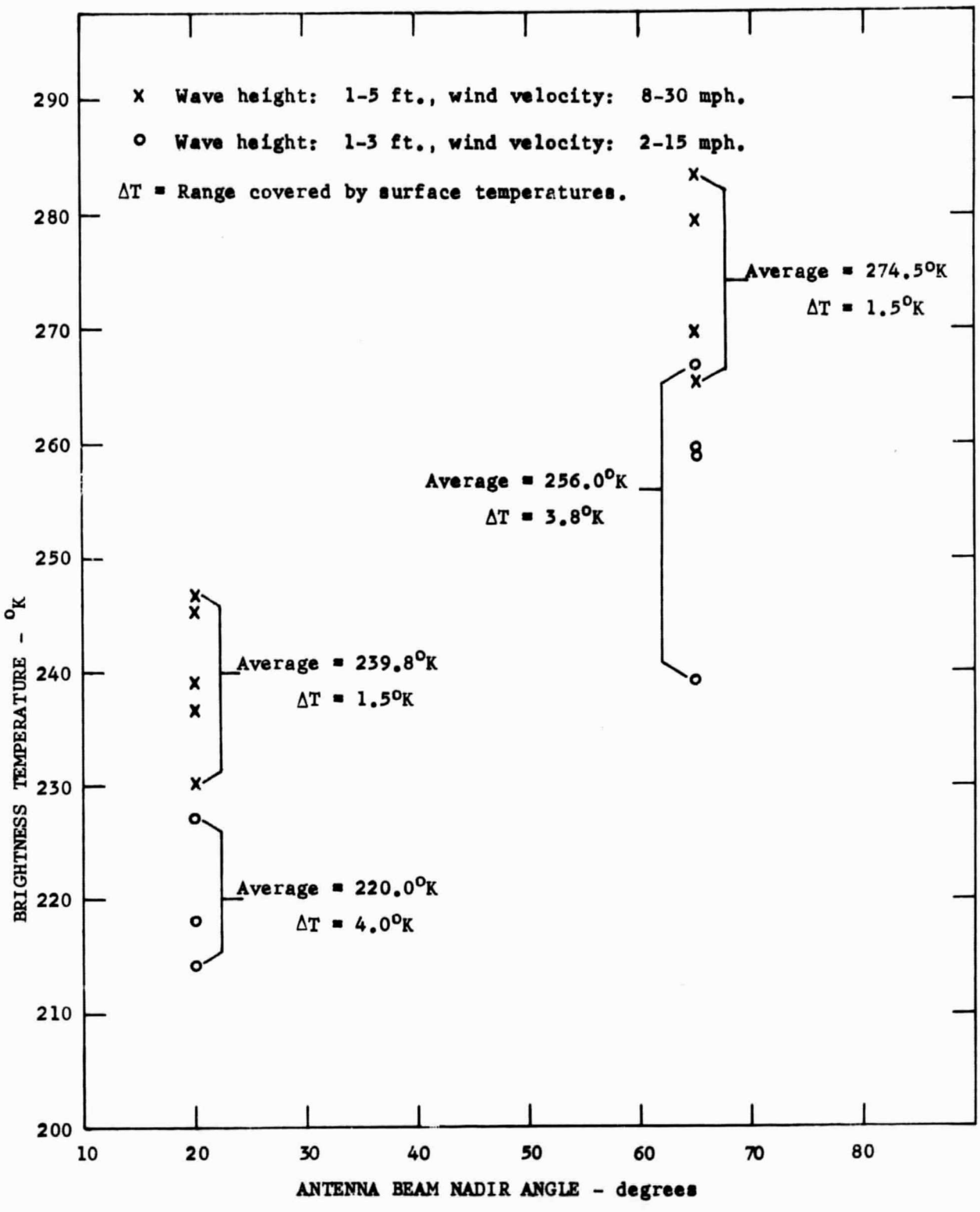


Figure 41 - Effects of Ocean Wave Height on Brightness Temperatures (94 GHz, Vert. Pol.).

2) At vertical polarization the emissivities are higher, in most cases, than for horizontal polarization, at both nadir angles. The largest increase is at 94 GHz, angle for angle.

3) The emissivities increase with frequency at angles of 20^{o} and 60^{o}, for both calm and rough seas and both polarizations. There is a small exception to this at 9.5 GHz, $\varphi = 20^{o}$, horizontal polarization; however, due to the scarcity of data at this frequency, this value should be ignored.

TABLE XXXIII

FREQUENCY DEPENDENCE OF DERIVED EMISSIVITIES

(Horizontal Polarization, Calm Sea - Wave Height = 1-3 ft.)

Frequency (GHz)	Surface Temperature (^{o}K)	Average Emissivity*	
		$\varphi = 20^{o}$	$\varphi = 60^{o}$
9.5	288.3	0.482	0.220
16.5	288.9	0.448	0.254
94	291.0	0.560	0.418
	Rough Sea —	Wave Height = 1-5 ft.	
16.5	288.9	0.408	0.288
94	291.0	0.560	0.446

* Averaged over several Runs.

TABLE XXXIV

FREQUENCY DEPENDENCE OF DERIVED EMISSIVITIES

(Vertical Polarization, Calm Sea - Wave Height = 1-3 ft.)

Frequency (GHz)	Surface Temperature (^{o}K)	Average Emissivity* $\varphi = 20^{o}$	$\varphi = 60^{o}$
9.5	288.6	0.371	0.551
16.5	288.4	0.455	0.640
94	289.7	0.724	0.753
Rough Sea — Wave Height = 1-5 ft.			
16.5	289.3	0.355	0.630
94	288.8	0.793	0.878

* Averaged over several Runs.

D. SALINES - DATA RESULTS AND ANALYSIS

Figure 42 and 43 present views of the saline material observed in Death Valley. Clearly, the material is very rough and is, essentially, a diffuse surface. The Formet sections, taken along and across the antenna line-of-sight, provide a quantitative indication of the surface roughness; these are shown in Figures 44 and 45.

The measured brightness temperatures and derived emissivities, both specular and diffuse, are discussed for each frequency in the following subsections.

1. 9.5 GHz Data

Figure 46 and Tables XXXV thru' XXXVII present measured data for horizontal polarization. The surface brightness temperatures, T_B, are relatively high and fairly constant with nadir angle, with most of the values lying in the range 235 to 271°K. The reduction of T_B to 198°K, at a nadir angle of 88°K, indicates a slight specularity at large nadir angles. An important item with regard to this data are the high surface temperatures. In this Run, the surface temperatures ranged from 310 to 311°K. This accounts for the high T_B values. The sky brightness temperatures are quite low, despite the high air temperature (108°F); this is due to the very low humidity at this location. Table XXXVI lists specular emissivities derived from brightness temperatures by means of Equation (31). The values are seen to range from 0.707 to 0.876 over a zenith angle range of 94 to 140°. Diffuse emissivities, obtained by means of Equations (33) thru' (39), are listed in Table XXXVIII and range from 0.757 to 0.875 over these zenith angles. Clearly, there is very little difference between these two sets of emissivities. A detailed comparison of emissivities derived with the two methods is presented in Subsection 5.

Figure 47 and Tables XXXIX thru' XLI present vertically polarized T_B's. It will be noted that this data is almost identical to the horizontally polarized data; most of the T_B's lie in the range 248 to 269°K, as compared with 235 to 271°K for horizontal polarization. Thus, a practically

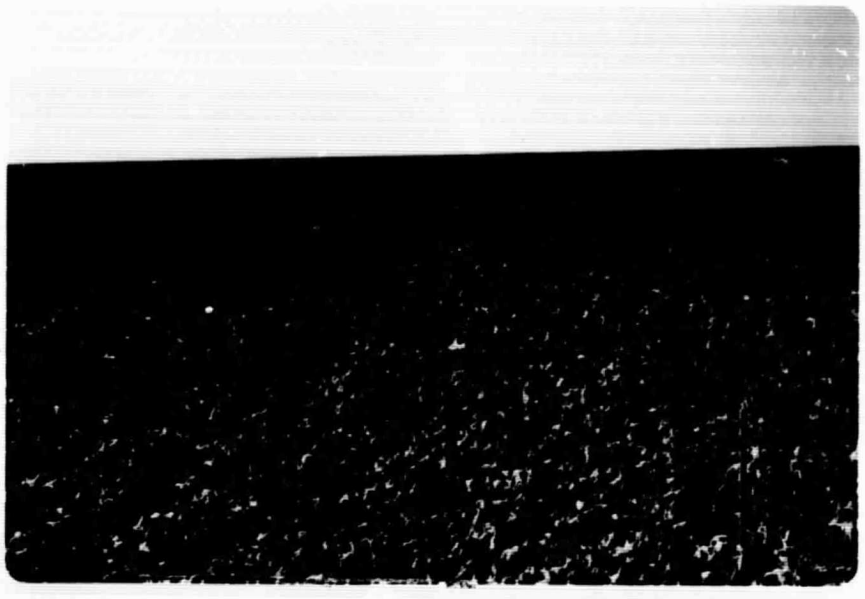


Figure 42 - Salines, Death Valley, California (Over-all View)

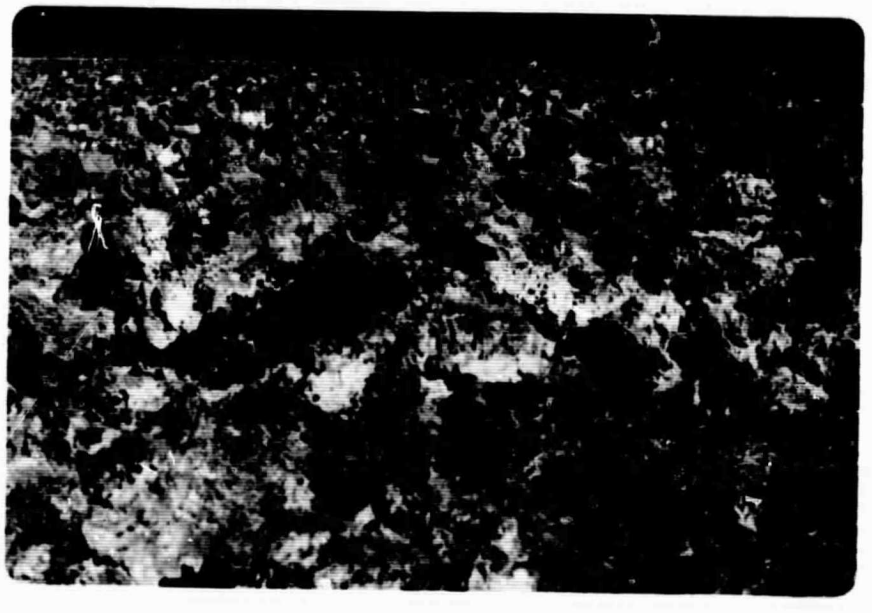


Figure 43 - Salines, Death Valley California (Close-up View)

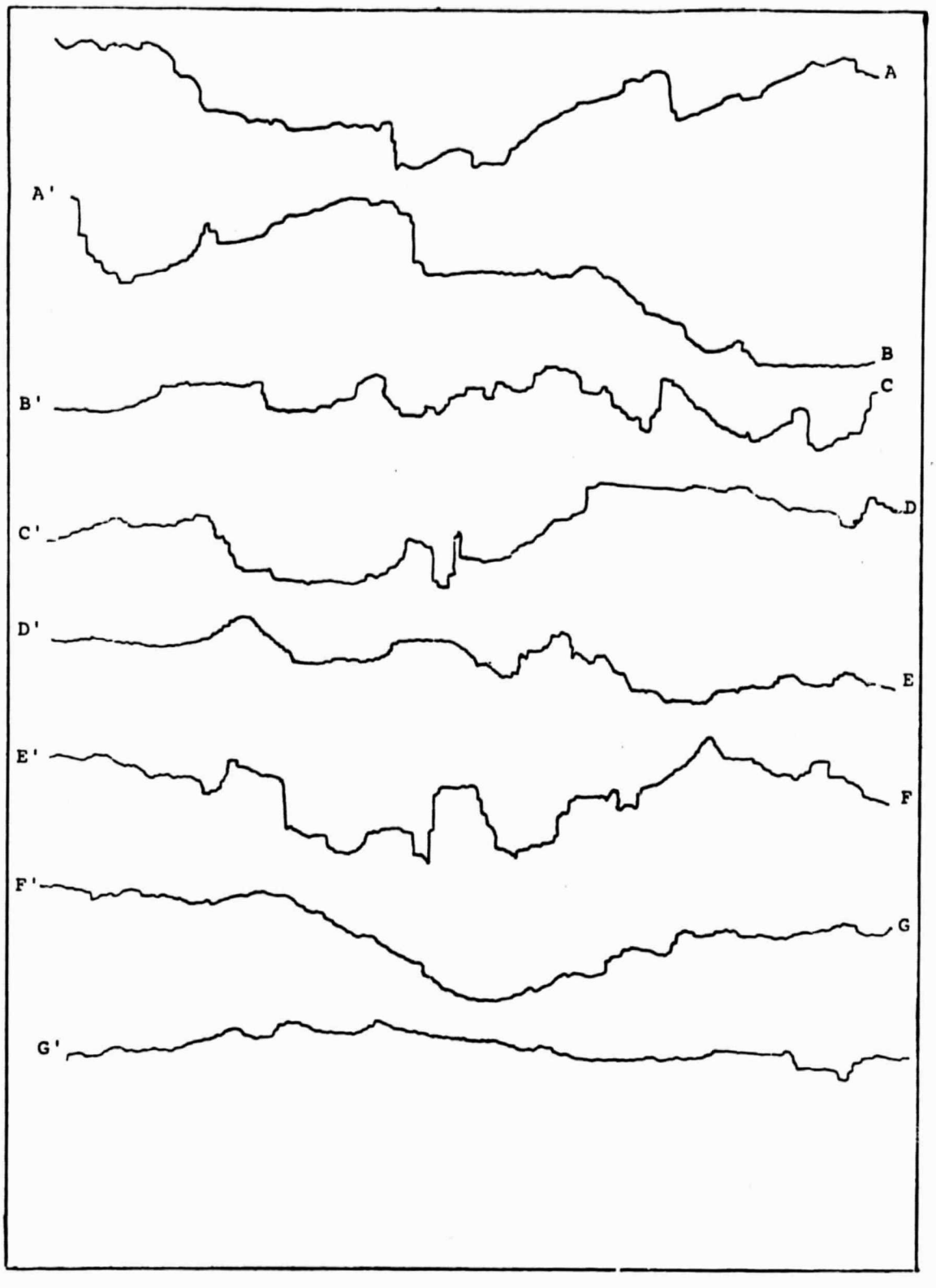


Figure 44 - North-South Format Section of Saline Rocks, Death Valley Site (Reduced to 85% of Actual Dimensions)

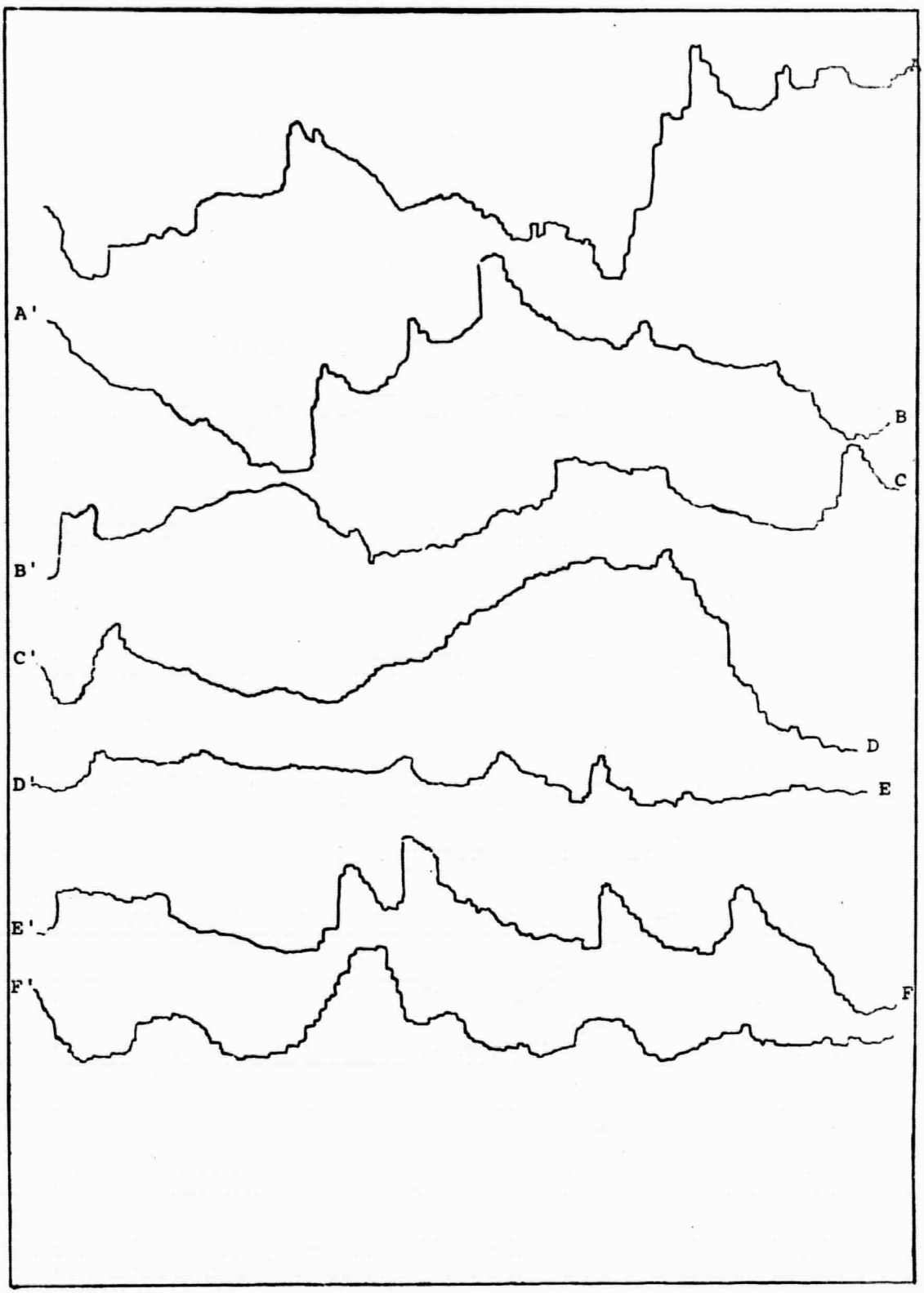


Figure 45 - East-West Formet Section of Saline Rocks, Death Valley Site
(Reduced to 85% of Actual Dimensions)

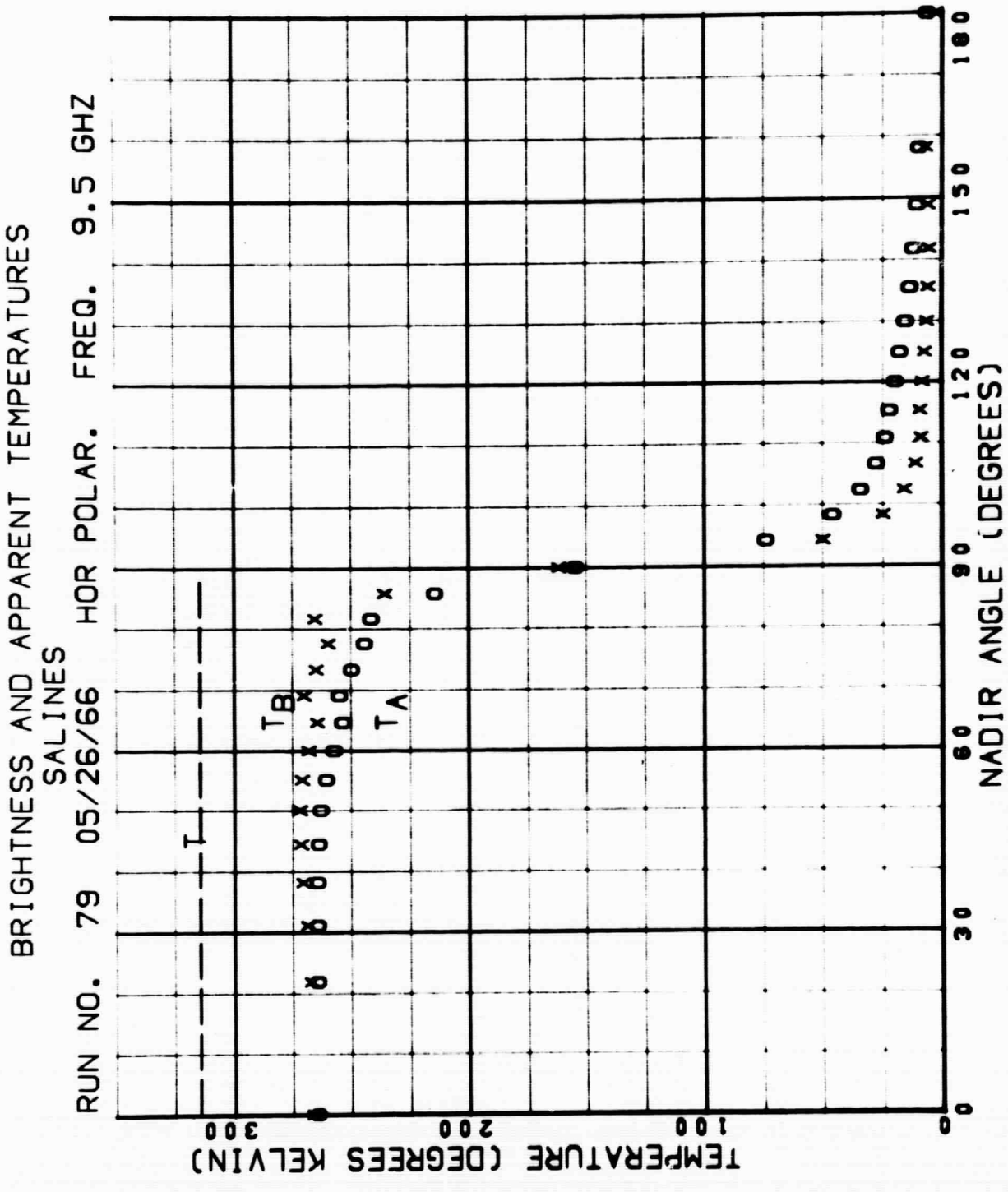


Figure 46 - Measured Salines Brightness Temperatures, 9.5 GHz, Hor. Pol.

PAGE 1 RUN 79

TARGET MATERIAL	SALINES
DATA DATE	05/26/66
START TIME	2045
FREQUENCY,GHZ	9.5
POLARIZATION	HOR
ANTENNA AZIMUTH,DEG	40
BAROMETRIC PRESSURE,IN.HG.	29.82
RELATIVE HUMIDITY,0/0	3
AIR TEMPERATURE,DEG F	108
WIND DIRECTION	SE
WIND SPEED,MPH	5
INTEGRATION TIME,SEC	1

THIRD CALIBRATION POINT 7.10DEG.K 6461.00MV.

INITIAL CALIBRATION DATA	
MINIMUM CAL.TEMP,DEG.K	318.52
MAXIMUM CAL.TEMP.DEG.K	402.42
K-FACTOR,DEG.K/MV.	0.56690
Y INTERCEPT	-3655.79

FINAL CALIBRATION DATA	
MINIMUM CAL.TEMP,DEG.K	318.53
MAXIMUM CAL.TEMP.DEG.K	402.43
K-FACTOR,DEG.K/MV.	0.56681
Y INTERCEPT	-3654.44

CALIBRATION CONSTANTS	INITIAL	FINAL	UNITS
HOT LOAD	403.00	403.00	DEG.K
ATTENUATOR	318.00	318.00	DEG.K
WAVE GUIDE SWITCH	317.00	316.50	DEG.K
ANTENNA	311.00	311.00	DEG.K
AVERAGE CAL.DATA-MIN.	7011.75	7004.45	MV.
-MAX.	7157.90	7161.30	MV.

COMMENTS
NIGHT TIME MEASUREMENT SKY DARK CLEAR MOON SHINING ON 2ND HALF

Table XXXV - Environmental and Calibration Data, Salines, 9.5 GHz, Hor. Pol.

TARGET MATERIAL SALINES
DATA DATE 05/26/66
START TIME 2045
FREQUENCY,GHZ 9.5
POLARIZATION HOR

ZENITH ANGLE DEG	BRIGHTNESS TEMP,HORIZONTAL DEG K	EMISSIVITY	TIME	READINGS MV	SURFACE TEMP	SLOPE ANGLE	1/2 IN TEMP DEG K	1 FT TEMP DEG K	2 FT TEMP DEG K	3 FT TEMP DEG K	3 IN TEMP DEG K	6 IN TEMP DEG K	12 IN TEMP DEG K
0.0	2.7		2045	6461.	0.0	0.0	0.0	0.0	0.0	0.0	0.0	0.0	0.0
10.0	4.6			6462.	0.0	0.0	0.0	0.0	0.0	0.0	0.0	0.0	0.0
20.0	6.5			6466.	0.0	0.0	0.0	0.0	0.0	0.0	0.0	0.0	0.0
30.0	6.0			6467.	0.0	0.0	0.0	0.0	0.0	0.0	0.0	0.0	0.0
40.0	5.6			6470.	0.0	0.0	0.0	0.0	0.0	0.0	0.0	0.0	0.0
50.0	6.5			6476.	0.0	0.0	0.0	0.0	0.0	0.0	0.0	0.0	0.0
55.0	7.5												
60.0	8.5			6483.	0.0	0.0	0.0	0.0	0.0	0.0	0.0	0.0	0.0
65.0	9.4			6488.	0.0	0.0	0.0	0.0	0.0	0.0	0.0	0.0	0.0
70.0	9.6			6491.	0.0	0.0	0.0	0.0	0.0	0.0	0.0	0.0	0.0
72.0	11.1												
74.0	12.5												
75.0	13.2			6500.	0.0	0.0	0.0	0.0	0.0	0.0	0.0	0.0	0.0
76.0	14.8												
78.0	18.0												
80.0	21.2			6516.	0.0	0.0	0.0	0.0	0.0	0.0	0.0	0.0	0.0
82.0	26.3			6531.	0.0	0.0	0.0	0.0	0.0	0.0	0.0	0.0	0.0
84.0	38.5		2050	6549.	0.0	0.0	0.0	0.0	0.0	0.0	0.0	0.0	0.0
86.0	52.7			6580.	0.0	0.0	0.0	0.0	0.0	0.0	0.0	0.0	0.0
88.0	107.3			6639.	0.0	0.0	0.0	0.0	0.0	0.0	0.0	0.0	0.0
90.0	161.8	0.0		6721.	310.0	0.0	310.0	0.0	0.0	0.0	0.0	0.0	0.0
92.0	198.2	0.448		6786.	310.0	0.0	310.0	0.0	0.0	0.0	0.0	0.0	0.0
94.0	234.5	0.707		6825.	310.0	0.0	310.0	0.0	0.0	0.0	0.0	0.0	0.0
96.0	249.8	0.778		6854.	310.0	0.0	310.0	0.0	0.0	0.0	0.0	0.0	0.0
98.0	264.0	0.838		6873.	310.0	0.0	310.0	0.0	0.0	0.0	0.0	0.0	0.0
100.0	263.2	0.835		6885.	311.0	0.0	310.0	0.0	0.0	0.0	0.0	0.0	0.0
102.0	260.7	0.828		6877.	311.0	0.0	296.0	0.0	0.0	0.0	314.0	313.0	313.0
104.0	262.1	0.835		6887.	311.0	0.0	310.0	0.0	0.0	0.0	0.0	0.0	0.0
106.0	264.5	0.844		6884.	311.0	0.0	310.0	0.0	0.0	0.0	0.0	0.0	0.0
108.0	266.9	0.856		6899.	310.0	0.0	310.0	0.0	0.0	0.0	0.0	0.0	0.0
110.0	269.4	0.865		6899.	310.0	0.0	310.0	0.0	0.0	0.0	0.0	0.0	0.0
115.0	265.4	0.852		6895.	310.0	0.0	310.0	0.0	0.0	0.0	0.0	0.0	0.0
120.0	268.7	0.863		6902.	310.0	0.0	310.0	0.0	0.0	0.0	0.0	316.0	316.0
125.0	271.4	0.872		6908.	310.0	0.0	310.0	294.0	310.0	310.0	316.0	316.0	316.0
130.0	272.3	0.876		6912.	310.0	0.0	310.0	0.0	0.0	0.0	0.0	0.0	0.0
140.0	271.0	0.872	2055	6914.	310.0	0.0	310.0	0.0	0.0	0.0	0.0	0.0	0.0

Table XXXVI - Brightness Temperatures, Salines, 9.5 GHz, Hor. Pol.

RUN NO. 79 05/26/66 HOR POLAR. 9.5 GHZ SALINES

ITERATION NUMBER 0

ZENITH ANGLE (DEG)	BRIGHTNESS TEMP. (DEG K)	APPARENT TEMP. (DEG K)	CORRECTION TEMP. (DEG K)
0.0	2.71	6.69	-3.9799
21.79	6.88	9.75	-2.8618
31.00	5.94	10.69	-4.7493
38.21	5.48	11.97	-6.4875
44.42	5.88	13.73	-7.8477
49.99	6.46	15.55	-9.0912
55.15	7.69	17.72	-10.0302
60.00	8.51	19.77	-11.2640
64.62	9.39	22.00	-12.6042
69.08	9.12	23.91	-14.7837
73.40	11.47	27.79	-16.3194
77.63	16.11	34.21	-18.1014
81.79	25.05	45.89	-20.8399
85.90	50.07	74.02	-23.9478
90.00	161.82	154.52	7.3042
94.10	236.23	214.43	21.7968
98.21	265.54	241.84	23.7078
102.37	260.19	244.46	15.7317
106.60	265.18	250.08	15.1002
110.92	270.57	255.29	15.2786
115.38	264.95	254.18	10.7710
120.00	268.68	257.87	10.8066
124.85	271.35	261.14	10.2098
130.01	272.30	263.14	9.1594
135.58	271.63	264.04	7.5876
141.79	270.79	264.75	6.0441
149.00	268.79	264.75	4.0364
158.21	267.37	264.75	2.6186
180.00	266.37	264.75	1.6177

ABS. CORRECTION = 1.12E 01 DEG. K

Table XXXVII - Brightness and Apparent Temperatures, Salines, 9.5 GHz, Hor. Pol.

RUN NO. 79 05/26/66 HOR POLAR. FREQ. 9.5 GHZ SALINES

OPTICAL DEPTH OF ATMOSPHERE= 0.009 NEPERS
AIR TEMPERATURE= 315.38 DEGREES K
SOIL TEMPERATURE= 31[illegible].25 DEGREES K

ZENITH ANGLE (DEGREES)	BRIGHTNESS TEMP. (DEG.K)	EMISSIVITY	SCATTERING COEFFICIENT
0.0	2.71		
21.79	6.88		
31.00	5.94		
38.21	5.48		
44.41	5.88		
49.99	6.46		
55.15	7.69		
60.00	8.51		
64.62	9.39		
69.07	9.12		
73.40	11.47		
77.63	16.11		
81.79	25.05		
85.90	5[illegible].07		
90.00	161.82	0.51331	1.94674
94.10	236.23	0.75736	0.97054
98.21	265.54	0.85353	0.58590
102.37	260.19	0.83597	0.65611
106.60	265.18	0.85234	0.59062
110.92	270.57	0.87000	0.51998
115.38	264.95	0.85158	0.59367
120.00	268.68	0.86380	0.54481
124.85	271.35	0.87256	0.50975
130.00	272.31	0.87569	0.49726
135.58	271.63	0.87348	0.50610
141.79	270.79	0.87075	0.51702
149.00	268.79	0.86416	0.54336
158.21	267.37	0.85951	0.56197
180.00	266.37	0.85623	0.57510

Table XXXVIII - Diffuse Emissivities, Salines, 9.5 GHz, Hor. Pol.

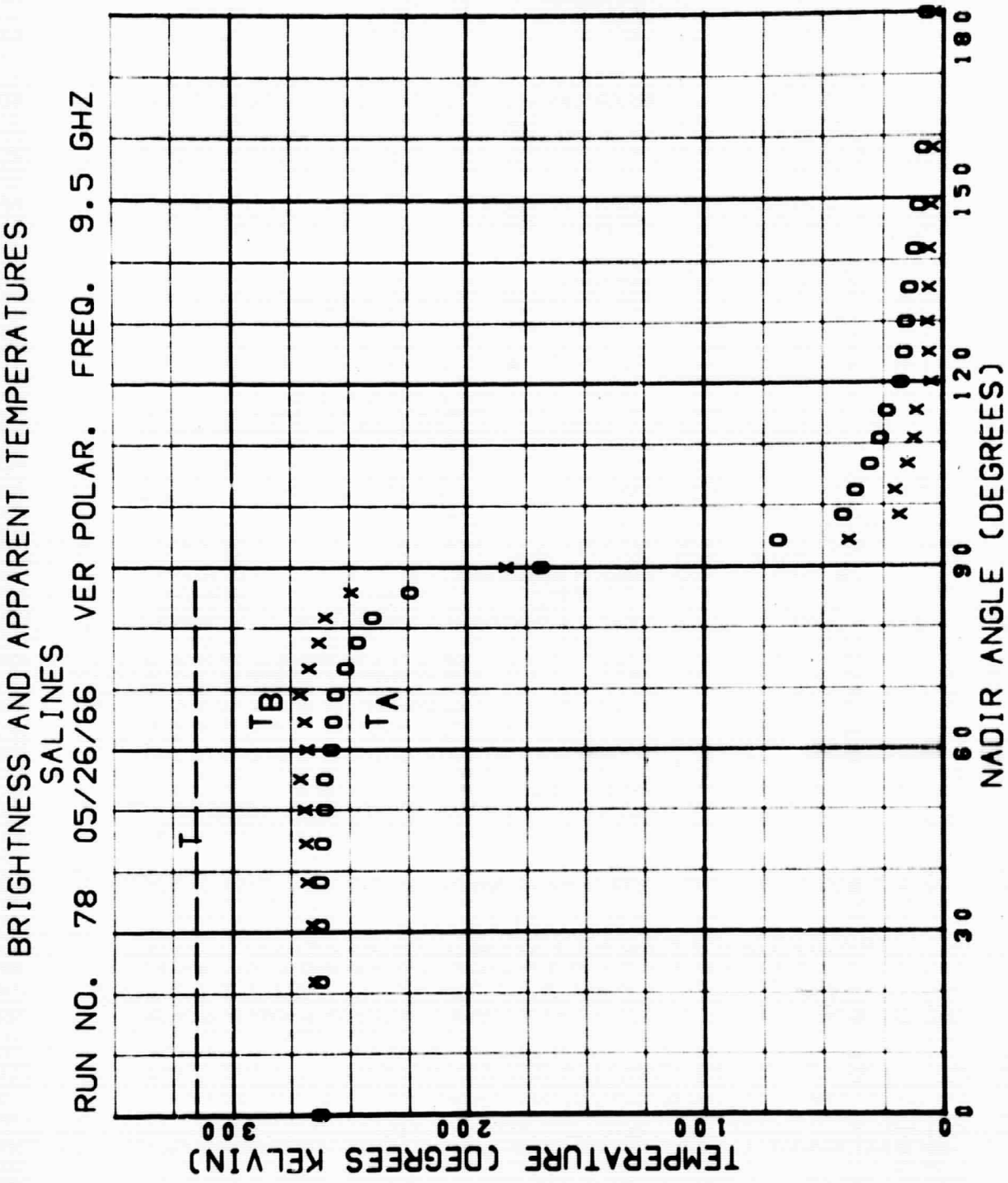


Figure 47 - Measured Salines Brightness Temperatures, 9.5 GHz, Vert. Pol.

PAGE 1 RUN 78

TARGET MATERIAL	SALINES
DATA DATE	05/26/66
START TIME	2030
FREQUENCY,GHZ	9.5
POLARIZATION	VER
ANTENNA AZIMUTH,DEG	40
BAROMETRIC PRESSURE,IN.HG.	29.80
RELATIVE HUMIDITY,0/0	4
AIR TEMPERATURE,DEG F	108
WIND DIRECTION	SE
WIND SPEED,MPH	5
INTEGRATION TIME,SEC	1

THIRD CALIBRATION POINT 7.10DEG.K 6470.00MV.

INITIAL CALIBRATION DATA	
MINIMUM CAL.TEMP,DEG.K	318.73
MAXIMUM CAL.TEMP.DEG.K	402.33
K-FACTOR,DEG.K/MV.	0.56473
Y INTERCEPT	-3646.54

FINAL CALIBRATION DATA	
MINIMUM CAL.TEMP,DEG.K	319.23
MAXIMUM CAL.TEMP.DEG.K	402.44
K-FACTOR,DEG.K/MV.	0.56922
Y INTERCEPT	-3675.15

CALIBRATION CONSTANTS	INITIAL	FINAL	UNITS
HOT LOAD	403.00	403.00	DEG.K
ATTENUATOR	318.30	318.70	DEG.K
WAVE GUIDE SWITCH	317.00	317.00	DEG.K
ANTENNA	313.00	311.80	DEG.K
AVERAGE CAL.DATA-MIN.	7020.20	7012.25	MV.
-MAX.	7170.60	7167.40	MV.

COMMENTS
SUNSET BLUE SKY NO CLOUDS 1/4 MOON OVERHEAD VERY DRY WIND

Table XXXIX - Environmental and Calibration Data, Salines, 9.5 GHz, Vert. Pol.

TARGET MATERIAL SALINES
DATA DATE 05/26/66
START TIME 2030
FREQUENCY,GHZ 9.5
POLARIZATION VER

ZENITH ANGLE DEG	BRIGHTNESS TEMP DEG K	EMISSIVITY VERTICAL	TIME	READINGS MV	SURFACE TEMP	SLOPE ANGLE	1/2 IN TEMP DEG K	1 FT TEMP DEG K	2 FT TEMP DEG K	3 FT TEMP DEG K	3 IN TEMP DEG K	6 IN TEMP DEG K	12 IN TEMP DEG K
0.0	4.1		2030	6470.	0.0	0.0	0.0	0.0	0.0	0.0	0.0	0.0	0JC
10.0	4.4			6469.	0.0	0.0	0.0	0.0	0.0	0.0	0.0	0.0	0JC
20.0	4.8			6472.	0.0	0.0	0.0	0.0	0.0	0.0	0.0	0.0	0JC
30.0	5.1			6474.	0.0	0.0	0.0	0.0	0.0	0.0	0.0	0.0	0JC
40.0	6.2			6480.	0.0	0.0	0.0	0.0	0.0	0.0	0.0	0.0	0JC
50.0	6.4			6484.	0.0	0.0	0.0	0.0	0.0	0.0	0.0	0.0	0JC
55.0	5.6												
60.0	4.9			6488.	0.0	0.0	0.0	0.0	0.0	0.0	0.0	0.0	0JC
65.0	11.2			6459.	0.0	0.0	0.0	0.0	0.0	0.0	0.0	0.0	0JC
70.0	12.6			6504.	0.0	0.0	0.0	0.0	0.0	0.0	0.0	0.0	0JC
72.0	14.4												
74.0	16.1												
75.0	17.0			6514.	0.0	0.0	0.0	0.0	0.0	0.0	0.0	0.0	0JC
76.0	17.4												
78.0	18.2												
80.0	19.1			6529.	0.0	0.0	0.0	0.0	0.0	0.0	0.0	0.0	0JC
82.0	19.3			6531.	0.0	0.0	0.0	0.0	0.0	0.0	0.0	0.0	0JC
84.0	29.6			6546.	0.0	0.0	0.0	0.0	0.0	0.0	0.0	0.0	0JC
86.0	42.7			6580.	0.0	0.0	0.0	0.0	0.0	0.0	0.0	0.0	0JC
88.0	113.3			6664.	0.0	0.0	0.0	0.0	0.0	0.0	0.0	0.0	0JC
90.0	183.9	0.0		6754.	311.0	0.0	311.0	0.0	0.0	0.0	0.0	0.0	0JC
92.0	216.0	0.520		6815.	311.0	0.0	311.0	0.0	0.0	0.0	0.0	0.0	0JC
94.0	248.1	0.766		6851.	311.0	0.0	311.0	0.0	0.0	0.0	0.0	0.0	0JC
96.0	254.7	0.800		6871.	311.0	0.0	311.0	0.0	0.0	0.0	0.0	0.0	0JC
98.0	260.0	0.825	2035	6879.	311.0	0.0	311.0	0.0	0.0	0.0	0.0	0.0	0JC
100.0	261.8	0.829		6888.	312.0	0.0	312.0	0.0	0.0	0.0	0.0	0.0	0JC
102.0	263.2	0.834		6889.	312.0	0.0	312.0	0.0	0.0	0.0	315.0	314.0	313JC
104.0	265.1	0.841		6899.	312.0	0.0	312.0	0.0	0.0	0.0	0.0	0.0	0JC
106.0	267.1	0.848		6899.	312.0	0.0	312.0	0.0	0.0	0.0	0.0	0.0	0JC
108.0	268.9	0.855		6903.	312.0	0.0	311.0	0.0	0.0	0.0	0.0	0.0	0JC
110.0	270.6	0.862		6908.	312.0	0.0	311.0	0.0	0.0	0.0	0.0	0.0	0JC
115.0	269.5	0.859		6909.	312.0	0.0	311.0	0.0	0.0	0.0	0.0	0.0	0JC
120.0	268.7	0.862		6911.	311.0	0.0	311.0	0.0	0.0	0.0	0.0	317.0	316JC
125.0	271.0	0.869		6915.	311.0	0.0	311.0	295.0	311.0	311.0	315.0	316.0	316JC
130.0	269.4	0.864		6915.	311.0	0.0	311.0	0.0	0.0	0.0	0.0	0.0	0JC
140.0	268.5	0.861	2040	6918.	311.0	0.0	311.0	0.0	0.0	0.0	0.0	0.0	0JC

Table XL - Brightness Temperatures, Salines, 9.5 GHz, Vert. Pol.

RUN NO. 78 05/26/66 VER POLAR. 9.5 GHZ SALINES

ITERATION NUMBER 0

ZENITH ANGLE (DEG)	BRIGHTNESS TEMP. (DEG K)	APPARENT TEMP. (DEG K)	CORRECTION TEMP. (DEG K)
0.0	4.11	7.21	-3.0966
21.79	4.84	8.49	-3.6427
31.00	5.13	10.12	-4.9915
38.21	6.14	12.41	-6.2728
44.42	6.27	14.08	-7.8119
49.99	6.36	15.48	-9.1201
55.15	6.17	16.62	-10.4516
60.00	4.93	17.70	-12.7714
64.62	11.16	23.27	-12.1032
69.08	11.97	26.27	-14.2981
73.40	15.02	30.64	-15.6112
77.63	20.79	36.71	-16.5213
81.79	18.21	41.68	-23.4691
85.90	39.33	68.86	-29.5289
90.00	183.89	168.73	15.1579
94.10	249.69	224.33	25.3631
98.21	260.53	240.46	20.0704
102.37	263.45	246.81	16.6398
106.60	267.75	252.23	15.5190
110.92	271.33	256.48	14.8487
115.38	269.34	257.19	12.1500
120.00	268.66	258.26	10.3974
124.85	271.09	260.83	10.2589
130.01	269.44	261.10	8.3346
135.58	269.12	261.97	7.1501
141.79	268.29	262.66	5.6291
149.00	266.33	262.66	3.6724
158.21	264.99	262.66	2.3304
180.00	264.02	262.66	1.3576

ABS. CORRECTION = 1.17E 01 DEG. K

Table XLI - Brightness and Apparent Temperatures, Salines, 9.5 GHz, Vert. Pol.

RUN NO. 78 05/26/66 VER POLAR. FREQ. 9.5 GHZ SALINES

OPTICAL DEPTH OF ATMOSPHERE= [illegible] NEPERS
AIR TEMPERATURE= 315.38 DEGREES K
SOIL TEMPERATURE= 311.5[illegible] DEGREES K

ZENITH ANGLE (DEGREES)	BRIGHTNESS TEMP. (DEG.K)	EMISSIVITY	SCATTERING COEFFICIENT
0.0	4.11		
21.79	4.84		
31.00	5.13		
38.21	6.14		
44.41	6.27		
49.99	6.36		
55.15	6.17		
60.00	4.93		
64.62	11.16		
69.07	11.97		
73.40	15.02		
77.63	20.19		
81.79	18.21		
85.90	39.33		
90.00	183.89	0.58320	1.66720
94.10	249.69	0.79812	0.80753
98.21	260.53	0.83351	0.66594
102.37	263.45	0.84306	0.62778
106.63	267.75	0.85709	0.57163
110.92	271.33	0.86880	0.52482
115.38	269.34	0.86229	0.55084
120.00	268.66	0.86007	0.55972
124.85	271.09	0.86801	0.52795
130.00	269.43	0.86261	0.54956
135.58	269.12	0.86158	0.55366
141.79	268.29	0.85887	0.56453
149.00	266.33	0.85247	0.59015
158.21	264.99	0.84809	0.60763
180.00	264.12	0.84491	0.62035

Table XLII - Diffuse Emissivities, Salines 9.5 GHz, Vert. Pol.

negligible polarization effect is evident; this is due to the very rough nature of the saline surface.

The specular and diffuse emissivities are again very similar. Figure 48 shows plots of derived and theoretical specular emissivities at 9.5 and 14 GHz, respectively. It was necessary to present theoretical data at 14 GHz due to the fact that the dielectric permittivity of the saline material was measured only at this frequency. Although the theoretical plot shows a fairly strong polarization effect, the derived horizontal and vertically polarized emissivity curves lie on top of one another. Thus, it appears that Equation (31) does not provide specular values of derived emissivities in the case of rough-surfaced materials. This is not difficult to understand since the values of T_B, used in that equation, represent diffuse brightness temperatures in this situation. A comparison of these emissivities with the diffuse emissivities, plotted in Figure 49, shows very little difference between the two pairs of curves. It would seem, therefore, that Equation (31) can be safely employed for the derivation of diffuse emissivities, over a broad range of nadir angles.

2. 16.5 GHz Data

Figures 50 thru' 54, together with Tables XLIII thru' L, present saline T_B's and emissivities at 16.5 GHz. This data is very similar to the 9.5 GHz data, although the T_B's are from 20 to 40°K higher, depending on polarization and nadir angle. Most of this increase is due to an average increase of about 15°K in surface temperature; the remainder is very likely due to a combination of errors in both calculated sky brightness temperatures, used for the third calibration point, and radiometer calibration.

Figure 52 shows plots of theoretical emissivities for the saline material at 14 GHz. Since the measured dielectric permittivity is at a relatively low value, the emissivities are rather high over a broad range of incidence angles. This feature, together with the high surface temperatures prevailing at the time of field measurements, permits a clearer understanding of the high brightness temperatures associated with this material.

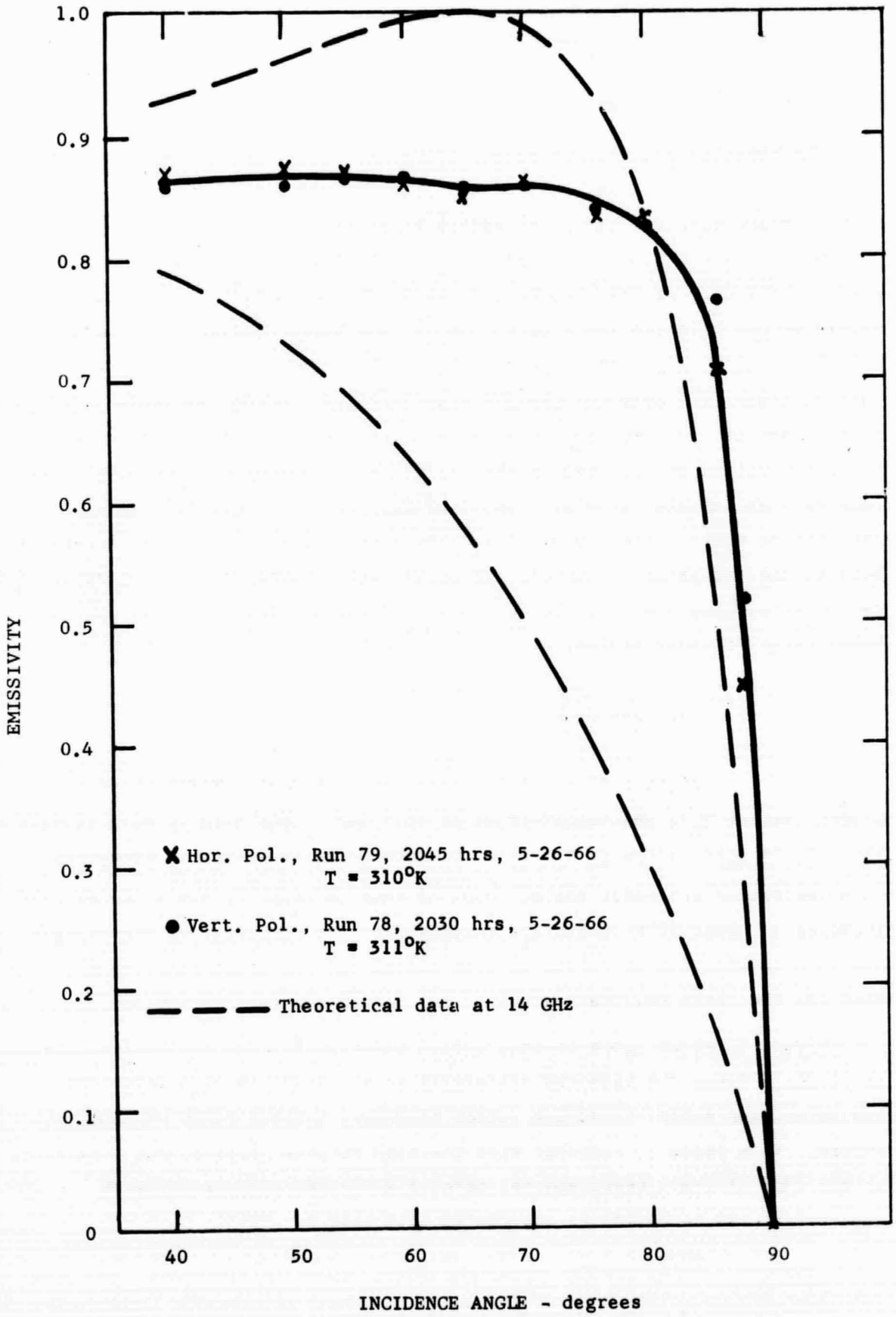


Figure 48 - Derived and Theoretical Specular Emissivities, Salines - 9.5 GHz

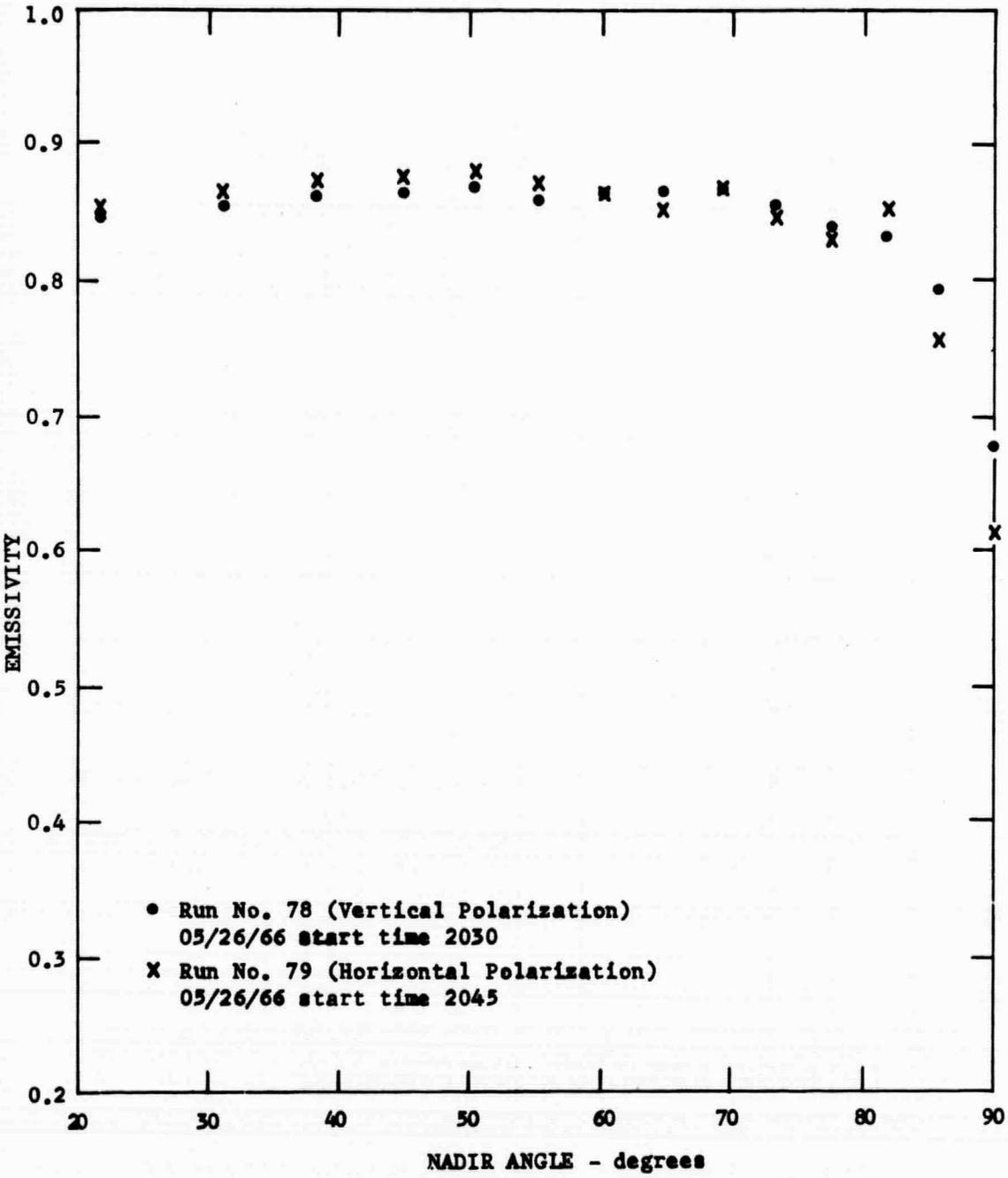


Figure 49 - Diffuse Emissivity vs Nadir Angle for Saline Surface at 9.5 GHz

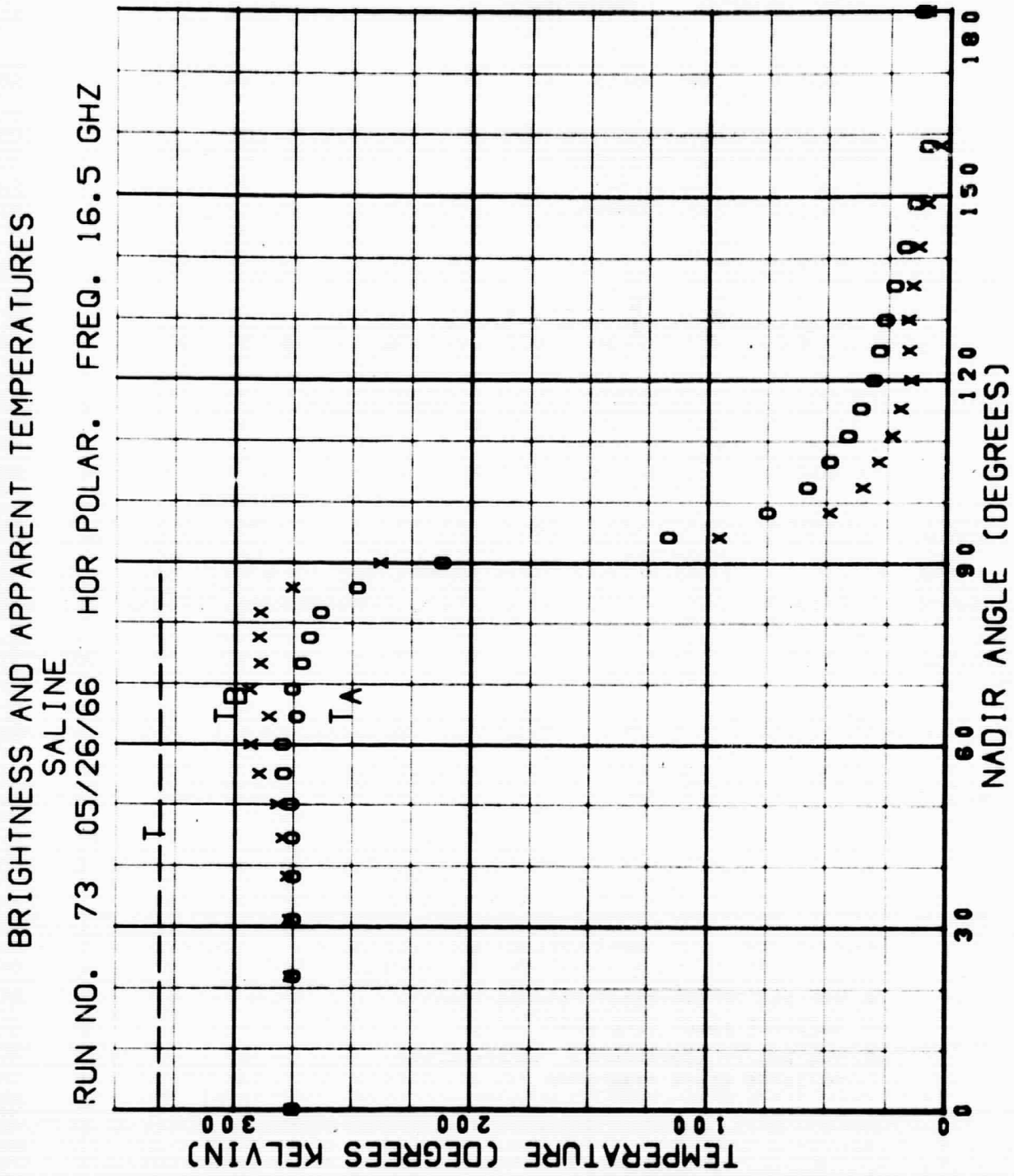


Figure 50 - Measured Salines Brightness Temperatures, 16.5 GHz, Hor. Pol.

PAGE 1 RUN 73

Table XLIII - Environmental and Calibration Data, Salines, 16.5 GHz, Hor. Pol.

TARGET MATERIAL	SALINE
DATA DATE	05/26/66
START TIME	1450
FREQUENCY,GHZ	16.5
POLARIZATION	HOR
ANTENNA AZIMUTH,DEG	40
BAROMETRIC PRESSURE,IN.HG.	29.86
RELATIVE HUMIDITY,0/0	6
AIR TEMPERATURE,DEG F	114
WIND DIRECTION	S
WIND SPEED,MPH	6
INTEGRATION TIME,SEC	1

THIRD CALIBRATION POINT 12.10DEG.K 6574.00MV.

INITIAL CALIBRATION DATA	
MINIMUM CAL.TEMP,DEG.K	320.83
MAXIMUM CAL.TEMP.DEG.K	389.26
K-FACTOR,DEG.K/MV.	0.71363
Y INTERCEPT	-4679.23

FINAL CALIBRATION DATA	
MINIMUM CAL.TEMP,DEG.K	320.87
MAXIMUM CAL.TEMP.DEG.K	390.74
K-FACTOR,DEG.K/MV.	0.70757
Y INTERCEPT	-4639.44

CALIBRATION CONSTANTS	INITIAL	FINAL	UNITS
HOT LOAD	391.50	393.00	DEG.K
ATTENUATOR	320.50	320.50	DEG.K
WAVE GUIDE SWITCH	321.00	320.50	DEG.K
ANTENNA	317.00	317.00	DEG.K
AVERAGE CAL.DATA-MIN.	7005.30	7009.50	MV.
-MAX.	7103.40	7109.85	MV.

COMMENTS
VERY LIGHT HAZE VERY BLUE SKY BACKGROUND VISIBILITY 18-20 MILES LIGHT LARGE PUFFY CLOUDS THIN BROKEN CLOUDS OVER THE MOUNTAINS

TARGET MATERIAL SALINE
DATA DATE 05/26/66
START TIME 1450
FREQUENCY,GHZ 16.5
POLARIZATION HOR

ZENITH ANGLE DEG	BRIGHTNESS TEMP,HORIZONTAL DEG K	EMISSIVITY	TIME	READINGS MV	SURFACE TEMP	SLOPE ANGLE	1/2 IN TEMP DEG K	1 FT TEMP DEG K	2 FT TEMP DEG K	3 FT TEMP DEG K	3 IN TEMP DEG K	6 IN TEMP DEG K	12 IN TEMP DEG K
0.0	5.9		1450	6573.	0.0	0.0	0.0	0.0	0.0	0.0	0.0	0.0	0.0
10.0	7.1			6571.	0.0	0.0	0.0	0.0	0.0	0.0	0.0	0.0	0.0
20.0	4.3			6569.	0.0	0.0	0.0	0.0	0.0	0.0	0.0	0.0	0.0
30.0	8.7			6576.	0.0	0.0	0.0	0.0	0.0	0.0	0.0	0.0	0.0
40.0	13.4			6584.	0.0	0.0	0.0	0.0	0.0	0.0	0.0	0.0	0.0
50.0	17.0			6594.	0.0	0.0	0.0	0.0	0.0	0.0	0.0	0.0	0.0
55.0	16.2												
60.0	15.5			6600.	0.0	0.0	0.0	0.0	0.0	0.0	0.0	0.0	0.0
65.0	19.9			6608.	0.0	0.0	0.0	0.0	0.0	0.0	0.0	0.0	0.0
70.0	24.0			6617.	0.0	0.0	0.0	0.0	0.0	0.0	0.0	0.0	0.0
72.0	26.8												
74.0	29.7												
75.0	31.1			6629.	0.0	0.0	0.0	0.0	0.0	0.0	0.0	0.0	0.0
76.0	33.4												
78.0	38.2												
80.0	42.9			6647.	0.0	0.0	0.0	0.0	0.0	0.0	0.0	0.0	0.0
82.0	51.0			6664.	0.0	0.0	0.0	0.0	0.0	0.0	0.0	0.0	0.0
84.0	73.6		1455	6686.	0.0	0.0	0.0	0.0	0.0	0.0	0.0	0.0	0.0
86.0	98.5			6722.	0.0	0.0	0.0	0.0	0.0	0.0	0.0	0.0	0.0
88.0	168.5			6754.	0.0	0.0	0.0	0.0	0.0	0.0	0.0	0.0	0.0
90.0	238.6	0.0		6855.	328.0	0.0	328.0	0.0	0.0	0.0	0.0	0.0	0.0
92.0	256.8	0.554		6886.	328.0	0.0	328.0	0.0	0.0	0.0	0.0	0.0	0.0
94.0	275.1	0.776		6906.	326.0	0.0	325.0	0.0	0.0	0.0	0.0	0.0	0.0
96.0	282.2	0.827		6920.	326.0	0.0	326.0	0.0	0.0	0.0	0.0	0.0	0.0
98.0	288.8	0.856		6928.	329.0	0.0	330.0	0.0	0.0	0.0	0.0	0.0	0.0
100.0	289.7	0.866		6931.	328.0	0.0	328.0	0.0	0.0	0.0	0.0	0.0	0.0
102.0	289.8	0.868		6936.	328.0	0.0	328.0	0.0	0.0	0.0	330.0	329.0	313.0
104.0	289.7	0.870		6935.	328.0	0.0	327.0	0.0	0.0	0.0	0.0	0.0	0.0
106.0	289.6	0.871		6939.	328.0	0.0	327.0	0.0	0.0	0.0	0.0	0.0	0.0
108.0	291.1	0.877		6943.	328.0	0.0	327.0	0.0	0.0	0.0	0.0	0.0	0.0
110.0	293.2	0.885		6947.	328.0	0.0	327.0	0.0	0.0	0.0	0.0	0.0	0.0
115.0	286.7	0.869		6943.	327.0	0.0	327.0	0.0	0.0	0.0	0.0	0.0	0.0
120.0	293.6	0.893		6952.	327.0	0.0	327.0	0.0	0.0	0.0	0.0	321.0	318.0
125.0	289.9	0.881		6952.	327.0	0.0	327.0	305.0	321.0	321.0	321.0	322.0	317.0
130.0	281.9	0.855		6947.	327.0	0.0	327.0	0.0	0.0	0.0	0.0	0.0	0.0
140.0	278.2	0.844	1500	6946.	327.0	0.0	327.0	0.0	0.0	0.0	0.0	0.0	0.0

Table XLIV - Brightness Temperatures, Saline, 16.5 GHz, Hor. Pol.

RUN NO. 73 05/26/66 HOR POLAR. 16.5 GHZ SALINE

ITERATION NUMBER 0

ZENITH ANGLE (DEG)	BRIGHTNESS TEMP. (DEG K)	APPARENT TEMP. (DEG K)	CORRECTION TEMP. (DEG K)
0.0	9.94	11.84	-1.8956
21.79	3.83	9.58	-5.7489
31.00	9.32	14.21	-4.8902
38.21	12.74	18.42	-5.6845
44.42	15.12	22.46	-7.3349
49.99	16.95	26.24	-9.2847
55.15	16.52	28.58	-12.0596
60.00	15.51	30.79	-15.2815
64.62	19.64	36.11	-16.4615
69.08	22.85	41.42	-18.5768
73.40	28.43	48.62	-20.1852
77.63	35.34	58.10	-22.7553
81.79	48.63	74.74	-26.1080
85.90	95.11	116.54	-21.4357
90.00	238.62	212.16	26.4655
94.10	275.93	248.32	27.6062
98.21	289.54	263.94	25.6003
102.37	289.82	268.58	21.1361
106.60	289.60	271.56	18.0354
110.92	294.14	276.20	17.9406
115.38	286.01	274.14	11.8694
120.00	293.60	280.03	13.5726
124.85	290.10	279.57	10.4325
130.01	281.91	276.26	5.6529
135.58	279.56	275.78	3.7771
141.79	277.67	275.41	2.2570
149.00	276.78	275.41	1.3733
158.21	276.22	275.41	0.8062
180.00	276.08	275.41	0.6665

ABS. CORRECTION = 1.29E 01 DEG. K

Table XLV - Brightness and Apparent Temperatures, Salines, 16.5 GHz, Hor. Pol.

RUN NO. 73 5/26/66 HOR POLAR. FREQ. 16.5 GHZ SALINE

OPTICAL DEPTH OF ATMOSPHERE= [illegible] 21 NEPERS
AIR TEMPERATURE= 318.72 DEGREES K
SOIL TEMPERATURE= 327.5[illegible] DEGREES K

ZENITH ANGLE (DEGREES)	BRIGHTNESS TEMP. (DEG.K)	EMISSIVITY	SCATTERING COEFFICIENT
0.0	9.94		
21.79	3.83		
31.00	9.32		
38.21	12.74		
44.41	15.12		
49.99	16.95		
55.15	16.52		
60.00	15.51		
64.62	19.64		
69.07	22.84		
73.40	28.43		
77.63	35.34		
81.79	48.63		
85.90	95.11		
90.00	238.62	0.71808	1.12769
94.10	275.93	0.83641	0.65435
98.21	289.54	0.87958	0.48167
102.37	289.82	0.88047	0.47811
106.60	289.60	0.87977	0.48193
110.92	294.14	0.89419	0.42325
115.38	286.11	0.86838	0.52646
120.00	293.60	0.89247	0.43012
124.85	29[illegible].1[illegible]	0.88137	0.47452
130.00	281.91	0.85539	0.57845
135.58	279.56	0.84793	0.60827
141.79	277.67	0.84192	0.63231
149.00	276.78	0.83912	0.64353
158.21	276.22	0.83732	0.65072
180.00	276.[illegible]8	0.83688	0.6525[illegible]

Table XLVI - Diffuse Emissivities, Salines, 16.5 GHz, Hor. Pol.

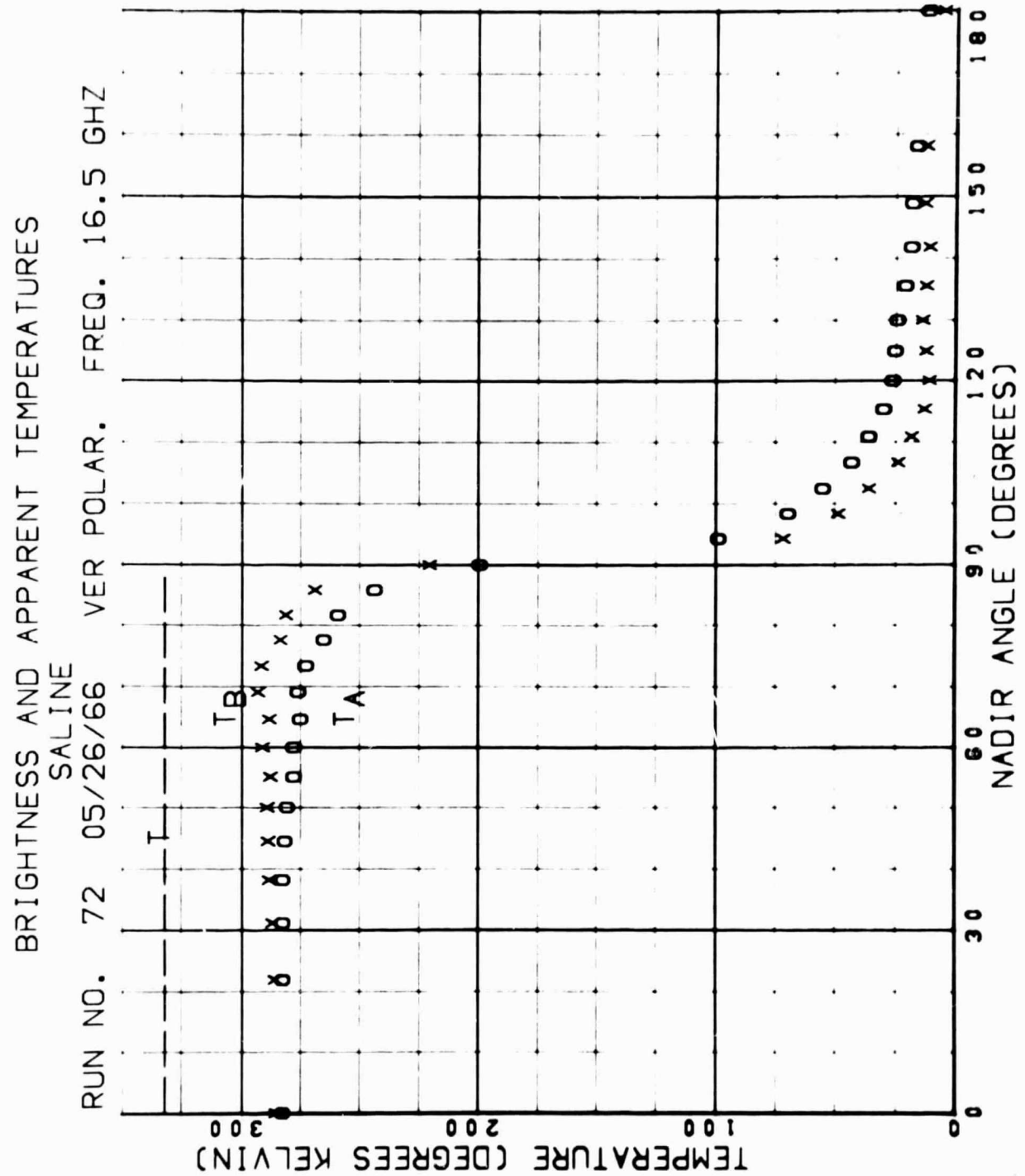


Figure 51 - Measured Salines Brightness Temperatures, 16.5 GHz, Vert. Pol.

Table XLVII - Environmental and Calibration Data, Salines, 16.5 GHz, Vert. Pol.

PAGE 1 RUN 72

TARGET MATERIAL	SALINE
DATA DATE	05/26/66
START TIME	1430
FREQUENCY,GHZ	16.5
POLARIZATION	VER
ANTENNA AZIMUTH,DEG	40
BAROMETRIC PRESSURE,IN.HG.	29.88
RELATIVE HUMIDITY,0/0	7
AIR TEMPERATURE,DEG F	112
WIND DIRECTION	S
WIND SPEED,MPH	8
INTEGRATION TIME,SEC	1

THIRD CALIBRATION POINT 12.20DEG.K 6570.00MV.

INITIAL CALIBRATION DATA

MINIMUM CAL.TEMP,DEG.K	321.31
MAXIMUM CAL.TEMP.DEG.K	392.14
K-FACTOR,DEG.K/MV.	0.71321
Y INTERCEPT	-4673.80

FINAL CALIBRATION DATA

MINIMUM CAL.TEMP,DEG.K	320.84
MAXIMUM CAL.TEMP.DEG.K	389.74
K-FACTOR,DEG.K/MV.	0.70644
Y INTERCEPT	-4629.16

CALIBRATION CONSTANTS	INITIAL	FINAL	UNITS
HOT LOAD	394.50	392.00	DEG.K
ATTENUATOR	321.00	320.50	DEG.K
WAVE GUIDE SWITCH	322.50	321.50	DEG.K
ANTENNA	317.00	316.50	DEG.K
AVERAGE CAL.DATA-MIN.	7005.60	7006.73	MV.
-MAX.	7101.54	7104.80	MV.

COMMENTS
SKY BACKGROUND VERY BLUE FEW LARGE PUFFY CLOUDS VISIBILITY 18-20 MILES LIGHT HAZE TOWARD THE HORIZON

TARGET MATERIAL SALINE
DATA DATE 05/26/66
START TIME 1430
FREQUENCY,GHZ 16.5
POLARIZATION VER

ZENITH ANGLE DEG	BRIGHTNESS TEMP DEG K	EMISSIVITY VERTICAL	TIME	READINGS MV	SURFACE TEMP	SLOPE ANGLE	1/2 IN TEMP DEG K	1 FT TEMP DEG K	2 FT TEMP DEG K	3 FT TEMP DEG K	9 IN TEMP DEG K	6 IN TEMP DEG K	12 IN TEMP DEG K
0.0	5.7		1432	6570.	0.0	0.0	0.0	0.0	0.0	0.0	0.0	0.0	0.0
10.0	8.8			6571.	0.0	0.0	0.0	0.0	0.0	0.0	0.0	0.0	0.0
20.0	11.9			6576.	0.0	0.0	0.0	0.0	0.0	0.0	0.0	0.0	0.0
30.0	13.1			6579.	0.0	0.0	0.0	0.0	0.0	0.0	0.0	0.0	0.0
40.0	11.6			6580.	0.0	0.0	0.0	0.0	0.0	0.0	0.0	0.0	0.0
50.0	14.2			6588.	0.0	0.0	0.0	0.0	0.0	0.0	0.0	0.0	0.0
55.0	12.6												
60.0	11.1			6590.	0.0	0.0	0.0	0.0	0.0	0.0	0.0	0.0	0.0
65.0	13.7			6596.	0.0	0.0	0.0	0.0	0.0	0.0	0.0	0.0	0.0
70.0	15.5			6605.	0.0	0.0	0.0	0.0	0.0	0.0	0.0	0.0	0.0
72.0	23.1												
74.0	26.8												
75.0	28.6			6618.	0.0	0.0	0.0	0.0	0.0	0.0	0.0	0.0	0.0
76.0	31.5												
78.0	37.5												
80.0	43.4			6642.	0.0	0.0	0.0	0.0	0.0	0.0	0.0	0.0	0.0
82.0	50.0			6653.	0.0	0.0	0.0	0.0	0.0	0.0	0.0	0.0	0.0
84.0	61.1			6664.	0.0	0.0	0.0	0.0	0.0	0.0	0.0	0.0	0.0
86.0	75.1			6654.	0.0	0.0	0.0	0.0	0.0	0.0	0.0	0.0	0.0
88.0	148.0			6752.	0.0	0.0	0.0	0.0	0.0	0.0	0.0	0.0	0.0
90.0	220.8	0.0		6834.	328.0	0.0	329.0	0.0	0.0	0.0	0.0	0.0	0.0
92.0	244.6	0.537	1437	6876.	328.0	0.0	329.0	0.0	0.0	0.0	0.0	0.0	0.0
94.0	268.4	0.770		6856.	326.0	0.0	326.0	0.0	0.0	0.0	0.0	0.0	0.0
96.0	275.1	0.81?		6812.	325.0	0.0	326.0	0.0	0.0	0.0	0.0	0.0	0.0
98.0	280.9	0.82.		6818.	329.0	0.0	331.0	0.0	0.0	0.0	0.0	0.0	0.0
100.0	282.5	0.84[illegible]		6826.	328.0	0.0	329.0	0.0	0.0	0.0	0.0	0.0	0.0
102.0	283.6	0.847		6827.	328.0	0.0	329.0	0.0	0.0	0.0	330.0	322.0	313.0
104.0	286.9	0.864		6832.	327.0	0.0	329.0	0.0	0.0	0.0	0.0	0.0	0.0
106.0	290.8	0.876		6838.	328.0	0.0	327.0	0.0	0.0	0.0	0.0	0.0	0.0
108.0	292.3	0.883		6840.	328.0	0.0	327.0	0.0	0.0	0.0	0.0	0.0	0.0
110.0	292.9	0.886		6844.	328.0	0.0	327.0	0.0	0.0	0.0	0.0	0.0	0.0
115.0	289.1	0.876		6842.	328.0	0.0	328.0	0.0	0.0	0.0	0.0	0.0	0.0
120.0	291.2	0.884		6846.	328.0	0.0	328.0	0.0	0.0	0.0	0.0	321.0	318.0
125.0	288.2	0.874		6847.	328.0	0.0	328.0	320.0	320.0	321.0	321.0	321.0	317.0
130.0	289.8	0.878	1442	6850.	328.0	0.0	328.0	0.0	0.0	0.0	0.0	0.0	0.0
140.0	288.6	0.876		6854.	328.0	0.0	328.0	0.0	0.0	0.0	0.0	0.0	0.0

Table XLVIII - Brightness Temperatures, Saline, 16.5 GHz, Vert. Pol.

RUN NO. 72 05/26/66 VER POLAR. 16.5 GHZ SALINE

ITERATION NUMBER 0

ZENITH ANGLE (DEG)	BRIGHTNESS TEMP. (DEG K)	APPARENT TEMP. (DEG K)	CORRECTION TEMP. (DEG K)
0.0	5.65	12.03	-6.3768
21.79	12.49	16.49	-4.0007
31.00	13.22	18.31	-5.0901
38.21	11.28	18.72	-7.4388
44.42	12.45	21.31	-8.8583
49.99	14.23	24.46	-10.2310
55.15	12.68	25.48	-12.8052
60.00	11.07	26.45	-15.3769
64.62	13.24	30.00	-16.7604
69.08	18.34	35.92	-17.5828
73.40	23.91	43.14	-19.2301
77.63	36.22	55.20	-18.9817
81.79	48.83	69.98	-21.1425
85.90	71.63	98.88	-27.2584
90.00	220.81	199.52	21.2934
94.10	269.52	244.00	25.5175
98.21	281.52	259.41	22.1156
102.37	283.79	265.52	18.2665
106.60	291.92	273.26	18.6617
110.92	293.16	276.33	16.8282
115.38	288.67	275.62	13.0519
120.00	291.21	278.36	12.8528
124.85	288.15	278.36	9.7859
130.01	289.77	280.89	8.8784
135.58	288.87	282.15	6.7227
141.79	288.53	283.14	5.3891
149.00	287.18	283.14	4.0441
158.21	286.35	283.14	3.2076
180.00	285.90	283.14	2.7641

Table XLIX - Brightness and Apparent Temperatures, Salines, 16.5 GHz, Vert. Pol.

ABS. CORRECTION = 1.31E 01 DEG. K

RUN NO. 72 05/26/66 VER POLAR. FREQ. 16.5 GHZ SALINE

OPTICAL DEPTH OF ATMOSPHERE= 0.022 NEPERS
AIR TEMPERATURE= 317.60 DEGREES K
SOIL TEMPERATURE= 327.70 DEGREES K

ZENITH ANGLE (DEGREES)	BRIGHTNESS TEMP. (DEG.K)	EMISSIVITY	SCATTERING COEFFICIENT
0.0	5.65		
21.79	12.49		
31.00	13.22		
38.21	11.28		
44.41	12.45		
49.99	14.23		
55.15	12.68		
60.00	11.07		
64.62	13.24		
69.07	18.34		
73.40	23.91		
77.63	36.22		
81.79	48.83		
85.90	71.62		
90.00	220.81	0.66061	1.35757
94.10	269.52	0.81526	0.73895
98.21	281.52	0.85338	0.58647
102.37	283.79	0.86058	0.55770
106.60	291.92	0.88639	0.45444
110.92	293.16	0.89032	0.43872
115.38	288.67	0.87609	0.49565
120.00	291.21	0.88414	0.46343
124.85	288.15	0.87441	0.50237
130.00	289.77	0.87956	0.48176
135.58	288.87	0.87670	0.49319
141.79	288.53	0.87562	0.49751
149.00	287.18	0.87135	0.51459
158.21	286.35	0.86870	0.52522
180.00	285.97	0.86729	0.53085

Table L - Diffuse Emissivities, Salines, 16.5 GHz, Vert. Pol.

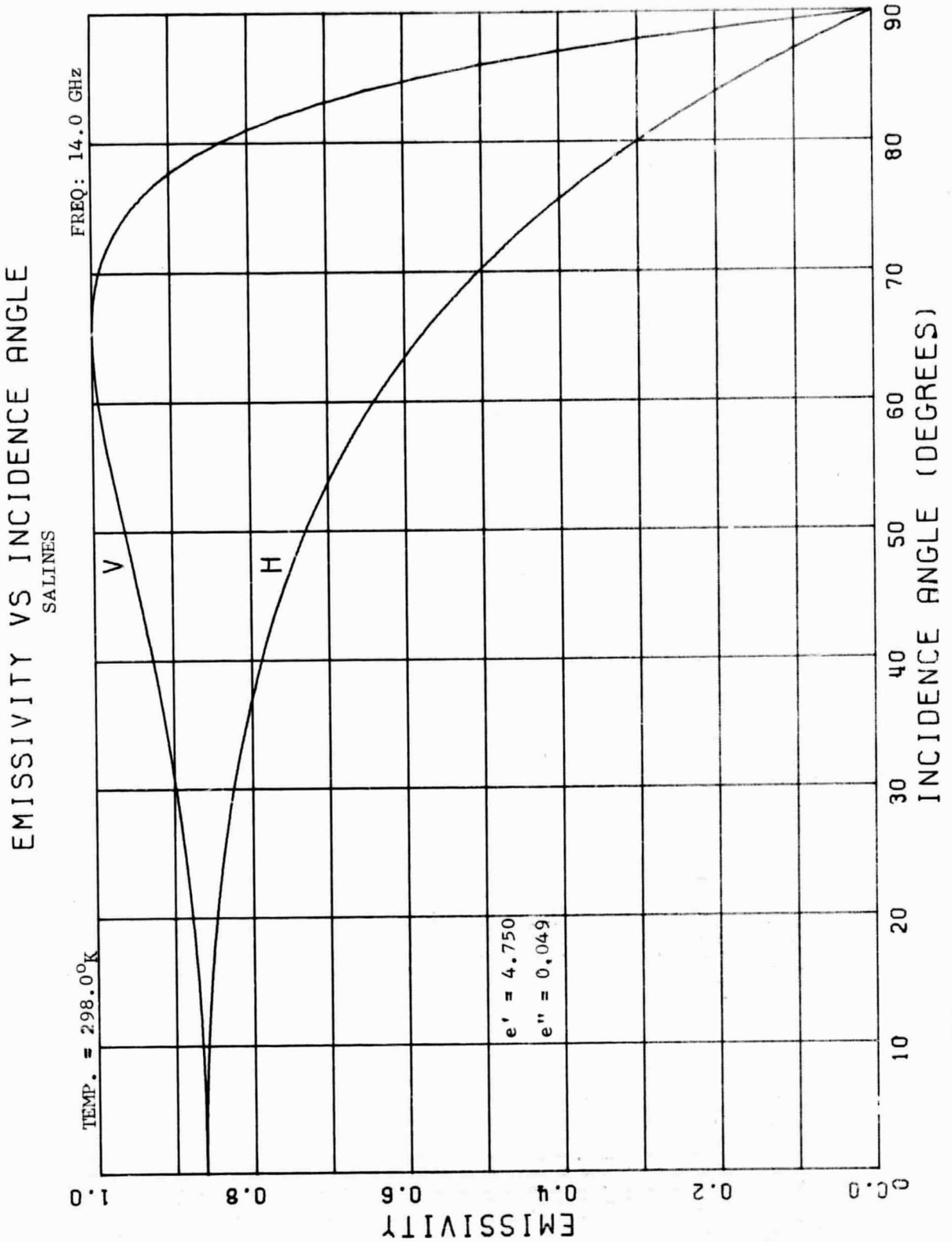


Figure 52 - Theoretical Emissivity of Salines - 14.0 GHz

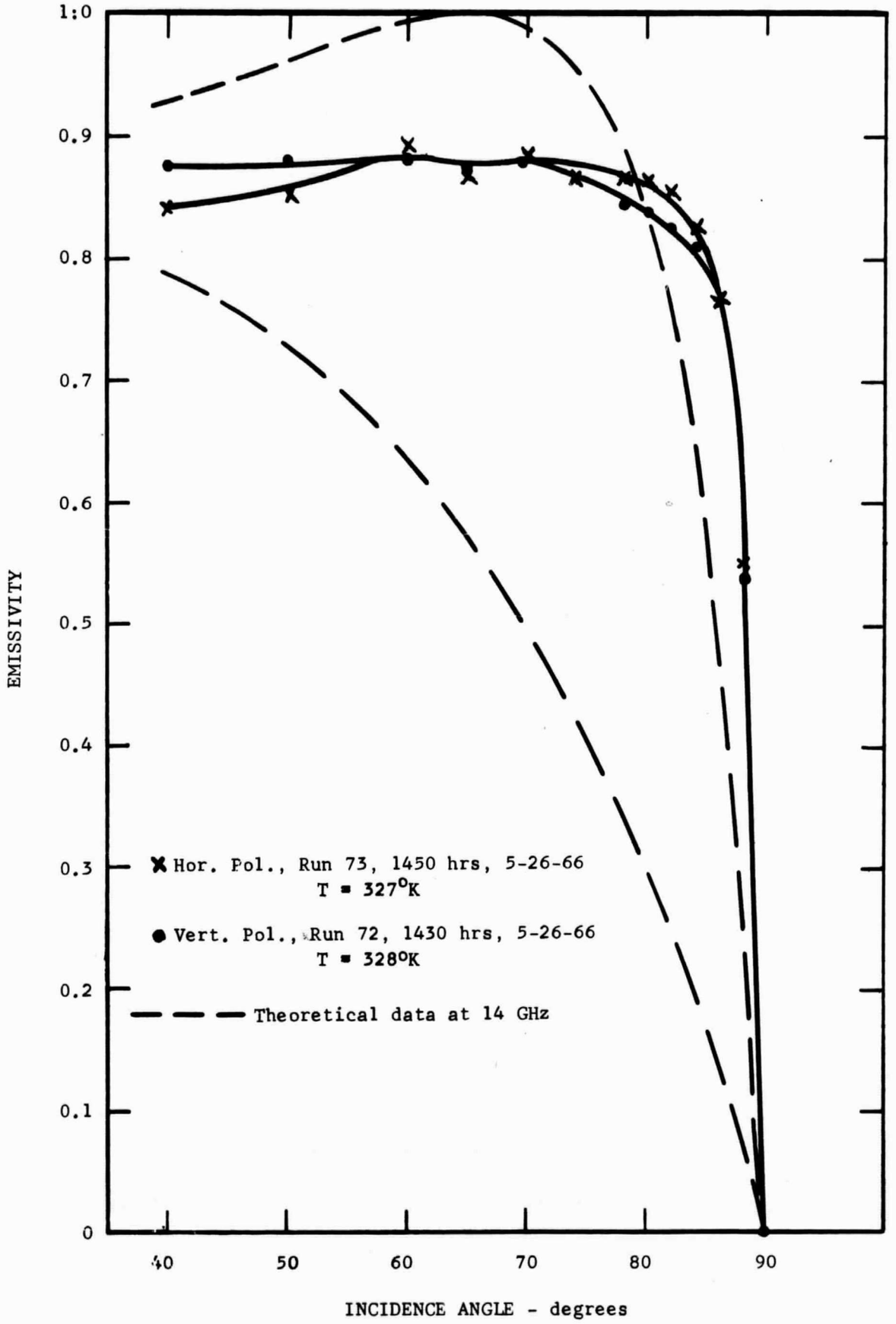


Figure 53 - Derived and Theoretical Specular Emissivities, Salines - 16.5 GHz

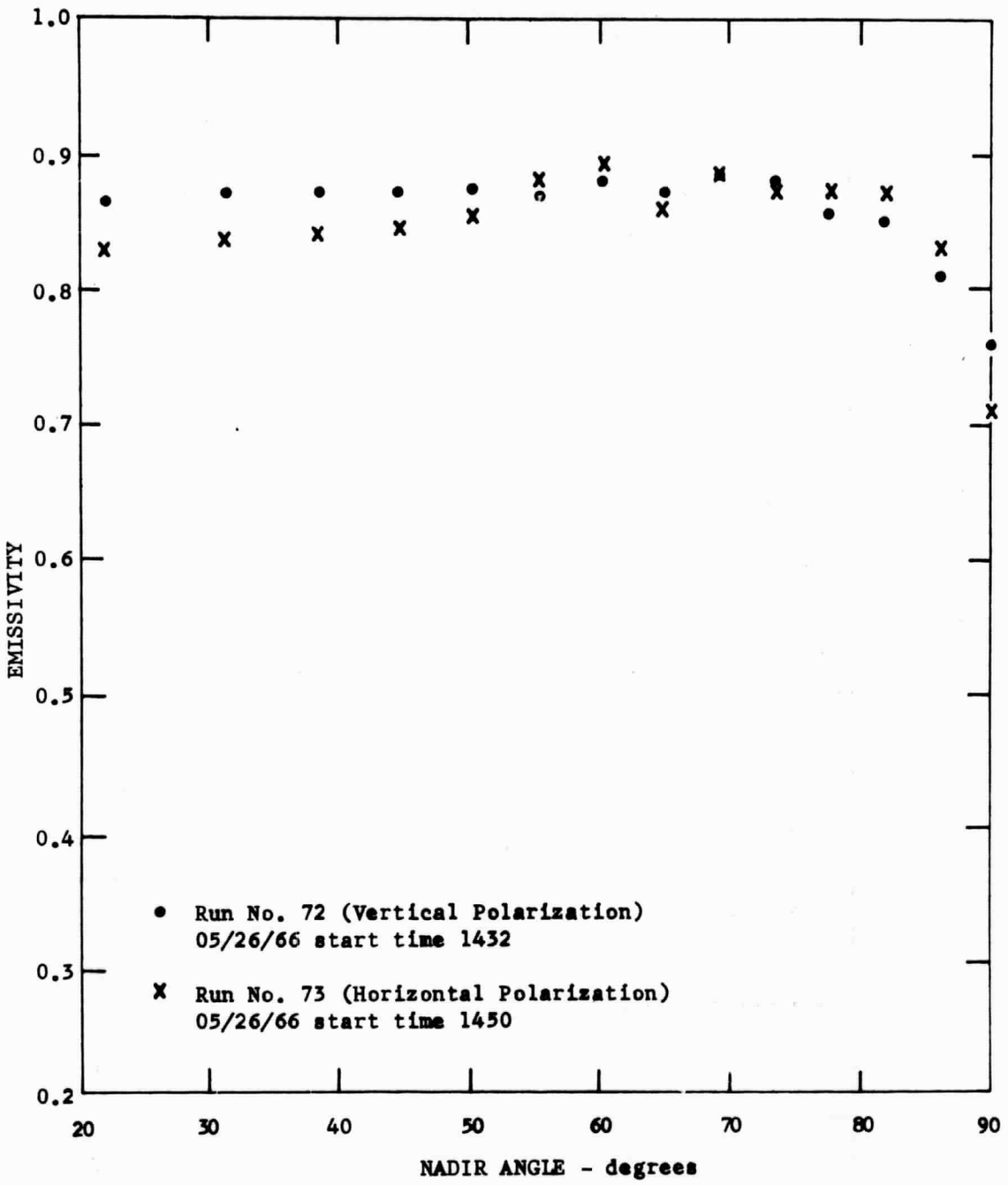


Figure 54 - Diffuse Emissivity vs Nadir Angle for Saline Surface at 16.5 GHz

As in the case of the 9.5 GHz specular and diffuse emissivities, there are relatively small differences between these at this frequency, as shown in Figures 53 and 54, respectively.

3. 94 GHz Data

Figure 55 and Tables LI thru' LIII present T_B's for horizontal polarization. These are even higher than those obtained at the two lower frequencies and are very constant with respect to nadir angle. This increase is due to a combination of a much shorter operating wavelength and considerably higher sky brightness temperatures. Referring to Figures 44 and 45, it appears that the small-scale surface roughness is comparable to the 3.2 millimeter operating wavelength of this radiometer. Thus, surface roughness effects should be more pronounced at 94 GHz than at the lower frequencies. This tends to increase the influence of sky brightness temperatures on observed T_B's since reflected sky radiation effectively emanates from a broader range of zenith angles.

Figure 56 and Tables LV thru' LVII show vertically polarized T_B's. These are very similar to the horizontally polarized T_B's, falling within 5°K of them over most of the nadir angle.

Figure 57 shows derived and theoretical specular emissivities of salines at 94 and 14 GHz, respectively. Since these frequencies are very widely separated there is no basis for comparison of the two pairs of curves. However, the derived emissivities are relatively high over a broad range of nadir angles. This is, basically, due to the small difference existing between brightness and surface temperature at a given angle - approximately 25°K. The small separation between the two polarization components is considered to be due partly to calibration error and partly to the influence of large variations in sky brightness temperature on emissivities calculated by means of Equation (31).

Table LVIII and Figure 58 present diffuse emissivities derived from the above T_B's. The average value and trend of the points are similar to the derived emissivities in Figure 57, except that a greater degree of

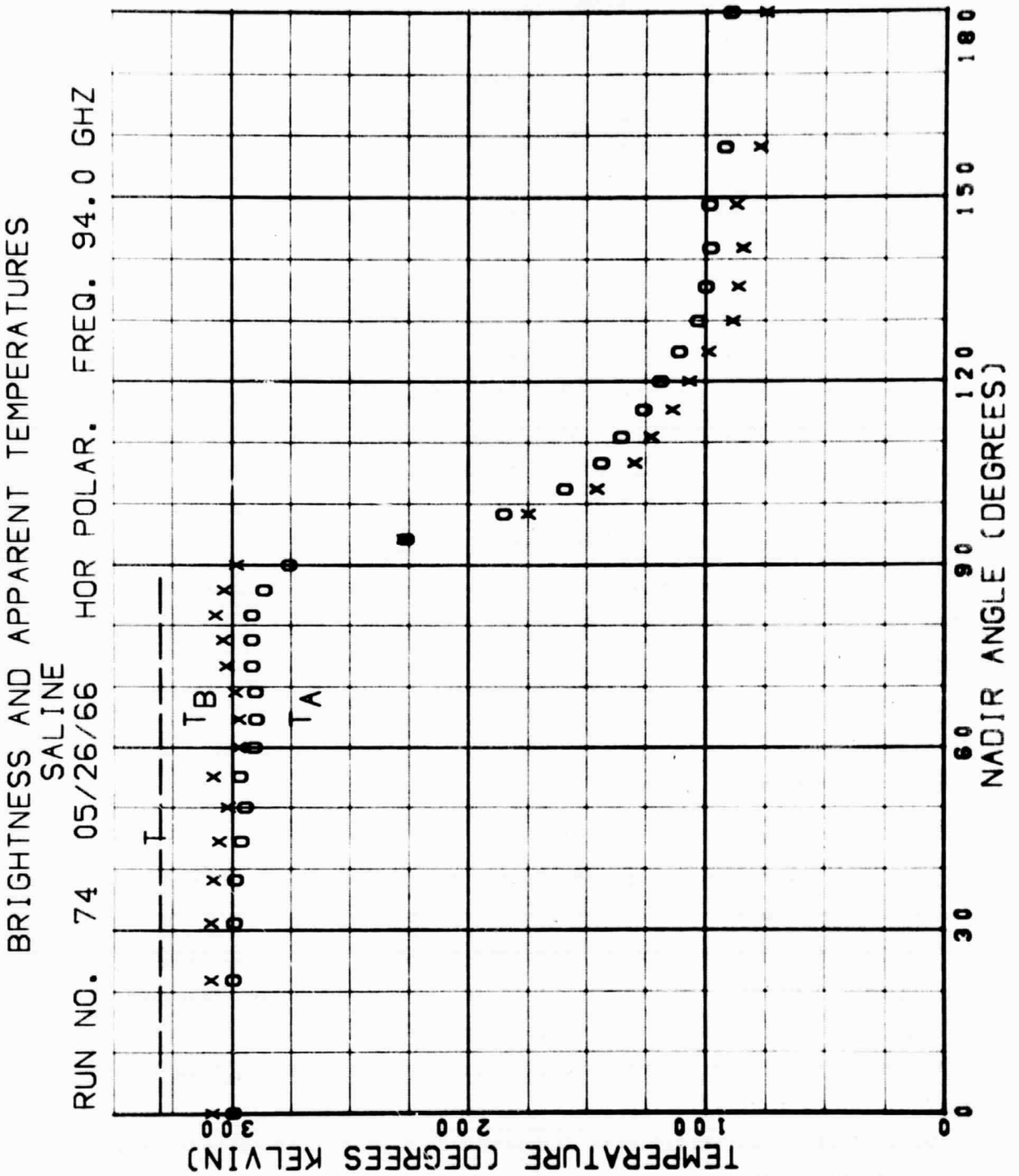


Figure 55 - Measured Salines Brightness Temperatures. 94 GHz, Hor. Pol.

Table LI - Environmental and Calibration Data, Salines, 94 GHz, Hor. Pol.

PAGE 1 RUN 74

TARGET MATERIAL	SALINE
DATA DATE	05/26/66
START TIME	1515
FREQUENCY,GHZ	94.0
POLARIZATION	HOR
ANTENNA AZIMUTH,DEG	220
BAROMETRIC PRESSURE,IN.HG.	29.82
RELATIVE HUMIDITY,0/0	5
AIR TEMPERATURE,DEG F	114
WIND DIRECTION	SE
WIND SPEED,MPH	8
INTEGRATION TIME,SEC	10

THIRD CALIBRATION POINT 89.30DEG.K 6573.00MV.

INITIAL CALIBRATION DATA

MINIMUM CAL.TEMP,DEG.K	321.03
MAXIMUM CAL.TEMP.DEG.K	385.42
K-FACTOR,DEG.K/MV.	0.52082
Y INTERCEPT	-3333.80

FINAL CALIBRATION DATA

MINIMUM CAL.TEMP,DEG.K	323.73
MAXIMUM CAL.TEMP.DEG.K	387.28
K-FACTOR,DEG.K/MV.	0.51728
Y INTERCEPT	-3310.78

CALIBRATION CONSTANTS	INITIAL	FINAL	UNITS
HOT LOAD	398.00	398.00	DEG.K
CAL WGS - MIN	321.00	322.00	DEG.K
CAL WGS - MAX	324.00	325.00	DEG.K
WAVE GUIDE SWITCH	319.00	319.00	DEG.K
ANTENNA	323.00	318.00	DEG.K
COLD LOAD	318.50	319.50	DEG.K
AVERAGE CAL.DATA-MIN.	7014.70	7026.20	MV.
-MAX.	7143.25	7149.20	MV.

COMMENTS
VERY LIGHT HAZE ON THE HORIZ FEW THIN BROKEN CLOUDS BLUE SKY BACKGROUND
VISIBILITY ABOUT 20 MILES

TARGET MATERIAL SALINE
DATA DATE 05/26/88
START TIME 1515
FREQUENCY,GHZ 94.0
POLARIZATION HOR

Table LII - Brightness Temperatures, Saline, 94 GHz, Hor. Pol.

ZENITH ANGLE DEG	BRIGHTNESS TEMP,HORIZONTAL DEG K	EMISSIVITY	TIME	READINGS MV	SURFACE TEMP	SLOPE ANGLE	1/2 IN TEMP DEG K	1 FT TEMP DEG K	2 FT TEMP DEG K	3 FT TEMP DEG K	3 IN TEMP DEG K	6 IN TEMP DEG K	12 IN TEMP DEG K
0.0	74.9		1515	6573.	0.0	0.0	0.0	0.0	0.0	0.0	0.0	0.0	0.0
10.0	76.0			6572.	0.0	0.0	0.0	0.0	0.0	0.0	0.0	0.0	0.0
20.0	77.1			6574.	0.0	0.0	0.0	0.0	0.0	0.0	0.0	0.0	0.0
30.0	86.2			6590.	0.0	0.0	0.0	0.0	0.0	0.0	0.0	0.0	0.0
40.0	84.8		1520	6589.	0.0	0.0	0.0	0.0	0.0	0.0	0.0	0.0	0.0
50.0	88.3			6599.	0.0	0.0	0.0	0.0	0.0	0.0	0.0	0.0	0.0
55.0	97.6												
60.0	106.9			6629.	0.0	0.0	0.0	0.0	0.0	0.0	0.0	0.0	0.0
65.0	114.3			6645.	0.0	0.0	0.0	0.0	0.0	0.0	0.0	0.0	0.0
70.0	124.4			6665.	0.0	0.0	0.0	0.0	0.0	0.0	0.0	0.0	0.0
72.0	128.9												
74.0	133.4												
75.0	135.7		1525	6684.	0.0	0.0	0.0	0.0	0.0	0.0	0.0	0.0	0.0
76.0	141.0												
78.0	151.7												
80.0	162.3			6729.	0.0	0.0	0.0	0.0	0.0	0.0	0.0	0.0	0.0
82.0	177.6		1535	6760.	0.0	0.0	0.0	0.0	0.0	0.0	0.0	0.0	0.0
84.0	203.0			6812.	0.0	0.0	0.0	0.0	0.0	0.0	0.0	0.0	0.0
86.0	228.8			6837.	0.0	0.0	0.0	0.0	0.0	0.0	0.0	0.0	0.0
88.0	263.6			6893.	0.0	0.0	0.0	0.0	0.0	0.0	0.0	0.0	0.0
90.0	298.4	0.0		6933.	326.0	0.0	326.0	0.0	0.0	0.0	0.0	0.0	0.0
92.0	300.8	0.597	1540	6952.	326.0	0.0	326.0	0.0	0.0	0.0	0.0	0.0	0.0
94.0	303.3	0.774		6952.	325.0	0.0	324.0	0.0	0.0	0.0	0.0	0.0	0.0
96.0	305.3	0.846		6966.	324.0	0.0	324.0	0.0	0.0	0.0	0.0	0.0	0.0
98.0	307.3	0.863		6964.	328.0	0.0	327.0	0.0	0.0	0.0	0.0	0.0	0.0
100.0	306.1	0.868	1545	6962.	328.0	0.0	327.0	0.0	0.0	0.0	0.0	0.0	0.0
102.0	304.4	0.871	1552	6964.	327.0	0.0	308.0	0.0	0.0	0.0	329.0	323.0	313.0
104.0	303.6	0.869		6963.	328.0	0.0	326.0	0.0	0.0	0.0	0.0	0.0	0.0
106.0	302.9	0.871		6965.	328.0	0.0	326.0	0.0	0.0	0.0	0.0	0.0	0.0
108.0	301.5	0.867		6963.	328.0	0.0	326.0	0.0	0.0	0.0	0.0	0.0	0.0
110.0	299.8	0.862		6962.	328.0	0.0	326.0	0.0	0.0	0.0	0.0	0.0	0.0
115.0	297.5	0.857	1557	6960.	328.0	0.0	326.0	0.0	0.0	0.0	0.0	0.0	0.0
120.0	297.7	0.871		6962.	326.0	0.0	326.0	0.0	0.0	0.0	0.0	321.0	318.0
125.0	300.2	0.922		6975.	326.0	0.0	326.0	365.0	321.0	321.0	322.0	322.0	318.0
130.0	302.2	0.950		6970.	326.0	0.0	326.0	0.0	0.0	0.0	0.0	0.0	0.0
140.0	307.7	0.924	1601	6978.	326.0	0.0	326.0	0.0	0.0	0.0	0.0	0.0	0.0
150.0	309.1	0.930		6980.	326.0	0.0	326.0	0.0	0.0	0.0	0.0	0.0	0.0

RUN NO. 74 05/26/66 HOR POLAR. 94.0 GHZ SALINE

ITERATION NUMBER 0

ZENITH ANGLE (DEG)	BRIGHTNESS TEMP. (DEG K)	APPARENT TEMP. (DEG K)	CORRECTION TEMP. (DEG K)
0.0	74.89	89.46	-14.5741
21.79	77.29	91.73	-14.4435
31.00	87.33	98.32	-10.9887
38.21	84.17	97.78	-13.6096
44.42	86.38	99.97	-13.5915
49.99	88.34	102.91	-14.5687
55.15	98.67	111.09	-12.4187
60.00	106.94	118.79	-11.8527
64.62	113.70	126.14	-12.4411
69.08	122.95	135.28	-12.3353
73.40	129.56	143.96	-14.3952
77.63	145.71	159.45	-13.7432
81.79	174.85	184.99	-10.1437
85.90	227.14	226.16	0.9833
90.00	298.36	276.09	22.2754
94.10	303.39	286.64	16.7540
98.21	307.54	292.00	15.5341
102.37	304.10	291.96	12.1382
106.60	302.71	292.08	10.6316
110.92	299.06	290.59	8.4696
115.38	297.31	289.91	7.3962
120.00	297.74	290.91	6.8300
124.85	308.38	297.23	11.1496
130.01	302.20	294.53	7.6731
135.58	305.87	296.81	9.0647
141.79	308.43	298.80	9.6232
149.00	309.14	299.59	9.5541
158.21	309.01	299.70	9.3098
180.00	308.88	299.70	9.1778

ABS. CORRECTION = 1.16E 01 DEG. K

Table LIII - Brightness and Apparent Temperatures, Salines, 94 GHz, Hor. Pol.

RUN NO. 74 05/26/66 HOR POLAR. FREQ. 94.0 GHZ SALINE

OPTICAL DEPTH OF ATMOSPHERE= 0.28 NEPERS
AIR TEMPERATURE= 318.72 DEGREES K
SOIL TEMPERATURE= 326.70 DEGREES K

ZENITH ANGLE (DEGREES)	BRIGHTNESS TEMP. (DEG.K)	EMISSIVITY	SCATTERING COEFFICIENT
0.0	74.89		
21.79	77.29		
31.00	87.33		
38.21	84.17		
44.41	86.38		
49.99	88.34		
55.15	98.67		
60.00	106.94		
64.62	113.70		
69.07	122.95		
73.40	129.56		
77.63	145.71		
81.79	174.85		
85.90	227.14		
90.00	298.36	0.86495	0.54020
94.10	303.39	0.88891	0.44436
98.21	307.54	0.90867	0.36534
102.37	304.10	0.89229	0.43084
106.60	302.71	0.88566	0.45736
110.92	299.06	0.86825	0.52701
115.38	297.31	0.85991	0.56037
120.00	297.74	0.86197	0.55211
124.85	308.38	0.91270	0.34921
130.00	302.25	0.88325	0.46699
135.58	305.87	0.90073	0.39706
141.79	308.43	0.91291	0.34837
149.00	309.14	0.91633	0.33468
158.21	309.01	0.91569	0.33726
180.00	308.88	0.91506	0.33977

Table LIV - Diffuse Emissivities, Saline, 94 GHz, Hor. Pol.

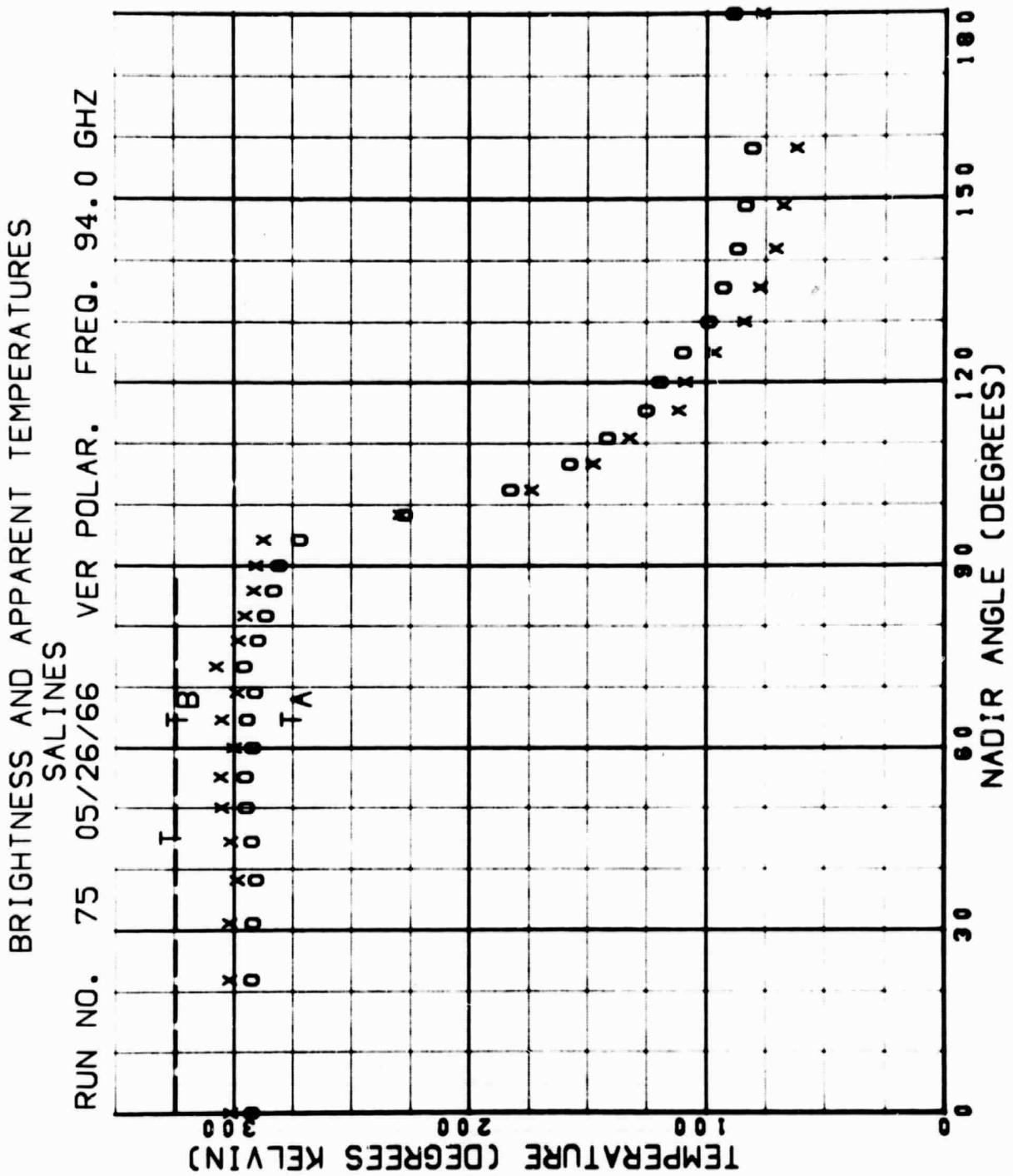


Figure 56 - Measured Salines Brightness Temperatures, 94 GHz, Vert. Pol.

Table LV - Environmental and Calibration Data, Salines, 94 GHz, Vert. Pol.

PAGE 1 RUN 75

TARGET MATERIAL	SALINES
DATA DATE	05/26/66
START TIME	1615
FREQUENCY,GHZ	94.0
POLARIZATION	VER
ANTENNA AZIMUTH,DEG	220
BAROMETRIC PRESSURE,IN.HG.	29.80
RELATIVE HUMIDITY,0/0	4
AIR TEMPERATURE,DEG F	112
WIND DIRECTION	SE
WIND SPEED,MPH	5
INTEGRATION TIME,SEC	10

THIRD CALIBRATION POINT 88.60DEG.K 6608.00MV.

INITIAL CALIBRATION DATA	
MINIMUM CAL.TEMP,DEG.K	323.99
MAXIMUM CAL.TEMP.DEG.K	387.70
K-FACTOR,DEG.K/MV.	0.56102
Y INTERCEPT	-3618.60

FINAL CALIBRATION DATA	
MINIMUM CAL.TEMP,DEG.K	324.91
MAXIMUM CAL.TEMP.DEG.K	389.22
K-FACTOR,DEG.K/MV.	0.57122
Y INTERCEPT	-3684.79

CALIBRATION CONSTANTS	INITIAL	FINAL	UNITS
HOT LOAD	398.00	398.00	DEG.K
CAL WGS - MIN	322.50	324.50	DEG.K
CAL WGS - MAX	325.50	327.50	DEG.K
WAVE GUIDE SWITCH	318.00	317.00	DEG.K
ANTENNA	318.00	317.00	DEG.K
COLD LOAD	319.20	318.00	DEG.K
AVERAGE CAL.DATA-MIN.	7026.90	7010.66	MV.
-MAX.	7141.70	7139.00	MV.

COMMENTS
SKY CLEAR FAIRLY BLUE BACKGROUND VERY LIGHT HAZE ON THE MOUNTAINS A SMALL THIN CLOUD OVERHEAD VISIBILITY ABOUT 20 MILES.

TARGET MATERIAL SALINES
DATA DATE 05/26/66
START TIME 1615
FREQUENCY,GHZ 94.0
POLARIZATION VER

ZENITH ANGLE DEG	BRIGHTNESS TEMP DEG K	EMISSIVITY VERTICAL	TIME	READINGS MV	SURFACE TEMP	SLOPE ANGLE	1/2 IN TEMP DEG K	1 FT TEMP DEG K	2 FT TEMP DEG K	3 FT TEMP DEG K	3 IN TEMP DEG K	6 IN TEMP DEG K	12 IN TEMP DEG K
0.0	76.5		1615	6608.	0.0	0.0	0.0	0.0	0.0	0.0	0.0	0.0	0.0
10.0	69.7			6601.	0.0	0.0	0.0	0.0	0.0	0.0	0.0	0.0	0.0
20.0	62.9			6592.	0.0	0.0	0.0	0.0	0.0	0.0	0.0	0.0	0.0
30.0	67.0			6598.	0.0	0.0	0.0	0.0	0.0	0.0	0.0	0.0	0.0
40.0	72.6			6606.	0.0	0.0	0.0	0.0	0.0	0.0	0.0	0.0	0.0
50.0	83.7		1620	6626.	0.0	0.0	0.0	0.0	0.0	0.0	0.0	0.0	0.0
55.0	96.2												
60.0	108.6			6662.	0.0	0.0	0.0	0.0	0.0	0.0	0.0	0.0	0.0
65.0	113.3			6673.	0.0	0.0	0.0	0.0	0.0	0.0	0.0	0.0	0.0
70.0	135.5			6708.	0.0	0.0	0.0	0.0	0.0	0.0	0.0	0.0	0.0
72.0	144.3												
74.0	153.2												
75.0	157.6			6740.	0.0	0.0	0.0	0.0	0.0	0.0	0.0	0.0	0.0
76.0	167.2												
78.0	186.5												
80.0	205.7		1625	6805.	0.0	0.0	0.0	0.0	0.0	0.0	0.0	0.0	0.0
82.0	232.8		1632	6860.	0.0	0.0	0.0	0.0	0.0	0.0	0.0	0.0	0.0
84.0	260.8			6898.	0.0	0.0	0.0	0.0	0.0	0.0	0.0	0.0	0.0
86.0	287.6			6933.	0.0	0.0	0.0	0.0	0.0	0.0	0.0	0.0	0.0
88.0	289.3			6942.	0.0	0.0	0.0	0.0	0.0	0.0	0.0	0.0	0.0
90.0	291.1	0.0	1637	6947.	325.0	0.0	325.0	0.0	0.0	0.0	0.0	0.0	0.0
92.0	291.4	0.060		6962.	325.0	0.0	325.0	0.0	0.0	0.0	0.0	0.0	0.0
94.0	291.8	0.111		6950.	326.0	0.0	324.0	0.0	0.0	0.0	0.0	0.0	0.0
96.0	293.6	0.511		6963.	325.0	0.0	324.0	0.0	0.0	0.0	0.0	0.0	0.0
98.0	295.4	0.658		6955.	326.0	0.0	327.0	0.0	0.0	0.0	0.0	0.0	0.0
100.0	296.9	0.745		6965.	328.0	0.0	327.0	0.0	0.0	0.0	0.0	0.0	0.0
102.0	298.2	0.790		6961.	328.0	0.0	328.0	0.0	0.0	0.0	327.0	322.0	314.0
104.0	302.2	0.850	1646	6961.	326.0	0.0	324.0	0.0	0.0	0.0	0.0	0.0	0.0
106.0	306.7	0.888	1650	6975.	326.0	0.0	324.0	0.0	0.0	0.0	0.0	0.0	0.0
108.0	305.1	0.885		6963.	326.0	0.0	324.0	0.0	0.0	0.0	0.0	0.0	0.0
110.0	300.8	0.868		6961.	326.0	0.0	324.0	0.0	0.0	0.0	0.0	0.0	0.0
115.0	304.9	0.901		6968.	326.0	0.0	324.0	0.0	0.0	0.0	0.0	0.0	0.0
120.0	300.2	0.906		6963.	320.0	0.0	322.0	0.0	0.0	0.0	0.0	321.0	318.0
125.0	306.1	0.938	1655	6969.	320.0	0.0	322.0	305.0	322.0	323.0	322.0	322.0	315.0
130.0	305.5	0.939		6968.	320.0	0.0	322.0	0.0	0.0	0.0	0.0	0.0	0.0
140.0	299.9	0.919		6960.	320.0	0.0	322.0	0.0	0.0	0.0	0.0	0.0	0.0
150.0	302.0	0.929	1700	6963.	320.0	0.0	322.0	0.0	0.0	0.0	0.0	0.0	0.0

Table LVI - Brightness Temperatures, Salines, 94 GHz, Vert. Pol.

RUN NO. 75 05/26/66 VER POLAR. 94.0 GHZ SALINES

ITERATION NUMBER 0

ZENITH ANGLE (DEG)	BRIGHTNESS TEMP. (DEG K)	APPARENT TEMP. (DEG K)	CORRECTION TEMP. (DEG K)
0.0	76.48	88.34	-11.8629
21.79	61.66	80.42	-18.7573
31.00	67.60	83.62	-16.0223
38.21	70.67	86.85	-16.1772
44.42	77.52	92.61	-15.0890
49.99	83.71	98.87	-15.1620
55.15	96.67	109.46	-12.7896
60.00	108.61	119.42	-10.8145
64.62	111.59	125.15	-13.5656
69.08	132.16	141.51	-9.3504
73.40	147.71	157.48	-9.7668
77.63	173.79	182.72	-8.9321
81.79	229.79	227.87	1.9186
85.90	287.51	272.05	15.4601
90.00	291.05	280.99	10.0622
94.10	291.86	283.57	8.2942
98.21	295.64	286.95	8.6904
102.37	298.50	290.08	8.4265
106.60	308.04	295.97	12.0726
110.92	298.85	291.42	7.4305
115.38	305.42	294.68	10.7390
120.00	300.16	292.25	7.9079
124.85	306.14	295.66	10.4793
130.01	305.50	295.35	10.1541
135.58	301.64	292.63	9.0101
141.79	299.13	290.88	8.2544
149.00	302.01	292.48	9.5332
158.21	302.01	292.70	9.3081
180.00	301.95	292.70	9.2473

ABS. CORRECTION = 1.09E 01 DEG. K

Table LVII - Brightness and Apparent Temperatures, Salines, 94 GHz, Vert. Pol.

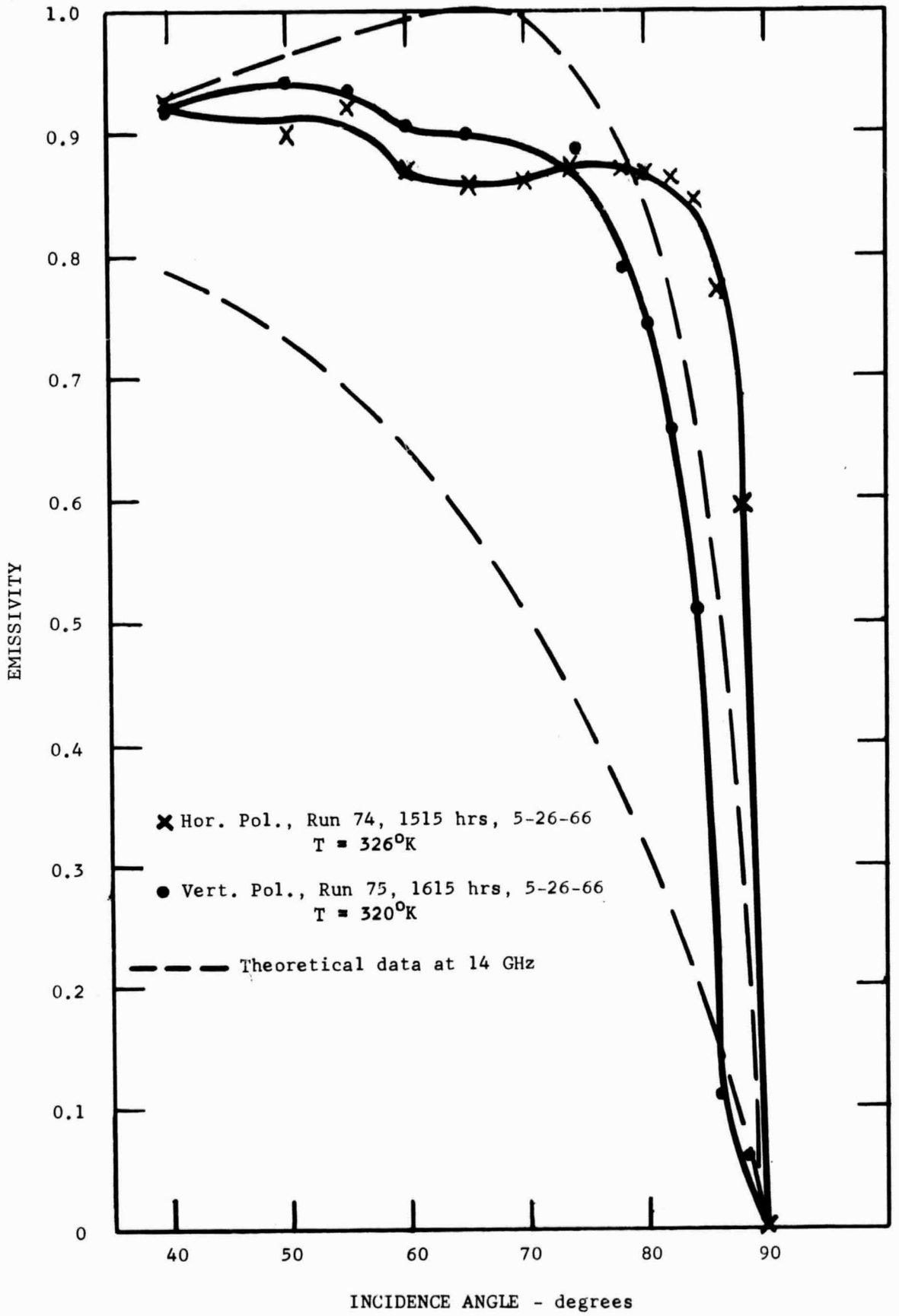


Figure 57 -Derived and Theoretical Specular Emissivities, Salines - 94 GHz

RUN NO. 75 05/26/66 VER POLAR. FREQ. 94.0 GHZ SALINES

OPTICAL DEPTH OF ATMOSPHERE= 0.288 NEPERS
AIR TEMPERATURE= 317.60 DEGREES K
SOIL TEMPERATURE= 324.30 DEGREES K

ZENITH ANGLE (DEGREES)	BRIGHTNESS TEMP. (DEG.K)	EMISSIVITY	SCATTERING COEFFICIENT
0.0	76.48		
21.79	61.66		
31.00	67.60		
38.21	70.67		
44.41	77.52		
49.99	83.71		
55.15	96.67		
60.00	108.60		
64.62	111.59		
69.07	132.16		
73.40	147.71		
77.63	173.79		
81.79	229.79		
85.90	287.51		
90.00	291.05	0.83823	0.64709
94.10	291.86	0.84218	0.63129
98.21	295.64	0.86055	0.55779
102.37	298.50	0.87449	0.50205
106.60	308.04	0.92088	0.31648
110.92	298.85	0.87615	0.49540
115.38	305.42	0.90814	0.36745
120.00	300.16	0.88253	0.46986
124.85	306.14	0.91165	0.35338
130.00	305.50	0.90853	0.36587
135.58	301.64	0.88975	0.44102
141.79	299.13	0.87754	0.48985
149.00	302.01	0.89154	0.43382
158.21	302.01	0.89154	0.43386
180.00	301.95	0.89124	0.43505

Table LVIII - Diffuse Emissivities, Salines, 94 GHz, Vert. Pol.

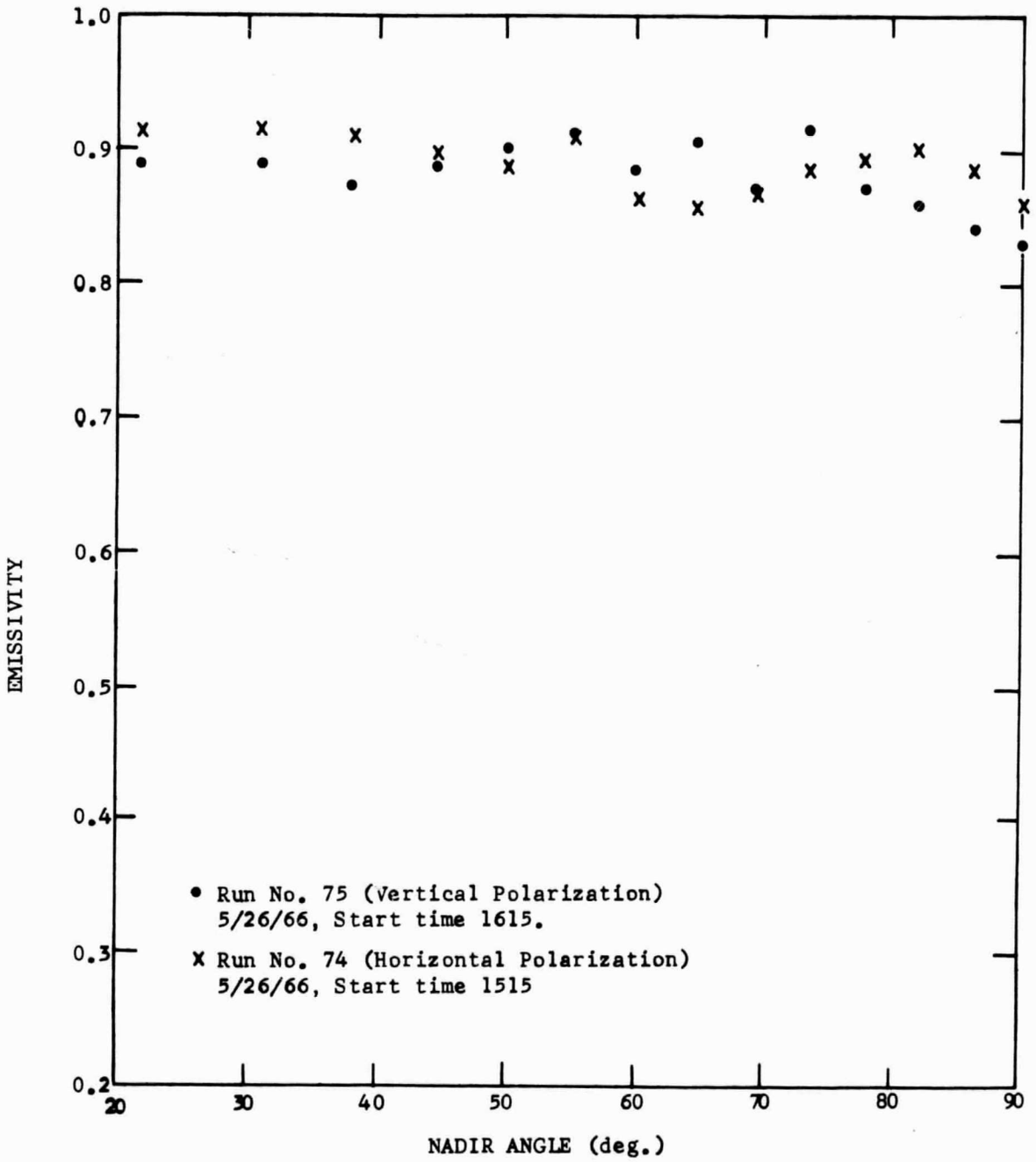


Figure 58 - Diffuse Emissivity vs. Nadir Angle for Saline Surface at 94 GHz.

interlacing between the polarization components is evident. This is, very likely, due to the similarity of T_B's at the two polarizations.

4. Comparison of Derived and Calculated Brightness Temperatures - Salines.

Figures 59 and 60 show comparisons of derived and calculated T_B's at 16.5 GHz, for salines at horizontal and vertical polarizations, respectively. As in the case of similar comparisons made for sea water data, the calculated values include measured surface temperatures and sky brightness temperatures. Specular emissivities, measured at 14 GHz, were used in the calculations. There is very poor agreement between derived and calculated T_B's, for horizontal polarization; the disparity increases with nadir angle. The reason for this is clear from an examination of the plots in Figure 53 — the difference between derived and theoretical emissivities increases markedly with incidence angle, for this polarization. In the case of vertically polarized data, shown in Figure 60, the agreement is considerably better. This is because the above-mentioned difference is smaller.

5. Comparison of Specular and Diffuse Emissivities - Salines

Table LIX presents a comparison of specular and diffuse emissivities at 9.5 GHz, for both polarizations. It is clear that very little difference exists between the emissivities derived by means of scattering coefficients and those derived by the simple relation given in Equation (31), except at a nadir angle of 90 degrees. The high emissivity values, at this nadir angle, appear to be in error since the main antenna lobe is actually viewing the atmosphere at this angle and only the minor lobes subtend the surface material.

Tables LX and LXI present similar comparisons of specular and diffuse emissivities at 16.5 and 94 GHz. The comments made above, for 9.5 GHz, apply equally well to emissivities listed at these frequencies.

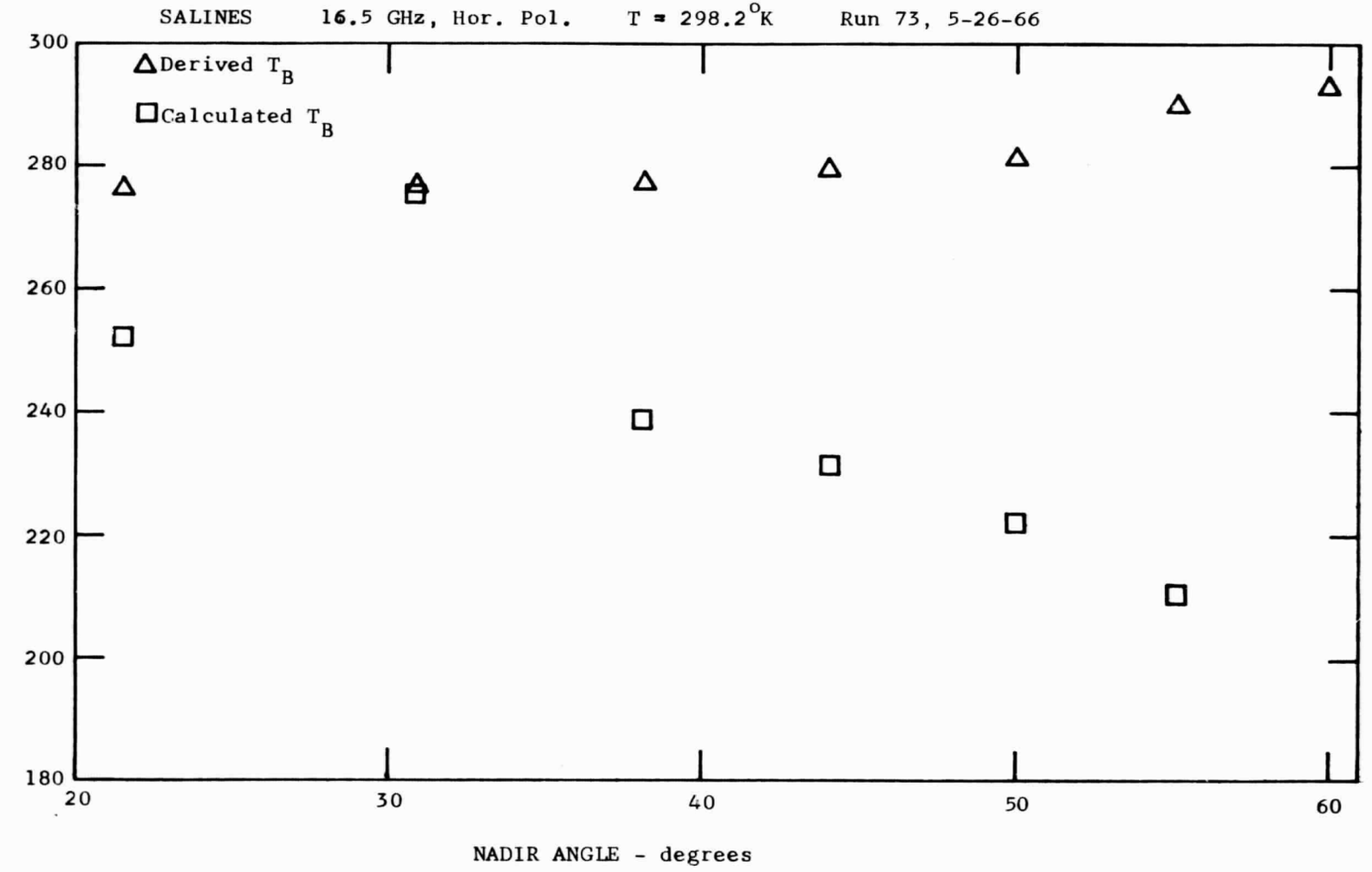


Figure 59 - Comparison of Derived and Calculated Brightness Temperatures at 16.5 GHz (Salines)

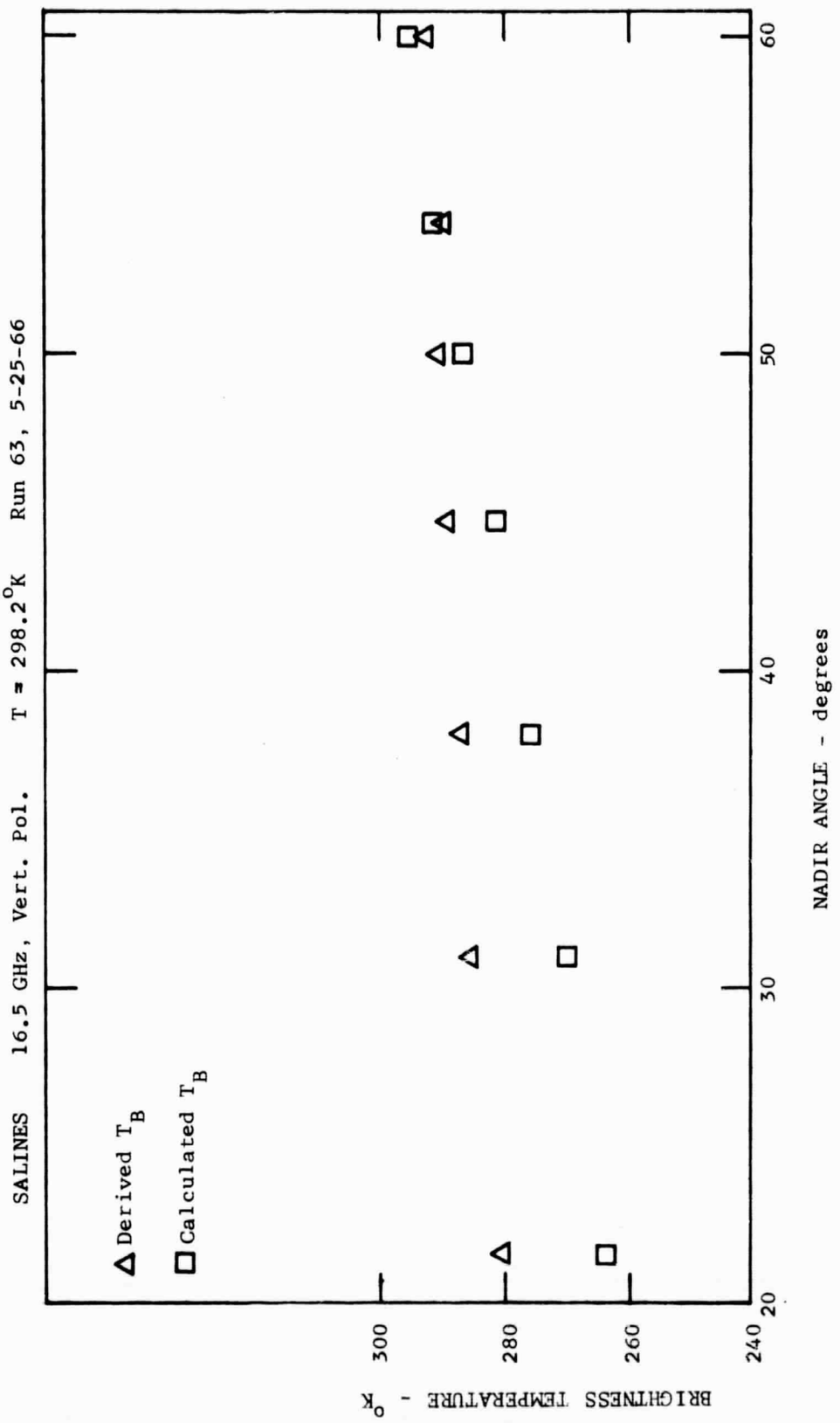


Figure 60 - Calculation of Derived and Calculated Brightness Temperatures at 16.5 GHz (Salines)

TABLE LIX

COMPARISON OF SPECULAR AND DIFFUSE

EMISSIVITIES - SALINES, 9.5 GHz

Run No. 81, Hor. Pol.

Antenna Nadir Angle (deg.)	Specular Emissivity	Diffuse Emissivity	Difference (Spec.-Diffuse)
40	0.869	0.859	0.01
50	0.875	0.874	0.001
60	0.884	0.883	0.001
70	0.866	0.874	-0.008
78	0.880	0.890	-0.010
90	0	0.952	-0.952
Run No. 80, Vert. Pol.			
40	0.888	0.881	0.007
50	0.909	0.905	0.004
60	0.873	0.872	0.001
70	0.865	0.860	0.005
78	0.852	0.856	-0.004
90	0	0.750	-0.750

TABLE LX

COMPARISON OF SPECULAR AND DIFFUSE

EMISSIVITIES - SALINES, 16.5 GHz

Antenna Nadir Angle (deg.)	Specular Emissivity	Diffuse Emissivity	Difference (Spec.-Diffuse)
Run No. 71, Hor. Pol.			
40	0.858	0.857	0.001
50	0.849	0.849	0.0
60	0.889	0.890	-0.001
70	0.894	0.900	-0.006
78	0.876	0.886	-0.010
90	0	0.735	-0.735
Run No. 70, Vert. Pol.			
40	0.871	0.869	0.002
50	0.880	0.879	0.001
60	0.887	0.885	0.002
70	0.895	0.903	-0.008
78	0.863	0.874	-0.001
90	0	0.658	-0.658

TABLE LXI

COMPARISON OF SPECULAR AND DIFFUSE

EMISSIVITIES - SALINES, 94 GHz

Run No. 68, Hor. Pol.

Antenna Nadir Angle (deg.)	Specular Emissivity	Diffuse Emissivity	Difference (Spec.-Diffuse)
40	0.913	0.910	0.003
50	0.899	0.892	0.007
60	0.896	0.897	-0.001
70	0.887	0.896	-0.009
78	0.855	0.883	-0.028
90	0	0.876	-0.876
Run No. 67 Vert. Pol.			
40	0.898	0.880	0.018
50	0.900	0.889	0.001
60	0.885	0.877	0.008
70	0.853	0.863	-0.010
78	0.819	0.884	-0.065
90	0	0.816	-0.816

E. QUARTZ SAND - DATA RESULTS AND ANALYSIS

Figure 61 shows a view of one of the quartz sand dunes at the Brawley site. The surface along the antenna line-of-sight (LOS) appears to be relatively smooth, with the exception of a few "dune buggy" tracks in the foreground. Thus, the brightness temperatures and emissivities should be fairly specular in nature; this is, in fact, the case. The sand dune profile was surveyed along two separate LOS's; the profiles are shown in Figures 62 and 63.

1. 9.5 GHz Data - Quartz Sand

Figure 64 and Tables LXII thru' LXV present measured data for horizontal polarization. It will be recalled that the quartz sand surface sloped downward and upward at slope angles as large as 21 degrees. For this reason, the antenna beam nadir angle, shown in Figure 64 and other similar plots, is not equivalent to the incidence angle, as would be the case with a horizontal surface. Thus, it is somewhat difficult to interpret the angular dependence of brightness and apparent temperatures. The simplest solution, therefore, is to examine the angular dependence in terms of emissivities, which are tabulated and plotted as a function of incidence angle. These are discussed in the following paragraph.

Referring to Figure 64, the surface temperature is shown to be at a rather high level, averaging about 314°K. However, the average brightness temperature is about 100°K lower, indicating a relatively low emissivity. Table LXIV lists emissivities versus incidence angle. The values range from 0.77 to 0.26 at incidence angles between 54° and 88°, respectively. Figure 65 shows a plot of these values. There is good agreement between these emissivities and the plotted 14 GHz data, over most of the angular range.

Figure 66 and Tables LXVI thru' LXIX furnish vertically polarized data. Here the T_B's are very close to the horizontally polarized values, at nadir angles between 20° and 40°, but are about 75°K higher over most of the remaining nadir angle, from 40° to 90°. This reinforces the conclusion

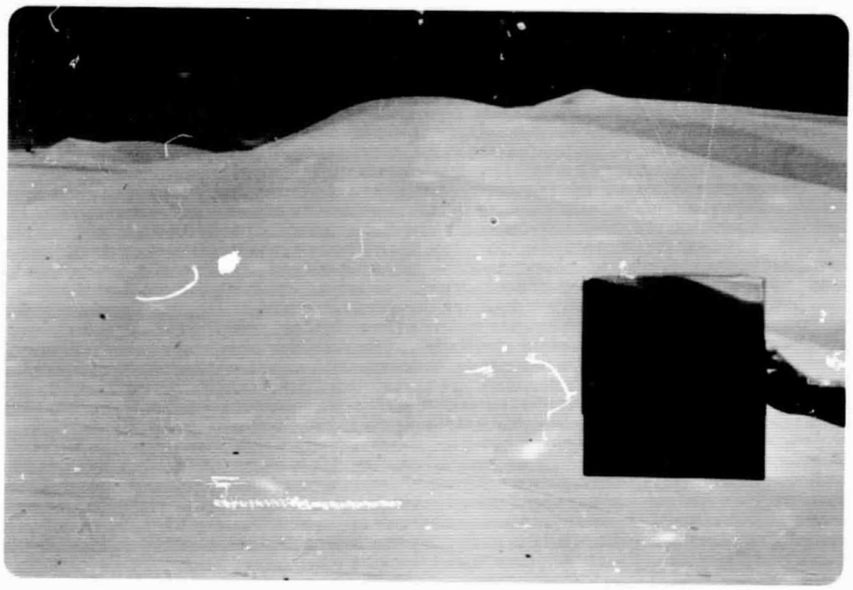


Figure 61 - Quartz Sand Dunes, Brawley, California

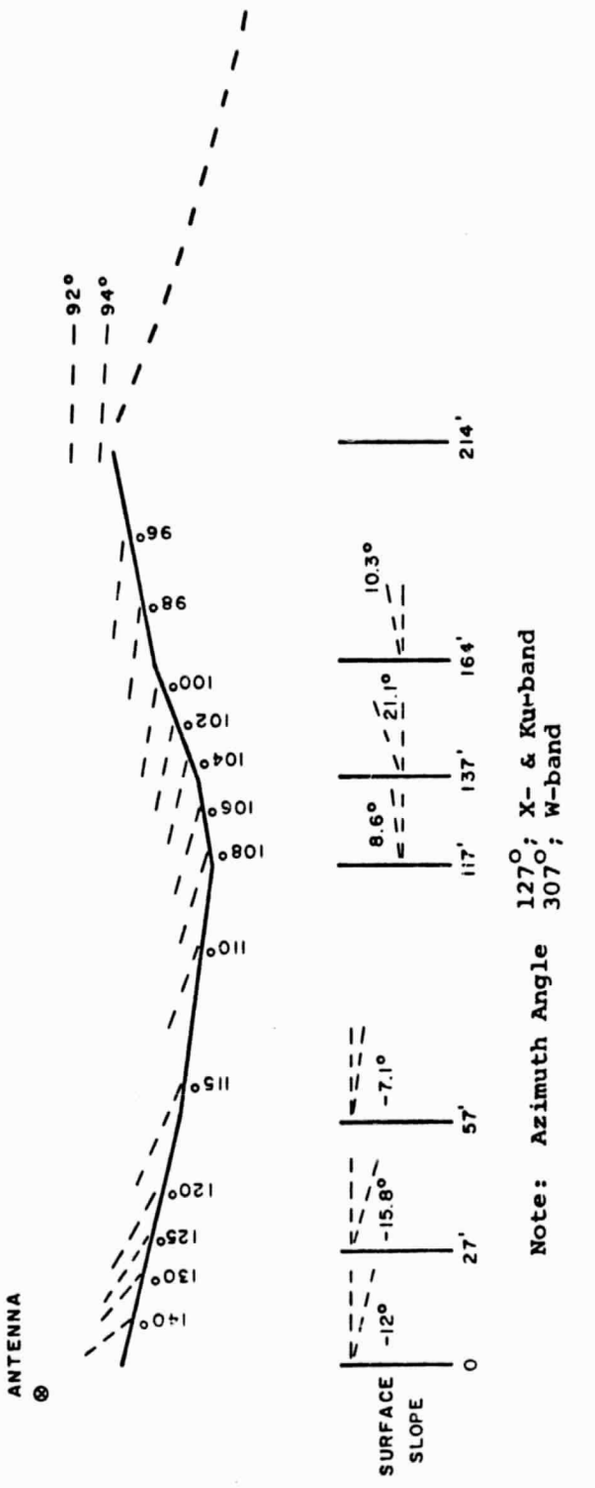


Figure 62 - Brawley Sand Dunes Profile - LOS No. 1

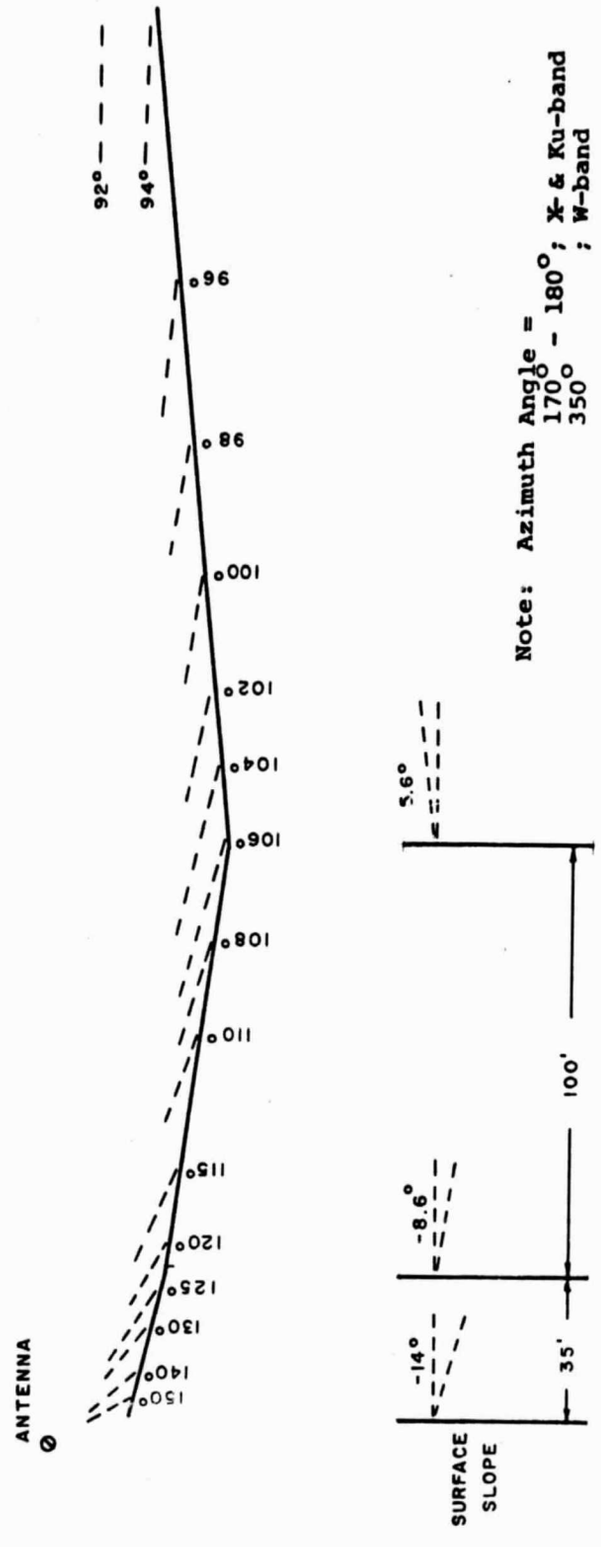


Figure 63 - Brawley Sand Dunes Profile - LOS No. 2

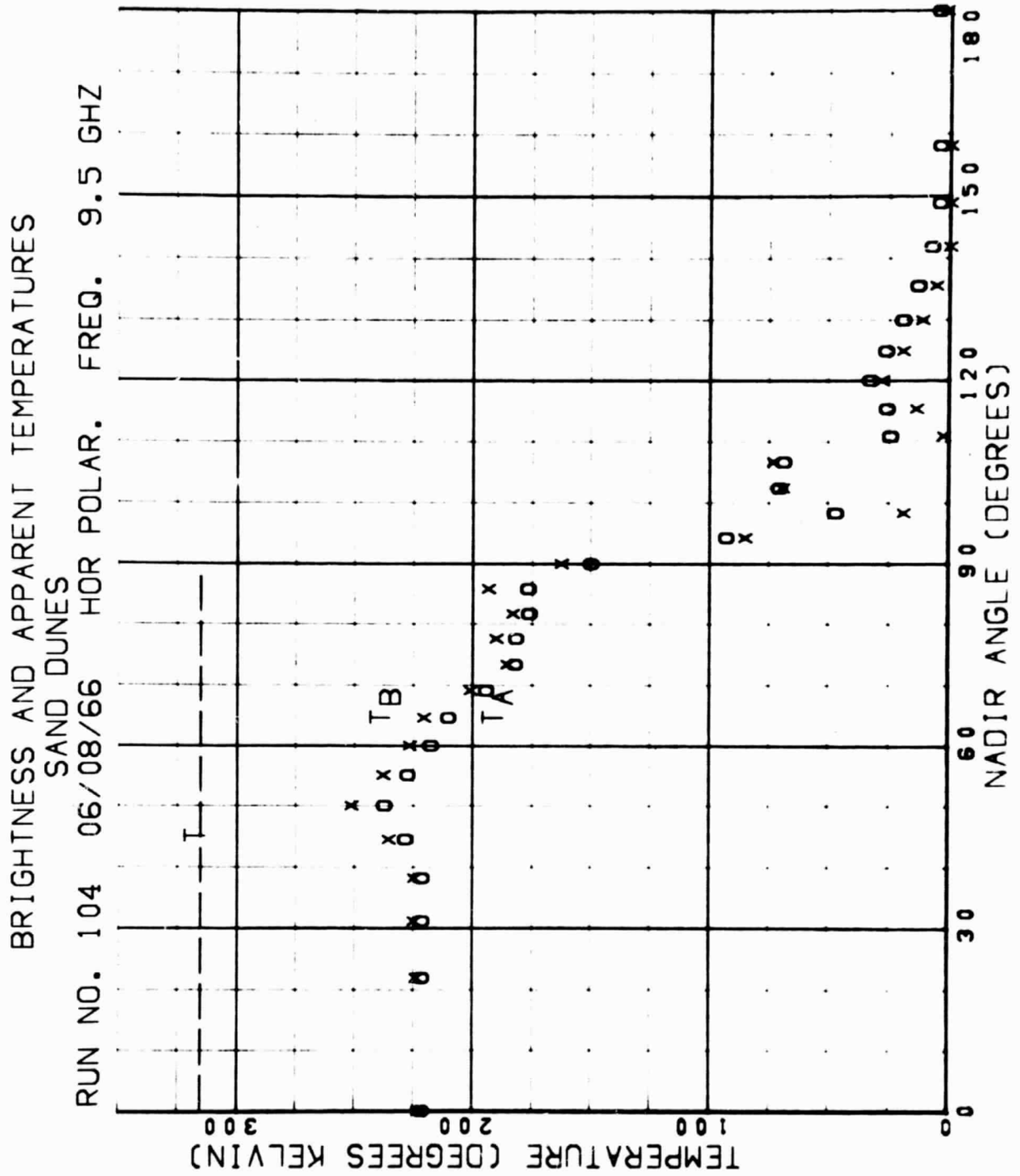


Figure 64 - Measured Quartz Sand Brightness Temperatures, 9.5 GHz, Hor. Pol.

Table IXII - Environmental and Calibration Data, Quartz Sand, 9.5 GHz, Hor. Pol.

TARGET MATERIAL	SAND DUNES
DATA DATE	06/08/66
START TIME	1430
FREQUENCY,GHZ	9.5
POLARIZATION	HOR
ANTENNA AZIMUTH,DEG	170
BAROMETRIC PRESSURE,IN.HG.	29.47
RELATIVE HUMIDITY,0/0	40
AIR TEMPERATURE,DEG F	87
WIND DIRECTION	
WIND SPEED,MPH	5
INTEGRATION TIME,SEC	

THIRD CALIBRATION POINT 3.81DEG.K 6139.00MV.

INITIAL CALIBRATION DATA	
MINIMUM CAL.TEMP,DEG.K	311.20
MAXIMUM CAL.TEMP.DEG.K	403.48
K-FACTOR,DEG.K/MV.	0.36438
Y INTERCEPT	-2232.27

FINAL CALIBRATION DATA	
MINIMUM CAL.TEMP,DEG.K	311.73
MAXIMUM CAL.TEMP.DEG.K	403.52
K-FACTOR,DEG.K/MV.	0.36437
Y INTERCEPT	-2231.78

CALIBRATION CONSTANTS	INITIAL	FINAL	UNITS
HOT LOAD	404.00	404.00	DEG.K
ATTENUATOR	310.50	311.00	DEG.K
WAVE GUIDE SWITCH	308.50	309.00	DEG.K
ANTENNA	301.00	301.00	DEG.K
AVERAGE CAL.DATA -MIN.	6970.82	6966.40	MV.
-MAX.	7240.85	7243.15	MV.

COMMENTS
SKY CLEAR SUNNY

AT ZENITH ANGLE 920.0 RADIATION ANGLE = 740.0 BUT WILL BE CONSIDERED 90 DEG BY THE PROGRAM

TARGET MATERIAL SAND DUNES
DATA DATE 06/08/66
START TIME 1430
FREQUENCY,GHZ 9.5
POLARIZATION HOR

ZENITH ANGLE DEG	BRIGHTNESS TEMP DEG K	TIME	READINGS MV	SURFACE TEMP	SLOPE ANGLE	1/2 IN TEMP DEG K	1 FT TEMP DEG K	2 FT TEMP DEG K	3 FT TEMP DEG K	3 IN TEMP DEG K	6 IN TEMP DEG K	12 IN TEMP DEG K
0.0	1.7	1430	6139.	0.0	0.0	0.0	[illegible]	0.0	0.0	0.0	0.0	0.0
10.0	1.5		6122.	0.0	0.0	0.0	[illegible]	0.0	0.0	0.0	0.0	0.0
20.0	-0.6		6125.	0.0	0.0	0.0	[illegible]	0.0	0.0	0.0	0.0	0.0
30.0	-2.4		6136.	0.0	0.0	0.0	[illegible]	0.0	0.0	0.0	0.0	0.0
40.0	1.8		6149.	0.0	0.0	0.0	[illegible]	0.0	0.0	0.0	0.0	0.0
50.0	11.5		6179.	0.0	0.0	0.0	[illegible]	0.0	0.0	0.0	0.0	0.0
60.0	28.3		6216.	0.0	0.0	0.0	[illegible]	0.0	0.0	0.0	0.0	0.0
62.8	19.5											
64.8	13.2											
65.0	12.6		6195.	0.0	0.0	0.0	[illegible]	0.0	0.0	0.0	0.0	0.0
66.8	14.4											
68.0	15.6											
68.8	16.4											
70.0	17.6		6193.	0.0	0.0	0.0	[illegible]	0.0	0.0	0.0	0.0	0.0
70.8	26.3											
72.8	48.0											
74.8	69.6											
75.0	71.8		6373.	0.0	0.0	0.0	[illegible]	0.0	0.0	0.0	0.0	0.0
77.2	58.1											
78.0	53.1											
80.0	40.6		6271.	0.0	0.0	0.0	[illegible]	0.0	0.0	0.0	0.0	0.0
82.0	22.4		6253.	0.0	0.0	0.0	[illegible]	0.0	0.0	0.0	0.0	0.0
82.2	25.6											
83.0	38.4											
84.0	54.4		6281.	0.0	0.0	0.0	[illegible]	0.0	0.0	0.0	0.0	0.0
85.0	86.6		6385.	0.0	0.0	0.0	[illegible]	0.0	0.0	0.0	0.0	0.0
87.2	109.4											
88.0	124.6		6468.	0.0	0.0	0.0	[illegible]	0.0	0.0	0.0	0.0	0.0
89.2	147.3											
91.0	162.5		6537.	310.0	0.0	307.0	[illegible]	0.0	0.0	0.0	0.0	0.0
92.0	177.6		6572.	310.0	0.0	307.0	[illegible]	0.0	0.0	0.0	0.0	0.0
94.0	192.6		6610.	310.0	5.6	307.0	[illegible]	0.0	0.0	0.0	0.0	0.0
96.0	188.7		6612.	310.0	5.6	307.0	[illegible]	0.0	0.0	0.0	0.0	0.0
98.0	183.7		6608.	317.0	5.6	313.0	[illegible]	0.0	0.0	0.0	0.0	0.0
100.0	186.3		6613.	309.0	5.6	318.0	[illegible]	0.0	0.0	0.0	0.0	0.0
102.0	189.8		6624.	318.0	5.6	320.0	[illegible]	0.0	0.0	0.0	0.0	0.0
104.0	188.6		6629.	318.0	5.6	318.0	[illegible]	0.0	0.0	0.0	0.0	0.0
106.0	186.3		6622.	318.0	5.6	315.0	[illegible]	0.0	0.0	0.0	0.0	0.0
108.0	190.6		6634.	311.0	-8.6	319.0	[illegible]	0.0	0.0	0.0	0.0	0.0
110.0	197.6		6650.	311.0	-8.6	319.0	[illegible]	0.0	0.0	0.0	0.0	0.0
115.0	219.2		6701.	310.0	-8.6	311.0	[illegible]	0.0	0.0	0.0	0.0	0.0
120.0	226.6		6723.	311.0	-8.6	310.0	[illegible]	306.0	309.0	310.0	302.0	300.0
125.0	238.3		6751.	311.0	-14.0	310.0	[illegible]	0.0	0.0	0.0	0.0	0.0
130.0	251.8		6776.	311.0	-14.0	310.0	[illegible]	0.0	0.0	0.0	0.0	0.0
140.0	228.1		6734.	311.0	-14.0	310.0	[illegible]	0.0	0.0	0.0	0.0	0.0

Table LXIII - Brightness Temperatures, Quartz Sand, 9.5 GHz, Hor. Pol.

PAGE 3 RUN 104

TARGET MATERIAL	SAND DUNES
DATA DATE	06/08/66
START TIME	1430
FREQUENCY, GHZ	9.5
POLARIZATION	HOR

ZENITH ANGLE DEG.	NADIR ANGLE DEG.	SLOPE ANGLE DEG.	INCIDENCE ANGLE DEG.	EMISSIVITY
90.0	90.0	0.0	90.0	0.0
92.0	88.0	0.0	88.0	0.286
94.0	86.0	5.6	80.4	0.512
96.0	84.0	5.6	78.4	0.537
98.0	82.0	5.6	76.4	0.541
100.0	80.0	5.6	74.4	0.581
102.0	78.0	5.6	72.4	0.578
104.0	76.0	5.6	70.4	0.575
106.0	74.0	5.6	68.4	0.559
108.0	72.0	-8.6	80.6	0.264
110.0	70.0	-8.6	78.6	0.438
115.0	65.0	-8.6	73.6	0.681
120.0	60.0	-8.6	68.6	0.666
125.0	55.0	-14.0	69.0	0.733
130.0	50.0	-14.0	64.0	0.771
140.0	40.0	-14.0	54.0	0.719

NOTES - NADIR ANGLE = 180 - ZENITH ANGLE

INCIDENCE ANGLE = NADIR ANGLE + OR - SLOPE ANGLE
(MINUS FOR UPSLOPE
PLUS FOR DOWNSLOPE)

Table LXIV - Emissivities of Quartz Sand, 9.5 GHz, Hor. Pol.

RUN NO. 104 06/08/66 HOR POLAR. 9.5 GHZ SAND DUNES

ITERATION NUMBER 0

ZENITH ANGLE (DEG)	BRIGHTNESS TEMP. (DEG K)	APPARENT TEMP. (DEG K)	CORRECTION TEMP. (DEG K)
0.0	1.69	4.75	-3.0582
21.79	-0.84	4.03	-4.8714
31.00	-2.63	4.21	-6.8387
38.21	0.15	7.66	-7.5104
44.42	5.78	13.24	-7.4623
49.99	11.47	19.20	-7.7382
55.15	19.20	26.28	-7.0731
60.00	28.33	32.93	-4.5969
64.62	13.49	25.80	-12.3068
69.08	2.49	24.55	-22.0600
73.40	73.24	69.01	4.2214
77.63	69.39	70.58	-1.1916
81.79	18.97	47.05	-28.0827
85.90	84.81	92.75	-7.9331
90.00	162.50	149.78	12.7232
94.10	193.36	176.68	16.6783
98.21	183.18	175.97	7.2138
102.37	190.41	181.89	8.5261
106.60	185.61	182.24	3.3788
110.92	200.90	194.60	6.3052
115.38	220.87	210.32	10.5543
120.00	226.63	217.87	8.7609
124.85	237.97	227.72	10.1598
130.01	251.83	237.35	14.4814
135.58	235.81	228.70	7.1158
141.79	224.92	221.85	3.0681
149.00	225.03	221.85	3.1841
158.21	224.08	221.85	2.2287
180.00	222.84	221.85	0.9866

ABS. CORRECTION = 8.29E 00 DEG. K

Table LXV - Brightness and Apparent Temperatures, Quartz Sand, 9.5 GHz, Hor. Pol.

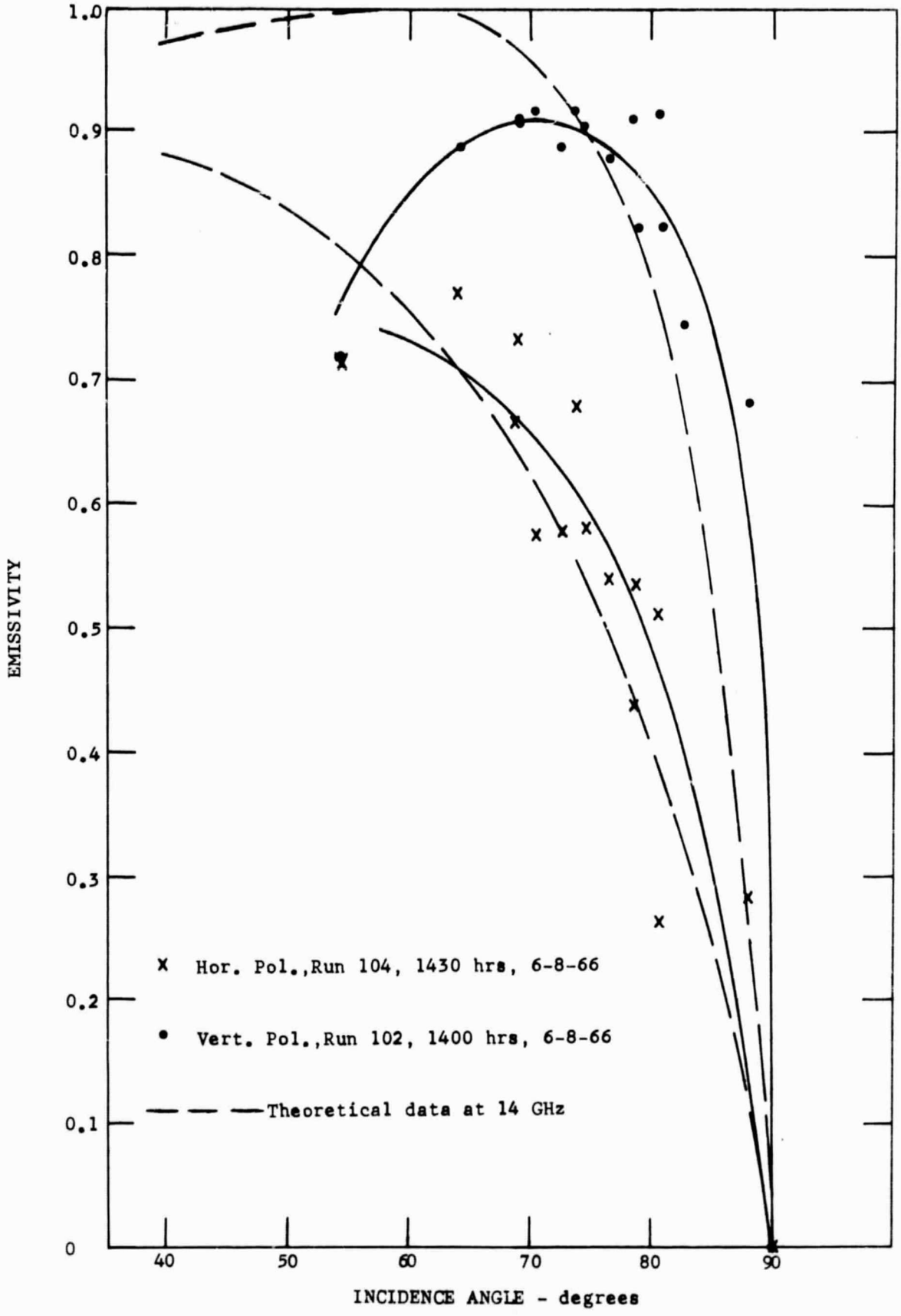


Figure 65 - Derived and Theoretical Emissivities, Quartz Sand - 9.5 GHz.

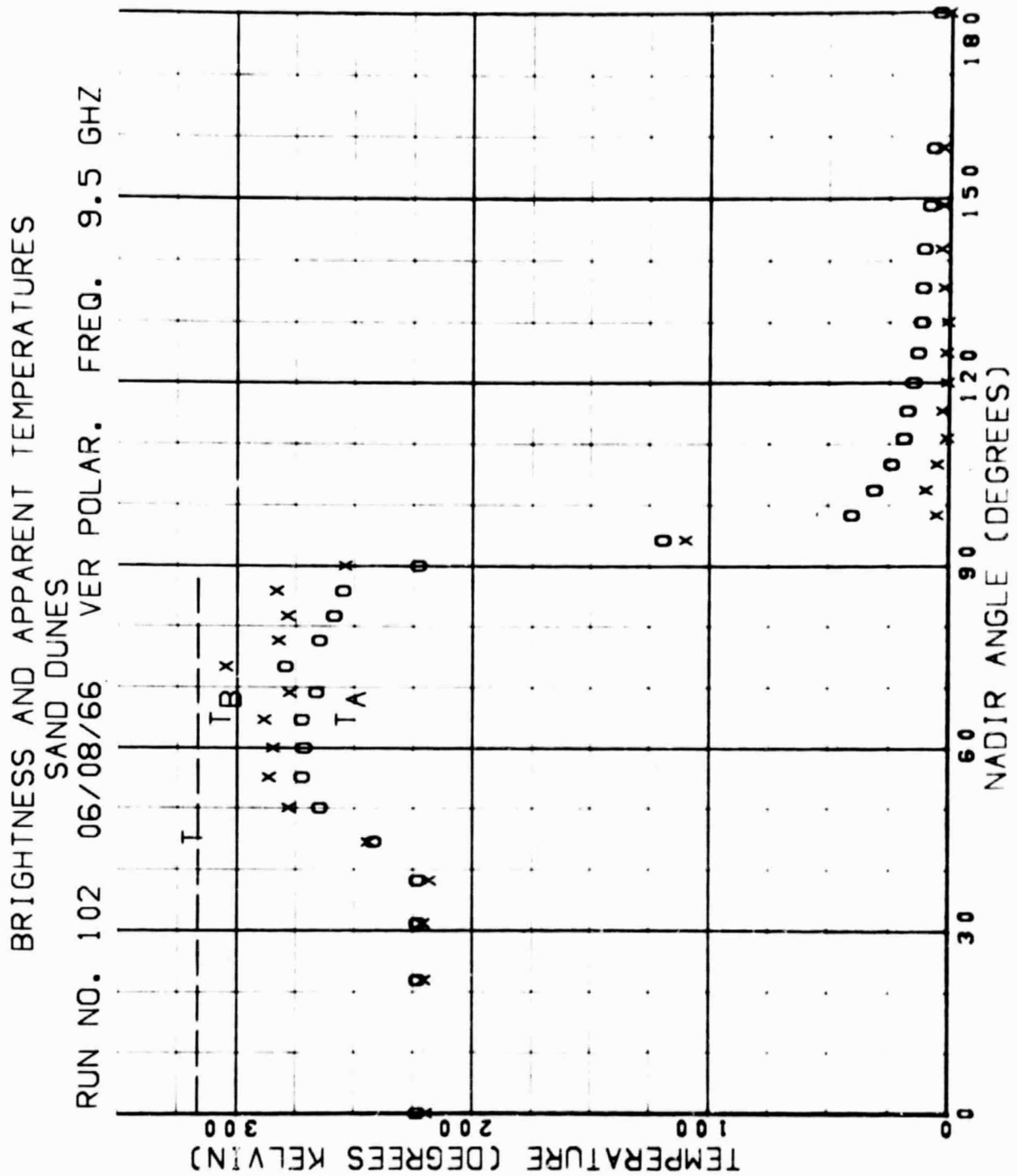


Figure 66 - Measured Quartz Sand Brightness Temperatures, 9.5 GHz, Vert. Pol.

PAGE 1 RUN 122

TARGET MATERIAL	SAND DUNES
DATA DATE	06/08/66
START TIME	1400
FREQUENCY,GHZ	9.5
POLARIZATION	VER
ANTENNA AZIMUTH,DEG	170
BAROMETRIC PRESSURE,IN.HG.	29.47
RELATIVE HUMIDITY,0/0	40
AIR TEMPERATURE,DEG F	87
WIND DIRECTION	
WIND SPEED,MPH	5
INTEGRATION TIME,SEC	

THIRD CALIBRATION POINT 3.81DEG.K 6121.00MV.

INITIAL CALIBRATION DATA

MINIMUM CAL.TEMP,DEG.K	310.61
MAXIMUM CAL.TEMP,DEG.K	403.39
K-FACTOR,DEG.K/MV.	0.35772
Y INTERCEPT	-2185.04

FINAL CALIBRATION DATA

MINIMUM CAL.TEMP,DEG.K	310.61
MAXIMUM CAL.TEMP,DEG.K	403.39
K-FACTOR,DEG.K/MV.	0.35854
Y INTERCEPT	-2190.20

CALIBRATION CONSTANTS	INITIAL	FINAL	UNITS
HOT LOAD	404.00	404.00	DEG.K
ATTENUATOR	310.00	310.00	DEG.K
WAVE GUIDE SWITCH	308.00	308.00	DEG.K
ANTENNA	302.00	302.00	DEG.K
AVERAGE CAL.DATA-MIN.	6967.85	6967.85	MV.
-MAX.	7242.45	7239.23	MV.

COMMENTS

AT ZENITH ANGLE 176. RADIATION ANGLE = 91.2 BUT WILL BE CONSIDERED 90 DEG BY THE PROGRAM

Table LXVI - Environmental and Calibration Data, Quartz Sand, 9.5 GHz, Vert. Pol.

REPRODUCIBILITY OF THE ORIGINAL PAGE IS POOR.

PAGE 2 RUN 172

TARGET MATERIAL SAND DUNES
DATA DATE 06/08/66
START TIME 1400
FREQUENCY,GHZ 9.5
POLARIZATION VER

ZENITH ANGLE DEG	BRIGHTNESS TEMP DEG K	TIME	READINGS MV	SURFACE TEMP	SLOPE ANGLE	1/2 IN TEMP DEG K	1 FT TEMP DEG K	2 FT TEMP DEG K	3 FT TEMP DEG K	3 IN TEMP DEG K	6 IN TEMP DEG K	12 IN TEMP DEG K
0.0	0.0	1400	6121.	0.0	0.0	0.0	0.0	0.0	0.0	0.0	0.0	0.0
10.0	2.0		6123.	0.0	0.0	0.0	0.0	0.0	0.0	0.0	0.0	0.0
20.0	3.0		6096.	0.0	0.0	0.0	0.0	0.0	0.0	0.0	0.0	0.0
30.0	2.7		6130.	0.0	0.0	0.0	0.0	0.0	0.0	0.0	0.0	0.0
40.0	3.3		6139.	0.0	0.0	0.0	0.0	0.0	0.0	0.0	0.0	0.0
50.0	0.9		6141.	0.0	0.0	0.0	0.0	0.0	0.0	0.0	0.0	0.0
60.0	1.1		6150.	0.0	0.0	0.0	0.0	0.0	0.0	0.0	0.0	0.0
64.8	2.4											
65.0	2.5		6158.	0.0	0.0	0.0	0.0	0.0	0.0	0.0	0.0	0.0
65.8	2.2											
68.0	2.0											
68.8	1.9											
70.0	1.7		6161.	0.0	0.0	0.0	0.0	0.0	0.0	0.0	0.0	0.0
70.8	2.5											
72.8	4.6											
74.8	6.6											
76.0	6.8		6181.	0.0	0.0	0.0	0.0	0.0	0.0	0.0	0.0	0.0
77.2	6.9											
78.0	7.0											
80.0	7.1		6206.	0.0	0.0	0.0	0.0	0.0	0.0	0.0	0.0	0.0
82.0	10.5		6223.	0.0	0.0	0.0	0.0	0.0	0.0	0.0	0.0	0.0
82.2	15.6											
83.0	36.0											
84.0	61.4		6284.	0.0	0.0	0.0	0.0	0.0	0.0	0.0	0.0	0.0
85.0	113.3		6450.	0.0	0.0	0.0	0.0	0.0	0.0	0.0	0.0	0.0
87.2	155.7											
88.0	184.0		6627.	0.0	0.0	0.0	0.0	0.0	0.0	0.0	0.0	0.0
89.2	226.3											
90.0	254.6		6731.	308.0	0.0	308.0	0.0	0.0	0.0	0.0	0.0	0.0
92.0	268.7		6843.	308.0	5.6	308.0	0.0	0.0	0.0	0.0	0.0	0.0
94.0	282.9		6821.	308.0	5.6	308.0	0.0	0.0	0.0	0.0	0.0	0.0
95.0	281.4		6821.	308.0	5.6	308.0	0.0	0.0	0.0	0.0	0.0	0.0
99.0	279.1		6831.	317.0	5.6	312.0	0.0	0.0	0.0	0.0	0.0	0.0
101.0	281.5		6845.	309.0	5.6	308.0	0.0	0.0	0.0	0.0	0.0	0.0
102.0	282.3		6847.	317.0	5.6	319.0	0.0	0.0	0.0	0.0	0.0	0.0
104.0	291.3		6860.	317.0	5.6	313.0	0.0	0.0	0.0	0.0	0.0	0.0
106.0	301.9		6903.	318.0	-8.6	316.0	0.0	0.0	0.0	0.0	0.0	0.0
108.0	296.4		6857.	311.0	-8.6	315.0	0.0	0.0	0.0	0.0	0.0	0.0
110.0	283.8		6849.	311.0	-8.6	311.0	0.0	0.0	0.0	0.0	0.0	0.0
115.0	237.9		6873.	312.0	-8.6	312.0	0.0	0.0	0.0	0.0	0.0	0.0
120.0	204.7		6867.	312.0	-8.6	311.0	305.0	305.0	306.0	306.0	305.0	305.0
125.0	206.6		6869.	312.0	-14.0	311.0	0.0	0.0	0.0	0.0	0.0	0.0
130.0	278.4		6849.	312.0	-14.0	311.0	0.0	0.0	0.0	0.0	0.0	0.0
140.0	225.9		6732.	312.0	-14.0	311.0	0.0	0.0	0.0	0.0	0.0	0.0

Table LXVII - Brightness Temperatures, Quartz Sand, 9.5 GHz, Vert. Pol.

TARGET MATERIAL	SAND DUNES
DATA DATE	06/08/66
START TIME	1400
FREQUENCY, GHZ	9.5
POLARIZATION	VER

ZENITH ANGLE DEG.	NADIR ANGLE DEG.	SLOPE ANGLE DEG.	INCIDENCE ANGLE DEG.	EMISSIVITY
90.0	90.0	0.0	90.0	0.0
92.0	88.0	0.0	88.0	0.684
94.0	86.0	5.6	80.4	0.917
96.0	84.0	5.6	78.4	0.912
98.0	82.0	5.6	76.4	0.880
100.0	80.0	5.6	74.4	0.907
102.0	78.0	5.6	72.4	0.890
104.0	76.0	5.6	70.4	0.918
106.0	74.0	-8.6	82.6	0.747
108.0	72.0	-8.6	80.6	0.827
110.0	70.0	-8.6	78.6	0.825
115.0	65.0	-8.6	73.6	0.919
120.0	60.0	-8.6	68.6	0.911
125.0	55.0	-14.0	69.0	0.908
130.0	50.0	-14.0	64.0	0.890
140.0	40.0	-14.0	54.0	0.722

NOTES - NADIR ANGLE = 180 - ZENITH ANGLE

INCIDENCE ANGLE = NADIR ANGLE + OR - SLOPE ANGLE
(MINUS FOR UPSLOPE
PLUS FOR DOWNSLOPE)

Table LXVIII - Emissivities of Quartz Sand, 9.5 GHz, Vert. Pol.

RUN NO. 102 06/08/66 VER POLAR. 9.5 GHZ SAND DUNES

ITERATION NUMBER 0

ZENITH ANGLE (DEG)	BRIGHTNESS TEMP. (DEG K)	APPARENT TEMP. (DEG K)	CORRECTION TEMP. (DEG K)
0.0	0.87	4.57	-3.7042
21.79	3.24	6.80	-3.5621
31.00	2.65	8.28	-5.6333
38.21	3.64	10.60	-6.9580
44.42	2.52	11.40	-8.8809
49.99	0.86	11.70	-10.8408
55.15	1.45	13.29	-11.8371
60.00	1.13	14.78	-13.6515
64.62	2.62	17.42	-14.7980
69.08	0.86	18.68	-17.8239
73.40	4.95	23.81	-18.8595
77.63	9.82	30.75	-20.9375
81.79	5.06	40.26	-35.2011
85.90	109.92	119.52	-9.6064
90.00	254.60	222.81	31.7910
94.10	283.58	255.21	28.3617
98.21	278.89	259.23	19.6661
102.37	282.61	265.38	17.2332
106.60	305.16	279.71	25.4462
110.92	278.02	266.62	11.4001
115.38	288.82	272.70	16.1188
120.00	284.73	271.66	13.0732
124.85	286.81	272.47	14.3330
130.01	278.43	265.22	13.2076
135.58	244.65	242.00	2.6451
141.79	218.26	223.63	-5.3693
149.00	220.99	223.63	-2.6361
158.21	220.56	223.63	-3.0658
180.00	219.74	223.63	-3.8866

ABS. CORRECTION = 1.35E 01 DEG. K

Table LXIX - Brightness and Apparent Temperatures, Quartz Sand, 9.5 GHz, Vert. Pol.

that this material is quite specular. In Table LXVIII, the emissivities range from 0.68 to 0.92 at incidence angles between 54° and 88°, with a broad peak between incidence angles of 68° and 80°. A plot of this data, in Figure 65, indicates the Brewster Angle to be at approximately 71°. This is considerably removed from the theoretical value of approximately 60° (at 14 GHz) and indicates the possibility of a higher dielectric permittivity at 9.5 GHz than at 14 GHz - the Brewster Angle position tends to increase directly with dielectric permittivity. There is considerable separation between derived emissivities, at the two polarizations, in the vicinity of the Brewster Angle, which confirms the specular nature of Quartz Sand at this frequency.

2. 16.5 GHz Data - Quartz Sand

Figure 67 and Tables LXX thru' LXXIII present data for horizontal polarization. The brightness temperatures appear to be approximately 15°K higher, between nadir angles of 20° and 45°, than the horizontally polarized 9.5 GHz values. Referring to Table LXXII, the emissivities are also somewhat higher, falling between 0.30 and 0.79 at incidence angles from 64° to 88°. Figure 68 shows a plot of these values. There is relatively poor agreement between derived and theoretical emissivities, although the latter are at 14 GHz. A possible reason for the lack of agreement is the broad scattering of data points in the derived values.

Figure 69 shows theoretical plots of Quartz Sand emissivities at 14 GHz. Due to the very low dielectric permittivity, the emissivities are quite high over a broad range of incidence angles; as a result the percentage polarization is relatively low - at an incidence angle of 60°, it is only approximately 14%.

Figure 70 and Tables LXXIV thru' LXXVII furnish measured data for vertical polarization. The brightness temperatures are considerably higher than those for horizontal polarization, with an average value of 285°K over a nadir angle range of 20° to 90°. In Table LXXVI the derived emissivities range from 0.56 to 0.94 in this angular interval.

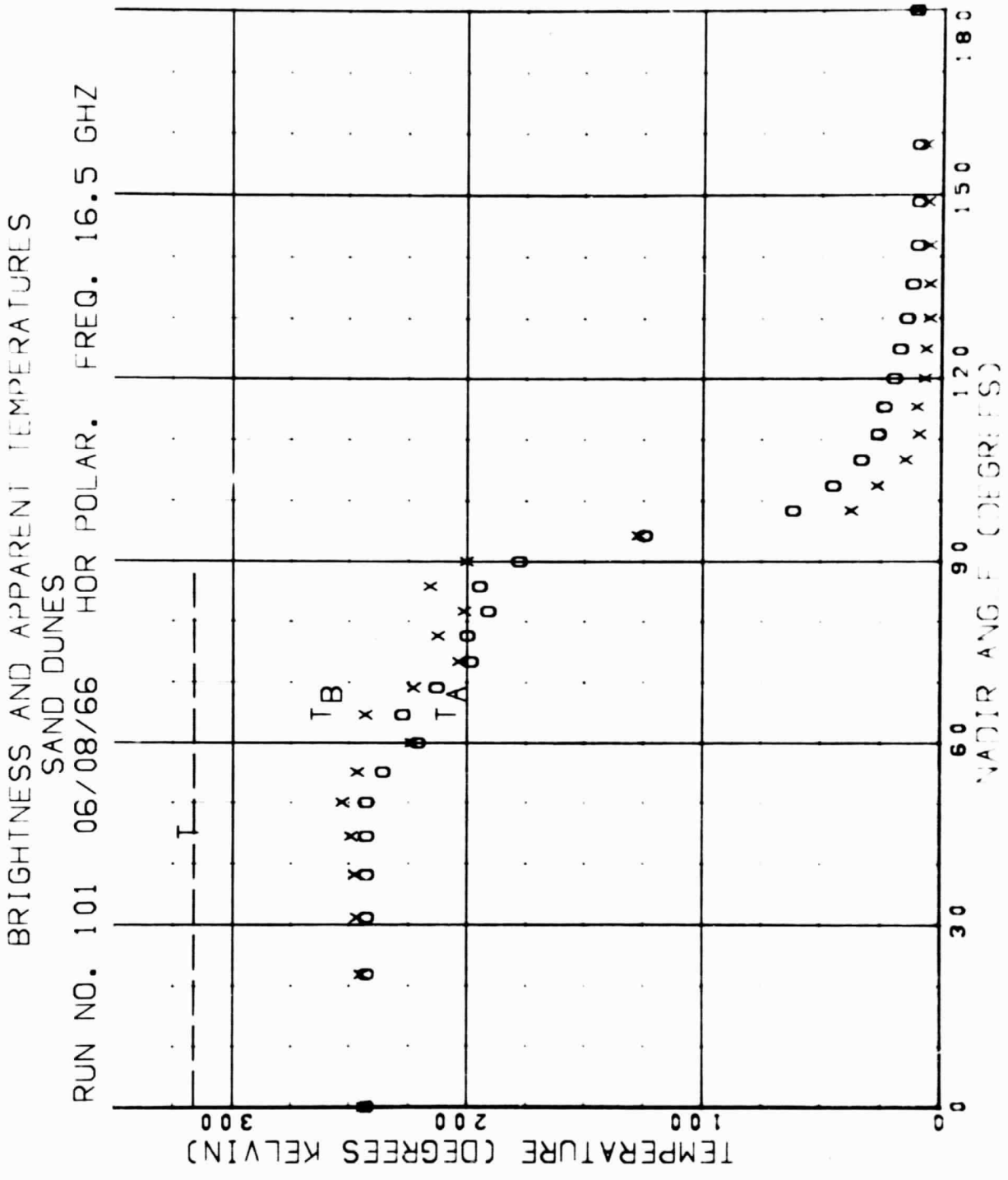


Figure 67 - Measured Quartz Sand Brightness Temperatures, 16.5 GHz, Hor. Pol.

PAGE 1 RUN 1?1

TARGET MATERIAL	SAND DUNES
DATA DATE	?6/?8/66
START TIME	1145
FREQUENCY,GHZ	16.5
POLARIZATION	HOR
ANTENNA AZIMUTH,DEG	17?
BAROMETRIC PRESSURE,IN.HG.	29.46
RELATIVE HUMIDITY,?/?	4?
AIR TEMPERATURE,DEG F	87
WIND DIRECTION	
WIND SPEED,MPH	5
INTEGRATION TIME,SEC	1

THIRD CALIBRATION POINT 11.63DEG.K 6572.?3MV.

INITIAL CALIBRATION DATA	
MINIMUM CAL.TEMP,DEG.K	3?8.8?
MAXIMUM CAL.TEMP,DEG.K	3?1.68
K-FACTOR,DEG.K/MV.	?.67?49
Y INTERCEPT	-4335.32
FINAL CALIBRATION DATA	
MINIMUM CAL.TEMP,DEG.K	3?7.43
MAXIMUM CAL.TEMP,DEG.K	389.34
K-FACTOR,DEG.K/MV.	?.69357
Y INTERCEPT	-4546.??

CALIBRATION CONSTANTS	INITIAL	FINAL	UNITS
HOT LOAD	394.??	392.??	DEG.K
ATTENUATOR	3?8.??	3?7.??	DEG.K
WAVE GUIDE SWITCH	3?4.??	3?7.??	DEG.K
ANTENNA	3?3.??	3?3.??	DEG.K
AVERAGE CAL.DATA-MIN.	7?19.7?	6993.85	MV.
-MAX.	7136.6?	7118.9?	MV.

COMMENTS
SUNNY THIN SCATTERED CLOUDS NOT ALONG LOS

Table LXXI - Brightness Temperatures, Quartz Sand, 16.5 GHz, Hor. Pol.

PAGE 2 RUN 101

TARGET MATERIAL SAND DUNES
DATA DATE 06/08/66
START TIME 1145
FREQUENCY,GHZ 16.5
POLARIZATION HOR

ZENITH ANGLE DEG	BRIGHTNESS TEMP DEG K	TIME	READINGS MV	SURFACE TEMP	SLOPE ANGLE	1/2 IN TEMP DEG K	1 FT TEMP DEG K	2 FT TEMP DEG K	3 FT TEMP DEG K	3 IN TEMP DEG K	6 IN TEMP DEG K	12 IN TEMP DEG K
0.0	11.0	1145	6572.	0.0	0.0	0.0	0.0	0.0	0.0	0.0	0.0	0.0
10.0	9.1		6572.	0.0	0.0	0.0	0.0	0.0	0.0	0.0	0.0	0.0
20.0	7.2		6570.	0.0	0.0	0.0	0.0	0.0	0.0	0.0	0.0	0.0
30.0	6.3		6570.	0.0	0.0	0.0	0.0	0.0	0.0	0.0	0.0	0.0
40.0	5.1		6571.	0.0	0.0	0.0	0.0	0.0	0.0	0.0	0.0	0.0
50.0	5.4		6577.	0.0	0.0	0.0	0.0	0.0	0.0	0.0	0.0	0.0
60.0	7.1		6585.	0.0	0.0	0.0	0.0	0.0	0.0	0.0	0.0	0.0
62.8	9.0											
64.8	10.3											
65.0	10.4		6591.	0.0	0.0	0.0	0.0	0.0	0.0	0.0	0.0	0.0
66.8	10.4											
68.8	10.5											
70.0	10.5		6594.	0.0	0.0	0.0	0.0	0.0	0.0	0.0	0.0	0.0
70.8	11.9											
72.8	15.5											
74.8	19.1											
75.0	19.4		6609.	0.0	0.0	0.0	0.0	0.0	0.0	0.0	0.0	0.0
77.2	25.3											
78.0	27.4											
80.0	32.7		6633.	0.0	0.0	0.0	0.0	0.0	0.0	0.0	0.0	0.0
82.0	42.0		6647.	0.0	0.0	0.0	0.0	0.0	0.0	0.0	0.0	0.0
82.2	46.4											
83.0	63.9											
84.0	85.8		6676.	0.0	0.0	0.0	0.0	0.0	0.0	0.0	0.0	0.0
86.0	129.3		6741.	0.0	0.0	0.0	0.0	0.0	0.0	0.0	0.0	0.0
87.2	150.7											
88.0	165.0		6785.	0.0	0.0	0.0	0.0	0.0	0.0	0.0	0.0	0.0
89.2	186.5											
90.0	200.8		6816.	309.0	0.0	308.0	0.0	0.0	0.0	0.0	0.0	0.0
92.0	208.1		6828.	309.0	0.0	308.0	0.0	0.0	0.0	0.0	0.0	0.0
94.0	215.5		6840.	309.0	5.6	308.0	0.0	0.0	0.0	0.0	0.0	0.0
95.0	219.1		6838.	309.0	5.6	308.0	0.0	0.0	0.0	0.0	0.0	0.0
98.0	232.1		6832.	315.0	5.6	310.0	0.0	0.0	0.0	0.0	0.0	0.0
100.0	236.2		6845.	308.0	5.6	308.0	0.0	0.0	0.0	0.0	0.0	0.0
102.0	241.7		6846.	316.0	5.6	308.0	0.0	0.0	0.0	0.0	0.0	0.0
104.0	239.3		6842.	316.0	5.6	308.0	0.0	0.0	0.0	0.0	0.0	0.0
105.0	235.1		6842.	319.0	5.6	315.0	0.0	0.0	0.0	0.0	0.0	0.0
108.2	218.0		6845.	311.0	-8.6	310.0	0.0	0.0	0.0	0.0	0.0	0.0
110.0	219.1		6858.	312.0	-8.6	310.0	0.0	0.0	0.0	0.0	0.0	0.0
116.0	241.7		6885.	312.0	-8.6	311.0	0.0	0.0	0.0	0.0	0.0	0.0
123.0	224.		6874.	312.0	-8.6	311.0	305.0	305.0	307.0	308.0	305.0	305.0
125.0	247.2		6896.	312.0	-14.1	311.0	0.0	0.0	0.0	0.0	0.0	0.0
130.0	253.3		6905.	312.0	-14.1	311.0	0.0	0.0	0.0	0.0	0.0	0.0

PAGE 3 RUN 1 1

TARGET MATERIAL	SAND DUNES
DATA DATE	6/ 8/66
START TIME	1145
FREQUENCY,GHZ	16.5
POLARIZATION	HOR

ZENITH ANGLE DEG.	NADIR ANGLE DEG.	SLOPE ANGLE DEG.	INCIDENCE ANGLE DEG.	EMISSIVITY
90.0	90.0	0.0	90.0	0.0
92.0	88.0	0.0	88.0	0.299
94.0	86.0	5.6	80.4	0.677
96.0	84.0	5.6	78.4	0.660
98.0	82.0	5.6	76.4	0.627
100.0	80.0	5.6	74.4	0.658
102.0	78.0	5.6	72.4	0.659
104.0	76.0	5.6	70.4	0.651
106.0	74.0	5.6	68.4	0.632
108.0	72.0	-8.6	80.6	0.189
110.0	70.0	-8.6	78.6	0.423
115.0	65.0	-8.6	73.6	0.735
120.0	60.0	-8.6	68.6	0.693
125.0	55.0	-14.0	69.0	0.739
130.0	50.0	-14.0	64.0	0.794

NOTES - NADIR ANGLE = 180 - ZENITH ANGLE

INCIDENCE ANGLE = NADIR ANGLE + OR - SLOPE ANGLE
(MINUS FOR UPSLOPE
PLUS FOR DOWNSLOPE)

Table LXXII - Emissivities of Quartz Sand, 16.5 GHz, Hor. Pol.

RUN NO. 101 06/08/66 HOR POLAR. 16.5 GHZ SAND DUNES

ITERATION NUMBER 0

ZENITH ANGLE (DEG)	BRIGHTNESS TEMP. (DEG K)	APPARENT TEMP. (DEG K)	CORRECTION TEMP. (DEG K)
0.0	11.01	11.38	-0.3668
21.79	6.89	9.62	-2.7345
31.00	6.27	9.95	-3.6761
38.21	5.10	10.51	-5.4135
44.42	5.20	12.33	-7.1304
49.99	5.38	14.46	-9.0790
55.15	6.62	17.19	-10.5792
60.00	7.14	19.77	-12.6251
64.62	10.50	23.94	-13.4400
69.08	9.23	26.15	-16.9126
73.40	15.04	33.14	-18.1025
77.63	26.67	45.15	-18.4827
81.79	37.31	61.71	-24.4000
85.90	127.53	124.58	2.9582
90.00	200.77	178.11	22.6565
94.10	215.81	194.80	21.0031
98.21	201.35	191.38	9.9699
102.37	212.76	199.88	12.8827
106.60	203.68	198.55	5.1302
110.92	223.13	213.05	10.0804
115.38	243.46	227.65	15.8078
120.00	224.02	220.94	3.0769
124.85	246.98	236.26	10.7211
130.01	253.30	243.06	10.2353
135.58	249.72	243.06	6.6554
141.79	248.05	243.06	4.9935
149.00	246.69	243.06	3.6309
158.21	245.42	243.06	2.3631
180.00	244.31	243.06	1.2515

ABS. CORRECTION = 9.87E 00 DEG. K

Table LXXIII - Brightness and Apparent Temperatures, Quartz Sand, 16.5 GHz, Hor. Pol.

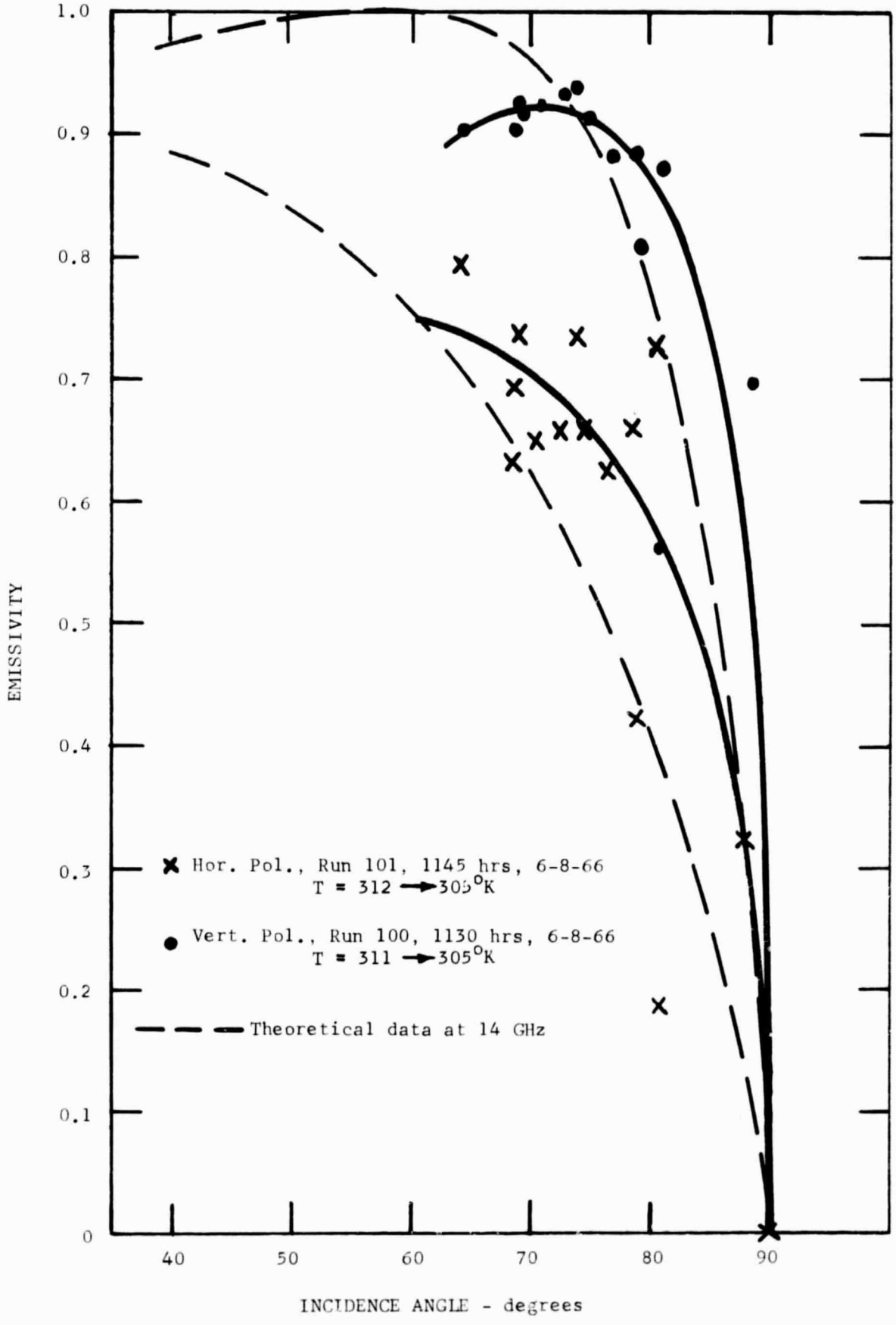


Figure 68 - Derived and Theoretical Specular Emissivities, Quartz Sand - 16.5 GHz

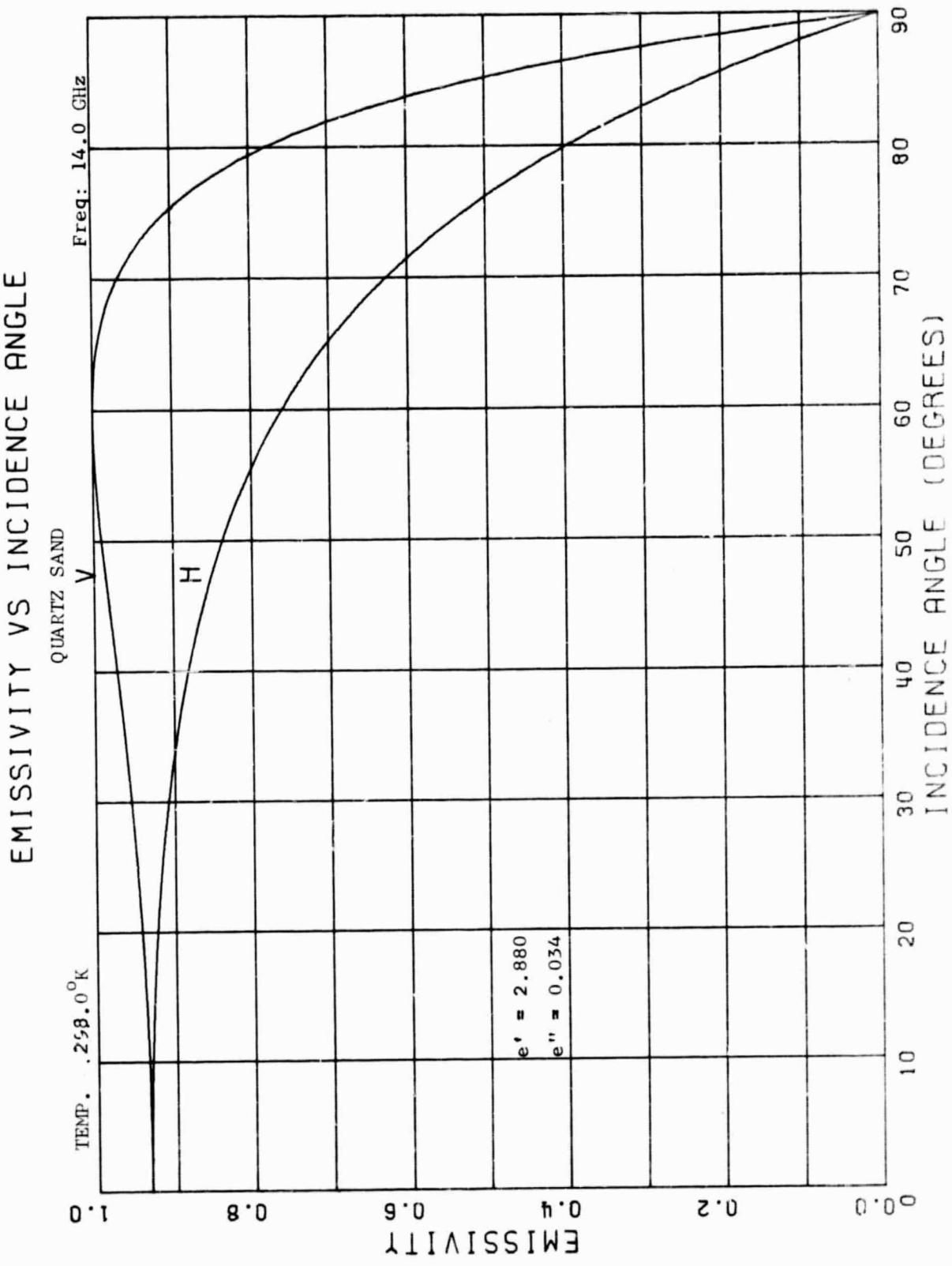


Figure 69 - Theoretical Emissivity of Quartz Sand - 14.0 GHz

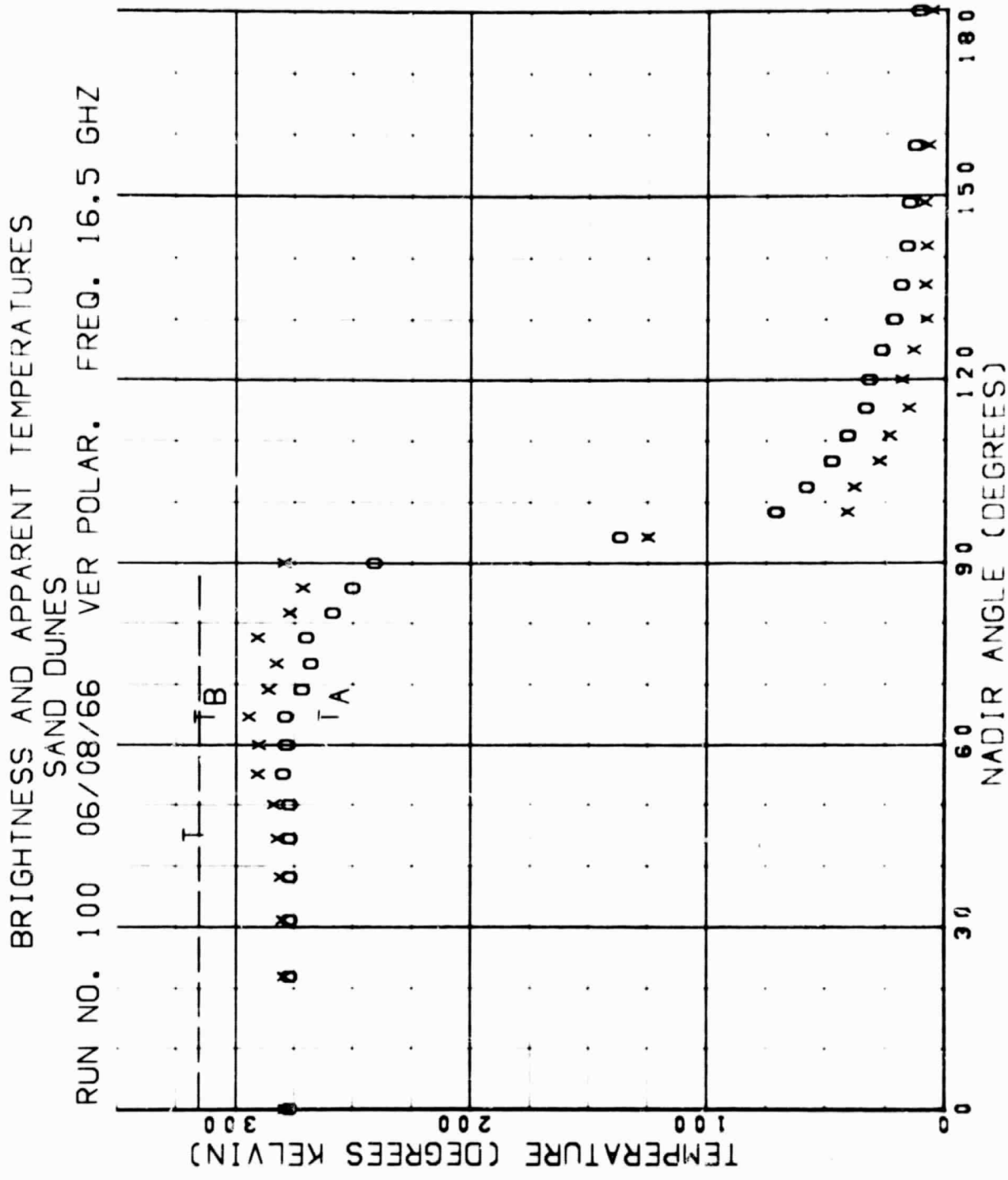


Figure 70 - Measured Quartz Sand Brightness Temperatures, 16.5 GHz, Vert. Pol.

PAGE 1 RUN 100

TARGET MATERIAL	SAND DUNES
DATA DATE	06/08/65
START TIME	1130
FREQUENCY,GHZ	16.5
POLARIZATION	VER
ANTENNA AZIMUTH,DEG	170
BAROMETRIC PRESSURE,IN.HG.	29.44
RELATIVE HUMIDITY,0/0	42
AIR TEMPERATURE,DEG F	85
WIND DIRECTION	WNW
WIND SPEED,MPH	4
INTEGRATION TIME,SEC	1

THIRD CALIBRATION POINT 11.50DEG.K 6577.00MV.

INITIAL CALIBRATION DATA	
MINIMUM CAL.TEMP,DEG.K	305.58
MAXIMUM CAL.TEMP.DEG.K	391.34
K-FACTOR,DEG.K/MV.	0.66547
Y INTERCEPT	-4365.11

FINAL CALIBRATION DATA	
MINIMUM CAL.TEMP,DEG.K	305.42
MAXIMUM CAL.TEMP.DEG.K	389.26
K-FACTOR,DEG.K/MV.	0.65432
Y INTERCEPT	-4292.38

CALIBRATION CONSTANTS	INITIAL	FINAL	UNITS
HOT LOAD	394.00	392.00	DEG.K
ATTENUATOR	305.00	305.00	DEG.K
WAVE GUIDE SWITCH	303.00	304.00	DEG.K
ANTENNA	301.00	302.00	DEG.K
AVERAGE CAL.DATA-MIN.	7016.65	7029.90	MV.
-MAX.	7149.15	7152.65	MV.

COMMENTS
SKY CLEAR SUNNY NO HAZE

Table LXXIV - Environmental and Calibration Data, Quartz Sand 16.5 GHz, Vert. Pol.

TARGET MATERIAL SAND DUNES
DATA DATE 16/ 8/66
START TIME 1130
FREQUENCY,GHZ 16.5
POLARIZATION VER

ZENITH ANGLE DEG	BRIGHTNESS TEMP DEG K	TIME	READINGS MV	SURFACE TEMP	SLOPE ANGLE	1/2 IN TEMP DEG K	1 FT TEMP DEG K	2 FT TEMP DEG K	3 FT TEMP DEG K	3 IN TEMP DEG K	6 IN TEMP DEG K	12 IN TEMP DEG K
[illegible]	6.7	1130	6577.	[illegible]	[illegible]	[illegible]	[illegible]	0.0	0.0	0.0	0.0	0.0
[illegible]	7.[illegible]		6576.	[illegible]	[illegible]	[illegible]	[illegible]	0.0	0.0	0.0	0.0	0.0
[illegible]	7.3		6578.	[illegible]	[illegible]	[illegible]	[illegible]	0.0	0.0	0.0	0.0	0.0
[illegible]	9.1		6582.	[illegible]	[illegible]	[illegible]	[illegible]	0.0	0.0	0.0	0.0	0.0
[illegible]	8.5		6585.	[illegible]	[illegible]	[illegible]	[illegible]	0.0	0.0	0.0	0.0	0.0
[illegible]	8.6		6592.	[illegible]	[illegible]	[illegible]	[illegible]	0.0	0.0	0.0	0.0	0.0
[illegible]	18.3		6608.	[illegible]	[illegible]	[illegible]	[illegible]	0.0	0.0	0.0	0.0	0.0
62.8	17.2											
64.8	16.4											
[illegible]	16.3		6610.	[illegible]	[illegible]	[illegible]	[illegible]	0.0	0.0	0.0	0.0	0.0
65.8	19.2											
68.8	22.5											
[illegible]	24.4		6623.	[illegible]	[illegible]	[illegible]	[illegible]	0.0	0.0	0.0	0.0	0.0
70.8	25.6											
72.8	28.4											
74.8	31.3											
[illegible]	31.6		6634.	[illegible]	[illegible]	[illegible]	[illegible]	0.0	0.0	0.0	0.0	0.0
77.2	35.1											
[illegible]	36.3											
[illegible]	39.5		6659.	[illegible]	[illegible]	[illegible]	[illegible]	0.0	0.0	0.0	0.0	0.0
[illegible]	45.[illegible]		6667.	[illegible]	[illegible]	[illegible]	[illegible]	0.0	0.0	0.0	0.0	0.0
82.2	49.1											
[illegible]	65.5											
[illegible]	85.9		6691.	[illegible]	[illegible]	[illegible]	[illegible]	0.0	0.0	0.0	0.0	0.0
[illegible]	128.6		6771.	[illegible]	[illegible]	[illegible]	[illegible]	0.0	0.0	0.0	0.0	0.0
87.2	173.9											
[illegible]	204.2		6891.	[illegible]	[illegible]	[illegible]	[illegible]	0.0	0.0	0.0	0.0	0.0
89.2	249.6											
[illegible]	279.9		6925.	307.[illegible]	[illegible]	317.[illegible]	[illegible]	0.0	0.0	0.0	0.0	0.0
[illegible]	275.8		6930.	307.[illegible]	[illegible]	317.[illegible]	[illegible]	0.0	0.0	0.0	0.0	0.0
[illegible]	271.8		6940.	307.[illegible]	5.6	317.[illegible]	[illegible]	0.0	0.0	0.0	0.0	0.0
[illegible]	274.3		6946.	307.[illegible]	5.6	317.[illegible]	[illegible]	0.0	0.0	0.0	0.0	0.0
[illegible]	277.1		6953.	310.[illegible]	5.6	318.[illegible]	[illegible]	0.0	0.0	0.0	0.0	0.0
[illegible]	283.2		6960.	307.[illegible]	5.6	317.[illegible]	[illegible]	0.0	0.0	0.0	0.0	0.0
[illegible]	289.8		6971.	309.[illegible]	5.6	312.[illegible]	[illegible]	0.0	0.0	0.0	0.0	0.0
[illegible]	288.[illegible]		6969.	310.[illegible]	5.6	312.[illegible]	[illegible]	0.0	0.0	0.0	0.0	0.0
[illegible]	284.3		6968.	313.[illegible]	5.6	312.[illegible]	[illegible]	0.0	0.0	0.0	0.0	0.0
[illegible]	284.1		6971.	311.[illegible]	-8.6	31[illegible]	[illegible]	0.0	0.0	0.0	0.0	0.0
[illegible]	285.5		6973.	312.[illegible]	-8.6	31[illegible]	[illegible]	0.0	0.0	0.0	0.0	0.0
[illegible]	294.[illegible]		6986.	31[illegible]	-8.6	31[illegible]	[illegible]	0.0	0.0	0.0	0.0	0.0
[illegible]	298.3		6985.	311.[illegible]	-8.6	31[illegible]	305.[illegible]	305.[illegible]	305.0	305.0	305.0	305.0
[illegible]	29[illegible].3		6988.	311.[illegible]	-14.[illegible]	31[illegible]	[illegible]	0.0	0.0	0.0	0.0	0.0
[illegible]	294.	1145	6984.	311.[illegible]	-14.[illegible]	31[illegible]	[illegible]	0.0	0.0	0.0	0.0	0.0

Table LXXV - Brightness Temperatures, Quartz Sand, 16.5 GHz, Vert. Pol.

Table LXXVI - Emissivities of Quartz Sand, 16.5 GHz, Vert. Pol.

TARGET MATERIAL	SAND DUNES
DATA DATE	(6/(8/66
START TIME	113(
FREQUENCY,GHZ	16.5
POLARIZATION	VER

ZENITH ANGLE DEG.	NADIR ANGLE DEG.	SLOPE ANGLE DEG.	INCIDENCE ANGLE DEG.	EMISSIVITY
90.0	90.0	0.0	90.0	0.0
92.0	88.0	0.0	88.0	0.697
94.2	86.(	5.6	80.4	0.872
96.(	84.(	5.6	78.4	0.883
98.(	82.0	5.6	76.4	0.884
100.0	80.(	5.6	74.4	0.917
102.0	78.(	5.6	72.4	0.934
104.0	76.0	5.6	70.4	0.925
106.0	74.0	5.6	68.4	0.903
108.2	72.2	-8.6	80.6	0.562
110.(	70.0	-8.6	78.6	0.808
115.0	65.4	-8.6	73.6	0.939
120.2	60.2	-8.6	68.6	0.925
125.2	55.2	-14.0	69.(	0.918
130.2	50.2	-14.(	64.(	0.902

NOTES - NADIR ANGLE = 18(- ZENITH ANGLE

INCIDENCE ANGLE = NADIR ANGLE + OR - SLOPE ANGLE
(MINUS FOR UPSLOPE
PLUS FOR DOWNSLOPE)

RUN NO. 100 06/09/66 VER POLAR. 16.5 GHZ SAND DUNES

ITERATION NUMBER 0

ZENITH ANGLE (DEG)	BRIGHTNESS TEMP. (DEG K)	APPARENT TEMP. (DEG K)	CORRECTION TEMP. (DEG K)
0.0	6.71	11.63	-4.9225
21.79	7.34	12.89	-5.5551
31.00	9.35	15.33	-5.9801
38.21	8.42	16.56	-8.1454
44.42	8.71	18.88	-10.1690
49.99	8.59	21.43	-12.8340
55.15	13.55	26.81	-13.2637
60.00	18.27	31.88	-13.6112
64.62	15.61	33.19	-17.5851
69.08	23.54	40.63	-17.0853
73.40	27.71	47.16	-19.4490
77.63	37.97	57.95	-19.9873
81.79	40.63	70.67	-30.0403
85.90	124.92	136.81	-11.8868
90.00	279.87	241.12	38.7461
94.10	271.58	250.88	20.6997
98.21	277.40	259.20	18.2063
102.37	291.02	270.14	20.8815
106.60	283.19	268.63	14.5556
110.92	286.08	272.38	13.7034
115.38	294.69	279.18	15.5114
120.00	290.31	278.60	11.7064
124.85	291.15	280.02	11.1310
130.01	284.04	277.20	6.8380
135.58	282.55	277.20	5.3532
141.79	281.24	277.20	4.0432
149.00	280.38	277.20	3.1849
158.21	279.69	277.20	2.4915
180.00	279.48	277.20	2.2787

ABS. CORRECTION = 1.31E 01 DEG. K

Table LXXVII - Brightness and Apparent Temperatures, Quartz Sand, 16.5 GHz, Vert. Pol.

Referring to Figure 68, these values exhibit less scattering than the horizontally polarized data. Although there is better agreement between the derived and theoretical emissivities at vertical polarization, the peak of the Brewster Angle is considerably removed from that of the theoretical curve at 14 GHz; there is an upward shift of approximately 12^{o} in its position. As in the case of the 9.5 GHz data, this indicates a possibly higher dielectric permittivity at 16.5 GHz versus the measured value at 14 GHz. Alternatively, the measurement error at 14 GHz, could account for this discrepancy.

3. 94 GHz Data - Quartz Sand

Figure 71 and Tables LXXVIII thru' LXXXI present measured data for horizontal polarization. The brightness temperatures are at a level quite close to those at 16.5 GHz, for the same polarization; however, the sky brightness temperatures are much higher, being similar to the Death Valley data.

Emissivities derived by means of Equation (31) are listed in Table LXXX and range from 0.11 to 0.74 over an incidence angle increment from 64^{o} to 88^{o}. The values are slightly lower than at 16.5 GHz (0.30 to 0.79). This is contrary to the expected results and is, very likely, due to the higher magnitudes of sky brightness temperatures, $T_{S\varphi}$, subtracted from the numerator and denominator in Equation (31). It appears, therefore, that a modified form of this equation should be employed for this purpose. Figure 72 shows plots of derived emissivities; theoretical data at 14 GHz is also shown for reference purposes.

Figure 73 and Tables LXXXII thru' LXXXV furnish vertically polarized data. It will be observed that the brightness temperatures are about $22^{o}K$ higher than those for horizontal polarization, over the nadir angle 20^{o} to 60^{o}; they are about $40^{o}K$ higher over the range 60^{o} to 90^{o}. As a result, the derived emissivities, listed in Table LXXXIV, are considerably higher, ranging from 0.48 to 0.89 over an incidence angle range of 64^{o} to 81^{o}. The plotted values, shown in Figure 72, indicate an unusual degree of specularity to this material at this high frequency. The Brewster Angle appears to be at approximately 70^{o}; this is very close to its

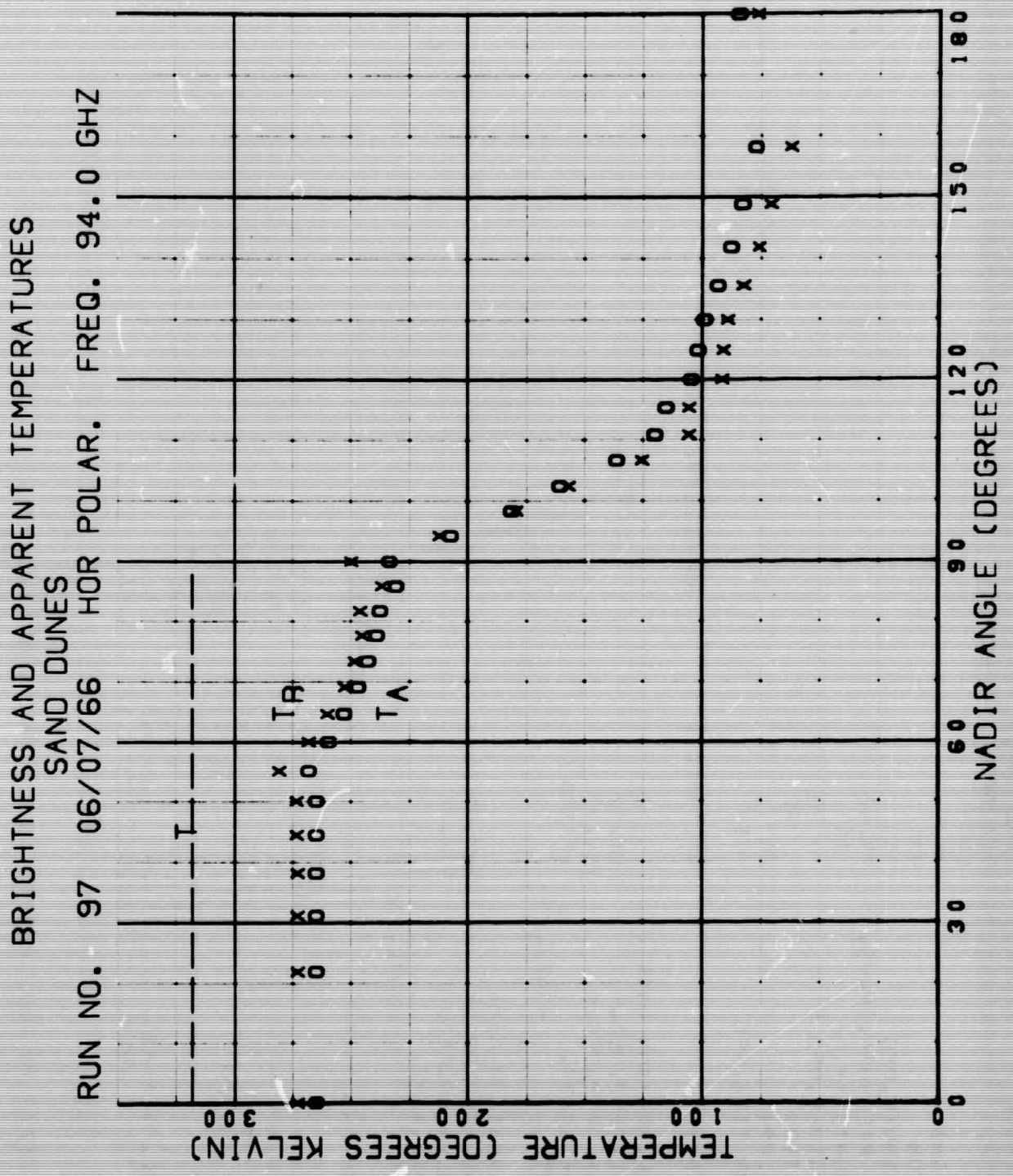


Figure 71 - Measured Quartz Sand Brightness Temperatures, 94 GHz, Hor. Pol.

Table LXXVIII - Environmental and Calibration Data, Quartz Sand, 94 GHz, Hor. Pol.

PAGE 1 RUN 97	
TARGET MATERIAL	SAND DUNES
DATA DATE	06/07/66
START TIME	1900
FREQUENCY,GHZ	94.0
POLARIZATION	HOR
ANTENNA AZIMUTH,DEG	350
BAROMETRIC PRESSURE,IN.HG.	29.42
RELATIVE HUMIDITY,0/0	33
AIR TEMPERATURE,DEG F	90
WIND DIRECTION	SE
WIND SPEED,MPH	25
INTEGRATION TIME,SEC	10

THIRD CALIBRATION POINT 85.00DEG.K 6565.00MV.

INITIAL CALIBRATION DATA	
MINIMUM CAL.TEMP,DEG.K	311.08
MAXIMUM CAL.TEMP.DEG.K	386.83
K-FACTOR,DEG.K/MV.	0.54186
Y INTERCEPT	-3472.73

FINAL CALIBRATION DATA	
MINIMUM CAL.TEMP,DEG.K	307.30
MAXIMUM CAL.TEMP.DEG.K	384.03
K-FACTOR,DEG.K/MV.	0.54472
Y INTERCEPT	-3492.24

CALIBRATION CONSTANTS	INITIAL	FINAL	UNITS
HOT LOAD	399.00	399.00	DEG.K
CAL WGS - MIN	311.11	306.50	DEG.K
CAL WGS - MAX	313.00	308.00	DEG.K
WAVE GUIDE SWITCH	306.50	306.50	DEG.K
ANTENNA	306.00	306.00	DEG.K
COLD LOAD	306.50	306.50	DEG.K
AVERAGE CAL.DATA-MIN.	6986.30	6983.93	MV.
-MAX.	7120.40	7109.53	MV.

COMMENTS
SKY SUNNY CLEAR NO HAZE HEAVY SANDS BLOWING ACROSS LOS

PAGE 2 RUN 97

TARGET MATERIAL SAND DUNES
DATA DATE 6/6 7/66
START TIME 1900
FREQUENCY,GHZ 94.[illegible]
POLARIZATION HOR

ZENITH ANGLE DEG	BRIGHTNESS TEMP DEG K	TIME	READINGS MV	SURFACE TEMP	SLOPE ANGLE	1/2 IN TEMP DEG K	1 FT TEMP DEG K	2 FT TEMP DEG K	3 FT TEMP DEG K	3 IN TEMP DEG K	6 IN TEMP DEG K	12 IN TEMP DEG K
2.2	76.5	1900	6565.	0.0	0.0	0.0	0.0	0.0	0.0	0.0	0.0	0.0
10.2	70.[illegible]		6547.	0.0	0.0	0.0	0.0	0.0	0.0	0.0	0.0	0.0
20.2	63.4		6550.	0.0	0.0	0.0	0.0	0.0	0.0	0.0	0.0	0.0
30.2	69.7		6561.	0.0	0.0	0.0	0.0	0.0	0.0	0.0	0.0	0.0
40.2	77.9		6573.	0.0	0.0	0.0	0.0	0.0	0.0	0.0	0.0	0.0
50.2	89.2		6592.	0.0	0.0	0.0	0.0	0.0	0.0	0.0	0.0	0.0
60.2	91.3		6602.	0.0	0.0	0.0	0.0	0.0	0.0	0.0	0.0	0.0
62.8	99.2											
64.8	104.8											
65.2	105.4		6623.	0.0	0.0	0.0	0.0	0.0	0.0	0.0	0.0	0.0
66.8	107.[illegible]											
68.8	108.8											
70.2	109.8		6632.	0.0	0.0	0.0	0.0	0.0	0.0	0.0	0.0	0.0
70.8	114.3											
72.8	125.3											
74.8	136.4											
75.2	137.5		6675.	0.0	0.0	0.0	0.0	0.0	0.0	0.0	0.0	0.0
77.2	151.8											
78.2	157.[illegible]											
80.2	169.9		6734.	0.0	0.0	0.0	0.0	0.0	0.0	0.0	0.0	0.0
82.2	181.3		6745.	0.0	0.0	0.0	0.0	0.0	0.0	0.0	0.0	0.0
82.2	182.9											
83.2	189.3											
84.2	197.3		6779.	0.0	0.0	0.0	0.0	0.0	0.0	0.0	0.0	0.0
86.2	213.3		6793.	0.0	0.0	0.0	0.0	0.0	0.0	0.0	0.0	0.0
87.2	224.4											
88.2	231.7		6825.	0.0	0.0	0.0	0.0	0.0	0.0	0.0	0.0	0.0
89.2	242.7											
90.2	250.1		6840.	315.6	0.0	312.0	0.0	0.0	0.0	0.0	0.0	0.0
92.2	243.8		6830.	315.0	0.0	312.0	0.0	0.0	0.0	0.0	0.0	0.0
94.2	237.6		6835.	315.0	5.6	312.0	0.0	0.0	0.0	0.0	0.0	0.0
96.2	241.6		6841.	315.0	5.6	312.0	0.0	0.0	0.0	0.0	0.0	0.0
98.2	246.1		6848.	316.0	5.6	317.0	0.0	0.0	0.0	0.0	0.0	0.0
100.2	246.1		6844.	316.0	5.6	317.0	0.0	0.0	0.0	0.0	0.0	0.0
102.2	245.5		6851.	316.0	5.6	316.0	0.0	0.0	0.0	0.0	0.0	0.0
104.2	246.7		6851.	316.0	5.6	316.0	0.0	0.0	0.0	0.0	0.0	0.0
106.2	248.4		6857.	314.0	5.6	311.0	0.0	0.0	0.0	0.0	0.0	0.0
108.2	250.3		6859.	314.0	-8.6	318.0	0.0	0.0	0.0	0.0	0.0	0.0
110.2	252.3		6863.	313.0	-8.6	318.0	0.0	0.0	0.0	0.0	0.0	0.0
115.2	259.7		6875.	309.0	-8.6	319.0	0.0	0.0	0.0	0.0	0.0	0.0
120.2	268.3		6888.	314.0	-8.6	313.0	0.0	0.0	0.0	312.0	310.0	310.0
125.2	281.0		6904.	314.0	-14.	313.0	0.0	0.0	0.0	0.0	0.0	0.0
130.2	296.6		6898.	314.0	-14.	313.0	0.0	0.0	0.0	0.0	0.0	0.0

Table LXXIX - Brightness Temperatures, Quartz Sand, 94 GHz, Hor. Pol.

TARGET MATERIAL	SAND DUNES
DATA DATE	6/ 7/66
START TIME	19[illegible]
FREQUENCY,GHZ	94.[illegible]
POLARIZATION	HOR

ZENITH ANGLE DEG.	NADIR ANGLE DEG.	SLOPE ANGLE DEG.	INCIDENCE ANGLE DEG.	EMISSIVITY
90.[illegible]	9[illegible].[illegible]	[illegible].[illegible]	9[illegible].[illegible]	0.0
92.[illegible]	88.[illegible]	[illegible].[illegible]	88.[illegible]	0.146
94.[illegible]	86.[illegible]	5.6	8[illegible].4	[illegible].567
96.[illegible]	84.[illegible]	5.6	78.4	[illegible].613
98.[illegible]	82.[illegible]	5.6	76.4	[illegible].654
1[illegible].[illegible]	8[illegible].[illegible]	5.6	74.4	[illegible].663
1[illegible]2.[illegible]	78.[illegible]	5.6	72.4	[illegible].663
1[illegible]4.[illegible]	76.[illegible]	5.6	7[illegible].4	[illegible].672
1[illegible]6.[illegible]	74.[illegible]	5.6	68.4	0.695
1[illegible]8.[illegible]	72.[illegible]	-8.6	8[illegible].6	[illegible].112
11[illegible].[illegible]	7[illegible].[illegible]	-8.6	78.6	[illegible].315
115.[illegible]	65.[illegible]	-8.6	73.6	[illegible].609
12[illegible].[illegible]	6[illegible].[illegible]	-8.6	68.6	[illegible].718
125.[illegible]	55.[illegible]	-14.[illegible]	69.[illegible]	0.736
13[illegible].[illegible]	5[illegible].[illegible]	-14.[illegible]	64.[illegible]	0.743

NOTES - NADIR ANGLE = 18[illegible] - ZENITH ANGLE

INCIDENCE ANGLE = NADIR ANGLE + OR - SLOPE ANGLE
(MINUS FOR UPSLOPE
PLUS FOR DOWNSLOPE)

Table LXXX - Emissivities of Quartz Sand, 94 GHz, Hor. Pol.

RUN NO. 97 06/07/66 HOR POLAR. 94.0 GHZ SAND DUNES

ITERATION NUMBER 0

ZENITH ANGLE (DEG)	BRIGHTNESS TEMP. (DEG K)	APPARENT TEMP. (DEG K)	CORRECTION TEMP. (DEG K)
0.0	76.52	84.48	-7.9586
21.79	62.25	77.49	-15.2418
31.00	70.57	82.78	-12.2114
38.21	76.03	87.57	-11.6435
44.42	82.60	93.28	-10.6847
49.99	89.21	98.84	-9.6390
55.15	91.03	101.78	-10.7428
60.00	91.32	104.53	-13.2134
64.62	105.34	115.16	-9.8233
69.08	105.54	119.73	-14.1926
73.40	125.61	136.45	-10.8414
77.63	157.04	160.83	-3.7966
81.79	179.63	181.25	-1.6267
85.90	212.45	207.37	5.0799
90.00	250.07	233.87	16.2042
94.10	237.31	231.10	6.2058
98.21	246.61	237.94	8.6640
102.37	245.37	239.40	5.9696
106.60	248.89	243.03	5.8611
110.92	253.20	247.32	5.8798
115.38	260.34	253.27	7.0683
120.00	268.26	259.93	8.3314
124.85	281.25	268.47	12.7878
130.01	273.57	265.10	8.4730
135.58	273.65	265.10	8.5457
141.79	273.35	265.10	8.2470
149.00	273.25	265.10	8.1523
158.21	273.28	265.10	8.1756
180.00	273.27	265.10	8.1723

ABS. CORRECTION = 9.03E 00 DEG. K

Table LXXXI - Brightness and Apparent Temperatures, Quartz Sand, 94 GHz, Hor. Pol.

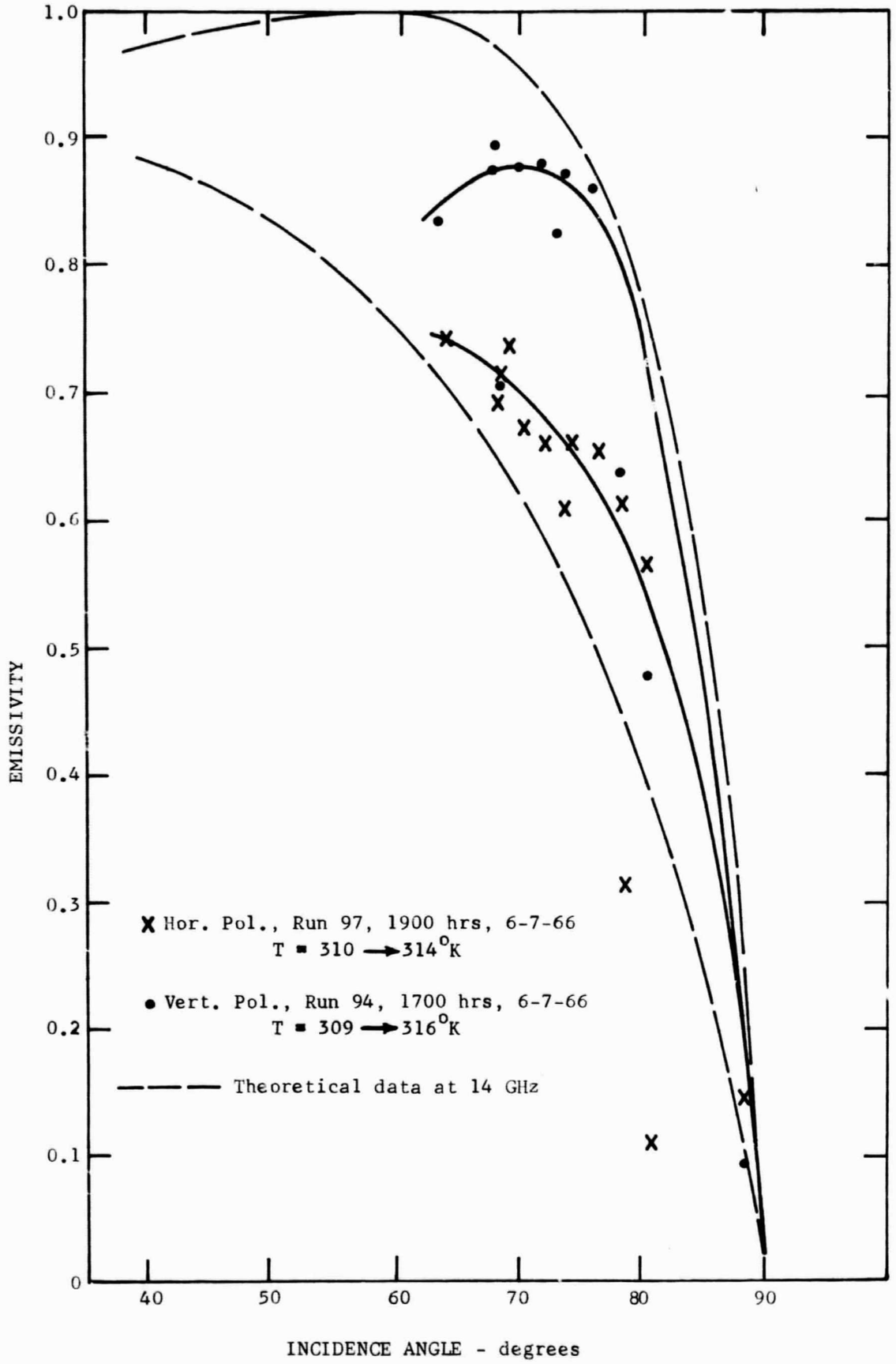


Figure 72 - Derived and Theoretical Specular Emissivities, Quartz Sand - 94 GHz

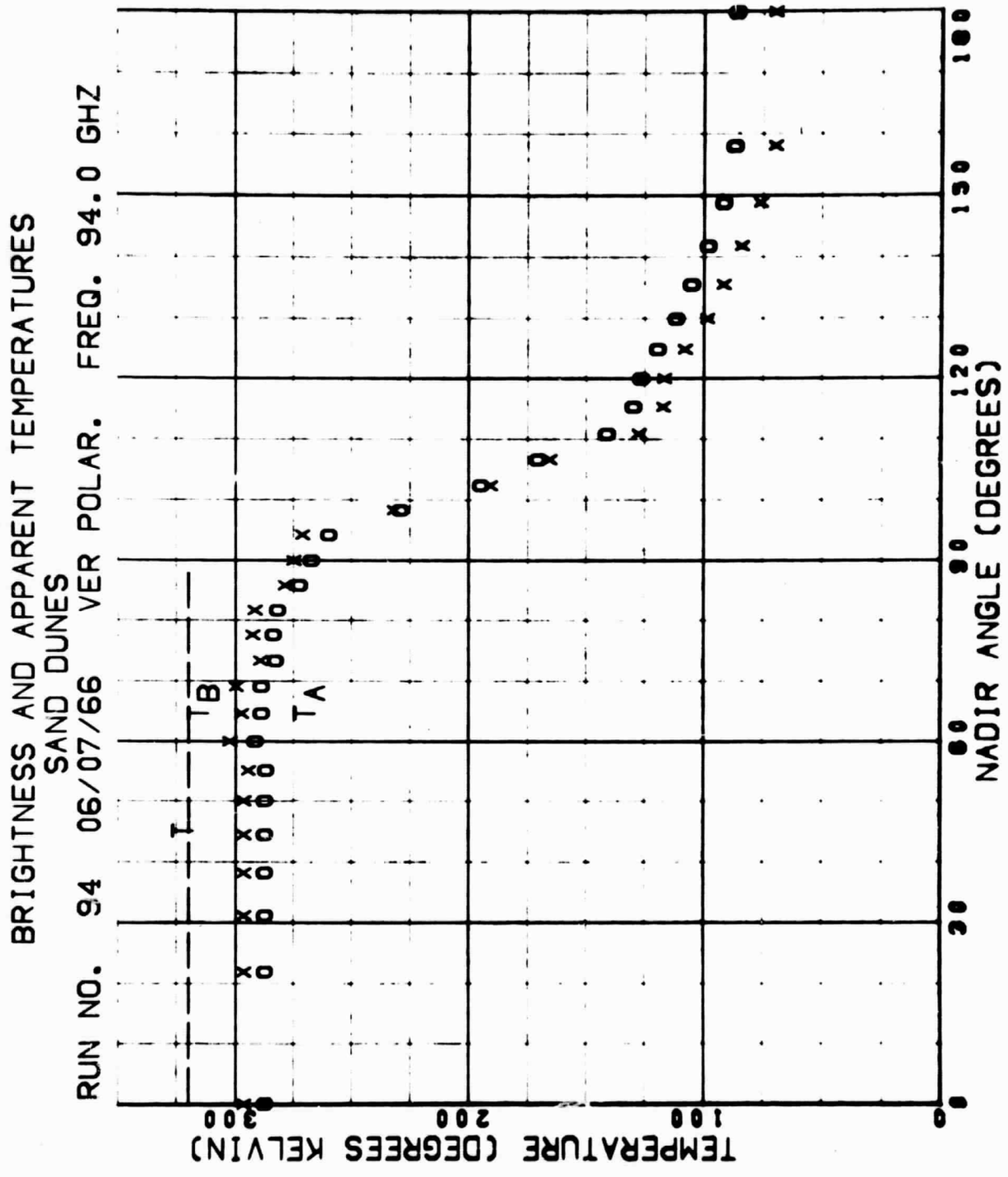


Figure 73 - Measured Quartz Sand Brightness Temperatures, 94 GHz, Vert. Pol.

Table LXXXII - Environmental and Calibration Data, Quartz Sand, 94 GHz, Vert. Pol.

PAGE 1 RUN 94

TARGET MATERIAL	SAND DUNES
DATA DATE	06/27/65
START TIME	17[illegible]
FREQUENCY,GHZ	94.
POLARIZATION	VER
ANTENNA AZIMUTH,DEG	350
BAROMETRIC PRESSURE,IN.HG.	29.46
RELATIVE HUMIDITY,P/O	36
AIR TEMPERATURE,DEG F	90
WIND DIRECTION	WNW
WIND SPEED,MPH	17
INTEGRATION TIME,SEC	10

THIRD CALIBRATION POINT 86.00DEG.K 6519.00MV.

INITIAL CALIBRATION DATA	
MINIMUM CAL.TEMP,DEG.K	304.94
MAXIMUM CAL.TEMP.DEG.K	383.50
K-FACTOR,DEG.K/MV.	0.49151
Y INTERCEPT	-3117.95

FINAL CALIBRATION DATA	
MINIMUM CAL.TEMP,DEG.K	304.94
MAXIMUM CAL.TEMP.DEG.K	383.50
K-FACTOR,DEG.K/MV.	0.48664
Y INTERCEPT	-3085.39

CALIBRATION CONSTANTS	INITIAL	FINAL	UNITS
HOT LOAD	399.00	399.00	DEG.K
CAL WGS - MIN	303.00	303.00	DEG.K
CAL WGS - MAX	306.00	306.00	DEG.K
WAVE GUIDE SWITCH	302.00	302.00	DEG.K
ANTENNA	304.00	304.00	DEG.K
COLD LOAD	303.00	303.00	DEG.K
AVERAGE CAL.DATA-MIN.	6965.85	6962.85	MV.
-MAX.	7122.55	7131.20	MV.

COMMENTS
SKY SUNNY CLEAR NO HAZE

TARGET MATERIAL SAND DUNES
DATA DATE 06/07/66
START TIME 1700
FREQUENCY,GHZ 94.0
POLARIZATION VER

ZENITH ANGLE DEG	BRIGHTNESS TEMP DEG K	TIME	READINGS MV	SURFACE TEMP	SLOPE ANGLE	1/2 IN TEMP DEG K	1 FT TEMP DEG K	2 FT TEMP DEG K	3 FT TEMP DEG K	3 IN TEMP DEG K	6 IN TEMP DEG K	12 IN TEMP DEG K
0.0	69.6	1700	6518.	0.0	0.0	0.0	0.0	0.0	0.0	0.0	0.0	0.0
10.0	69.8		6518.	0.0	0.0	0.0	0.0	0.0	0.0	0.0	0.0	0.0
20.0	70.0		6518.	0.0	0.0	0.0	0.0	0.0	0.0	0.0	0.0	0.0
30.0	75.4		6528.	0.0	0.0	0.0	0.0	0.0	0.0	0.0	0.0	0.0
40.0	86.1		6546.	0.0	0.0	0.0	0.0	0.0	0.0	0.0	0.0	0.0
50.0	98.6		6570.	0.0	0.0	0.0	0.0	0.0	0.0	0.0	0.0	0.0
60.0	116.9		6601.	0.0	0.0	0.0	0.0	0.0	0.0	0.0	0.0	0.0
62.8	117.4											
64.8	117.8											
65.0	117.8		6608.	0.0	0.0	0.0	0.0	0.0	0.0	0.0	0.0	0.0
65.8	124.2											
68.8	131.2											
70.0	135.5	1710	6635.	0.0	0.0	0.0	0.0	0.0	0.0	0.0	0.0	0.0
70.8	141.8											
72.8	157.6											
74.8	173.4											
75.0	175.0		6716.	0.0	0.0	0.0	0.0	0.0	0.0	0.0	0.0	0.0
77.2	192.2											
78.0	198.4											
80.0	214.1		6763.	0.0	0.0	0.0	0.0	0.0	0.0	0.0	0.0	0.0
82.0	233.8		6816.	0.0	0.0	0.0	0.0	0.0	0.0	0.0	0.0	0.0
82.2	235.7											
83.0	243.4											
84.0	253.0		6859.	0.0	0.0	0.0	0.0	0.0	0.0	0.0	0.0	0.0
85.0	271.3	1730	6874.	0.0	0.0	0.0	0.0	0.0	0.0	0.0	0.0	0.0
87.2	272.5											
88.0	273.2		6879.	0.0	0.0	0.0	0.0	0.0	0.0	0.0	0.0	0.0
89.2	274.4											
90.0	275.1		6889.	314.0	0.0	310.0	0.0	0.0	0.0	0.0	0.0	0.0
92.0	276.8		6901.	314.0	0.0	310.0	0.0	0.0	0.0	0.0	0.0	0.0
94.0	278.5		6898.	314.0	5.6	310.0	0.0	0.0	0.0	0.0	0.0	0.0
96.0	284.7		6916.	314.0	5.6	310.0	0.0	0.0	0.0	0.0	0.0	0.0
98.0	291.2	1740	6918.	316.0	5.6	312.0	0.0	0.0	0.0	0.0	0.0	0.0
100.0	292.3		6923.	316.0	5.6	312.0	0.0	0.0	0.0	0.0	0.0	0.0
102.0	292.7		6922.	316.0	5.6	312.0	0.0	0.0	0.0	0.0	0.0	0.0
104.0	291.4		6926.	316.0	5.6	312.0	0.0	0.0	0.0	0.0	0.0	0.0
106.0	289.8		6919.	315.0	5.6	312.0	0.0	0.0	0.0	0.0	0.0	0.0
108.0	288.7		6925.	313.0	-8.6	312.0	0.0	0.0	0.0	0.0	0.0	0.0
110.0	287.5		6935.	312.0	-8.6	310.0	0.0	0.0	0.0	0.0	0.0	0.0
115.0	287.6		6934.	311.0	-8.6	311.0	0.0	0.0	0.0	0.0	0.0	0.0
120.0	292.5		6939.	316.0	-8.6	316.0	0.0	0.0	0.0	315.0	311.0	309.0
125.0	294.8		6937.	316.0	-14.0	316.0	0.0	0.0	0.0	0.0	0.0	0.0
130.0	296.5	1810	6931.	316.0	-14.0	316.0	0.0	0.0	0.0	0.0	0.0	0.0

Table LXXXIII - Brightness Temperatures, Quartz Sand, 94 GHz, Vert. Pol.

TARGET MATERIAL	SAND DUNES
DATA DATE	6/07/66
START TIME	170
FREQUENCY,GHZ	94.0
POLARIZATION	VER

ZENITH ANGLE DEG.	NADIR ANGLE DEG.	SLOPE ANGLE DEG.	INCIDENCE ANGLE DEG.	EMISSIVITY
90.0	90.0	0.0	90.0	0.0
92.0	88.0	0.0	88.0	0.088
94.0	86.0	5.6	80.4	0.748
96.0	84.0	5.6	78.4	0.813
98.0	82.0	5.6	76.4	0.858
100.0	80.0	5.6	74.4	0.871
102.0	78.0	5.6	72.4	0.878
104.0	76.0	5.6	70.4	0.876
106.0	74.0	5.6	68.4	0.873
108.0	72.0	-8.6	80.6	0.475
110.0	70.0	-8.6	78.6	0.634
115.0	65.0	-8.6	73.6	0.822
120.0	60.0	-8.6	68.6	0.891
125.0	55.0	-14.0	69.0	0.708
130.0	50.0	-14.0	64.0	0.834

NOTES - NADIR ANGLE = 180 - ZENITH ANGLE

INCIDENCE ANGLE = NADIR ANGLE + OR - SLOPE ANGLE
(MINUS FOR UPSLOPE
PLUS FOR DOWNSLOPE)

Table LXXXIV - Emissivities of Quartz Sand, 94 GHz, Vert. Pol.

RUN NO. 94 06/07/66 VER POLAR. 94.0 GHZ SAND DUNES

ITERATION NUMBER 0

ZENITH ANGLE (DEG)	BRIGHTNESS TEMP. (DEG K)	APPARENT TEMP. (DEG K)	CORRECTION TEMP. (DEG K)
0.0	69.61	85.63	-16.0212
21.79	70.01	86.51	-16.5016
31.00	76.10	91.51	-15.4093
38.21	83.88	98.14	-14.2549
44.42	91.60	104.94	-13.3403
49.99	98.57	111.45	-12.8862
55.15	107.80	119.33	-11.5339
60.00	116.90	126.74	-9.8411
64.62	116.96	129.62	-12.6662
69.08	127.28	140.90	-13.6180
73.40	165.53	170.37	-4.8405
77.63	190.49	195.12	-4.6356
81.79	231.79	229.14	2.6467
85.90	271.25	260.10	11.1534
90.00	275.11	267.72	7.3898
94.10	278.60	272.53	6.0697
98.21	291.89	282.01	9.8830
102.37	292.74	283.81	8.9331
106.60	289.35	282.86	6.4887
110.92	299.75	289.32	10.4217
115.38	297.41	289.07	8.3381
120.00	302.46	291.67	10.7904
124.85	294.77	287.24	7.5300
130.01	296.51	287.74	8.7686
135.58	296.43	287.74	8.6924
141.79	296.43	287.74	8.6938
149.00	296.43	287.74	8.6925
158.21	296.43	287.74	8.6926
180.00	296.43	287.74	8.6876

ABS. CORRECTION = 9.91E 00 DEG. K

Table LXXXV - Brightness and Apparent Temperatures, Quartz Sand, 94 GHz, Vert. Pol.

position at the two lower frequencies. It appears, therefore, that the dielectric permittivity of Quartz Sand is at a fairly constant value from 9.5 to 94 GHz.

4. Comparison of Derived and Calculated Brightness Temperatures - Quartz Sand

Figures 74 and 75 show plots of derived and calculated brightness temperatures at 16.5 GHz, for horizontal and vertical polarizations, respectively. There is practically no agreement between derived and calculated T_B's, for horizontal polarization, and limited agreement over a narrow range of angles for vertical polarization. This disparity is evident from the scattering of emissivity data points, as shown in Figure 68. The data scattering is, very likely, due to inaccurate surveys of the sand dune profiles - it is rather difficult to perform an accurate profile survey on a soft, shifting material.

F. LIMESTONE - DATA RESULTS AND ANALYSIS

These measurements were performed at a limestone quarry and involved a powdery form of the material and an area with a pebbled texture. Views of the antenna lines-of-sight are shown for each texture in Figures 76 and 77. A plaster cast of the pebbled limestone is shown in Figure 78. Although the field records stated that both powdered and pebbled lines-of-sight were level, there are deep vehicle tracks in the powdered material. In addition, an examination of the horizontally polarized brightness temperature plots reveals the usual horizon peak at a nadir angle of 85 degrees instead of 90 degrees, which indicates that the radiometer van was not level i.e., the antenna horizontal axis was tilted up 5 degrees from the true horizontal, with respect to the plane of the material.

Figures 79 and 80 show Formet sections of the pebbled material in the antenna LOS. The surface roughness ranges from 0.1 to 1 cm, indicating a possibly significant effect on the brightness temperatures at 94 GHz (λ = 0.32 cm).

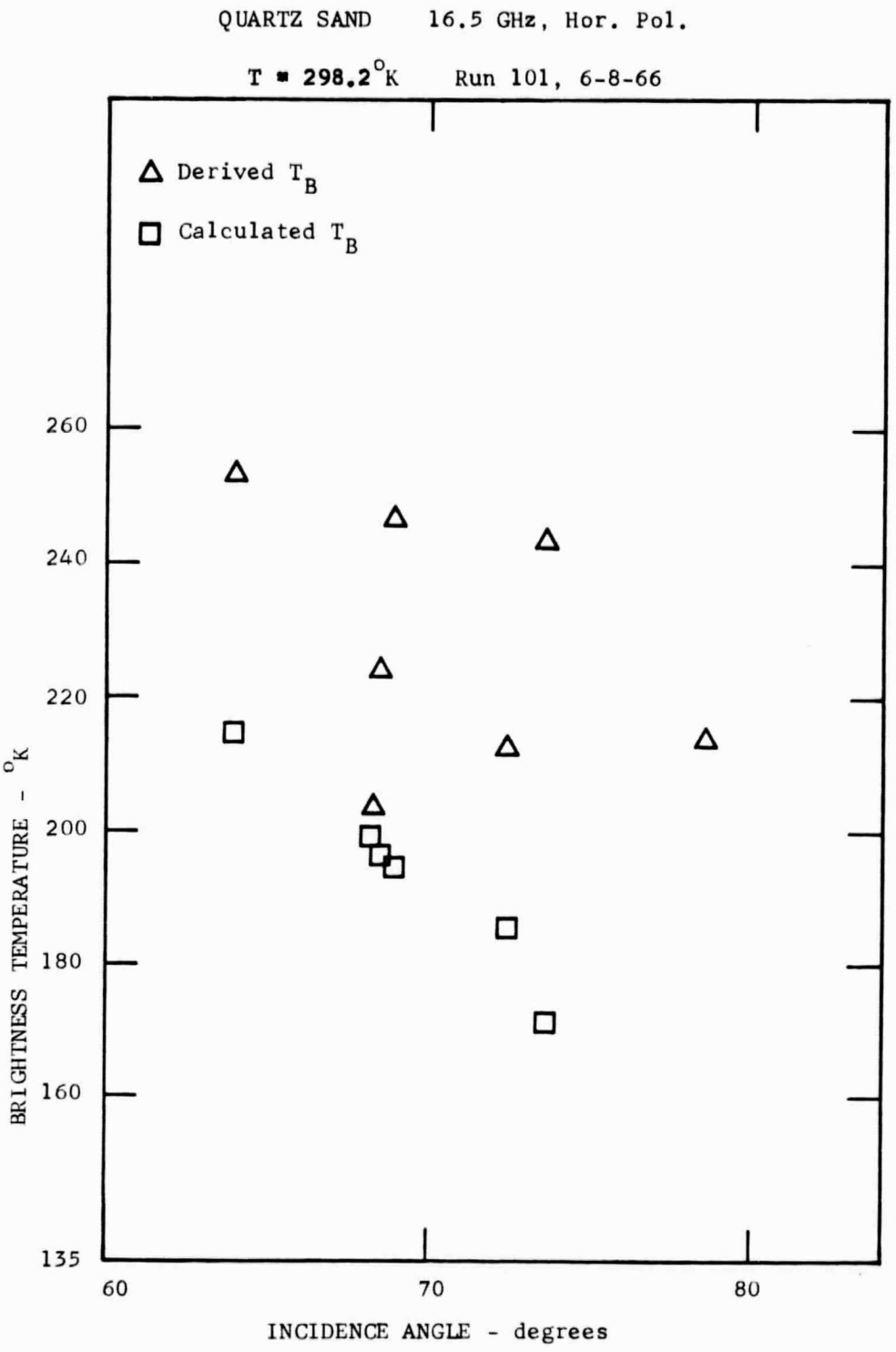


Figure 74 - Comparison of Derived and Calculated Brightness Temperatures at 16.5 GHz (Quartz Sand)

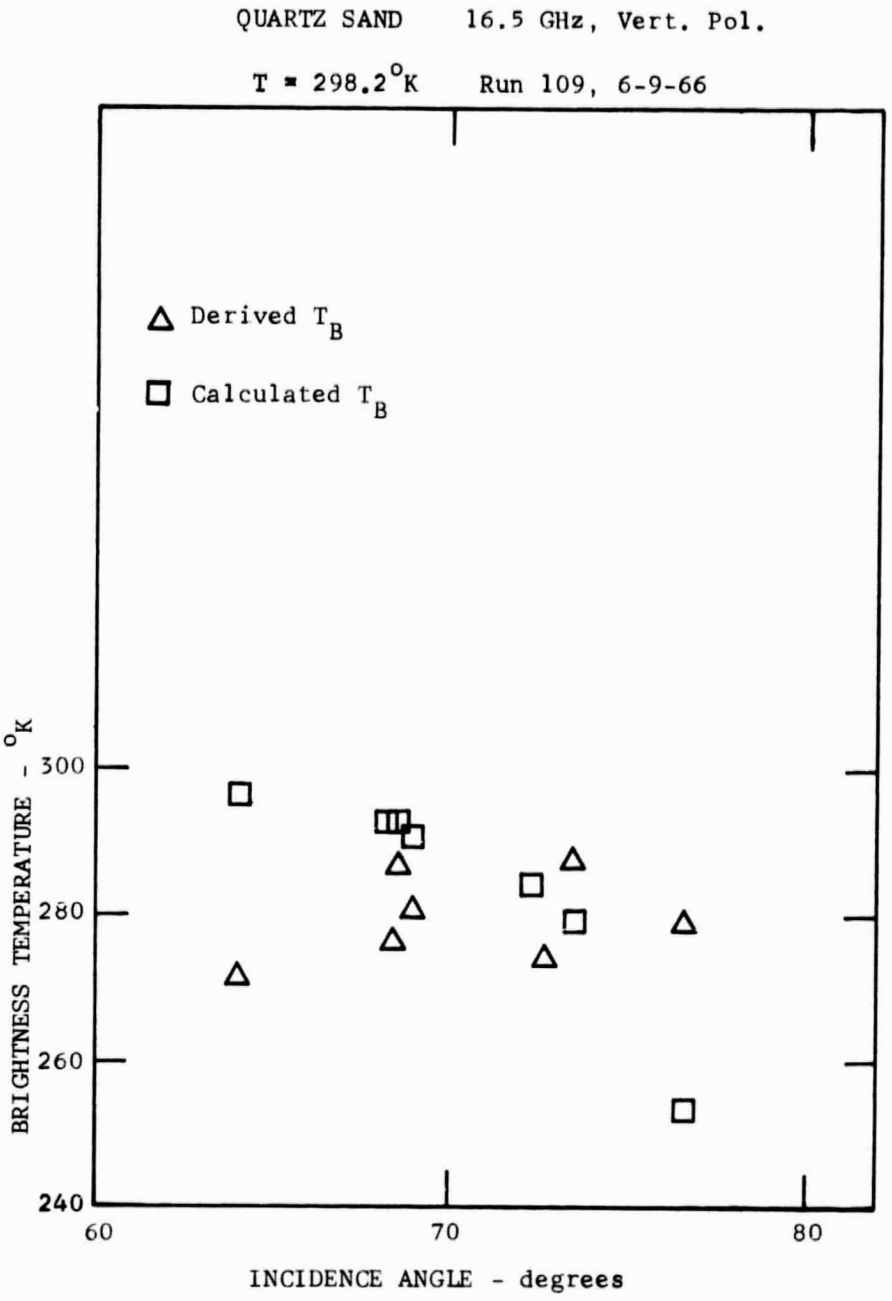


Figure 75 - Comparison of Derived and Calculated Brightness Temperatures at 16.5 GHz (Quartz Sand)



Figure 76 - Powdered Limestone, Lucerne Valley, California

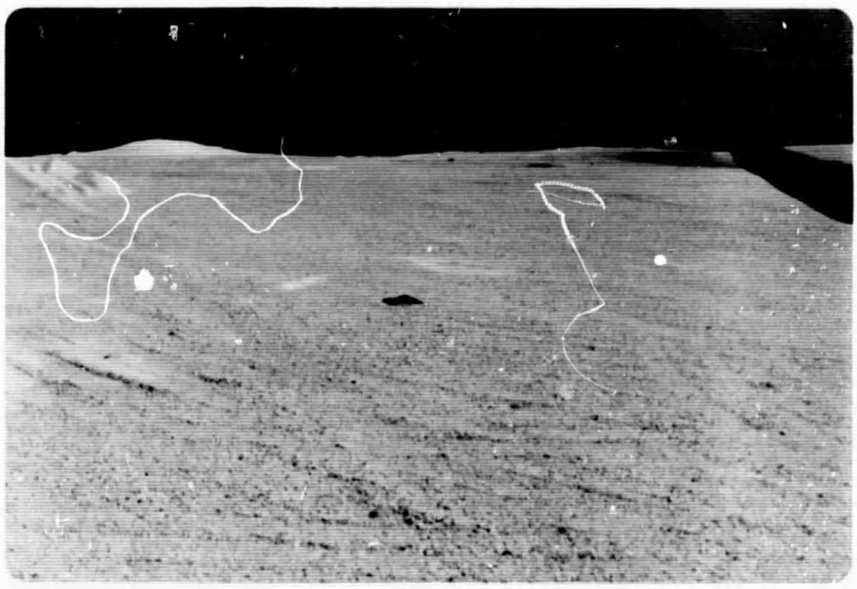


Figure 77 - Pebbled Limestone, Lucerne Valley, California



Figure 78 - Plaster Cast of Pebbled Limestone Surface, Lucerne Valley, California

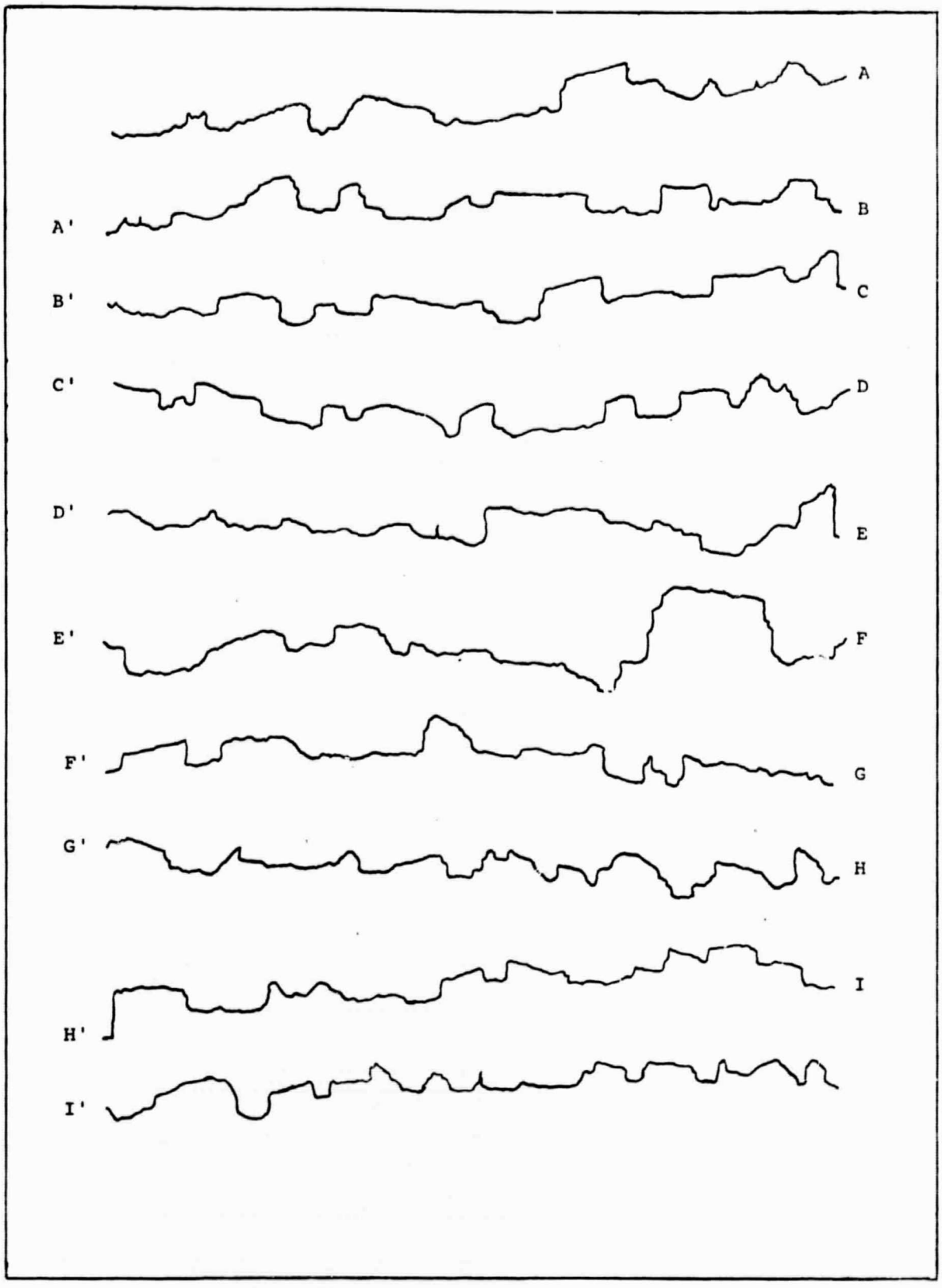


Figure 79 - North-South Formet Section of Lucerne Valley Limestone Pebble Dump (Reduced to 85% of Actual Dimensions)

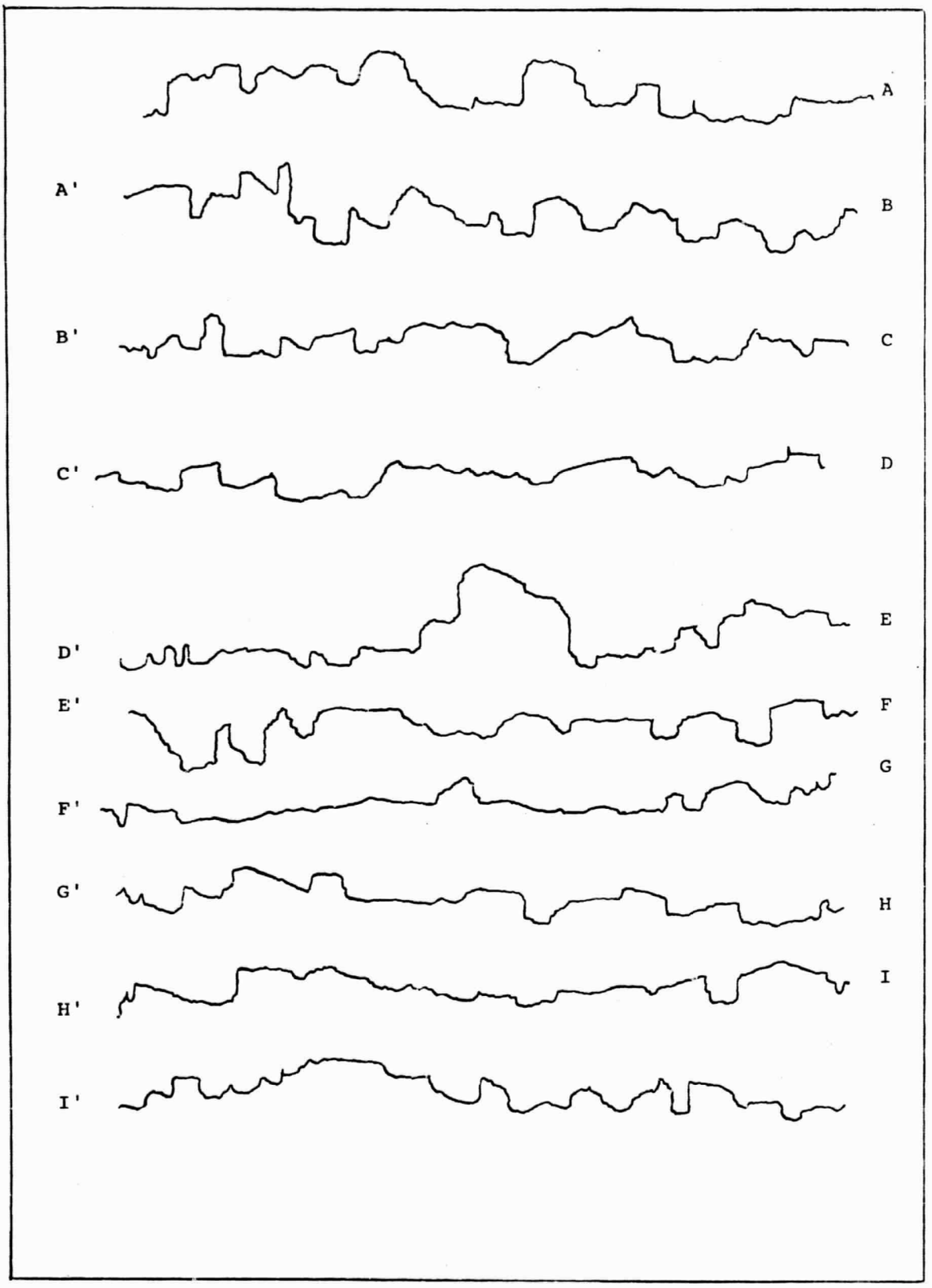


Figure 80 - East-West Formet Section of Lucerne Valley Limestone Pebble Dump (Reduced to 85% of Actual Dimensions)

1. 9.5 GHz Data - Powdered Limestone

Figure 81 and Tables LXXXVI thru' LXXXVIII present horizontally polarized data. The brightness temperatures lie at a somewhat high level - 260°K to 240°K between nadir angles of 20° and 60°, respectively. It should be noted, however, that the surface temperature is also rather high - 302°K. A curving off of the T_B's, beyond 60°, indicates a specular characteristic in the brightness temperatures. The derived emissivities are fairly high, ranging from 0.87 to 0.59, over a nadir angle range of 45° to 78°, respectively. Data beyond 78° is unreliable.

Figure 82 and Tables LXXXIX thru' XCI furnish vertically polarized data for the powdered material. The T_B values are generally higher than for horizontal polarization, ranging from 270°K to 296°K over the nadir angle range 20° to 60°, respectively, for the same surface temperature. A clear peak at a nadir angle of 60° places the Brewster Angle at this position.

Figure 83 shows plots of derived emissivities for this material, together with theoretical data at 14 GHz. Due to the previously mentioned 5 - degree tilt to the radiometer antenna horizontal axis, the emissivity values show extraneous peaks at an incidence angle of 85°. This is the result of similar peaks in the brightness temperatures at a nadir angle of 85°. Apart from this undesired effect, the two polarizations are widely separated, indicating considerable specularity to the powdered limestone at 9.5 GHz.

2. 9.5 GHz Data - Pebbled Limestone

Figure 84 and Tables XCII thru' XCIV furnish horizontally polarized data. Although the T_B's follow a similar curve to those for powdered limestone, they are at a lower level, ranging from 237°K to 215°K, between nadir angles of 20° and 60°, respectively. This is principally due to a reduction of 13°K in the surface temperature. The derived emissivities are slightly lower than for the powdered material, lying in

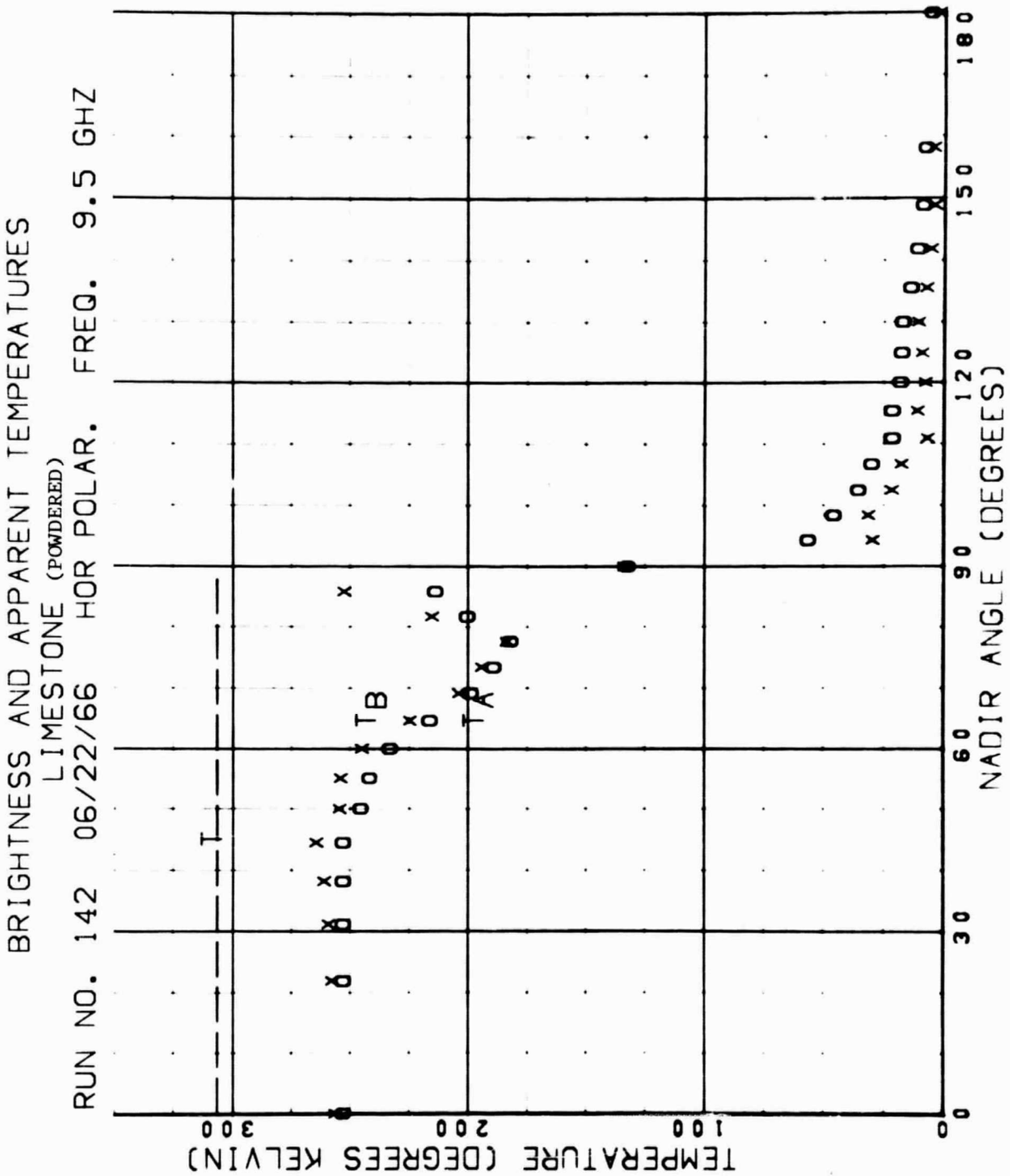


Figure 81 - Measured Brightness Temperatures, Powdered Limestone, 9.5 GHz, Hor. Pol.

REPRODUCIBILITY OF THE ORIGINAL PAGE IS POOR.

PAGE 1 RUN 142

TARGET MATERIAL	LIMESTONE
DATA DATE	06/22/66
START TIME	1[illegible]
FREQUENCY,GHZ	9.5
POLARIZATION	HOR
ANTENNA AZIMUTH,DEG	
BAROMETRIC PRESSURE,IN.HG.	3[illegible].69
RELATIVE HUMIDITY,%	27
AIR TEMPERATURE,DEG F	84
WIND DIRECTION	N
WIND SPEED,MPH	13
INTEGRATION TIME,SEC	1

THIRD CALIBRATION POINT 6.00DEG.K 6[illegible]89.30MV.

INITIAL CALIBRATION DATA			
MINIMUM CAL.TEMP,DEG.K	394.44		
MAXIMUM CAL.TEMP,DEG.K	402.15		
K-FACTOR,DEG.K/MV.	0.34514		
Y INTERCEPT	-2095.33		
FINAL CALIBRATION DATA			
MINIMUM CAL.TEMP,DEG.K	395.46		
MAXIMUM CAL.TEMP,DEG.K	401.20		
K-FACTOR,DEG.K/MV.	0.35345		
Y INTERCEPT	-2144.37		
CALIBRATION CONSTANTS	INITIAL	FINAL	UNITS
HOT LOAD	403.30	402.00	DEG.K
ATTENUATOR	394.33	395.[illegible]	DEG.K
WAVE GUIDE SWITCH	392.00	392.[illegible]	DEG.K
ANTENNA	299.[illegible]	300.[illegible]	DEG.K
AVERAGE CAL.DATA-MIN.	6954.66	6915.60	MV.
-MAX.	7235.[illegible]	7213.53	MV.

COMMENTS
BLOWING LIMESTONE DUST IN LDS

Table LXXXVI - Environmental and Calibration Data, Powdered Limestone, 9.5 GHz, Hor. Pol.

TARGET MATERIAL LIMESTONE
DATA DATE 06/22/66
START TIME 1000
FREQUENCY,GHZ 9.5
POLARIZATION HOR

ZENITH ANGLE DEG	BRIGHTNESS TEMP, HORIZONTAL DEG K	EMISSIVITY	TIME	READINGS MV	SURFACE TEMP	SLOPE ANGLE	1/2 IN TEMP DEG K	1 FT TEMP DEG K	2 FT TEMP DEG K	3 FT TEMP DEG K	3 IN TEMP DEG K	6 IN TEMP DEG K	12 IN TEMP DEG K
0.0	2.4		1000	6088.	0.0	0.0	0.0	0.0	0.0	0.0	0.0	0.0	0.0
10.0	3.5			6109.	0.0	0.0	0.0	0.0	0.0	0.0	0.0	0.0	0.0
20.0	4.5			6102.	0.0	0.0	0.0	0.0	0.0	0.0	0.0	0.0	0.0
30.0	4.2			6095.	0.0	0.0	0.0	0.0	0.0	0.0	0.0	0.0	0.0
40.0	6.1			6104.	0.0	0.0	0.0	0.0	0.0	0.0	0.0	0.0	0.0
45.0	8.3												
50.0	10.6			6120.	0.0	0.0	0.0	0.0	0.0	0.0	0.0	0.0	0.0
55.0	9.3												
60.0	8.0			6123.	0.0	0.0	0.0	0.0	0.0	0.0	0.0	0.0	0.0
65.0	10.9			6132.	0.0	0.0	0.0	0.0	0.0	0.0	0.0	0.0	0.0
70.0	9.2			6131.	0.0	0.0	0.0	0.0	0.0	0.0	0.0	0.0	0.0
72.0	13.2												
74.0	17.1												
75.0	19.1			6167.	0.0	0.0	0.0	0.0	0.0	0.0	0.0	0.0	0.0
76.0	20.7												
78.0	23.9												
80.0	27.2			6177.	0.0	0.0	0.0	0.0	0.0	0.0	0.0	0.0	0.0
82.0	31.4			6204.	0.0	0.0	0.0	0.0	0.0	0.0	0.0	0.0	0.0
84.0	30.5			6194.	0.0	0.0	0.0	0.0	0.0	0.0	0.0	0.0	0.0
86.0	32.1			6234.	0.0	0.0	0.0	0.0	0.0	0.0	0.0	0.0	0.0
88.0	83.0			6313.	0.0	0.0	0.0	0.0	0.0	0.0	0.0	0.0	0.0
90.0	134.0	0.0		6449.	302.0	0.0	0.0	0.0	0.0	0.0	0.0	0.0	0.0
92.0	192.2	0.498		6571.	302.0	0.0	0.0	0.0	0.0	0.0	0.0	0.0	0.0
94.0	250.4	0.809		6681.	302.0	0.0	0.0	0.0	0.0	0.0	0.0	0.0	0.0
96.0	235.7	0.756		6680.	302.0	0.0	0.0	0.0	0.0	0.0	0.0	0.0	0.0
98.0	217.4	0.688		6645.	302.0	0.0	0.0	0.0	0.0	0.0	0.0	0.0	0.0
100.0	201.9	0.636		6602.	302.0	0.0	0.0	0.0	0.0	0.0	0.0	0.0	0.0
102.0	186.7	0.585		6585.	302.0	0.0	0.0	0.0	0.0	0.0	0.0	0.0	0.0
104.0	188.0	0.595		6600.	302.0	0.0	0.0	0.0	0.0	0.0	0.0	0.0	0.0
106.0	193.1	0.618		6601.	302.0	0.0	0.0	0.0	0.0	0.0	0.0	0.0	0.0
108.0	197.6	0.639		6619.	302.0	0.0	0.0	0.0	0.0	0.0	0.0	0.0	0.0
110.0	201.9	0.658		6623.	302.0	0.0	0.0	0.0	0.0	0.0	0.0	0.0	0.0
115.0	223.0	0.728		6677.	302.0	0.0	0.0	0.0	0.0	0.0	0.0	0.0	0.0
120.0	245.3	0.807		6729.	302.0	0.0	0.0	0.0	0.0	0.0	0.0	0.0	0.0
125.0	254.2	0.837		6755.	302.0	0.0	0.0	0.0	0.0	0.0	0.0	0.0	0.0
130.0	254.9	0.838		6763.	302.0	0.0	0.0	0.0	0.0	0.0	0.0	0.0	0.0
135.0	253.8	0.834		6784.	302.0	0.0	0.0	0.0	0.0	0.0	0.0	0.0	0.0

Table LXXXVII - Brightness Temperatures, Powdered Limestone, 9.5 GHz, Hor. Pol.

RUN NO. 142 06/22/66 HOR POLAR. 9.5 GHZ LIMESTONE

ITERATION NUMBER 0

ZENITH ANGLE (DEG)	BRIGHTNESS TEMP. (DEG K)	APPARENT TEMP. (DEG K)	CORRECTION TEMP. (DEG K)
0.0	2.41	5.80	-3.3905
21.79	4.70	7.76	-3.0655
31.00	4.16	8.84	-4.6752
38.21	5.41	11.18	-5.7733
44.42	7.68	14.16	-6.4809
49.99	10.62	17.19	-6.5668
55.15	9.43	17.68	-8.2531
60.00	7.98	18.15	-10.1667
64.62	11.30	21.40	-10.0945
69.08	6.94	21.36	-14.4147
73.40	17.68	29.87	-12.1828
77.63	21.45	35.77	-14.3213
81.79	31.45	45.87	-14.4183
85.90	29.68	56.72	-27.0393
90.00	133.97	132.65	1.3183
94.10	253.15	214.22	38.9299
98.21	215.50	200.50	14.9991
102.37	183.85	182.41	1.4405
106.60	194.63	189.46	5.1709
110.92	203.86	199.10	4.7668
115.38	224.74	216.33	8.4121
120.00	245.33	233.32	12.0135
124.85	254.19	242.30	11.8847
130.01	254.92	245.83	9.0877
135.58	264.84	253.52	11.3212
141.79	261.33	253.52	7.8068
149.00	259.39	253.52	5.8666
158.21	258.09	253.52	4.5744
180.00	256.62	253.52	3.1008

ABS. CORRECTION = 9.71E 00 DEG. K

Table LXXXVIII - Brightness and Apparent Temperatures, Powdered Limestone, 9.5 GHz, Hor. Pol.

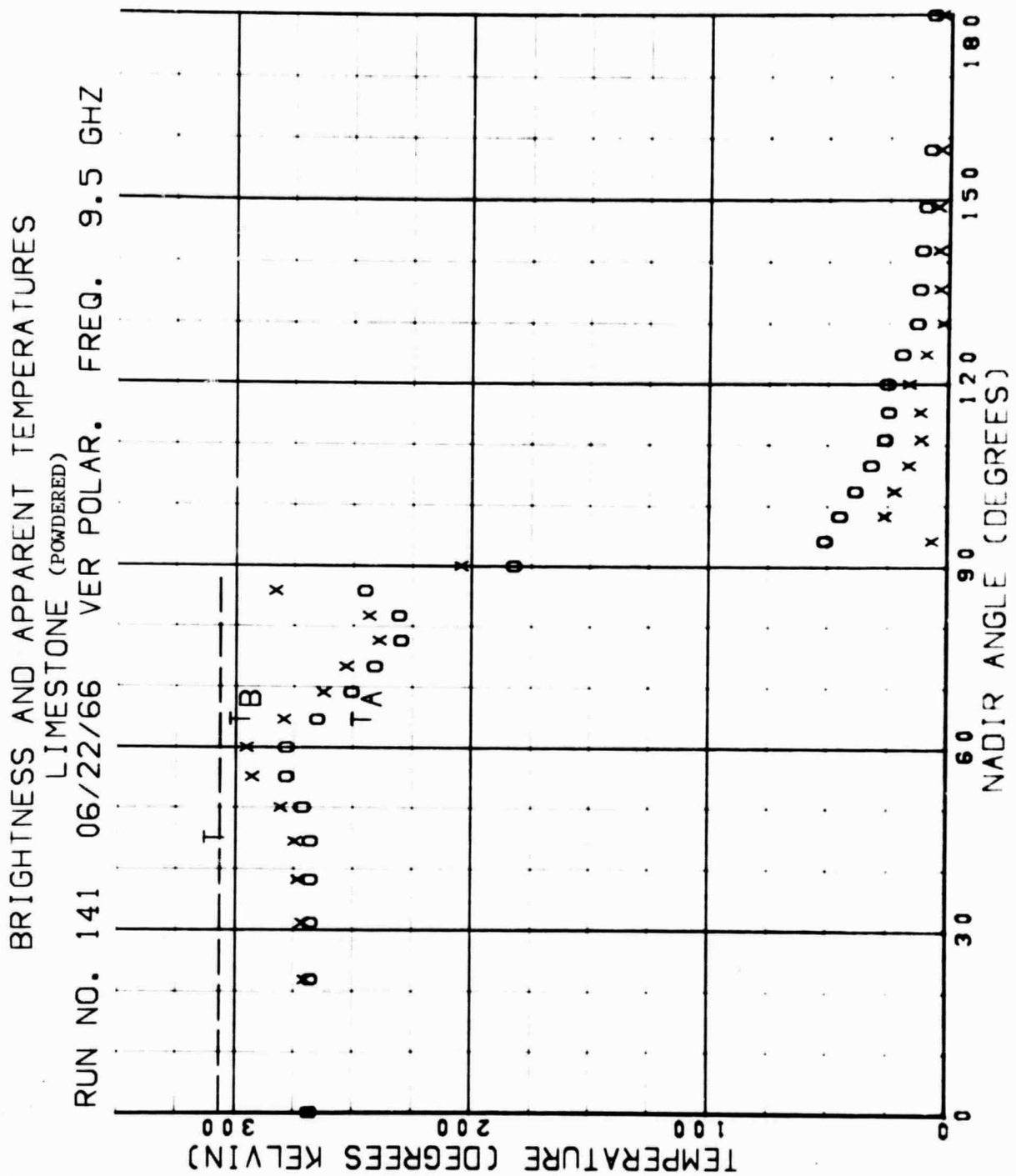


Figure 82 - Measured Brightness Temperatures, Powdered Limestone, 9.5 GHz, Vert. Pol.

PAGE 1 RUN 141

TARGET MATERIAL	LIMESTONE
DATA DATE	06/22/66
START TIME	1[illegible]
FREQUENCY,GHZ	9.5
POLARIZATION	VER
ANTENNA AZIMUTH,DEG	
BAROMETRIC PRESSURE,IN.HG.	30.7[illegible]
RELATIVE HUMIDITY,%	3[illegible]
AIR TEMPERATURE,DEG F	82
WIND DIRECTION	NNW
WIND SPEED,MPH	13
INTEGRATION TIME,SEC	1

THIRD CALIBRATION POINT 6.1[illegible]DEG.K 6111.[illegible]MV.

INITIAL CALIBRATION DATA	
MINIMUM CAL.TEMP,DEG.K	3[illegible].44
MAXIMUM CAL.TEMP.DEG.K	4[illegible].15
K-FACTOR,DEG.K/MV.	[illegible].34956
Y INTERCEPT	-2129.47

FINAL CALIBRATION DATA	
MINIMUM CAL.TEMP,DEG.K	3[illegible].42
MAXIMUM CAL.TEMP.DEG.K	402.13
K-FACTOR,DEG.K/MV.	[illegible].35378
Y INTERCEPT	-2155.21

CALIBRATION CONSTANTS	INITIAL	FINAL	UNITS
HOT LOAD	4[illegible].[illegible]	4[illegible].[illegible]	DEG.K
ATTENUATOR	3[illegible].[illegible]	3[illegible].[illegible]	DEG.K
WAVE GUIDE SWITCH	3[illegible].[illegible]	3[illegible].[illegible]	DEG.K
ANTENNA	3[illegible].[illegible]	299.[illegible]	DEG.K
AVERAGE CAL.DATA-MIN.	6962.12	6945.53	MV.
-MAX.	7253.[illegible]	7233.73	MV.

COMMENTS
BLOWING LIMESTONE DUST IN LBS

REPRODUCIBILITY OF THE ORIGINAL PAGE IS POOR.

ZENITH ANGLE DEG	EMISSIVITY TEMP VERTICAL DEG K	TIME	READINGS MV	SURFACE TEMP	SLEEVE ANGLE	1/2 IN TEMP DEG K	1 FT TEMP DEG K	2 FT TEMP DEG K	3 FT TEMP DEG K	6 IN TEMP DEG K	12 IN TEMP DEG K
0.0	0.0	1000	e111e	0.0	0.0	0.0	0.0	0.0	0.0	0.0	0.0
10.0	0.0		e1C4e	0.0	0.0	0.0	0.0	0.0	0.0	0.0	0.0
20.0	0.0		e113e	0.0	0.0	0.0	0.0	0.0	0.0	0.0	0.0
30.0	0.0		e1C2e	0.0	0.0	0.0	0.0	0.0	0.0	0.0	0.0
40.0	0.0		e12Ae	0.0	0.0	0.0	0.0	0.0	0.0	0.0	0.0
50.0	0.0		e17Ce	0.0	0.0	0.0	0.0	0.0	0.0	0.0	0.0
60.0	0.0		e1E4e	0.0	0.0	0.0	0.0	0.0	0.0	0.0	0.0
70.0	0.0		e1E2e	0.0	0.0	0.0	0.0	0.0	0.0	0.0	0.0
72.0	0.0		e1E8e	0.0	0.0	0.0	0.0	0.0	0.0	0.0	0.0
74.0	0.0		e15Ce	0.0	0.0	0.0	0.0	0.0	0.0	0.0	0.0
76.0	0.0		e2C2e	0.0	0.0	0.0	0.0	0.0	0.0	0.0	0.0
78.0	0.0		e221e	0.0	0.0	0.0	0.0	0.0	0.0	0.0	0.0
80.0	0.0		e25Ae	0.0	0.0	0.0	0.0	0.0	0.0	0.0	0.0
81.0	0.0		e23Be	0.0	0.0	0.0	0.0	0.0	0.0	0.0	0.0
82.0	0.0		e3E4e	0.0	0.0	0.0	0.0	0.0	0.0	0.0	0.0
83.0	0.0		e41Ce	0.0	0.0	0.0	0.0	0.0	0.0	0.0	0.0
84.0	0.0		e71Ae	0.0	0.0	0.0	0.0	0.0	0.0	0.0	0.0
85.0	0.0		e75Ce	0.0	0.0	0.0	0.0	0.0	0.0	0.0	0.0
86.0	0.0		e75Ae	0.0	0.0	0.0	0.0	0.0	0.0	0.0	0.0
87.0	0.0		e73Ae	0.0	0.0	0.0	0.0	0.0	0.0	0.0	0.0
88.0	0.0		e73Ee	0.0	0.0	0.0	0.0	0.0	0.0	0.0	0.0
89.0	0.0		e77Ae	0.0	0.0	0.0	0.0	0.0	0.0	0.0	0.0
90.0	0.0		e773e	0.0	0.0	0.0	0.0	0.0	0.0	0.0	0.0
91.0	0.0		e76Ae	0.0	0.0	0.0	0.0	0.0	0.0	0.0	0.0
92.0	0.0		e75Ae	0.0	0.0	0.0	0.0	0.0	0.0	0.0	0.0
93.0	0.0		e74Ae	0.0	0.0	0.0	0.0	0.0	0.0	0.0	0.0
94.0	0.0		e6F1e	0.0	0.0	0.0	0.0	0.0	0.0	0.0	0.0
95.0	0.0		e6F4e	0.0	0.0	0.0	0.0	0.0	0.0	0.0	0.0
96.0	0.0		e6E1e	0.0	0.0	0.0	0.0	0.0	0.0	0.0	0.0
97.0	0.0		e6E4e	0.0	0.0	0.0	0.0	0.0	0.0	0.0	0.0
98.0	0.0		e6E1e	0.0	0.0	0.0	0.0	0.0	0.0	0.0	0.0
99.0	0.0		e6E4e	0.0	0.0	0.0	0.0	0.0	0.0	0.0	0.0

Table XC - Brightness Temperatures, Powdered Limestone, 9.5 GHz, Vert. Pol.

RUN NO. 141 06/22/66 VER POLAR. 9.5 GHZ LIMESTONE

ITERATION NUMBER 0

ZENITH ANGLE (DEG)	BRIGHTNESS TEMP. (DEG K)	APPARENT TEMP. (DEG K)	CORRECTION TEMP. (DEG K)
0.0	3.60	6.80	-3.2047
21.79	3.98	7.83	-3.8554
31.00	4.80	9.69	-4.8857
38.21	4.32	11.06	-6.7401
44.42	3.81	12.19	-8.3758
49.99	2.37	13.19	-10.8204
55.15	9.56	19.40	-9.8442
60.00	16.25	25.25	-8.9956
64.62	11.75	24.74	-12.9882
69.08	11.25	26.45	-15.1982
73.40	16.38	31.91	-15.5317
77.63	22.02	38.51	-16.4841
81.79	26.30	45.12	-18.8163
85.90	6.45	51.04	-44.5860
90.00	204.76	182.08	22.6863
94.10	283.62	245.57	38.0510
98.21	243.42	230.79	12.6315
102.37	239.45	230.21	9.2368
106.60	253.63	241.48	12.1449
110.92	262.64	251.34	11.3022
115.38	279.50	265.77	13.7329
120.00	295.63	278.60	17.0351
124.85	293.12	278.77	14.3440
130.01	280.91	271.86	9.0540
135.58	274.87	268.32	6.5493
141.79	273.73	268.32	5.4138
149.00	271.94	268.32	3.6247
158.21	270.72	268.32	2.4049
180.00	269.15	268.32	0.8305

ABS. CORRECTION = 1.24E 01 DEG. K

Table XCI - Brightness and Apparent Temperatures, Powdered Limestone, 9.5 GHz, Vert. Pol.

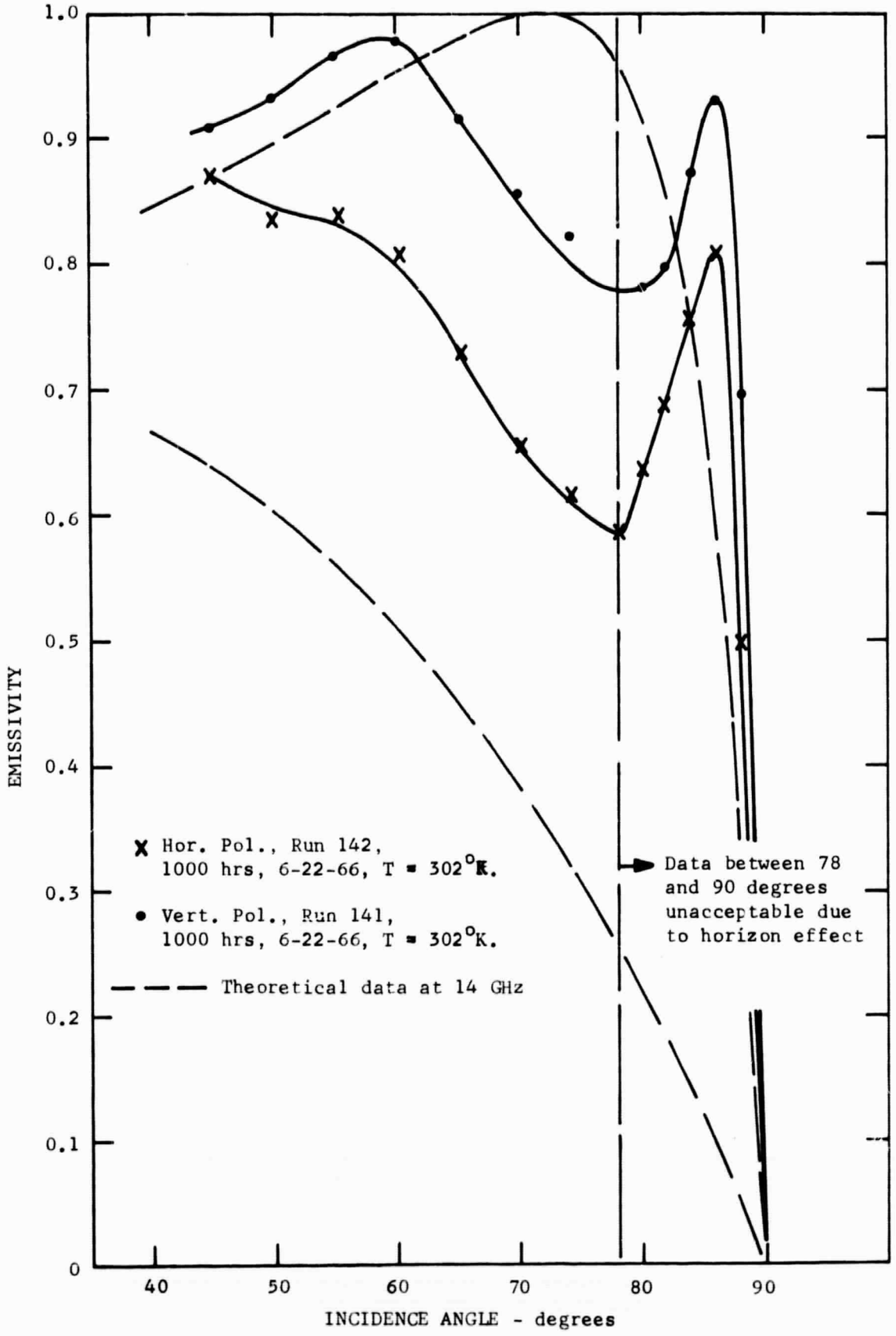


Figure 83 - Derived and Theoretical Specular Emissivities, Powdered Limestone - 9.5 GHz.

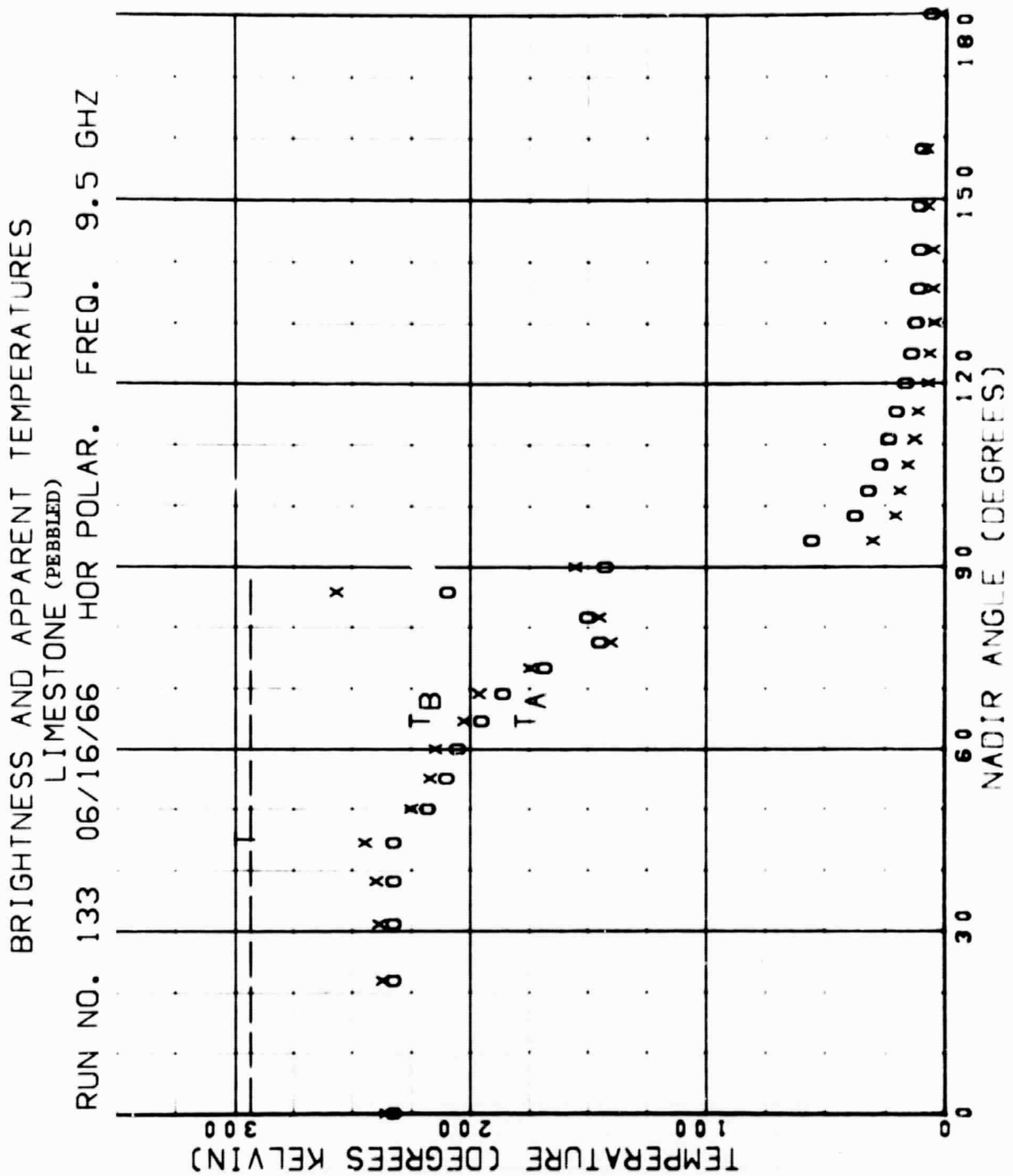


Figure 84 - Measured Brightness Temperatures, Pebbled Limestone, 9.5 GHz, Hor. Pol.

Table XCII - Environmental and Calibration Data, Pebbled Limestone, 9.5 GHz, Hor. Pol.

PAGE 1 RUN 133

TARGET MATERIAL	LIMESTONE
DATA DATE	06/16/66
START TIME	2345
FREQUENCY,GHZ	9.5
POLARIZATION	HOR
ANTENNA AZIMUTH,DEG	
BAROMETRIC PRESSURE,IN.HG.	30.84
RELATIVE HUMIDITY,%	37
AIR TEMPERATURE,DEG F	81
WIND DIRECTION	SE
WIND SPEED,MPH	3
INTEGRATION TIME,SEC	

THIRD CALIBRATION POINT 6.30DEG.K 6937.00MV.

INITIAL CALIBRATION DATA

MINIMUM CAL.TEMP,DEG.K	299.57
MAXIMUM CAL.TEMP.DEG.K	404.19
K-FACTOR,DEG.K/MV.	0.32709
Y INTERCEPT	-1926.38

FINAL CALIBRATION DATA

MINIMUM CAL.TEMP,DEG.K	299.57
MAXIMUM CAL.TEMP.DEG.K	404.19
K-FACTOR,DEG.K/MV.	0.31648
Y INTERCEPT	-1904.26

CALIBRATION CONSTANTS	INITIAL	FINAL	UNITS
HOT LOAD	405.00	405.00	DEG.K
ATTENUATOR	299.00	299.00	DEG.K
WAVE GUIDE SWITCH	297.00	297.00	DEG.K
ANTENNA	292.00	292.00	DEG.K
AVERAGE CAL.DATA-MIN.	6957.50	6962.80	MV.
-MAX.	7278.60	7294.53	MV.

COMMENTS
SKY DARK CLEAR

PAGE 4 RUN 122

TABLET MATERIAL LIMESTONE
DATA DATE 06/18/80
START TIME 2345
FREQUENCY,GHZ 9.5
POLARIZATION HOR

ZENITH ANGLE DEG	EMISSIVITY TEMP,HORIZONTAL DEG K	TIME	READINGS MV	SURFACE TEMP	SLOPE ANGLE	1/2 IN TEMP DEG K	1 FT TEMP DEG K	2 FT TEMP DEG K	3 FT TEMP DEG K	3 IN TEMP DEG K	6 IN TEMP DEG K	12 IN TEMP DEG K
0.0	2.1	2345	6C37.	0.0	0.0	0.0	0.0	0.0	0.0	0.0	0.0	0.0
10.0	4.9		6C56.	0.0	0.0	0.0	0.0	0.0	0.0	0.0	0.0	0.0
20.0	7.6		6C45.	0.0	0.0	0.0	0.0	0.0	0.0	0.0	0.0	0.0
30.0	7.4		6C52.	0.0	0.0	0.0	0.0	0.0	0.0	0.0	0.0	0.0
40.0	5.2		6C51.	0.0	0.0	0.0	0.0	0.0	0.0	0.0	0.0	0.0
45.0	5.0											
50.0	4.7		6C56.	0.0	0.0	0.0	0.0	0.0	0.0	0.0	0.0	0.0
55.0	5.5											
60.0	7.2		6C65.	0.0	0.0	0.0	0.0	0.0	0.0	0.0	0.0	0.0
65.0	11.2		6C83.	0.0	0.0	0.0	0.0	0.0	0.0	0.0	0.0	0.0
70.0	13.4		6C93.	0.0	0.0	0.0	0.0	0.0	0.0	0.0	0.0	0.0
72.0	14.8											
74.0	16.2											
75.0	16.8		6107.	0.0	0.0	0.0	0.0	0.0	0.0	0.0	0.0	0.0
76.0	17.5											
78.0	18.7											
80.0	20.0		6126.	0.0	0.0	0.0	0.0	0.0	0.0	0.0	0.0	0.0
82.0	21.3		6136.	0.0	0.0	0.0	0.0	0.0	0.0	0.0	0.0	0.0
84.0	25.5		6158.	0.0	0.0	0.0	0.0	0.0	0.0	0.0	0.0	0.0
86.0	33.1		6154.	0.0	0.0	0.0	0.0	0.0	0.0	0.0	0.0	0.0
88.0	34.3		6254.	0.0	0.0	0.0	0.0	0.0	0.0	0.0	0.0	0.0
90.0	155.5		6467.	289.0	0.0	289.0	0.0	0.0	0.0	0.0	0.0	0.0
92.0	205.2	0.570	655C.	289.0	0.0	289.0	0.0	0.0	0.0	0.0	0.0	0.0
94.0	255.0	0.667	6662.	289.0	0.0	289.0	0.0	0.0	0.0	0.0	0.0	0.0
96.0	295.4	0.660	6595.	290.0	0.0	290.0	0.0	0.0	0.0	0.0	0.0	0.0
98.0	150.8	0.464	6456.	289.0	0.0	289.0	0.0	0.0	0.0	0.0	0.0	0.0
100.0	143.1	0.456	6449.	290.0	0.0	290.0	0.0	0.0	0.0	0.0	0.0	0.0
102.0	141.0	0.451	6476.	290.0	0.0	290.0	0.0	0.0	0.0	0.0	0.0	0.0
104.0	153.8	0.500	6498.	290.0	0.0	290.0	0.0	0.0	0.0	0.0	0.0	0.0
106.0	170.0	0.562	653E.	290.0	0.0	290.0	0.0	0.0	0.0	0.0	0.0	0.0
108.0	181.8	0.607	6574.	290.0	0.0	289.0	0.0	0.0	0.0	0.0	0.0	0.0
110.0	191.7	0.644	66CC.	290.0	0.0	289.0	0.0	0.0	0.0	0.0	0.0	0.0
115.0	202.5	0.684	6631.	290.0	0.0	289.0	0.0	0.0	0.0	0.0	0.0	0.0
120.0	215.0	0.737	6666.	289.0	0.0	289.0	0.0	0.0	0.0	0.0	0.0	0.0
125.0	217.6	0.745	66E1.	289.0	0.0	289.0	292.0	292.0	292.0	297.0	299.0	299.0
130.0	225.3	0.772	67C7.	289.0	0.0	289.0	0.0	0.0	0.0	0.0	0.0	0.0
135.0	243.1	0.833	6752.	289.0	0.0	289.0	0.0	0.0	0.0	0.0	0.0	0.0

Table XCIII - Brightness Temperatures, Pebbled Limestone, 9.5 GHz, Hor. Pol.

RUN NO. 133 06/16/66 HOR POLAR. 9.5 GHZ LIMESTONE

ITERATION NUMBER 0

ZENITH ANGLE (DEG)	BRIGHTNESS TEMP. (DEG K)	APPARENT TEMP. (DEG K)	CORRECTION TEMP. (DEG K)
0.0	2.12	6.03	-3.9092
21.79	8.13	9.94	-1.8122
31.00	7.31	10.70	-3.3829
38.21	5.33	10.60	-5.2740
44.42	4.99	11.26	-6.2709
49.99	4.72	12.13	-7.4083
55.15	6.45	14.29	-7.8403
60.00	7.17	16.32	-9.1472
64.62	11.06	20.38	-9.3149
69.08	12.82	23.46	-10.6407
73.40	15.60	27.11	-11.5118
77.63	18.87	31.63	-12.7639
81.79	20.84	37.42	-16.5875
85.90	30.21	55.60	-25.3971
90.00	155.47	143.07	12.4002
94.10	257.36	210.05	47.3161
98.21	145.02	150.43	-5.4117
102.37	140.58	145.36	-4.7846
106.60	174.89	168.80	6.0867
110.92	196.22	186.65	9.5722
115.38	203.07	195.46	7.6026
120.00	214.97	205.58	9.3886
124.85	217.34	210.16	7.1827
130.01	225.35	218.35	6.9998
135.58	245.20	232.67	12.5284
141.79	240.48	232.67	7.8081
149.00	238.72	232.67	6.0541
158.21	237.52	232.67	4.8518
180.00	236.24	232.67	3.5737

ABS. CORRECTION = 9.75E 00 DEG. K

Table XCIV - Brightness and Apparent Temperatures, Pebbled Limestone, 9.5 GHz, Hor. Pol.

the range 0.84 to 0.45, over a nadir angle range of 45° to 78°, respectively. Thus, there appears to be a rather small difference between horizontally polarized data for the powdered and pebbled limestone, except at large incidence angles. It could be stated that, since the emissivities fall off at a slightly faster rate with incidence angle in the case of the pebbled limestone, this texture is somewhat more specular than the powdered material. However, since this is contrary to expectations, such a conclusion can only be made on the basis of a more comprehensive comparison of a large number of data Runs. Such a comparison is presented in Subsection 6.

Vertically polarized data, for pebbled limestone, is shown in Figure 85 and Tables XCV thru' XCVII. The T_B's are at about the same level as for horizontal polarization, except in the vicinity of 65° (nadir angle) where they rise to a peak of 265°K. The derived emissivities range from 0.84 to 0.68 over a nadir angle range of 45° to 78°, respectively, with a peak of 0.91 at the Brewster Angle (65°). This Brewster Angle position is 5 degrees higher than for the powdered material, indicating a possibly higher dielectric permittivity in the pebbled limestone.

Figure 86 shows plots of derived emissivities. Although both polarizations are slightly lower than the powdered limestone curves, the separation between them is similar, except at large incidence angles where the vertical component drops off at a steeper rate than its powdered limestone counterpart. This results in better agreement with the shape of the theoretical curve at 14 GHz.

3. 16.5 GHz Data - Pebbled Limestone

There were no powdered limestone measurements at this frequency. Figure 87 and Tables XCVIII thru' C show horizontally polarized data for the pebbled material. It will be observed that the T_B's are about 20°K lower than the 9.5 GHz values shown in Figure 84. Since the surface temperatures are similar in both cases, this difference is difficult to reconcile, unless the dielectric permittivity is higher at 16.5 GHz. Unfortunately, since measured values of dielectric permittivity are available only at 14 GHz, the frequency dependence of this parameter, for dry limestone, is unknown. The derived emissivities are

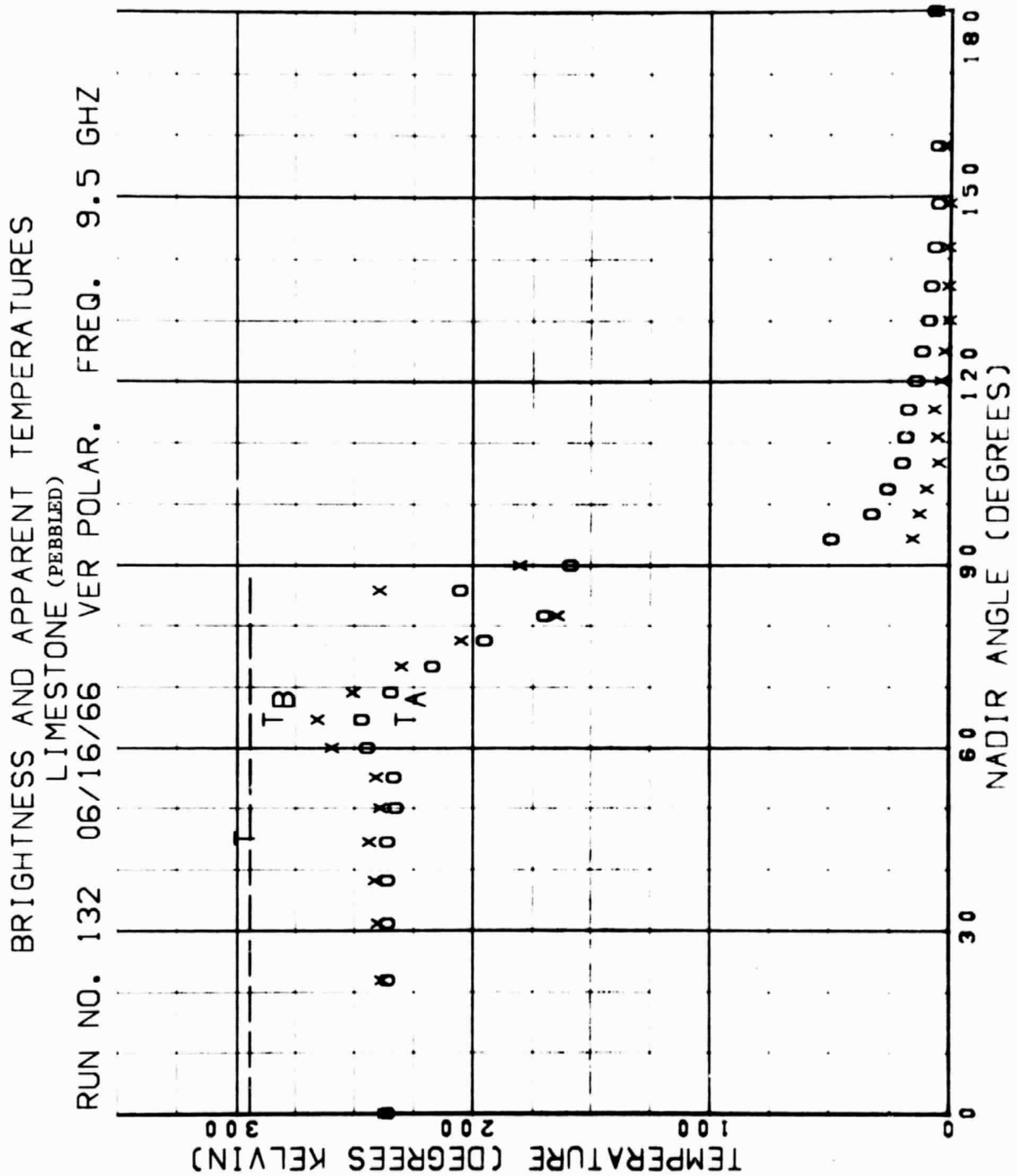


Figure 85 - Measured Brightness Temperatures, Pebbled Limestone, 9.5 GHz, Vert. Pol.

PAGE 1 RUN 132

TARGET MATERIAL	LIMESTONE
DATA DATE	06/16/66
START TIME	2330
FREQUENCY,GHZ	9.5
POLARIZATION	VER
ANTENNA AZIMUTH,DEG	
BAROMETRIC PRESSURE,IN.HG.	30.83
RELATIVE HUMIDITY,%	37
AIR TEMPERATURE,DEG F	81
WIND DIRECTION	SE
WIND SPEED,MPH	3
INTEGRATION TIME,SEC	

THIRD CALIBRATION POINT 6.30DEG.K 6[illegible]54.00MV.

INITIAL CALIBRATION DATA	
MINIMUM CAL.TEMP,DEG.K	299.51
MAXIMUM CAL.TEMP.DEG.K	404.13
K-FACTOR,DEG.K/MV.	0.32831
Y INTERCEPT	-1980.67
FINAL CALIBRATION DATA	
MINIMUM CAL.TEMP,DEG.K	299.51
MAXIMUM CAL.TEMP.DEG.K	404.13
K-FACTOR,DEG.K/MV.	0.32639
Y INTERCEPT	-1969.13

CALIBRATION CONSTANTS	INITIAL	FINAL	UNITS
HOT LOAD	405.00	405.00	DEG.K
ATTENUATOR	299.00	299.00	DEG.K
WAVE GUIDE SWITCH	297.30	297.00	DEG.K
ANTENNA	293.30	293.01	DEG.K
AVERAGE CAL.DATA-MIN.	6938.40	6944.60	MV.
-MAX.	7258.85	7275.60	MV.

COMMENTS
SKY DARK CLEAR

Table XCV - Environmental and Calibration Data, Pebbled Limestone, 9.5 GHz, Vert. Pol.

REPRODUCIBILITY OF THE ORIGINAL PAGE IS POOR.

PAGE 2 [illegible]

TARGET WITH-IAL LIMESTONE
DATA DATE 08/16/78
START TIME 2330
FREQUENCY,GHZ 9.5
POLARIZATION VER

ZENITH ANGLE DEG	BRIGHTNESS TEMP DEG K	EMISSIVITY VERTICAL	TIME	READINGS MV	SURFACE TEMP	SLOPE ANGLE	1/2 IN TEMP DEG K	1 FT TEMP DEG K	2 FT TEMP DEG K	3 FT TEMP DEG K	3 IN TEMP DEG K	6 IN TEMP DEG K	12 IN TEMP DEG K
0.0	5.5		2330	6654.	0.0	0.0	0.0	0.0	0.0	0.0	0.0	0.0	0.0
1.0	4.4			6653.	0.0	0.0	0.0	0.0	0.0	0.0	0.0	0.0	0.0
2.0	3.0			6650.	0.0	0.1	0.0	0.0	0.0	0.0	0.0	0.0	0.0
3.0	0.6			6648.	0.0	0.0	0.0	0.0	0.0	0.0	0.0	0.0	0.0
4.0	0.8			6654.	0.0	0.0	0.0	0.0	0.0	0.0	0.0	0.0	0.0
4.5	0.6												
5.0	0.5			6660.	0.0	0.0	0.0	0.0	0.0	0.0	0.0	0.0	0.0
5.5	2.1												
6.0	3.7			6675.	0.0	0.0	0.0	0.0	0.0	0.0	0.0	0.0	0.0
6.5	4.7			6687.	0.0	0.0	0.0	0.0	0.0	0.0	0.0	0.0	0.0
7.0	5.1			6695.	0.0	0.0	0.0	0.0	0.0	0.0	0.0	0.0	0.0
7.5	5.7												
7.5	6.3												
7.5	6.6			6696.	0.0	0.0	0.0	0.0	0.0	0.0	0.0	0.0	0.0
7.6	7.6												
7.8	9.6												
8.0	11.6			6725.	0.0	0.0	0.0	0.0	0.0	0.0	0.0	0.0	0.0
8.5	13.0			6732.	0.0	0.0	0.0	0.0	0.0	0.0	0.0	0.0	0.0
8.5	14.3			6745.	0.0	0.0	0.0	0.0	0.0	0.0	0.0	0.0	0.0
8.6	15.4			6765.	0.0	0.0	0.0	0.0	0.0	0.0	0.0	0.0	0.0
8.8	100.0			6814.	0.0	0.0	0.0	0.0	0.0	0.0	0.0	0.0	0.0
9.0	180.5	0.0		6518.	2920.0	0.0	2920.0	0.0	0.0	0.0	0.0	0.0	0.0
9.2	209.4	0.570		6526.	2920.0	0.0	2920.0	0.0	0.0	0.0	0.0	0.0	0.0
9.4	218.3	0.FC2		6544.	2920.0	0.0	2920.0	0.0	0.0	0.0	0.0	0.0	0.0
9.6	204.9	0.E85		6566.	2910.0	0.0	2910.0	0.0	0.0	0.0	0.0	0.0	0.0
9.8	168.2	0.E55		6551.	2910.0	0.0	2910.0	0.0	0.0	0.0	0.0	0.0	0.0
10.0	191.8	0.EC5		6565.	2910.0	0.0	2910.0	0.0	0.0	0.0	0.0	0.0	0.0
10.2	201.4	0.EE1		6625.	2910.0	0.0	2910.0	0.0	0.0	0.0	0.0	0.0	0.0
10.4	214.5	0.721		6655.	2910.0	0.0	2910.0	0.0	0.0	0.0	0.0	0.0	0.0
10.6	227.6	0.7F5		6651.	2910.0	0.0	2910.0	0.0	0.0	0.0	0.0	0.0	0.0
10.8	237.2	0.E12		6715.	2910.0	0.0	2910.0	0.0	0.0	0.0	0.0	0.0	0.0
11.0	246.6	0.E45		6744.	2910.0	0.0	2910.0	0.0	0.0	0.0	0.0	0.0	0.0
11.5	254.5	0.5C4		6751.	2910.0	0.0	2910.0	0.0	0.0	0.0	0.0	0.0	0.0
12.0	259.8	0.E55		6763.	2900.0	0.0	2900.0	0.0	0.0	0.0	0.0	0.0	0.0
12.5	241.1	0.E30		6749.	2900.0	0.0	2900.0	2920.0	2920.0	2920.0	2970.0	2990.0	2990.0
13.0	229.6	0.E22		6747.	2900.0	0.1	2900.0	0.0	0.0	0.0	0.0	0.0	0.0
13.5	243.8	0.E40		6758.	2900.0	0.0	2900.0	0.0	0.0	0.0	0.0	0.0	0.0

Table XCVI - Brightness Temperatures, Pebbled Limestone, 9.5 GHz, Vert. Pol.

RUN NO. 132 06/16/66 VER POLAR. 9.5 GHZ LIMESTONE

ITERATION NUMBER 0

ZENITH ANGLE (DEG)	BRIGHTNESS TEMP. (DEG K)	APPARENT TEMP. (DEG K)	CORRECTION TEMP. (DEG K)
0.0	5.86	6.88	-1.0231
21.79	2.71	5.58	-2.8715
31.00	0.31	5.05	-4.7344
38.21	0.79	6.53	-5.7462
44.42	0.81	7.81	-7.0023
49.99	0.49	8.96	-8.4715
55.15	2.51	11.53	-9.0186
60.00	3.73	13.95	-10.2157
64.62	6.79	17.37	-10.5780
69.08	5.18	18.16	-12.9746
73.40	4.66	19.79	-15.1277
77.63	9.86	25.56	-15.6968
81.79	12.86	32.22	-19.3621
85.90	15.56	49.14	-33.5806
90.00	180.54	158.85	21.6897
94.10	239.69	205.47	34.2215
98.21	164.37	170.03	-5.6536
102.37	205.00	195.34	9.6616
106.60	230.69	217.30	13.3894
110.92	250.95	235.02	15.9282
115.38	266.19	247.54	18.6475
120.00	259.82	244.98	14.8414
124.85	241.18	234.03	7.1508
130.01	239.62	233.06	6.5612
135.58	244.27	236.68	7.5868
141.79	241.92	236.68	5.2407
149.00	240.37	236.68	3.6896
158.21	239.08	236.68	2.3965
180.00	237.76	236.68	1.0809

ABS. CORRECTION = 1.12E 01 DEG. K

Table XCVII - Brightness and Apparent Temperatures, Pebbled Limestone, 9.5 GHz, Vert. Pol.

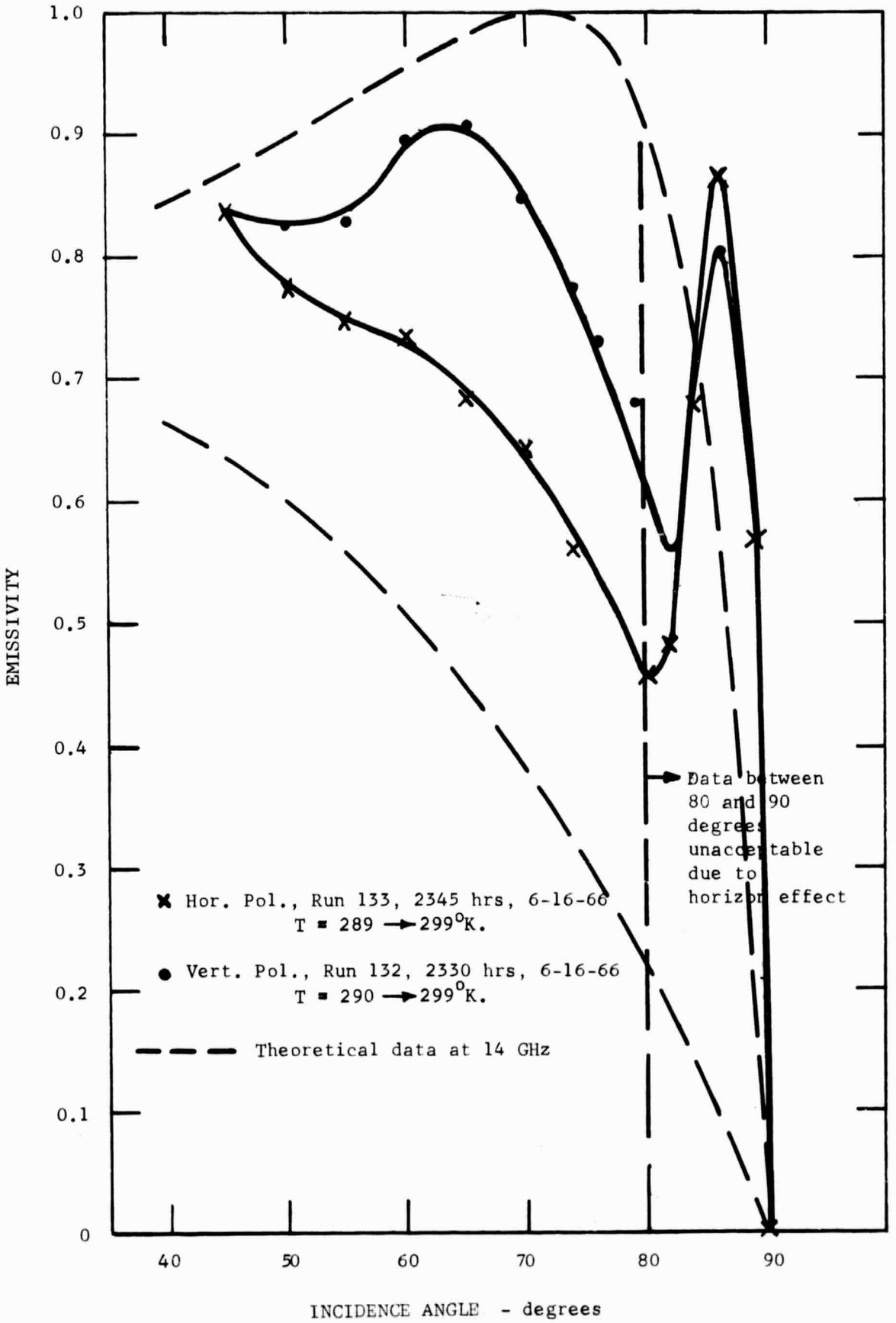


Figure 86 - Derived and Theoretical Specular Emissivities, Pebbled Limestone - 9.5 GHz

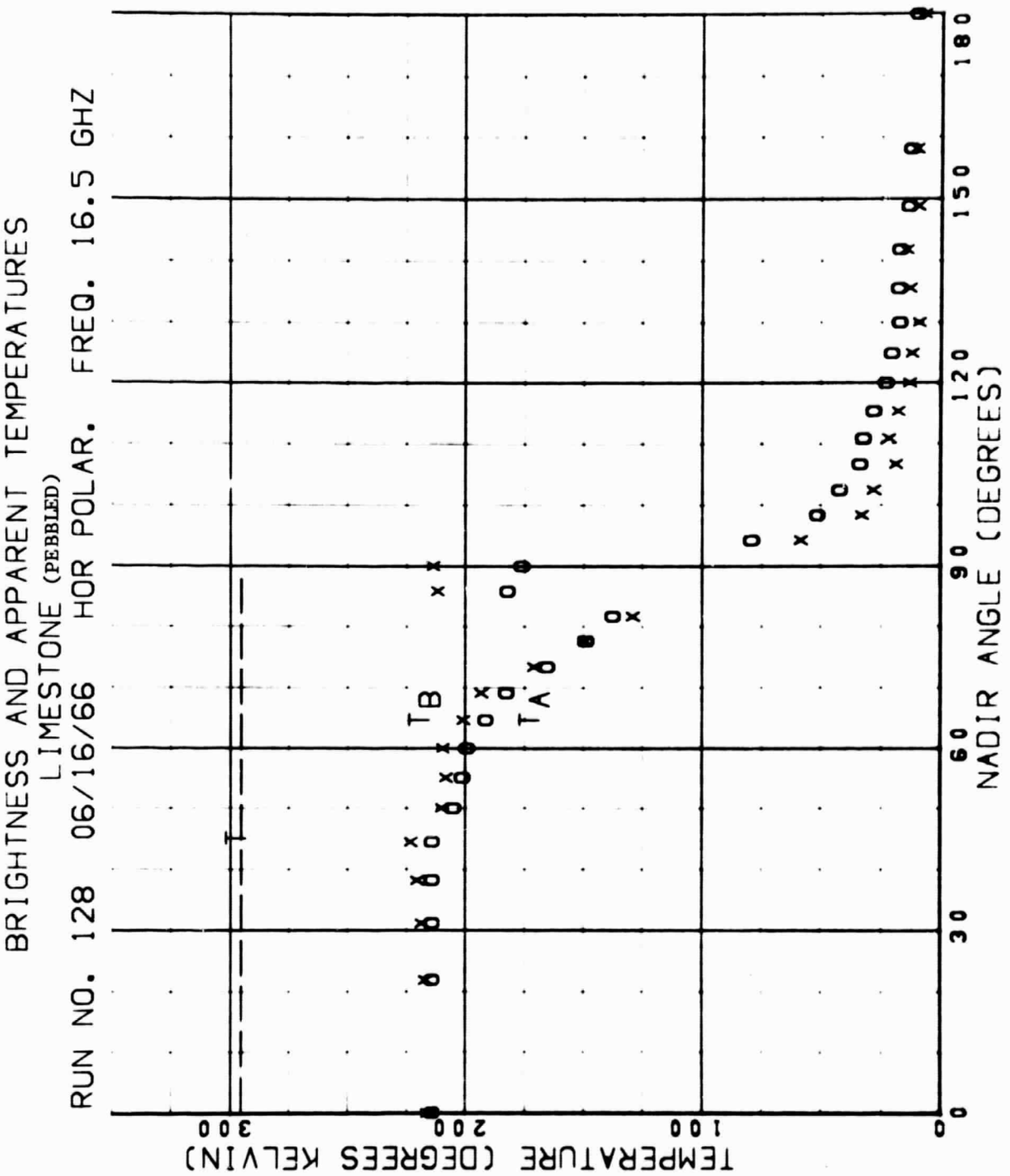


Figure 87 - Measured Brightness Temperatures, Pebbled Limestone, 16.5 GHz, Hor. Pol.

PAGE 1 RUN 128

TARGET MATERIAL	LIMESTONE	
DATA DATE	06/16/66	
START TIME	2130	
FREQUENCY,GHZ	16.5	
POLARIZATION	HOR	
ANTENNA AZIMUTH,DEG		
BAROMETRIC PRESSURE,IN.HG.	30.84	
RELATIVE HUMIDITY,%	33	
AIR TEMPERATURE,DEG F	80	
WIND DIRECTION		
WIND SPEED,MPH		
INTEGRATION TIME,SEC	1	
THIRD CALIBRATION POINT	10.10DEG.K	6659.00MV.

INITIAL CALIBRATION DATA

MINIMUM CAL.TEMP,DEG.K	297.84
MAXIMUM CAL.TEMP.DEG.K	393.24
K-FACTOR,DEG.K/MV.	0.78674
Y INTERCEPT	-5228.58

FINAL CALIBRATION DATA

MINIMUM CAL.TEMP,DEG.K	297.84
MAXIMUM CAL.TEMP.DEG.K	393.24
K-FACTOR,DEG.K/MV.	0.79101
Y INTERCEPT	-5258.02

CALIBRATION CONSTANTS	INITIAL	FINAL	UNITS
HOT LOAD	396.00	396.00	DEG.K
ATTENUATOR	297.00	297.00	DEG.K
WAVE GUIDE SWITCH	295.00	295.00	DEG.K
ANTENNA	290.10	290.10	DEG.K
AVERAGE CAL.DATA-MIN.	7023.20	7027.85	MV.
-MAX.	7146.66	7141.35	MV.

COMMENTS
SKY DARK CLEAR

PAGE 2 RUN 122

TARGET MATERIAL LIMESTONE
DATA DATE 06/16/66
START TIME 2130
FREQUENCY,GHZ 16.5
POLARIZATION HOR

ZENITH ANGLE DEG	EMISSIVITY TEMP,PERPENDICULAR DEG K	TIME	READINGS MV	SURFACE TEMP	SLOPE ANGLE	1/2 IN TEMP DEG K	1 FT TEMP DEG K	2 FT TEMP DEG K	3 FT TEMP DEG K	3 IN TEMP DEG K	6 IN TEMP DEG K	12 IN TEMP DEG K
0.0	7.7	2130	.6559	0.0	0.0	0.0	0.0	0.0	0.0	0.0	0.0	0.0
10.0	9.7		.6561	0.0	0.0	0.0	0.0	0.0	0.0	0.0	0.0	0.0
20.0	10.0		.6555	0.0	0.0	0.0	0.0	0.0	0.0	0.0	0.0	0.0
30.0	9.9		.6563	0.0	0.0	0.0	0.0	0.0	0.0	0.0	0.0	0.0
40.0	14.1		.6565	0.0	0.0	0.0	0.0	0.0	0.0	0.0	0.0	0.0
45.0	11.8											
50.0	9.5		.6568	0.0	0.0	0.0	0.0	0.0	0.0	0.0	0.0	0.0
55.0	11.3											
60.0	13.1		.6575	0.0	0.0	0.0	0.0	0.0	0.0	0.0	0.0	0.0
65.0	14.1		.6582	0.0	0.0	0.0	0.0	0.0	0.0	0.0	0.0	0.0
70.0	21.0		.6588	0.0	0.0	0.0	0.0	0.0	0.0	0.0	0.0	0.0
72.0	21.5											
74.0	22.1											
75.0	22.3		.6595	0.0	0.0	0.0	0.0	0.0	0.0	0.0	0.0	0.0
76.0	24.0											
78.0	27.3											
80.0	30.6		.6709	0.0	0.0	0.0	0.0	0.0	0.0	0.0	0.0	0.0
82.0	34.1		.6712	0.0	0.0	0.0	0.0	0.0	0.0	0.0	0.0	0.0
84.0	46.7		.6723	0.0	0.0	0.0	0.0	0.0	0.0	0.0	0.0	0.0
86.0	52.4		.6748	0.0	0.0	0.0	0.0	0.0	0.0	0.0	0.0	0.0
88.0	138.3		.6800	0.0	0.0	0.0	0.0	0.0	0.0	0.0	0.0	0.0
90.0	214.2	0.0	.6830	2510.0	0.0	287.0	0.0	0.0	0.0	0.0	0.0	0.0
92.0	213.3	0.0491	.6857	2510.0	0.0	297.0	0.0	0.0	0.0	0.0	0.0	0.0
94.0	212.4	0.0556	.6875	2510.0	0.0	290.0	0.0	0.0	0.0	0.0	0.0	0.0
95.0	174.0	0.0521	.6852	2510.0	0.0	291.0	0.0	0.0	0.0	0.0	0.0	0.0
96.0	133.7	0.0384	.6821	2510.0	0.0	291.0	0.0	0.0	0.0	0.0	0.0	0.0
100.0	138.0	0.0414	.6824	2510.0	0.0	290.0	0.0	0.0	0.0	0.0	0.0	0.0
102.0	147.7	0.0455	.6832	2510.0	0.0	290.0	0.0	0.0	0.0	0.0	0.0	0.0
104.0	157.7	0.0503	.6845	2510.0	0.0	290.0	0.0	0.0	0.0	0.0	0.0	0.0
106.0	167.6	0.0544	.6852	2510.0	0.0	290.0	0.0	0.0	0.0	0.0	0.0	0.0
108.0	175.3	0.0584	.6867	2510.0	0.0	290.0	0.0	0.0	0.0	0.0	0.0	0.0
110.0	138.2	0.0424	.6876	2510.0	0.0	290.0	0.0	0.0	0.0	0.0	0.0	0.0
115.0	200.5	0.0671	.6895	2510.0	0.0	290.0	0.0	0.0	0.0	0.0	0.0	0.0
120.0	210.1	0.0705	.6906	2510.0	0.0	291.0	0.0	0.0	0.0	0.0	0.0	0.0
125.0	208.4	0.0708	.6902	2510.0	0.0	291.0	296.0	292.0	291.0	297.0	297.0	296.0
130.0	210.6	0.0714	.6907	2510.0	0.0	291.0	0.0	0.0	0.0	0.0	0.0	0.0
135.0	222.3	0.0754	.6919	2510.0	0.0	291.0	0.0	0.0	0.0	0.0	0.0	0.0

Table XCIX - Brightness Temperatures, Pebbled Limestone, 16.5 GHz, Hor. Pol.

RUN NO. 128 06/16/66 HOR POLAR. 16.5 GHZ LIMESTONE

ITERATION NUMBER 0

ZENITH ANGLE (DEG)	BRIGHTNESS TEMP. (DEG K)	APPARENT TEMP. (DEG K)	CORRECTION TEMP. (DEG K)
0.0	7.37	10.33	-2.9561
21.79	10.29	12.48	-2.1895
31.00	9.89	13.58	-3.6890
38.21	14.55	17.30	-2.7448
44.42	12.99	17.93	-4.9429
49.99	9.48	17.56	-8.0783
55.15	11.99	20.42	-8.4306
60.00	13.10	23.12	-10.0174
64.62	17.82	28.02	-10.1981
69.08	21.57	32.33	-10.7637
73.40	18.95	33.68	-14.7279
77.63	27.89	42.20	-14.3156
81.79	32.72	51.51	-18.7952
85.90	58.80	79.35	-20.5499
90.00	214.25	176.11	38.1381
94.10	212.36	182.34	30.0234
98.21	129.38	137.83	-8.4453
102.37	149.46	148.87	0.5868
106.60	170.93	165.43	5.4965
110.92	193.65	182.96	10.6977
115.38	201.15	191.67	9.4808
120.00	210.08	199.71	10.3679
124.85	208.36	201.40	6.9633
130.01	210.58	205.33	5.2465
135.58	223.70	214.81	8.8855
141.79	220.61	214.81	5.7958
149.00	218.96	214.81	4.1523
158.21	217.58	214.81	2.7683
180.00	216.35	214.81	1.5355

ABS. CORRECTION = 9.69E 00 DEG. K

Table C - Brightness and Apparent Temperatures, Pebbled Limestone, 16.5 GHz, Hor. Pol.

lower than at 9.5 GHz, lying between 0.75 and 0.46 in the nadir angle range 45^{o} to 78^{o}, respectively.

Figure 88, together with Tables CI thru' CIII, shows vertically polarized data. Here, the T_B's are approximately equal to the horizontally polarized values except in the vicinity of the Brewster Angle, which is centered at a nadir angle of 65^{o}. Derived emissivities lie between 0.73 and 0.67 for nadir angles of 45^{o} to 78^{o}, respectively, with a peak of 0.80 at the Brewster Angle.

The derived emissivities are shown plotted in Figure 89, together with theoretical data at 14 GHz. Perhaps the most notable feature is the small separation between the two polarizations, compared with the 9.5 GHz data shown in Figure 86. This implies a smaller degree of specularity for the pebbled limestone at 16.5 GHz. Referring to the roughness characteristic of this material in Figures 79 and 80, the convergence of the two polarizations is understandable at this frequency.

Figure 90 shows plots of theoretical emissivities of limestone at 14 GHz. It will be noted that the emissivities are generally lower for this material than for Salines or Quartz Sand. This is due to the higher dielectric permittivity - 8.63 versus 4.75 and 2.88 for Salines and Quartz Sand, respectively. The Brewster Angle is at an incidence angle of approximately 71^{o}, which is 6^{o} higher than its position at 16.5 and 9.5 GHz, respectively, for the pebbled material; it is 11^{o} higher than its position at 9.5 GHz, for the powdered material.

4. Comparison of Derived and Calculated Brightness Temperatures - Pebbled Limestone

Figures 91 and 92 show plots of derived and calculated T_B's at 16.5 GHz for horizontal and vertical polarization, respectively. The agreement between derived and calculated values is rather poor for horizontal polarization, indicating that the specular emissivities employed in the latter do not represent satisfactory values for the pebbled material. The disparity between specular and derived emissivities is clearly shown in Figure 89 - the specular values are from 0.12 to 0.22 lower than the derived values. At a temperature of $298.2^{o}K$, these represent

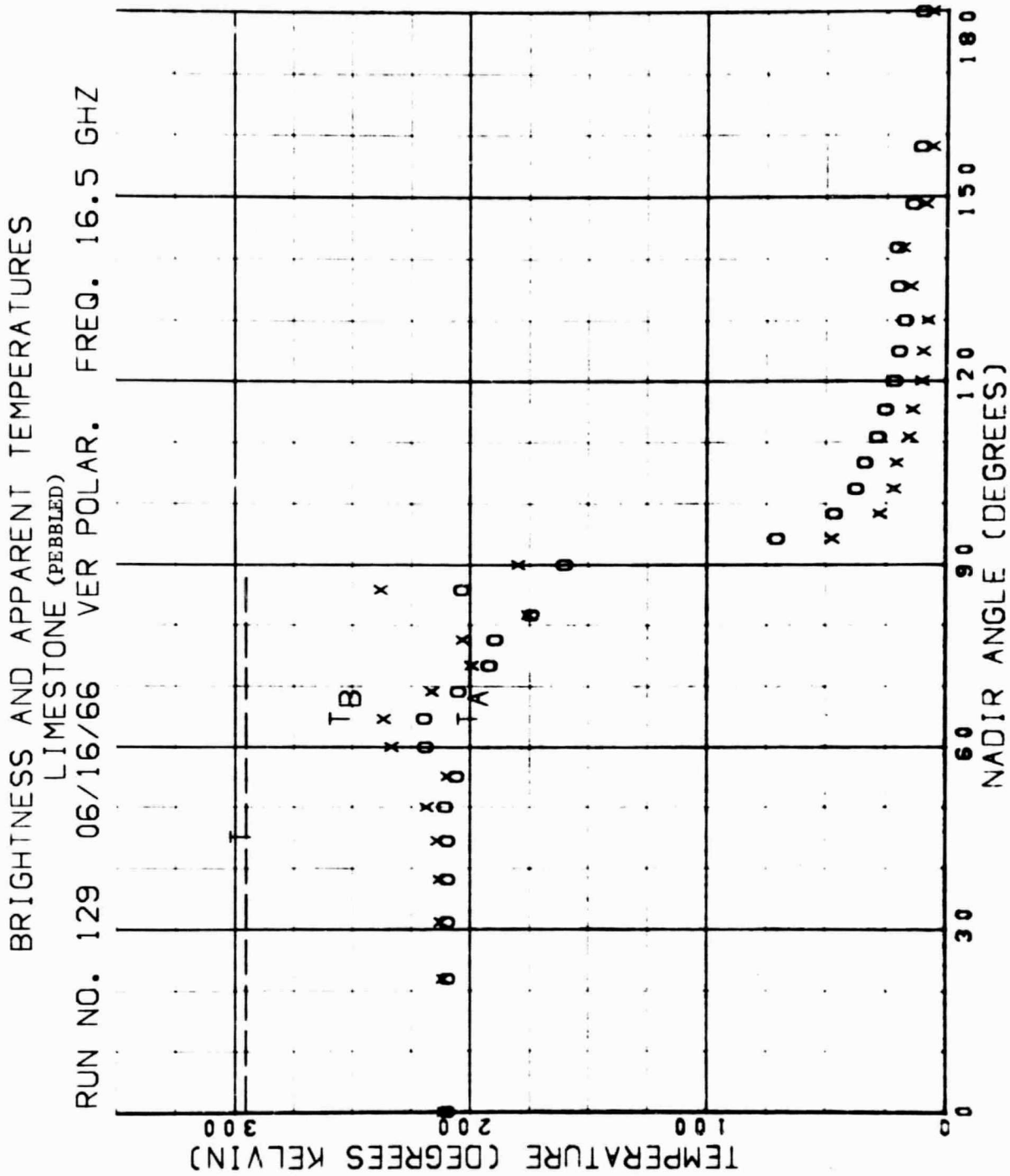


Figure 88 - Measured Brightness Temperatures, Pebbled Limestone, 16.5 GHz, Vert. Pol.

Table CI - Environmental and Calibration Data, Pebbled Limestone, 16.5 GHz, Vert. Pol.

PAGE 1 RUN 129

TARGET MATERIAL	LIMESTONE
DATA DATE	06/16/66
START TIME	2204
FREQUENCY,GHZ	16.5
POLARIZATION	VER
ANTENNA AZIMUTH,DEG	
BAROMETRIC PRESSURE,IN.HG.	30.05
RELATIVE HUMIDITY,%/0	32
AIR TEMPERATURE,DEG F	80
WIND DIRECTION	
WIND SPEED,MPH	
INTEGRATION TIME,SEC	1

THIRD CALIBRATION POINT 9.90DEG.K 6664.03MV.

INITIAL CALIBRATION DATA

MINIMUM CAL.TEMP,DEG.K	295.53
MAXIMUM CAL.TEMP.DEG.K	391.90
K-FACTOR,DEG.K/MV.	0.79058
Y INTERCEPT	-5257.93

FINAL CALIBRATION DATA

MINIMUM CAL.TEMP,DEG.K	295.53
MAXIMUM CAL.TEMP.DEG.K	391.90
K-FACTOR,DEG.K/MV.	0.79274
Y INTERCEPT	-5272.77

CALIBRATION CONSTANTS	INITIAL	FINAL	UNITS
HOT LOAD	395.00	395.00	DEG.K
ATTENUATOR	295.00	295.00	DEG.K
WAVE GUIDE SWITCH	295.00	295.00	DEG.K
ANTENNA	290.00	290.00	DEG.K
AVERAGE CAL.DATA-MIN.	7021.25	7023.65	MV.
-MAX.	7148.90	7146.50	MV.

COMMENTS
SKY DARK CLEAR

TARGET MATERIAL LIMESTONE
DATA DATE 06/16/66
START TIME 2200
FREQUENCY,GHZ 16.5
POLARIZATION VER

ZENITH ANGLE DEG	BRIGHTNESS TEMP DEG K	EMISSIVITY VERTICAL	TIME	READINGS MV	SURFACE TEMP	SLOPE ANGLE	1/2 IN TEMP DEG K	1 FT TEMP DEG K	2 FT TEMP DEG K	3 FT TEMP DEG K	3 IN TEMP DEG K	6 IN TEMP DEG K	12 IN TEMP DEG K
0.0	6.4		2200	6664.	0.0	0.0	0.0	0.0	0.0	0.0	0.0	0.0	0.0
10.0	6.3			6667.	0.0	0.0	0.0	0.0	0.0	0.0	0.0	0.0	0.0
20.0	6.2			6664.	0.0	0.0	0.0	0.0	0.0	0.0	0.0	0.0	0.0
30.0	8.8			6667.	0.0	0.0	0.0	0.0	0.0	0.0	0.0	0.0	0.0
40.0	17.3			6679.	0.0	0.0	0.0	0.0	0.0	0.0	0.0	0.0	0.0
45.0	12.7												
50.0	8.2			6673.	0.0	0.0	0.0	0.0	0.0	0.0	0.0	0.0	0.0
55.0	9.1												
60.0	10.1			6678.	0.0	0.0	0.0	0.0	0.0	0.0	0.0	0.0	0.0
65.0	14.3			6683.	0.0	0.0	0.0	0.0	0.0	0.0	0.0	0.0	0.0
70.0	16.4			6688.	0.0	0.0	0.0	0.0	0.0	0.0	0.0	0.0	0.0
72.0	18.3												
74.0	20.2												
75.0	21.1			6697.	0.0	0.0	0.0	0.0	0.0	0.0	0.0	0.0	0.0
76.0	21.9												
78.0	23.5												
80.0	25.1			6700.	0.0	0.0	0.0	0.0	0.0	0.0	0.0	0.0	0.0
82.0	28.8			6711.	0.0	0.0	0.0	0.0	0.0	0.0	0.0	0.0	0.0
84.0	38.3			6718.	0.0	0.0	0.0	0.0	0.0	0.0	0.0	0.0	0.0
86.0	50.5			6742.	0.0	0.0	0.0	0.0	0.0	0.0	0.0	0.0	0.0
88.0	115.3			6785.	0.0	0.0	0.0	0.0	0.0	0.0	0.0	0.0	0.0
90.0	180.1	0.0		6853.	291.0	0.0	287.0	0.0	0.0	0.0	0.0	0.0	0.0
92.0	208.6	0.531		6898.	291.0	0.0	287.0	0.0	0.0	0.0	0.0	0.0	0.0
94.0	247.1	0.776		6909.	291.0	0.0	290.0	0.0	0.0	0.0	0.0	0.0	0.0
96.0	209.5	0.677		6896.	291.0	0.0	291.0	0.0	0.0	0.0	0.0	0.0	0.0
98.0	179.1	0.573		6871.	291.0	0.0	291.0	0.0	0.0	0.0	0.0	0.0	0.0
100.0	187.0	0.613		6870.	290.0	0.0	290.0	0.0	0.0	0.0	0.0	0.0	0.0
102.0	200.8	0.665		6885.	290.0	0.0	290.0	0.0	0.0	0.0	0.0	0.0	0.0
104.0	201.8	0.671		6896.	290.0	0.0	290.0	0.0	0.0	0.0	0.0	0.0	0.0
106.0	200.1	0.667		6892.	290.0	0.0	290.0	0.0	0.0	0.0	0.0	0.0	0.0
108.0	205.0	0.687		6897.	290.0	0.0	290.0	0.0	0.0	0.0	0.0	0.0	0.0
110.0	212.7	0.716		6906.	290.0	0.0	290.0	0.0	0.0	0.0	0.0	0.0	0.0
115.0	235.3	0.802		6929.	290.0	0.0	290.0	0.0	0.0	0.0	0.0	0.0	0.0
120.0	233.9	0.797		6928.	291.0	0.0	291.0	0.0	0.0	0.0	0.0	0.0	0.0
125.0	210.1	0.713		6911.	291.0	0.0	291.0	291.0	292.0	291.0	297.0	297.0	296.0
130.0	218.7	0.744		6917.	291.0	0.0	291.0	0.0	0.0	0.0	0.0	0.0	0.0
135.0	214.7	0.728		6916.	291.0	0.0	291.0	0.0	0.0	0.0	0.0	0.0	0.0

Table CII - Brightness Temperatures, Pebbled Limestone, 16.5 GHz, Vert. Pol.

RUN NO. 129 06/16/66 VER POLAR. 16.5 GHZ LIMESTONE

ITERATION NUMBER 0

ZENITH ANGLE (DEG)	BRIGHTNESS TEMP. (DEG K)	APPARENT TEMP. (DEG K)	CORRECTION TEMP. (DEG K)
0.0	6.39	10.19	-3.7969
21.79	6.14	10.76	-4.6196
31.00	9.09	14.01	-4.9137
38.21	18.23	20.67	-2.4358
44.42	14.92	20.22	-5.2942
49.99	8.18	17.56	-9.3820
55.15	9.79	19.51	-9.7144
60.00	10.10	21.34	-11.2448
64.62	14.16	25.43	-11.2636
69.08	15.29	28.40	-13.1135
73.40	20.72	33.88	-13.1633
77.63	21.69	37.71	-16.0253
81.79	27.75	46.51	-18.7576
85.90	47.43	70.95	-23.5173
90.00	180.11	160.17	19.9380
94.10	238.44	203.73	34.6601
98.21	175.85	174.34	1.5036
102.37	203.23	189.72	13.5133
106.60	199.61	191.87	7.7437
110.92	216.32	205.01	11.3075
115.38	237.04	219.95	17.0899
120.00	233.94	219.29	14.6529
124.85	209.85	206.15	3.7025
130.01	218.66	210.98	7.6345
135.58	214.21	209.79	4.4222
141.79	213.36	209.79	3.5677
149.00	212.56	209.79	2.7665
158.21	211.71	209.79	1.9191
180.00	211.52	209.79	1.7343

APS. CORRECTION = 1.01E 01 DEG. K

Table CIII - Brightness and Apparent Temperatures, Pebbled Limestone, 16.5 GHz, Vert. Pol.

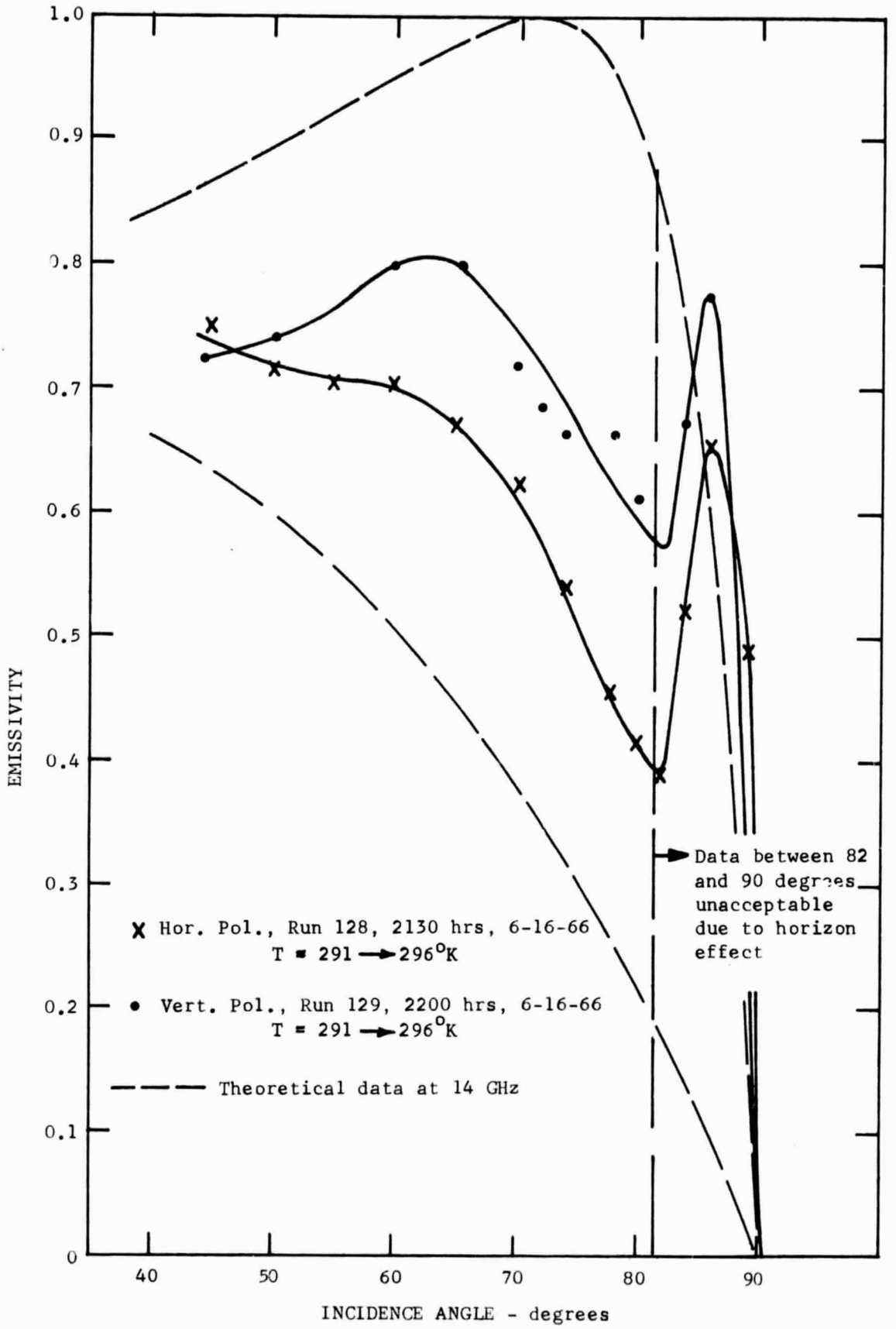


Figure 89 - Derived and Theoretical Specular Emissivities, Pebbled Limestone - 16.5 GHz

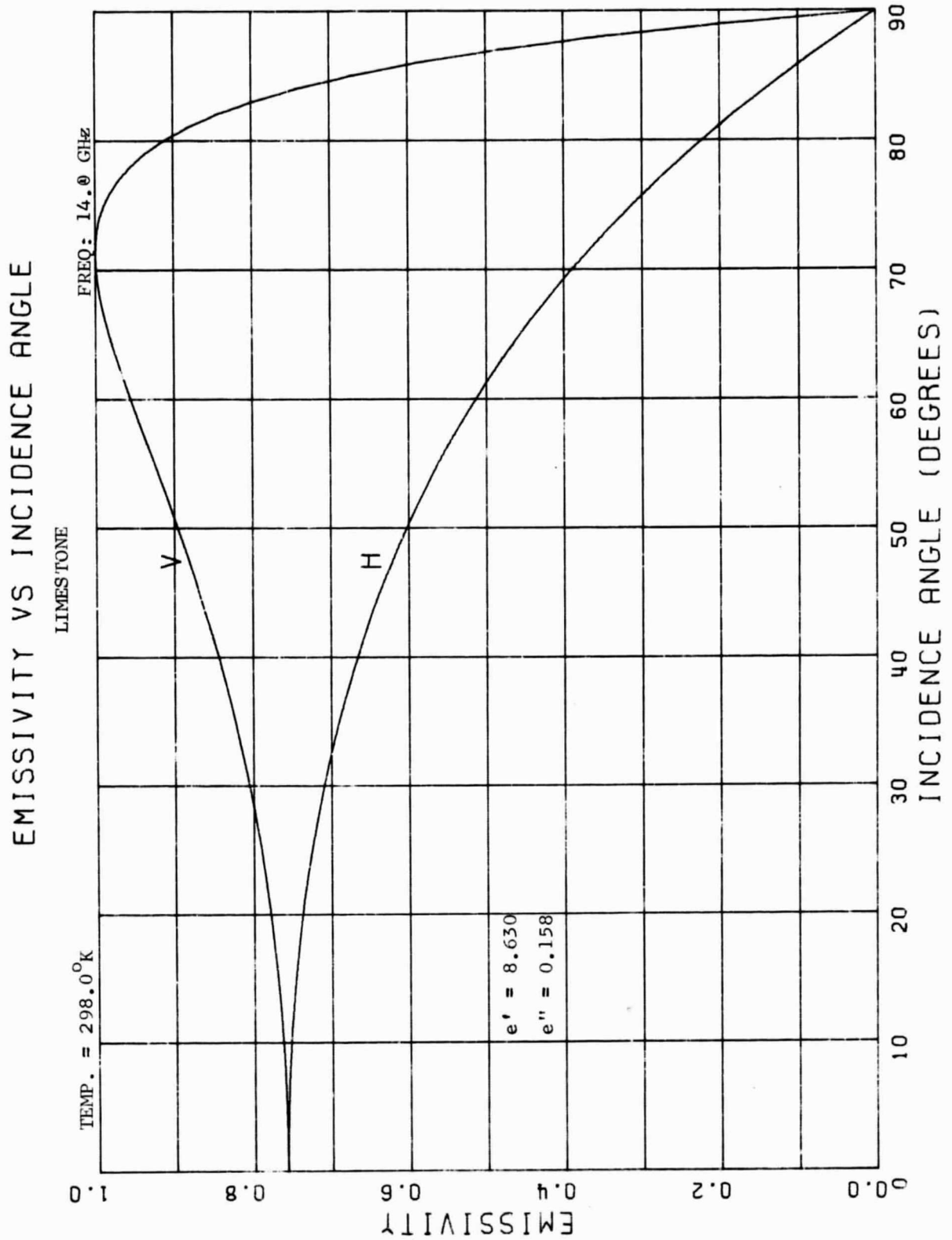


Figure 90 - Theoretical Emissivity of Limestone - 14.0 GHz

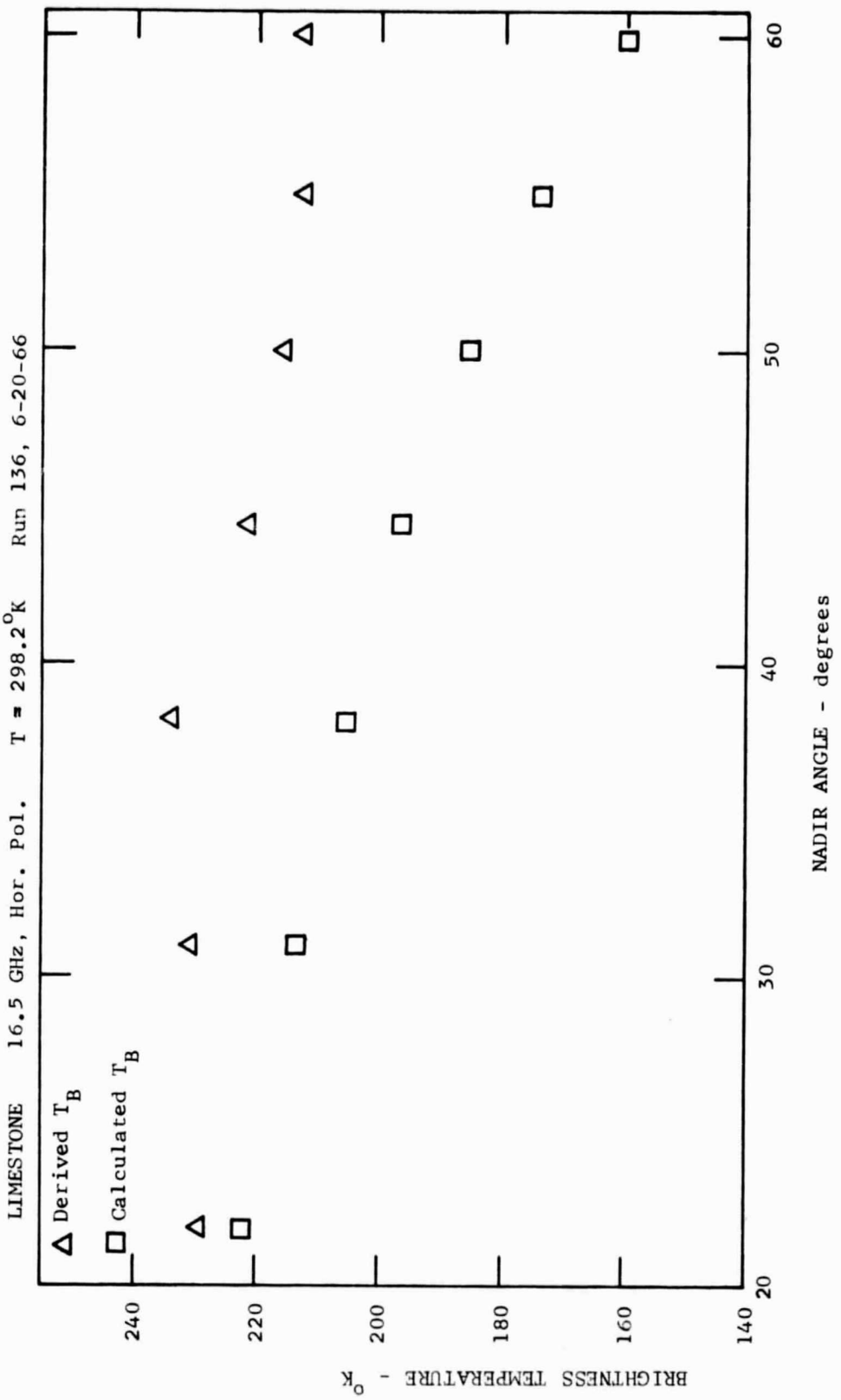


Figure 91 - Comparison of Derived and Calculated Brightness Temperatures at 16.5 GHz (Limestone)

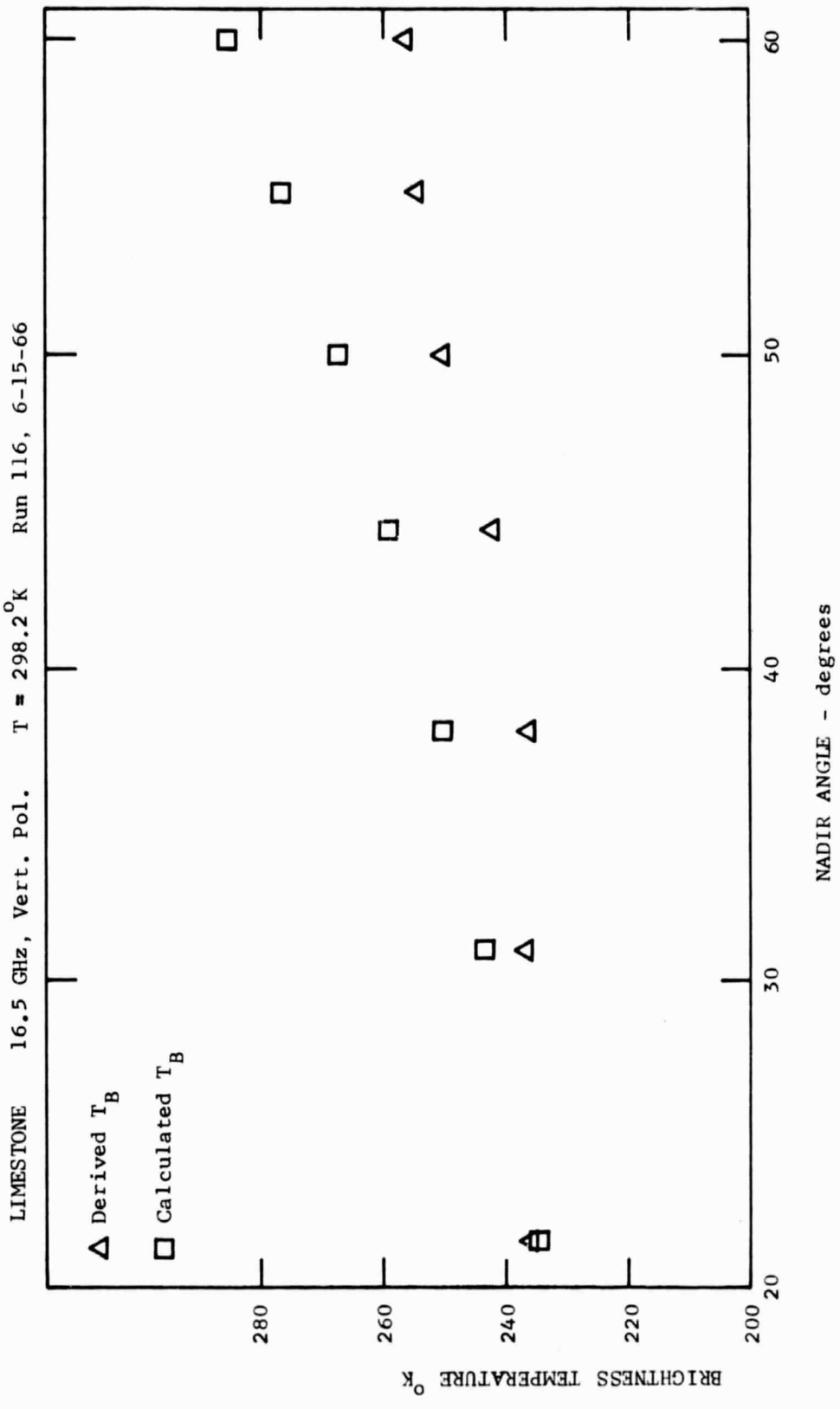


Figure 92 - Comparison of Derived and Calculated Brightness Temperatures at 16.5 GHz (Limestone)

brightness temperatures that are from 36°K to 66°K lower than the measured values. The differences in T_B's, plotted in Figure 91, are thus properly accounted for.

Smaller differences are apparent between derived and calculated T_B's for vertical polarization, as shown in Figure 92; however, the disparities range from 20 to 30°K in the nadir angle range 40° - 60°. This is also due to the considerable differences between specular and derived emissivities, for the pebbled material, as shown in Figure 89.

5. 94 GHz Data - Pebbled Limestone

The brightness temperatures obtained at this frequency show relatively modest variations, as a function of antenna beam nadir angle, and generally indicate the effects of surface roughness. The T_B levels are fairly high and the difference between polarizations is limited. Figure 93 and Tables CIV thru' CVI show horizontally polarized data. The T_B's range from 246 to 208°K, over nadir angles from 45° to 78°; the corresponding emissivities range from 0.79 to 0.56. The latter are not too different from the 9.5 GHz emissivities, for the powdered material (see Subsection 1) although the range is slightly narrower.

Figure 94 and Tables CVII thru' CIX present vertically polarized data. The T_B levels are quite high in this Run, ranging from 273 to 248°K over nadir angles from 45° to 78°, with a Brewster Angle barely discernable at a nadir angle of 60°. The derived emissivities lie in the range 0.91 to 0.69, over the above nadir angle span. There is a similarity between these emissivities and the 9.5 GHz powdered limestone values which range from 0.91 to 0.78.

Figure 95 shows plots of derived emissivities for both polarizations. It is clear that, although the T_B's and emissivities are both fairly high at this frequency, the pebbled material exhibits as much specularity at 94 GHz as at 9.5 and 16.5 GHz. Thus, a somewhat invariant frequency characteristic appears to hold for pebbled limestone. In addition, referring to the powdered limestone emissivity plots in Figure 83, it can be stated that fine-textured limestone does not enhance specularity

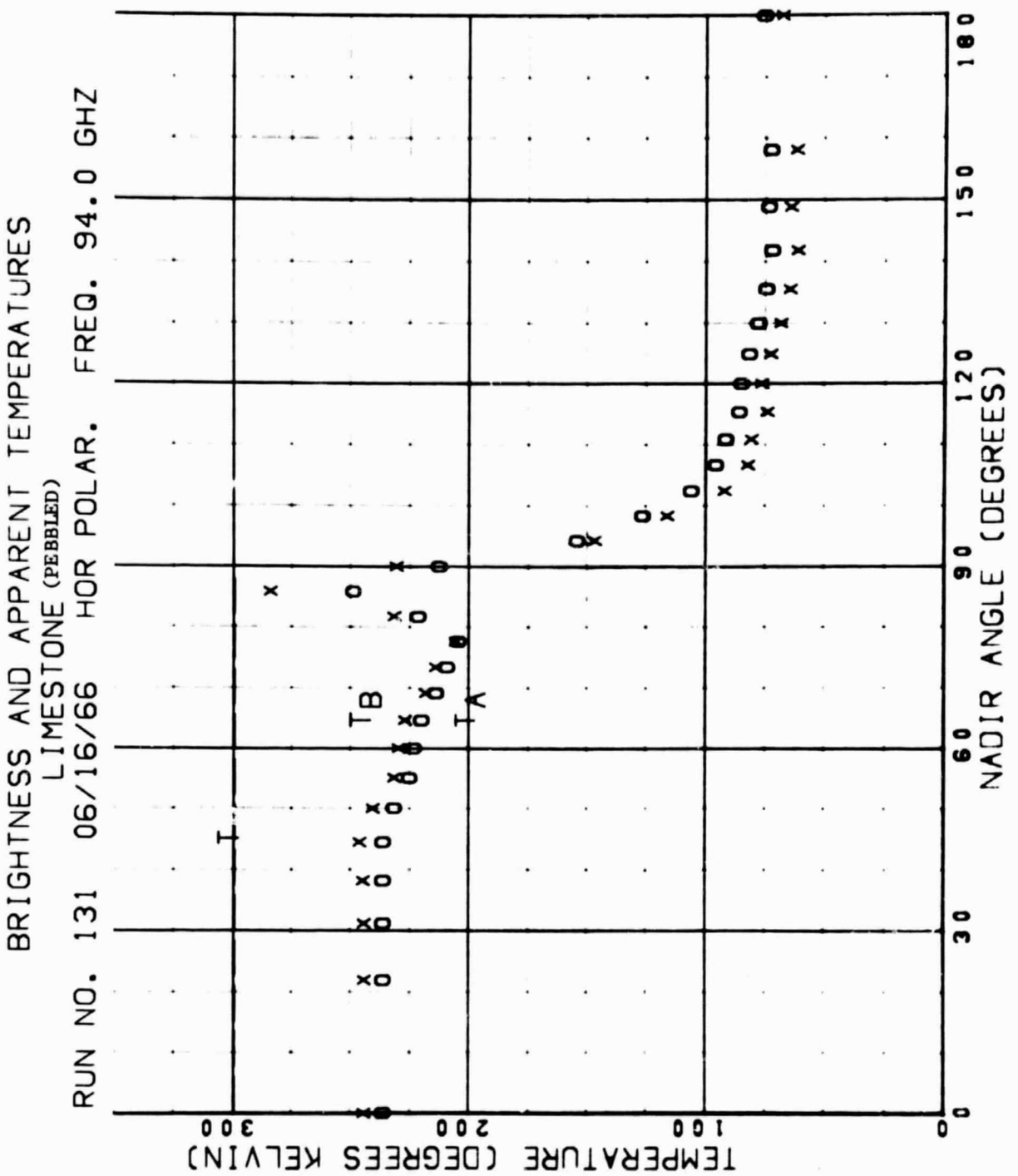


Figure 93 - Measured Brightness Temperatures, Pebbled Limestone, 94 GHz, Hor. Pol.

Table CIV - Environmental and Calibration Data, Pebbled Limestone, 94 GHz, Hor. Pol.

PAGE 1 RUN 131

TARGET MATERIAL	LIMESTONE
DATA DATE	06/16/66
START TIME	2303
FREQUENCY,GHZ	94.1
POLARIZATION	HOR
ANTENNA AZIMUTH,DEG	
BAROMETRIC PRESSURE,IN.HG.	30.85
RELATIVE HUMIDITY,PCT	27
AIR TEMPERATURE,DEG F	81
WIND DIRECTION	SE
WIND SPEED,MPH	3
INTEGRATION TIME,SEC	5

THIRD CALIBRATION POINT 75.30DEG.K 6609.00MV.

INITIAL CALIBRATION DATA

MINIMUM CAL.TEMP,DEG.K	306.90
MAXIMUM CAL.TEMP.DEG.K	385.95
K-FACTOR,DEG.K/MV.	0.57803
Y INTERCEPT	-3744.68

FINAL CALIBRATION DATA

MINIMUM CAL.TEMP,DEG.K	306.90
MAXIMUM CAL.TEMP.DEG.K	385.95
K-FACTOR,DEG.K/MV.	0.56483
Y INTERCEPT	-3657.05

CALIBRATION CONSTANTS	INITIAL	FINAL	UNITS
HOT LOAD	399.00	399.00	DEG.K
CAL WGS - MIN	301.00	301.00	DEG.K
CAL WGS - MAX	312.00	312.00	DEG.K
WAVE GUIDE SWITCH	295.00	295.00	DEG.K
ANTENNA	294.00	294.00	DEG.K
COLD LOAD	295.00	295.00	DEG.K
AVERAGE CAL.DATA-MIN.	7097.73	7013.65	MV.
-MAX.	7147.33	7161.20	MV.

COMMENTS
SKY DARK CLEAR

REPRODUCIBILITY OF THE ORIGINAL PAGE IS POOR.

TARGET MATERIAL LIMESTONE
DATA DATE 06/16/66
START TIME 2300
FREQUENCY,GHZ 94.0
POLARIZATION HOR

ZENITH ANGLE DEG	BRIGHTNESS TEMP, HORIZONTAL DEG K	EMISSIVITY	TIME	READINGS MV	SURFACE TEMP	SLOPE ANGLE	1/2 IN TEMP DEG K	1 FT TEMP DEG K	2 FT TEMP DEG K	3 FT TEMP DEG K	3 IN TEMP DEG K	6 IN TEMP DEG K	12 IN TEMP DEG K
0.0	66.0		2300	6605.	0.0	0.0	0.0	0.0	0.0	0.0	0.0	0.0	0.0
10.0	65.2			6606.	0.0	0.0	0.0	0.0	0.0	0.0	0.0	0.0	0.0
20.0	62.5			6603.	0.0	0.0	0.0	0.0	0.0	0.0	0.0	0.0	0.0
30.0	63.8			6605.	0.0	0.0	0.0	0.0	0.0	0.0	0.0	0.0	0.0
40.0	62.3			6603.	0.0	0.0	0.0	0.0	0.0	0.0	0.0	0.0	0.0
45.0	65.4												
50.0	68.5			6613.	0.0	0.0	0.0	0.0	0.0	0.0	0.0	0.0	0.0
55.0	72.4												
60.0	76.3			6625.	0.0	0.0	0.0	0.0	0.0	0.0	0.0	0.0	0.0
65.0	74.7			6627.	0.0	0.0	0.0	0.0	0.0	0.0	0.0	0.0	0.0
70.0	80.7			6619.	0.0	0.0	0.0	0.0	0.0	0.0	0.0	0.0	0.0
72.0	82.6												
74.0	84.6												
75.0	85.5			6646.	0.0	0.0	0.0	0.0	0.0	0.0	0.0	0.0	0.0
76.0	89.6												
78.0	97.6												
80.0	105.7			6676.	0.0	0.0	0.0	0.0	0.0	0.0	0.0	0.0	0.0
82.0	117.8			6700.	0.0	0.0	0.0	0.0	0.0	0.0	0.0	0.0	0.0
84.0	132.6			6722.	0.0	0.0	0.0	0.0	0.0	0.0	0.0	0.0	0.0
86.0	148.6			6748.	0.0	0.0	0.0	0.0	0.0	0.0	0.0	0.0	0.0
88.0	189.6			6757.	0.0	0.0	0.0	0.0	0.0	0.0	0.0	0.0	0.0
90.0	231.0	0.0		6845.	293.0	0.0	293.0	0.0	0.0	0.0	0.0	0.0	0.0
92.0	257.0	0.651		6919.	293.0	0.0	293.0	0.0	0.0	0.0	0.0	0.0	0.0
94.0	283.0	0.924		6914.	294.0	0.0	294.0	0.0	0.0	0.0	0.0	0.0	0.0
96.0	260.1	0.795		6895.	294.0	0.0	294.0	0.0	0.0	0.0	0.0	0.0	0.0
98.0	234.8	0.664		6868.	294.0	0.0	294.0	0.0	0.0	0.0	0.0	0.0	0.0
100.0	220.7	0.600		6846.	295.0	0.0	295.0	0.0	0.0	0.0	0.0	0.0	0.0
102.0	207.9	0.562		6837.	294.0	0.0	294.0	0.0	0.0	0.0	0.0	0.0	0.0
104.0	208.7	0.583		6833.	294.0	0.0	294.0	0.0	0.0	0.0	0.0	0.0	0.0
106.0	212.7	0.612		6839.	294.0	0.0	294.0	0.0	0.0	0.0	0.0	0.0	0.0
108.0	215.4	0.628		6857.	294.0	0.0	294.0	0.0	0.0	0.0	0.0	0.0	0.0
110.0	217.5	0.642		6850.	294.0	0.0	294.0	0.0	0.0	0.0	0.0	0.0	0.0
115.0	226.3	0.691		6864.	294.0	0.0	294.0	0.0	0.0	0.0	0.0	0.0	0.0
120.0	230.1	0.703		6870.	295.0	0.0	295.0	0.0	0.0	0.0	0.0	0.0	0.0
125.0	232.1	0.717		6874.	295.0	0.0	295.0	296.0	296.0	297.0	297.0	298.0	298.0
130.0	240.6	0.760		6885.	295.0	0.0	295.0	0.0	0.0	0.0	0.0	0.0	0.0
135.0	245.8	0.786		6893.	295.0	0.0	295.0	0.0	0.0	0.0	0.0	0.0	0.0

Table CV - Brightness Temperatures, Pebbled Limestone, 94 GHz, Hor. Pol.

RUN NO. 131 06/16/66 HOR POLAR. 94.0 GHZ LIMESTONE

ITERATION NUMBER 0

ZENITH ANGLE (DEG)	BRIGHTNESS TEMP. (DEG K)	APPARENT TEMP. (DEG K)	CORRECTION TEMP. (DEG K)
0.0	67.97	75.61	-7.6405
21.79	61.98	72.40	-10.4217
31.00	64.04	73.33	-9.2832
38.21	61.43	72.30	-10.8607
44.42	64.56	74.67	-10.1108
49.99	68.56	78.00	-9.4405
55.15	72.58	81.55	-8.9752
60.00	76.27	84.90	-8.6276
64.62	74.20	85.65	-11.4496
69.08	80.38	91.38	-11.0010
73.40	81.79	95.60	-13.8119
77.63	91.69	105.87	-14.1778
81.79	116.19	126.33	-10.1330
85.90	146.66	154.35	-7.6905
90.00	230.99	212.90	18.0868
94.10	284.21	249.44	34.7666
98.21	232.14	221.82	10.3140
102.37	205.51	204.93	0.5764
106.60	213.91	209.64	4.2779
110.92	218.52	214.14	4.3839
115.38	227.01	220.40	6.6108
120.00	230.13	223.34	6.7903
124.85	231.79	225.54	6.2524
130.01	240.63	231.90	8.7234
135.58	246.44	236.42	10.0229
141.79	245.12	236.42	8.7036
149.00	244.71	236.42	8.2947
158.21	244.49	236.42	8.0694
180.00	244.47	236.42	8.0450

ABS. CORRECTION = 9.92E 00 DEG. K

Table CVI - Brightness and Apparent Temperatures, Pebbled Limestone, 94 GHz, Hor. Pol.

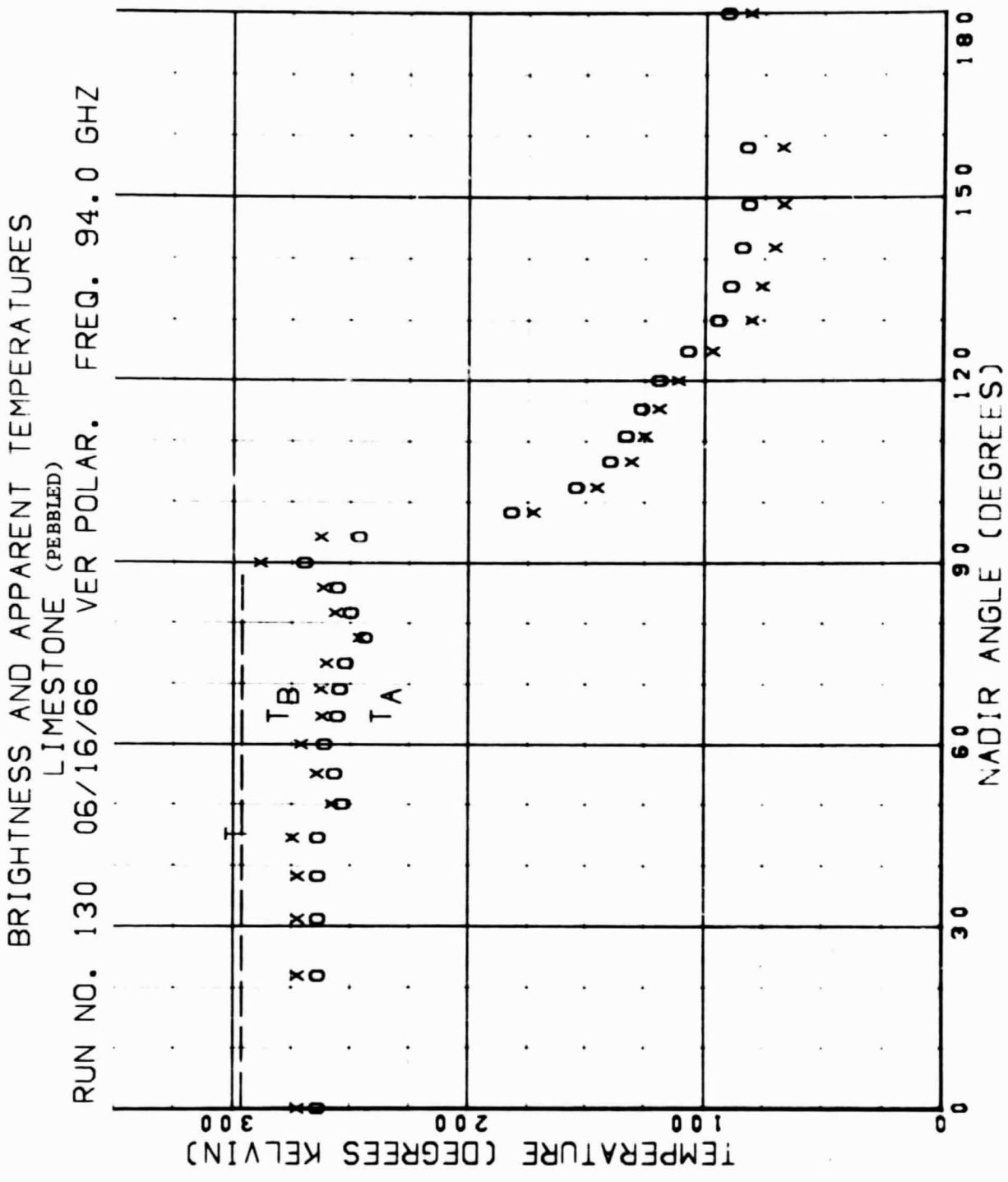


Figure 94 - Measured Brightness Temperatures, Pebbled Limestone, 94 GHz, Vert. Pol.

Table CVII - Environmental and Calibration Data, Pebbled Limestone, 94 GHz, Vert. Pol.

PAGE 1 RUN 136

TARGET MATERIAL	LIMESTONE
DATA DATE	06/16/66
START TIME	223[illegible]
FREQUENCY,GHZ	94.
POLARIZATION	VER
ANTENNA AZIMUTH,DEG	
BAROMETRIC PRESSURE,IN.HG.	30.85
RELATIVE HUMIDITY,%	38
AIR TEMPERATURE,DEG F	81
WIND DIRECTION	SE
WIND SPEED,MPH	4
INTEGRATION TIME,SEC	5

THIRD CALIBRATION POINT 90.80DEG.K 6545.00MV.

INITIAL CALIBRATION DATA

MINIMUM CAL.TEMP,DEG.K	310.50
MAXIMUM CAL.TEMP.DEG.K	388.21
K-FACTOR,DEG.K/MV.	0.51758
Y INTERCEPT	-3297.26

FINAL CALIBRATION DATA

MINIMUM CAL.TEMP,DEG.K	310.50
MAXIMUM CAL.TEMP.DEG.K	388.21
K-FACTOR,DEG.K/MV.	0.48736
Y INTERCEPT	-3099.68

CALIBRATION CONSTANTS	INITIAL	FINAL	UNITS
HOT LOAD	399.00	399.00	DEG.K
CAL WGS - MIN	306.00	306.00	DEG.K
CAL WGS - MAX	317.00	317.00	DEG.K
WAVE GUIDE SWITCH	297.00	297.00	DEG.K
ANTENNA	295.00	295.00	DEG.K
COLD LOAD	296.00	296.00	DEG.K
AVERAGE CAL.DATA-MIN.	6973.80	7012.39	MV.
-MAX.	7118.13	7152.85	MV.

COMMENTS
SKY DARK CLEAR

PAGE [illegible]

TARGET MATERIAL: LIMESTONE
DATA DATE: 06/16/66
START TIME: 2220
FREQUENCY,GHZ: 94.0
POLARIZATION: VER

ZENITH ANGLE DEG	BRIGHTNESS TEMP DEG K	EMISSIVITY VERTICAL	TIME	READINGS MV	SURFACE TEMP	SLOPE ANGLE	1/2 IN TEMP DEG K	1 FT TEMP DEG K	2 FT TEMP DEG K	3 FT TEMP DEG K	3 IN TEMP DEG K	6 IN TEMP DEG K	12 IN TEMP DEG K
0.0	81.3		2220	6545.	0.0	0.0	0.0	0.0	0.0	0.0	0.0	0.0	0.0
10.0	74.9			6526.	0.0	0.0	0.0	0.0	0.0	0.0	0.0	0.0	0.0
20.0	69.5			6530.	0.0	0.0	0.0	0.0	0.0	0.0	0.0	0.0	0.0
30.0	67.2			6527.	0.0	0.0	0.0	0.0	0.0	0.0	0.0	0.0	0.0
40.0	72.2			6535.	0.0	0.0	0.0	0.0	0.0	0.0	0.0	0.0	0.0
45.0	76.1												
50.0	80.0			6552.	0.0	0.0	0.0	0.0	0.0	0.0	0.0	0.0	0.0
55.0	85.4												
60.0	110.6			6601.	0.0	0.0	0.0	0.0	0.0	0.0	0.0	0.0	0.0
65.0	119.6			6618.	0.0	0.0	0.0	0.0	0.0	0.0	0.0	0.0	0.0
70.0	126.3			6631.	0.0	0.0	0.0	0.0	0.0	0.0	0.0	0.0	0.0
72.0	130.3												
74.0	134.3												
75.0	136.3			6647.	0.0	0.0	0.0	0.0	0.0	0.0	0.0	0.0	0.0
76.0	141.2												
78.0	150.5												
80.0	160.6			6651.	0.0	0.0	0.0	0.0	0.0	0.0	0.0	0.0	0.0
82.0	176.9			6730.	0.0	0.0	0.0	0.0	0.0	0.0	0.0	0.0	0.0
84.0	220.5			6774.	0.0	0.0	0.0	0.0	0.0	0.0	0.0	0.0	0.0
86.0	263.3			6855.	0.0	0.0	0.0	0.0	0.0	0.0	0.0	0.0	0.0
88.0	275.9			6859.	0.0	0.0	0.0	0.0	0.0	0.0	0.0	0.0	0.0
90.0	283.6	0.0		6902.	0.0	0.0	292.0	0.0	0.0	0.0	0.0	0.0	0.0
92.0	275.5	-0.0028		6857.	0.0	0.0	292.0	0.0	0.0	0.0	0.0	0.0	0.0
94.0	262.4	-0.0031		6876.	0.0	0.0	292.0	0.0	0.0	0.0	0.0	0.0	0.0
96.0	259.6	0.0544		6867.	0.0	0.0	292.0	0.0	0.0	0.0	0.0	0.0	0.0
98.0	257.2	0.0551		6866.	0.0	0.0	292.0	0.0	0.0	0.0	0.0	0.0	0.0
100.0	252.5	0.0700		6867.	0.0	0.0	292.0	0.0	0.0	0.0	0.0	0.0	0.0
102.0	247.6	0.0885		6851.	0.0	0.0	292.0	0.0	0.0	0.0	0.0	0.0	0.0
104.0	252.0	0.0735		6871.	0.0	0.0	292.0	0.0	0.0	0.0	0.0	0.0	0.0
106.0	259.6	0.0788		6873.	0.0	0.0	292.0	0.0	0.0	0.0	0.0	0.0	0.0
108.0	251.3	0.0915		6876.	0.0	0.0	291.0	0.0	0.0	0.0	0.0	0.0	0.0
110.0	262.2	0.0825		6875.	0.0	0.0	291.0	0.0	0.0	0.0	0.0	0.0	0.0
115.0	262.4	0.0833		6881.	0.0	0.0	291.0	0.0	0.0	0.0	0.0	0.0	0.0
120.0	271.5	0.0887		6854.	0.0	0.0	292.0	0.0	0.0	0.0	0.0	0.0	0.0
125.0	264.6	0.0861		6866.	0.0	0.0	292.0	0.0	293.0	293.0	297.0	298.0	298.0
130.0	258.2	0.0841		6881.	0.0	0.0	292.0	0.0	0.0	0.0	0.0	0.0	0.0
135.0	273.2	0.0919		6902.	0.0	0.0	292.0	0.0	0.0	0.0	0.0	0.0	0.0

Table CVIII - Brightness Temperatures, Pebbled Limestone, 94 GHz, Vert. Pol.

RUN NO. 130 06/16/66 VER POLAR. 94.0 GHZ LIMESTONE

ITERATION NUMBER 0

ZENITH ANGLE (DEG)	BRIGHTNESS TEMP. (DEG K)	APPARENT TEMP. (DEG K)	CORRECTION TEMP. (DEG K)
0.0	81.28	90.26	-8.9764
21.79	67.34	82.33	-14.9842
31.00	67.23	81.58	-14.3556
38.21	70.63	84.32	-13.6954
44.42	76.09	88.96	-12.8700
49.99	80.03	93.97	-13.9347
55.15	96.35	106.79	-10.4434
60.00	110.82	118.87	-8.0531
64.62	119.05	126.74	-7.6840
69.08	125.09	132.84	-7.7512
73.40	130.85	139.68	-8.8293
77.63	145.20	153.99	-8.7959
81.79	172.21	182.01	-9.7990
85.90	262.72	246.40	16.3181
90.00	288.55	269.74	18.8124
94.10	261.81	255.65	6.1560
98.21	256.96	250.16	6.7978
102.37	246.64	244.05	2.5920
106.60	260.59	252.36	8.2308
110.92	262.67	254.91	7.7651
115.38	262.40	255.83	6.5683
120.00	271.50	261.23	10.2737
124.85	264.80	257.34	7.4628
130.01	258.28	254.07	4.2073
135.58	274.90	264.15	10.7481
141.79	272.70	264.15	8.5470
149.00	272.62	264.15	8.4725
158.21	272.61	264.15	8.4641
180.00	272.61	264.15	8.4613

ABS. CORRECTION = 9.66E 00 DEG. K

Table CIX - Brightness and Apparent Temperatures, Pebbled Limestone, 94 GHz, Vert. Pol.

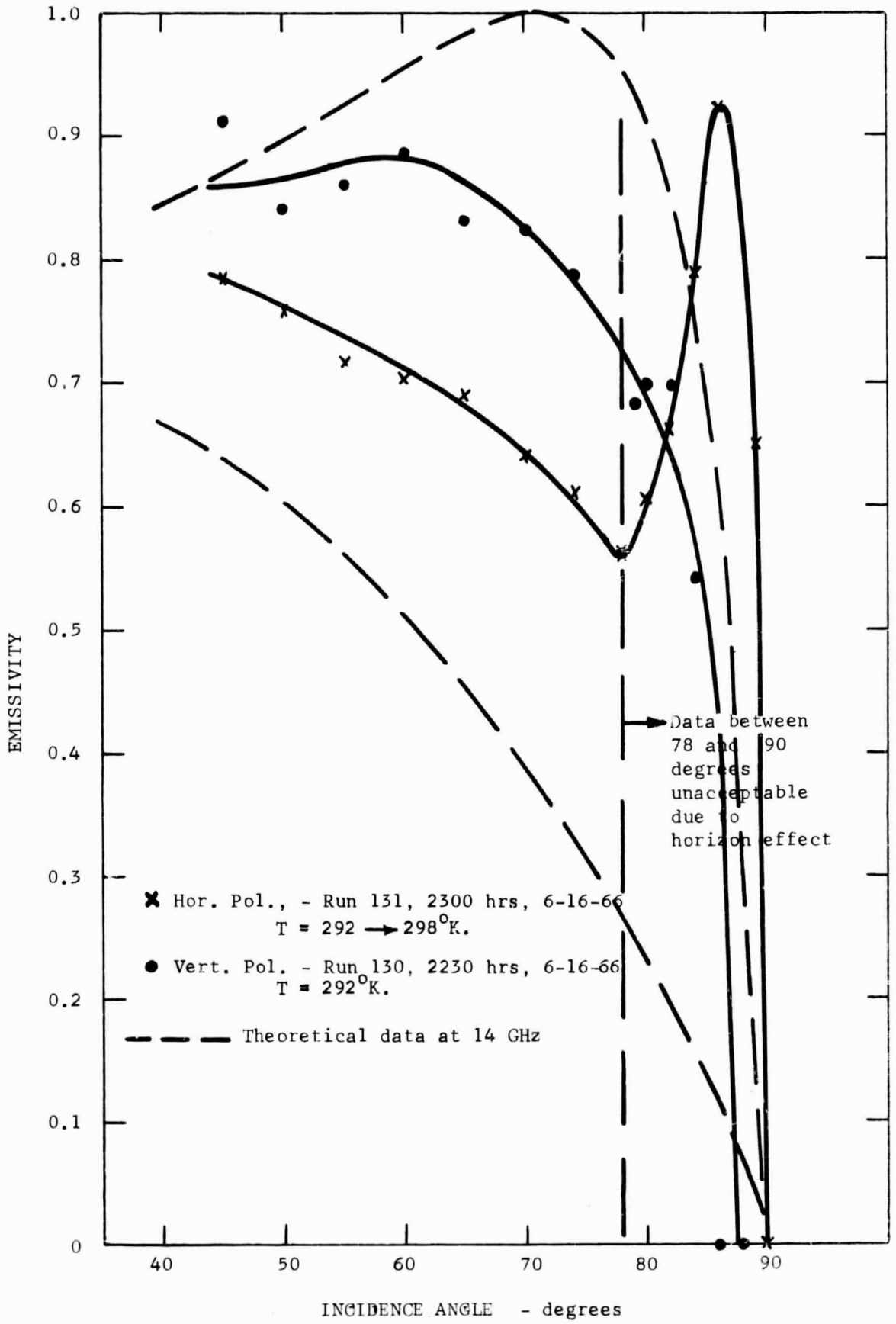


Figure 95 - Derived and Theoretical Specular Emissivities, Pebbled Limestone - 94 GHz

in any significant manner. Thus, as far as this characteristic is concerned, powdered limestone is sufficiently similar to pebbled limestone for it to be placed in the same class, in terms of invariance with frequency.

6. Polarization and Frequency Dependence of Brightness Temperatures and Emissivities - Limestone

TABLE CX

POLARIZATION AND FREQUENCY DEPENDENCE OF BRIGHTNESS TEMPERATURES AND EMISSIVITIES

(a) Pebbled Limestone, Incidence Angle = 55°

Frequency GHz	Polarization	Averaged T_B(°K)	ΔT_B (°K)	Averaged ϵ	$\Delta\epsilon$
9.5	Hor.	218.5	6.1	0.690	0.024
9.5	Vert.	244.4	3.4	0.788	0.010
16.5	Hor.	217.0	13.0	0.657	0.037
16.5	Vert.	224.6	14.7	0.704	0.018
94	Hor.	246.9	13.6	0.682	0.026
94	Vert.	273.8	11.7	0.807	0.049
(b) Powdered Limestone, Incidence Angle = 55°					
9.5	Hor.	262.3	9.5	0.823	0.028
9.5	Vert.	291.3	0	0.917	0

Table CX furnishes averaged brightness temperatures and emissivities, together with their dispersions ΔT_B and $\Delta\epsilon$, respectively, for pebbled and powdered limestone, at an incidence angle of 55°. Referring to the pebbled limestone portion, the T_B's are similar at 9.5 and 16.5 GHz, at each polarization, with slightly lower values at 16.5 GHz; however, there is a considerable increase in the 94 GHz T_B's over those at the lower frequencies. The dispersions in the T_B's are quite low at 9.5 GHz and considerably higher at the two other frequencies, with little difference between them.

At a given polarization, the emissivities fall within a rather narrow range. At horizontal polarization, for example, the total spread with respect to frequency is 0.033. Vertically polarized emissivities exhibit a somewhat greater spread - 0.103. Within each frequency the dispersion, $\Delta\epsilon$, is also small, except at 94 GHz, vertical polarization. It is interesting to note that, at 9.5 and 16.5 GHz, $\Delta\epsilon$ is larger for horizontal polarization. This is probably due to a greater sensitivity to surface roughness at this polarization.

Referring to the powdered limestone portion of the Table, the average T_B for horizontal polarization is 29°K lower than for vertical polarization, indicating a good degree of specularity in this material at 9.5 GHz. However, the brightness temperature dispersion is rather high for horizontal polarization. The averaged emissivities differ by almost 0.1, between the two polarizations. As in the case of the ΔT_B's, the emissivity dispersion is rather large for horizontal polarization.

G. INFLUENCE OF SURFACE ROUGHNESS ON BRIGHTNESS TEMPERATURES OF SOLID MATERIALS

This analysis includes Salines, Quartz Sand, Powdered Limestone and Pebbled Limestone. A measure of the influence of surface roughness on brightness temperatures is the extent to which T_B's for horizontal and vertical polarization converge at a given nadir angle. A criterion has been established for classifying specular and diffuse materials. The criterion is based on the degree of separation between the two polarizations at a nadir angle of 55 degrees, for all materials except Quartz Sand. In the case of this material, it was necessary to specify an incidence angle, since various slopes are associated with this material. Thus, an incidence angle of 68.6 degrees was selected for this analysis of Quartz Sand data. It is considered reasonable to use a separation of 15°K between the two polarizations as a criterion for classifying specular and diffuse surfaces for Salines, Powdered Limestone and Pebbled Limestone. For Quartz Sand, the criterion is 25°K.

Table CXI presents averaged results for each material and frequency. Based on the above criteria, all materials are specular at all three frequencies, except Salines; the separation exceeds 15°K for Limestone and 25°K for Quartz Sand. The Salines are obviously diffuse since the small separations are far below the 15°K level.

TABLE CXI

INFLUENCE OF SURFACE ROUGHNESS ON

BRIGHTNESS TEMPERATURE OF SOLID MATERIALS

Incidence Angle = 55°

Material	Frequency (GHz)	T_{Bv}(Averaged) (°K)	T_{Bh}(Averaged) (°K)	$T_{Bv} - T_{Bh}$ (°K)
Powdered Limestone	9.5	292.36	262.33	30.03
	16.5	--	--	--
	94	--	--	--
Pebbled Limestone	9.5	244.35	218.33	26.02
	16.5	232.12	216.00	16.12
	94	278.20	240.05	38.15
Salines	9.5	271.55	272.62	-1.07
	16.5	289.23	291.82	-2.59
	94	303.57	301.53	2.04
Quartz Sand*	9.5	285.28	235.30	49.98
	16.5	291.95	219.08	72.87
	94	308.39	273.44	34.95

* Incidence Angle = 68.6°

H. EFFECTS OF SURFACE AND SUBSURFACE TEMPERATURES ON BRIGHTNESS TEMPERATURES AND EMISSIVITIES

As indicated in Equation (30), surface temperature contributes directly to brightness temperature. The degree to which subsurface temperature contributes to T_B is dependent on the attenuation coefficient of the material under consideration. The attenuation coefficient, α, is expressed by,

$$\alpha = \frac{2\pi\mu_o\lambda_o\nu^2\, e''}{\left[\frac{(2e' + e'')}{2}\right]^{1/2}} \qquad (43)$$

where,

μ_o = permeability of free space, 0.927×10^{-20} erg/gauss

λ_o = free space wavelength of the radiation under consideration

ν = frequency under consideration

e', e'' = real and imaginary parts of the dielectric constant, respectively.

Values of α have been calculated using measured values of e' and e" at 14 GHz for Salines, Limestone and Quartz Sand, and are tabulated in Table CXII. The tabulated data is based on the assumption that e' and e" of these materials are relatively constant with frequency.

TABLE CXII

CALCULATED ATTENUATIONS VERSUS FREQUENCY

Frequency → / Material	9.5 GHz	16.5 GHz	94 GHz
Salines	$0.357 cm^{-1}$	$0.620 cm^{-1}$	$3.53 cm^{-1}$
Limestone	0.866 "	1.504 "	8.57 "
Quartz Sand	0.334 "	0.581 "	3.31 "

The above data shows that Quartz Sand has the lowest attenuation, followed by Salines and Limestone, at a given frequency. Thus, attenuation is directly related to the real part of the dielectric permittivity, in a dry material. It will be recalled that e' has values of 2.88, 4.75 and 8.63 for Quartz Sand, Salines and Limestone, respectively, at 14 GHz.

Representative data Runs were analyzed for surface and subsurface temperature effects on T_B's. The results are summarized in the following paragraphs.

1. Limestone

At 9.5 GHz, vertical polarization, between 0900 and 2330 hours, a brightness temperature decrease of 6.7°K was observed while surface temperature dropped by 15°K and subsurface temperature increased by 4°K. The dominant influence here is the decrease in surface temperature.

At 16.5 GHz, vertical polarization, between 1130 and 2200 hours, T_B decreased 24.2°K while surface temperature decreased 18°K and subsurface temperature increased 1°K. Here again, the prime influence is surface temperature.

At 94 GHz, vertical polarization, a T_B decrease of 2.9°K was accompanied by a surface temperature decrease of 4°K and subsurface temperature increase of 1°K. The surface temperature effect is also dominant in this example.

2. Salines

This material is considerably more susceptible to subsurface temperature effects than Limestone. This is due to the lower attenuation coefficient in this material.

At 16.5 GHz, vertical polarization, a T_B decrease of 5.5°K was accompanied by a surface temperature decrease of 10°K and a subsurface temperature increase of 2°K. It appears that the surface temperature decrease was sufficiently large to override the effect of a small change in subsurface temperature. For horizontal polarization the opposite effect was observed - T_B decreased

by 2.1°K while subsurface temperature dropped by 4°K; there was no change in surface temperature. Thus, a subsurface effect was clearly responsible for the drop in T_B.

At 94 GHz, vertical polarization, T_B increased by 5.1°K while surface temperature decreased by 2°K and subsurface temperature increased by 10°K. In this case, the subsurface effect is quite pronounced.

3. Quartz Sand

No positive conclusions could be drawn for this material due to the scattering of data, resulting from slope uncertainties.

V. DETERMINATION OF DIELECTRIC CONSTANTS OF SPECULAR MATERIALS

The purpose of this Section is to present a technique for manipulation of radiometric data so that the dielectric properties of a material can be determined. The problem is examined theoretically, using some simplifying physical assumptions. A specific method for dry materials, any material with a small value for the imaginary part of the dielectric permittivity, is devised. The method is then applied to limestone data at 16.5 GHz. As a result of the considerations involved in developing the method, certain general predictions can be made concerning the feasibility and potential accuracy of deriving dielectric permittivities from radiometric data.

A. THEORETICAL CONSIDERATIONS

In this study certain simplifying constraints are imposed:

1) Specular reflection - this enables use of simple equations relating brightness temperature, T_B, incidence angle, φ, the real part of the dielectric permittivity, e', and the imaginary part, e".

2) Materials considered are dry solids - this places e' and e" in specific ranges, which leads to an important elimination of e" as a variable.

3) The selected frequency is 16.5 GHz - this is because values of e' and e" are available for dry solids at an adjacent frequency ..e., 14 GHz.

On the basis of the first assumption, the specular expression for brightness temperature is used:*

$$T_B = \epsilon T + (1 - \epsilon)\, T_{s\varphi} \qquad (44)$$

where, ϵ is the emissivity of the material

*Note, subscripts h and v are used to indicate horizontally and vertically polarized radiation data, respectively.

T_B is its brightness temperature - from the reduced radiometric data

T is the measured temperature of material

$T_{s\varphi}$ is the influencing sky brightness temperature.

The second assumption establishes the following ranges for e' and e", based upon laboratory measurement of dielectric permittivities:

$$e' = 2.0 \text{ to } 9.0$$

$$e'' = 0 \quad \text{to } 0.16$$

The above values are based on data presented in Table CXIII.

TABLE CXIII

MEASURED VALUES OF DIELECTRIC PERMITTIVITIES

Material	e'	e"
Quartz Sand	2.88	0.034
Salines	4.75	0.049
Limestone	8.63	0.158

It should be noted that different materials affect measured brightness temperatures via ε. That is, if it is assumed that all the materials have the same geometry, the variations in e' and e" affect only ε directly. The theoretical expressions for ε_v and ε_h given in Equations (C-6) thru' (C-9) in Appendix C, describe the dependence of these two variables on e' and e". The values of ε_v and ε_h have been calculated by computer, as both e' and e" are varied over the prescribed range. Table CXIV shows values of ε_v and ε_h for e' fixed at the three values (2.0, 5.5, and 8.5) and e" varied at 0.01 intervals from 0 to 0.19. Data was calculated for $\varphi = 0^\circ$ to $\varphi = 70^\circ$ at 10° intervals. The Table shows results for three angles only. On the basis of the tabulated data, e" can be reasonably disregarded as a variable in these considerations, since variations in e" over the entire range encountered for dry solids, produces a negligible change in the values of ε_v and ε_h. Typically, at $\varphi = 40^\circ$ and e' = 5.5, the following shifts in ε_v and ε_h are evident:

TABLE CXIV

DEPENDENCE OF ϵ_v AND ϵ_h ON VARIATIONS IN e''

φ = 0 degrees								
e' = 2.0			e' = 5.5			e' = 8.5		
e''	ϵ_v	ϵ_h	e''	ϵ_v	ϵ_h	e''	ϵ_v	ϵ_h
0.0	0.9706	0.9706	0.0	0.8383	0.8383	0.0	0.7607	0.7607
0.01	0.9706	0.9706	0.01	0.8383	0.8383	0.01	0.7607	0.7607
0.02	0.9706	0.9706	0.02	0.8383	0.8383	0.02	0.7607	0.7607
0.03	0.9705	0.9705	0.03	0.8383	0.8383	0.03	0.7607	0.7607
0.04	0.9705	0.9705	0.04	0.8383	0.8383	0.04	0.7607	0.7607
0.05	0.9705	0.9705	0.05	0.8383	0.8383	0.05	0.7607	0.7607
0.06	0.9705	0.9705	0.06	0.8383	0.8383	0.06	0.7607	0.7607
0.07	0.9704	0.9704	0.07	0.8383	0.8383	0.07	0.7607	0.7607
0.08	0.9704	0.9704	0.08	0.8383	0.8383	0.08	0.7607	0.7607
0.09	0.9704	0.9704	0.09	0.8383	0.8383	0.09	0.7607	0.7607
0.10	0.9703	0.9703	0.10	0.8382	0.8382	0.10	0.7607	0.7607
0.11	0.9702	0.9702	0.11	0.8382	0.8382	0.11	0.7607	0.7607
0.12	0.9702	0.9702	0.12	0.8382	0.8382	0.12	0.7606	0.7606
0.13	0.9701	0.9701	0.13	0.8382	0.8382	0.13	0.7606	0.7606
0.14	0.9701	0.9701	0.14	0.8382	0.8382	0.14	0.7606	0.7606
0.15	0.9700	0.9700	0.15	0.8382	0.8382	0.15	0.7606	0.7606
0.16	0.9699	0.9699	0.16	0.8382	0.8382	0.16	0.7606	0.7606
0.17	0.9698	0.9698	0.17	0.8382	0.8382	0.17	0.7606	0.7606
0.18	0.9697	0.9697	0.18	0.8381	0.8381	0.18	0.7606	0.7606
0.19	0.9696	0.9696	0.19	0.8381	0.8381	0.19	0.7606	0.7606
φ = 40 degrees								
0.0	0.9905	0.9406	0.0	0.9084	0.7570	0.0	0.8463	0.6687
0.01	0.9905	0.9406	0.01	0.9084	0.7570	0.01	0.8463	0.6687
0.02	0.9905	0.9406	0.02	0.9084	0.7570	0.02	0.8463	0.6687
0.03	0.9905	0.9406	0.03	0.9084	0.7570	0.03	0.8463	0.6687
0.04	0.9905	0.9405	0.04	0.9084	0.7570	0.04	0.8463	0.6687
0.05	0.9905	0.9405	0.05	0.9084	0.7570	0.05	0.8463	0.6687
0.06	0.9904	0.9504	0.06	0.9084	0.7570	0.06	0.8463	0.6687
0.07	0.9904	0.9404	0.07	0.9084	0.7570	0.07	0.8463	0.6687
0.08	0.9904	0.9403	0.08	0.9084	0.7570	0.08	0.8463	0.6687
0.09	0.9904	0.9402	0.09	0.9084	0.7570	0.09	0.8463	0.6687
0.10	0.9904	0.9401	0.10	0.9084	0.7570	0.10	0.8463	0.6687
0.11	0.9903	0.9400	0.11	0.9083	0.7570	0.11	0.8463	0.6687
0.12	0.9903	0.9399	0.12	0.9083	0.7569	0.12	0.8463	0.6687
0.13	0.9903	0.9398	0.13	0.9083	0.7569	0.13	0.8463	0.6687
0.14	0.9903	0.9397	0.14	0.9083	0.7569	0.14	0.8463	0.6687
0.15	0.9902	0.9396	0.15	0.9083	0.7569	0.15	0.8463	0.668
0.16	0.9902	0.9394	0.16	0.9083	0.7569	0.16	0.8463	0.6687
0.17	0.9902	0.9393	0.17	0.9083	0.7569	0.17	0.8462	0.6686
0.18	0.9901	0.9391	0.18	0.9083	0.7568	0.18	0.8462	0.6686
0.19	0.9901	0.9389	0.19	0.9083	0.7568	0.19	0.8462	0.6686

TABLE CXIV (continued)

DEPENDENCE OF ϵ_v AND ϵ_h ON VARIATIONS IN e"

φ = 60 degrees								
e' = 2.0			e' = 5.5			e' = 8.5		
e"	ϵ_v	ϵ_h	e"	ϵ_v	ϵ_h	e"	ϵ_v	ϵ_h
0.0	0.9969	0.8541	0.0	0.9866	0.6071	0.0	0.9566	0.5163
0.01	0.9969	0.8541	0.01	0.9866	0.6071	0.01	0.9566	0.5163
0.02	0.9969	0.8541	0.02	0.9866	0.6071	0.02	0.9566	0.5163
0.03	0.9969	0.8540	0.03	0.9866	0.6071	0.03	0.9566	0.5163
0.04	0.9969	0.8540	0.04	0.9866	0.6071	0.04	0.9566	0.5163
0.05	0.9969	0.8539	0.05	0.9866	0.6071	0.05	0.9566	0.5163
0.06	0.9969	0.8538	0.06	0.9866	0.6071	0.06	0.9565	0.5163
0.07	0.9969	0.8537	0.07	0.9866	0.6071	0.07	0.9565	0.5163
0.08	0.9969	0.8535	0.08	0.9866	0.6071	0.08	0.9565	0.5163
0.09	0.9969	0.8534	0.09	0.9866	0.6071	0.09	0.9565	0.5163
0.10	0.9969	0.8532	0.10	0.9866	0.6071	0.10	0.9565	0.5163
0.11	0.9968	0.8530	0.11	0.9866	0.6071	0.11	0.9565	0.5163
0.12	0.9968	0.8528	0.12	0.9866	0.6070	0.12	0.9565	0.5163
0.13	0.9968	0.8526	0.13	0.9866	0.6070	0.13	0.9565	0.5163
0.14	0.9968	0.8523	0.14	0.9866	0.6070	0.14	0.9565	0.5163
0.15	0.9968	0.8521	0.15	0.9866	0.6070	0.15	0.9565	0.5163
0.16	0.9968	0.8518	0.16	0.9865	0.6070	0.16	0.9565	0.5162
0.17	0.9968	0.8515	0.17	0.9865	0.6069	0.17	0.9565	0.5162
0.18	0.9968	0.8512	0.18	0.9865	0.6069	0.18	0.9565	0.5162
0.19	0.9967	0.8508	0.19	0.9865	0.6069	0.19	0.9565	0.5162

e"	ϵ_v	ϵ_h
0	0.9084	0.7570
0.19	0.9083	0.7568

$\Delta\epsilon_v = 0.0001$

$\Delta\epsilon_h = 0.0002$

Therefore, e" can be set at 0.1. This is an important elimination since it leaves only two unknowns in Equation (44). Thus two independent sets of data are required, providing an equal number of independent equations.

A visualization of the variation of ϵ_v and ϵ_h, as functions of φ and e', is shown in Figure 96 , for e" = 0. Curves for e" = 0.08 and 0.16 are presented in Figures 97 and 98 . Numerical data for Figure 96 is presented in Table CXV . It can be seen that the variation in ϵ_h, for the range e' = 2.0 thru' e' = 8.9, is approximately constant with φ and is equal to approximately 0.3. $\Delta\epsilon_v$, however, decreases with increasing φ. Since a large value of $\Delta\epsilon$ is desired, to improve the resolution on e', guidelines have been established for selecting the necessary data sets. Two possibilities arise:

1) Horizontally polarized data at $\varphi \approx 60^o$
   and at $\varphi = 0^o$

and 2) Horizontally polarized data at $\varphi \approx 60^o$
   and vertically polarized data at $\varphi = 0^o$.

Both possibilities provide reasonable values of $\Delta\epsilon$. A method which can be used for both cases will now be developed.

B. METHOD FOR CALCULATION OF e' AND T

Beginning with specific versions of Equation (44),

$$T_{Bh} = \epsilon_h T + (1 - \epsilon_h)\, T_{s\varphi} \tag{45}$$

and

$$T_{B2} = \epsilon_2 T + (1 - \epsilon_2)\, T_{s\varphi} \tag{46}$$

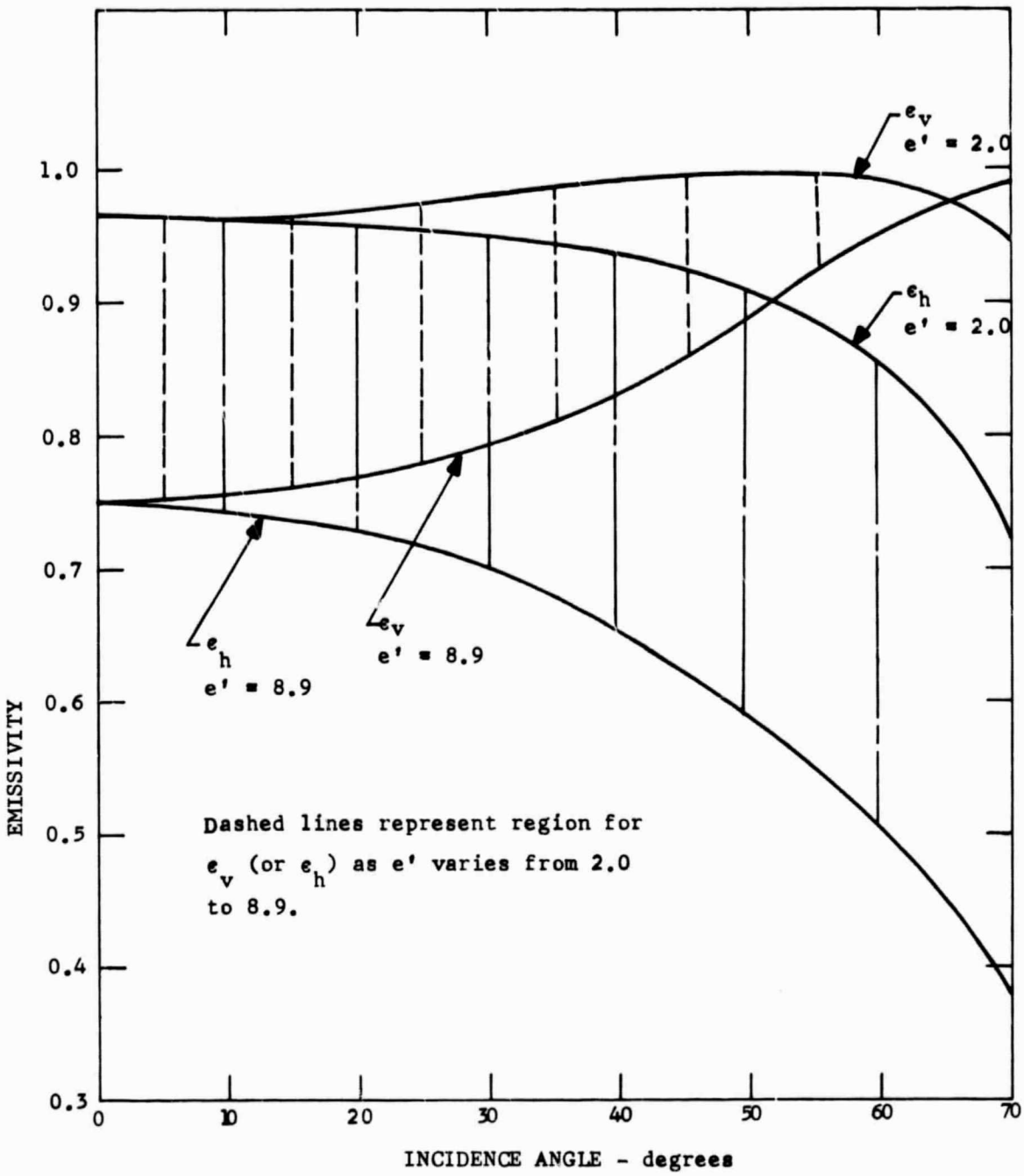


Figure 96 - Emissivity Variations as a Function of Incidence Angle, for a Range of e' (Dry Solids, e" = 0).

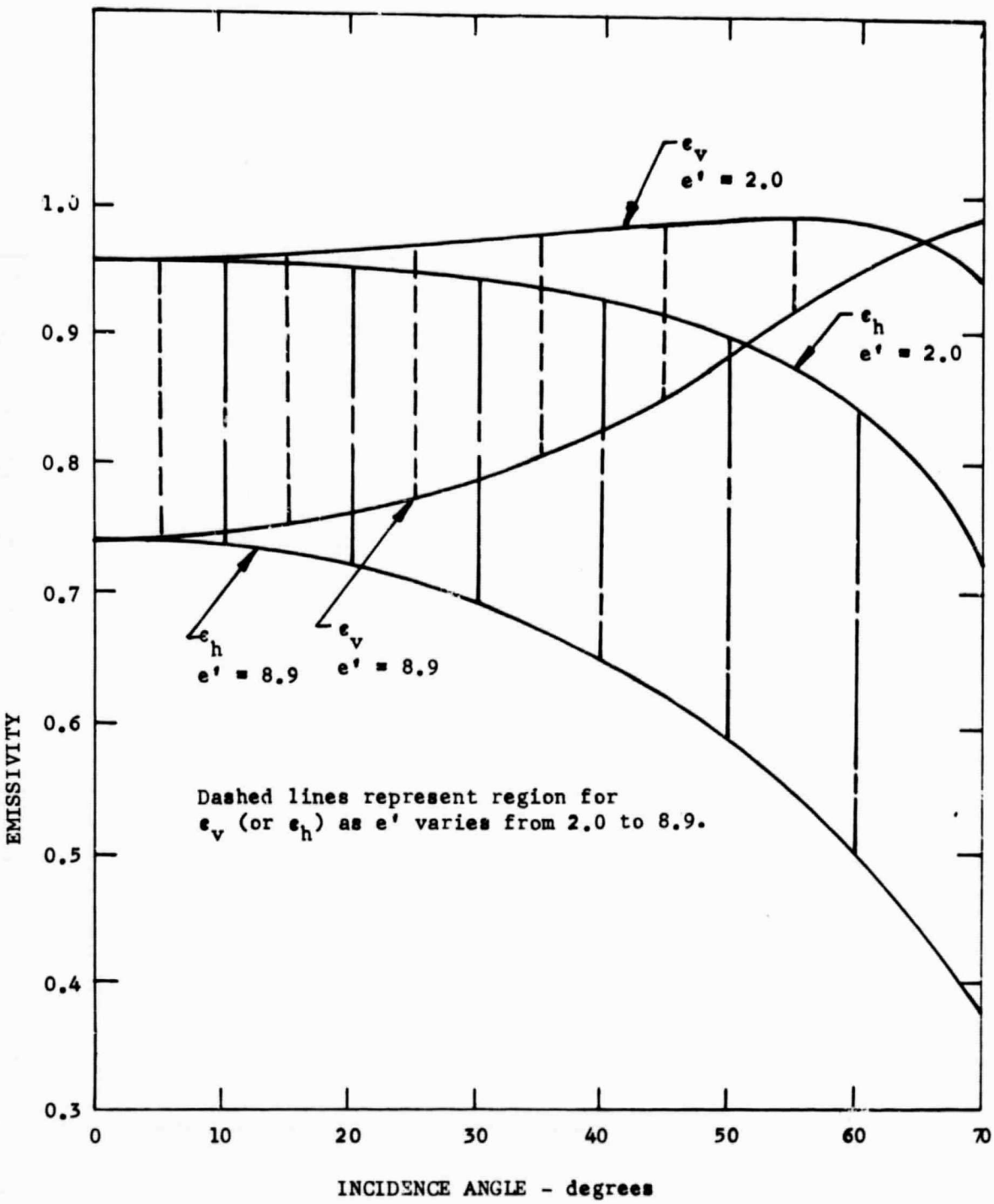


Figure 97 - Emissivity Variations as a Function of Incidence Angle, for a Range of e' (Dry Solids, e" = 0.08).

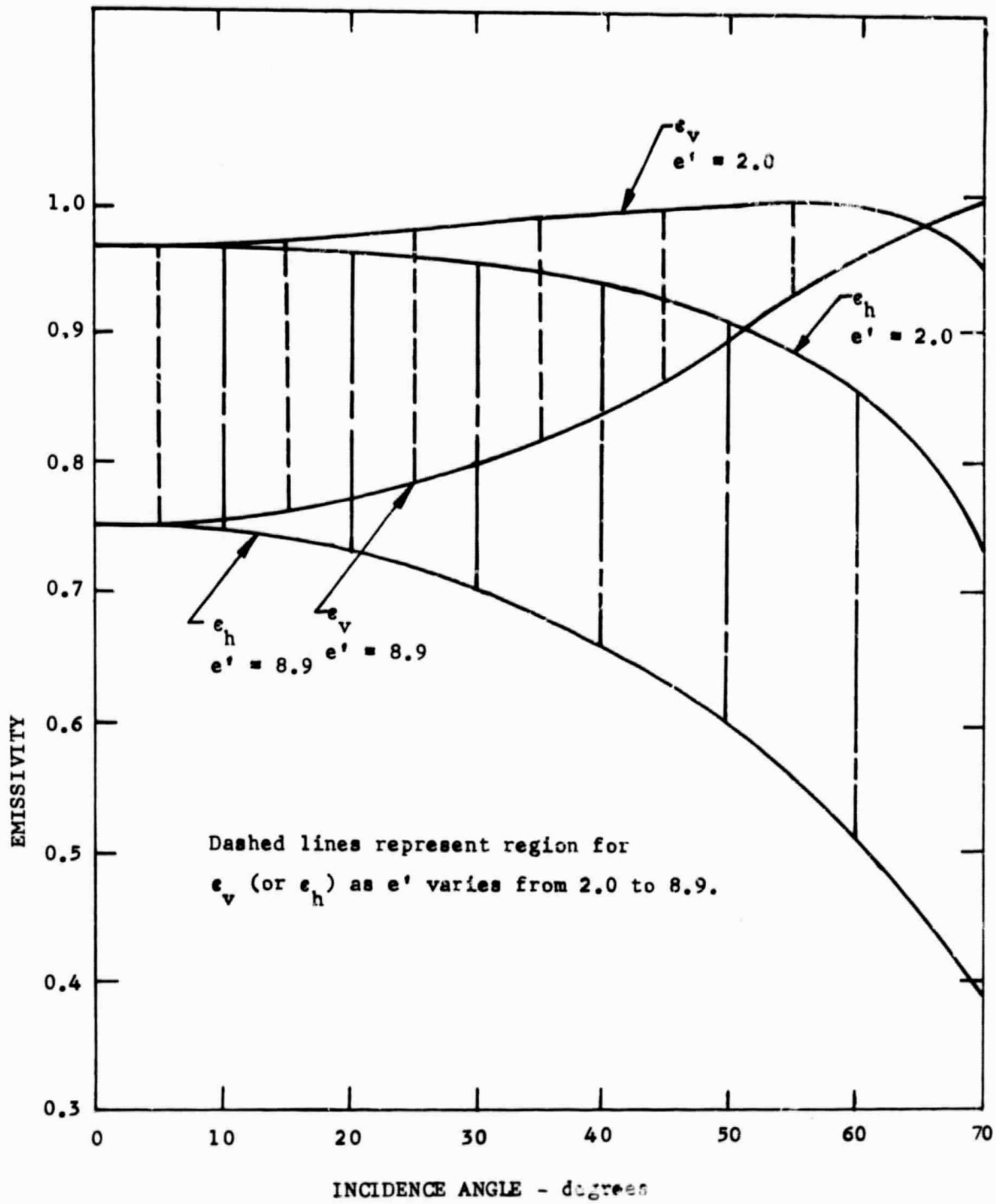


Figure 98 - Emissivity Variations as a Function of Incidence Angle, for a Range of e' (Dry Solids, e" = 0.16).

TABLE CXV

DRY SOLIDS - EMISSIVITY VERSUS INCIDENCE ANGLE

	ϵ_v		ϵ_h	
Incidence Angle - deg.	e' = 2.0	e' = 8.9	e' = 2.0	e' = 8.9
0	.9706	.7521	.9706	.7521
10	.9718	.7572	.9693	.7470
20	.9757	.7727	.9650	.7311
30	.9821	.7996	.9564	.7029
40	.9905	.8390	.9406	.6594
50	.9485	.8912	.9111	.5963
60	.9969	.9523	.8541	.5073
70	.9541	.9987	.7389	.3846

In this Table, e" = 0.

Equation (45) is for horizontal polarization at $\varphi \approx 60^{\circ}$ and Equation (46) corresponds to either vertical or horizontal polarization for $\varphi = 0^{\circ}$. Solving for T in Equation (45) and substituting into Equation (46),

$$T_{B2} = \epsilon_2 \left[\frac{T_{Bh} - T_{s\varphi}}{\epsilon_h} + T_{s\varphi} \right] + (1 - \epsilon_2)\, T_{s\varphi} \qquad (47)$$

Equation (47) involves one unknown, e'. A computer program, using an iteration technique, solves for the value of e' that yields the correct value of T_{B2}. This calculation is explained in detail in Appendix D. The computer program provides values of e' and T which satisfy Equations (45) and (46) simultaneously for the given data sets. A problem arises here with deviations of measured T_B's from calculated T_B's, which are obtained by means of Equation (45) and known values of e' and T. If, however, this deviation can be accounted for in a systematic manner, the problem will be eliminated. Using data at 16.5 GHz for limestone, the following deviations were found:

TABLE CXVI

DEVIATION OF MEASURED T_B's FROM CALCULATED T_B's

(HORIZONTALLY POLARIZED COMPONENT)

Run No. → / Incidence Angle, deg.	117	125	136	128	Approx. Average ($^{\circ}$K)
	T = 307 - 310°K			T = 291°K	
40	27.4	25.5	22.2	31.4	-25.5
50	39.3	28.1	26.2	31.1	-31.0
60	55.9	50.5	48.1	54.1	-52.0
70	54.4	54.6	52.1	62.4	-55.0

TABLE CXVII

DEVIATION OF MEASURED T_B's FROM CALCULATED T_B's

(VERTICALLY POLARIZED COMPONENT)

Run No. → / Incidence Angle, deg.	116	124	135	129	Approx. Average (^oK)
	T = 307 - 310^oK			T = 291^oK	
40	22.7	27.3	30.4	34.5	28.0
50	25.6	45.7	44.8	42.8	44.0
60	37.2	48.4	53.9	44.6	49.0
70	73.8	76.9	79.3	77.8	77.0

From the above data, it can be seen that the deviations are approximately the same for a given incidence angle, and for a range of T. The fact that approximately the same deviation is involved at a given angle enables the use of a "correction" on the data, which effectively aligns it with the theoretical values. Ideally, if the data is "corrected" to an exact theoretical value, the program will yield the exact corresponding values of e' and T. Using an approximate average, a correction set has been established for four angles (last column in above Tables) for both polarizations. If both corrected and uncorrected T_B data were to be plotted as a function of φ, it would be apparent that the correction effectively spreads apart the curves for T_{Bv} and T_{Bh}. That is, the plotted values of measured T_{Bh} and T_{Bv} are closer together than the theoretical curves. This is an effect that appears in measured sea water data - the curves are "pushed" toward each other as surface roughness increases. Curves due to Hollinger are given in Appendix D and show this effect. See Figures D-4, D-5, D-6 and D-7. Effectively, it can be stated that the deviations summarize the roughness of the observed surface. If this is the case, however, different "correction" curves may be expected for different roughness conditions. In fact it can be stated that the signature of the roughness is represented by the correction curve used. In addition to limestone, some quartz sand data was also examined, the roughness characteristics of which are

quite different from limestone. Table CXVIII shows "correction" sets for quartz sand. Comparing Tables CXVI, CXVII and CXVIII, the "corrections" are markedly different from each other. The difference between these curves can be primarily ascribed to different scattering geometries. The fact that the curves are different indicates that the primary reason for the observed curves lying closer together than the theoretical curves is not the fault of the radiometer, since any discrepancies would be uniform and independent of the material under observation.

TABLE CXVIII

DEVIATION OF MEASURED T_B's FROM CALCULATED T_B's (16.5 GHz)

(VERTICALLY POLARIZED COMPONENT)

Run.No. → / Incidence Angle (deg.)	84 T = 318°K	88 T = 307°K	92 T = 317°K	Approx. Average (°K)
44	19.70	---	---	---
54	18.23	18.49	34.00	22.0
64	11.00	7.80	20.17	14.0

(HORIZONTALLY POLARIZED COMPONENT)

Run No. → / Incidence Angle (deg.)	85 T = 318°K	89 T = 307°K	93 T = 317°K	Approx. Average (°K)
54	2.37	2.88	7.12	3.5
64	22.96	27.79	27.48	24.0

C. ANALYSIS OF LIMESTONE CALCULATIONS

Using measured limestone data at 16.5 GHz, calculations of e' and T have been performed. The value of e" was set at 0.1, although actually e" = 0.158 for limestone. Many calculations were performed using horizontal-horizontal

(h-h)and horizontal-vertical (h-v) data sets, at several combinations of incidence angle. These are tabulated in Table CXIX.

TABLE CXIX

CALCULATION OF e' AND T USING MEASURED

LIMESTONE BRIGHTNESS TEMPERATURES AT 16.5 GHz (h-v DATA)

φ_h	φ_2	Calculated e'	Calculated T(°K)	Measured T(°K)	Run No.
70	40	7.990	303.97	309	124 - 125
70	50	7.742	300.23	"	"
70	60	8.125	305.99	"	"
60	40	8.765	309.10	"	"
60	50	8.321	303.26	"	"
60	60	8.660	307.73	"	"
50	40	9.101	311.09	"	"
50	50	8.508	304.22	"	"
40	40	8.099	304.74	"	"
70	40	8.048	300.70	310	135 - 136
70	50	8.266	303.90	"	"
70	60	8.008	300.12	"	"
60	40	9.515	310.09	"	"
60	50	9.536	310.34	"	"
60	60	8.968	303.46	"	"
50	40	10.100	313.67	"	"
50	50	9.999	312.62	"	"
40	40	9.351	309.07	"	"
70	45	5.631	261.52	291	128 - 129
70	50	6.919	283.91	"	"
70	60	7.408	291.80	"	"
60	45	6.415	265.79	"	"
60	50	8.217	290.36	"	"
60	60	8.642	295.74	"	"
50	45	6.412	265.56	"	"
50	50	8.729	292.92	"	"
45	45	4.868	257.33	"	"
70	40	11.341	329.76	307	116 - 117
60	40	8.236	310.26	"	"

TABLE CXX

CALCULATION OF e' AND T USING

MEASURED BRIGHTNESS TEMPERATURES AT

16.5 GHz (h-h DATA)

φ_h	φ_2	Calculated e'	Calculated T(°K)	Measured T(°K)	Run No.
70	40	8.089	305.45	309	124 - 125
70	50	6.141	274.31	"	"
60	40	10.522	330.83	"	"
70	40	7.000	284.66	310	135 - 135
60	40	9.765	313.06	"	"
70	45	6.871	283.12	291	128 - 129
60	45	13.900	353.51	"	"
70	45	47.896	595.00	309	116 - 117
60	45	12.936	367.11	"	"

Some conclusions may be drawn from the results of these calculations:

1) The (h-v) data sets are considerably more stable and accurate than the (h-h) data sets. This is reasonable since, in fact, the equations are more independent for the h-v case.

2) On the basis of a modest amount of data, restricted to incidence angles in the range 40 to 70 degrees, it is clear that the most successful combination is $\varphi_h = 60^\circ$ and $\varphi_v = 50^\circ$ and 40°. Table CXXI summarizes the results at these angles.

TABLE CXXI

CALCULATION OF e' AND T FOR LIMESTONE

f = 16.5 GHz. Actual e' = 8.63.

Run Nos.	φ_h(deg.)	φ_v(deg.)	Calc. e'	Calc. T (°K)	Meas. T (°K)
124 - 125	60	40	8.77	309.1	309
	60	50	8.32	303.3	309
135 - 139	60	40	9.52	310.1	310
	60	50	9.54	310.3	310
128 - 129	60	45	6.42	265.8	291
	60	50	8.22	290.4	291
	60	60	8.64	295.7	291
116 - 117	60	40	8.24	310.3	307

Considering the above results with reference to Equation (44) , it is apparent that a discrepancy exists between measured and theoretical values of T_B. A correction has been introduced into Equation (44) as follows:

$$T_B = \epsilon T + (1 - \epsilon)\, T_{s\varphi} + \alpha\,(\varphi, p, g) \qquad (48)$$

where, α is a correction dependent on, φ, the angle of incidence; p, the polarization of the received radiation; and, g, the scattering geometry (surface roughness).

In the preceding calculations, α was deduced by obtaining an approximate match between measured and theoretical values of T_B. The usefulness of this procedure is predicated on the consistency of the function, α, for all situations and specified values of φ, p and g. Since there is an insufficient amount of data at 16.5 GHz, there is no satisfying way of testing this. Thus, a need exists for additional measured data to permit examination of the following questions:

1) Does α depend on T (there are only two values of T available)? If this is the case the method would necessarily require revision.

2) Is α sufficiently consistent for small variations in g?

Since measured data exists at 9.5 GHz, for limestone, it has been possible to examine the possibility of a frequency dependence in α. Table CXXII shows the results of this investigation.

Considerable discrepancies appear, in the above Table, between the derived and measured values of T. Although there is no measured data for e' at 9.5 GHz, the derived values of e' appear to be low, if it is assumed that e' is not strongly frequency dependent. Therefore, a logical conclusion is that the function, α, is not correcting properly at this frequency i.e., α is frequency dependent. Thus, frequency should be included as one of the parameters affecting α. Thus,

$$\alpha = \alpha(\varphi, p, g, f) \tag{49}$$

Of the four parameters, three (φ, p, and f) are specified by the measurement - only g is unknown at the outset. Hence,

$$\alpha = \alpha(g)$$

TABLE CXXII

CALCULATED VALUES OF e' AND T USING CORRECTION,

OBTAINED FOR LIMESTONE AT 16.5 GHz, FOR 9.5 GHz DATA

φ_h(deg.)	φ_2(deg.)	Calculated e'	Calculated T(°K)	Measured T(°K)	Run No.
60	45	6.654	335.34	302	141 - 142
60	50	7.983	358.45	"	"
60	60	7.930	357.57	"	"
60	45	4.493	325.64	302	143 - 145
60	50	5.298	344.75	"	"
60	60	5.528	349.92	"	"
60	45	5.776	327.78	302	144 - 146
60	50	7.000	351.36	"	"
60	60	6.751	346.75	"	"
60	50	7.276	310.58	307	137 - 138
60	55	6.809	303.02	"	"
60	60	8.570	330.34	"	"
60	45	9.850	325.50	305	121 - 127
60	50	10.834	337.80	"	"
60	60	11.273	343.09	"	"
60	45	8.972	315.28		
60	50	9.403	320.89		
60	60	9.952	327.83		

Different scattering geometries will produce different α functions. Using measured data, as in the case of limestone, α could be determined for other materials. Equipped with the various α's one could input the data into computer programs and perform calculations of e' and T. If α_1 is the limestone correction, then only limestone data would be expected to result with e' and T within the appropriate range. Bearing in mind that, for limestone, e' = 8.63, one could establish criteria for the identification of limestone so that, say, 90% of the data predicts $7.5 < e' < 9.5$. This is strictly a qualitative statement couched in quantitative terms. Data for Quartz Sand input into the program, using the limestone correction, is tabulated in Table CXXIII.

It will be noted that the prediction for e' shows considerable deviations from the measured value of 2.88. However, it is expected that if the Quartz Sand data were manipulated using a value of α appropriate for this material, a consistent picture would emerge. Thus, if two different materials exhibit the same α, one would obtain the appropriate range of e' by means of that α and incorrect values of e' with α's pertaining to other materials.

The following difficulties may arise:

1) α may not provide sufficiently distinct e' values to distinguish some materials.

2) Data for material A may appear within the criteria for material B, using the criteria for B. This possibility requires further analysis and the establishment of corrections of interest.

It is felt that, within the constraints imposed by somewhat limited data, the feasibility of determining the dielectric constants of specular materials from brightness temperatures has been demonstrated. However, it has not been possible to prove the workability of the method. To accomplish this, the following recommendations are in order:

1) A complete set of measured brightness temperatures, for a variety of materials, is required. A large amount of data would permit the development of a technique which would not be sensitive to unusual data fluctuations.

TABLE CXXIII

CALCULATION OF e' FOR QUARTZ SAND, USING CORRECTIONS FOR LIMESTONE

φ_h	φ_2	Calculated e'	Calculated T(°K)	Measured T(°K)	Run No.	Freq. (GHz)
64.0	64.0	4.688	333.16	310	100 - 101	16.5
64.0	44.0	5.503	345.56	318	84 - 85	"
64.0	54.0	5.999	357.04	"	84 - 85	"
64.0	64.0	5.845	353.53	"	84 - 85	"
64.0	54.0	5.361	342.08	307	88 - 89	"
64.0	64.0	5.496	345.28	"	88 - 89	"
62.0	52.0	5.429	341.02	"	92 - 93	"
62.0	62.0	5.585	344.62	"	"	"
62.0	64.3	5.240	336.60	"	"	"
63.4	52.0	14.531	391.93	"	"	"
63.4	62.0	12.272	366.13	"	"	"
63.4	64.3	10.882	349.03	"	"	"
64.0	54.0	1.687	230.35	311	98 - 99	9.5
64.0	64.4	3.508	300.27	311	98 - 99	"
64.0	54.0	2.638	270.41	312	102 - 104	"
64.0	64.0	4.399	327.44	312	102 - 104	"
64.0	54.0	2.308	253.07	310	105 - 106	"
64.0	64.0	4.142	314.11	310	105 - 106	"

2) A set of α values should be established for the above materials at several frequencies.

3) Experimental measurements should be performed to determine e' and e" for the materials concerned at the frequencies of interest. The unavailability of such data, at the frequencies employed in the field measurements, made it necessary to limit most of the analysis to a single frequency.

VI. CONCLUSIONS

Since a considerable wealth of information is included in this report, a number of conclusions and comments are summarized here for purposes of convenience. These are presented in the order in which the detailed information appears in the preceding Sections.

A. CORRECTION OF CALIBRATION ERRORS

The use of a third calibration point, consisting of a calculated value of zenith sky brightness temperature in each data Run, is considered to be very worthwhile, in that the measured data was effectively stabilized in this manner. All negative and excessively positive values of measured zenith sky brightness temperatures, T_{So}, were thus eliminated. A critical examination of all reduced data on the basis of reasonable T_{So} values (referred to established tolerances) resulted in rejection of approximately 15% of the data. The remaining data is considered to be quite consistent compared with the first reduction performed in 1966. It should be stressed that this method of data stabilization is best suited to clear sky conditions; cloud models are difficult to establish accurately when measured atmospheric profiles are not available at the measurement site, as was the case in the field measurement program.

B. SEA WATER DATA

The measured sea water brightness temperatures exhibit a high degree of specularity at 9.5, 16.5 and 94 GHz, with an inverse relationship prevailing between specularity and frequency.

There is better agreement between derived and theoretical emissivities at vertical polarization than horizontal polarization, at 9.5 and 16.5 GHz. In the case of 94 GHz, agreement is better for horizontal polarization. The derived emissivity magnitudes display a direct relationship with frequency, at vertical incidence. This is consistent with theory.

Calculations of sea water dielectric permittivities show a strong inverse shift with respect to frequency and a relatively small direct relationship with temperature. Theoretical emissivities show a very small inverse temperature dependence at the two lower frequencies, with a slightly greater dependence at 94 GHz. Results derived from measured data agree with these relationships.

Conversion of apparent temperatures to brightness temperatures appears to have been worthwhile, since reasonably good agreement exists between measured and theoretical brightness temperatures, especially for vertical polarization. The difference between T_A's and T_B's tends to increase with frequency, with relatively small differences evident at 9.5 GHz.

Surface roughness generally increases sea water brightness temperatures at both 16.5 and 94 GHz. The increase is greater at low antenna beam nadir angles, at both polarizations. However, there is some uncertainty as to any increase at large nadir angles for vertical polarization; this effect is more pronounced at 16.5 GHz.

C. SALINES DATA

The very rough nature of the Saline material has resulted in high brightness temperatures at all three frequencies, with essentially constant values over a broad range of nadir angles at each frequency. In addition, the very small separation between polarizations classifies this surface as a diffuse reflector.

In the derivation of emissivities for this material it was noted that, basically, the same results are obtained when using an inverted form of the specular equation for brightness temperature (Equation (31)) and when using scattering coefficients (Equation (33)). Thus, it would appear that the former equation can be safely employed when deriving emissivities of very rough surfaces.

There is very little agreement between derived and theoretical emissivities, although the latter are available at only 14 GHz*. The

---

* The frequency dependence of emissivities of dry materials is considered to be very small, over the frequency range covered in this study.

reason for this is the very rough nature of the Saline surface. Hence, there is little agreement between measured and theoretical brightness temperatures.

D. QUARTZ SAND DATA

The Quartz Sand material surface was fairly smooth; as a result the brightness temperatures and emissivities exhibit a definite specularity at all three frequencies. However, the material is somewhat less specular at 94 GHz than at the lower frequencies.

There is fair agreement between derived and theoretical emissivities, at larger incidence angles, at all frequencies. The lack of better agreement is considered to be due to possible errors in the survey of the sand dune profiles. A point worth noting is that the derived emissivity magnitudes are fairly invariant with frequency. Finally, the Brewster Angle is positioned about 10 degrees higher in the derived emissivity plots, compared with its position in the theoretical plot. This indicates a somewhat higher dielectric permittivity than that measured in the laboratory at 14 GHz.

Due to the scattered nature of the brightness temperature data points, there is rather limited agreement between these and calculated T_B's, at 16.5 GHz, except in a narrow angular range at vertical polarization.

E. LIMESTONE DATA

These observations involved both powdered and pebbled limestone textures; measurements were performed on both at 9.5 GHz only. Although both sets of data show a definite specular characteristic, the T_B's and derived emissivities are considerably higher for the powdered limestone.

The 16.5 and 9.5 GHz data are similar for the pebbled material, except that the derived emissivities are slightly lower at 16.5 GHz. There is some similarity between the 94 GHz pebbled limestone data and the 9.5 GHz powdered limestone information. At all frequencies, however, regardless of surface texture, the Brewster Angle is positioned from 6^o

to 11° below its position in the theoretical emissivity plot. Thus, it appears that the correct value of dielectric permittivity could be somewhat lower than the measured value at 14 GHz (e' = 8.63 at this frequency). Finally, at all frequencies, there is limited agreement between derived and theoretical emissivities, in terms of magnitude, but reasonable agreement with respect to shape. This is probably due to surface roughness effects.

Due to considerable differences between the magnitudes of derived and theoretical emissivities, the differences between measured and calculated T_B's are sizeable, except at lower nadir angles for vertical polarization. Although the comparison is made only at 16.5 GHz, the same comment very likely applies to the other frequencies.

F. OTHER CONCLUSIONS

An analysis of the influence of surface roughness on brightness temperatures permits listing the observed materials, in terms of decreasing specularity, for each frequency. The results are shown in the Table below.

TABLE CXXIV

INFLUENCE OF SURFACE ROUGHNESS

(In Terms Of Decreasing Specularity)

Incidence Angle = 55°

9.5 GHz	16.5 GHz	94 GHz
Sea Water	Sea Water	Sea Water
Quartz Sand*	Quartz Sand*	Pebbled Limestone
Powdered Limestone	Pebbled Limestone	Quartz Sand*
Pebbled Limestone	Salines	Salines
Salines		

*Incidence Angle = 68.6°.

The above data shows that, with the exception of powdered limestone, the order is the same at 9.5 and 16.5 GHz; however, at 94 GHz the Pebbled Limestone is more specular than Quartz Sand. This is rather significant since the incidence angle, at which the quantity ($T_{Bv} - T_{Bh}$) was taken for Quartz Sand, was greater than for Limestone - 68.6° versus 55°, respectively. It has not been possible to reconcile this apparent anomaly.

In a brief study of the effects of surface and subsurface temperatures on brightness temperatures, it was noted that attenuation in dry materials is directly proportional to frequency. Thus, in a given material, the influence of subsurface temperatures on T_B's is expected to diminish with increasing frequency. Due to restrictions on time, it was not possible to substantiate this with measured data during the course of the study. However, it was observed that subsurface temperatures did influence T_B's of the Saline material at both 16.5 and 94 GHz. The clear effect at both frequencies was, very likely, due to the associated low attenuations in this material.

During the study an attempt was made to develop a method of determining dielectric constants of specular materials from brightness temperatures. Although feasibility was demonstrated to a limited degree, it was not possible to prove the workability of the method. Additional effort is required to develop a satisfactory technique.

An attempt was made to correlate brightness temperatures and geological information, presented in Reference (2) report, for solid materials. Apart from a few correlations of T_B's with surface and subsurface temperatures, it was difficult to find any relationship between T_B and such items as density; specific gravity; percent insolubles; modal analyses; chemical analyses; thermal gravimetric and differential thermal analyses; particle size distribution; and, roundness and sphericity. Some of these items are automatically accounted for through the dielectric permittivity of a given material; however, individual contributions to brightness temperatures (or emissivities) can only be determined by somewhat specialized observations. The field measurements, performed under the original program in 1966, did not fall in this category.

VII. RECOMMENDATIONS

A detailed examination of the reduced data reveals considerable consistency within each frequency, with relatively smooth curves of brightness temperatures versus incidence angle. In addition, the frequency dependence of the data is quite clear. Thus, it can be stated that the brightness temperatures and emissivities are of sufficient quality to warrant their use in further studies. Such studies should exploit the data in specific applications, thereby ensuring full benefit from the current data manipulations and analyses. It is therefore recommended that consideration be give to the following work:

1) Continue the investigation of techniques for determining the dielectric constants of specular and diffusely reflecting surfaces, and apply these techniques, wherever possible, to the measured data.

2) In connection with Item (1) obtain, by measurement, additional dielectric permittivities of limestone and quartz sand at, or near, the lower frequencies used in the field measurement program (9.5 and 16.5 GHz). Ideally, these measurements should be performed at several frequencies, encompassing these, to obtain the frequency dependence of dielectric permittivities. Facilities are available at the Massachusetts Institute of Technology for measurements at 1, 3, 8.5, 14 and 24 GHz. Other materials, for which apparent or brightness temperatures are available, should be included in this investigation.

3) The results of Items (1) and (2) should be applied in an investigation of techniques for radiometric identification of materials. This item could not be included in the current study.

4) The influence of subsurface moisture and temperature on the brightness temperatures of solid materials should be investigated with the aid of, both, data generated during this study and measured dielectric permittivities. Such a study would require additional material samples (for laboratory measurements of dielectric constants) and the development of mathematical expressions for calculation of emissivities and reflectivities of layered media. The mathematical models must take into account internal

reflections and attenuations influencing the final emissivity and reflectivity of the particular soil model.

Brightness temperatures should be calculated as required for each soil model, at frequencies of interest, as a function of incidence angle with polarization and atmospheric models as parameters. This information should be furnished, both, at the surface and at a specified altitude. The results of this work should be discussed in terms of the utility of microwave radiometers, operating at specified frequencies, for sensing subsurface moisture in soils and subsurface moisture distribution from a given altitude. This information is expected to be of considerable value to the Earth Resources Program.

5) Additional analyses should be performed on ocean surface roughness effects, by examining the 16.5 GHz data printout-for-printout. In the current study, the brightness temperatures represent an average of fifteen individual printouts by the digital voltmeter. These have been entered on the data cards. The data reduction program can be modified to provide T_B's for each entry; thus, a new T_B value would be available every second, since the radiometer time constant was one (1) second. This approach would permit a dynamic analysis of ocean roughness effects, including various statistical investigations.

REFERENCES

1. Porter, R.A., and T. E. Servey, "Microwave Radiometer Field Measurement Program" (Sea Water) Raytheon Co. Report FR-66-293, 31 August 1966.

2. Porter, R.A., and T.E. Servey, "Microwave Radiometer Field Measurement Program (Saline, Sand and Limestone)", Raytheon Co. Report FR-66-379, 16 December 1966.

3. Porter, R.A., and T.E. Servey, "Radiometer System Accuracy Analysis", Raytheon Co. Report FR-66-293 Addendum No. 1, 22 November 1966.

4. "Radiometric Measurement Program" (Computer Program) Raytheon Report U67-4125, 4 January 1967.

5. Staelin, D.H. (1966): Measurement and interpretation of the microwave spectrum of the terrestrial atmosphere near 1 cm wavelength. J. Geo. Res., 71, 12, 2875.

6. Valley, S.L. (ed.) (1965): Handbook of Geophysics and Space Environments. Air Force Cambridge Research Lab., Bedford, Mass.

7. Neiburger, M. (1949): Reflection, absorption, and transmission of insolation by stratus cloud, J. Meteor., 6, in Mason Physics of Clouds.

8. Mason, B.J. (1957): The Physics of Clouds. Clarendon Press, Oxford.

9. Houghton, H. G., and W.H. Radford (1938): On the measurement of drop size and liquid water content in fogs and clouds, M.I.T., Pap. Phys. Oceanog. and Met., 6, 4, in Mason, Physics of Clouds.

10. Goldstein, H., in Propagation of Short Radio Waves, (ed. Kerr), Radiation Laboratory Series, M.I.T., 13, McGraw-Hill, New York (1951).

11. Weickmann, H.K., and H.J. Aufm Kampe (1953): Physical properties of cumulus clouds, J. Meteor., 10, in Mason, Physics of Clouds.

12. Borovikov, A. M. (1963): Cloud Physics, Israel Program for Scientific Translation, Jerusalem, 1963.

13. Scarborough, J.B., "Numerical Mathematical Analysis", Baltimore, 1958.

14. Chen, S.N.C. and W.H. Peake, "Apparent Temperatures of Smooth and Rough Terrain", IRE Transaction on Antennas and Propogation, pp. 567-572, November 1961.

15. Cosgriff, R.L., W.H. Peake and R.C. Taylor, "Terrain Scattering Properties for Sensor System Design", (Terrain Handbook II), Engineering Experiment Station Bulletin 181, The Ohio State University (May 1960).

16. Peake, W.H., "The Microwave Radiometer as a Remote Sensing Instrument", Tech. Report 1903-8 under contract NSR-36-008-27, Ohio State University, January 17, 1969.

17. Wulfsberg, K.N., "Atmospheric Attenuation at mm Wavelengths", Radio Sci. 2 (New Series), 1967.

18. Hogg, D.C. and R.A. Semplak, "The Effect of Rain and Water Vapor on Sky Noise at Centimeter Wavelengths", The Bell Telephone Journal, p. 1334, September 1961.

19. Hasted, J.B., D.M. Ritson and C.H. Collie, "Dielectric Properties of Aqueous Ionic Solutions, Parts I and II", J. Chemical Physics, Vol. 16, No. 1, January 1948.

20. Paris, J.F., "Microwave Radiometry and its Application to Marine Meteorology and Oceanography", Texas A & M Univ. report prepared under ONR Contract Nonr 2119(04), January 1969.

21. Liebermann, L.N. "Other Electromagnetic Radiation", The Sea, Vol. 1, Interscience Publishers, 1962.

22. Stogryn, A., "The Apparent Temperature of the Sea at Microwave Frequencies", IEEE Transactions on Antennas and Propagation, Vol. AP-15,No.2.

APPENDIX A

ANTENNA PATTERN CORRECTION

1. Geometry

The gain patterns of microwave and millimeter-wave antennas is simply the manifestation of diffraction of electromagnetic waves by a finite aperture. Most of the power received by the antenna is contained in the main lobe of the diffraction pattern. The remaining power is received via the side and back lobes.

If one were investigating astronomical radio sources of very small angular extent, it would be important to remove the effect of the main lobe "pattern". However, for extended sources, such as the atmosphere and terrestrial materials, the brightness temperature variation within the main lobe half-width is not sufficient to necessitate the removal of the main lobe effects. The following discussion will concentrate on the correction for side and back lobe effects.

The geometry of the situation is indicated in Figure (A-1). Environmental temperatures are given in the $(\hat{x}, \hat{y}, \hat{z})$ coordinate system where the unit vector $\hat{z}$ is oriented in the zenith direction. The antenna axis is inclined at angle θ_o to the zenith and defines the unit vector $\hat{z}'$. If the $\hat{x}'$ direction is chosen to coincide with the $\hat{x}$ direction, the set $(\hat{x}', \hat{y}', \hat{z}')$ defines Cartesian coordinates in the antenna-centered frame.

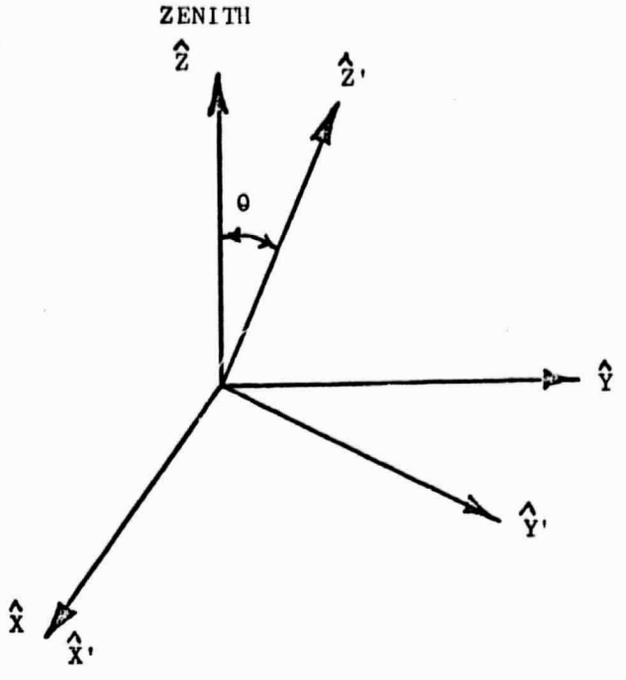


Figure A-1 Antenna Pattern and Environment Coordinates

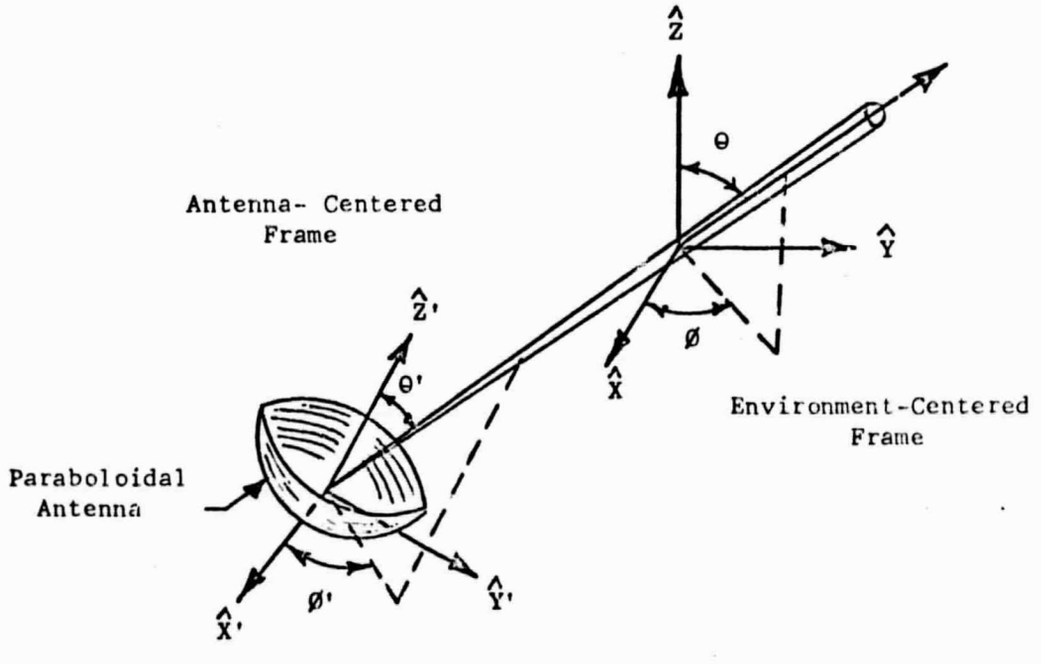


Figure A-2 Angular Coordinates of Antenna Pencil Beam in Antenna and Environment-Centered Frames.

Polar angles in either frame are defined with respect to the z axes, while azimuthal angles are defined with respect to the x axes. Figure A-2 shows the angular coordinates of a pencil beam in both environment and antenna-centered frames.

2. Analytical Approach

The apparent (measured) temperature seen by an antenna oriented at a zenith angle θ_o is given by

$$T_A(\theta_o) = \frac{\int T_B(\theta, \phi)\, g(\theta', \phi')\, d\Omega'}{\int g(\theta', \phi')\, d\Omega'} \qquad \text{(A-1)}$$

where

$T_B(\theta, \phi)$ = brightness temperature of environment at zenith angle θ and azimuthal angle ϕ

θ' = polar angle of environmental point in antenna-centered coordinates

ϕ' = azimuthal angle in antenna-centered coordinates

g = antenna gain function in antenna-centered system

$d\Omega'$ = element of solid angle in antenna system

If one assumes the environment to be azimuthally symmetric (certainly true for clear skies), then T_B depends on θ only and Equation (A-1) can be written

$$T_A(\theta_o) = \int_0^{\pi} K(\theta_o, \theta)\, T_B(\theta)\, d\theta \qquad \text{(A-2)}$$

where

$$K(\theta_o, \theta) = \frac{\sin\theta \int_0^{2\pi} g(\theta', \phi')\, d\phi}{\int_0^{\pi}\int_0^{2\pi} g(\theta', \phi') \sin\theta'\, d\phi'\, d\theta'} \qquad \text{(A-3)}$$

Equation (A-2) is a Fredholm integral equation of the first kind with kernal K. It can be solved numerically in the following way.

First, one introduces a quadrature rule to change the integral in Equation (A-2) into a sum:

$$T_A(\theta_o) = \sum_j k_j(\theta_o)\, T_B(\theta_j) \qquad \text{(A-4)}$$

The set of finite angles $\{\theta_i\}$ may be chosen to be equidistant if desired. If the antenna temperature T_A is also measured at these angles, then a set of linear matrix equations results:

$$T_A(\theta_i) = \sum_j G_{ij}\, T_B(\theta_j) \qquad \text{(A-5)}$$

where G_{ij} is a m x m matrix derived from K.

Since T_A and T_B are very close in magnitude, it is convenient to calculate their difference. Equation (A-5) can be written

$$T_A(\theta_i) = T_B(\theta_i) + \sum_j (G_{ij} - \delta_{ij})\, T_B(\theta_j)$$

where, δ_{ij} is the unit matrix; or in symbolic matrix notation

$$T_B = T_A - (G - I)T_B \tag{A-6}$$

Equation (A-6) has a formal solution which may be expressed as an infinite series:

$$T_B = T_A - (G - I)T_A + (G - I)(G - I)T_A - \ldots \tag{A-7}$$

In Equation (A-6) and (A-7), I represents the unit matrix.

Truncation of the series in Equation (A-7) is equivalent to solving the following iterative set

$$T_B^{(\ell)} = T_A - (G - I)\, T_B^{(\ell-1)}$$

$$T_B^{(o)} = T_A \tag{A-8}$$

Usually only one or two iterations are necessary in order to achieve a satisfactory solution to Equation (A-5) if T_A is given by empirical data.

An obvious method to calculate G_{ij} involves using a quadrature rule based on equidistant intervals in θ. This approach leads to the form

$$k_i(\theta_o) = w_i K(\theta_o, \theta_i),$$

where, w_i is an appropriate weight. Because of the highly peaked nature of K, the important sum condition

$$\sum_i k_i(\theta_o) = 1$$

does not hold sufficiently well to insure the accuracy needed for solution of Equation (A-6). A better method of calculation involves writing Equation (A-2) as

$$T_A(\theta_o) = \int_o^{\pi} T_B(\theta)\, dP(\theta, \theta_o) \qquad \text{(A-9)}$$

where

$$P(\theta, \theta_o) = \int_o^{\theta} K(\theta_o, \bar{\theta})\, d\bar{\theta} \qquad \text{(A-10)}$$

Then the trapezodial rule may be applied to Equation (A-9). yielding

$$T_A(\theta_o) = \sum_i T_B(\theta_i)\ 1/2\ [P(\theta_{i+1}, \theta_o) - P(\theta_{i-1}, \theta_o)] \qquad \text{(A-11)}$$

or

$$G_{ij} = 1/2[P(\theta_{j+1}, \theta_i) - P(\theta_{j-1}, \theta_i)] \ . \qquad \text{(A-12)}$$

Next it is necessary to indicate the method of computing P. Using Equation (A-3)and (A-10) we write,

$$P(\bar{\theta}, \theta_o) = \int H\ (\bar{\theta}-\theta)\ g(\theta',\phi')\ d\Omega' \ / \int g(\theta',\phi')\ d\Omega' \qquad \text{(A-13)}$$

where, $H(\bar{\theta})$ is the Heaviside unit step function. The solid angle integration in the numerator of Equation (A-13) has been written in the antenna-centered system instead of the zenith-centered system. One may interpret Equation (A-13) as saying that $P(\bar{\theta},\theta_o)$ is the fraction of the received power entering the cone with half-angle $\bar{\theta}$ centered on the zenith.

Now if $\theta_o = 0$, then $\theta = \theta'$, and Equation (A-13) becomes

$$P(\bar{\theta}, 0) = \frac{\int_0^{\bar{\theta}} \int_0^{2\pi} g(\theta', \phi')\, d\phi' \sin\theta' \, d\theta'}{\int_0^{\pi} \int_0^{2\pi} g(\theta', \phi')\, d\phi' \sin\theta' \, d\theta'} \qquad \text{(A-14)}$$

A great simplication is acheived by specializing to the case where the antenna is azimuthally symmetrical i.e., there is no gain dependence on ϕ'. In this case, Equation (A-14) becomes

$$P(\bar{\theta}, 0) = \frac{\int_0^{\bar{\theta}} g(\theta') \sin\theta' \, d\theta'}{\int_0^{\pi} g(\theta') \sin\theta' \, d\theta'} \qquad \text{(A-15)}$$

and Equation (A-13) can be written

$$P(\bar{\theta}, \theta_o) = \int_0^{\pi} \frac{\Delta\phi(\theta_o, \bar{\theta}, \theta')}{2\pi} \, dP(\theta', 0) \qquad \text{(A-16)}$$

where,

$$\Delta\phi\ (\theta_o,\bar{\theta},\theta') = \int_0^{2\pi} H(\bar{\theta} - \theta)d\phi'$$

$$= \Phi_1'(\theta_o,\bar{\theta},\theta') - \Phi_2'\ (\theta_o,\bar{\theta},\theta') \qquad \text{(A-17)}$$

Now the angles $\Phi_i'\ (\theta_o,\theta,\theta')$ represent the azimuthal angles corresponding to the intersections of two cones: the first cone is defined in the antenna-centered frame by constant polar angle θ'; the second cone is defined in the environment-centered frame by constant polar angle θ. In order to determine the analytic relations for Φ_i, the geometrical configuration of Figure A-2 can be used to express the transformation of coordinates between antenna and environment-centered frames:

$$\sin\theta' \cos\phi' = \sin\theta \cos\phi \qquad \text{(A-18)}$$

$$\sin\theta' \sin\phi' = \cos\theta_o \sin\theta \sin\phi - \sin\theta_o \cos\theta \qquad \text{(A-19)}$$

$$\cos\theta' = \sin\theta_o \sin\theta \sin\phi + \cos\theta_o \cos\theta \qquad \text{(A-20)}$$

The angles ϕ' defined by fixed values of θ_o, θ, and θ' can be found from Equation (A-18) if values of ϕ are already determined; these latter must be obtained by solving Equation (A-20). The set of Equations (A-18), (A-19), and (A-20) are invariant under the transformation

$$\phi \rightarrow \pi - \phi, \quad \phi' \rightarrow \pi - \phi' \ ; \qquad \text{(A-21)}$$

hence, the two solutions in Equation (A-17) are related. By rewriting Equation (A-20) as,

$$\sin\phi = \frac{\cos\theta' - \cos\theta_o \cos\theta}{\sin\theta_o \sin\theta} \qquad \text{(A-22)}$$

one can see that it has two solutions: ϕ_2 and $\phi_1 = \pi - \phi_2$. The final result is obtained by inserting either value in Equation (A-18) in the form, for example,

$$\phi_2'(\theta_o,\theta,\theta') = \cos^{-1}\left(\frac{\sin\theta \cos\phi_2}{\sin\theta'}\right) \qquad \text{(A-23)}$$

The other branch of the solution is given by

$$\phi_1'(\theta_o,\theta,\theta') = \pi - \phi_2'(\theta_o,\theta,\theta') \qquad \text{(A-24)}$$

3. Calculations

Two computer programs have been coded to perform the antenna pattern removal.

The first program has the task of calculating the matrix elements G_{ij} from Equation (A-12). The matrix

$$M = G - 1 \qquad \text{(A-25)}$$

is output on punched cards or magnetic tape for use with the second program. In the course of calculation the condition

$$\sum_j M_{ij} = 0 \qquad \text{(A-26)}$$

is tested.

The second program, APCOR4, has the task of solving for brightness temperatures by the iterative method presented in Equation (A-8). It accepts the matrix elements, M, and performs a given number of iterations on the apparent temperture data. which are obtained at the specified angular mesh $\{\theta_i\}$ by polynomial interpolation. The mesh chosen for the present data consisted of 29 angles defined by

$$\cos\theta_n = \frac{n - 15}{14}$$

This set appeared to give adequate resolution near the horizon, while keeping computer time to a reasonable level.

The results of the iterative method applied to 20 cases are presented elsewhere in this report. For the X-band data, an averaged gain pattern was used for both polarizations. In the K_u- and W-band cases seperate antenna patterns were employed for both polarizations, and the computer performed the azimuthal averaging.

From preliminary calculations it was concluded that satisfactory antenna pattern correction may be obtained with one iteration. Therefore, all the processed data show a single application of Equation (A-8).

Figures A-3, A-4 and A-5 show actual (measured) antenna patterns for the 9.5, 16.5 and 94 GHz radiometers, respectively.

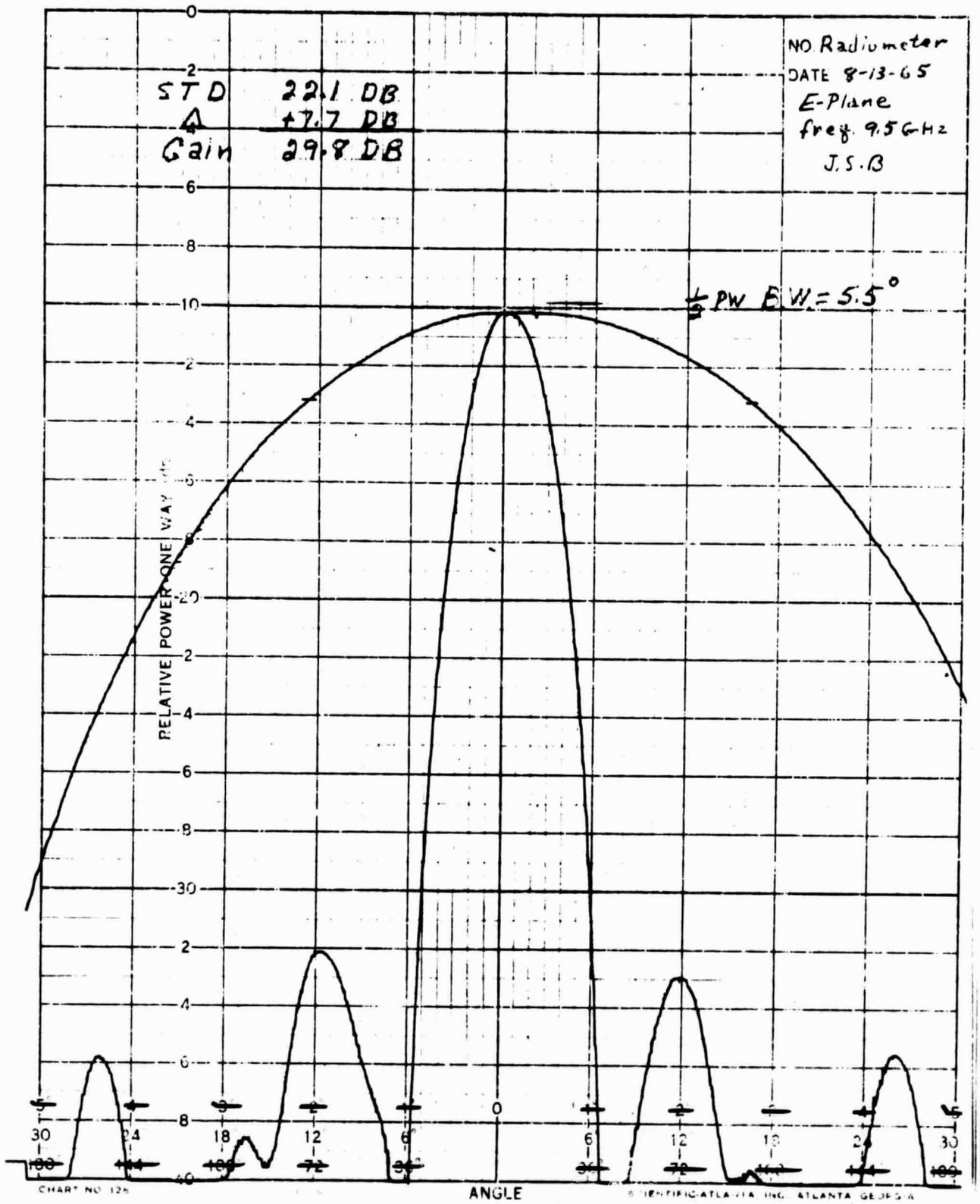


Figure A-3a - 9.5 Ghz Radiometer Antenna Pattern (enlarged). E-Plane Polarization. (See also Figures A-3b thru' A-3d).

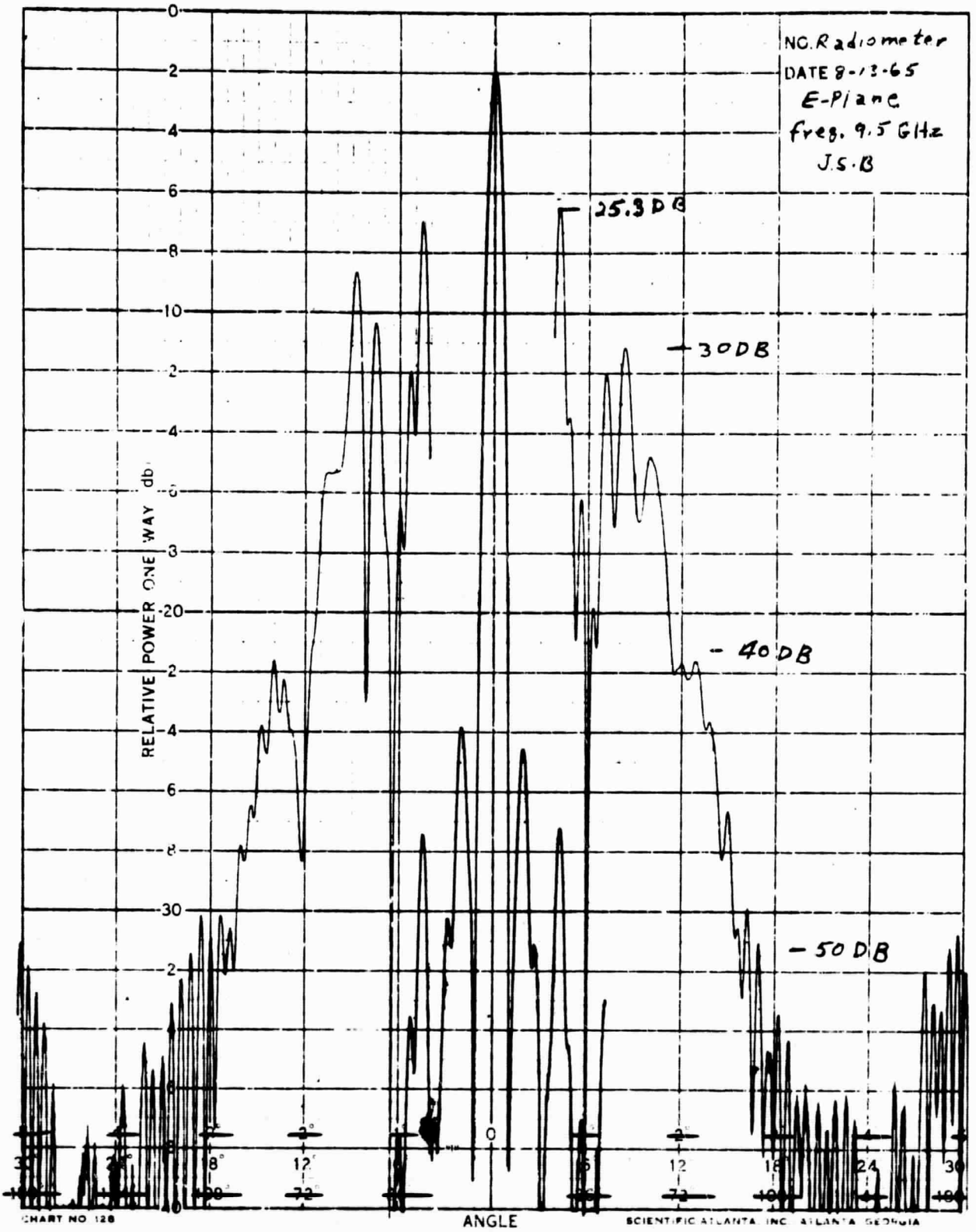


Figure A-3b - 9.5 Ghz Radiometer Antenna Pattern, E-Plane Polarization

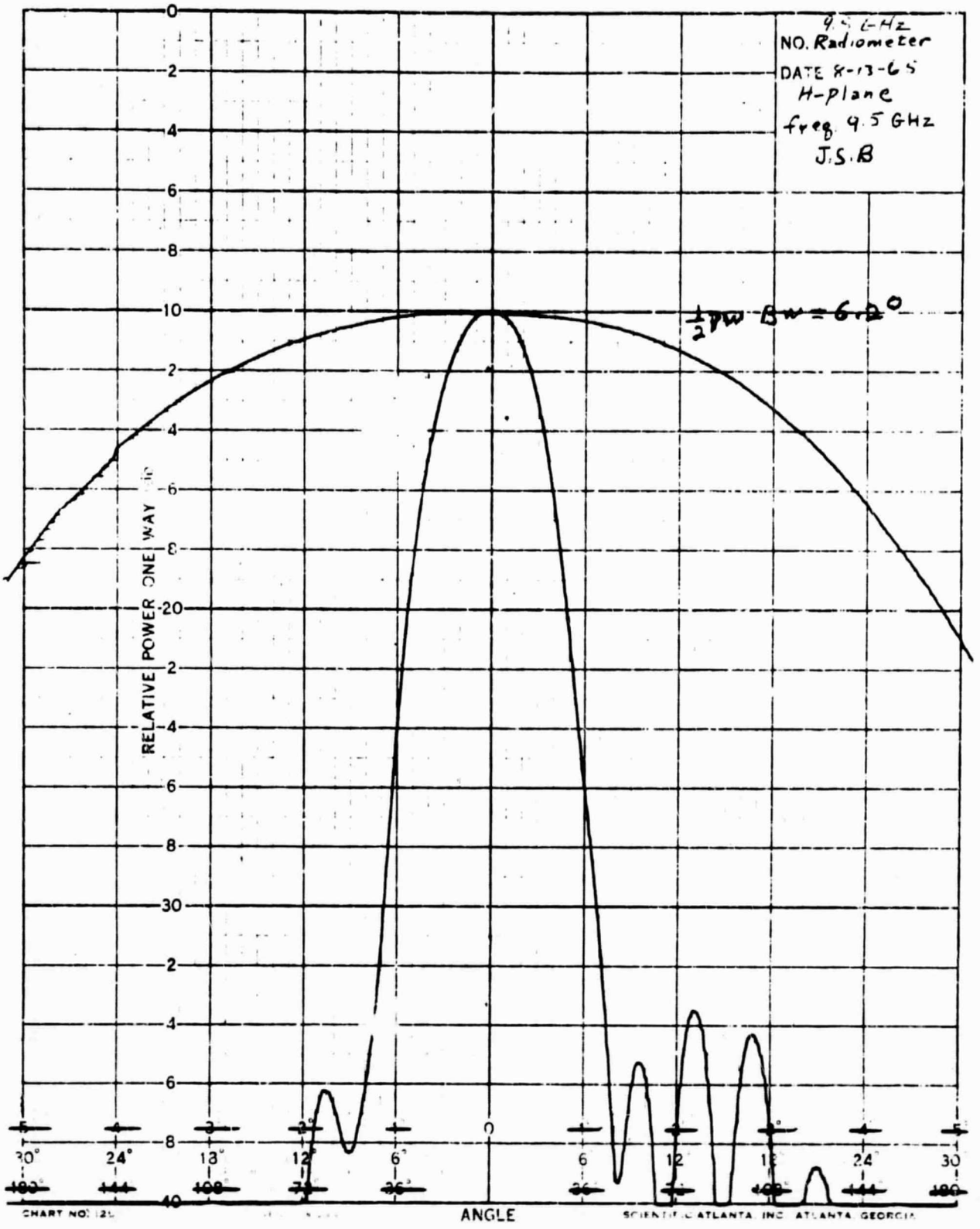


Figure A-3c - 9.5 GHz Radiometer Antenna Pattern (enlarged) H-Plane Polarization

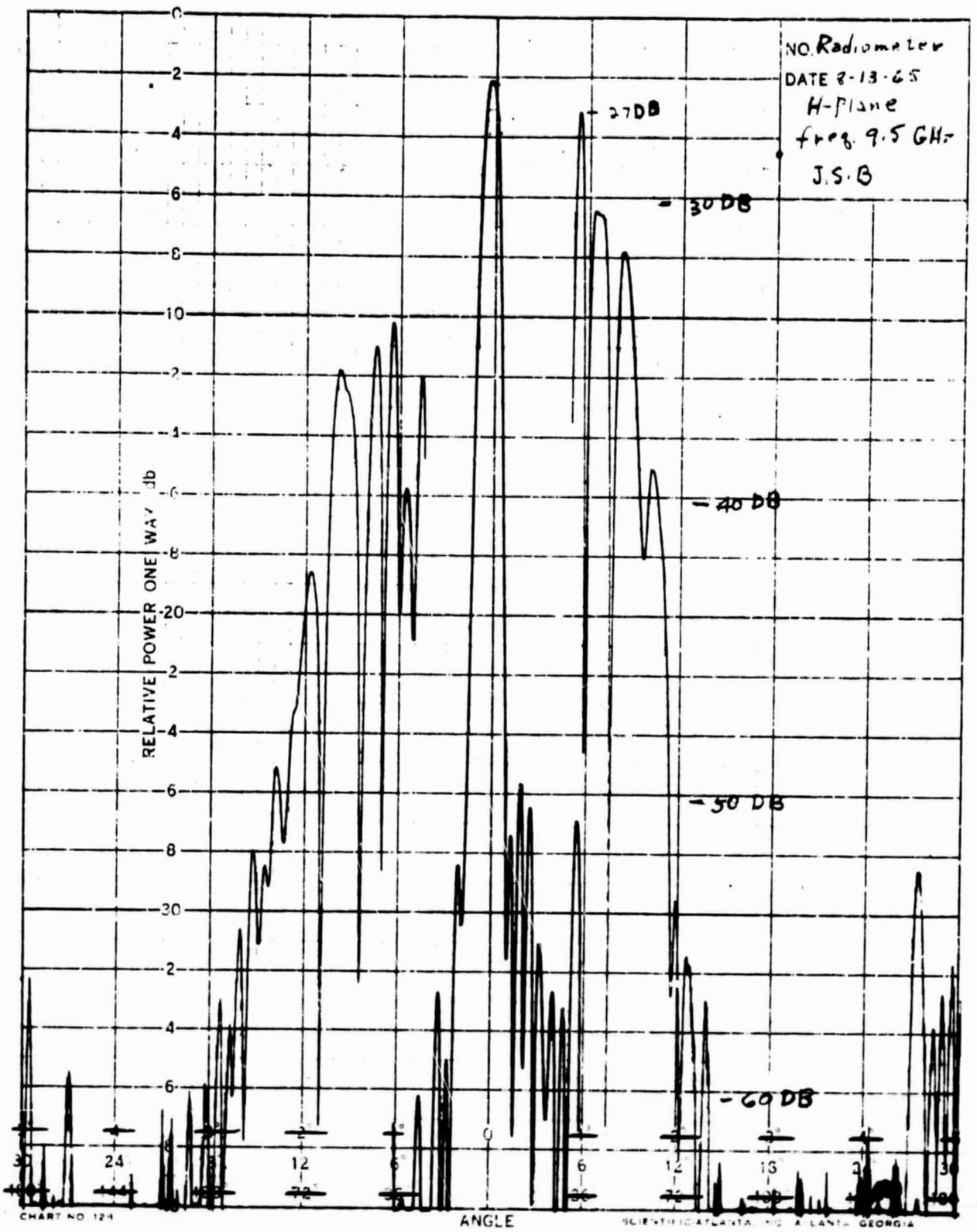


Figure A-3d - 9.5 GHz Radiometer Antenna Pattern, H-Plane Polarization

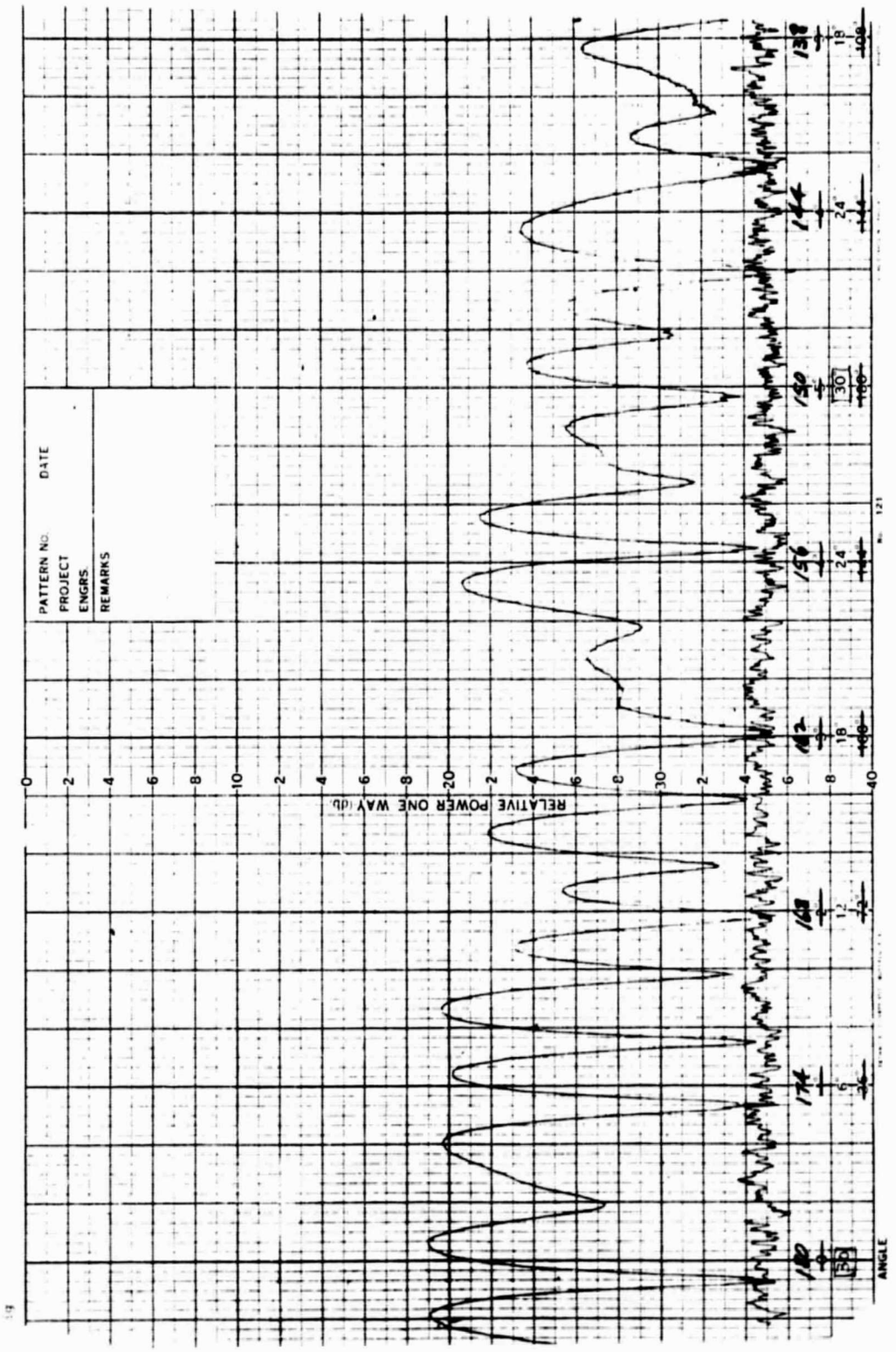


Figure A-4a - 16.5 GHz Radiometer Antenna Pattern (enlarged) E-Plane Polarization. (See also Figures A-4b thru' A-4h).

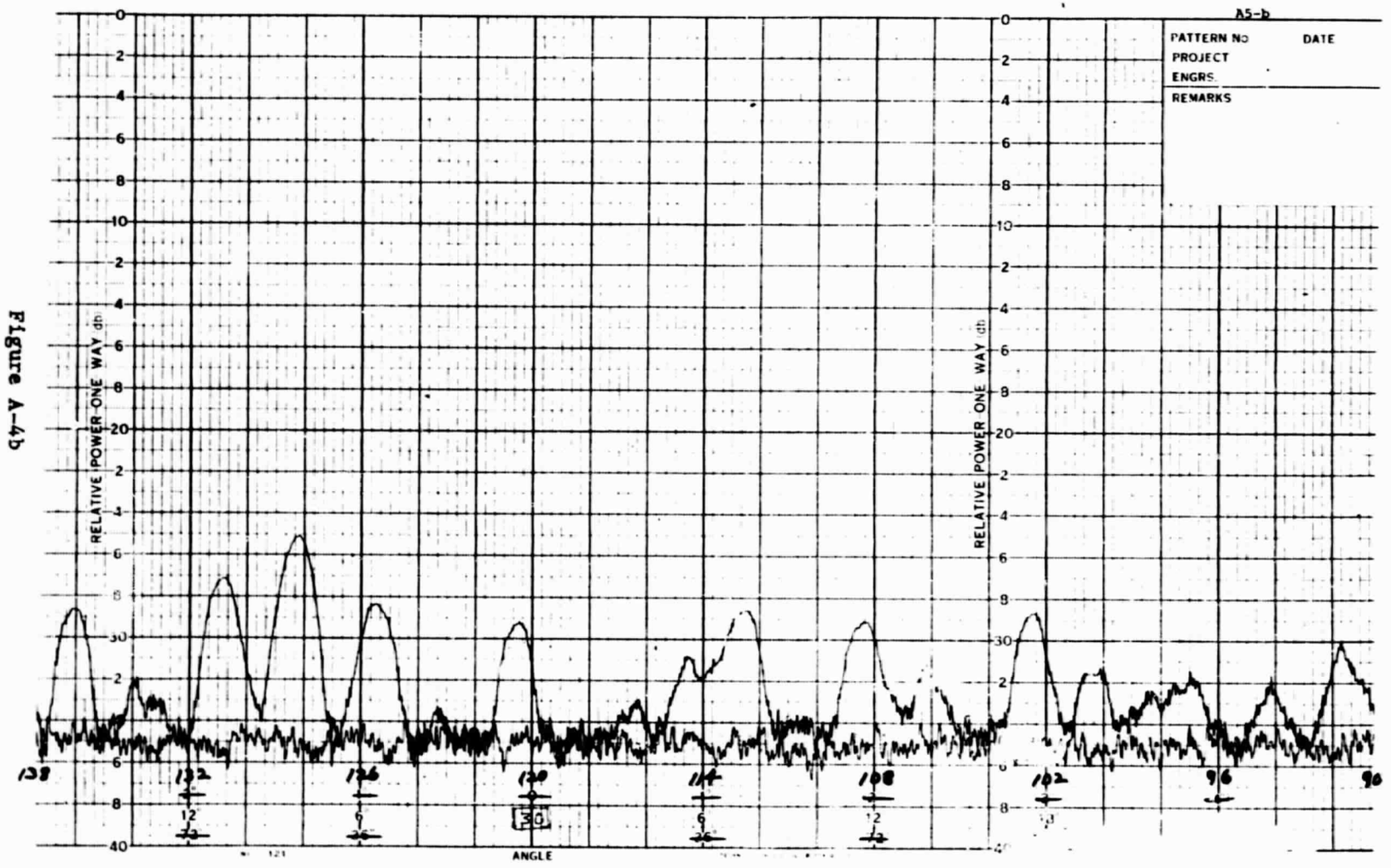

A5-b
PATTERN NO
DATE
PROJECT
ENGRS
REMARKS
RELATIVE POWER ONE WAY db
RELATIVE POWER ONE WAY db
ANGLE
138
132
126
120
114
108
102
96
90
30

Figure A-4b

Figure A-4c

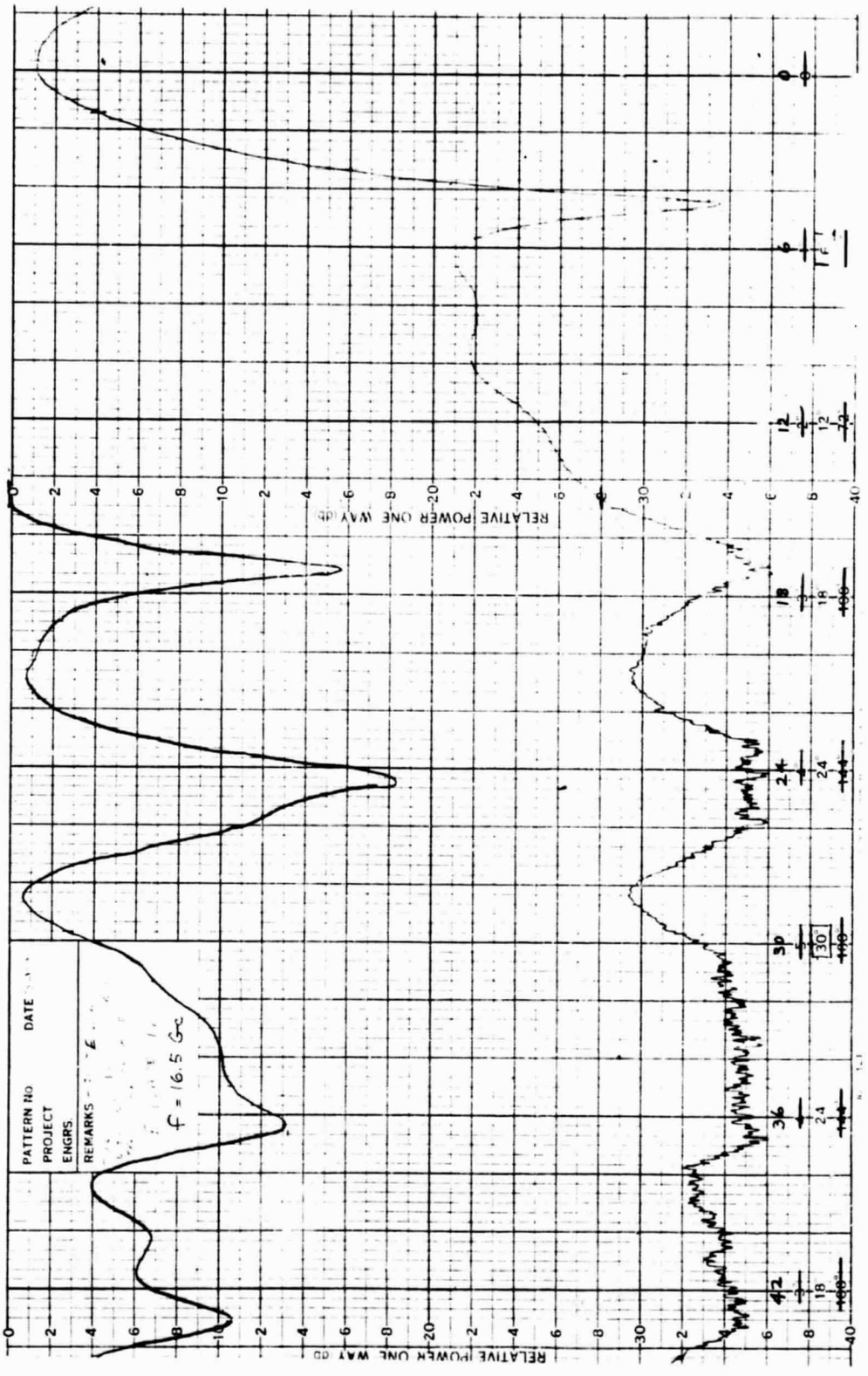

PATTERN NO
DATE
PROJECT
ENGRS
REMARKS
f = 16.5 Gc
RELATIVE POWER ONE WAY dB
RELATIVE POWER ONE WAY dB

Figure A-4d

RELATIVE POWER ONE WAY (db)
RELATIVE POWER ONE WAY (db)
PATTERN NO.
PROJECT
ENGRS
REMARKS
DATE

Figure A-4e

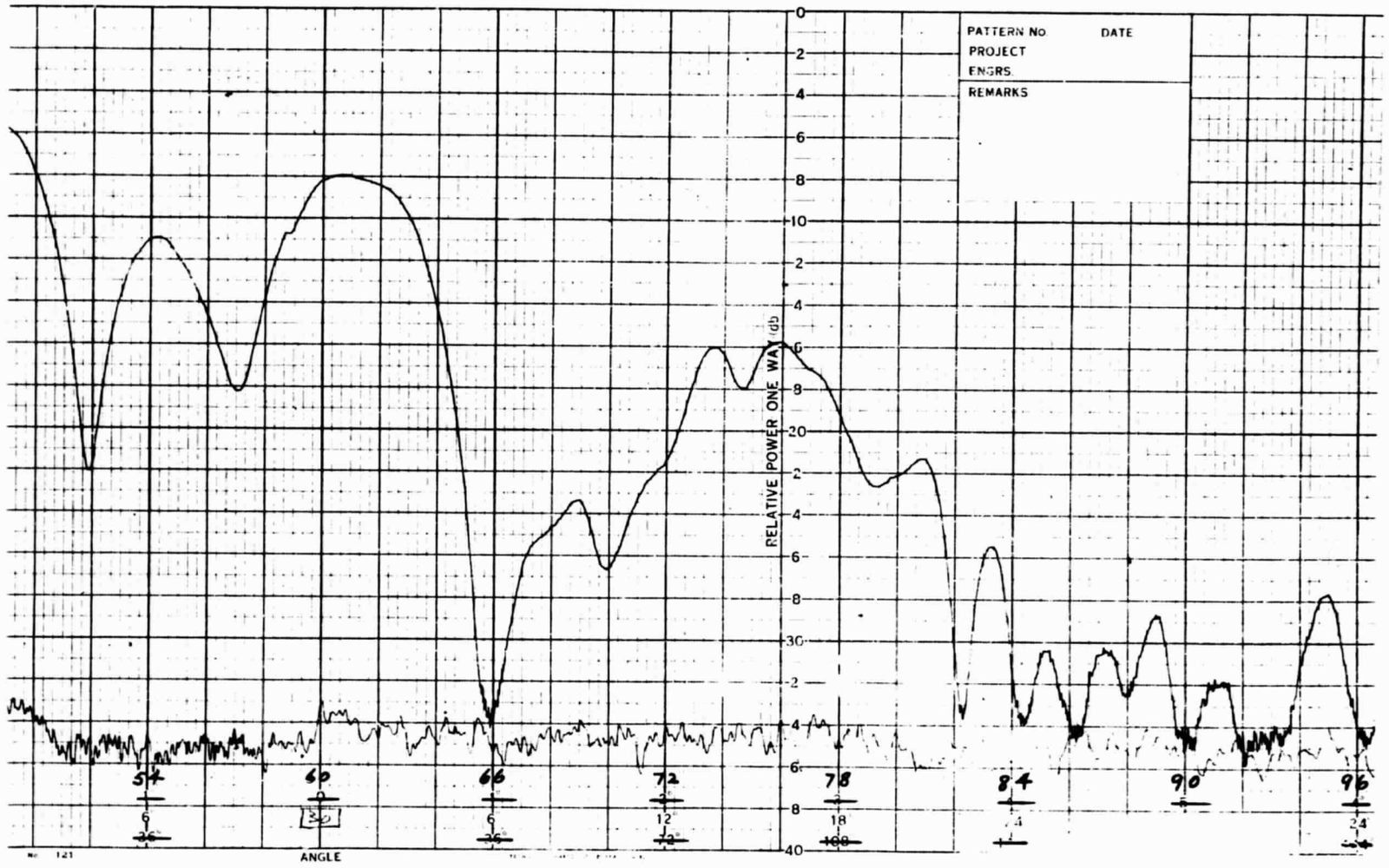

PATTERN NO.
DATE
PROJECT
ENGRS.
REMARKS
RELATIVE POWER ONE WAY (dB)
0
2
4
6
8
10
2
4
6
8
20
2
4
6
8
30
2
4
6
8
40
54
60
66
72
78
84
90
96
6
6
12
18
24
ANGLE

Figure A-4f

PATTERN
PROJECT
ENGRS
REMARKS
RELATIVE POWER ONE WAY (db)
RELATIVE POWER ONE WAY (db)
ANGLE

Figure A-4g

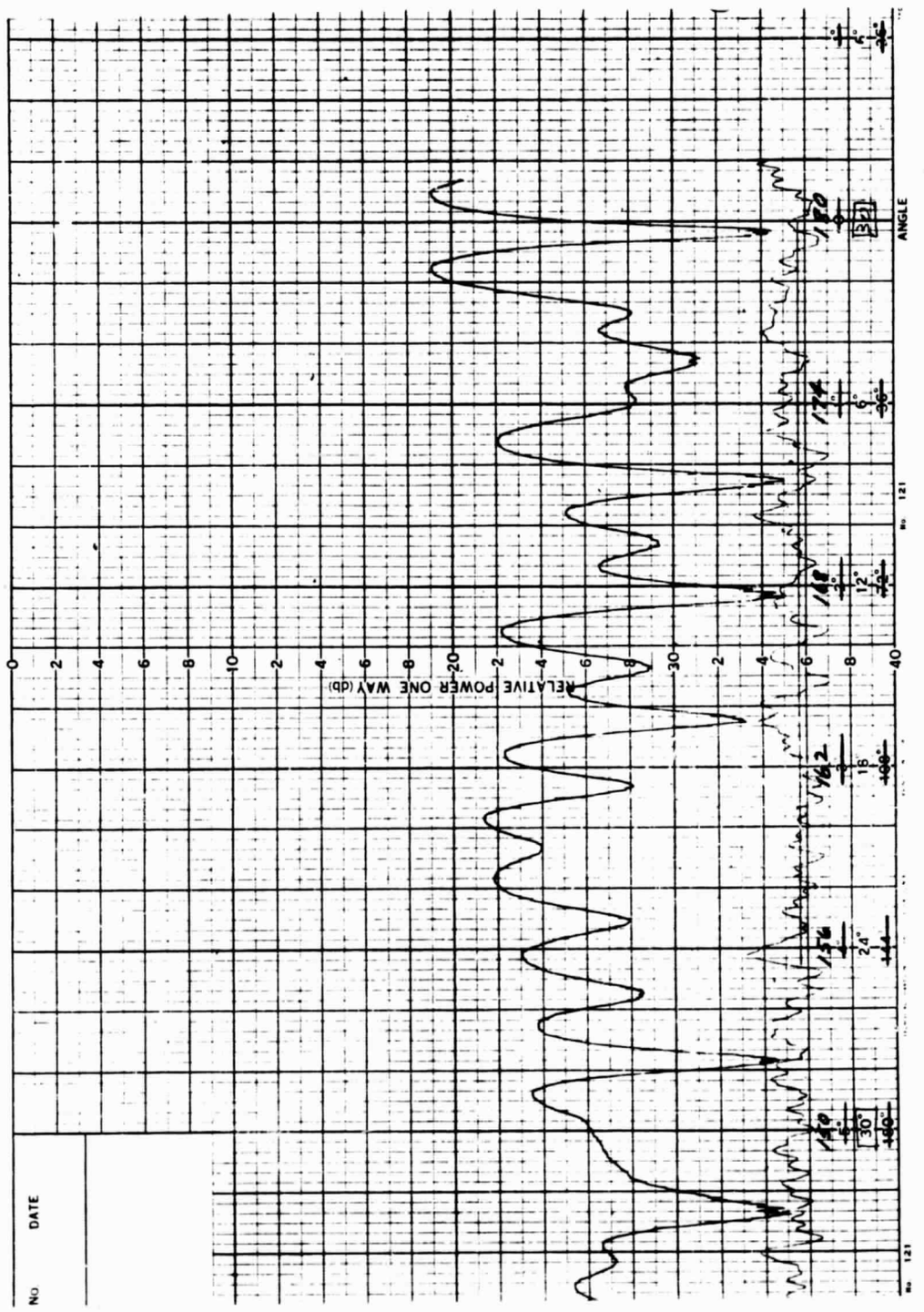


Figure A-4h

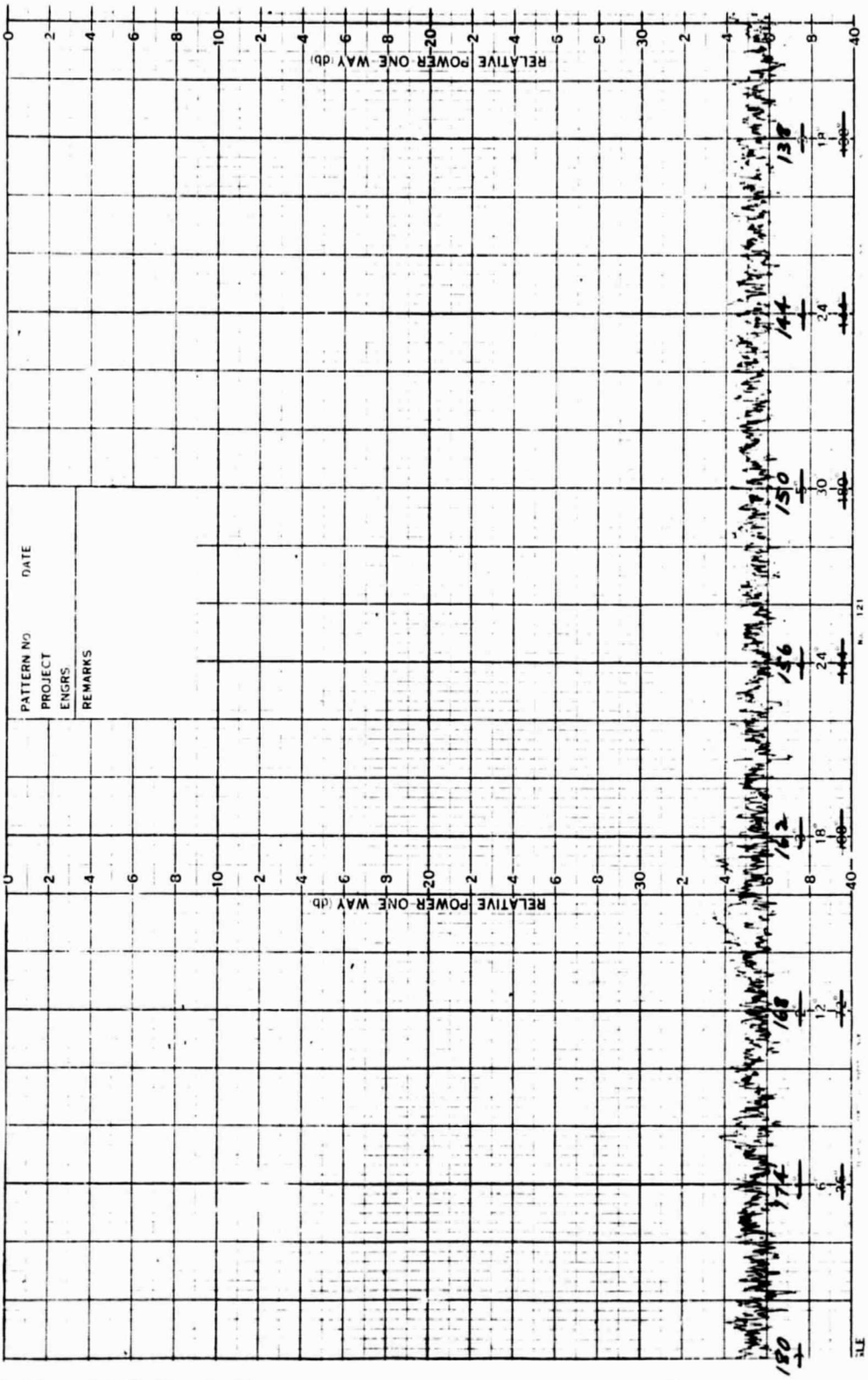


Figure A-4i - 16.5 GHz Radiometer Antenna Pattern (enlarged) H-Plane Polarization. (See also Figures A-4j thru' A-4p).

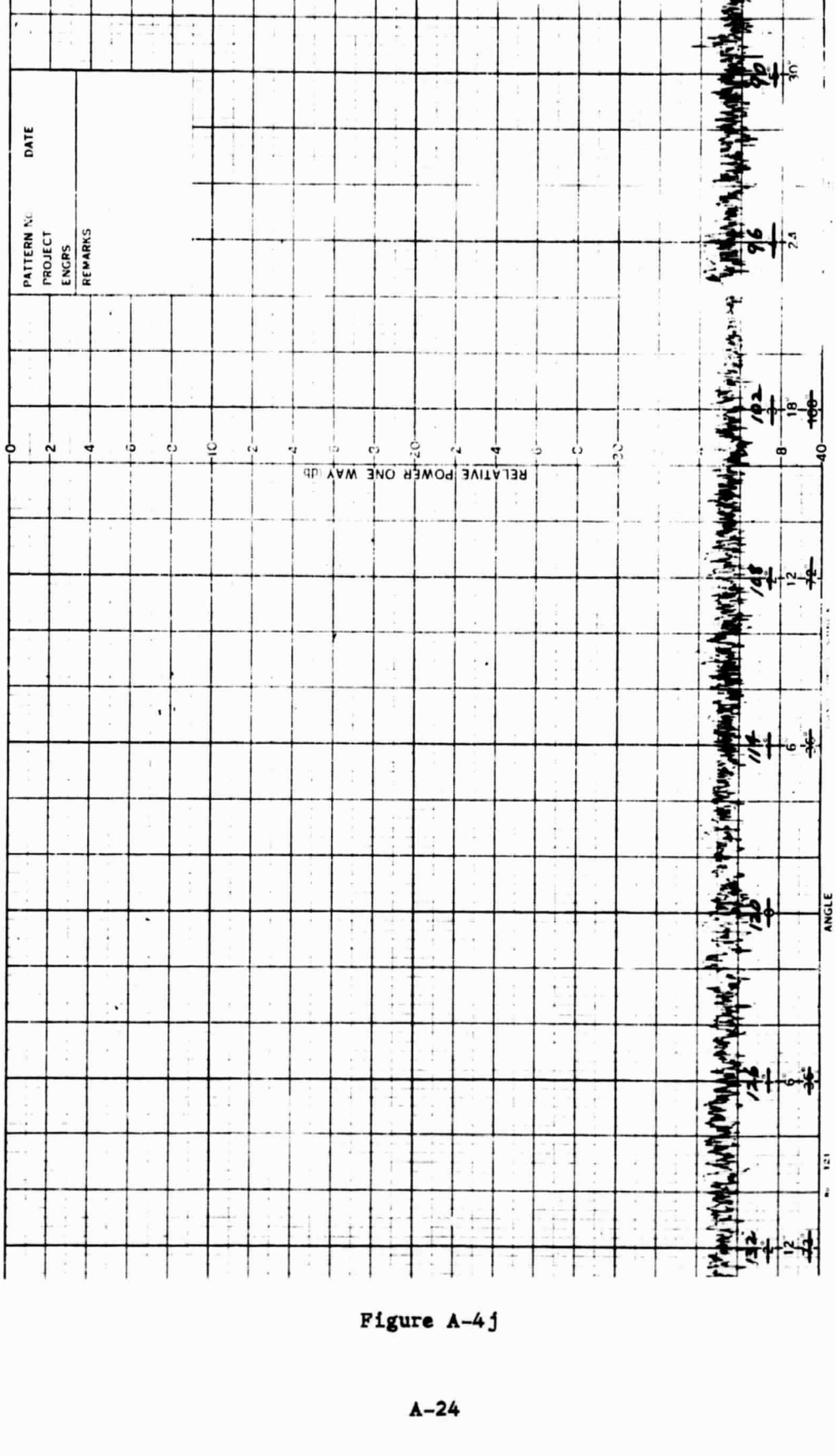

PATTERN NO.
DATE
PROJECT
ENGRS
REMARKS
RELATIVE POWER ONE WAY dB
ANGLE

Figure A-4j

Figure A-4k

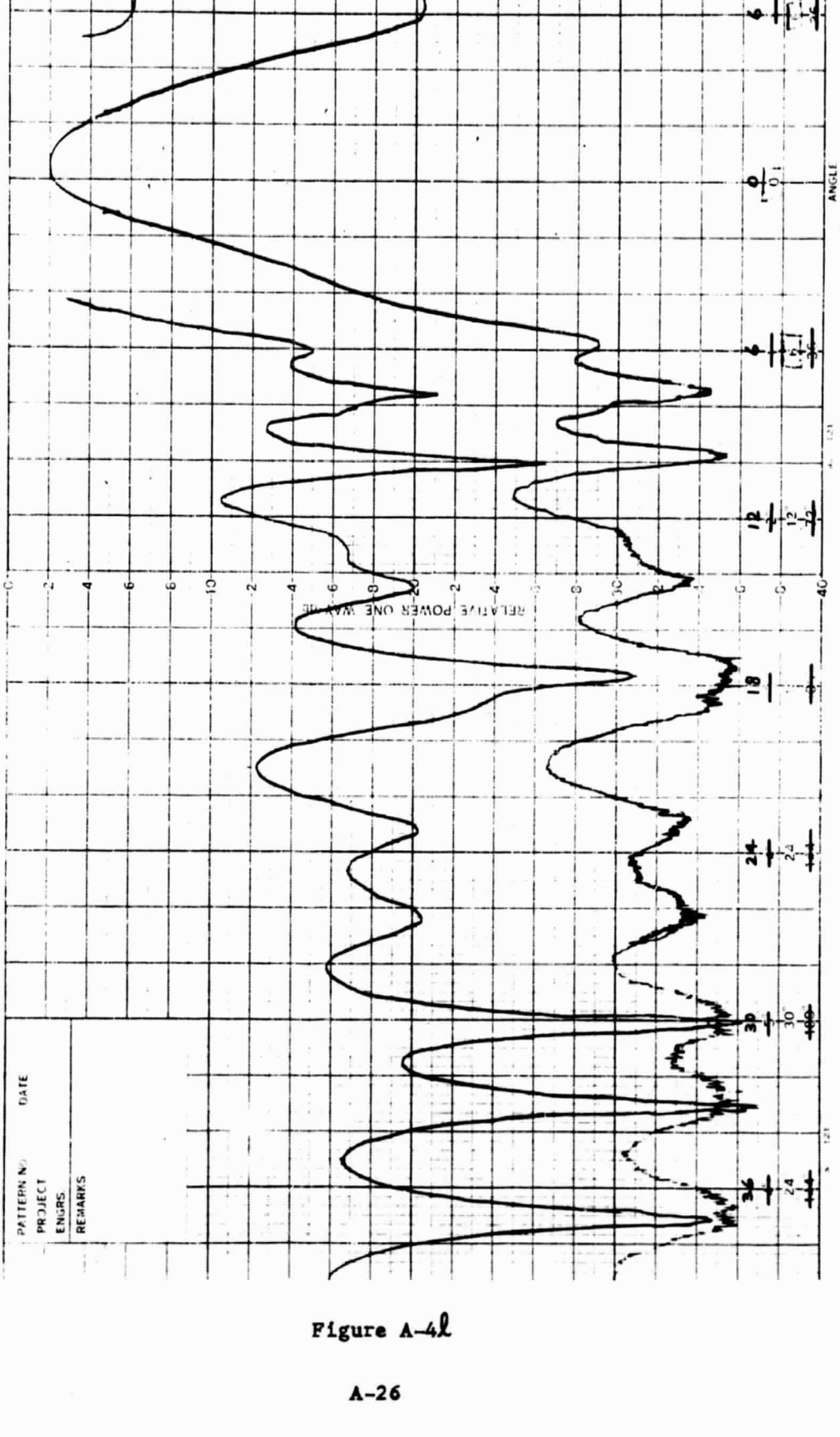

PATTERN NO.
DATE
PROJECT
ENGRS
REMARKS
RELATIVE POWER ONE WAY DB
ANGLE

Figure A-4ℓ

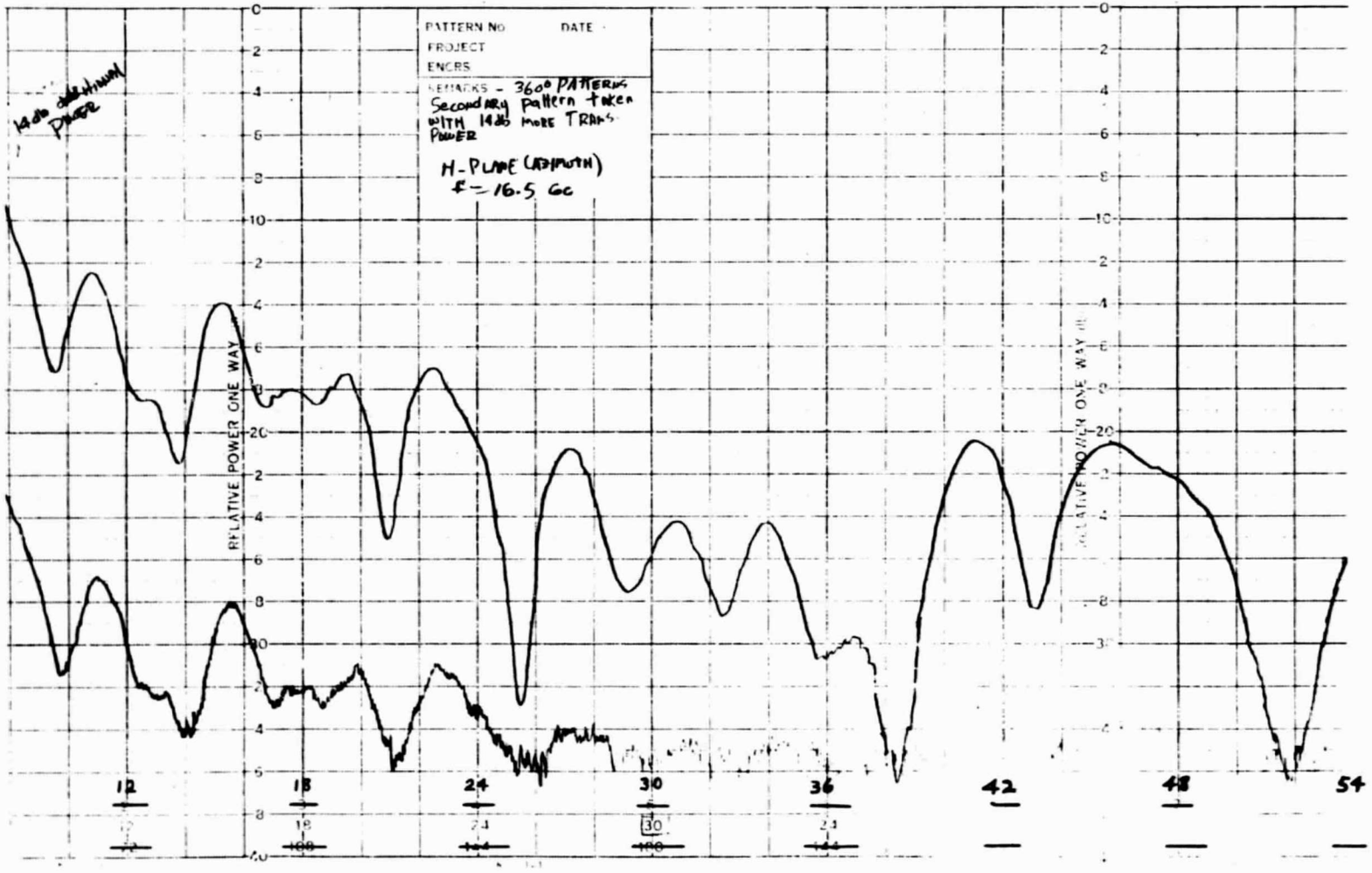

PATTERN NO DATE
PROJECT
ENGRS
REMARKS - 360° PATTERN
Secondary pattern taken
WITH 14db more TRANS
POWER
H-PLANE (AZIMUTH)
f = 16.5 Gc
14db additional Power
RELATIVE POWER ONE WAY
RELATIVE POWER ONE WAY
0
2
4
6
8
10
20
30
12
18
24
30
36
42
48
54

Figure A-4m

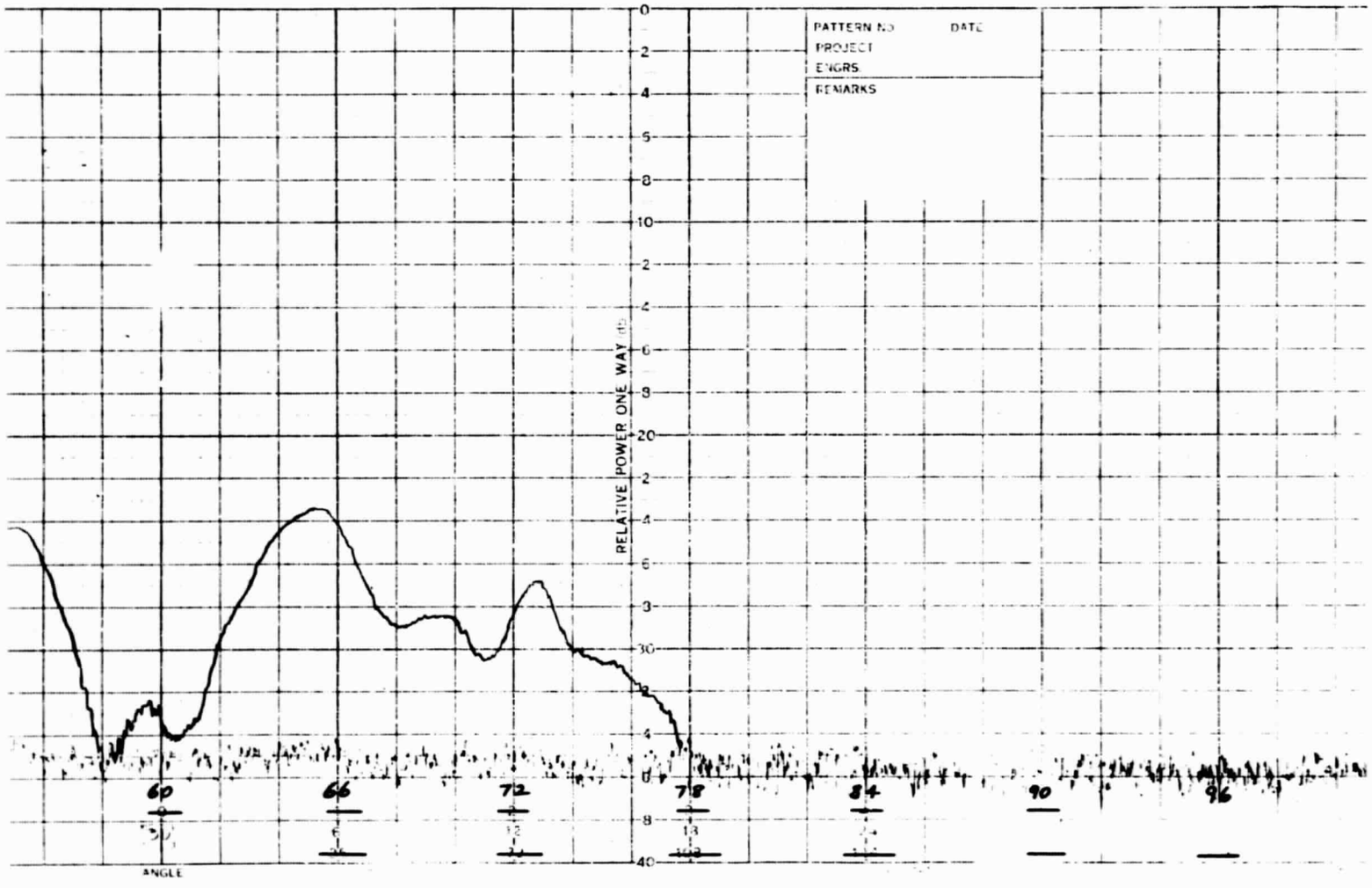

PATTERN NO.
DATE
PROJECT
ENGRS.
REMARKS
RELATIVE POWER ONE WAY (dB)
0
2
4
5
8
10
2
4
6
8
20
2
4
6
3
30
4
0
8
40
60
66
72
78
84
90
96
ANGLE

Figure A-4n

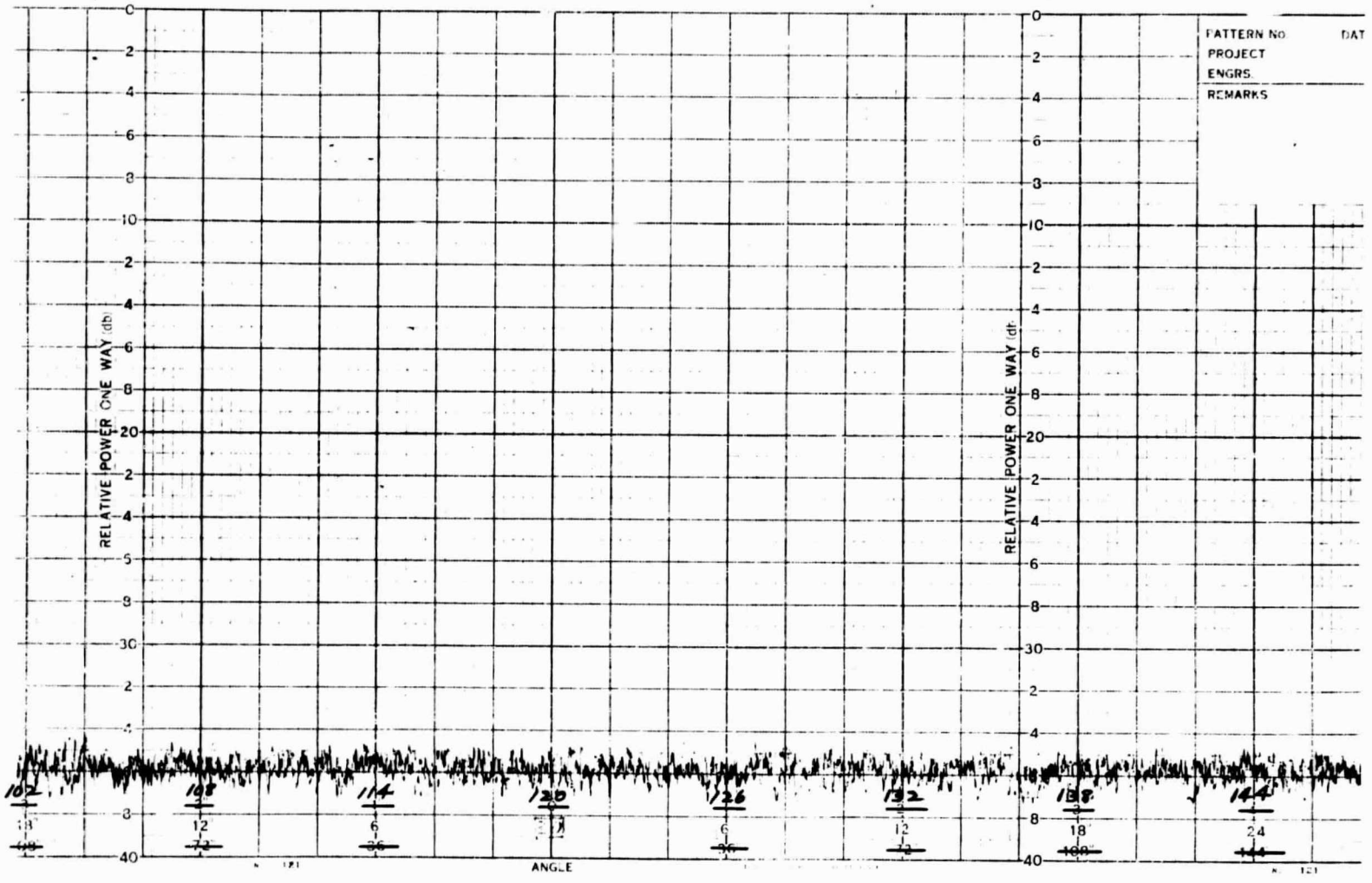

PATTERN No
DAT
PROJECT
ENGRS.
REMARKS
RELATIVE POWER ONE WAY (db)
RELATIVE POWER ONE WAY (db)
ANGLE
102
108
114
120
126
132
138
144

Figure A-40

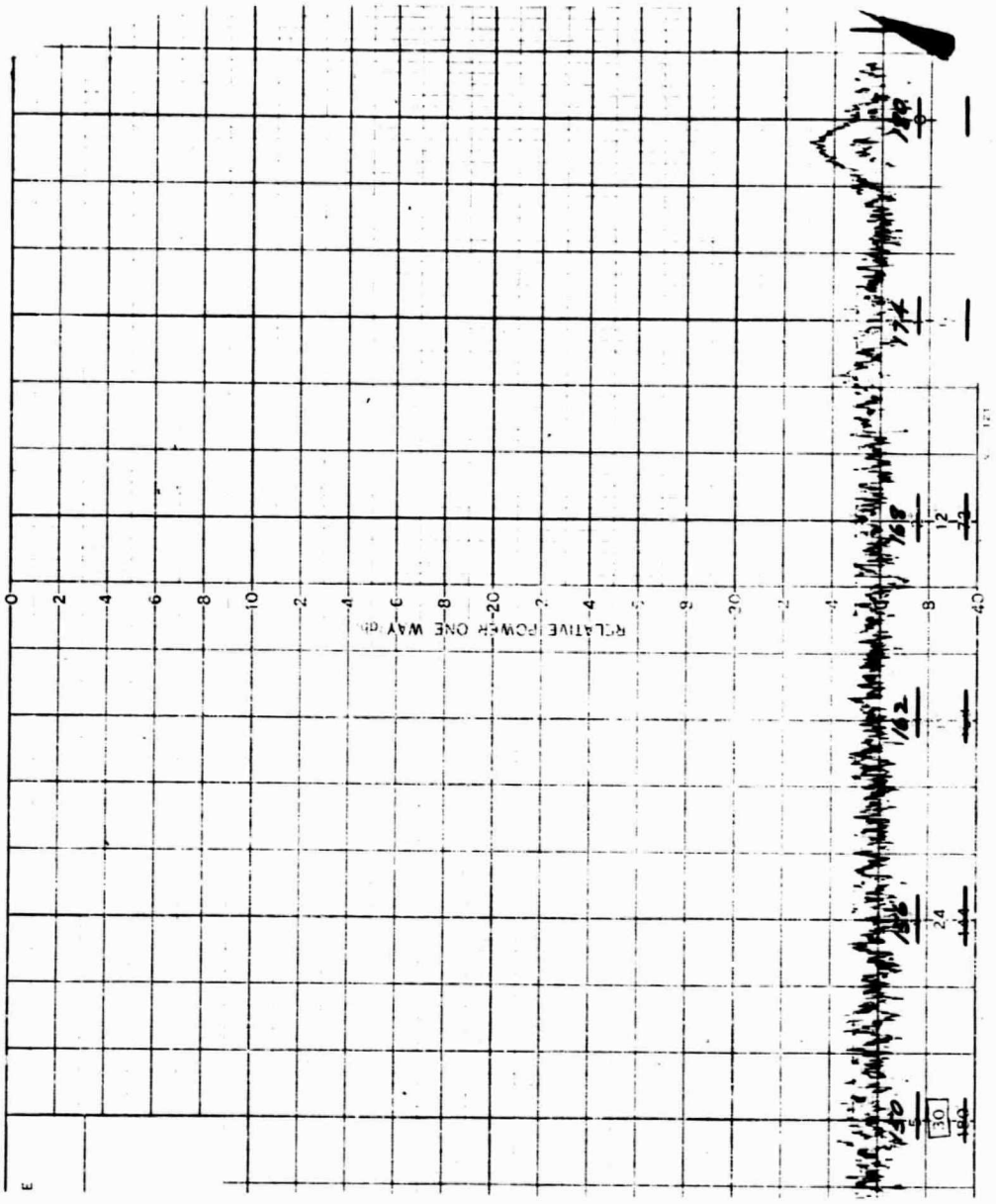


Figure A-4p

REPRODUCIBILITY OF THE ORIGINAL PAGE IS POOR.

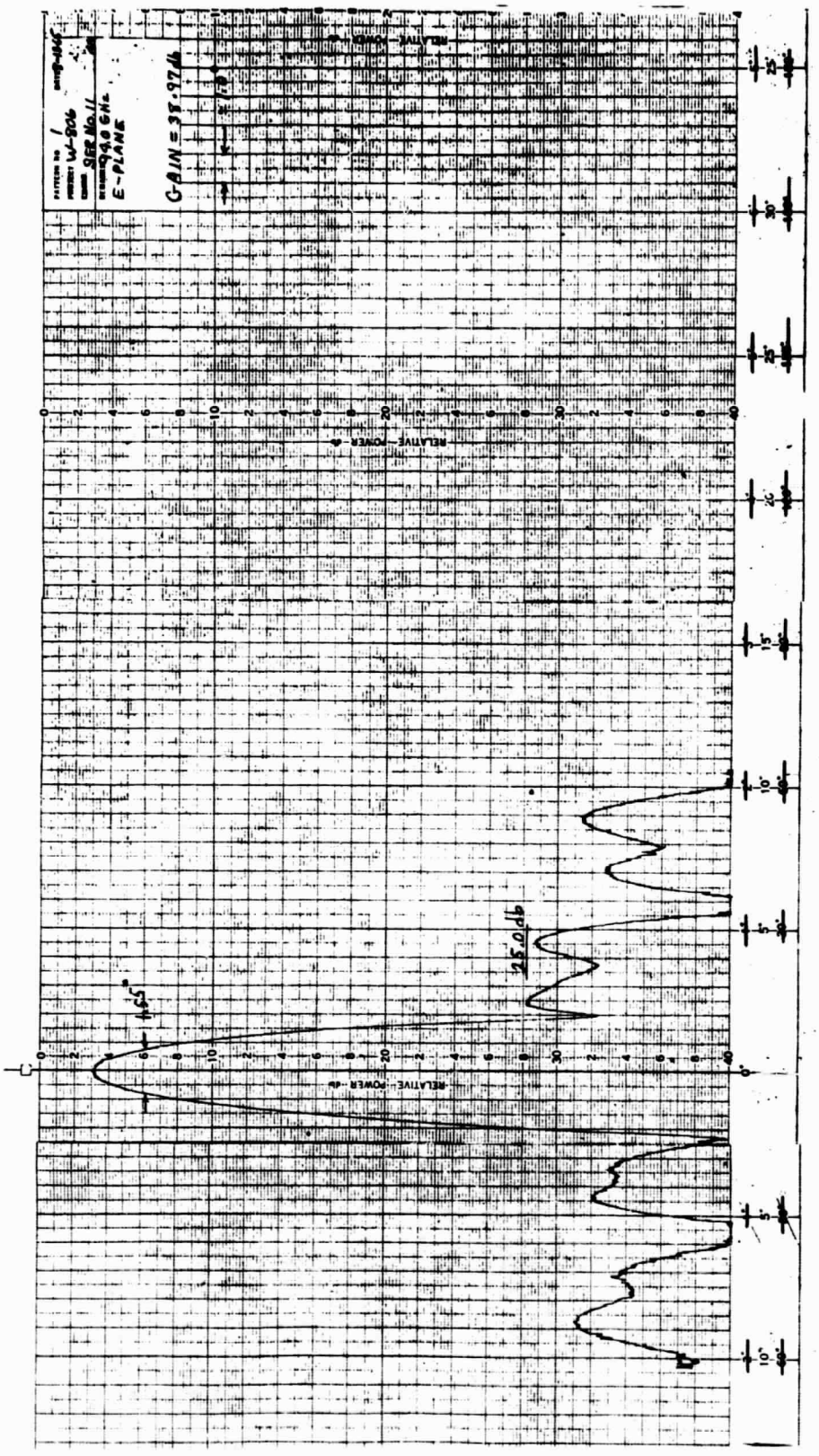


Figure A-5a - 94 GHz Radiometer Antenna Pattern (enlarged) E-Plane Polarization. (See also Figures A-5b thru' A-5d).

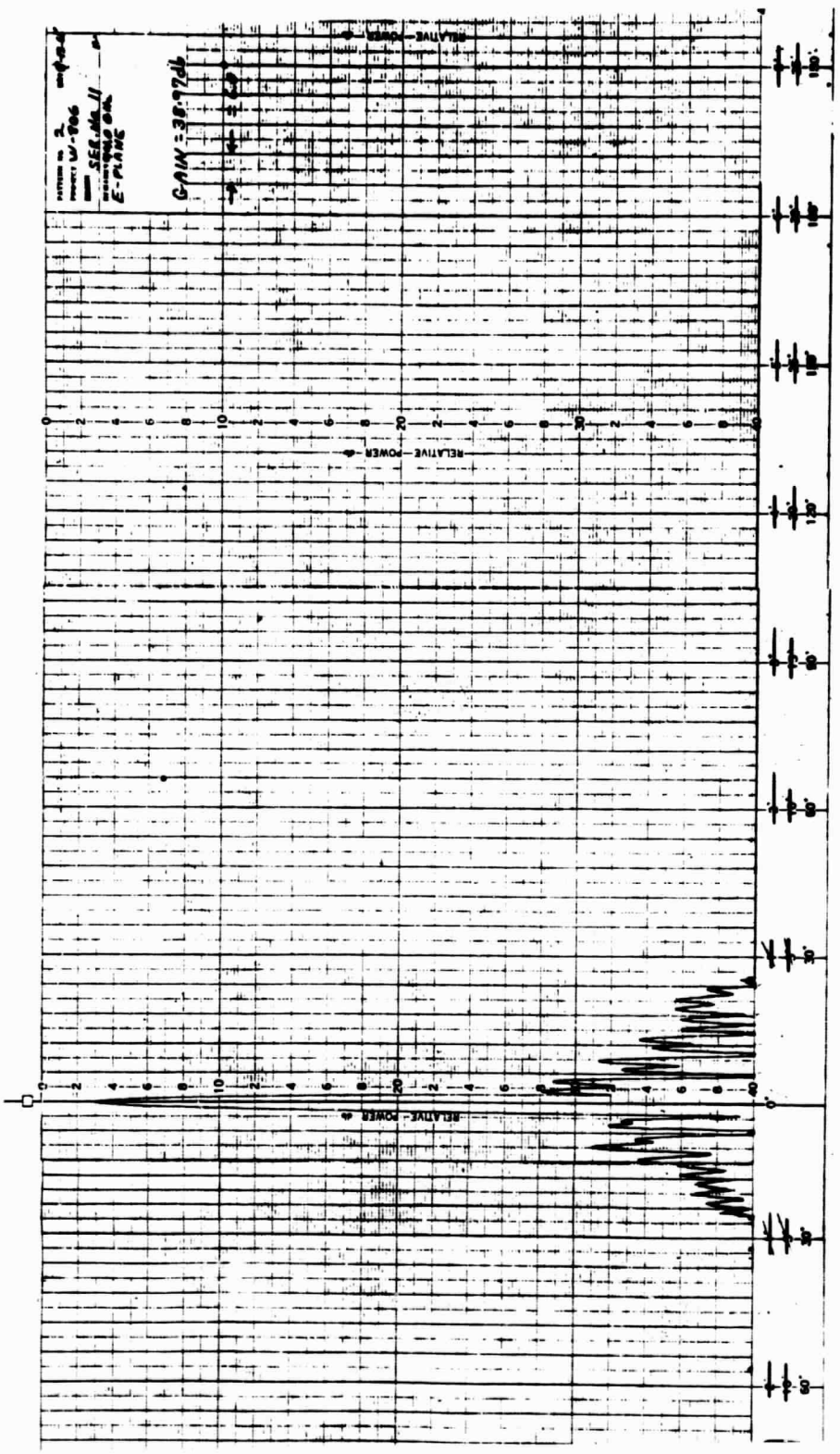


Figure A-5b - 94 GHz Radiometer Antenna Pattern, E-Plane Polarization

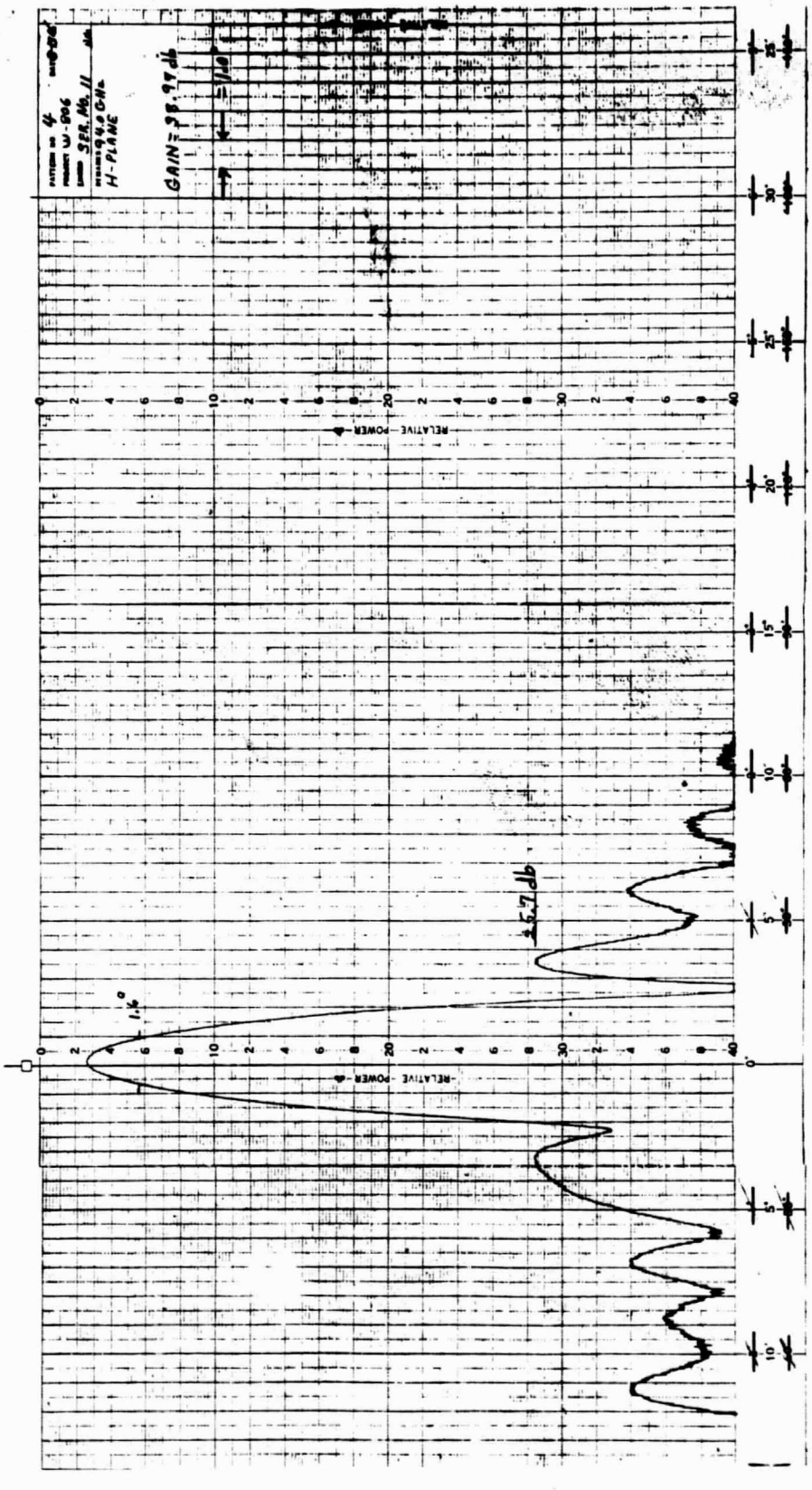


Figure A-5c - 94 GHz Radiometer Antenna Pattern (enlarged) H-Plane Polarization

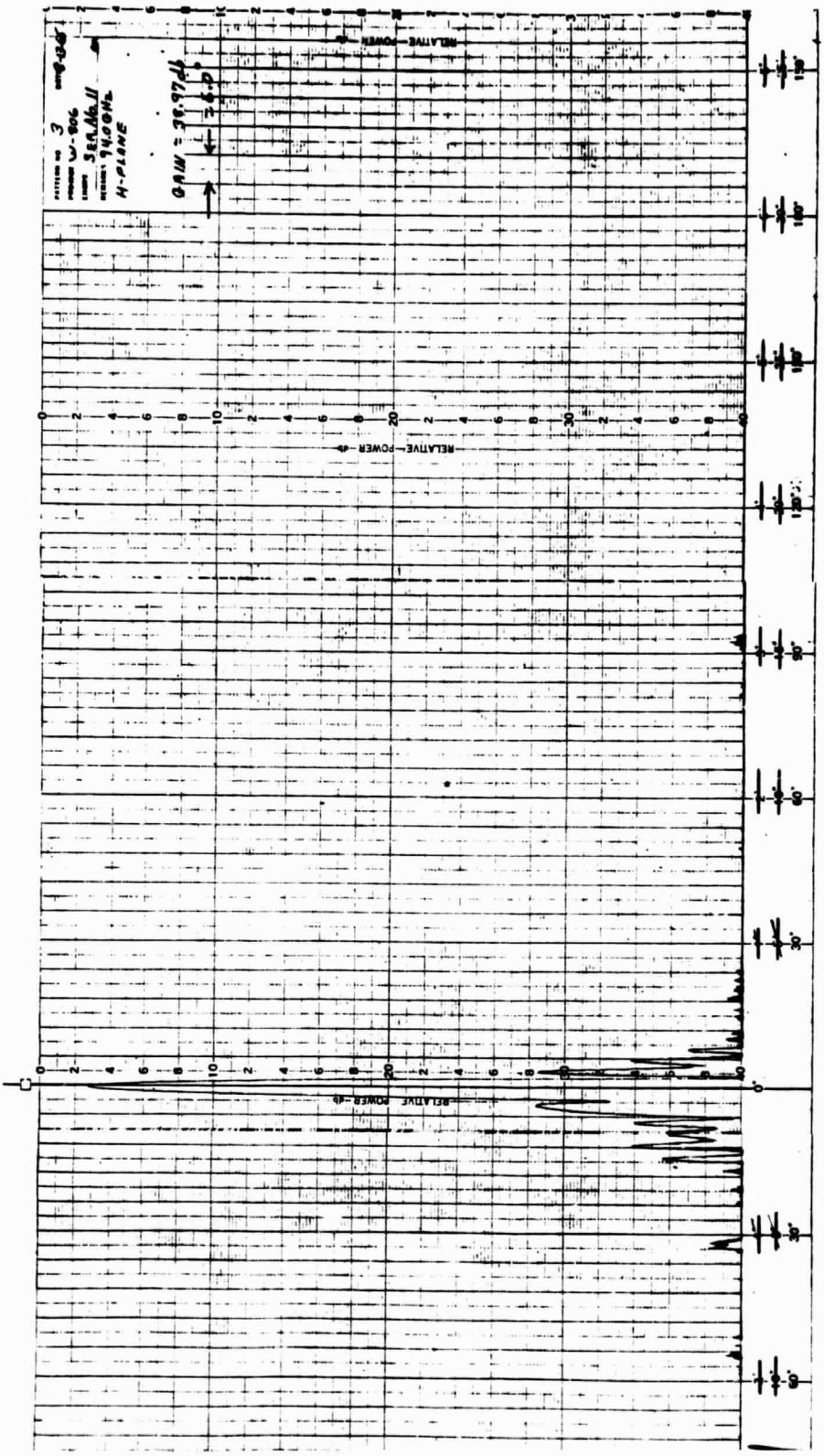


Figure A-5d - 94 GHz Radiometer Antenna Pattern, H-Plane Polarization

APPENDIX B

COMPUTER PROGRAMS FOR ANTENNA PATTERN CORRECTION

Two computer programs have been coded to perform the task of antenna pattern correction. Here we will briefly describe the operation of these program They have been integrated in such a way that appropriate changesin subroutine may be made to facilitate universality.

1. ANTPTI

The first program, termed ANTPTI, has the task of calculating the matrix elements of Mij. The method of calculation has been described above; here we mention only one important point. The quadrature used in Equation (A-16) in Appendix A,

$$P(\bar{\theta},\theta_o) = \int_o^{\pi} \frac{\Delta\phi\ (\theta_o,\bar{\theta},\theta^1)}{2\pi}\ dP\ (\theta^1,0) \qquad \text{(B-1)}$$

involves singularities of the integrand at $\theta^1 = |\theta \pm \theta_o|$. Although the singularities are integrable, they pose a difficulty for numerical quadrature.

It was determined that the use of Simpson's rule in Equation (B-1) could minimize the quadrature error. Thus the set of angles $\{\theta^1_k\}$ used in the numerical quadrature is chosen to permit the application of Simpson's rule. The program has been written to calculate the set $\{\theta^1_k\}$, so that an even number of equally spaced

intervals are generated between angles $\{\theta_i\}$. But while one can utilize equally spaced intervals of θ_1 in Equation (B-1), it would appear that equal spacing in P would give better accuracy. Hence, the option of correcting the midpoints θ_{2k} for the non-linearity of $P(\theta_1, 0)$ has been incorporated into the ANTPTI program. If the variable INDX is set equal to zero, no correction is made; if INDX = 1, then the midpoint correction is made.

Program ANTPTI requires three subroutines which may be adapted to the nature of the antenna pattern data. The subroutine READAP is employed to read in the pattern data. The function subroutine ANTPOW is used to calculated the gain $g(\theta_1)$ as a function of the argument $\{\theta_1\}$. Either pattern models or interpolation may be employed in coding ANTPOW. The subroutine DEMESH has the task of calculating the set of angles θ_i for which matrix elements are desired. The total number of angles, including $\theta = 0°, 180°$, is the first argument of DEMESH. This number is given by (2 * MESH + 1). The second argument is the set of variable angles ZANT, whose dimensions are defined in the main program.

Table B-1 documents the input to ANTPTI. A subroutine CORMAT is needed for output of the matrix Mij. Either punched cards or magnetic tape may be used for the output. CORMAT will test for satisfaction of sum condition Equation (A-26) if IREFIN = 1.

2. APCOR 4

The task of this program is to calculate brightness temperatures from apparent temperatures. Three subroutines are needed: RDMAT

reads in the matrix elements calculated by ANTPTI and stores them in the labeled common block BMAT. Subroutine DFMESH has been treated alone.

Subroutine APTEMP generates apparent temperatures at the angles $\{\theta_i\}$. The present version of APTEMP uses polynomial interpolation on tabular values of T_B.

Basic parameters are input to APCOR 4 through Namelist ANTPRM. MESH has the same significance as in ANTPTI; FREQ is frequency in GHz. KASES is the number of cases to be treated with one antenna pattern. Setting MESH = 0 causes the program to stop.

Each case treated must have a title card followed by the necessary input for subroutine APTEMP. When a batch of cases has been completed, the main program reads in a new set of parameters through ANTPRM.

One must specify the total number of iterations desired. Zero iterations is considered to mean one correction. The variable ITER gives the maximum number of iterations; it is read in by Namelist ANTPRM.

Program APCOR 4 calculates the mean absolute correction:

$$\Delta T_m^{(k)} = \sum_{i=1}^{m} \left| T_B^{(k+1)}(\theta_i) - T_B^{(k)}(\theta_i) \right| / m$$

This value is printed as well as the individual corrections at each angle.

TABLE B-1

INPUT FOR PROGRAM ANTPTI

Variable (Dimension)	Description
Namelist ANTPRM	
MESH	Number of zenith angles in interval $0 \leq \theta < 90^{\circ}$.
INORM	Indicator for printout of normalized gain pattern; INORM = 0 means skip printout
INDX	Indicator for midpoint correction; INDX = 0 means no correction, INDX = 1 means correction
IPATT	Indicator for printout of pattern; IPATT = 0 means skip printout
IREFIN	Indicator for matrix elements; IREFIN = 0 gives only results on punched cards, IREFIN = 1 means sum condition is checked and elements are printed, IREFIN > 1 means calculation is repeated with new mesh

TABLE B-1 (cont.)

MZEN ( )	Number of sub-divisions in quadrature subinterval

TITLE CARD

NAME	Title, 60 characters long
FREQ	Frequency (GHz) in FORMAT F 5.3

CALCULATION OF EMISSIVITY FOR SPECULARLY REFLECTING MATERIALS

The emissivity of a specular surface is derived from the refectivity by Kirchoff's law.

$$e = 1 - \rho \tag{C-1}$$

The reflectivity for horizontally polarized waves, is given by the Fresnel formula,

$$\rho_h = \left| \frac{\cos \varphi - \bar{e}^{1/2} \cos \psi}{\cos \varphi + \bar{e}^{1/2} \cos \psi} \right|^2 \tag{C-2}$$

where,

φ = incidence angle

ψ = angle of transmitted beam with respect to normal.

$\bar{e} = e' - je''$ = complex dielectric permittivity

For vertical polarization a similar expression obtains,

$$\rho_v = \left| \frac{\bar{e} \cos \varphi - \bar{e}^{1/2} \cos \psi}{\bar{e} \cos \varphi + \bar{e}^{1/2} \cos \psi} \right|^2 \tag{C-3}$$

In order to reduce Equations (C-2) and (C-3) to real form, Snells law is employed.

$$\bar{e}^{1/2} \sin \psi = \sin \varphi \qquad \text{(C-4)}$$

The polar form for the complex number is then introduced:

$$\bar{e} \cos^2 \psi = \bar{e} - \sin^2 \varphi = r\, e^{-j\zeta} \qquad \text{(C-5)}$$

The polar quantities can be calculated explicitly as follows:

$$r = \left[e' - \sin^2 \varphi)^2 + (e'')^2\right]^{1/2} \qquad \text{(C-6)}$$

$$\zeta = \tan^{-1} \left[e'' / (e' - \sin^2 \varphi)\right] \qquad \text{(C-7)}$$

Using the definition in Equation (C-5), the absolute values in Equations (C-2) and C-3) can be evaluated. Substituting these results in Equation (C-1), yields after some manipulation,

$$\epsilon_h = \frac{4 \cos \varphi\, r^{1/2} \cos (\zeta/2)}{\left[\cos \varphi + r^{1/2} \cos (\zeta/2)\right]^2 + r \sin^2 \zeta/2} \qquad \text{(C-8)}$$

$$\epsilon_v = \frac{4 \cos \varphi\, r^{1/2} \left[\cos (\zeta/2)\, e' + \sin (\zeta/2)\, e''\right]}{\left[e' \cos \varphi + r^{1/2} \cos (\zeta/2)\right]^2 + \left[e'' \cos \varphi + r^{1/2} \sin (\zeta/2)\right]^2} \qquad \text{(C-9)}$$

Some simplication of Equations (C-8) and (C-9) is possible by introduction of two auxiliary parameters:

$$a = r^{1/2} \cos (\zeta/2) \qquad \text{(C-10)}$$

$$b = r^{1/2} \sin (\zeta/2) \qquad \text{(C-11)}$$

For the case of normal incidence, ($\varphi = 0$), these parameters are readily identified. From Equation (C-5),

$$\bar{e} = r \exp(-j\zeta)$$

so that ζ is the so-called dielectric loss angle. Hence, a is the refractive index and b is often called the "absorption" coefficient. For non-normal incidence, a and b differ slightly from these values.

Substituting equations (C-10) and (C-11) in Equations (C-8) and (C-9) yields:

$$e_h = \frac{4\, a \cos\varphi}{(\cos\varphi + a)^2 + b^2} \qquad \text{(C-12)}$$

and

$$e_v = \frac{4 \cos\varphi\, (a\, e' + b\, e'')}{(e' \cos\varphi + a)^2 + (e'' \cos\varphi + b)^2} \qquad \text{(C-13)}$$

Equations (C-8) and (C-9) have been employed in calculations of specular emissivities of sea water, salines, quartz sand and limestone utilizing dielectric permittivities at appropriate frequencies and temperatures. In the case of sea water, dielectric permittivities were calculated in accordance with References (19) and (20) at 9.5, 14, 16.5 and 94 GHz, at temperatures encountered in the original project. With regard to solid materials, the permittivities were those measured by the Massachusetts Institute of Technology, at a temperature of 298°K. Since the permittivities were obtained at 14 GHz, it was necessary to confine the emissivity calculations to this frequency, due to the fact that extrapolation of solid material permittivities to other frequencies is not possible.

Calculated sea water permittivities are in reasonable agreement with measured values, as shown in Table C-I.

TABLE C-I

COMPARISON OF SEA WATER PERMITTIVITIES

Freq.: 14 GHz, T = 299.4°K

Item	Measured Value	Calculated Value	Difference (%)
e'	43.0	47.6	+ 10.7
e"	31.4	36.6	+ 16.5

Mr. William B. Westphal, of the MIT Insulation Laboratory, states that the errors in the measured values of e' and e" are approximately $\pm$15%; thus the above calculated values are considered to be reasonable.

Tables C-II thru' C-VIII list calculated emissivities of sea water at 9.5, 16.5, 94 and 14 GHz as a function of incidence angle, with temperature and polarization as parameters. Tables C-IX thru' C-XI present emissivities of salines, quartz sand and limestone at 14 GHz for a temperature of 298.0°K.

TABLE C-II

CALCULATED VALUES OF EMISSIVITY FOR

SEA WATER

f = 9.5 GHz, e' = 52.634, e" = 38.100, T = 288.4°K

Incidence Angle	Vertical Polarization	Horizontal Polarization
0	0.377	0.377
10	0.382	0.373
20	0.396	0.359
30	0.421	0.337
40	0.461	0.304
50	0.522	0.263
60	0.614	0.211
70	0.756	0.150
80	0.947	0.079
82	0.972	0.064
83	0.976	0.056
84	0.969	0.048
85	0.946	0.040
86	0.899	0.033
87	0.813	0.025

TABLE C-III

CALCULATED VALUES OF EMISSIVITY FOR

SEA WATER

f = 16.5 GHz, e' = 34.987, e" = 37.820, T = 287.7 ^{o}K

Incidence Angle	Vertical Polarization	Horizontal Polarization
0	0.401	0.401
10	0.405	0.396
20	0.420	0.382
30	0.446	0.358
40	0.487	0.324
50	0.549	0.280
60	0.642	0.226
70	0.780	0.161
80	0.945	0.085
82	0.958	0.069
83	0.954	0.061
84	0.938	0.052
85	0.906	0.044
86	0.850	0.035
87	0.756	0.026

TABLE C-IV

CALCULATED VALUES OF EMISSIVITY FOR

SEA WATER

f = 16.5 GHz, e' = 36.943, e" = 37.878 T = 289.9°K

Incidence Angle	Vertical Polarization	Horizontal Polarization
0	0.398	0.398
10	0.403	0.394
20	0.418	0.380
30	0.444	0.356
40	0.485	0.322
50	0.547	0.279
60	0.640	0.224
70	0.778	0.160
80	0.946	0.085
82	0.960	0.068
83	0.957	0.060
84	0.943	0.052
85	0.912	0.043
86	0.856	0.035
87	0.764	0.026

TABLE C-V

CALCULATED VALUES OF EMISSIVITY FOR

SEA WATER

f = 16.5 GHz, e' = 39.039, e" = 37.754, T = 292.7°K

Incidence Angle	Vertical Polarization	Horizontal Polarization
0	0.396	0.396
10	0.401	0.392
20	0.415	0.378
30	0.442	0.354
40	0.483	0.321
50	0.544	0.277
60	0.637	0.223
70	0.776	0.159
80	0.948	0.084
82	0.963	0.068
83	0.961	0.060
84	0.947	0.051
85	0.917	0.043
86	0.863	0.035
87	0.771	0.026

TABLE C-VI

CALCULATED VALUES OF EMISSIVITY FOR

SEA WATER

f = 94.0 GHz, e' = 6.606, e" = 11.340, T = 288.2°K

Incidence Angle	Vertical Polarization	Horizontal Polarization
0	0.616	0.616
10	0.621	0.610
20	0.639	0.593
30	0.669	0.563
40	0.713	0.519
50	0.774	0.459
60	0.850	0.380
70	0.924	0.279
72	0.933	0.256
74	0.937	0.232
76	0.934	0.206
78	0.920	0.180
80	0.890	0.153
85	0.680	0.080

TABLE C-VII

CALCULATED VALUES OF EMISSIVITY FOR

SEA WATER

f = 94.0 GHz, e' = 7.025, e" = 12.490, T = 292.4°K

Incidence Angle	Vertical Polarization	Horizontal Polarization
0	0.598	0.598
10	0.603	0.592
20	0.621	0.575
30	0.651	0.546
40	0.695	0.502
50	0.757	0.443
60	0.836	0.366
70	0.916	0.267
73	0.931	0.234
75	0.935	0.210
77	0.930	0.185
80	0.896	0.146
83	0.806	0.105
85	0.693	0.076

TABLE C-VIII

CALCULATED VALUES OF EMISSIVITY FOR

SEA WATER

f = 14.0 GHz, e' = 47.579, e" = 36.614, T = 299.4°K

Incidence Angle	Vertical Polarization	Horizontal Polarization
0	0.388	0.388
10	0.392	0.383
20	0.406	0.369
30	0.432	0.346
40	0.473	0.313
50	0.534	0.271
60	0.627	0.218
70	0.768	0.155
80	0.951	0.082
82	0.972	0.066
83	0.973	0.058
84	0.963	0.050
85	0.937	0.042
86	0.887	0.034
87	0.798	0.025

TABLE C-IX

CALCULATED VALUES OF EMISSIVITY FOR

SALINES

f = 14.0 GHz, e' = 4.750, e" = 0.049 T = 298.0°K

Incidence Angle	Vertical Polarization	Horizontal Polarization
0	0.862	0.862
10	0.866	0.858
20	0.878	0.846
30	0.898	0.823
40	0.926	0.786
50	0.960	0.729
60	0.993	0.640
64	0.999	0.593
65	1.000	0.579
66	1.000	0.566
67	0.999	0.551
70	0.991	0.505
80	0.837	0.301
85	0.580	0.165

TABLE C-X

CALCULATED VALUES OF EMISSIVITY FOR

QUARTZ SAND

f = 14.0 GHz, e' = 2.880, e" = 0.034 T = 298.0°K

Incidence Angle	Vertical Polarization	Horizontal Polarization
0	0.933	0.933
10	0.936	0.931
20	0.943	0.923
30	0.955	0.908
40	0.972	0.881
50	0.990	0.837
58	1.000	0.779
59	1.000	0.770
60	1.000	0.760
61	1.000	0.750
65	0.993	0.703
70	0.968	0.628
80	0.780	0.397
85	0.522	0.224

TABLE C-XI

CALCULATED VALUES OF EMISSIVITY FOR

LIMESTONE

f = 14.0 GHz, e' = 8.630, e" = 0.158 T = 298.0°K

Incidence Angle	Vertical Polarization	Horizontal Polarization
0	0.758	0.758
10	0.763	0.753
20	0.778	0.737
30	0.805	0.709
40	0.844	0.666
50	0.895	0.602
60	0.955	0.513
69	0.997	0.404
70	0.999	0.390
71	1.000	0.375
72	1.000	0.360
75	0.988	0.312
80	0.912	0.222
85	0.673	0.119

APPENDIX D

COMPUTER PROGRAM FOR CALCULATION OF e' AND T

Beginning with the following equations,

$$T_{Bh} = \epsilon_h T + (1 - \epsilon_h) T_{s\varphi} \tag{D-1}$$

$$T_{B2} = \epsilon_2 T + (1 - \epsilon_2) T_{s\varphi} \tag{D-2}$$

and the known functional dependence of ϵ_h and ϵ_v on e', e'', φ, as given in Equations (C-8) and (C-9) in Appendix C,

$$T_{B2} = \epsilon_2 \left(\frac{T_{Bh} - T_{s\varphi}}{\epsilon_h} + T_{s\varphi} \right) + (1 - \epsilon_2) T_{s\varphi} \tag{D-3}$$

If e'' is set to 0.1, Equation (D-3) is an implicit expression for variable e'. Thus,

$$T_{B2} = T_{B2}(e', \varphi_h, \varphi_2, T_{Bh}, T_{s\varphi}) \tag{D-4}$$

(data: φ_h, φ_2, T_{Bh}, $T_{s\varphi}$; function: $T_{B2}(e', \ldots)$)

The task is to find the value of e' which satisfies the above relationship for given values of T_{B2}, φ_h, φ_2, T_{Bh} and $T_{s\varphi}$.

Consider a function T_{Bc}

$$T_{Bc} = T_{B2}(e', \varphi_h, \varphi_2, T_{Bh}, T_{s\varphi}) \tag{D-5}$$

or

$$T_{Bc} = T_{Bc}(e')$$

It is desired to find e' such that

$$T_{B2} = T_{Bc}(e'_o) \tag{D-6}$$

where, e'_o is the value of e' which satisfies this relation, and therefore also the value which satisfies Equations (D-1) and (D-2). To calculate for the remaining variable, Equation (D-1) is solved for T:

$$T_o = \frac{T_{Bh} - T_{s\varphi}}{\epsilon_h(e'_o)} + T_{s\varphi} \tag{D-7}$$

Here e'_o is used to evaluate ϵ_h. T_o and e'_o are the two simultaneous solutions to Equations (D-1) and (D-2).

A. DETERMINATION OF e'_o

A computer program has been devised which determines the value of e'_o for a specified T_{B2}.

Consider the function T_{Bc}, depicted in Figure D-1 as a function of e'. The correct value of e' is the intersection of the curve T_{Bc} and the data T_{B2}, represented by a straight horizontal line. Using the limits suggested by the set of materials under consideration, values of T_{Bc} are calculated at a low and high value of e'. In the program these are $e'_1 = 2.0$ and $e'_2 = 8.9$, respectively.

The program now has co-ordinates of Points (1) and (2) and proceeds as follows:

1) Finds the intersection of a straight line connecting Points (1) and (2) and the horizontal line T_{B2}. In Figure D-1 this is Point (3), and locates e'_3.

2) Using this value of e' ($= e'_3$), T_{Bc} is calculated. This is shown as T_{Bc3} in Figure D-1.

3) Program compares value of T_{Bc3} and T_{B2}. If $\left|T_{Bc3} - T_{B2}\right| < 0.2$, e'_3 is named e'_o, the desired value, and then proceeds to calculate T_o using Equation (D-7). If this requirement is not met, e'_1 is renamed e'_3 and T_{Bc1} is renamed T_{Bc3}.

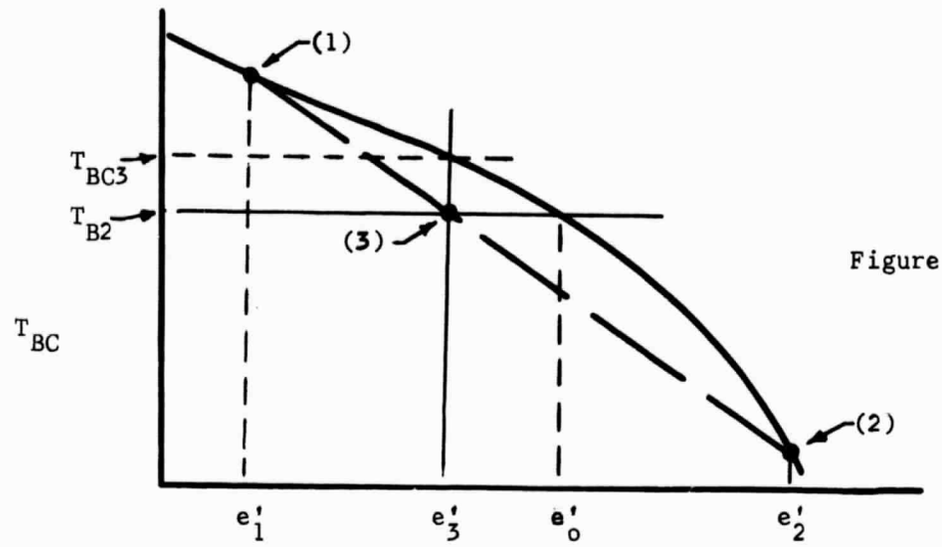


Figure D-1

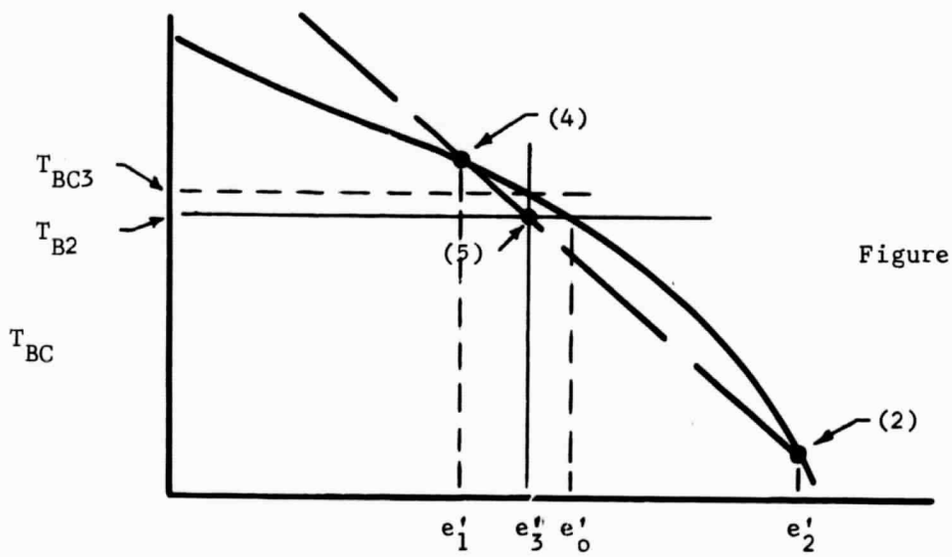


Figure D-2

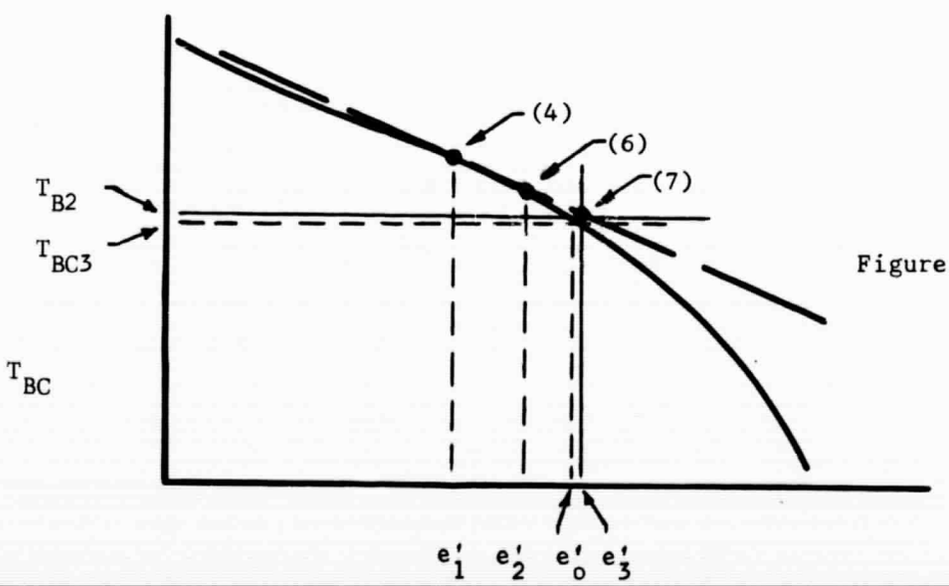


Figure D-3

Using the new values of e_1' and T_{Bc1}, a straight line is drawn between Points (4) & (2) and find its intersection with T_{B2}, as shown in Figure D-2. This intersection provides the new e_3', Point (5). The corresponding T_{Bc3} is now calculated and compared with T_{B2}. If the requirements are still not met, e_2' is renamed e_3' and T_{Bc2} is renamed T_{Bc3} and the process is repeated. The maximum and minimum values of e' are renamed alternately and the process repeated. The result is a very fast convergence on the correct values as indicated in Figure D-3. In general, a maximum of 6 repetitions of the above process will achieve matching to within 0.2.

As a test of the validity of the method a brief calculation was performed using calculated T_B data. The results are tabulated in Table D-I.

TABLE D-I

TEST DATA AND RESULTS FROM

COMPUTER PROGRAM (h - h DATA)

e'	T (^oK)	φ_h (deg.)	T_{Bh} (^oK)	φ_2 (deg.)	T_{B2} (^oK)	Input T (^oK)
8.597	290.93	70	126.40	40	198.59	291
8.592	290.89	60	155.93	40	198.59	291
8.591	306.87	70	143.44	40	209.08	307
8.589	306.84	60	164.69	40	209.08	307
			(h - v Data)			
8.600	290.98	70	126.40	40	248.41	291
8.594	290.90	70	126.40	50	261.49	291
8.597	306.95	70	143.44	40	260.81	307
8.597	306.95	60	164.69	40	260.81	307

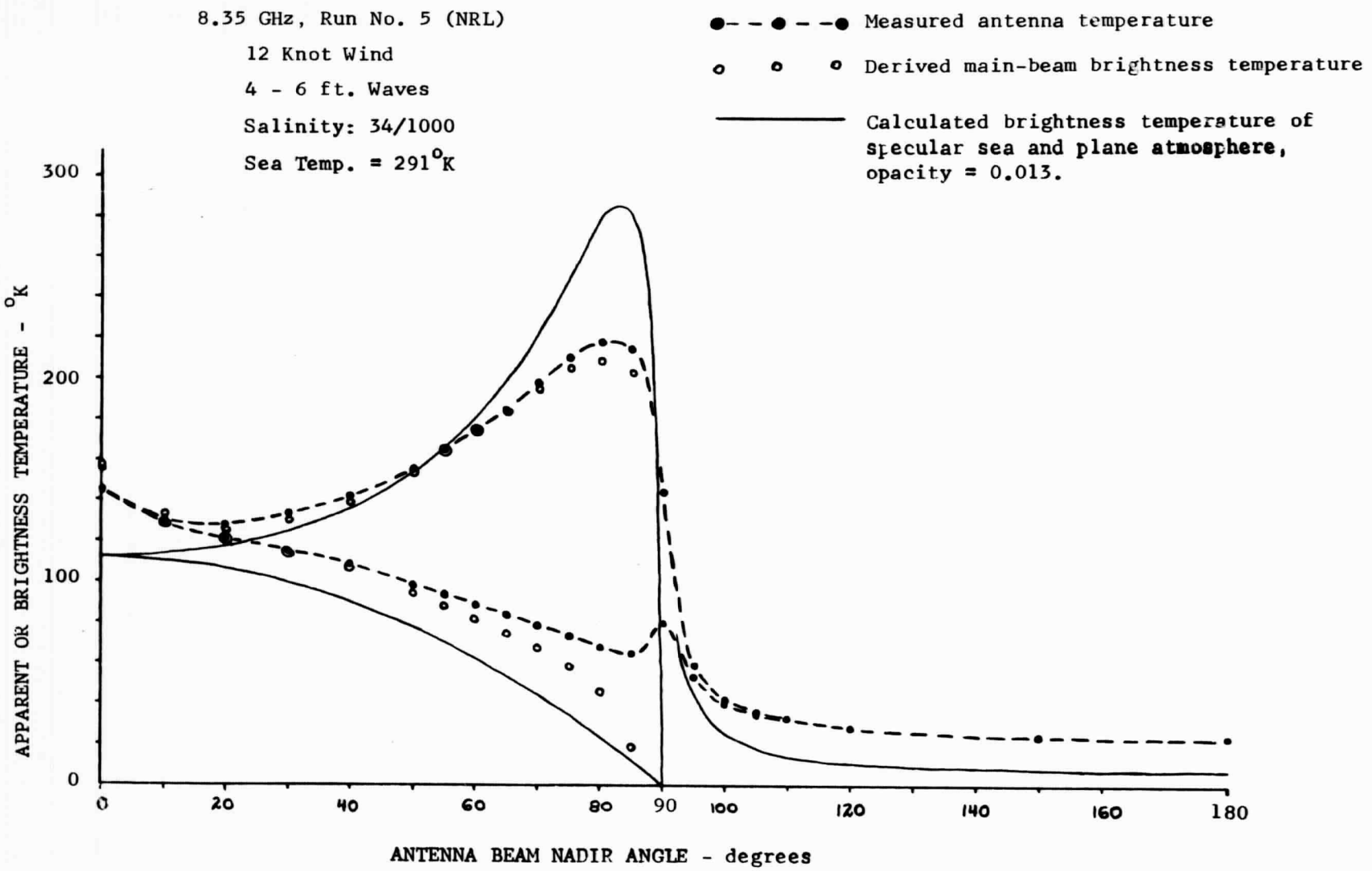


Figure D-4 Apparent and Brightness Temperatures at 8.35 GHz (J. Hollinger, NRL)

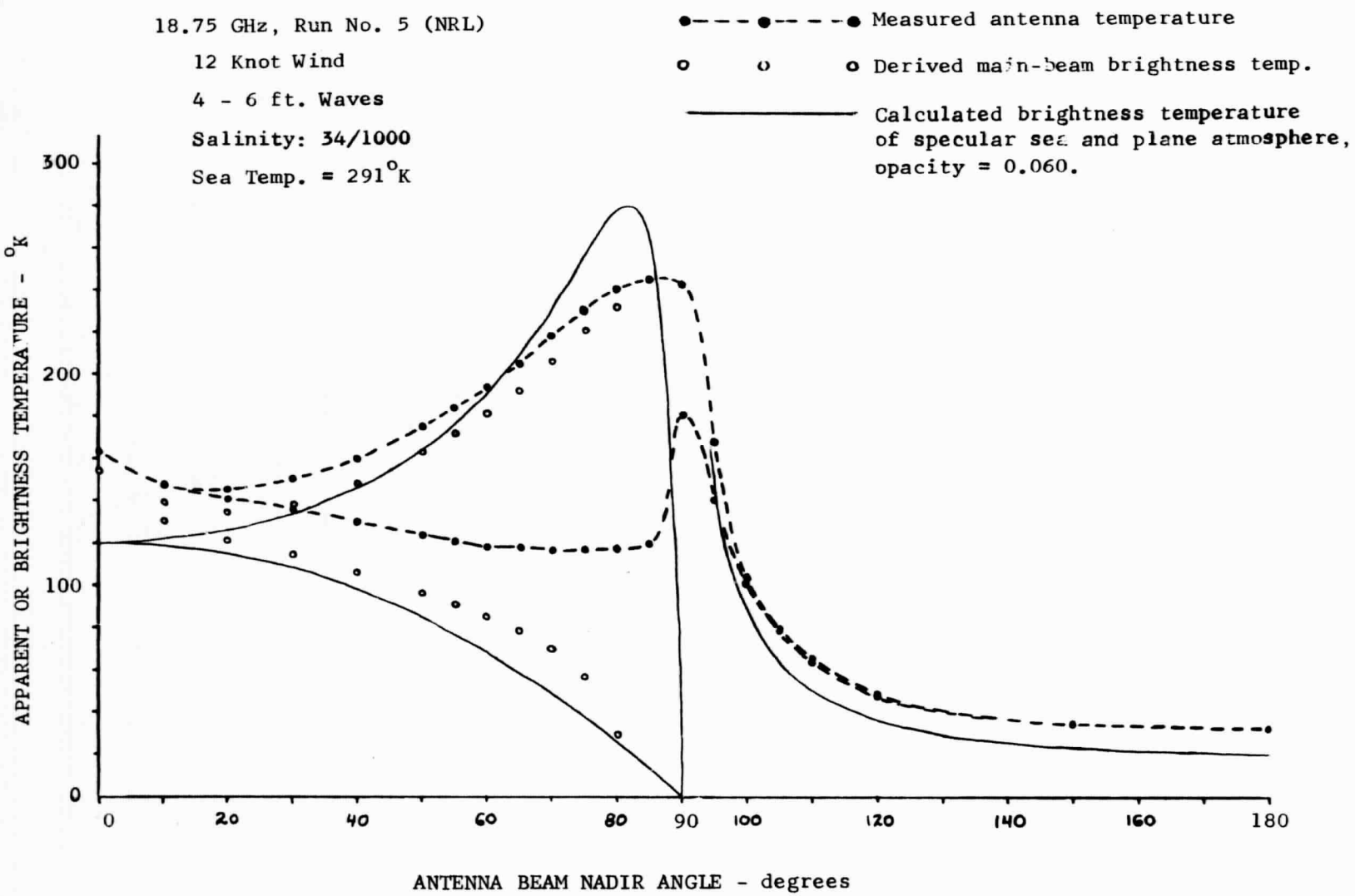


Figure D-5 Apparent and Brightness Temperatures at 18.75 GHz (J. Hollinger, NRL)

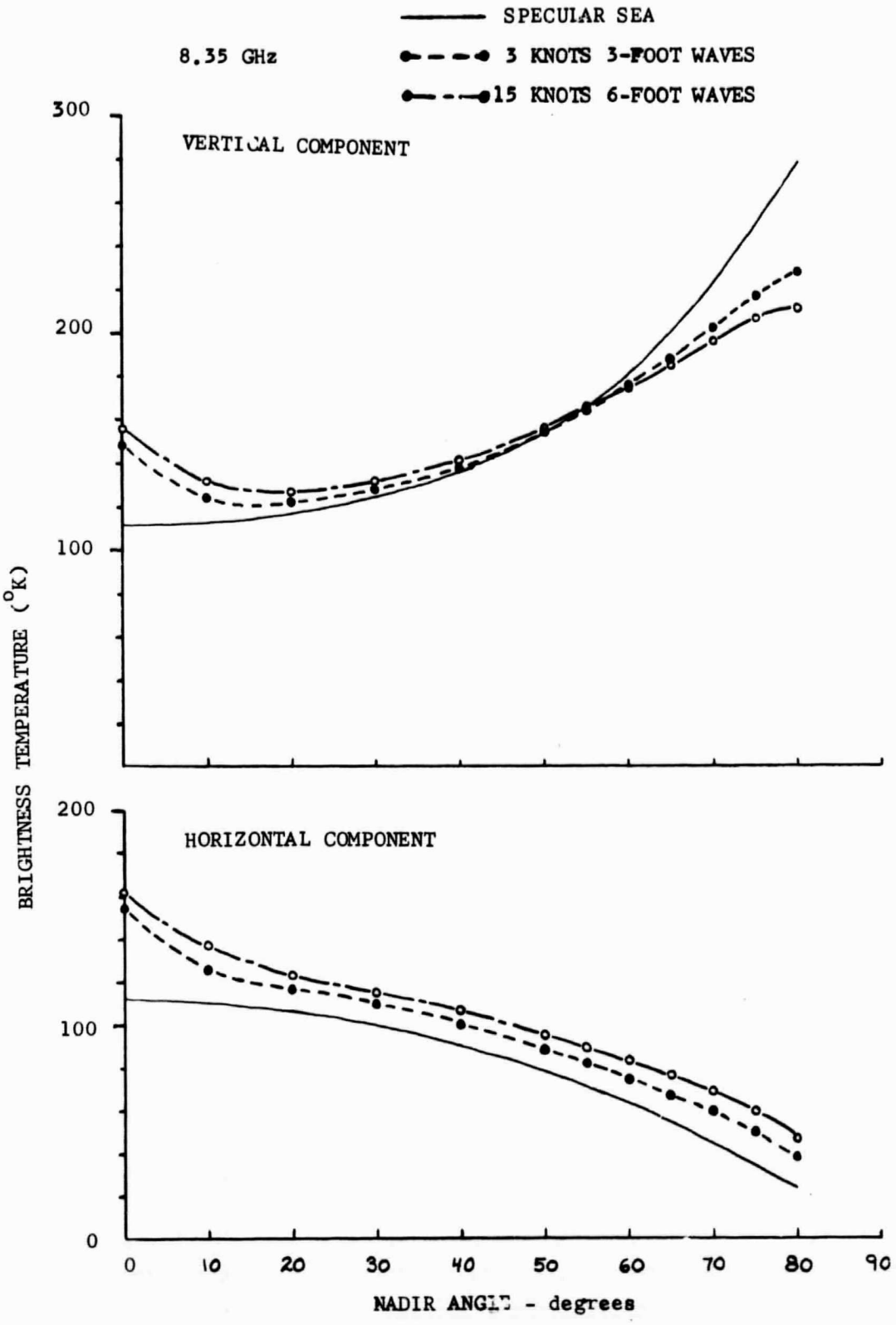


Figure D-6 Brightness Temperatures at 8.35 GHz, for Various Sea Surface Roughnesses (J. Hollinger, NRL).

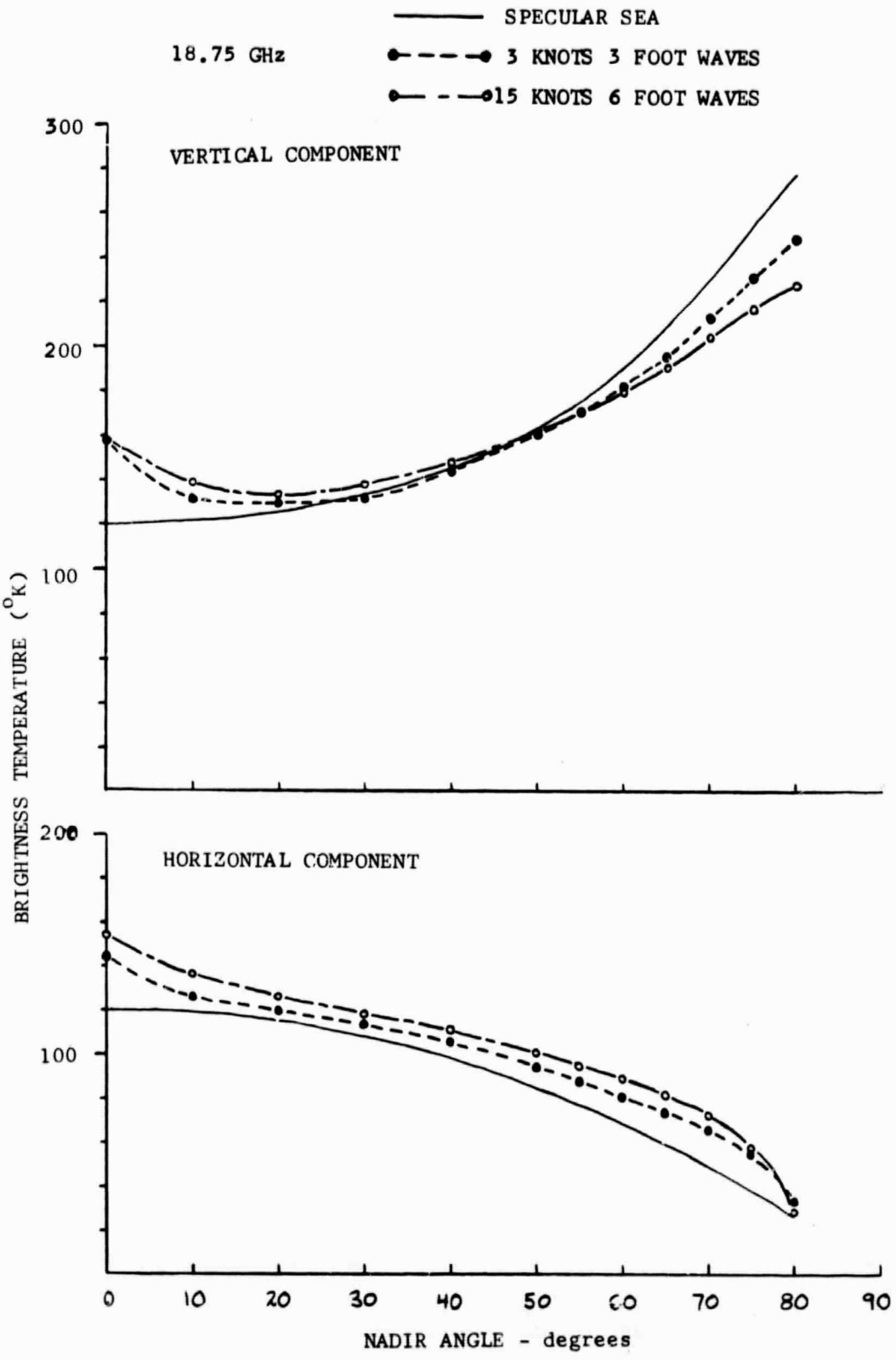


Figure D-7 Brightness Temperatures at 18.75 GHz, for Various Sea Surface Roughnesses (J. Hollinger, NRL).